Modelling Embryonic Haematopoiesis Using *In Vitro* State-of-art Gastruloid Culture

Chun Wai Suen

Homerton College

Department of Genetics

University of Cambridge

This thesis is submitted for the degree of
Doctor of Philosophy

March 2022

This thesis is the result of my own work except for the analysis of single-cell SMART sequencing in chapter 6.3 was conducted by Dr Gabriel Torregrosa Cortés from Universitat Pompeu Fabra.

This thesis is not substantially the same as any works submitted for a degree or diploma, or other qualification at any other University. I further state that no part of this thesis has already been or is being concurrently submitted for any such degree, diploma or other qualification.

This thesis does not exceed the prescribed word limit for the Biology Degree Committee.

Abstract

Haematopoietic stem cell progenitor cells (HSPCs) have substantial research and therapeutic value, but the *in vitro* production of HSPCs from pluripotent stem cells remains elusive. A novel 3D culture method, known as a gastruloid, can mimic gastrulation in embryogenesis, which is crucial to the emergence of HSPC precursors, highlighting the potential to develop this protocol as an *in vitro* platform for haematopoietic research. This project aims to adapt the previously published gastruloid culture protocol and develop it into a haemogenic gastruloid protocol to produce HSPCs from mouse ES cells and model haematopoiesis which occurs at the aorta-gonad-mesonephros (AGM) region of the mouse embryo.

In this project, the gastruloid culture protocol is modified to maintain a gastruloid (gastrulation organoid) for up to 216 hr by introducing a 2iLIF pretreatment and a panel of cytokines throughout the culture. Under the new culture conditions, gastruloids can generate haemogenic endothelium and pro- and pre-HSCs in sequential order, as detected by a combination of markers in flow cytometry assays (Flk-1, c-Kit, CD41 and CD45). Concomitant use of cytokines VEGF and FGF_2 can facilitate the emergence of cells with the property of haemogenic endothelial cells, pro-HSCs and type 1 pre-HSCs from 96 to 144 hr. Applying Shh, Flt-3l, TPO, and SCF accordingly can promote the formation $CD45^+$ cells, which is indicative of the formation of type 2 pre-HSCs at 192 and 216 hr. The emergence of these haematopoietic makers suggests stepwise haematopoiesis is recapitulated in the haemogenic gastruloid.

The AGM-like haematopoietic clusters are observed at 192 and 216 hr under confocal imaging, further suggesting that definitive haematopoiesis likely occurs in the gastruloid under the optimised protocol. The CFC assay shows that gastruloid cells have the potential to form multipotential myeloid and lymphoid haematopoietic progenitors. The $CD45^+$ cells from the 216 hr gastruloids can occasionally be enriched in OP9 co-culture, and they can also sometimes form committed B-cell linage progenitors with OP9 cells. The chick embryo chorioallantoic membrane (CAM) assay and mouse transplantation experiments imply that the haemogenic gastruloid cells may possess engraftment capability.

Single cell SMART sequencing data confirms that gastruloids have haematopoietic gene expression profiles similar to the AGM region of the mouse embryo and captures successive progenitors with erythroid, myeloid-lymphoid and HSC-like signatures. Finally, this

haemogenic gastruloid protocol has been applied to other mouse ES cell lines to generate gastruloids, and they can also recapitulate stepwise haematopoiesis.

This study has successfully developed a haemogenic gastruloid protocol with a cocktail of haematopoietic cytokines. This haemogenic gastruloid is able to form AGM-like haematopoietic clusters and recapitulate stepwise definitive haematopoiesis to produce haematopoietic progenitors. In the future, this protocol could be developed to validate and reduce the use of animals in scientific research. The results from this study could also be useful preliminary data for developing a human haemogenic gastruloid protocol. Finally, this protocol could be applied as a drug screening or disease modelling tool, such as an infant leukaemia disease model.

This thesis is dedicated to my parents,

Yip-Po Suen and Wan-Ping Chan,

and my siblings,

Jackie Chun-Lung Suen and Yvonne Wing-Yung Suen,

for their endless love, support and encouragement throughout my pursuit for this PhD degree.

Acknowledgements

I would like to express my deepest appreciation to my supervisor, Dr Cristina Pina, for offering me the opportunity to pursue this PhD in her group. Her valuable and unceasing inspiration, advice and guidance have been particularly important in every stage of my research, especially during the covid pandemic. I would also like to thank her for all the help and suggestions she has provided for my thesis write-up. I appreciate Dr Shikha Gupta and Ana Filipa Domingues for their advice on experiments, particularly their assistance in setting up the C57BL/6 mice model for gastruloid transplantation. The summer student Oliver Davies also deserves credit for his preliminary studies.
I express my heartfelt gratitude to Professor Alfonso Martinez Arias for welcoming me to work in his lab and later becoming my second supervisor. His enduring encouragement and care have been an important source of support for me during this process. Credit must also be given to Tina Balayo for the gastruloids culture training and Dr David Turner for the assistance with fluorescence microscopy and confocal imagining. Gratitude should be given to Dr Peter Baillie-Benson and Dr Suzanne Van den Brink for their advice and their work, which formed the vital foundation for my research. I also want to thank Dr Naomi Moris for sharing her insights on gastruloids from time to time.

I would like to extend my gratitude towards Dr Ben Steventon for being my supervisor in the final year of my PhD. He was always willing to offer me much-needed help and advice when my research progress was delayed due to the Covid pandemic and on extending my thesis submission deadline. I am also thankful to Dr Chaitanya Dingare for the assistance in tissue culture and expertise on gastruloid culture.

I am grateful to Joana Ceveira from the Flow Cytometry Facility, Department of Pathology, for providing training on the flow cytometer, assisting with the plate sorting for gene sequencing and being extremely helpful every time I faced a problem with the analyser. I would like to thank Professor Kamil Kranc, Dr Natacha Bohin and Andrea Tavosanis from Barts Cancer Centre for working on the c-Kit mutant NSG mice model for gastruloid transplantation. I am also thankful to Dr Gabriel Torregrosa Cortés from Universitat Pompeu Fabra for his help in analysing the gastruloid data for single-gene SMART sequencing.

I am truly blessed to have Dr Shikha Gupta, Dr Liliana Arede and Dr Keti Zeka and thank them for being my best lab mates. Whether at the lab bench or in the café, their companionship has left me with a wonderful memory of my time in Cambridge. Finally, I would like to say a big thank you to the best friends I gained throughout this PhD journey, from Dr Andy Tseng, Dr Jeremy Chang, Dr Lancelot Peng, Dr Louis Wu, Jefferson Chan, Kris Wu and Yi-Hsuan Kuo. The friendships I formed with them are priceless. I really appreciated their help when I was going through hard times and the joy we had shared together when we celebrated our accomplishments.

List of figures

List of tables

Abbreviations

2iLIF	2 Inhibitors & LIF
3D	Three dimensions
AC	Activin A & Chiron
Act A	Activin A
ADA-SCID	Adenosine deaminase deficiency
AGM	Aorta-gonad-mesonephros
AVE	Anterior visceral endoderm
BFU-E	Burst forming unit-erythroid
BMP	Morphogenetic protein
CAM	Chick chorioallantoic membrane
CD	Cluster of differentiation
cDNA	Complementary DNA
CFC Assay	Colony forming cell assay
CFU-M	Colony-forming unit-myeloid
CFU-S	Spleen colony-forming cell
Chi	Chiron
C-kit	SCF receptor
CLPs	Common lymphoid progenitors
CMPs	Common myeloid progenitors
DE	Differential expression
DMSO	Dimethylsulfoxide
DNA	Deoxyribonucleic acid
dpf	Days post fertilisation
DVE	Distal visceral endoderm
EBs	Embryoid bodies
ECM	Extracellular matrix
EDTA	Ethylenediaminetetraacetic acid
eGFP	Enhanced green fluorescent protein
EHT	Endothelial-to-hematopoietic transition
EMPs	Erythroid/myeloid progenitors
EMT	Epithelial to mesenchymal transition

EPI	Epiblast-like
EPO	Erythropoietin
ERK	Extracellular signal–regulated kinases
ES Cells	Embryonic stem cells
FACS	Fluorescence-activated cell sorting
FGF	Fibroblast growth factor
FISH	fluorescence in situ hybridisation
Flk-1	Vascular endothelial growth factor receptor
Flt3-L	Fms-like tyrosine kinase receptor 3 ligand
FSC	Forward scatter
GAPDH	Glyceraldehyde 3-phosphate dehydrogenase
GMPs	Granulocyte/macrophage progenitors
Gsk3	Glycogen synthase kinase 3
Hbb	Haemoglobin beta
Hh	Hedgehog
HPP-CFC	High proliferative potential CFC
HSCs	Haematopoietic stem cells
HSPCs	Hematopoietic stem/progenitor cells
IL	Interleukin
iPSCs	Induced pluripotent stem cells
IT-HSCs	Intermediate-HSCs
LIF	Leukaemia inhibitory factor
LMPPs	Lymphoid-primed multipotent progenitors
LMPs	Lympho-myeloid progenitors
LSCs	Leukaemic stem cells
LT-HSCs	Long term-HSCs
M-CSF	Macrophage-colony stimulating factor
MEK	Mitogen-activated protein kinase kinase enzymes
MEPs	Megakaryocyte/erythrocyte progenitors
MPPs	multipotent progenitors
OoC	Organ-on-a-chip
PBS	Phosphate-buffered saline
PC	Principal component

PCR	Polymerase chain reaction
PSA	Penicillin-Streptomycin Amphotericin
PSC	Pluripotent stem cells
qPCR	Quantitative real-time polymerase chain reaction
RNA	Ribonucleic acid
RNA	Ribonucleic acid
SCF	Stem cell factor
Shh	Sonic hedgehog
SLAM	Signaling lymphocytic activation molecule
Smad	Mothers against decapentaplegic homolog
SP	Side population
SSC	Side scatter
ST-HSCs	Short-term-HSCs
TAE	Tris-acetate-EDTA
TGFβ	Transforming growth factor-β
TPO	Thrombopoietin
UV	Ultraviolet
VeCAD	Vascular endothelial cadherin
VEGF	Vascular endothelial growth factor

Table of contents

Chapter 1: Introduction

1.1 Haematopoiesis

1.1.1 Haematopoietic system and embryonic haematopoiesis

The blood circulatory system is one of the most important methods of transporting nutrients to tissues, providing immune protection against infection and regulating the body's homeostasis. Blood cells are categorised into two lineages, myeloid and lymphoid. Myeloid lineage cells are erythrocytes, megakaryocytes, macrophages, and granulocytes, a majority of which are components of the non-specific defence system against infectious agents and foreign particles, known as the innate immune system (Alberts *et al*., 2002). T cells, B cells, and natural killer cells are lymphoid cells. T and B cells are vital members of the adaptive immune system, which provides an acquired response to eliminate specific pathogens by targeting their antigens (Bonilla & Oettgen, 2020). Continuous production of such functional blood cells throughout life relies on a pool of multipotent haematopoietic stem cells (HSCs). HSCs are the foundation of the haematopoietic system as they generate all of the cellular components of the blood to replenish and maintain the blood and immune system (Kondo *et al*., 2003).

In the adult haematopoietic system, HSCs primarily reside in the bone marrow and continuously initiate haematopoiesis. The pool of HSCs is precisely balanced between self-renewal to generate multipotent daughter HSCs, or differentiation into committed progenitors (Ng & Alexander, 2017). Embryonic haematopoiesis differs from the adult one, with waves of haematopoiesis that occur spatially and temporally during early embryogenesis. Each wave generates a cohort of blood cell progenitors with higher blood lineage potential and complexity.

The primitive haematopoietic cells emerge as the first wave in the extraembryonic region in the yolk sac (Palis *et al*., 1999). Primitive haematopoietic cells originate from the blood islands of the yolk sac mesoderm and generate short-lived cells. Primitive haematopoiesis gives rise to lineage-restricted blood cell types including primitive erythrocytes, macrophages, and megakaryocyte progenitors (Tobe *et al*., 2007). The second wave, pro-definitive haematopoiesis, originates from the vasculature of the yolk sac and generates hematopoietic progenitors that contribute blood cells to the embryo until birth. Erythroid/myeloid progenitors (EMPs), lymphoid-restricted progenitors, and multilineage lymphoid-myeloid progenitors (LMPs) emerge at the yolk sac endothelium and colonise the foetal liver (Gomez Perdiguero *et al*., 2015).

When the structure of the growing embryo becomes complex, a more advanced haematopoietic system is required to support the increasing nutrient and oxygen needs. The third wave of haematopoiesis, leading to long term adult HSC production, begins when the aorta-gonad-mesonephros (AGM) region is developed and definitive HSPCs are intraembryonically derived from the haemogenic endothelium in the AGM (Kauts *et al*., 2016). HSPCs are haematopoietic cells with a robust, long-term multilineage reconstitution potential which undergo expansion and maturation at the foetal liver (Batsivari *et al*., 2017). The switching from primitive to pro-definitive to definitive haematopoiesis occurs gradually in mice and definitive HSCs are subsequently present at the placenta and foetal liver (Eaves, 2015). Finally, HSCs migrate to the bone marrow to contribute to the life-long adult haematopoiesis after birth (Mahony & Bertrand, 2019).

However, it remains unclear on the specific cell lineages and the origins of haemogenic endothelium cells developed from the dorsal aorta. The early hypothesis suggested that endothelial and haematopoietic bi-potent haemangioblast originates from extraembryonic yolk sac blood islands (Maximow, 1909; Sabin, 1920). Nevertheless, the blood-forming area forms a belt-like structure encircling the yolk sac in the whole-mount preparations of the E8 embryo, suggesting that haemangioblast may not arise from the yolk sac (Ferkowicz and Yoder, 2005). Instead, it is suggested that the haemogenic endothelium-forming haemangioblast migrates from the intraembryonic splanchnic mesoderm to the aorta (Medvinsky *et al.*, 2011). The identification of endothelial and haematopoietic blast colony-forming cells (BL-CFC) *in vivo* and single-cell labelling assay revealed haemangioblast's role as a bipotential precursor (Vogeli *et al.*, 2006). During the BL-CFC development, the haemogenic endothelium forming population transiently presented, and they can form HSCs in further culture, suggesting the close link between haemangioblast and haemogenic endothelium (Lancrin *et al.*, 2009). Although the origin of the aortic haemogenic endothelium cells is still controversial, a recent review used avian models to illustrate that haemangioblast is the common origin of yolk sac blood islands and aortic haemogenic endothelium cells (Seco *et al.*, 2020).

The placenta is a large and highly vascularised tissue for foetal-maternal exchange during pregnancy and it is also an important foetal haematopoietic organ. The placenta can generate

HSCs and their progenitors de novo and establish a major reservoir of HSCs in the conceptus to protect them from premature differentiation (Gekas *et al.*, 2010). Mouse placenta at E8.0 to E9.0 develops many haematopoietic progenitors which can form colonies and replatable in high proliferative potential CFC (HPP-CFC) assay (Alvarez-Silva *et al.*, 2003). Both prefusion allantois and chorion tissues have intrinsic hematopoietic potential by forming clonogenic haematopoietic progenitors and expressing haematopoietic markers 48hr after explant culture (Zeigler *et al.*, 2006). Both placenta and AGM concomitantly have definitive HSCs presented at E10.5 and 11.0 (Gekas *et al.*, 2005). By E12.5, the placenta develops a substantial definitive HSCs pool which will translocate to foetal liver by E15.5 (Ottersbach & Dzierzak, 2005; Robin *et al.*, 2009).

1.1.2 Murine Primitive and pro-definitive Haematopoiesis

The first wave of haematopoiesis occurs in the mouse from E7.0 onwards. Production of the primitive blood cells begins when mesodermal progenitors differentiate into vascular and hematopoietic cells and organise themselves into the yolk sac blood islands (Ferkowicz & Yoder, 2005). The mouse blood islands in the extraembryonic yolk sac at E7.25 contain a pool of bipotential megakaryocyte/erythroid progenitors (MEPs) that can generate primitive erythrocytes and megakaryocytes between E7.5 to E10.5 (Tober *et al*., 2007). In contrast to their adult equivalents, the primitive erythrocytes are larger, nucleated and contain embryonic haemoglobin, *Hbb-epsilon*. In addition, these erythrocytes are characterised by erythrocyte colony-forming unit cells, BFU-E, detectable exclusively within the yolk sac at E8.25 (Palis *et al*., 1999).

Aside from a large population of primitive erythrocytes, most haemangioblast precursors have megakaryocyte-forming potential during early gastrulation. Progenitors with megakaryocyte lineage can be detected in the yolk sac at E9.5 and decline at E10.5 (Tober *et al*., 2007). Diploid proplatelets form in the E10.5 yolk sac and reticulated platelets are released and identifiable in the embryonic blood at E11 (Potts *et al*., 2014). The yolk sac is the primary source of embryonic platelets, in contrast to polyploid megakaryocytes which are formed in the foetal liver at a later stage.

The yolk sac blood islands also contain unipotent primitive macrophage progenitors, and macrophages emerge from E9.0 onwards (Palis *et al*., 1999). The surrogate marker of monocytic intermediates, endogenous peroxidase activity, is absent at this stage which suggests that these macrophages are primitive and bypass monocytic intermediates (Hoeffel & Ginhoux, 2015). These primitive macrophages either remain in the yolk sac or invade the embryo, which becomes the origin of tissue-resident macrophages, such as future brain microglia (Ginhoux *et al*., 2013).

Pro-definitive haematopoiesis is the second wave of haematopoiesis, and arises in the yolk sac vasculature. This wave is occasionally referred to as transient definitive haematopoiesis as the multipotent progenitors generated at this wave can only transiently reconstitute to the adult mouse with bone marrow ablation. The shift from primitive to pro-definitive haematopoiesis happens coincidently with the onset of the pulsatile systemic circulation and synchronous heart beating (Hirschi, 2012). Multipotent progenitors are initiated rapidly in the yolk sac, and this second wave of haematopoietic cells is more complex than the progenitor cells of the first wave, and includes erythroid/myeloid progenitors (EMPs) emerging at E8.25, and lymphoid-restricted progenitors and lymphoid potential progenitors (LMPs) present at E9.5 (Palis *et al*., 1999). However, it is unclear whether these progenitors are derived from the same pool or a distinct subpopulation of haemogenic endothelium, a specialised endothelium in the aorta, which is committed to hematopoietic lineage following endothelial to hematopoietic transition (EHT) (Hadland & Yoshimoto, 2018).

The EMPs are developed at the c-Kit expressing cluster in the venous and arterial vessels of the yolk sac, though EMP-derived erythrocytes contain adult haemoglobins (Frame *et al*., 2016). With the establishment of blood circulation by E10.5, EMPs colonise the foetal liver and yield more foetal-like haematopoietic cells including enucleated erythrocytes containing foetal-type haemoglobin, *Hbb-bh1* (Gomez Perdiguero *et al*., 2015). EMPs differentiate into monocytes which infiltrate other organs and form tissue-resident macrophages (Hoeffel & Ginhoux, 2018). From E12.5 onwards, macrophages formed during this wave gradually replace those formed in primitive haematopoiesis and become the majority of tissue-resident macrophages, except microglia due to the blood-brain barrier (Ginhoux & Guiliams, 2016).

In parallel to EMPs, lymphoid-restricted progenitors and multilineage LMPs also emerge at approximately E9.5 in the yolk sac, and migrate to the foetal liver by E11.5 onwards (Böiers *et al*., 2013). Lymphoid progenitors differentiate into B and T cells in the foetal liver and circulate to multiple organs, becoming tissue specific. For example, innate lymphocytes may become B-1a lymphocytes in the lung and gut, or γδ T cells in the lung and skin (Kobayashi *et al*., 2014). The E9 yolk sac has also been discovered to give rise to AA4.1^{+} CD19^{+} B220$^{low/-}$ B progenitor cells, which are associated with innate B-1 cells and marginal zone B cells in the adult spleen (Yoshimoto *et al*., 2011). In the E14.5 foetal liver, AA4.1^{+} multipotential progenitors with T cell, B cell and macrophage forming potential were observed (Lacaud *et al*., 1998). Granulocytes and monocytes are also derived from the foetal liver in the E14.5 yolk sac (Böiers *et al*., 2013).

The presence of CD41^{+} cells in the foetal liver was reported, and the co-expression of CD41, c-Kit and CD16 are regarded as the selection criterion to separate EMPs from B-1 forming lymphoid progenitors (McGrath *et al*., 2015). These EMPs not only have the potential to form erythrocytes, macrophages, megakaryocytes, and neutrophils but also can transiently reconstitute adult erythrocytes in immune-compromised adult mice (McGrath *et al*., 2015).

1.1.3 Murine Definitive Haematopoiesis and AGM

Haematopoietic stem and progenitor cells differentiate hierarchically in the bone marrow. This hierarchy is first established in embryos with a unique and rare population of HSCs, which emerge from the AGM region during definitive haematopoiesis (de Bruijn *et al*., 2000). The generation of definitive multilineage HSCs is suggested to begin at the mesoderm. The mesodermal layer is formed after the gastrulation of the embryo. The mesodermal cells generate endothelial cells, which subsequently transform into haemogenic endothelial cells (Era *et al*., 2008). Intraembryonic haematopoiesis, which contributes to the foetal liver and bone marrow, begins in the AGM region with the budding off of the endothelium and specialisation into hemogenic endothelium at approximately E9 (Gekas *et al*., 2005).

Lineage-tracing studies suggest that mesodermal progenitor cells with co-expression of Brachyury and the receptor for the vascular endothelial growth factor (Flk-1) have the potency to differentiate into mesodermal lineages and haematopoietic progenitor cells (Figure 1.1.1) (Motoike *et al*., 2003). Flk-1 is first detected in the yolk sac mesoderm and later in AGM. Flk-1^+ vascular endothelium gives rise to the expression of the endothelial cell marker CD31 and vascular endothelial cadherin (VeCAD) (Kauts *et al*., 2016). Mouse embryo-derived $VeCAD^+$ $CD45^-$ endothelial cells can differentiate into myeloid and lymphoid cells *in vitro*, and eventually, HSCs are generated to colonise the hematopoietic sites of the embryo *in vivo* (Nishikawa *et al*., 1998; Zovein *et al*., 2008).

Endothelial-to-hematopoietic transition (EHT) is the hallmark of definitive haematopoiesis in AGM, in which endothelial cells acquire specification to form haematopoietic progenitor cells, driven by the upregulated transcription factor Runx1 and Gata2 (North et al., 1999). Although Runx1 is expressed in yolk sac, aorta and in variety of haematopoietic cells, Runx1only specify the haemogenic potential of the non-haemogenic endothelium in a very short developmental window (E7.5-E8.5) in the yolk sac and the dorsal aorta (Yzaguirre et al., 2018). Gata2 expression is initiated in the primitive streak, and then in major haematopoietic sites (yolk sac, aorta, intra-aortic hematopoietic clusters and fetal liver) (Minegishi *et al.*, 2003). When compared with Runx1, Gata2 take a more predominant role which is not restricted to haemogenic endothelium formation and on endowing hematopoietic activity through the promotion of EHT (Kang *et al*., 2018).

Haemogenic endothelium expresses the growth factor receptor of mast/stem cell, c-Kit. Flk-1^{+} $VeCAD^{+}$ c-Kit^{+} cells specifically represent haemogenic endothelium and show multilineage hematopoietic potential at a clonal level (Goldie *et al*., 2008). Pro-HSCs ($VeCAD^{+}$ c-Kit^{+} $CD41^{low}$) emerge from the haemogenic endothelium at E9.5 and subsequently transform into a type 1 pre-HSC population, which display $VeCAD^{+}$ c-kit^{+} $CD41^{low}CD43^{+}$ in the AGM region at E10.5 (Batsivari *et al*., 2017; Cao & Zhao, 2016).

Type 1 pre-HSC will slow down their cycling at the base of intra-aortic clusters and persist to E11 (Batsivari *et al*., 2017). Type 2 pre-HSC ($VeCAD^{+}$ $CD31^{+}$ $CD41^{low}CD45^{+}$) begin to emerge at E11.5 and exhibit multi-lineage hematopoietic colony-forming activity (Goldie *et al*., 2008; Nadin *et al*., 2003). Type 2 pre-HSCs are located at more apical positions in the intra-aortic clusters and cycle more actively than Type 1 pre-HSCs (Batsivari *et al*., 2017). The Flk-1 is critical to the initiation of haematopoiesis as it is involved in the migration of cells from the posterior primitive streak to the yolk sac and, possibly, to the intraembryonic sites of definitive haematopoiesis. Although Flk-1 is highly expressed in the haemogenic endothelium, it begins to be downregulated in haematopoietic progenitors with the onset of haematopoiesis (Shalaby *et al*., 1997).

In the AGM, type 2 pre-HSCs continue to proliferate and mature into long-term repopulating definitive HSCs. The proliferative organisation of intra-aortic clusters is maintained in the AGM region during the development of HSCs to support the maturation of the haematopoietic system. Flk-1^{-} $CD45^{+}$ HSCs begin to relocate to the foetal liver at E11.5, triggering HSCs to significantly expand for several days before being released into the circulating blood, which eventually reaches the bone marrow and spleen (Wang *et al*., 2016).

To drive the definitive haematopoiesis, haematopoietic gene regulatory networks are supported by a panel of transcription factors. By using human iPSCs in mouse engraftment study, seven transcriptional factors (*ERG, HOXA5, HOXA9, HOXA10, LCOR, RUNX1* and *SPI1*) are identified that their expressions are enough to drive the differentiation of haemogenic endothelium to HSCs with myeloid engraftment potentials (Sugimura *et al.*, 2017). In mouse endothelial cells, the transient expression of *FOSB, GFI1, RUNX1* and *SPI1* (collectively FGRS) can initiate endogenous Runx1 expression and yields cells similar to adult HSCs. Also, the activation of *CXCR4* and *BMP* or inhibition of *TGFβ* and *CXCR7* signalling can promote the formation of these adult HSCs-like cells (Lis *et al.*, 2017).

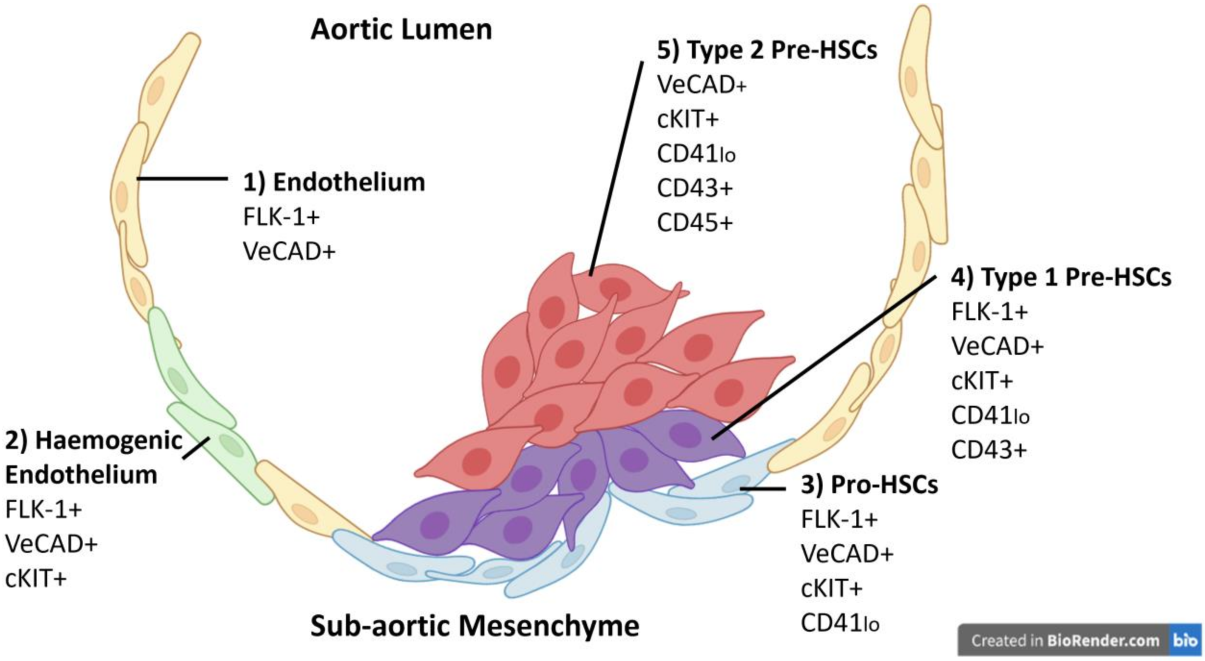

Figure 1.1.1. Illustration of mouse definitive haematopoiesis in AGM.

Stepwise specification of early embryonic haematopoietic progenitor cells at the intra-aorta cluster in the AGM.

The pre-HSCs mature into HSCs in the AGM and subsequently home to the foetal liver via blood circulation, while some pro-HSCs and pre-HSCs also migrate to the foetal liver for maturation into HSCs (Rybtsov *et al*., 2016). Mature HSCs have the capacity for long-term reconstitution in adult mice, and immature pre-HSCs and mature HSCs can be detected in the foetal liver from E10.5 (Kumaravelu *et al*., 2002). From E11.5, the foetal liver becomes the main organ for haematopoietic activities as it recruits EMPs and lymphoid progenitors from the yolk sac's first two waves, in parallel to the expansion of definitive HSCs. After birth, HSCs migrate from the foetal liver to the bone marrow for life-long haematopoiesis (Laurenti & Göttgens, 2018). Functional HSCs with long-term repopulation capabilities only appear in foetal bone marrow at E16.5, and the interaction with osteo-lineage cells is required to sustain multilineage progenitors in the bone marrow (Coşkun *et al*., 2014).

However, the maintenance and homeostasis of HSCs are not well understood, as many previous studies were based on the assumption that all haematopoietic cells and progenitors differentiate from HSCs (Kawamoto & Katsura, 2009). Previous studies have used CD41 and AA4.1 as makers to distinguish early hematopoietic precursors, unfortunately many multipotential progenitors, including the EMPs and LMPs, share these phenotypes with pre-HSC and HSCs (Mikkola & Orkin, 2006). Sca-1 is a stem cell antigen which has a role in haematopoietic stem cell self-renewal (Ito *et al*., 2003). Applying Sca-1 and c-Kit together with lineage markers and signalling lymphocyte activation molecule (SLAM) family markers (CD150, CD48 and CD244) helped to clarify the characterisation of adult bone marrow HSCs, defined as $Lin^{-}c\text{-}Kit^{+}Sca\text{-}1^{+}CD150^{+}CD48^{-}CD244^{-}$ cells (Oguro *et al*., 2013). However, no evidence suggests that these markers have the same significance in AGM HSCs.

1.1.4 Haematopoietic hierarchy

HSCs can self-renew and give rise to all blood lineages through sequential lineage-restriction events in a hierarchically organised manner, in which the hierarchy resembles a tree-like branched roadmap (Figure 1.1.2) (Eaves, 2015). The hierarchy is established stepwise and starts from multilineage long term-HSCs (LT-HSCs). LT-HSCs are a quiescent rare bone marrow population and have a long-term reconstitution capability in irradiated recipients (Osawa *et al*., 1996). Activated LT-HSCs lose their self-renewal ability and differentiate into the intermediate-HSCs (IT-HSCs) (Yamamoto *et al*., 2013). IT-HSCs are transient and become short-term-HSCs (ST-HSCs), which only have a short-term reconstitution capability (8–12 weeks post-transplantation) (Yang *et al*., 2005).

IT-HSCs subsequently transform into populations of multipotent progenitors (MPPs), which have robust differentiation activity, while IT-HSCs are very similar to MPP1s, a subpopulation of MPPs (Pietras *et al*., 2015). MPP2s, MPP3s and MPP4s are subgroups of MPPs that have different kinetics depending on the haematopoietic demands. MPP2s and MPP3s are distinct myeloid-biased MPPs, which coordinate with lymphoid-biased MPP4s to maintain a steady production of blood (Pietras *et al*., 2015). MPP4s also have comparable surface markers to lymphoid-primed multipotent progenitors (LMPPs), which show upregulated Flt3 expression (Boyer *et al*., 2011).

Common myeloid progenitors (CMPs) are downstream of the MPPs and CMPs, which further derive into megakaryocyte/erythrocyte progenitors (MEPs) and granulocyte/ macrophage progenitors (GMPs). Common lymphoid progenitors (CLPs) derived from the MPPs developed only to have lymphoid-restricted differentiation ability (Na Nakorn *et al*., 2002). GMPs and CLPs constitute the remainder of the haemopoietic system, which includes dendritic cells, myeloid lineage cells (macrophages, granulocytes, and monocytes), and lymphoid lineage cells (natural killer cells, B lymphocytes, and T lymphocytes) (Figure 1.1.2) (Eaves, 2015).

Pronk and his colleagues used functional analysis to explore the processes of myeloid cell differentiation and show a series of novel intermediate progenitors (Pronk *et al.*, 2007). This new approach has redefined the classical CMPs and MEPs into four subpopulations, megakaryocyte/erythroid precursors (pre-MegEs), pre-CFU-Es, CFU-Es and granulocyte-macrophage precursors (pre-GMs) (Figure 1.1.3) (Pronk *et al.*, 2007). MPPs can produce

CMPs and LMPPs and possibly pre-MegEs. Pre MegEs give rise to megakaryocyte progenitors (MkP) and Pre-CFU-E, the precursor to CFU-E. CMPs have the bi-potential to differentiate into either pre-MegEs or LMPPs. LMPPs act upstream of CLPs and Pre-GM, which subsequently generate GMPs (Pronk *et al.,* 2007). This model has suggested a hierarchical progression constructed by a set of intermediate progenitors and demonstrated that hematopoietic progenitors have multiple possible routes to take in the generation of megakaryocyte, macrophage, erythroid and granulocyte cell lineage.

According to a single-cell sequencing study, haematopoiesis is not always a discrete and stepwise process, and can happen dynamically from HSCs to the differentiated cells in a continuous process (Alemany *et al*., 2018). Additionally, certain cell lineage can be segregated in early haematopoiesis; for example, megakaryocytes can be formed directly from HSCs by bypassing MPPs, CMPs, and MEPs (Notta *et al*., 2016). The lineage segregation that happens in HSCs further suggests the heterogeneity of HSCs. The distinct fate-predetermined HSCs display the same expression of HSCs signature genes, but they differ in self-renewal ability, surface markers, and lineage differentiation programs and outputs *in vivo* (Dykstra *et al*., 2007; Buenrostro *et al*., 2018). Heterogenous HSCs can be characterised by CD150, in which $CD150^{high}$ HSCs display myeloid-biased reconstitution ability, while the $CD150^{neg}$ HSC subpopulation is expected to provide lymphoid-biased outputs (Morita *et al*., 2010). The pre-HSCs and pro-HSCs in the AGM at E11 have already shown heterogeneous differentiation, in addition to a complex signalling network and epigenetic modifications throughout haematopoiesis. In combination, these three reasons explain why HSC subpopulations are heterogeneous (He & Liu, 2016; Ye *et al*., 2017).

The hematopoietic hierarchy is an organised stepwise process by which LT-HSCs differentiate into the committed progenitors and then mature blood cells. However, downstream lineage-committed progenitors also have self-renewal capacity suggesting that they may also form a long-lived pool, which challenges the concept of hematopoietic hierarchy. A longitudinal analysis of clonal dynamics in adult mice demonstrated that steady blood production is predominantly maintained by a large number of long-lived committed progenitors (Sun *et al*., 2014). However, another group also found that adult LT-HSCs contribute robustly to the continuous influx of blood cells in steady-state haematopoiesis (Chapple *et al*., 2018). These results suggest that the contribution of LT-HSCs and committed progenitors in adult haematopoiesis require further investigation.

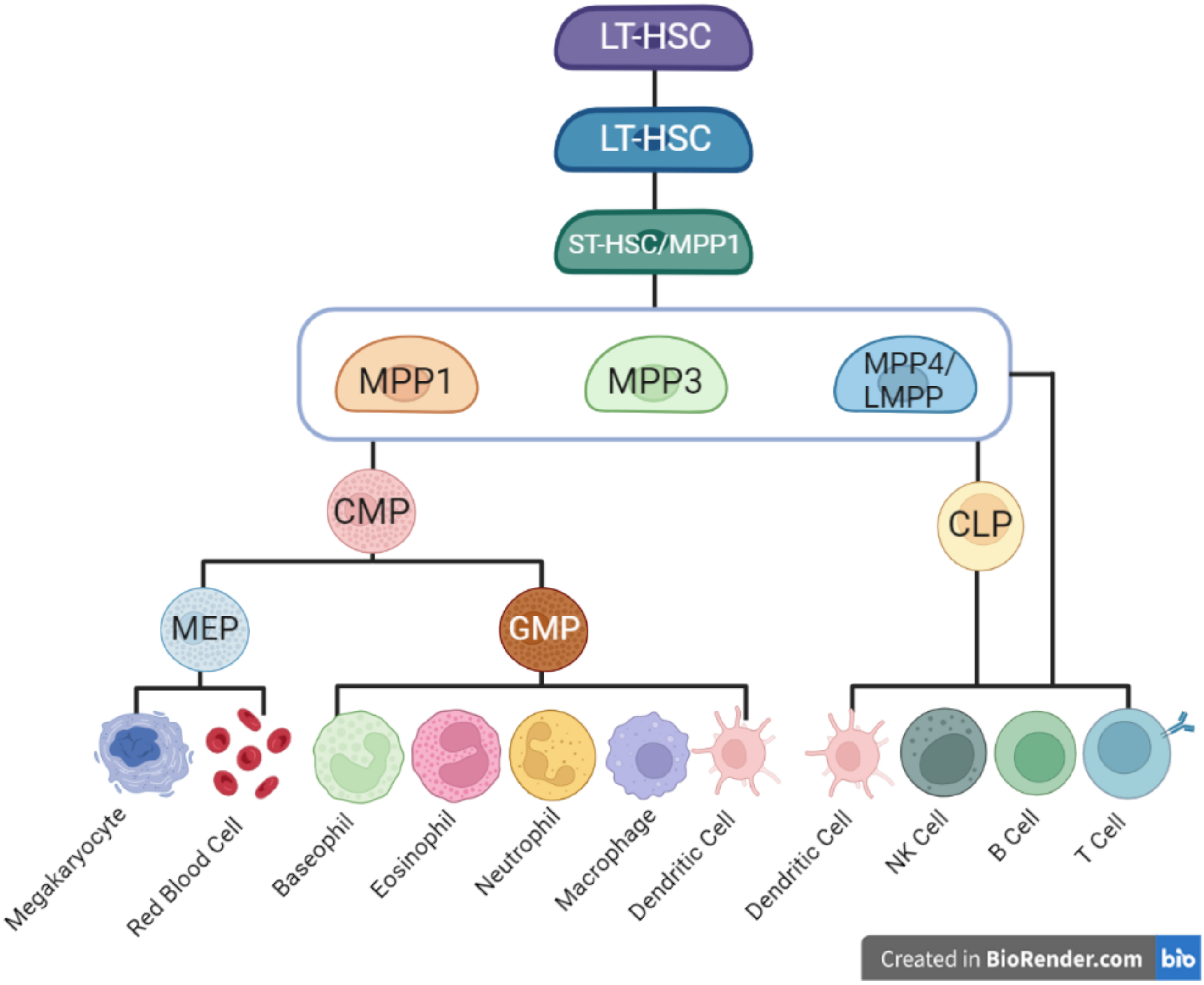

Figure 1.1.2. Roadmaps of haematopoietic hierarchy (Zhang et al., 2018).

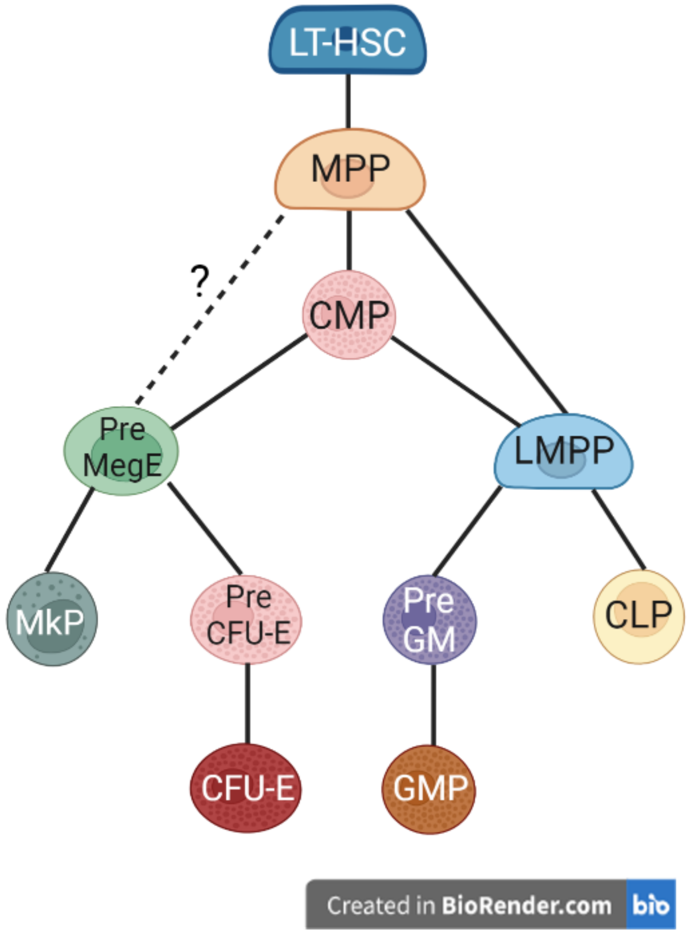

Figure 1.1.3. Revised roadmaps of intermediate hematopoietic progenitors hierarchy (Pronk et al., 2007).

1.1.5 Murine Definitive Haematopoiesis Niche

Definitive HSCs are located on the floor of the dorsal aorta, which is dependent on the aortic haematopoietic niche. Apart from the localisation of HSCs, the maintenance and specification of HSCs are also regulated by cell signalling, although the key pathways remain incompletely understood. Several signalling pathways have been studied and shown to have a role in the dynamic haematopoietic microenvironment. These pathways are bone morphogenetic protein (BMP), fibroblast growth factor (FGF), vascular endothelial growth factor (VEGF), hedgehog (Hh), tyrosine-protein kinase kit (c-Kit), Fms-like tyrosine kinase receptor 3 (Flt3), and thrombopoietin (TPO).

BMP signalling belongs to the superfamily of transforming growth factor-β (TGFβ), which have critical roles in embryogenesis during gastrulation, mesoderm specification, and HSC emergence. The subaortic mesenchyme around the developing dorsal aorta expresses *BMP4* suggesting that BMP4 is the key determinant of polarisation in HSC formation (Durand *et al*., 2007). It has been discovered that BMP4 and its antagonist (Noggin) are spatially segregated to regulate the polarisation of HSCs. The presence of BMP4 is predominantly underneath the aortic endothelium, while Noggin is mainly expressed in haematopoietic clusters located at the ventral floor of the dorsal aorta (Ivanovs *et al*., 2014; Souilhol *et al*., 2016). BMP4 is required in the HSCs specification during the earlier stage at approximately E8.5, while the downregulation of BMP targets accompany the *in vivo* transition of type I to type II pre-HSC, suggesting that BMP activity is downregulated with the progression of HSCs specification (Souilhol *et al*., 2016; Wilkinson *et al*., 2009).

FGF regulates the emergence and maintenance of HSCs in the dorsal aorta by counteracting the BMP activity. FGF is absent in the aortic region which expresses *BMP4*, and conversely, BMP4 is absent in the aortic region if *FGF* is overactivated (Pouget *et al*., 2014). *Smad-1* is the downstream activator of the BMP pathway, and it transactivates *Runx1* activity, indicating *BMP4* is directly upstream of *Runx1* (Pimanda *et al*., 2007). Inhibiting FGF activity results in the expression of *Runx1* in the dorsal aorta, while the loss of FGF signalling does not affect the dorsal polarisation of the dorsal aorta (Pouget *et al*., 2014). It has been demonstrated that FGF signalling acts upstream and represses the primitive emergence of HSCs. However, FGF contradictorily promotes the HSC proliferation in adult haematopoiesis, implying that the FGF pathway has variable roles at multiple stages of HSCs development (Pouget *et al*., 2014; Lee *et al*., 2014).

VEGF signalling is critical to the gastrulation and axis formation of the embryo, which is vital to endothelial cells(Yamaguchi *et al*., 1993; Flamme *et al*., 1995). Flk-1 is a member of the VEGF receptor family and is expressed in the stage from mesodermal to endothelial cells to initiate *Runx1* expression for the development of haemogenic endothelial cells (Hirai *et al*., 2005). *Runx1* activity subsequently leads to the silencing of the *Flk-1* promoter and expression, which is consistent with downregulation of *Flk-1* in type 2 pre-HSCs. The interplay between Notch and VEGF signalling pathways is also required for the specifications of aortic and HSCs. Activated Notch signalling is involved in the downregulation of *Flk-1* expression, reducing their response to VEGF signalling (Suchting *et al*., 2007). Knocking down the regulator of VEGF, *ETO2*, in embryogenesis also leads to the absence of *Notch 1* expression and subsequently the failure of HSC specification in the dorsal aorta (Leung *et al*., 2013). *Notch 1* mutant explants display impaired haematopoietic colony formation, and transplantation studies showed that Notch 1 is required to generate HSCs from haemogenic endothelial cells (Marcelo *et al*., 2013).

Similarly, hedgehog signalling pathways are involved in a wide range of haematopoietic events. Sonic hedgehog (Shh) acts upstream of VEGF signalling and promotes the specification of the arterial endothelial cell and haematopoietic patterning (Pouget *et al*., 2014; Lawson *et al*., 2002). The dorsal domain of dorsal aorta tissue contains notochord, which is a rich source of Shh (Echelard *et al*., 1993). Shh signalling demonstrates a stage-specific effect in HSCs development which acts almost exclusively to the type 1 pre-HSC at around E10.5 (Rybtsov *et al*., 2011). Although the dissected dorsal domain of the dorsal aorta presented enhanced expression of Shh receptors at E10.5, they were downregulated in E11.5, which may explain why Shh is a stage-specific HSCs inducer (Souilhol *et al*., 2016). Shh, which BMP4 can downregulate, may form a positive feedback loop with Noggin, a BMP4 antagonist, to support the maturation of HSCs (Souilhol *et al*., 2016).

C-kit is uniquely expressed when endothelial cells are specified to acquire haematopoietic potential. *C-kit* is co-expressed with *Flk-1* in the haematogenic endothelium of the haematopoietic clusters in the dorsal aorta, proving the importance of c-kit in definitive haematopoiesis (Yoshida *et al*., 1998). C-Kit belongs to the family of growth factor receptors stimulated by stem cell factor (SCF). SCF is such a major HSC maturation factor that SCF alone can induce the maturation of vascular endothelium at E9.5 and type 1 pre-HSCs at E10.5, which is consistent with the decline of HSC activity in SCF mutant mice (Rybtsov *et al*., 2014; Ding *et al*., 2012). At E11.5, SCF in combination with interleukin-3 (IL-3) is shown to potentiate the development of type 2 pre-HSCs (Rybtsov *et al*., 2014). Higher levels of polarised SCF expression in the ventral root of the dorsal aorta and urogenital ridges support its proposed role in regulating the polarisation of HSCs (Souilhol *et al*., 2016).

Flt3 gene expression is highly restricted in the early lymphoid progenitors and its role in regulating LMPPs, CLPs and subsequent B and T lymphopoiesis has been demonstrated in *Flt3* conditional knockout mice (Zriwil *et al*., 2018). Flt-3 ligand (Flt-3l) can bind and activate Flt-3 and subsequent signalling pathways. Flt-3l is a haematopoietic growth factor that promotes the proliferation of hematopoietic progenitor cells of both lymphoid and myeloid origin in the foetal liver (Dong *et al*., 2002). A high level of Flt-3l was also found in $CD45^{+}$ and $Ter119^{+}$ hematopoietic cells (Yumine *et al*., 2017). Moreover, SCF, Flt-3l and IL-3 can successfully maintain the E11.5 *ex vivo* haematopoietic capability of dissociated and reaggregated AGM region from HSCs (Taoudi *et al*., 2008). In the erythropoietic niche, the gene encoding of critical cytokines, *SCF, Flt-3l, EPO* and *TPO*, were remarkably upregulated in the E12.5 foetal liver, implying their roles support the haematopoietic expansion to the foetal liver (Yumine *et al*., 2017).

Thrombopoietin (TPO) is a ligand of its receptor, Mpl, which plays a functional role in establishing definitive mouse haematopoiesis in the AGM region. The gene *Mpl* is expressed in the haematopoietic cluster in the AGM region and foetal liver in E10.5, and the lack of Mpl could delay the production of HSCs (Petit-Cocault *et al*., 2007). TPO is essential in the regulation of *Runx1* expression and activation for the transition of haemogenic endothelial cells to HSCs in the AGM region in E10.5 (Fleury *et al*., 2010). The *Mpl* gene is highly expressed in $CD45^{low}$c-Kit^{high} cells among Sox-17-transduced AGM cells, and more Mpl protein is found in intra-aortic hematopoietic cell clusters, which suggests that TPO is critical to the formation and maintenance of haematopoietic cell clusters in the AGM (Harada *et al*., 2017). In addition, TPO is a vital cytokine in haematopoiesis that all megakaryocyte-primed progenitors, including HSCs, CMPs, and MEPs, express alongside Mpl. *TPO* and *Mpl* gene knockout mice displayed a global decrease in HSCs production (Noetzli *et al*., 2019).

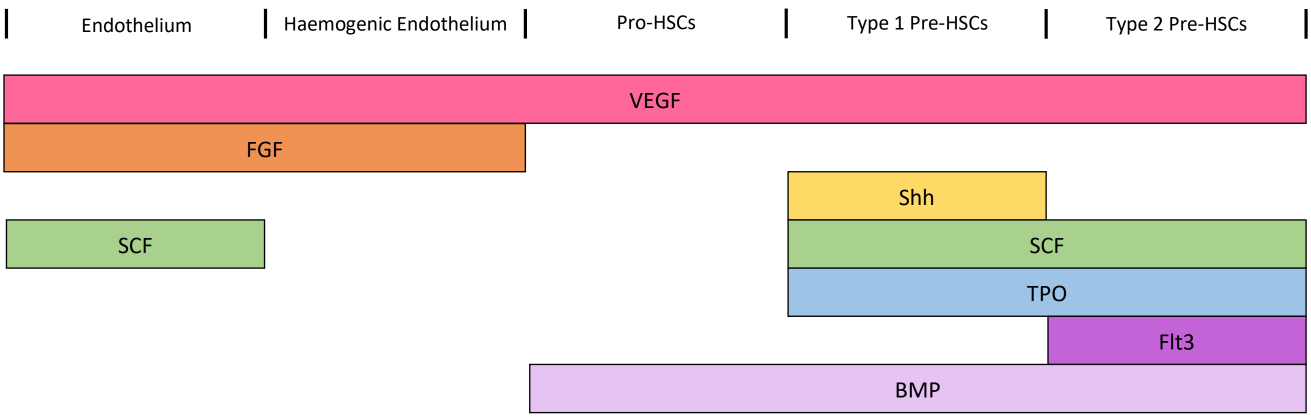

Figure 1.1.4. Overview of important signalling pathways during definitive haematopoiesis in mouse AGM in vivo.

Important signalling pathways include bone morphogenetic protein (BMP), fibroblast growth factor (FGF), vascular endothelial growth factor (VEGF), sonic hedgehog (Shh), system cell factor (SCF), Fms-like tyrosine kinase receptor 3 (Flt3), and thrombopoietin (TPO).

1.1.6 Current Production of HSCs and Progenitors in Research

HSPCs are characterised by having multipotency, self-renewal and a repopulating capability, which has attracted great enthusiasm. Transplantation of HSCs has already been widely applied as a well-established medical procedure for patients with the haematopoietic disease to regenerate and maintain a functional haemopoietic system. Although gene therapy for adenosine deaminase deficiency (ADA-SCID), which uses genetically engineered HSCs, has market approval for clinical use, the transplantation still relies on HSCs aspirated from human bodies which restricts the applications of HSCs therapeutics (Wang & Rivière, 2017). Aside from the clinical setting, a standardised and homogeneous source of HSPCs is also sought by those in research as studies in haematopoietic stem cells rely on HSCs harvested from animal models, which causes heterogeneity of cell samples and constrains the scale of the studies.

Genetical programming strategies have been applied to generate HSCs from mouse and human pluripotent stem cells *in vitro*. The enforced expression of a panel of transcription factors can differentiate human pluripotent stem cells (PSC) into haemogenic endothelium cells and be converted into HSCs that can engraft myeloid, B and T cells in mouse recipients (Sugimura *et al*., 2017). By transiently expressing transcription factors using reprogramming strategies, mouse fibroblasts and lineage-committed progenitors can generate HSC-like cells, which demonstrate HSCs' gene expression profiles, cell surface phenotype, and colony forming capabilities (Pereira *et al*., 2013; Riddell *et al*., 2014). However, the mechanism of the reprogramming process still has not been fully elucidated, and viruses are required to manipulate the expression of transcription factors. Consequently, the HSCs generated from programming strategies are not *bona fide* HSCs that can be used to study genuine haematopoiesis.

Stroma cell co-culture has been widely applied to research the generation of blood progenitors from ES cells. Stromal cells are derived from bone marrow which facilitates the differentiation of HSCs by secreting cytokines to influence the lineage output. OP9 cells are the most commonly studied cell line, and do not release macrophage colony-stimulating factor (M-CSF). ES cells gain lymphoid potential through co-culture with OP9 cells to generate B cell lineages, and with OP9-DL1 cells to form T cell lineages (Holmes & Zúñiga-Pflücker, 2009). Another group also have developed a stepwise non-serum protocol to generate definitive human HSCs through a monolayer culture method (Kim *et al*., 2017). Although co-culturing can provide the pivotal extracellular environment and cell-cell interaction to facilitate haematopoiesis, such 2D culture struggles to provide gene expression and morphology comparable to the *in vivo* culture, restricting the application of co-culturing in haematopoietic studies.

Aggregation of embryonic bodies (EBs) is another protocol used to study the production of blood cells and progenitors using ES cells. In 1985, the cystic blood island structure was identified in liquid culture, and this EB is analogous to the yolk sac displaying erythroid and myeloid lineages (Burkert *et al*., 1991). Cells derived within EBs can release various haematopoietic cytokines to initiate haematopoiesis, and the exogenous addition of serum and cytokines can support the development of specific mature lineages (Wang *et al*., 2005). A stepwise culture protocol has recently been reported to develop mouse ES cells to adult-type HSCs by utilising the EBs and stroma co-culture (Matsumoto *et al*., 2009). Although EBs can generate definitive hematopoietic progenitors, one of the challenges that remains unresolved is modelling the three-dimensional (3D) haematopoietic complex. Topographical analysis of the emergence of haematopoietic cells from cell clusters in EBs as no clear mesodermal structures are differentiated (Wang *et al*., 2018). Lastly, a significant limitation of the EBs assay is that the EB-derived haematopoietic progenitors do not have the repopulation capability to engraft into the bone marrow without genetic manipulation.

Although early-stage haematopoiesis can be partly recapitulated using mouse and human pluripotent stem cells *in vitro*, it remains a challenge to generate LT-HSCs like those differentiated from the AGM region without genetic reprogramming. The microenvironment of definitive haematopoiesis is composed of stromal cell contacts, paracrine factors, and physical forces which vary throughout embryonic development, though they have not yet been clearly defined. A novel haematopoietic cluster-forming 3D culture system that can regenerate definite HSC niches similar to the AGM region in a serum-free, stroma-free method awaits development to facilitate the advancement of haematological research.

1.2 Gastruloid

1.2.1 Application of organoid culture in biological research

2D cell culture protocols have been successfully applied to a wide variety of biological research in the past fifty years, including disease modelling, infectious disease and cancer pathology, in addition to novel drug discovery and development. However, many studies have proven that the 2D culture failed to recapitulate the *in vivo* environment and cell signalling networks and thus, the results from 2D *in vitro* studies are not representative enough. Furthermore, the 2D culture cannot mimic the organisation, structure, and cell-to-cell interactions critical to the *in vivo* cell development. The importance of 3D cell culture in biological research, especially in drug development, cell differentiation and signalling modelling, has been widely recognised in the past twenty years. The recent development of organoids has introduced new culture systems to stem cell research, and these efforts were highlighted in the Method of 2017 by Nature Methods (Nature Methods, 2018).

The first research highlighting the importance of 'three-dimensional culture models' were the assays developed by Barcellos-Hoff in 1990. However, it also can be dated back to the hanging drop culture technique invented by Harrison (Barcellos-Hoff *et al*., 1989; Harrison, 1906). Organoid culture previously meant a 3D culture that encapsulates small fragments of tissues/organs in gels (for example, collagen, hydrogel, or laminin gel) to generate an organ-like structure that reassembles the original tissues/organs (Simian *et al*., 2001). As organoid and 3D culture gained more recognition over time, the meaning of 'organoid' also evolved and became a cell culture technique that grows a stem cell-derived cluster *in vitro* which the cells aggregate to, to form an organised structure of self-renewal and self-organisation.

The first group directly applying stem cells to create organoids was Dontu from the field of the mammary gland (Dontu *et al*., 2003). They proved that the mammary progenitors could differentiate into luminal and/or myoepithelial lineages and form ductal/acinar structures when the progenitors are seeded in low-density Matrigel (Dontu *et al*., 2003). Sato has successfully generated stem cells from intestinal tissue and produced crypt-villus structured organoids (Sato *et al*., 2009). Sato's intestinal epithelium forming protocol has subsequently inspired the development of organoid cultures using stomach, colon, pancreas, and liver tissues (Barker *et al*., 2010; Huch *et al*., 2013; Boj *et al*., 2015). The induced PSCs (iPSCs) have further leveraged the organoid as a developmental tool on morphogenesis, in which cerebral organoids were made using iPSCs derived from skin fibroblasts (Lancaster *et al*., 2013).

With the development of organoids, bioengineering approaches, such as tissue engineering and cell niche engineering, have been applied to assist in organoid formation. The *in vivo* behaviour of stem cells is regulated by the local microenvironment, which consists of extrinsic biochemical and biophysical signals. The advancement of microfluidic and microfabrication technology demonstrates the possibility of imitating the key structural and physiological features of tissues for the study of more complex biological systems on organoids. The advanced microfluidic technologies can fabricate microchannels for fluid flow among multiple organoids on one chip at a rate comparable to *in vivo,* also known as 'organ-on-a-chip'. This technique has been used to understand the complex biological system *in vivo,* such as inter-organ responses (liver, heart, and lung) to the administration of a drug (Skardal *et al*., 2017).

Genome editing technology has also been performed on organoid culture in which human stem cell-derived primary intestinal organoids were genome-edited using the CRISPR/Cas9 technique (Schwank *et al*., 2013). CRISPR gene editing has been applied to study tumour metastasis and progression by introducing multiple mutations into human intestinal epithelial organoids and transplanting them to mice recipients (Matano *et al*., 2015). The techniques in genome editing have evolved very rapidly, and next-generation organoids with genome editing will advance the study of pathology, stem cell differentiation, organogenesis, drug screening and even organoid based therapies.

1.2.2 Development and research on gastruloid protocol

In early mammalian embryogenesis, gastrulation is an essential developmental stage, in which the single-layered epithelial cells transform into a multiple-layered structure, and the formation of a primitive streak marks the beginning of this process. The endodermal and mesodermal progenitors ingress through the primitive streak from a single-layered epithelium, undergo the epithelial to mesenchymal transition (EMT) and form the three germ layers (Acloque *et al*., 2009). These three germ layers are the endoderm, mesoderm, and ectoderm, and each layer is committed to specific systems during embryogenesis. Gastrulation has a mechanism which generates a multi-level body plan with the establishment of axis formation on dorsal/ventral and posterior/anterior axes and left/right symmetry (Lu *et al*., 2001). The symmetry breaking is coordinated by a series of signalling pathways, such as TGFB, Wnt, Nodal, and BMPs signalling, which initiate the migration of distal visceral endoderm (DVE) to anterior visceral endoderm (AVE) and form the anterior/posterior axis (Tam & Loebel, 2007).

Currently, there are several *in vitro* embryo models, including micropatterned 2D cultures, blastoids, ETS- and iETX-embryo and the human epiblast model (van den Brink & van Oudenaarden, 2021). The micropatterning system plates cells on dishes with micropatterns for cell attachment, while the blastoids model is an aggregate modelling the blastocyst-stage mouse conceptus (Warmflash *et al*., 2014; Rivron *et al*., 2018). ETS- and iETX-embryo is a model which seeds mouse ES cells and trophoblast stem cells in a 3D scaffold that can recapitulate the E6.5 mouse conceptus (Amadei *et al*., 2021). The human epiblast model can resemble the 10-days post fertilisation (dpf) human epiblast by seeding human ES cells in polymeric hydrogels supplemented with Matrigel (Simunovic *et al*., 2019). These models are easy to upscale the screening numbers and are accessible for genetic modification on cells, advancing the research on embryogenesis in developmental biology. However, gastrulation is a process which occurs in a manner of multi-layer and three-division. There will be a significant advance if the organoid culture can be applied in embryo models.

Using the EB cultures, Marikawa and his colleagues discovered mesodermal formation and elongation morphogenesis in the EBs derived from mouse embryonic carcinoma cells (Marikawa *et al*., 2009). This result has inspired the Martinez Arias Group to develop a novel specific organoid culture. This protocol can generate organoids with gastrulation features, known as gastruloid (Figure 1.2.1) (Baillie-Johnson *et al*., 2015; van den Brink *et al*., 2014). The mouse ES cell-derived gastruloid generated with the first protocol displayed elongation, specification of all three-germ layers and a clear axis formation (Beccari *et al*., 2018).

Since the gastruloid protocol was developed, many research groups have used this tool to understand organogenesis and provide new insights into gastrulation. Girgin and his colleagues showed the development of anterior neural tissues in gastruloids by removing the Wnt activation (Girgin *et al*., 2021). In the ordinary gastruloid protocol, the 24-hour pulse of Chiron is added to the gastruloid at 48 hr to provide the gastruloid with a high level of Wnt activation (Baillie-Johnson *et al*., 2015; van den Brink *et al*., 2014). However, it is believed that such Wnt activation resulted in the lack of anterior embryonic regions, which is critical for brain development. Girgin seeded mouse ES cells in a hydrogel well and successfully generated a post-implantation epiblast-like (EPI) gastruloid (Girgin *et al*., 2021). The EPI gastruloid exhibited symmetry break, axially elongation, differentiation towards both anterior ectoderm and meso-endoderm lineages and crucially, anterior brain-like tissues through the inhibition of Wnt signalling during the early stage of gastruloid culture (Girgin *et al*., 2021).

It has been reported that embedding the 96 hr mouse ES cell-derived gastruloid in Matrigel drives the morphogenesis of trunk-like structures comprising the somites and neural tube (Veenvliet *et al*., 2020). The somites and neural tube displayed dorsal-ventral patterning comparable to the notochord in embryos (Veenvliet *et al*., 2020). Van den Brink and her colleagues also successfully induced the formation of somites with correct rostral-caudal patterning in the Matrigel-embed gastruloid. The somites rhythmically appeared one-by-one in anterior-to-posterior, comparable to the embryo pattern (van den Brink *et al*., 2020). Extraembryonic endoderm cells produce extracellular matrix (ECM) and assist the surrounding embryos to form somite and neural tube (Rozario & DeSimone, 2010). Matrigel has a similar characteristic as ECM and thus, it may function as an ECM to support the somites and neural tube formation in gastruloids.

In addition to forming brain-like structures and somite and neutral tube-like structures, cardiac structures can also be derived in the gastruloid protocol. Rossi and his colleagues showed cardiogenesis using gastruloids made with mouse-ES cells (Rossi *et al*., 2021a). By exposing the gastruloid to the cocktail of cardiogenic cytokines, they captured early heart organogenesis with a temporal and spatial accuracy to *in vivo* embryonic carcinogenesis. The gastruloids displayed morphogenesis of an anterior cardiac crescent-like structure with Ca^{2+}

related heart beating, comparable to foetal cardiomyocytes. The shaking helps to extend the gastruloid protocol to 168 hr, and this is equivalent to E9.5, during which cardiogenesis is initiated in the embryo.

With the efforts from different research groups, the gastruloid culture protocol is well validated and has proved to be a next-generation mouse embryonic research tool with great potential. Additional studies on gastruloids utilising imaging-based characterisations (for example fluorescence microscopy, immunostaining and confocal microscopy, and *in situ* hybridisation) and further studies on embryonic gene expression profiles are needed. Several studies have included single-cell RNA sequencing in their investigation to benchmark the gene expression profiles of gastruloid cells with *in vivo* embryonic tissues. Results from the sequencing confirmed the emergence of most embryonic cell types, from endothelial, head mesenchymal, neuro-mesodermal progenitor to primordial germ cell-like cells (van den Brink *et al*., 2020; Rossi *et al*., 2021a; Veenvliet *et al*., 2020). When analysing the results of microscopic characterisations and sequencing together, spatial transcriptomics revealed that the spatial and temporal patterns of *Hox* gene expression were correct and resulted in the embryonic cells forming at the right location along their anterior-posterior axis in mouse gastruloids (van den Brink *et al*., 2020; Veenvliet *et al*., 2020; Beccari *et al*., 2018).

With the success of the mouse gastruloid cultures in recapitulating the *in vivo* embryonic developments, the concept of gastruloids has been extended to human ES cells. Human gastruloid cultures need Chiron + ROCKi pre-treatment, and the aggregation takes only 1 hour, unlike mouse gastruloids which require 48 hours for aggregation (Figure 1.2.1) (van den Brink *et al*., 2014; Moris *et al*., 2020). The human gastruloid culture is shorter than mouse culture, but is equivalent to 18-21 dpf (Carnegie Stage 8-9) and is equivalent to mouse E8 or E9 (Xue *et al*., 2013; Moris *et al*., 2020). Similarly to the mouse gastruloids, human gastruloids can also form three germ layers in the spatial location comparable to the post-occipital region of 18–21 dpf human embryos (Moris *et al*., 2020). However, only node-like structures are reported in human gastruloid, and further studies on the morphogenesis of brain, somite, and tube structures are yet to be carried out.

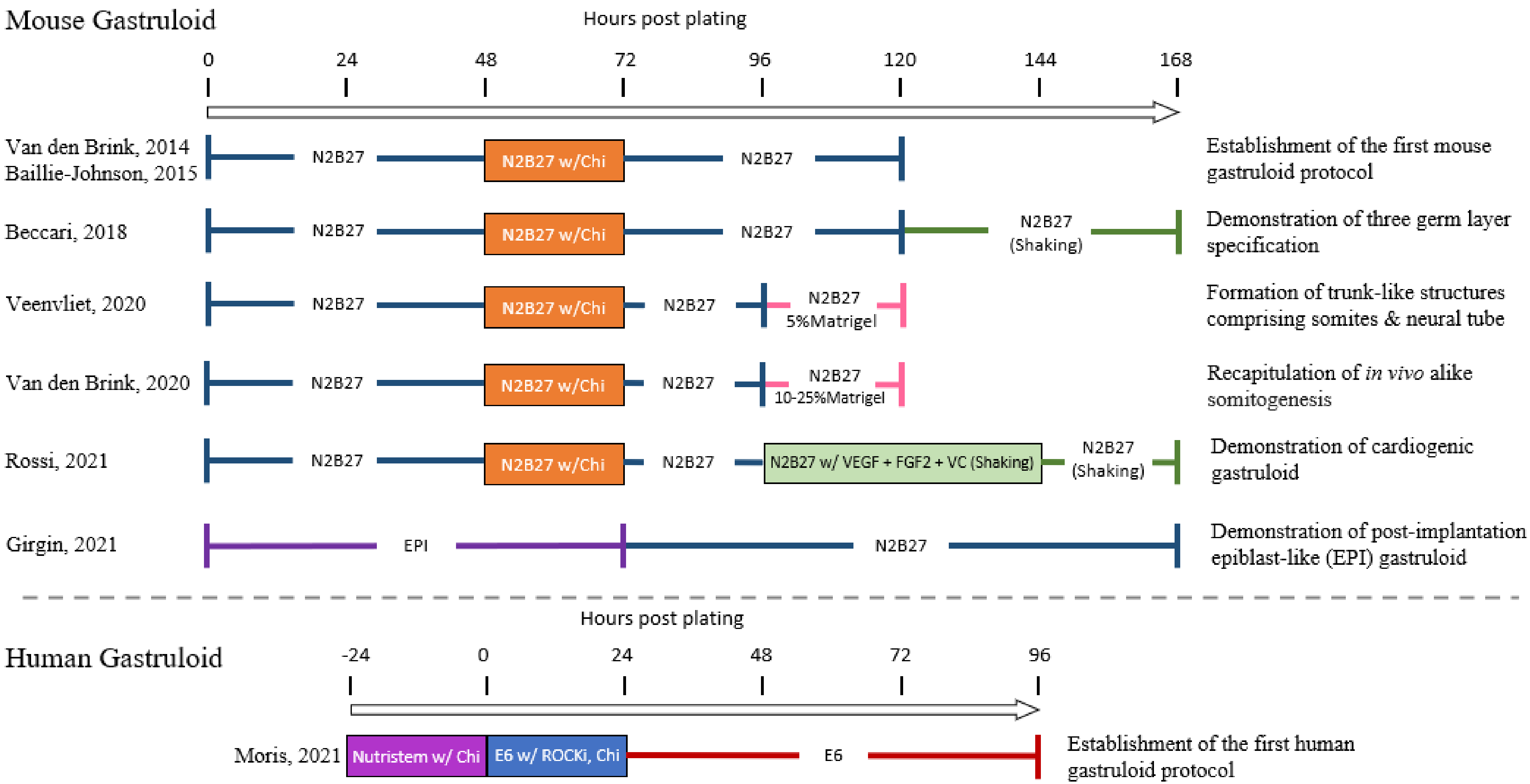

Figure 1.2.1. Overview of currently available mouse and human gastruloid protocols.

1.2.3 Developing gastruloid protocol for haematopoietic research

In the field of haematopoietic research, the use of EBs is a common culture protocol that has been applied to ES cells to generate definitive HSCs. Although EBs are a 3D aggregate culture method to generate HSCs, EBs require thousands of cells which is too large to represent the early stage of the embryo and it grows in a disordered manner meaning only limited architectural organisation of the embryo is preserved (Chen *et al*., 2014; Wiles & Keller, 1991). Since the creation of the organoid culture protocol, it has been widely applied in many organogenesis studies and a range of organ structures have already been recapitulated, including cerebral, intestinal and lung organoids. Organoid culture have great potential for further development as a tool for haematopoietic research. Specifically, organoids may be used to study the emergence of definitive haematopoietic cells from the AGM region, which no *in vitro* assays have recapitulated yet.

Gastrulation is critical to initiate the haematopoiesis in the embryo as the mesodermal germ layer drives haematopoietic specification and subsequent differentiation of haematopoietic progenitors (Shiratori & Hamada, 2006; Ivanovs *et al*., 2017). There is significant elucidation of extrinsic signals involved in establishing the niche required for developing HSCs at these early time points, and the first wave of haematopoiesis occurs at the time of mesodermal patterning (Souilhol *et al*., 2016). Mesoderm cells can specify into primordial endothelial cells in a process called vasculogenesis through extrinsic and intrinsic signals (Marcelo *et al*., 2103). Endothelial cells are well characterised by their critical role in deriving the haematopoietic progenitors via EHT. Since gastruloids can recapitulate the formation of the mesodermal layer, it suggests gastruloids may be able to recapitulate this progress under specific, tightly controlled extrinsic signals.

Flk-1 is a marker of mesodermal cells, which mesodermal progenitor cells co-expressing Brachyury and the receptor for Flk-1 have a potency to differentiate into and haematopoietic progenitor cells (Motoike *et al*., 2003). Flk-1 is first detected in the yolk sac mesoderm and later in the AGM. (Kauts *et al*., 2016). Rossi and her colleagues have revealed that the *Flk-1* gene can be upregulated in gastruloids using single-cell RNA sequencing and proved the formation of Flk-1^{+} cells in fluorescence microscopy (Rossi *et al*., 2021a). The expression of Flk-1 emerges in the embryo at E7.5 and it occurs in the gastruloid at 96 hr, while the formation of the AGM begins at E9 and the emergence of type 2 pre-HSCs starts at E11.5

(Gekas *et al*., 2005; Wang *et al*., 2016). Since the emergence of Flk-1 also occurs in the gastruloid at 96hr, if the gastruloid protocol could be extended to 168 hr or even later, it may be equivalent to few embryonic days later(Rossi *et al*., 2021a). At later time points the gastruloid may be able to recapitulate the formation of an AGM-like structure and perhaps type 2 pre-HSCs under exposure to signalling comparable to the microenvironment in the AGM region.

Cardiac progenitors are specified shortly after the gastrulation of the embryo at E7.5 and localised anteriorly. Studies have revealed that cardiovascular lineage cells have Flk-1 expression (Ema *et al*., 2006). Flk-1^{+} cardiovascular progenitor cells are multipotent and can derive to cardiomyocyte, endothelial, and vascular smooth muscle lineages when culturing with cardiogenic cytokines (Kattman *et al*., 2006). Common Flk-1^{+} progenitors also display the potential to form both haematopoietic and cardiovascular progeny (Huber *et al*., 2004). Gastruloids cultured in the extended protocol can generate a heart-beating structure, indicating that the common Flk-1^{+} progenitors may also have haematopoietic potentials (Rossi *et al*., 2021a).

Since *in vitro* assays could not generate LT-HSCs and the AGM region, the definitive haematopoiesis still has not been fully elucidated, and studies must rely on animal models to harvest cells from the AGM region for any analysis. While various embryonic structures have been generated in gastruloids, if a gastruloid is cultured with haematopoietic cytokines, they may form structures comparable to the organ generated in an *in vivo* animal model. Haemogenic gastruloid culture can be an alternative to the animal model, which relieves the demand for animal study and provides a more flexible, economical, and easy-to-maintain model for haematopoietic research. A haemogenic gastruloid culture protocol will create a great opportunity to model the development of a definitive haematopoietic system at the AGM region, which can then be a novel alternative tool to explore the cellular and molecular interaction in haematopoiesis.

1.3 Hypothesis

The gastruloid culture protocol has been characterised to generate organoids with gastrulation features including elongation, all three-germ layer specifications and a clear axis formation. The mesodermal layer is critical to the formation of haematopoietic progenitors, and the mesodermal cells formed in the gastruloid may have the potential to raise the progenitors with haematopoietic linage. In addition, the *Flk-1* gene is upregulated, and common Flk-1^{+} progenitors are derived in the gastruloid at 96 hr (equivalent to E7.5), which is close to E9, the day when the AGM region is reported in the mouse embryo (Gekas *et al*., 2005; Rossi *et al*., 2021a). I hypothesise that gastruloids can generate AGM-like haematopoietic clusters, which can derive definitive haematopoietic stem cells and/or progenitors if the mouse gastruloid culture protocol can be extended and optimised using haematopoietic extrinsic signals temporally similar to the mouse AGM region.

To test this hypothesis, Flk-1::GFP mouse ES cells have been kindly provided by Alexander Medvinsky (CIRM, University of Edinburgh) in collaboration with my co-supervisor, Alfonso Martinez Arias, to initiate the gastruloid culture protocol. The culture regimens and growth factor cocktails were optimised and the haematopoietic output in terms of molecular phenotypes was measured (e.g., haemoglobin switching, haemopoietic transcription factors, and lineage markers). Flow cytometry analysis has been extensively utilised to identify the formation of haematopoietic progenitors over time and to quantify the individual and combinatorial efficiency of haematopoietic cytokines in driving haematopoiesis.

To investigate whether the haematopoietic cluster formed in the gastruloid, fluorescence microscopy has been used to study the morphogenesis of the structure in the gastruloid over time. In addition, confocal microscopy has been applied to confirm the haematopoietic identity of the clusters and structures formed in the gastruloid. Gastruloid cells were seeded onto a colony-forming cell assay to discover whether the gastruloids can produce multipotent haematopoietic progenitors. To identify if the gastruloid generates haematopoietic progenitors with engraftment capability, they were injected into mice for transplantation.

Lastly, to scrutinise whether the gastruloid can recapitulate the embryonic transcriptional activities and demonstrate similar differentiation trajectories as the AGM region of the mouse embryo, single-cell SMART sequencing has been performed on gastruloids collected over time and analysed with sequencing data acquired from the AGM region of the mouse embryo.

1.4 Objective

This project aims to adapt the gastruloid culture protocol initially developed by the Martinez Arias Group to recapitulate developmental haematopoiesis and optimise this protocol as a novel, stroma-free, and genetic modification-free 3D differentiation system for haematopoietic research and the *in vitro* generation of definitive haematopoietic progenitors.

Objectives:

- To adapt the gastruloid culture protocol and stably extend the protocol for the emergence of the AGM region and definitive haematopoiesis.
- To optimise the gastruloid culture conditions and the cocktail of haematopoietic cytokines to recapitulate a mouse AGM-like haematopoietic niche
- To recapitulate the formation of mouse AGM-like haematopoietic clusters for supporting the specification of definitive haematopoietic progenitors.

1.5 Thesis Structure

Chapter One is the introduction of the thesis, which begins with a literature review on the three waves of haematopoiesis in mice, haematopoietic hierarchy, haematopoietic niches, and the current model for haematopoietic research in the field. The second section of the introduction is a literature review on the development of organoid and gastruloid culture in addition to the possibility of developing gastruloid culture to model the AGM-like development of haematopoietic progenitors. Chapter two includes all of the protocols used in this doctoral project, from the protocol for ordinary gastruloid, finalised haemogenic gastruloid, flow cytometry, the CFC assay, and transplantation study to single-cell RNA sequencing.

Chapters three to six are the results from experiments and analyses of the haemogenic gastruloid culture protocols. Chapter three focuses on adapting the ordinary gastruloid to generate mesodermal cells and haematopoietic precursors. qPCR analysis and PCR-gel electrophoresis suggested that adding VEGF and FGF_2 between 72 and 144 hr can drive haemoglobin switching. Fluorescence microscopy revealed the polarised pattern of Flk-1$^+$ signalling at 96 hr and the formation of structures in the gastruloid since 120 hr. The CFC assay has revealed that the gastruloid cultured with VEGF and FGF_2 between 72 and 144 hr can form erythroid and myeloid progenitors. Flow cytometry analysis proved VEGF and FGF_2 could increase the formation of VeCAD, c-Kit$^+$ and CD41 cells, featuring haemogenic endothelium and pro-HSCs.

Chapter four demonstrates how to extend the haemogenic gastruloid culture protocol to 216 hr to allow the formation of AGM-like haematopoietic clusters and cells with important definitive haematopoietic markers such as CD45. By switching to cell culture plates coated with low adherence hydrophobic surfaces, the gastruloid culture can be further extended to 216 hr without shaking. Fluorescence microscopy and flow cytometry confirmed that the gastruloids are still viable, and the Flk-1$^+$ pattern in the gastruloid declines in a similar manner as in the mouse AGM region. The 24-hour 2iLIF pre-treatment was added before plating to provide a more homogeneous cells population, and the addition of a 24-hour pulse of Shh at 144 hr can raise the VeCAD$^+$ and CD45$^+$ cells in the gastruloid. A haematopoietic cluster with CD45, c-Kit and CD31 expression in the 192 hr gastruloid was revealed using immunostaining and confocal microscopy. Gastruloid cells were injected into irradiated mice, and demonstrated short-term engraftment capability to bone marrow.

Chapter five aims to finalise the scheme of the haemogenic gastruloid culture protocol and characterise the proposed $CD45^+$ type 2 pre-HSCs with a series of assays. The addition of SCF and TPO together with Flt-3L was found to boost the formation of $CD45^+$ cells at 216 hr. By comparing the percentage of CD45 formed at 192 and 216 hr, on average, gastruloids at 192 hr displayed more $CD45^+$ cells but also had greater discrepancy than those at 216 hr. Sca-1^+ and $EPCR^+$ cells were also observed in the 216 hr gastruloid using flow cytometry. Confocal microscopy and immunostaining have shown a clearer image of the haematopoietic cluster with CD45, c-Kit and Flk-1 expression in the 216 hr gastruloid. The lymphohaematopoietic potential of the 216 hr gastruloid was also tested using OP9 and OP9-DL1 co-culturing. The entire 216 hr gastruloid has been shown to engraft the CAM and maintain the CD45 expression. However, the 192 hr gastruloid failed to display engraftment in non-irradiated mice.

Chapter six is the final chapter of the result, and focuses on characterising the gastruloids across various time points. Gastruloid cells were collected across time and tested using a CFC assay in which multipotent progenitors such as CFU-GEMM and late-stage progenitors like CFU-E were observed. Flow cytometry was intensively carried out, and demonstrated that an AGM-like hematopoietic differentiation was recapitulated in the gastruloid, from the endothelium, haemogenic endothelium, pro-HSCs, and type 1 pre-HSCs to the type 2 pre-HSCs. The finalised haemogenic culture protocol was also applied to create gastruloids with E14 cells and its derivatives TBra::GFP cells, and KH2 cells derivative Sox17::GFP cells. They recapitulate the formation of $CD45^+$ cells in Flk-1::GFP-made gastruloids. Finally, single-cell SMART sequencing was applied to gastruloids collected over time, and the data from the gastruloids was compared with the data from the mouse AGM region. Sequencing results suggested the gastruloid and the AGM region of the mouse embryo displayed similarity in their gene expression profiles. Additionally, the gastruloid captures a successive generation of erythroid progenitors, myeloid-lymphoid progenitors and HSC-like cells.

Chapter Seven is the discussion section, which includes the insights developed from this project, the future applications in research and the restrictions of this project. Also, future works that can be carried out with this mouse haemogenic gastruloid culture protocol are discussed, such as adapting this protocol to human ES cells and developing this protocol to generate a mouse infant leukaemia model.

Chapter 2: Materials and Methods

2.1 Ordinary gastruloid protocol

The ordinary gastruloid culture was prepared using the published protocol (Baillie-Johnson *et al*., 2015) (Turner *et al*., 2016).

2.1.1 Cell culture conditions prior to generation of gastruloids

Mouse ES cells are maintained in 5mL of ESLIF medium (Glasgow MEM BHK-21 (Gibco) supplemented with 10% FBS (Biosera), 1% GlutaMax (Gibco), 1% MEM Non-essential amino acid (Gibco/Invitrogen), 1% sodium pyruvate (Gibco), 0.2% 2-Mercaptoethanol (Gibco/Invitrogen) and 550 U/mL LIF (Qkine)) on 0.1% gelatin/PBS (Fisher Scientific) coated T25 tissue-culture flask in a humidified incubator at 37 °C and 5% CO_2. The cells are passaged when it reaches 60-70% confluency. Cells are grown at least two passages post thawing before plating for making gastruloid.

For cryopreservation, ES cells were centrifuged at 2000rpm for 5 minutes, and each sample was resuspended with 900uL of ESLIF medium and 100uL of Dimethylsulfoxide (DMSO) (Sigma). Cell suspension is transferred to a cryopreservation vial and stored in Mr Frosty freezing container at -80°C for three days and then in liquid nitrogen for long term storage.

2.1.2 Generation of gastruloids

The culture medium from the tissue culture flask is aspirated and rinsed gently with 5 mL of PBS ($Ca2^+$, $Mg2^+$) (Sigma). PBS is then discarded, and 1 mL of pre-warmed Trypsin-EDTA (0.25%) (Gibco) is added to dissociate the cell. After being in the incubator for less than 5 minutes or until cells have fully detached, 5mL of pre-warmed ESLIF medium is added to neutralise the trypsin. If cells do not detach from the flask after 5 minutes, tapping the flask or pipetting up and down with a P1000 pipette helps detach cells. After pipetting up and down ten times to wash down the cells and dislodge any clumps, the cell suspension is transferred to a 15mL falcon tube and spun down at 1000rpm for 5 minutes.

The cell pellet is gently washed with 5mL of PBS twice by repeating the process - discard the supernatant, add PBS, and spin down the cells. Resuspend the cell pellet with 1mL of pre-warmed N2B27 (Takara) and prepare 5mL of cell suspension (1 x 10^4 cells/mL) using pre-warmed N2B27. The cell suspension is transferred to a sterile reservoir, and a 40uL droplet is pipetted into the bottom of each well of 'U'-bottomed 96-well plate using a multichannel pipette.

2.1.3 Applying stimuli and changing medium for gastruloids

After 48 hours of incubation in a humidified incubator at 37 °C and 5% CO_2 for aggregation, 150uL fresh N2B27 with 3uM of Chiron (Qkine) is added to each well of 96-well plate (Greiner Bio-One) for a 24-hour stimulation pulse. To remove the medium after 24 hours, 150uL of the medium was removed from each well in a 96 wells plate using a multichannel pipette. Medium is removed very gently with a speed of around 50uL per second, and the multichannel pipette is held at an angle (approximately 30°) to prevent accidental removal of gastruloids. Medium is changed every 24 hours until the time-course is complete (the typical length of a gastruloid culture is 120 hours or 144 hours).

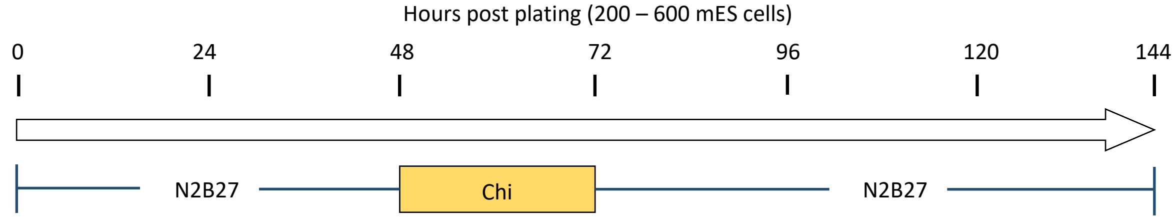

Figure 2.1.1. The culture scheme of ordinary mouse gastruloid protocol.

2.2 Haemogenic gastruloid protocol

2.2.1 Cell culture conditions prior to generation of haemogenic gastruloids

For normal cell culture maintenance, the procedure from 2.1.1 is followed (Figure 2.2.1 (i)). 2iLIF pre-treatment is applied to precondition mESCs prior to aggregation. 300,000 of mESCs is seeded with 5mL of ESLIF medium on 0.1% gelatin-coated T25 tissue-culture flask. At the 24 hours before generating gastruloid, all ESLIF medium is removed, and 2iLIF-supplemented N2B27 medium (1uM PD03 (abcr), 3uM Chiron (Qkine) and 550U/mL LIF (Qkine)) is added to the flask for 24-hour pre-treatment (Figure 2.2.1 (ii)).

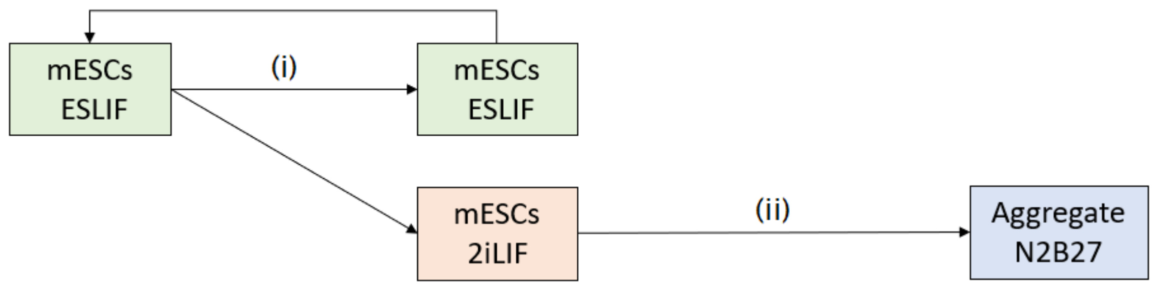

Figure 2.2.1. Cells Culture Conditions for maintaining mESCs cell line and preconditioning mESCs prior to the aggregation.

2.2.2 Generation of haemogenic gastruloids

2iLIF treated mES cells are used to generate haemogenic gastruloid following the procedure from 2.1.2., except cell suspension with fewer cells (6.25×10^3 cells/mL) are prepared for seeding 250 mES cells to each well of 96-well plate and CELLSTAR Cell Repellent U-bottom 96-well plate (Greiner Bio-one) is used.

2.2.3 Applying stimuli and changing medium for haemogenic gastruloids

After 48 hours of incubation in a humidified incubator at 37 °C and 5% CO_2 for aggregation, 150uL fresh N2B27 with 3uM Chiron and 100ng/mL Activin A (Qkine) is added to each well of 96-well plate for a 24-hour stimulation pulse. Medium supplemented with cytokines is changed every 24 hours until the time-course is complete. Between 72 and 168 hr, 5ng/mL VEGF (PeproTech) and 5ng/mL FGF_2 (PeproTech) are added to the N2B27, and 20ng/mL Shh (PeproTech) is additionally added to N2B27 between 144 and 168 hr. Between 168 and 216 hr, N2B27 is supplemented with 5ng/mL VEGF, 100ng/mL SCF (PeproTech), 20ng/mL TPO (PeproTech) and 100ng/mL Flt3L (PeproTech) (Figure 2.2.2).

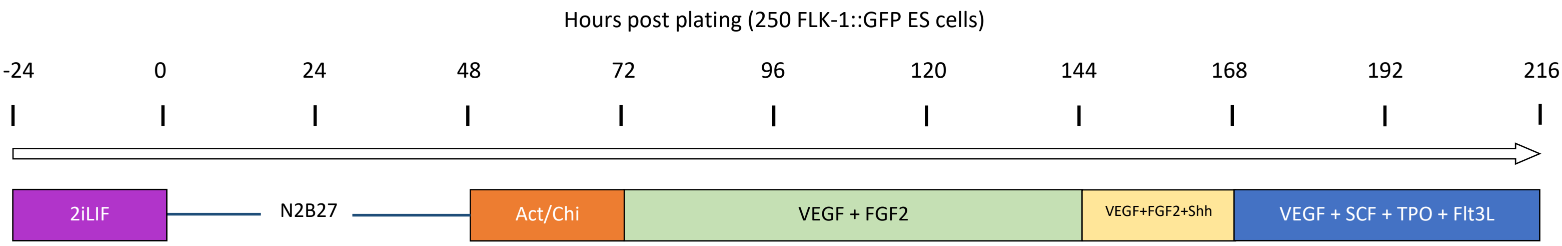

Figure 2.2.2. The culture scheme of mouse haemogenic gastruloid protocol.

2.2.4 Collection and dissociation of gastruloid cells

After removing 100uL medium from each well of 96-well plate using a multichannel pipette, The remaining medium and gastruloids are transferred into a 1.5mL Eppendorf tube with a P1000 pipette. Gastruloids are then washed with PBS (-$Ca2^+$, -$Mg2^+$) (Sigma), and 100-200uL Triple Express (Gibco) are added to the Eppendorf tube to trypsinise gastruloids to single cells in the incubator. If there are any cell pellets or clumps, they can be dislodged by pipetting up and down with a P1000 pipette. To neutralise the Triple Express, 1mL of ESLIF medium is added to the Eppendorf and spun down at 1000rpm at 5 minutes. Finally, The single-cell suspension of gastruloid is prepared by resuspending the cell pellet with either PBS or medium (volume subject to be changed) according to the subsequent assays.

2.3 Immunofluorescence staining and confocal microscopy

The ordinary protocol of gastruloid immunostaining and confocal microscopy analysis was set up according to previously published literature (Baillie-Johnson *et al*., 2015).

2.3.1 Gastruloid fixations

After removing 100uL medium from each well of 96-well plate using a multichannel pipette, The remaining medium and gastruloids are transferred into a 1.5mL Eppendorf tube with a P1000 pipette. Gastruloids are washed with PBS (-Ca2^{+}, -Mg2^{+}) twice. If the fluorescent protein of the cell line, such as eGFP reporter, is to be detectable on confocal microscopy, formaldehyde (PFA) (4%) (Sigma) can be used for fixation to avoid denaturing the fluorescent protein. After removing the PBS from the Eppendorf with a P1000 pipette, 1 ml fresh formaldehyde (4%) dissolved in PBS is added and incubated for 4 hours at 4 °C on an orbital shaker set to a low speed. After PFA-fixation, 4% PFA is aspirated, and the gastruloids are washed with 1mL of PBS twice on an orbital shaker set to a low speed for 10 minutes.

If the experimental design does not include detecting the fluorescent protein of the cell line, methanol can be applied to denature the fluorescent protein. After removing the PBS from the Eppendorf with a P1000 pipette, 1 ml pre-cold methanol is added and incubated for 30 minutes at 4 °C on an orbital shaker set to a low speed. After methanol-fixation, methanol is aspirated with a P1000 pipette which the tip is pre-coated with FBS. The gastruloids are washed with 1mL of PBS twice at 4 °C on an orbital shaker set to a low speed for 10 minutes. Methanol-fixed gastruloids tend to be floating on the surface of PBS and stick to P1000 pipette tip, pre-coating the pipette tip can prevent gastruloids from getting stuck in the tip, but caution should still be taken not to remove gastruloid accidentally during PBS washing.

The PBS is aspirated, and the gastruloids are washed with PBSFT (10% FBS (Biosera) and 0.2% Triton X-100 (Thermo Fisher)) twice at 4 °C on an orbital shaker set to a low speed for 10 minutes. The gastruloids are blocked with PBSFT at 4 °C on an orbital shaker set to a low speed for 1 hour. After blocking, PBSFT is aspirated, and gastruloids is stored with PBS at 4 °C. Gastruloids is stored with PBS to avoid contamination.

2.3.2 Primary and secondary antibody incubation

The gastruloids are transferred to a single plate or 9-well glass plate with a P1000 pipette which the tip is pre-coated with FBS. The PBS is aspirated, and the gastruloids are washed with PBSFT (10% FBS and 0.2% Triton X-100) at 4 °C on an orbital shaker set to a low speed for 1 hour. The PBSFT is then aspirated, and the gastruloids are incubated with 500 µl of PBSFT containing the required primary antibodies overnight at 4 °C on an orbital shaker set to low speed (Table 2.3.1). The glass plate is covered with paraffin film to prevent evaporation.

After overnight, the primary antibody solution is aspirated and washed with PBSFT twice for 5 minutes, twice for 15 minutes, and four times for 1 hour at 4 °C on an orbital shaker set to a low speed. The PBSFT is then aspirated, and the gastruloids are incubated with 500 µl of PBSFT containing the required secondary antibodies and Hoechst 42 overnight at 4 °C on an orbital shaker set to low speed.

Description	Target Species	Host Species	Conjugate / Format	Dilution Ratio	Supplier
CD45.2	Anti-Mouse	Mouse	PE	1:200	BD Biosciences
cKIT	Anti-Mouse	Goat	Biotin	1:250	R&D Systems
CD31	Anti-Mouse	Rat	N/A	1:200	BD Biosciences
CD45	Anti-Mouse	Rat	Biotin	1:250	BD Biosciences
Hoechst42	N/A	N/A	N/A	1:1000	Thermo Fisher
N/A	Anti-Rat	Donkey	AF-568	1:500	Thermo Fisher
N/A	Anti-Goat	Donkey	AF-633	1:500	Thermo Fisher
N/A	Anti-Rat	Donkey	AF-488	1:500	Thermo Fisher
N/A	Anti-Goat	Donkey	AF-568	1:500	Thermo Fisher
N/A	Anti-Rat	Donkey	AF-647	1:500	Thermo Fisher

Table 2.3.1 List of primary and secondary antibodies used for confocal microscopy.

2.3.3 Clearing and mounting

Again, after overnight, the secondary antibody solution is aspirated and washed with PBSFT twice for 5 minutes, twice for 15 minutes and four-time for 1 hour at 4 °C on an orbital shaker set to a low speed. The PBSFT is then aspirated, and the gastruloids are incubated with 100uL of ScaleS4 clearing solution overnight at 4 °C on an orbital shaker set to low speed. Each gastruloid is pipetted onto a 22 x 40mm glass coverslip as a 15 µl droplet, and double-sided tape is foldback on itself four times as a spacer on each end of the coverslip. After all, gastruloids are placed on the coverslip; the top coverslip is placed upon the spacers.

2.3.4 Confocal microscopy

Mounted gastruloid is taken for confocal microscopy imaging. Gastruloid were imaged using LSM700 on a Zeiss Axiovert 200 M with Zeiss EC "Plan-Neofluar" 10x/0.30 M27 and Zeiss LD "Plan-Neofluar" 20x/0.4 M27 objective lens. The fluorescent proteins were sequentially excited with 405, 488, 555 and 639 nm diode lasers, respectively(Table 2.3.1). Gastruloid image capturing and analysis were carried out using Zen2010 v6 (Zeiss).

2.4 Flow cytometry analysis

2.4.1 Antibodies staining

Gastruloid cells that had been trypsinised from gastruloid to a single-cell suspension were resuspended in 100 uL of PBE (PBS supplemented with 2mM EDTA and 0.5% BSA) containing a panel of antibodies for staining at 4°C for 20 minutes. After the cells are washed with PBE and spun down, if the biotinylated antibody is included in the staining panel, staining will be repeated with 100 uL of PBE containing streptavidin antibodies in 4°C for another 20 minutes. After washing, the cells pellet was resuspended with 300 uL of PBE containing Hochest 58 as viability dye.

Description	Conjugate / Format	Dilution Ratio	Supplier
AA4.1	PerCP/Cy5.5	1:100	Biolegend
B220	AF700	1:100	Biolegend
CD11b	PE	1:150	Biolegend
CD19	PE/Cy7	1:100	Biolegend
CD4	PE	1:150	Biolegend
CD41	Biotin	1:100	Biolegend
CD41	PE Dazzle594	1:100	Biolegend
CD43	PE	1:150	BD Biosciences
CD45	PB	1:100	Biolegend
CD45	APC	1:100	Biolegend
CD45.1	BV711	1:100	Biolegend
CD45.2	PerCP	1:100	Biolegend
CD8	PE/Cy7	1:100	Biolegend
cKit	APC/Cy7	1:100	Biolegend
EPCR	PE	1:150	Biolegend
Sca-1	PE/Cy7	1:100	Biolegend
Ter119	APC	1:100	Biolegend
VeCAD	APC	1:100	Biolegend
Streptavidin	BV421	1:200	Biolegend
Streptavidin	BV510	1:200	Biolegend
Streptavidin	AF594	1:200	Biolegend

Table 2.4.1 List of rat anti-mouse antibodies used for flow cytometry.

2.4.2 Flow cytometry analysis

Stained cells suspension was analysed using Attune™ NxT Flow Cytometer and Attune™ NxT Software (Thermofisher, US) or Gallios Flow Cytometer and Kaluza Analysis Software (Beckman Coulter, US). Regarding the gating strategy, cell debris was first excluded at the bottom left of the forward scatter area (FSC-A) vs side scatter area (SSC-A) density plot (Figure 2.4.1). The cells were then further gated to remove the doublets on the forward scatter height (FSC-H) vs FSC-A density plot. Finally, living singlet cells were selected on the SSC vs Hoechst 58 density plot. All flow cytometry data used this gating strategy unless specified. Living singlet cells were then further analysed according to the design of the experiments, and the dot plots in the results show the corresponding gating strategies.

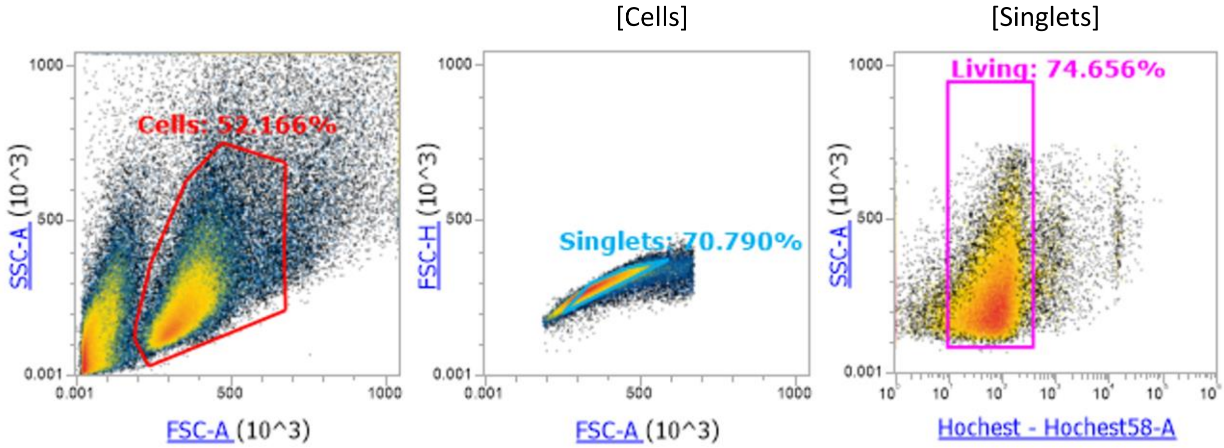

Figure 2.4.1 Gating Strategy in flow cytometry analysis.

Cell debris was first excluded in FSC-A/SSC-A plot, and then doublets were removed in FSC-A/FSC-H. Finally living singlets cells were selected using Hocehst 58 dye.

2.5 Fluorescence microscopy analysis

For fluorescence and bright-field colour imaging, lively gastruloids were imaged by Nikon Ti2 inverted microscope in a humidified CO2 incubator (37°C, 5% CO2). 150uL of N2B27 medium is changed 30 minutes before imaging. Fluorescent eGFP were sequentially excited with 488 nm diode lasers. Images were taken with fluorescence cubes and 10x or 20x objectives and analysed using Nikon NIS-Elements Imaging and ImageJ Software.

2.6 Animal transplantation assay

2.6.1 Gastruloid cells Injection into mice

The single-cell suspension of gastruloid cells is acquired and resuspended in 300uL of PBS following step 2.2.4. For the animal study in chapter 4.5, ~2x10^5 of CD45.1 bone marrow cells were injected with ~6x10^5 of bulk gastruloid cells or ~2x10^3 sorted gastruloid cells into the experimental mice (Figure 2.6.1). Only ~2x10^5 of CD45.1 bone marrow cells were injected into the control mice. For the animal study (PPL number: PP4153210) in chapter 5.4.3, ~5x10^5 of gastruloid cells were injected into the experimental mice, and ~1x10^4 of CD45.1$^+$CD45.2$^+$ bone marrow cells were injected into the control mice (Figure 2.6.2).

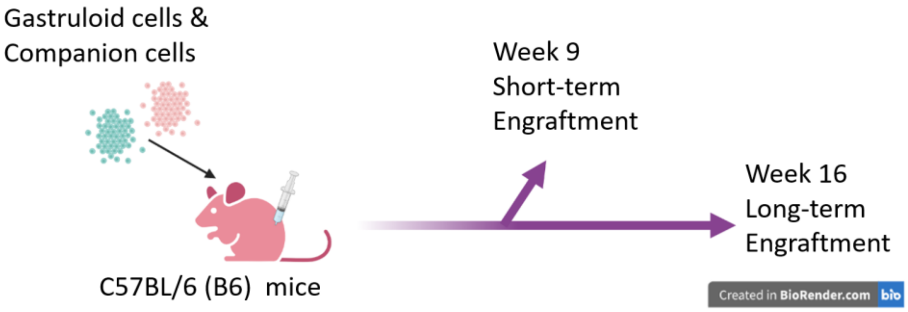

Figure 2.6.1 Experimental plan for the transplantation of gastruloid cells in chapter 4.5.

Gastruloid cells and companion cells were injected into irradiated C57BL/6 mice. Mice were culled either on week 9 to check the short-term engraftment or on week 16 to check the long-term engraftment.

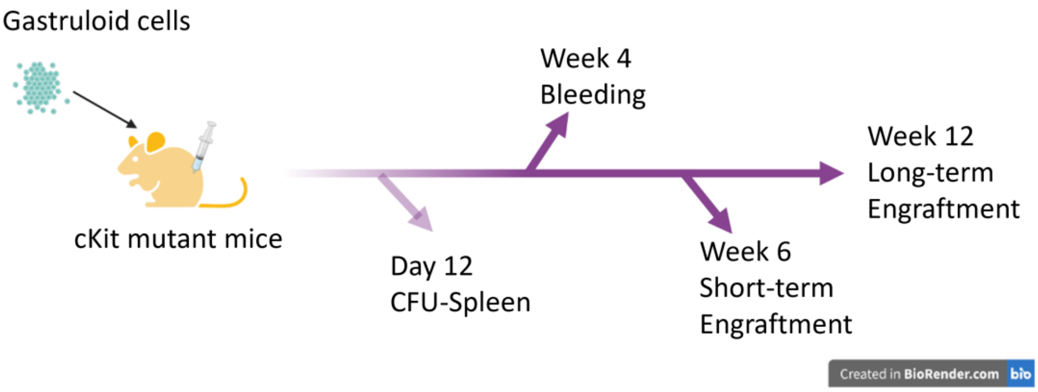

Figure 2.6.2 Experimental plan for the transplantation of gastruloid cells to in chapter 5.4.3.

Gastruloid cells were injected into non-irradiated c-Kit mutant mice. Mice were bled on week 4 to check the presence of gastruloid cells in the peripheral blood. Mice were culled on either on day 12 to check the CFU-Spleen, week 6 to check the short-term engraftment or on week 12 to check the long-term engraftment.

The cell suspension was adjusted to 200uL for the mouse injection based on the required number of cells per mouse. Mice were secured in the holder, and anaesthetic was applied on the tail's surface. The 200uL Bone marrow and/or gastruloid cells were slowly injected into the lateral vein of the tail using a 30 G needle (VWR) with an insulin syringe (BD).

2.6.2 Peripheral blood collection and processing

Post-transplantation Peripheral blood was collected every four-week using the saphenous vein method. Mice were warmed in a temperature-regulated chamber at 37°C for 15 minutes which helped the blood vessel dilate for bleeding. Bleeding is done on the mice one by one, and the mouse was made comfortable in a restrainer for assessing the tail vein. After applying the anaesthetics on the tail's surface, the vein was punctured with a 30G needle (VWR) and blood was collected using a capillary tube (Sarstedt).
Collected peripheral blood samples were analysed with Vet abc automated counter (Scil Animal Care, Viernheim, Germany) for measuring the different haematological parameters. 50ul of blood sample was first diluted with PBS (1:1 ratio), and 100uL of RBC lysis buffer (Invitrogen) was added to lyse the red blood cells in the blood sample. After 10 minutes of RBC lysis, samples were spun down at 2000rpm for 5 minutes and resuspended with 100µl of PBS. The cell suspension was stained antibodies for flow cytometry accordingly following protocol in step 2.5.

2.6.3 Bone and spleen collection and processing

Experimental mice were culled using cervical dislocation, which is a physical euthanasia method by applying pressure to the neck of the mouse to dislocate the spinal column from the skull. The 70% ethanol was sprayed over the mouse before dissection. When the mouse was dissected, muscles were removed using forceps and scalpel blade and femur, tibia and spleen were collected in I10 medium (IMDM (Thermo Fisher) supplemented with 10% FBS (Thermo Fisher), 2mg/mL L-Glutamine (Thermo Fisher), and 1% Penicillin-Streptomycin Amphotericin (Sigma). Extraction of bone marrow and spleen cells were conducted inside the laboratory hood.
Scissors, forceps and scalpel blade was used to scrape out any flesh attached to the femur and tibia. Femur and tibia were crashed in 10mL of I10 medium using mortar and pestle. Samples are ground until the crashed bone debris turn white, and no large red strain is visible. The extract was filtered using 40µM cell strainer (Fisher Scientific) to a 50mL falcon tube. 10mL of I10 was added to bone debris for washing and filtered to the same 50mL falcon tube.
To extract cells from the spleen, 40µM cell strainer on a 50mL falcon tube was first wet with 2mL of I10 medium, and the spleen was gently ground on the cell strainer using the pestle. The cell strainer is rinsed with 2mL of I10 medium time to time to wash down the spleen

cells. Spleen was gently ground until the debris turned white, and cell strainer and debris were discarded after being rinsed with 2mL of I10 medium three times.

Bone marrow cells and spleen cells extract was put on ice from time to time to prevent the aggregation of cells. The cells extract was centrifuged at 2000rpm for 5 minutes at 4°C and resuspended with 2mL of RBC lysis buffer red blood cells lysis on ice. After 5 minutes of RBC lysis, samples were spun down at 2000rpm for 5 minutes and resuspended with 1mL of PBS. The cell suspension was either stained with antibodies for flow cytometry accordingly (step 2.5), taken for OP9 co-culture (step 2.8.2), or cryopreserved.

For cryopreservation, bone marrow and spleen cells were centrifuged at 2000rpm for 5 minutes, and each sample was resuspended with 0.5mL of I10 medium and 0.5mL of freezing medium (FBS supplemented with 20% DMSO). The cell suspension is transferred to a cryopreservation vial and stored in Mr Frosty freezing container at -80°C for three days and then in liquid nitrogen for long term storage.

2.7 Chick chorioallantoic membrane (CAM) assay

2.7.1 Egg cultures and gastruloids grafting

The pathogen-free embryonated eggs were acquired from the Department of Zoology, University of Cambridge and incubated in a 50% humidified incubator at 37 °C for 7 days. On day 7, the egg was kept horizontally and taped with adhesive tape on the top to prevent over-craking of the egg. A hole is cracked within the taped area on the top using sterilised tweezers, and the cracked open was trimmed into rectangles window using scissors. The 216 hr Gastuloid were collected at 1.5mL Eppendorf and washed with 1mL of PBS. The gastruloid was stained with 1mL of PBS containing 5uL of stained with Vybrant DiO-dye (Thermo Fisher) in a humidified incubator at 37 °C and 5% CO_2 for 30 minutes. After washing with PBS twice and checking under fluorescence microscopy, ~10 gastruloids were engrafted directly on the CAM. The window of the eggs was covered with parafilm, and the eggs were incubated in a 50% humidified incubator at 37 °C for another 7 days.

2.7.2 Fluorescence and confocal microscopic imaging

On day 14, the engrafted eggs were taken out for fluorescence microscopy imaging to confirm if the gastruloids (shown in GFP fluorescence) had engrafted and if they engrafted adjacent to any vascularity on the CAM. If there are any engraftments, CAM around the engrafted gastruloid was cut and sampled using tweezers and scissors. Sampled CAM was fixed in 4%PFA in a 35mm glass-bottom culture dish (ibidi) for 4 hours at 4 °C on an orbital shaker set to a low speed. Fixed CAM and engrafted gastruloid were immunostained with CD45 antibody using the method in Chapter 2.3.2 and confocal imaged according to the method in Chapter 2.3.4.

2.8 OP9 and OP9-DL1 co-culture

The OP9 and OP9-DL1 co-culture were prepared using the published protocol (Holmes & Zúñiga-Pflücker, 2009).

2.8.1 OP9 and OP9-DL1 cell co-culture

OP9 cells and OP-DL1 are maintained in 5mL of OP9 medium (α-MEM (Thermo Fisher) supplemented with 20% FBS and 1% Pen-Strep (Thermo Fisher)) on T25 tissue-culture flask in a humidified incubator at 37 °C and 5% CO_2. The cells are passaged before it reaches 80% confluency. Cells are maintained by splitting at a ratio of 1-to-4 and passaged every two days. Cells are grown at least two passages post thawing before plating for OP9 co-culturing. For OP9 co-culturing with gastruloid or bone marrow, OP9 and OP9-DL1 cells are seed in the well of a 48-well plate.

For cryopreservation, OP9 or OP9-DL1 cells were centrifuged at 2000rpm for 5 minutes, and each cell line was resuspended with 1 mL of OP9 freezing medium (OP9 medium supplemented with 10% DMSO and 40% FBS). The cell suspension is transferred to a cryopreservation vial and stored in Mr Frosty freezing container at -80°C for three days and then in liquid nitrogen for long term storage.

2.8.2 Initiation of bone marrow or gastruloid cells co-culture

The method in step 2.6.3 is followed to extract the bone marrow from the mouse femur and tibia. 1 x 10^4 bone marrow cells or 30-Gastruloid-equivalent single cells suspension is seeded to a well in a 48-well plate pre-seeded with 80% confluent OP9 or OP9-DL1 cells 1.5 mL conditioned OP9 medium, which is supplemented with 5 ng/mL Flt-3L (PeproTech) and 1 ng/mL IL-7 (PeproTech).

On days 5, 8 and 12 (or in every 4-day intervals), cells are disaggregated without using trypsin just by pipetting up and down with a P1000 pipette until OP9 or OP9-DL1 monolayer is completely disrupted into many small pieces. Dislodged cells suspension is filtered through a 40-µm cell strainer (Greiner Bio-one) into a 15mL falcon tube, and the well and cell strainer are rinsed with 3mL PBS twice. After centrifugation, cells were resuspended with 1mL of conditioned OP9 medium and 100uL of cell suspension was taken for flow cytometry analysis (method in step 2.5). The remaining cell suspension (~900uL) are seeded into wells of a 48-well plate of 80% confluent OP9 or OP9-DL1 cells.

2.9 Colony forming cell (CFC) assay

MethoCult™ M3434 Methylcellulose medium (Stemcell Technologies) aliquots (~3mL) were thawed at room temperature in advance, and the single-cell suspension of gastruloid cells is acquired following step 2.2.4. The number of gastruloid cells that is equivalent to five gastruloids were resuspended with 300uL of I10 medium and vigorously mixed with a methylcellulose medium aliquot (~3mL) using a vortex. After 30 minutes and when most of the bubbles were off, the medium was split into two, which medium (~1.5mL) was transferred into a 35 mm gridded tissue culture dish (Sarstedt), gently using a 5mL glass pipette. Four sample dishes and an uncovered dish containing 3mL of PBS were placed in a 100mm culture dish with cover. After 7 days or 14 days of incubation at 37 °C and 5% CO_2 (accordingly to the design of the experiment), sample dishes were scored on the number and type of colonies formed on the medium under the ZEISS Axio Observer microscope with a 10x and a 20x objectives. Imagines of the colonies were taken when necessarily with ZEISS Axiocam ERc 5s camera attached to the microscope.

2.10 Quantification of RNA on qPCR analysis

2.10.1 RNA extraction

Gastruloids were trypsinised, and RNA was extracted in 1mL of TRIzol (Life Technologies) at room temperature for 5 minutes. After adding 0.2mL chloroform (Sigma) to the cells and incubating for 3 minutes, cell lyses was spun down at 12000g at 4 °C for 5 minutes. The aqueous layer is moved to a new tube and 0.5mL isopropanol (Sigma) for 10 minutes incubator. After centrifugation, 1mL of 75% ethanol (Sigma) is added to resuspend the RNA pellet for washing, and it is spun down at 7500g at 4 °C for 5 minutes. The ethanol washing is repeated, but with 100% ethanol and RNA pellet are air-dried in the hood for 10 minutes. 50uL of RNase-free water (Qiagen) is added to dissolve the RNA pellet, and the concentration of RNA is measured using NanoDrop™ 2000/2000c Spectrophotometers (ThermoFisher).

2.10.2 qPCR analysis

Complementary DNA (cDNA) synthesis was performed with total RNA extract equivalent to 100,000 cells using the SuperScript III First-Strand Synthesis System (Thermo Fisher). Each RNA/primer mixture is prepared with 2uL RNA, 1uL of 50 μM oligo(dT) primer, 1uL 10mM sNTP mix and 6uL DEPC-treated water and is incubated at 65°C for 5 minutes then on ice for 1 minute. After incubation, 10uL of cDNA synthesis Mix (2uL of RT buffer, 4uL od 25uM $MgCl_2$, 2uL of 0.1M DTT, 1uL of RNaseOUT and 1uL of SuperScript III RT) is added to each sample mixture. The Reverse transcription is finished by treating the mixture at 50°C for 50 minutes and at 85°C for 5 minutes to terminate the reactions.

The quantitative real-time polymerase chain reaction (qPCR) reactions were run in triplicate, each sample using 10 μL Takyon Low Rox SYBR MasterMix (Eurogentec), 2.5 μL cDNA, 0.5 μL primer mix (100 μm) and 7 μL dH2O. Primer pairs used in the qPCR are shown in the table 2.10.1. Technical repeats were averaged and normalised to GAPDH levels. Standard errors were propagated accordingly. Cycling conditions for the RT-PCR thermocycler: initial denaturation at 95°C for 3 minutes, followed by 40 cycles of denaturation at 95°C for 10 seconds and annealing/extension at 60°C for 30 seconds. Melt curves were generated between 60 and 95°C, holding for 5 seconds for each step. The triplicate CT values from the qPCR were analysed using $2^{-\Delta\Delta Ct}$ method to quantify the relative gene expressions.

Gene	Forward Primer (5' -3')	Reverse Primer(5' -3')
Hbb-bh1	AGGAGAAACTCTGGGAAGGCTC	TTGCCATGGGCTCTAATCCG
Hbb-Y	GTGGATCCTGAGAACTTCAAACTC	AAAGGAGGCATAGCGGACAC
Hbb-B1	GCACCTTTGCCAGCCTCAGT	AACCATTGTTCACAGGCAAGAGC
GAPDH	AACTTTGGCATTGTGGAAGG	GGATGCAGGGATGATGTTCT
Pou5f1	TCTTTCCACCAGGCCCCCGGCTC	TGCGGGCGGACATGGGGAGATCC
Sox2	GGCAGCTACAGCATGATGCAGGAGC	CTGGTCATGGAGTTGTACTGCAGG
Sox17	AGCTCCAGAAACTGCAGACCAGAA	AGCTCCAGAAACTGCAGACCAGAA
Runx1	ACTCACTGGCGCTGCAACAA	AAGCTCTTGCCTCTACCGCT
Sfpi1	AACCACTTCACAGAGCTGCA	CAAGCCATCAGCTTCTCCAT
Gata1	CATTGGCCCCTTGTGAGGCCAGAGA	ACCTGATGGAGCTTGAAATAGAGGC
Gata2	GACTATGGCAGCAGTCTCTTCC	GGTGGTTGTCGTCTGACAATT
Tal1	ATGGAGATTTCTGATGGTCCTCAC	AAGTGTGCTTGGGTGTTGGCTC
Flk1	CACCTGGCACTCTCCACCTTC	GATTTCATCCCACTACCGAAAG
VeCad	CGTGAGCATCCAGGCAGTGGT	GAGCCGCCGCCGCAGGAAG

Table 2.10.1 List of primers (Sigma) used for qPCR analysis.

2.11 PCR and gel electrophoresis

2.11.1 PCR

The RNA extraction of the gastruloids and cDNA synthesis was followed using the method in step 2.10. The polymerase chain reaction (PCR) was run using HotStarTaq Master Mix Kit (Qiagen). Each reaction mixture is prepared using 2uL of cDNA, 10uL of HotStarTaq Master Mix, 0.2 µL primer mix (100 µM) and 7.8 uL RNase-free water. Cycling conditions for the PCR thermocycler are set below, initial denaturation at 95°C for 15 minutes, and final extension at 72°C for 10 minutes. The 40 cycles included denaturation at 94°C for 30 seconds, annealing at 60°C for 30 seconds, and the extension set at 72°C for 1 minute.

2.11.1 Electrophoresis

A 1.5% agarose gel was prepared by dissolving 1.05g agarose powder in 70 mL TAE (1x) buffer and microwaved for 1 minute with swirling in between. 10uL of SYBR™ Safe DNA Gel Stain (Thermo Fisher) is added to the agarose mixture. Wait a few minutes until the mixture is not boiling hot; the mixture is poured into the gel rig with the combs and waited for 1 hour for the gel to set. 10uL of DNA sample from the PCR was mixed with 2uL of DNA Gel Loading Dye (6X) (Thermo Fisher), and 10uL of it was added to the well of the gel. The Electrophoresis was run at 80v for 25 minutes or until the bands of the 10,000x DNA ladder (Thermo Fisher) were well separated, checked using the UV transilluminator.

2.12 Single-cell SMART sequencing

2.12.1 FACS sorting

Gastruloid have been collected daily from 120 to 216 hr, and single-cell suspension of gastruloid cells is acquired for flow cytometry following the method in step 2.2.4. The antibodies CD45-APC, CD41-PE Dazzle 594, cKIT-APC/Cy7 and Sca1-PE/Cy7 were used in the stained following the method in step 2.4.1. FACS sorting have been carried out in BD FACSAria™ III high sensitivity flow cytometer inside a CL2 hood. Regarding the gating strategy for sorting, dead cells were first excluded at the bottom of the forward scatter area (FSC-A) vs Hoechst 58 density plot (Figure 2.12.1). The cell debris was excluded at the bottom left of the FSC-A vs side scatter area (SSC-A) density plot to identify the cells with the size and complexity of interest. The pulse geometry gatings were further applied to remove the doublets on the FSC-A vs forward scatter height (FSC-H) density plot and then on SSC-A vs side scatter height (SSC-H) density plot. Living singlet cells were then further analysed and sorted accordingly.

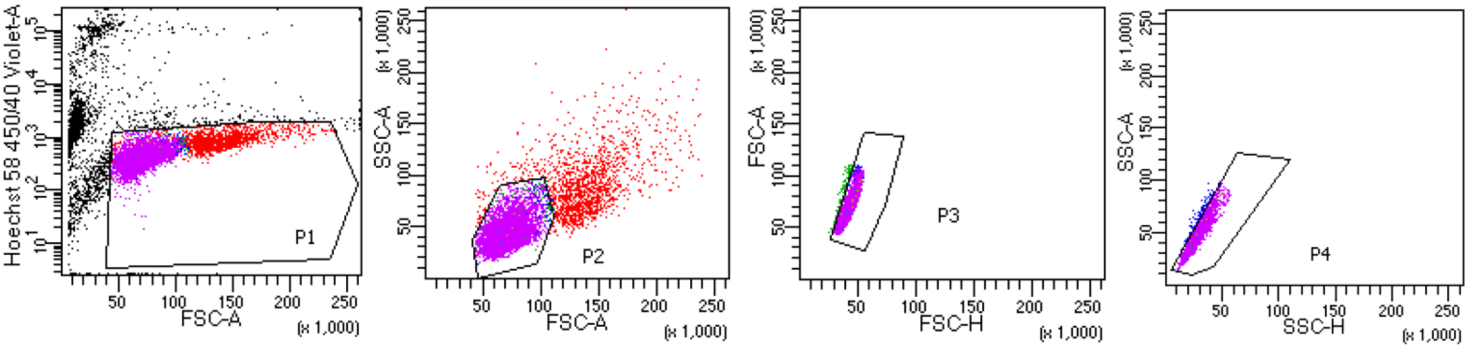

Figure 2.12.1 Gating Strategy in flow cytometry analysis and sorting.

Living cells were first selected using Hocehst 58 dye and Cell debris was excluded in FSC-A/SSC-A plot. Doublets were removed in FSC-A/FSC-H and SSC-A/SSC-H plots.

Sorting used 70uM nozzle, and the single cell was sorted to Eppendorf twin.tec® 96 wells PCR plates containing 2uL of lysis buffer (0.2% Triton X-100 (Thermo Fisher), 1U/µl RNase inhibitor(Promega)). Lysis buffer plates were spun down 2000rpm at 4 °C for 2 minutes before and after the sorting. Sorted plates were stored at -80°C and delivered to the Centro Nacional de Análisis Genómico on dry ice for analysis.

2.12.2 Library preparation and sequencing

Full-length single-cell RNA-seq libraries were prepared using the Smart-seq2 protocol with minor modifications (Picelli *et al*., 2013). Reverse transcription was performed using SuperScript II (Thermo Fisher Scientific) in the presence of 1 µM oligo-dT30VN (IDT), 1 µM Template-switching oligonucleotides (Qiagen), and 1 M betaine. cDNA was amplified using the KAPA Hifi Hotstart ReadyMix (Kapa Biosystems) and IS PCR primer (IDT), with 22 cycles of amplification. Following purification with Agencourt Ampure XP beads (Beckmann Coulter), product size distribution and quantity were assessed on a Bioanalyzer using a High Sensitivity DNA Kit (Agilent Technologies). A total of 140 pg of the amplified cDNA was fragmented using Nextera XT (Illumina) and amplified with double indexed Nextera PCR primers (IDT). Products of each well of the 96-well plate were pooled and purified twice with Agencourt Ampure XP beads (Beckmann Coulter). Final libraries were quantified and checked for fragment size distribution using a Bioanalyzer High Sensitivity DNA Kit (Agilent Technologies). Pooled Sequencing of Nextera libraries was carried out using a NovaSeq6000 (Illumina) to an average sequencing depth of 0.5 million reads per cell. Sequencing was carried out as paired-end (PE150) reads with library indexes corresponding to cell barcodes.

2.12.3 Sequencing data analysis

The Seurat algorithm with default properties was first applied to select the highly variable genes, followed by elbow method to select the first 10 principal components (PCs) in both the whole and sorted gastruloid subsets (Satija *et al*., 2015). The UMAP plots of the clustering were performed with the Leiden algorithm with a resolution of 0.5 on the whole gastruloid and sorted gastruloid subpopulation cells data.

In the correlation analyses, the KNN graph was computed by using a KNN classifier with 15 neighbours with maximum vote criteria to classify the cell by clusters. The metric employed for computing distances is correlation metric in the first 15 PCAs components space. Based on the KNN graph, the proportion of cells from the gastruloid clusters and mean distance (correlation distance) to the cluster over the cells were computed.

2.13 Statistical analysis

All experiments were done in at least duplicates ($n \geq 2$) except where mentioned. The data from experiments were analysed with Student's paired or unpaired t test using GraphPad Prism 7.0 software. The data is plotted as Mean ± Standard deviation with an error bar using GraphPad Prism 7.0 and Microsoft Excel software.

Chapter 3: Early adaption of gastruloid protocol to produce haemogenic endothelium and haematopoietic precursors

3.1 Overview

In this chapter, the ordinary gastruloid protocol was studied to determine whether this protocol could be adapted to form gastruloids with haematopoietic potentials. Since Activin A is critical to the initiation of meso-endodermal commitment in embryos, Activin A was added, together with Chiron, to the gastruloid culture after aggregation to study if they could initiate the expression of a mesodermal marker, Flk-1, detected by GFP fluorescence.

After testing the importance of the Activin A and Chiron (A+C) impulse in raising the mesodermal potential, an investigation into the effect of adding VEGF and FGF_2 to the gastruloid culture followed. VEGF and FGF_2 signalling plays a vital role in the gastrulation and HSC specification in early haematopoiesis. Therefore, gastruloids were treated with VEGF and FGF_2 for 48 hours after the A+C pulse, with the help of Mr Oliver Davies. Mr Davies also helped carry out qPCR to study whether VEGF and FGF_2 can initiate haematopoietic-related transcriptional activities in gastruloids at 120 hr. Other hematopoietic cytokines such as SCF are as crucial as VEGF to haematopoiesis in the AGM region. Following the A+C pulse, gastruloids were grown with or without SCF and FGF_2. Gel electrophoresis-based PCR analysis and qPCR analysis were applied on gastruloid cells to determine if the cytokines can facilitate haemoglobin switching between 72 and 120 hr during developmental haematopoiesis, in which embryonic and foetal haemoglobins are replaced by adult haemoglobins. In addition to the haemoglobin switching study, Flk-1/GFP expression patterns in a gastruloid from 72 to 144 hr was imaged by fluorescence microscopy.

Since Noggin and Shh are believed to work on BMP and VEGF signalling respectively at the aorta endothelium in early-stage definitive haematopoiesis, gastruloids were grown with SCF, Noggin and/or Shh to study haemoglobin switching using qPCR analysis. Gastruloids cultured with SCF, Noggin, or Shh were also seeded in a CFC assay at 144 hr to examine whether these cytokines could potentiate the haematopoietic colony-formation, ensuring progenitor content. To understand more about the expression of haemopoietic markers in gastruloids, they were collected at 144 hr and the expression of Flk-1/GFP, CD45, c-Kit and CD41 were analysed using flow cytometry. Finally, flow cytometry was also utilised to understand if the addition of Shh or SCF between 120 and 144 hr could elevate the expression of Flk-1/GFP, VeCAD and CD41.

3.2 Adaptation of ordinary gastruloid protocol

The standard gastruloid protocol has been adapted by adding cytokines that are important to maintain the haematopoietic microenvironment to the culture in a temporal control. To study the feasibility of adapting this protocol to generate a haematopoietic gastruloid, 250 Flk-1::GFP cells with N2B27 medium were plated onto a 96-well U bottom plate and the cells clustered to form a gastruloid (Figure 3.2.1).

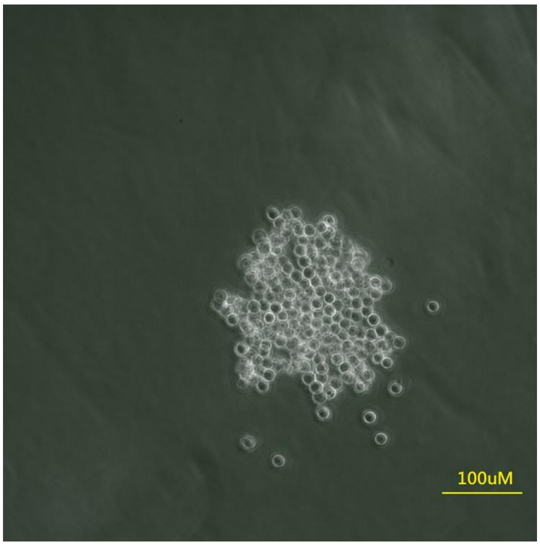

Figure 3.2.1. Image of Flk-1::GFP cells at 0 hour (250 cells, magnification: 20x).

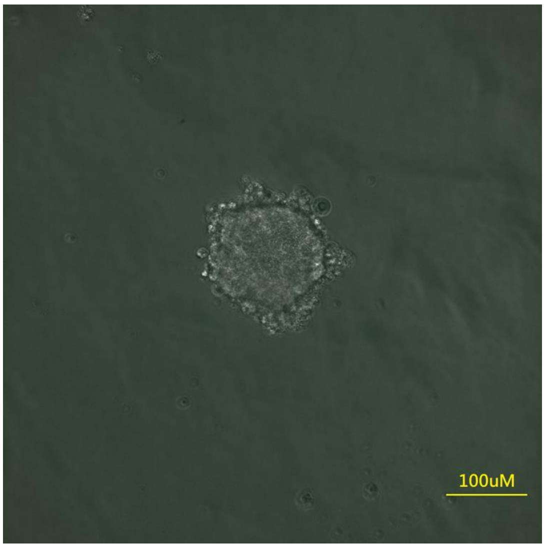

Figure 3.2.2. Image of gastruloid at 48 hour (250 cells, magnification: 20x).

The plate containing mES cells was cultured in the incubator undisturbed for 48 hours to allow the cells to settle at the bottom of the wells. These mES cells attached to the surrounding cells and self-organised to form a spherical aggregate as if an embryo in the early stage of embryonic development (Figure 3.2.2). Mammalian embryos at this stage go through gastrulation, a process which transforms a group of cells into an ensemble of tissues. The embryo is shaped to form an organised three-layered structure spatiotemporally, and the cells in these three germ layers begin differentiation to establish distinct cell lineages. These coordinated movements of cells help to set up the organisation of the embryo along anteroposterior, dorsoventral and left-right axes, resulting in symmetry breaking and elongation (Nowotschin & Hadjantonakis, 2011).

In the ordinary gastruloid protocol, the aggregates are treated with Wnt agonist Chiron for 24 hours. Chiron provides local activation of symmetry-breaking signals, which initiates the polarisation process and results in the elongation of the gastruloid (van den Brink *et al*., 2014). Gastruloids treated with Chiron displayed enhanced levels of T/Brachyury, which is an important protein in defining the midline and regulating the anterior-posterior axis and thus, is an important topological marker of gastruloid cultures (Turner *et al*., 2017). The practice of treating gastruloids with the 24-hour pulse of Chiron after aggregation is adapted, but it is worth studying should the protocol also include Activin A in this pulse.

Activin A belongs to the TGFβ superfamily and applying this cytokine in ES cells can drive the cells into a meso-endodermal fate (Pauklin & Vallier, 2015). Activin A can activate the Activin/Nodal signalling pathway and directly modulates corresponding developmental regulator expression, alongside orchestrating the commitment of mouse ES cells towards the meso-endodermal lineage at the end. In the haematopoietic microenvironment, Activin A, expressed by mesenchyme, promotes hematopoietic fated mesoderm development (Cerdan *et al*., 2012). However, since Activin A showed repression to the differentiation of several blood lineages such as the B-cell lineage, it could only be applied earlier when adapting this cytokine into the gastruloid protocol to prevent unwanted restrictions on blood lineage development (Shav-Tal & Zipori, 2002).

Flk-1::GFP cells were plated to form a gastruloid as Flk-1 is critical to the initiation of haematopoiesis, and was found to be highly expressed in the haemogenic endothelium in previous studies (Motoike *et al*., 2003). The mouse ES cell line E14TG2a was used to customise the Flk-1::GFP cells, with an eGFP reporter inserted into the initiation codon of the *Flk-1* locus (Jakobsson *et al*., 2010). The expression of *Flk1* in the gastruloid was regarded as the initiation of haemogenic differentiation, and its pattern was shown by GFP fluorescence which was captured by fluorescence microscopy.

At 48 hrs of the culture, gastruloids were treated with A) an A+C pulse, B) Chiron only, or C) Activin A only. At 72 hr, all groups of gastruloid were treated with naïve N2B27 medium, and group C was additionally treated with a Chiron pulse (Figure 3.2.3). At 96 hr, gastruloids were analysed under fluorescence microscopy to investigate if they displayed GFP fluorescence.

Together these results indicated that applying Activin A together with Chiron is critical to endothelial development as significant Flk-1/GFP expression was shown on the fluorescence image of the gastruloid in group A at 96 hr. In addition, A+C pulsed gastruloids had an elongated ovoid shape and displayed polarised GFP fluorescence at 96 hr (Figure 3.2.4 A).

Without Activin A, no GFP fluorescence was observed, suggesting that Activin/Nodal signalling is

essential to trigger Flk-1 expression in gastruloids (Figure 3.2.4 B). In addition, a fine temporal of the Wnt signalling and Activin/Nodal signalling is necessary for Flk-1 expression, as no GFP fluorescence was observed in group C where the Chiron pulse was 24 hours delayed after the addition of Activin A at 48 hr (Figure 3.2.4 C).

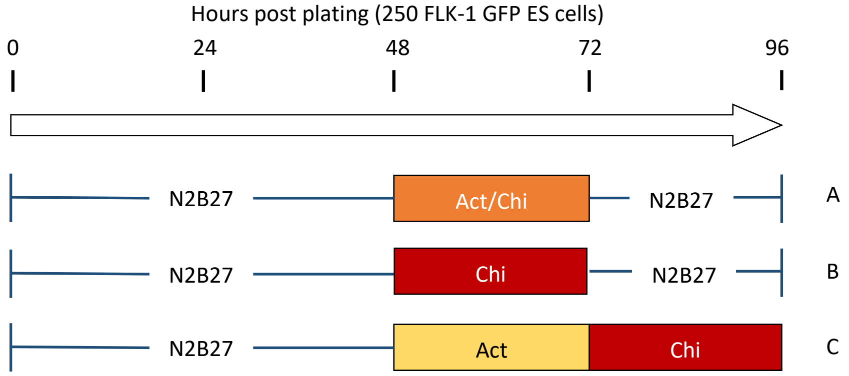

Figure 3.2.3. The culture scheme of gastruloids used to investigate whether Activin A (Act) and Chiron (Chi) are essential to the Flk-1 expression in gastruloid at 96hr.

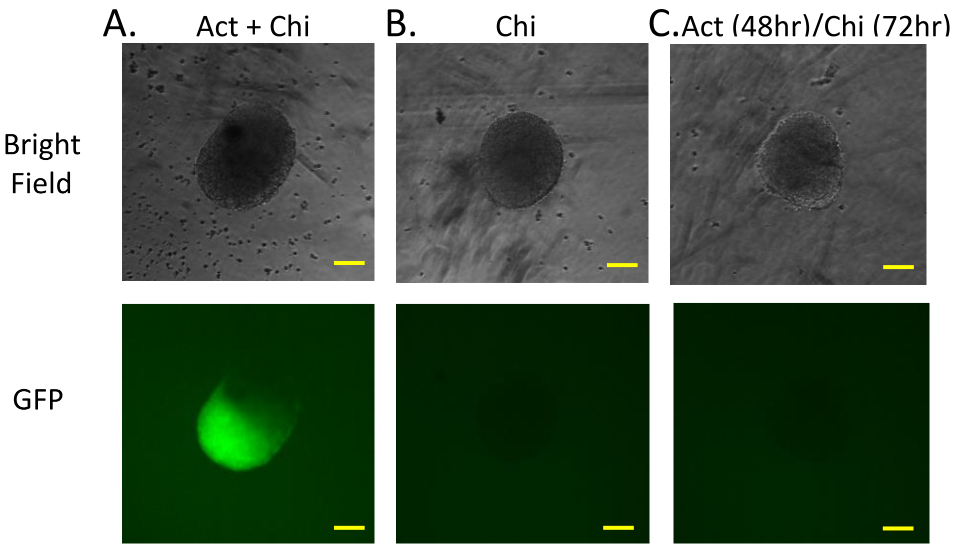

Figure 3.2.4. Fluorescence microscopy images of 96 hr gastruloids with either or both Activin A and Chiron added.

Bright-field (top panels) and GFP fluorescence (bottom panels) microscopy images of a representative 96 hr gastruloid, with either or both Act and Chi added to the culture. (A) Gastruloid with Act+Chi pulse between 48 and 72 hr is ovoid-shaped and shows polarised GFP fluorescence at the posterior end (n=20). (B) With Chi only between 48 and 72 hr, no GFP fluorescence has been observed (n=18). (C) No GFP is detected in the gastruloid if the Act A pulse (48 and 72 hr) is added separately with the Chi pulse (72 and 96 hr) (n=18). (Magnification: 20x; scale bar: 100uM)

3.3 Characterisation of early-stage haemogenic gastruloids

3.3.1 Adding VEGF and FGF_2 to gastruloid culture between 72 and 120 hr initiate gene expressions related to haematopoietic activities

Aside from adding Activin A and Chiron to trigger elongation and Flk-1 expression in gastruloids shown in Figure 3.1.4, other cytokines are also necessary to maintain the haematopoietic microenvironment for the gastruloid to differentiate the haematopoietic progenitors. VEGF, FGF_2 and SCF are the possible haematopoietic cytokines that were added to the culture after 72 hours, the time point following the A+C pulse and as the gastruloid is beginning to upregulate the Flk-1 expression.

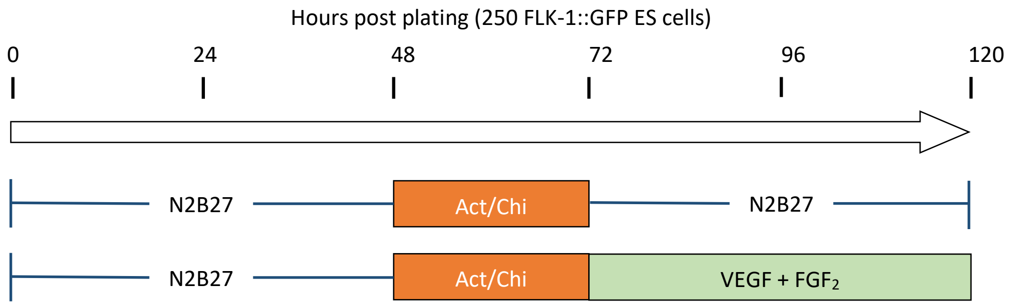

Figure 3.3.1. The culture scheme of gastruloids used to investigate if VEGF and FGF_2 can upregulate expression of the haematopoietic and endothelial genes in the gastruloids at 120hr.

VEGF signalling is critical to the gastrulation and axis formation of the embryo, which is essential to endothelial cells(Yamaguchi *et al*., 1993; Flamme *et al*., 1995). Flk-1 is a member of the VEGF receptor family, and Flk-1 is expressed in the stage from mesodermal to endothelial cells to initiate the development of haemogenic endothelial cells (Hirai *et al*., 2005). VEGF is also a signalling protein that promotes the growth of vascular endothelial cells and has an essential role in maintaining the survival of haematopoietic stem cells (Gerber *et al*., 2002). FGF_2 is another hematopoietic cytokine as important as VEGF during early haematopoiesis. FGF_2 regulates the emergence and maintenance of HSCs at the dorsal aorta (Pouget et al., 2014). FGF_2 is required for HSC specification through its actions in neighbouring somitic tissues during early somitogenesis, but also contradictorily promotes HSC proliferation in adult haematopoiesis, suggesting the FGF pathway has variable roles at multiple stages of HSCs development (Lee *et al*., 2014).

Thus, it is interesting to investigate whether adding VEGF and FGF_2 from 72 hr would help to promote haematopoietic and endothelial markers in the gastruloid, which can be regarded as a critical step in haematopoiesis. With the assistance of Mr Oliver Davies from Dr Cristina Pina's group at the University of Cambridge, a plate of gastruloids was made using Flk::1GFP ES cells, and qPCR analysis was performed on gastruloids treated with only a A+C pulse and those treated with VEGF and FGF_2 following the A+C pulse (Figure 3.3.1). It is unsurprising that the qPCR analysis revealed that the expression of haematopoietic and endothelial markers (*Sox 17, Runx1, Flk-1 and Gata1*) were upregulated because of the VEGF and FGF_2 (Figure 3.3.2). The stemness marker expression (*Pou5f1*) was downregulated, and haemoglobin expression (*bH-globin*) was also upregulated in the gastruloid treated with $VEGF_2$ from 72 to 120 hr. Genes that are critical for EHT, Sfpi1 is downregulated while Gata2 is marginally upregulated. These results show that VEGF and FGF_2 can promote the transcriptional activities in gastruloids, and facilitate the differentiation of embryonic stem cells into the precursor of haematopoietic cells.

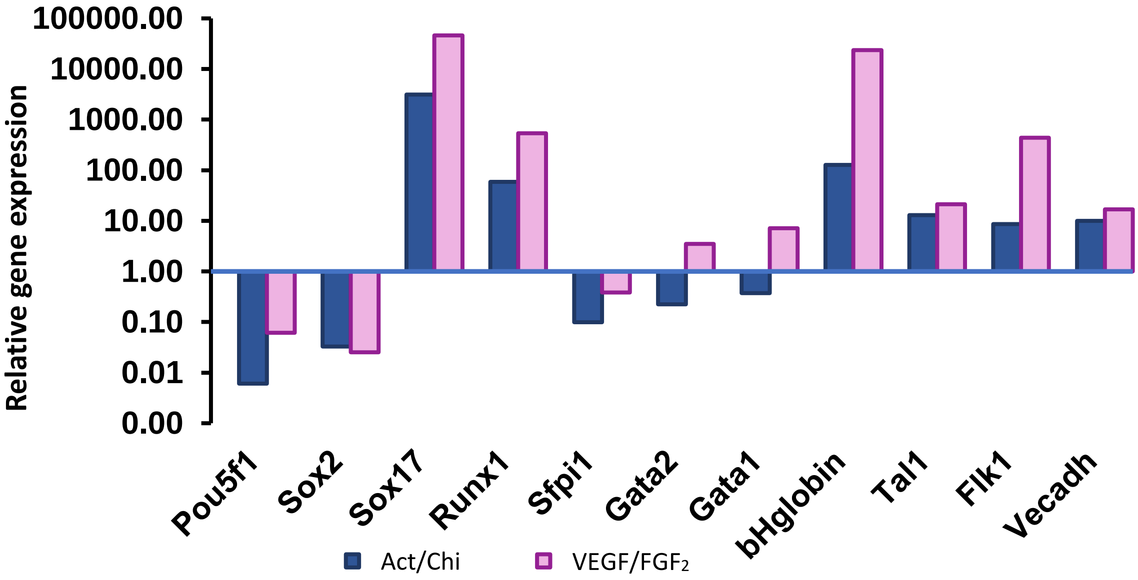

Figure 3.3.2. qPCR Analysis of relative gene expressions at the 120 hr gastruloid

The gastruloids were cultured with A+C pulse only and A+C pulse followed by VEGF and FGF2. Gastruloids were collected at 120 hr and the expressions of Sox2, Sox 17, Runx1, Flk-1, Gata1, Gata2,, Sfpi1, Pou5f1, bH-globin and Tai1were anaylsed by qPCR using 2-△△Ct method (Credit to Mr Oliver Davies) (n=2).

3.3.2 Adding VEGF and FGF_2 to gastruloid culture between 72 and 120 hr promotes haemoglobin switching

In addition to VEGF and FGF_2, SCF is another hematopoietic cytokine as important in early haematopoiesis. SCF is such a significant HSCs maturation factor that SCF alone can induce the maturation of vascular endothelium at E9.5 and type 1 pre-HSCs at E10.5, which is consistent with the decline of HSC activity in SCF mutant mice (Rybtsov *et al*., 2014). Since SCF plays a role in fetal haematopoiesis, SCF may aid the development of a microenvironment that is favourable to the haematopoiesis in the gastruloids. Throughout murine embryonic development, the composition of the haemoglobin subunits changes and it leads to the assembly of haemoglobin having various lineage-restricted physiological properties (Sankaran *et al*., 2010). These developmental haemoglobin swtichings are regulated by the expression of embryonic ζ-globin (*Hbb-bh1*) and γ-globin (*Hbb-y*), and adult β-globin (*Hbb-b1*) genes (Sankaran *et al*., 2010). Examining the expression of these haemoglobin genes in the gastruloid culture helps evaluate what culture condition is favourable to the haematopoietic differentiation of the gastruloids.

To further understand the role of VEGF, FGF_2 and SCF in promoting the differentiation in the gastruloid revealed by the haemoglobin switching, gastruloids were cultured in three different conditions followed by qPCR analysis.At 48 hr of the gastruloid, Actin and Chiron were added accordingly to the culture. Five schedules were set throughout the 120 hours of culture, which are 1) control, without any cytokines, 2) A+C pulse between 48 and 72 hr, 3) A+C pulse with FGF_2 from 72 and 120 hr, 4) A+C pulse with VEGF and FGF_2 from 72 and 120 hr and 5) A+C pulse with VEGF, FGF_2 and SCF from 72 and 120 hr (Figure 3.3.3). Gastruloids from different conditions were collected at 120 hr and analysed with qPCR, RT-PCR, and gel electrophoresis.

The gel electrophoresis results revealed that gastruloids cultured without any haematopoietic cytokines did not express any globin genes (Figure 3.3.4, lane 1). Even with the assistance of Activin and Chiron, the gastruloids did not have any globin gene expressions (lane 2). Adding FGF_2 from 72 to 120 hr slightly promoted the expression of *Hbb-bh1* and *Hbb-b1*, suggesting that differentiation of gastruloids could be facilitated under stimulation from haematopoietic cytokines (lane 3). Furthermore, adding VEGF and FGF_2 to gastruloids from 72 to 120 hr may further upregulate all three *Hbb* genes, and clear and bright bands were visible on all three gels, which is consistent with the qPCR analysis that *Hbb* can be upregulated with VEGF (lane 4). However, an additional 24-hour SCF pulse did not promote but repressed the expression of *Hbb* genes and resulted in a dimer band on the gel, repression was also particularly obvious on *Hbb-y* and *Hbb-b1* (lane 5).

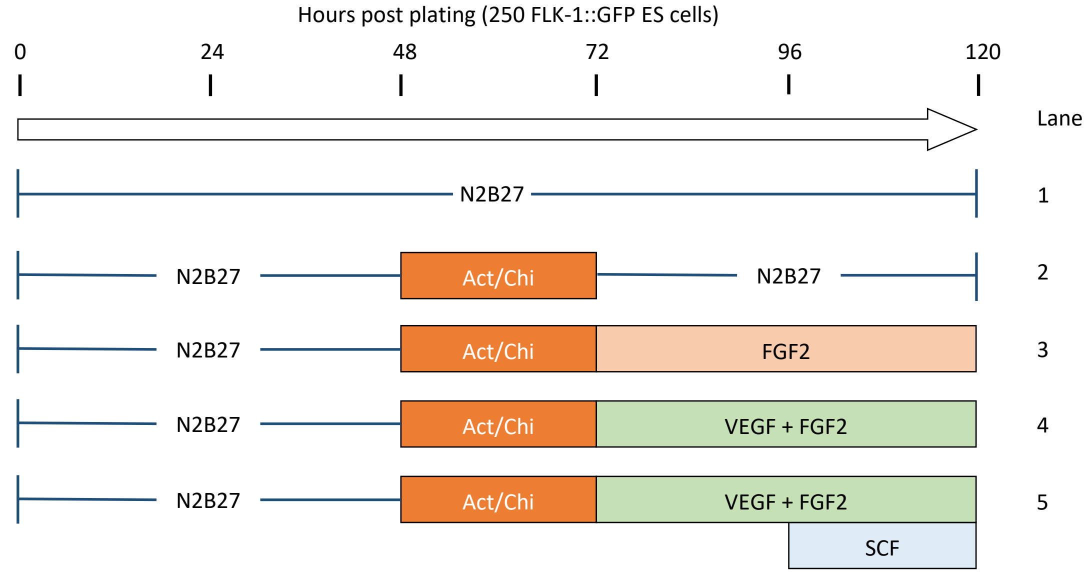

Figure 3.3.3 The culture scheme of gastruloids used to investigate if VEGF, FGF_2 and SCF can promote the differentiation of the gastruloids and haemoglobin switching at 120hr.

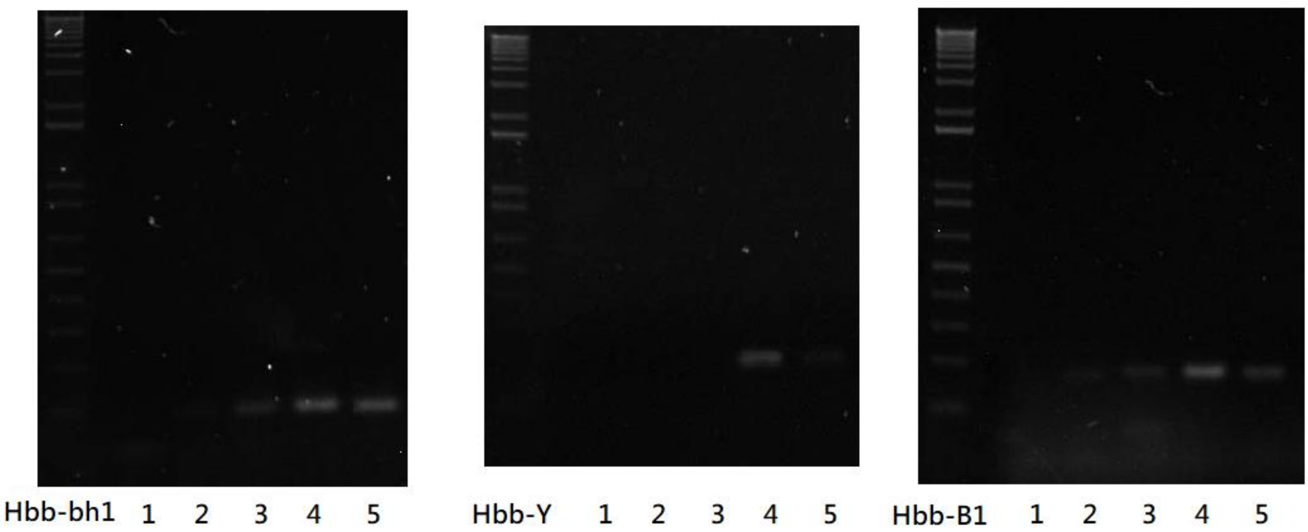

Figure 3.3.4 Result of RT-PCR with gel electrophoresis on RNA from 120hr gastruloids treated with different culture conditions.

RT-PCR with gel electrophoresis of RT-PCR products primers Hbb-bh1 (left), Hbb-Y (middle) and Hbb-B1 (right). Refer to the figure for the information regarding the gastruloid culture conditions. Lane 1 is the control without any cytokines; lanes 2 to 5 are treated with Activin and Chiron from 48 to 72hr. Lane 3 is treated with FGF_2 from 72 to 120hr; lane 4 is VEGF and FGF_2 from 72 to 120hr; lane 5 is VEGF and FGF_2 from 72 to 120hr and SCF from 96 to 120hr.

The RT-PCR and gel electrophoresis results are fascinating as they suggest FGF_2, VEGF, and SCF may facilitate haematopoiesis and haemoglobin switching (Figure 3.3.5). Gastruloids from conditions 3, 4 and 5 were taken for RNA extraction and qPCR analysis to quantitatively study if FGF_2, VEGF and SCF in combination can initiate the transcriptional program haemoglobin and its switching. From the result of qPCR from condition 3, only FGF_2 was added between 72 and 120 hr, suggesting that FGF_2 alone is not sufficient to trigger the haematopoietic program to drive the haematopoiesis in gastruloids as all haemoglobin genes are relatively lowly expressed.

In comparison, with the help of VEGF, the gastruloid in condition 4 displayed elevated expression of haemoglobin, of which the embryonic ζ-globin (*Hbb-bh1*) was the highest, followed by γ-globin (*Hbb-y*), and adult β-globin (*Hbb-b1*) last. This result is consistent with the results from RT-PCR and gel electrophoresis that VEGF has a critical role in triggering haematopoiesis and mediating haemoglobin switching as *Hbb-b1* was upregulated. However, adding SCF at 96 hr may be too premature as embryonic ζ-globin (*Hbb-bh1*) was further upregulated, while adult β-globin (*Hbb-b1*) was downregulated. Although SCF is well known to be an important HSCs maturation marker, the embryonic date of the gastruloid may be too early. Consequently, adding SCF at this time might have delayed the haemoglobin switching, and it may subsequently delay haematopoietic development of the gastruloid.

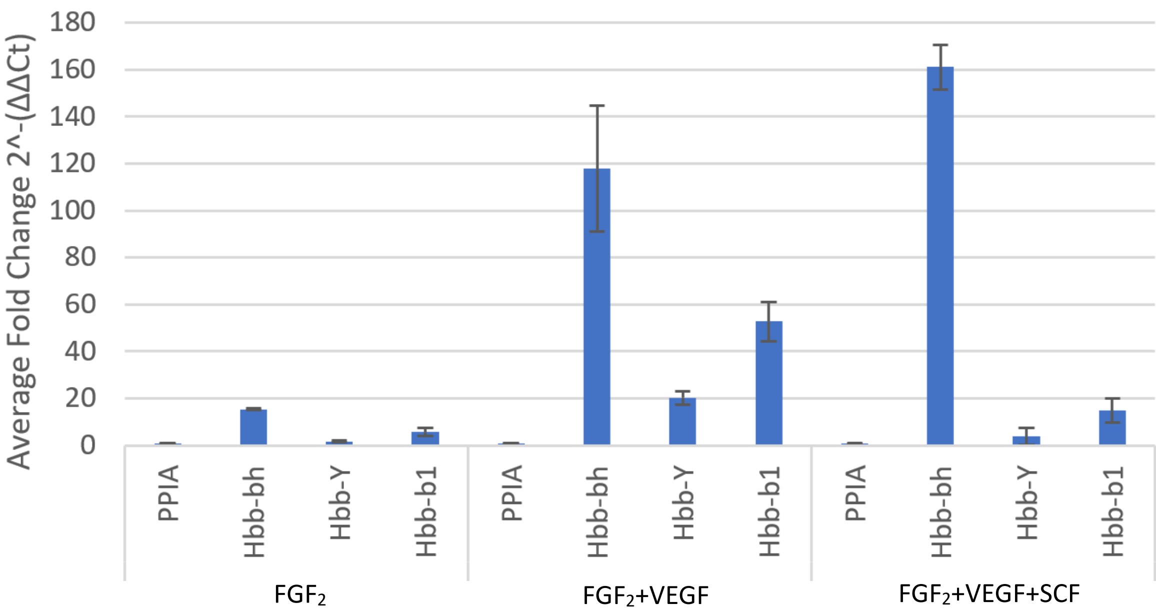

Figure 3.3.5 qPCR Analysis of gene expressions of haemoglobin at the 120 hr gastruloids.

Gastruloids were cultured with VEGF, FGF2 and SCF between 72 and 120 hr and analysed by qPCR on the expressions of Hbb-bH, Hbb-Y and Hbb-b1 using 2-△△Ct method (n=2).

3.3.3 Fluorescence microscopic images showing the Flk-1 expression pattern in gastruloids between the 96 and 144 hr

qPCR analysis has suggested that adding FGF_2 and VEGF from 72 to 120 hr can promote haematopoiesis and activate the expression of the adult globin chain, while adding SCF at 96 hrs did not further promote the switching. To date, experiments have only studied adding SCF for a 24-hour pulse at 96 hr, thus it remains unknown if adding the SCF pulse at 120 hr or extending the pulse into 48-hour can help promote the haematopoietic potentials.

As discussed above, under fluorescence microscopy Flk-1::GFP cells of the gastruloid displayed GFP fluorescence, indicating *Flk1* expression in the gastruloid and initiation of haemogenic differentiation. Therefore, gastruloids were cultured in several conditions, with SCF added at different times and for various durations. All gastruloids were cultured with VEGF and FGF_2 between 72 and 144 hr, with 1) no SCF added, 2) SCF added between 96 to 120 hr, 3) SCF added between 120 to 144 hr and 4) SCF added between 96 to 144 hr (Figure 3.3.6). Fluorescence microscopy images of gastruloids were taken at 72 hr, 96 hr, 120 hr and 144 hr.

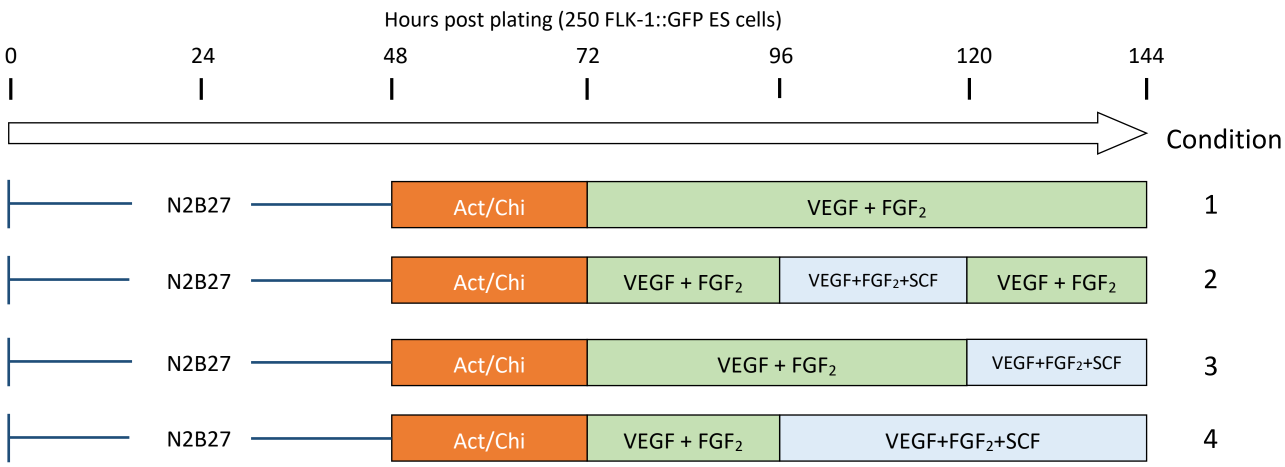

Figure 3.3.6 The culture scheme of gastruloids used to investigate if adding SCF promote the haematopoietic differentiation at 144hr.

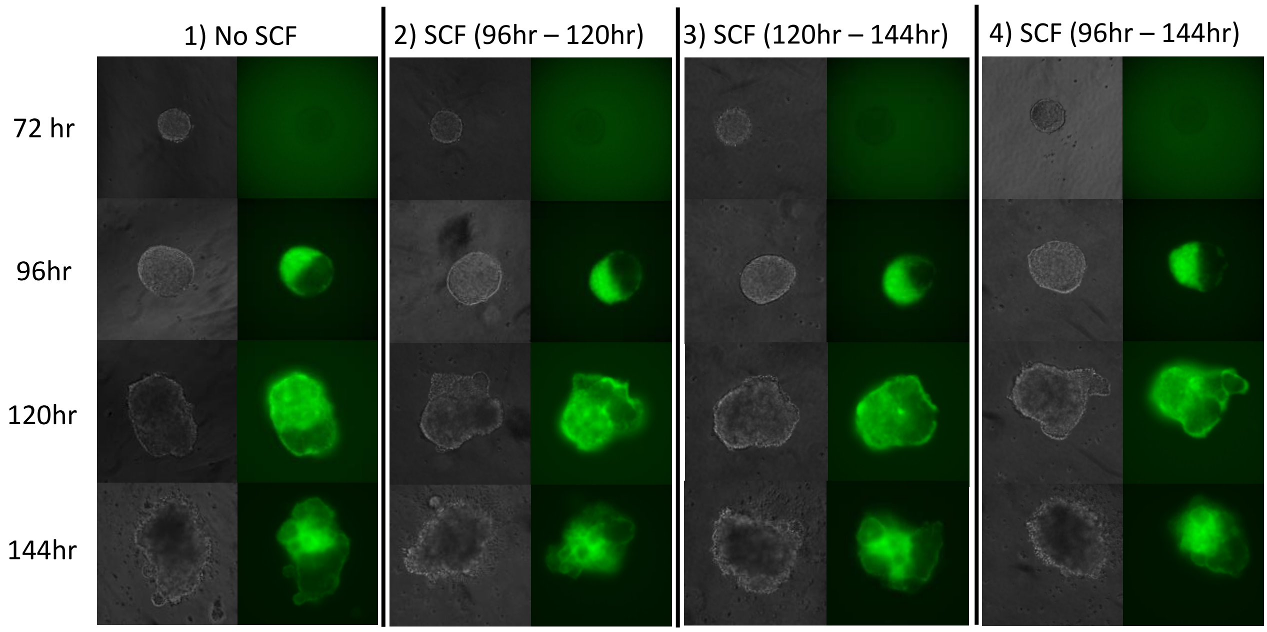

Figure 3.3.7. Time course fluorescent microscopy images of 72, 96, 120 and 144hr gastruloids with SCF added at different time.

Bright-field (left panels) and GFP fluorescence (right panels) microscopy images of representative gastruloids at 72 hr, 96 hr, 120 hr and 144 hr, with SCF added at different time. All gastruloids were treated with an Act+Chi pulse between 48 and 72 hr, and VEGF and FGF2 between 72 and 144 hr and 1) with no SCF added (n=43), 2) With SCF between 96 and 120 hr (n=45), 3) with SCF between 120 and 144 hr (n=40), and 4) with SCF between 96 and 144 hr (n=45).

Gastruloids in all conditions showed a spheroid shape (~100um) at 72 hr, but no GFP fluorescence was detected (Figure 3.3.7). At 96 hr, the gastruloids had doubled in size (~200um), were ovoid-shaped and had polarised GFP pattern in all conditions. The 96 hr results are consistent with the previous results (Figure 3.2.4; Figure 3.3.7). After 24 hours, all gastruloids continued to grow and started to develop irregularly shaped budding. During this time GFP fluorescence was present at the whole gastruloid but remained polarised, the patterning displayed that compartmentations or structures started forming in the gastruloid. Finally, at 144 hr, the overall intensity of GFP fluorescence of all gastruloids was maintained, but the bright GFP sections remained in the gastruloids. The structures in the gastruloid became more established, developed and observable under the microscope.

Across all conditions, no significant difference in their morphology can be observed, including elongation, GFP fluorescence (Flk-1 expression), shape and the development of structures in the gastruloids. Gastruloids treated with SCF for 48 hours are generally, subtly smaller than others, but this minor difference is negligible and inconclusive.

3.4 Optimisation of the cytokine schedule between 96 and 144 hr

3.4.1 Haemoglobin gene switching is downregulated on the 144 hr gastruloid by hematopoietic cytokines (SCF Shh and Noggin

To establish an embryonic haematopoietic microenvironment *in vitro*, simply applying VEGF and FGF_2 may not be enough to stimulate the definitive haematopoiesis. It has been discovered that other cytokines including SCF, Noggin and Shh also are crucial to early-stage definitive haematopoiesis in embryos (Rybtsov *et al.*, 2014; Rybtsov *et al.*, 2014; Souilhol *et al.*, 2016). BMP signalling has a critical role in the HSC emergence, and BMP4 is predominantly found underneath the aortic endothelium, while its antagonist Noggin is mainly expressed in haematopoietic clusters in the dorsal aorta (Ivanovs *et al*., 2014). Sonic Hedgehog (Shh) acts upstream of the VEGF signalling, and promotes the specification of the arterial endothelial cell and haematopoietic patterning (Lawson *et al*., 2002). Apart from the dorsal aorta tissue being a rich source of Shh, Shh signalling has a stage-specific effect in HSCs development, almost exclusively affecting early-stage definitive haematopoiesis (Rybtsov *et al*., 2011).

To further understand these cytokines, SCF, Shh and Noggin were added to the gastruloid culture either at 96 or 120 hr (Figure 3.4.1). Gastruloids were collected at 144 hr, and the expression of haemoglobin genes (*Hbb-y, Hbb-bh1* and *Hbb-b1)* were analysed through qPCR. The qPCR results have been normalised to GAPDH, and the average fold change of genes is relative to the expression of genes cultured with the VEGF and FGF_2 only group.

The qPCR result prove that individually adding these cytokines between 96 and 144 hr cannot promote the VEGF and FGF_2-induced switch of haemoglobin (Figure 3.4.2). The addition of Noggin even significantly silenced the expression of haemoglobin genes, suggesting Noggin should not be added at this time. Since definitive haematopoiesis is under tight temporal control of signalling pathways, the ES cells may not have developed into the progenitor cells that are responsive to these cytokines individually, slowing down the haemoglobin switching.

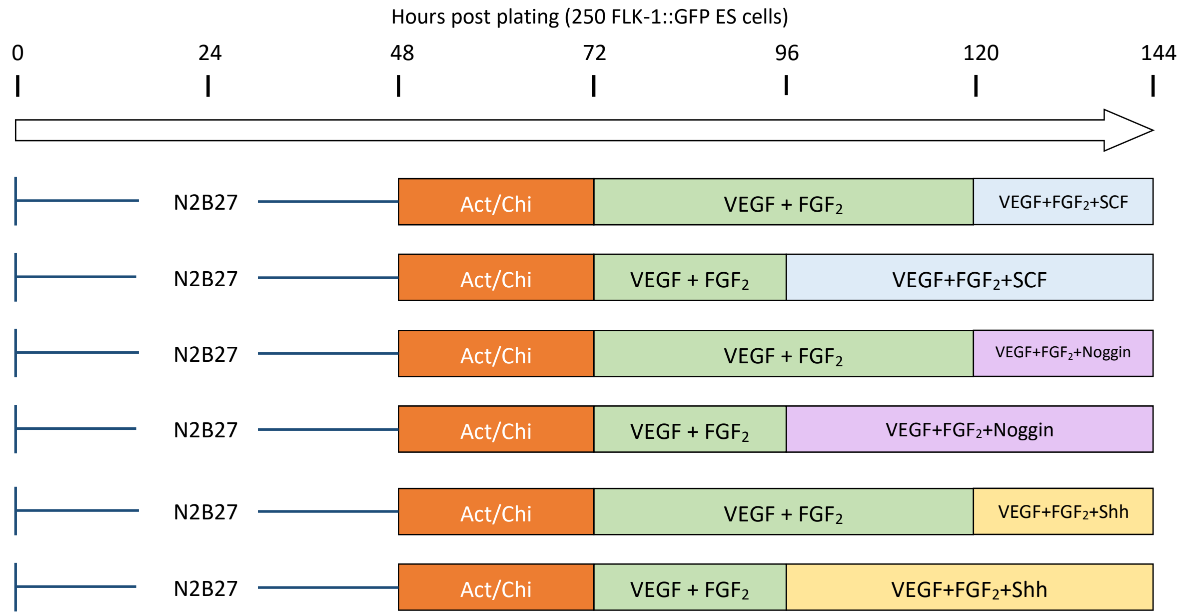

Figure 3.4.1. The culture scheme of gastruloids used to investigate if adding SCF, Shh, and/or Noggin for last 24 or 48hr can enhance switching of haemoglobin at 144hr.

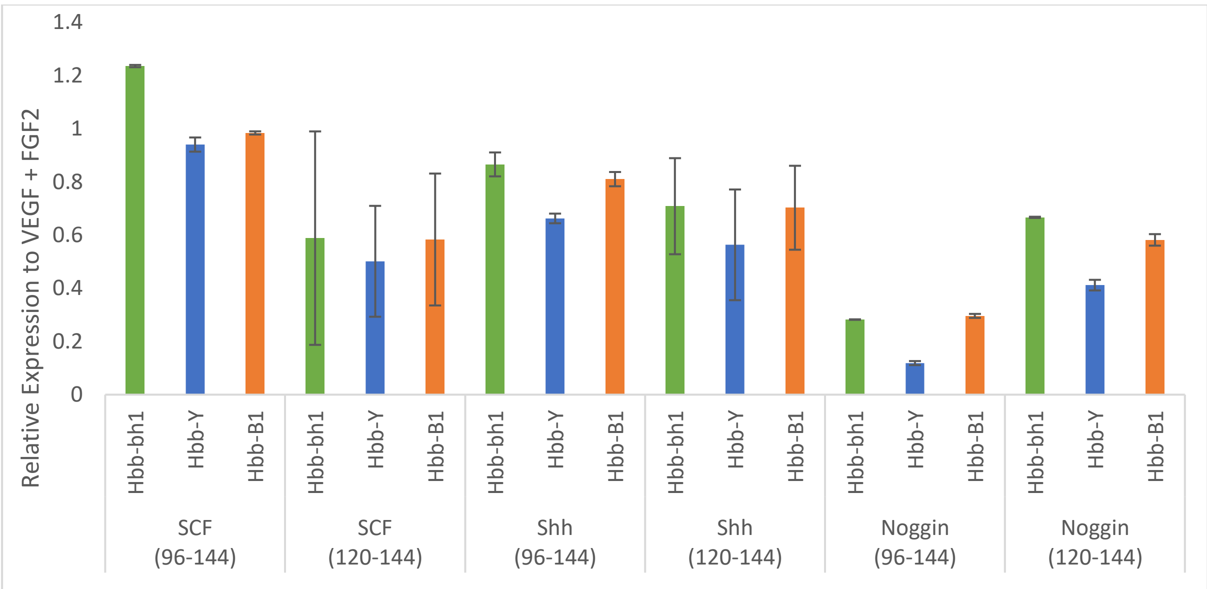

Figure 3.4.2. qPCR Analysis of gene expressions of haemoglobin at the 144 hr gastruloid treated with Shh, SCF and/or Noggin in the last 24 or 48 hr.

Gene expression analysis of gastruloids treated with Shh, SCF or Noggin for 24 or 48 hours (SCF, Shh,noggin (96-144), n=3; SCF, Shh, noggin (120-144), n=6). Gastruloids were analysed by qPCR on the expressions of Hbb-bH, Hbb-Y and Hbb-b1 relative to the expression of the control, VEGF + FGF_2 only using 2-△△Ct method (n=3 or 6).

Numerous cytokines are involved in the haematopoietic microenvironment *in vivo*, and they may have a synergistic effect in promoting haematopoiesis. Although the qPCR analysis in Figure 3.4.2 did not show these cytokines can drive the haemoglobin switching in the gastruloid, these cytokines may have synergy to drive the haematopoiesis and haemoglobin switching. Different combinations of SCF, Shh and Noggin were added to the gastruloid culture at 120 hr and collected at 144 hr to study if adding them in combination can be synergistic in upregulating the haematopoietic transcriptional activities. (Figure 3.4.3).

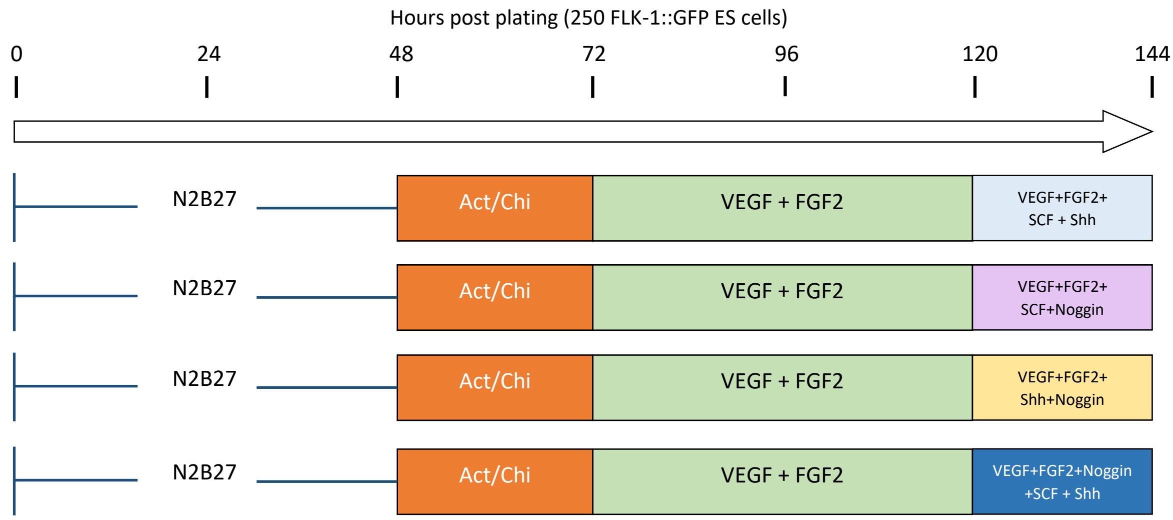

Figure 3.4.3. The culture scheme of gastruloids used to investigate if adding SCF, Shh or Noggin in the last 24 hr can enhance switching of haemoglobin at 144hr.

Gastruloids were collected at 144 hr, and the expression of haemoglobin genes (*Hbb-y*, *Hbb-bh1* and *Hbb-b1)* were analysed using qPCR analysis. However, even adding these cytokines in combination, regardless of adding SCF + Shh, SCF + Noggin or Shh + Noggin, no combination can promote the transcriptional activities of haemoglobin switching (Figure 3.4.4). Gastruloids with Shh and Noggin together notably displayed lower expression of haemoglobin. However, adding all three cytokines together could rescue a certain degree of haemoglobin expression silencing observed with pairs of cytokines, suggesting some synergy among them. In addition, the full combination failed to improve adult haemoglobin production relative to VEGF and FGF_2 alone. As mentioned previously, adding these cytokines to the gastruloid at these timepoints may be too early, and the progenitor cells responsive to these cytokines might not have been differentiated yet.

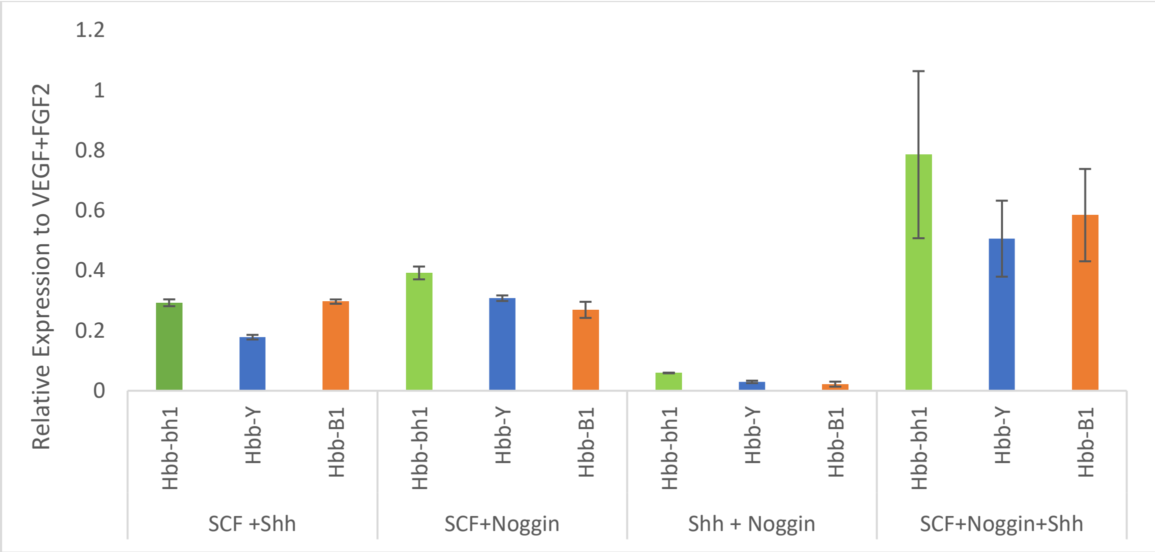

Figure 3.4.4. qPCR Analysis of gene expressions of haemoglobin at the 144 hr gastruloids treated with Shh, SCF and/or Noggin in the last 24 hr.

Gene expression analysis of gastruloids treated with a combination of Shh/SCF/Noggin for 24 hours (SCF+Shh, SCF+Noggin, Shh+Noggin, n=3; SCF+Noggin+Shh, n=6). Gastruloids were analysed by qPCR on the expressions of Hbb-bH, Hbb-Y and Hbb-b1 relative to the expression of the control, VEGF + FGF_2 only using 2-△△Ct method (n=3 or 6).

3.4.2 CFC Assay on the 144 hr gastruloid cells grew with different hematopoietic cytokines (SCF, Shh and Noggin)

Many signalling pathways have been associated with definitive haematopoiesis, while their mechanisms and interactions in promoting the haematopoietic potential have not been well elucidated. Some studies have reported that c-Kit, Shh and BMP4 signalling pathways can interact to mediate the endothelial-to-haematopoietic (EHT) transition and HSC maturation in the AGM region (Marshall *et al*., 2007; Wilkinson *et al*., 2009). A study has also found that the interplay among these three signalling pathways is under tight spatial and temporal control to regulate the activities of each other and mediate the definite haematopoiesis occurring in the AGM region (Souilhol *et al*., 2016).

Although it is shown that adding the key cytokines involved in these pathways, including SCF (c-Kit ligand), Noggin (BMP4 antagonist), and Shh to the gastruloid at 96 and 120 hr is too early to mediate the transcriptional program of haemoglobin switching, the haematopoietic progenitor potential of gastruloids cultured with these cytokines have not yet been studied. HSC progenitors are capable of differentiating into a full lineage of blood cells. It is helpful to examine the differentiation pattern of gastruloid cells to determine whether haematopoiesis is taking place in the gastruloid due to the addition of these cytokines into the culture.

The colony forming cell (CFC) assay can be applied to the gastruloids to examine the proliferation and differentiation potential of ES cells by their ability to form colonies in a semisolid medium. The methylcellulose used is optimised to support the growth and differentiation of HSPCs by containing hematopoietic cytokines such as SCF, IL-3, IL-6, and EPO (STEMCELL Technologies Inc., 2018). Gastruloids were cultured in five conditions for 144 hr in which all conditions have a 24-hour A+C pulse at 48 hr and conditions 2) to 5) have VEGF and FGF_2 between 72 and 144 hr. For conditions 3) to 5), Shh, SCF and Noggin have been added to the culture at 120 hr, respectively (Figure 3.4.5). At 144 hr, six gastruloids from each condition were collected, trypsinised and replated in methylcellulose medium (M3434) for a CFC assay for 20 days.

The results of the CFC assay indicated that the concomitant application of VEGF and FGF_2 can significantly promote the differentiation potential of ES cells in gastruloid culture for 144 hours (Figure 3.4.6; Figure 3.4.7). Activin A and Chiron treated gastruloids only had a residual specification of burst forming unit-erythroid (BFU-E) and colony-forming unit-myeloid (CFU-M) progenitors, while treating the gastruloid with VEGF and FGF_2 significantly promoted the haematopoietic potential of gastruloid cells to form BFU-E and CFU-M-type colonies (Figure 3.4.6). The addition of SCF at 120 hr did not increase the formation of either colony, suggesting that SCF does not enhance the haematopoietic potential at this time point.

The addition of Shh did not affect the BFU-E forming potential but reduced the CFU-M colonies, while adding Noggin reduced all colonies formed by the gastruloid cells (Figure 3.4.7). VEGF and FGF_2 cultured gastruloids had BFU-E and CFU-M, suggesting that the gastruloid cells had erythropoietic and myeloid potential. Only gastruloid cells treated with Shh exhibited mixed colonies of erythroid and myeloid, which corresponds to the earliest progenitor associated with definitive haematopoiesis, specifically the yolk sac EMP (Frame *et al*., 2016). This suggests that Shh can further enhance the hematopoietic potential of gastruloids cultured with VEGF and FGF_2 (Figure 3.4.7).

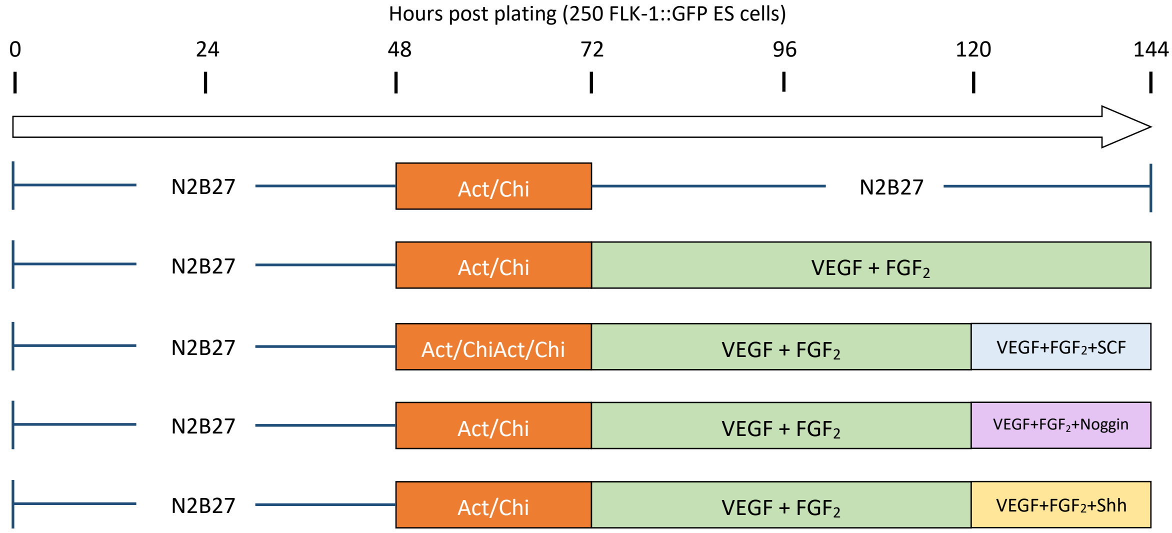

Figure 3.4.5. The culture scheme of gastruloids used to investigate if adding SCF, Shh or Noggin last 24 hr can promote the haematopoietic potential of 144hr gastruloids on a CFC assay.

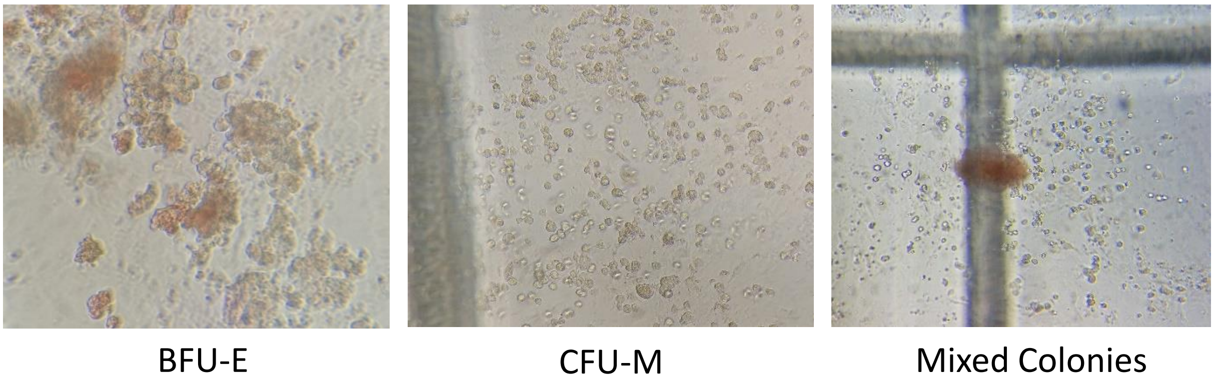

Figure 3.4.6. Images of colonies formed by the 144hr gastruloid cells

Images of burst forming unit-erythroid (BFU-E) (left) and colony-forming unit-myeloid (CFU-M) (middle) formed by the 144hr gastruloid cells (magnification: 20x). Mixed colonies were observed in ES cells cultured with Shh (right) (magnification: 10x)

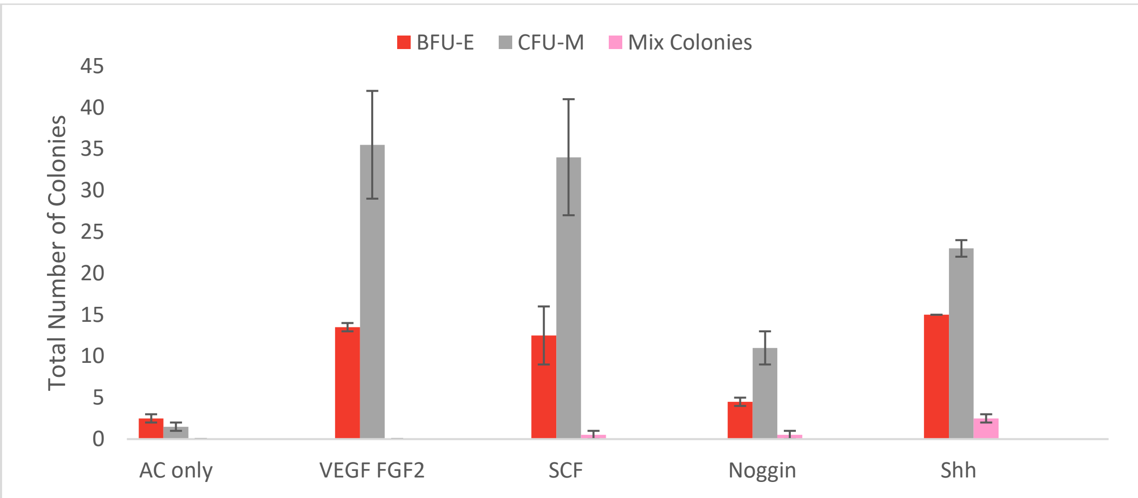

Figure 3.4.7. Summarised CFC assay result of colonies formed by 144hr gastruloid treated with different culture conditions

Total number of BFU-E and CFU-M formed by gastruloids treated with (1) A+C pulse only; (2) A+C pulse then VEGF+FGF$_2$; A+C pulse then VEGF+FGF$_2$ and (1) SCF, (2) Shh, and (3) noggin (120-144hr). (n=2)

3.4.3 GFP$^+$ (low & high) level and c-Kit$^+$CD41$^+$ expression throughout 96 to 144 hr

Previous investigations have focused on studying which cytokines need to be added during the 144 hours of gastruloid culture to establish a haematopoietic microenvironment to drive definitive haematopoiesis in the gastruloid. Aside from using a CFC assay to study the haematopoietic potential, the emergence of cells carrying haematogenic cell surface markers during gastruloid culture should also be studied to estimate the stage of haematopoiesis by understanding which HSC progenitors have formed.

Flow cytometry (FACS) analyses were carried out to characterise the expression of haematogenic cell surface markers, Flk-1, CD41, CD45, c-Kit and VeCAD, in the gastruloid throughout the time course of 96 to 144 hr. Analysing the haematopoietic subpopulation cross-time may display the progress and dynamics of haematopoietic events in the gastruloids. Initially, two culture conditions were included, one with only the A+C pulse at 48hr, while the second condition included VEGF and FGF from 72 hr to the end of culture, 144 hr (Figure 3.4.8).

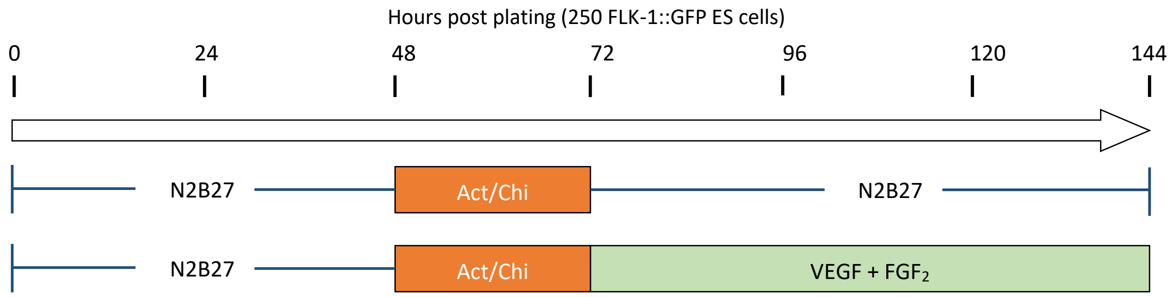

Figure 3.4.8. The culture scheme of gastruloids used to investigate the expression of haematopoietic markers in the gastruloids over time, at 96, 120 and 144hr.

Since the initiation codon of the *Flk-1* locus in ES cells is inserted with an eGFP reporter, fluorescence microscopy can recognise this GFP fluorescence, which is also detectable through flow cytometry, indirectly indicating the expression of Flk-1. At 96 hr, both conditions showed a significant (~40%) portion of GFP$^+$ cells, consistent with the results from fluorescence microscopy (Figure 3.2.4; Figure 3.3.7). The initiation of Flk-1 indicates the differentiation of mesodermal progenitors in the gastruloid, which is preliminary to the formation of haemato-endothelial progenitors and subsequent differentiation of the haemogenic endothelium (Figure 3.4.9 A and D). After 24 hours, the expression of GFP peaked at around 60% in both conditions (Figure 3.4.9 B and E), subsequently dropping to

~45% in the culture with the A+C pulse only, while remaining around ~55% in the culture with VEGF and FGF_2 (Figure 3.4.9 C and F) at 144hr. In addition, two populations of GFP (low and high) were observed in the VEGF and FGF groups from 120 hr (Figure 3.4.9 E and F). No CD45 population was observed in any gastruloid, with both conditions showing no sign of the emergence of definitive haematopoiesis before 144 hr, suggesting no haematopoietic stem cells progenitors were developed.

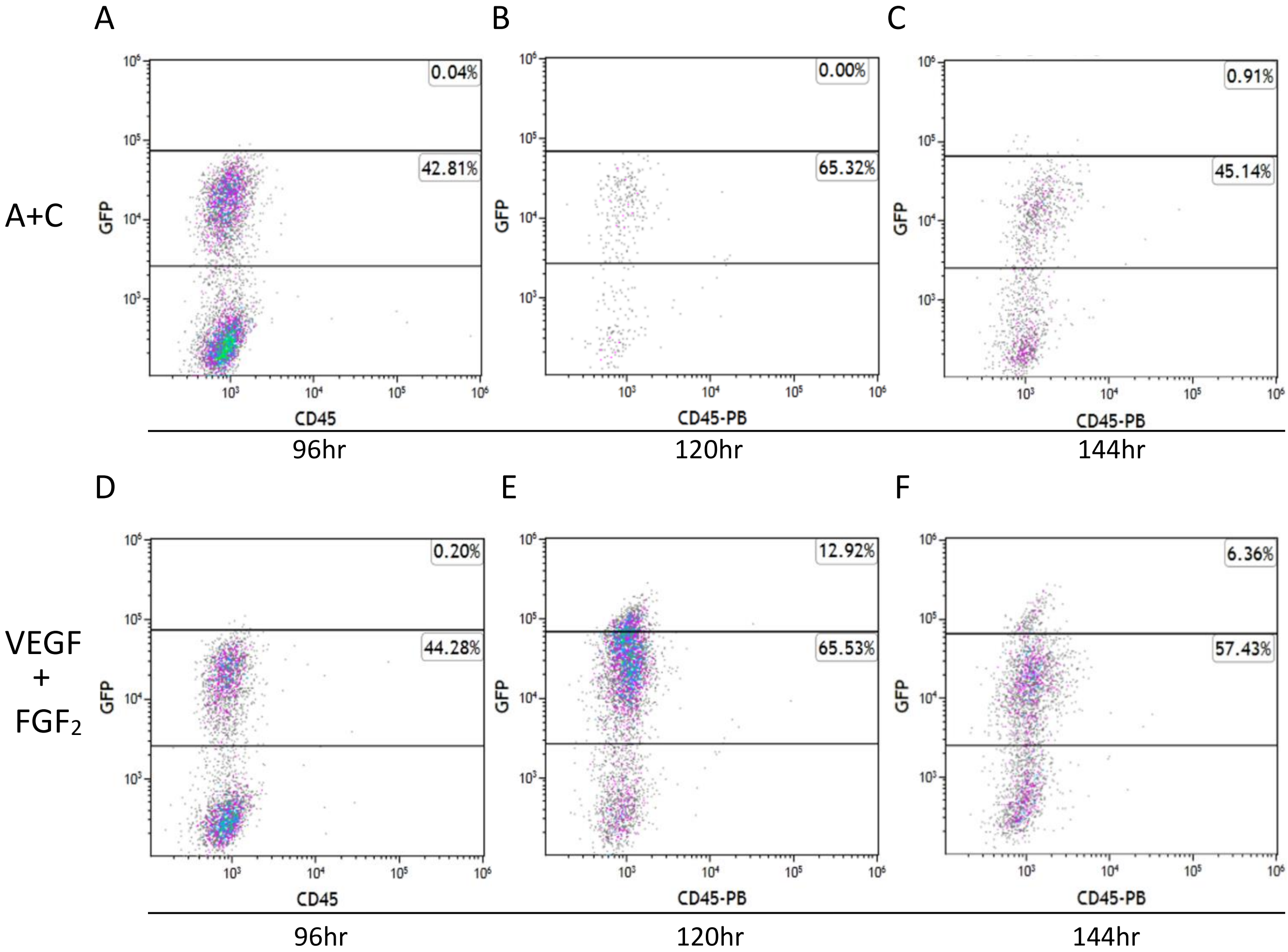

Figure 3.4.9. Time course flow cytometry results of gastruloids at 96, 120 and 144hr (CD45 vs GFP)

Representative dot plots from flow cytometry which GFP subpopulation is identified throughout the time course. Gastruloids are cultured with either an A+C pulse only and collected at 96hr (A), 120hr (B) and 144hr(C) or an A+C pulse followed by VEGF+FGF_2 and collected at 96hr (D), 120hr (E) and 144hr (F) (n=2).

In order to have a better understanding of the haemogenic differentiation happening in the gastruloid, the gastruloids were further stained with CD41, a marker of Pro-HSCs, and c-Kit, the stem cell marker for endothelial/haematopoietic progenitors. At 96 hr, both A+C and VEGF+FGF_2 groups displayed very minimal expression of either marker (Figure 3.4.10 A and D), suggesting an undifferentiated state that precedes the differentiation of endothelial and haematopoietic cells. At 120 hr, the c-Kit population was remarkably raised in the VEGF+FGF_2 group, while this emergence is missing in the A+C group (Figure 3.4.10 A and D), proving that VEGF and FGF_2 are necessary to promote the differentiation potentials of gastruloid cells. In addition, the CD41 population appeared to be reduced in the A+C group, indicating that VEGF and FGF_2 are critical to maintaining the haemogenic differentiation.

At 144 hr, the GFP subpopulations were highlighted in different colours to help further study the stemness and haemogenic differentiation of the gastruloids. Although the c-Kit population presented in the gastruloid treated with Activin and Chiron, these c-Kit$^+$ cells are all CD41$^-$, which means that endothelial differentiation may have occurred, but the differentiation of Pro-HSCs was absent (Figure 3.4.10 C and F). For the group of gastruloids with VEGF and $FGF_{2,}$ the GFP^{high} population (bright green) are primarily c-Kit$^+$ and spread across CD41$^-$ and CD41$^+$, while the GFP^{low} populations (brown) have a distinctive CD41$^+$ c-Kit$^-$ expression (Figure 3.4.10 F). The GFP^{high}CD41$^-$c-Kit$^+$ population indicated the endothelial stem cell progenitors, and the presence of the GFP^{high}CD41$^+$c-Kit$^+$ population confirmed endothelial stem cell progenitors have undergone endothelial-to-haematopoietic transition (EHT), and become the Pro-HSCs population (North *et al*., 1999; Batsivari *et al*., 2017)..

These results have laid the foundation of the adaptation of this protocol, the critical role of VEGF and FGF_2 in initiating the endothelial-to-haematopoietic transition, and the early-stage haematopoietic potential of gastruloids.

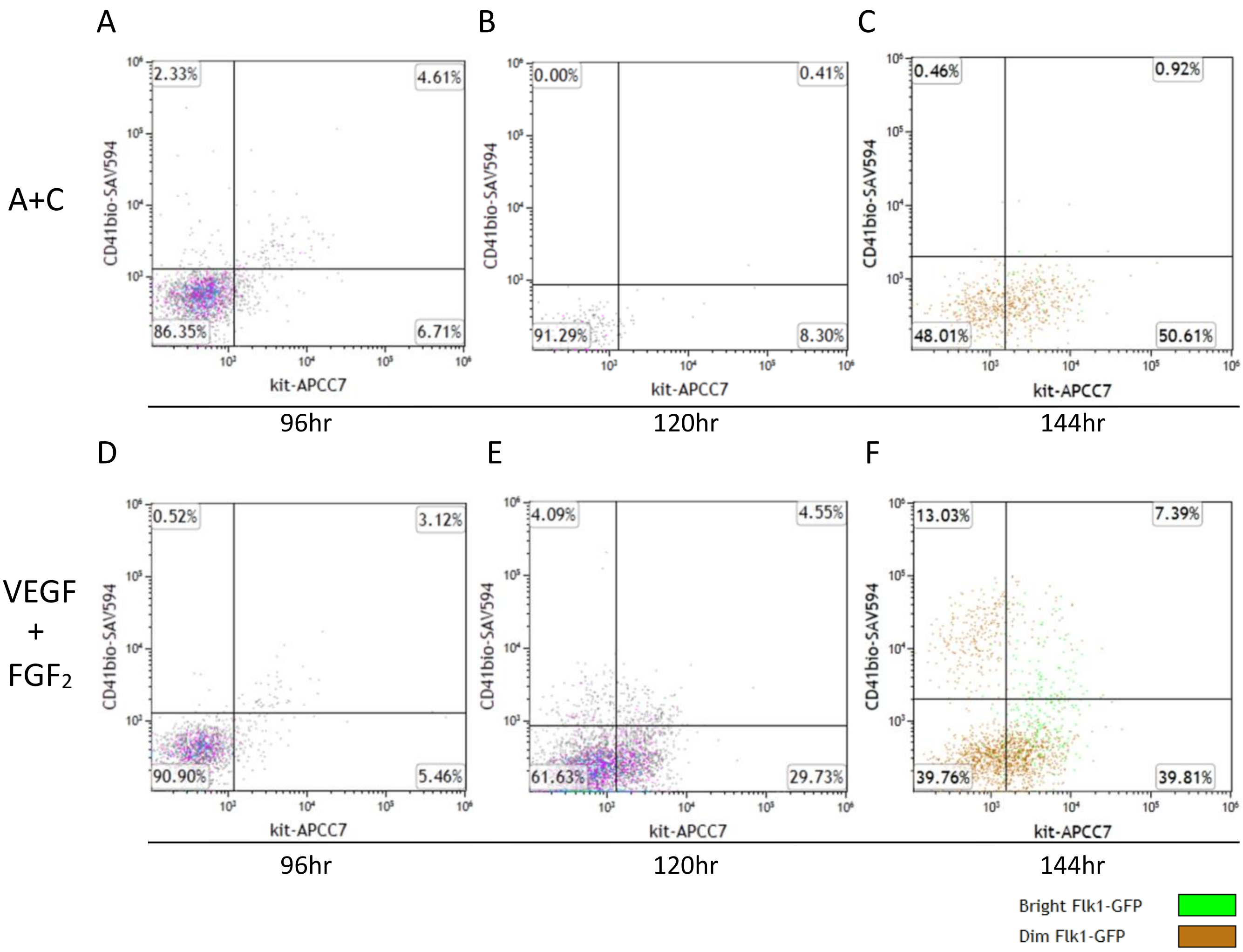

Figure 3.4.10. Time course flow cytometry results of gastruloids at 96, 120, 144 hr (cKit vs CD41)

Representative Flk-1/GFP gated dot plots of FACS analysis on the gastruloid stained with CD41-biotin, streptavidin 594 and cKit-APC/Cy7 antibodies. Gastruloids were cultured with either an A+C pulse only and collected at 96hr (A), 120hr (B) and 144hr(C) or an A+C pulse followed by VEGF +FGF_2 and collected at 96hr (D), 120hr (E) and 144hr (F). Cells at 144hr were highlighted with GFP^{high} signal (bright green) and GFP^{low} signal (brown) (n=2).

3.4.4 Shh provides better promotion than SCF in forming more cells with haematopoietic progenitors' signatures in gastruloids at the 144 hr

It has been found that VEGF and FGF_2 can initiate the formation of two distinct GFP/Flk-1 populations in gastruloids, indicating gastruloid cells have heterogeneously lineage-committed at the 144 hr. Also, a CFC assay has tested whether Shh and SCF are able to facilitate the haematopoietic differentiation in gastruloids. Flow cytometry was performed to analyse the c-Kit, CD41, and CD45 expression of gastruloids with Shh or SCF added at the 120 hr, which can explain the expression of haemogenic markers in gastruloids in response to these cytokines.

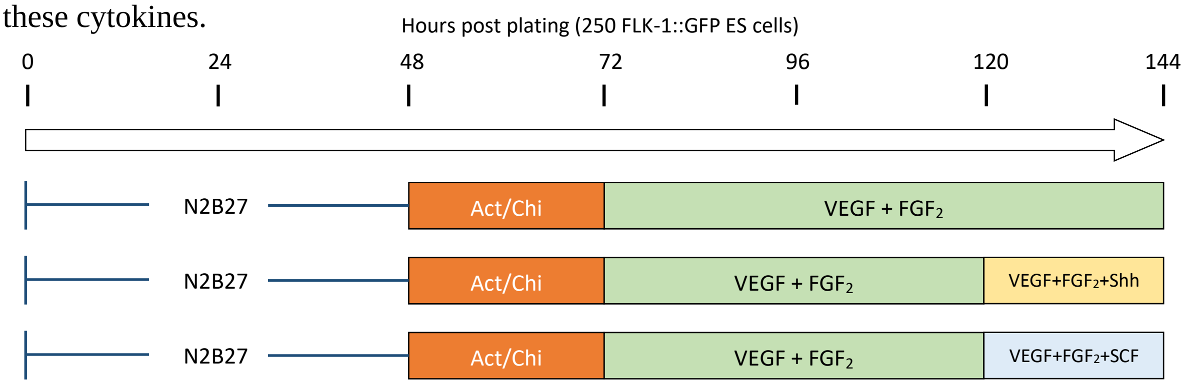

Figure 3.4.11. The culture scheme of gastruloids used to investigate if Shh and SCF can promote the haematopoietic differentiation at 144hr.

All gastruloids demonstrated a similar expression pattern of two distinct GFP populations, indicating that SCF and Shh cannot regulate Flk-1 expression in gastruloids during 120 and 144hr (Figure 3.4.12 A, B and C). In addition, Shh and SCF cannot promote the potential into definitive haematopoiesis as no CD45 expression was observed in the gastruloid during the 120 and 144 hr. Shh and SCF can facilitate the differentiation into GFP_{Low} $CD41_{high}$ and GFP_{High} $CD41_{low}$, and Shh had higher efficacy than SCF in promoting the formation of these two subpopulations (Figure 3.4.12 D, E and F).

Shh displayed better promotion than SCF on GFP^{Low} $CD41^{High}$ and GFP^{High} $CD41^{low}$ populations, and these populations had different expressions of VeCAD and c-Kit (Figure 3.4.12 E, F, H and I). The GFP^{Low} $CD41^{high}$ cells were VeCAD negative, and only part of them expressed c-Kit, while almost all GFP^{High} $CD41^{low}$ cells were positive for c-Kit and some co-expressed VeCAD and c-Kit (Figure 3.4.12 H). Shh was also more effective than SCF in promoting the generation of both $VeCAD^{+}$ $c\text{-}Kit^{+}$ and $VeCAD^{-}$ $c\text{-}Kit^{+}$ cells (Figure 3.4.12 H and I).

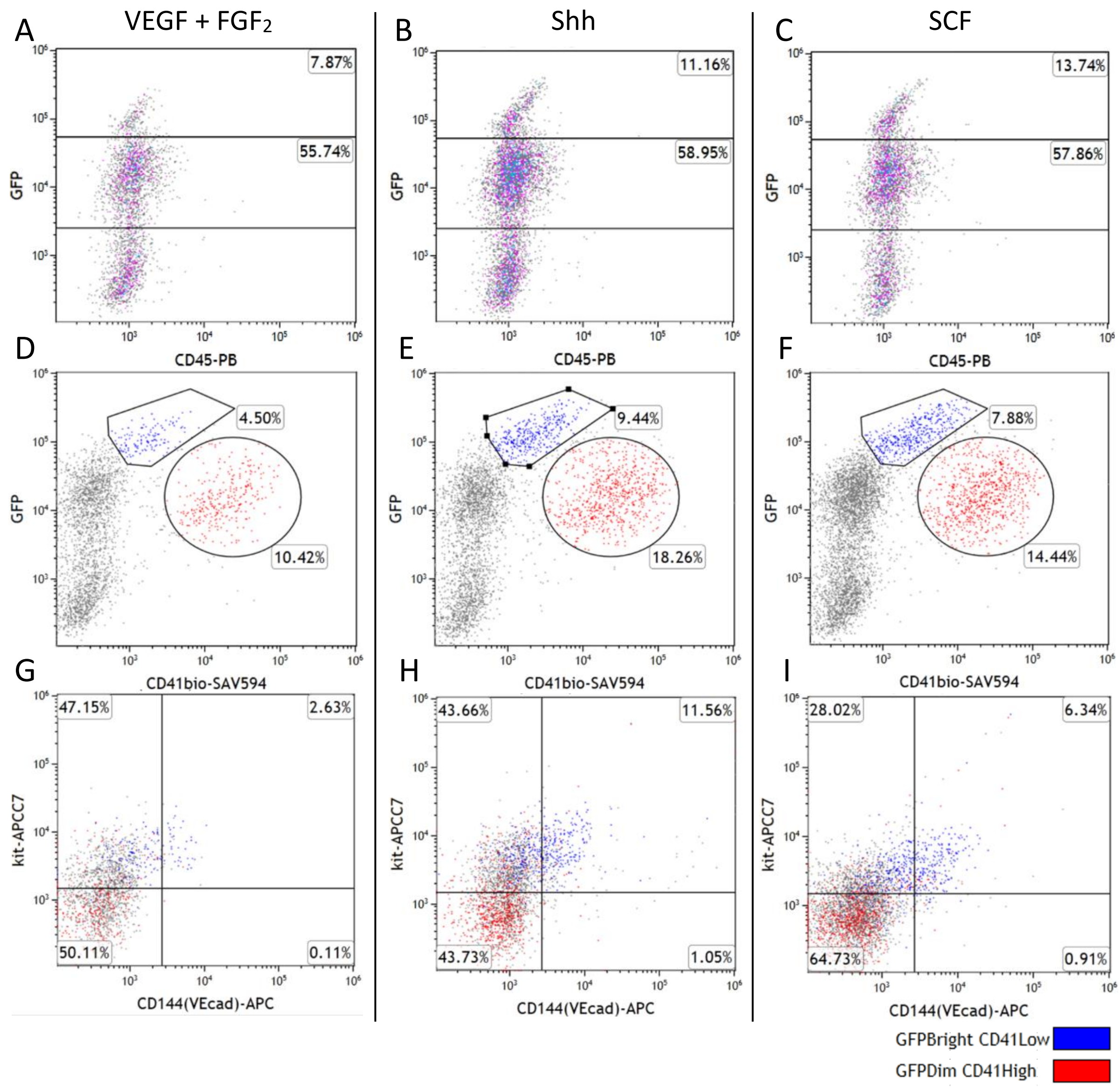

Figure 3.4.12. Flow cytometry results of 144 hr gastruloids treated with either Shh or SCF on various haematopoietic markers.

Representative Flk-1/GFP gated dot plots of FACS analysis on the 144hr-gastruloids cultured with either VEGF +FGF$_2$ (A, D & G), and with the addition of Shh (B, E & H) or SCF (C, F & I). Shh and SCF facilitate the differentiation into GFP^{Low} CD41^{high} (red) and GFP^{High} CD41^{low}(blue) Gastruloid cells were stained with VeCAD-APC, CD41-biotin, streptavidin Alexa-fluor 594 and cKit-APC/Cy7 antibodies (n=2).

3.5 Conclusion

This chapter contains the preliminary results to investigate if it is possible to adapt the ordinary gastruloid protocol to fit this project. Since Activin A is important to initiate the Flk-1 and Chiron is crucial to trigger the mesodermal differentiation, adding them to the gastruloid culture at 48 hr form the foundation of this project, signifying the feasibility of adapting this protocol for haematopoietic research (Pauklin & Vallier, 2015; Cerdan, *et al.*, 2012). The discovery of GFP_{Low} and GFP_{High} populations in gastruloid suggests that more than one progenitor is developing in the gastruloid. A subpopulation of $GFP_{Low\ has}$ a distinctive CD41 expression indicating they are the endothelial stem cell progenitors and suggest the GFP_{Low} population probably are the group having haematopoietic potential that may lead to definitive haematopoiesis if culture is extended. Although the GFP^{high} subpopulation has cKIT expression, its CD41 expression is much more uncertain, implying that the GFP^{high} subpopulation may belong to other non-haematopoietic progenitors.

VEGF and FGF_2 are important cytokines in haematopoiesis and adding them to the culture is intended to upregulate haematopoietic-related transcriptional activities. The qPCR analysis and haemoglobin switching suggested that the addition of VEGF and FGF_2 to the gastruloid displayed facilitated switching to adult haemoglobin, and it is worth optimising their additions in the later experiments. The Flk-1/GFP expression pattern in gastruloids from 72 to 144 hr was visualised using fluorescence microscopy, which further supported the internal development of gastruloids, such as forming lumen-like structures. The ETH happens when the endothelium of the lumen transforms into haemogenic endothelium by acquiring haematopoietic characteristics, and the formation of lumen-like structures in gastruloid hints the resembling of this event in gastruloid (North et al., 1999).

Although previous literatures suggested that SCF and Noggin have an important role in early haematopoiesis, adding these two cytokines did not promote haemoglobin switching in the gastruloid shown in qPCR analysis (Ivanovs *et al*., 2014; Souilhol *et al*., 2016). These results suggested that adding SCF and Noggin to gastruloids before 144hr is likely to be too early, or other members in haematopoietic signalling pathways (BMP, Notch, etc) should also be considered together with SCF and Noggin.

These findings lay a critical foundation of this project since they proved that the recapitulation of early haematopoiesis in the gastruloid is possible. However, limited by the length of the culture, CD45, the marker of type 2 pre-HSCs, are yet to be observed in the gastruloid. Additional work will attempt to extend the gastruloid culture protocol and validate whether the haematopoietic potential increases when the protocol is extended.

Chapter	Main Findings
3.2	The 24-hr pulse of activin A and chiron at 48hr triggers the expression of a mesodermal marker, Flk-1, in gastruloid at 96hr.
3.3.1	VEGF and FGF2 upregulate haematopoietic and endothelial markers in the gastruloid at 120hr.
3.3.2	VEGF and FGF2 promote haemoglobin switching at 120hr
3.3.3	Gastruloid breaks the shape symmetry and mimics early embryonic polarisation in Flk-1/GFP expression since 96hr.
3.4.1	Adding SCF Shh and Noggin would not promote haemoglobin switching before 120hr
3.4.2	Gastruloid cells show colony (BFU-E and CFU-M) formation potential
3.4.3	Gastruloid start showing cKIT+ cells from 120hr and show CD41+ cells at 144hr.
3.4.4	Shh promotes the haematopoietic progenitors' signatures in gastruloids at 144hr

Table 3.5.1. Summary of the main findings in chapter 3.

Chapter 4: Extension of haemogenic gastruloid protocol to generate more committed haematopoietic progenitors

4.1 Introduction

Since previous studies have demonstrated no CD45 expression in gastruloids at 144 hr, the haemogenic gastruloid protocol is extended to allow more time for the emergence of $CD45^+$ cells, which indicates definitive haematopoietic progenitor cells. Since gastruloids grown on normal U-bottomed 96-well plates collapse at 168 hr, gastruloids were grown on ultra-low attachment coated U-bottom 96-well plates to study whether they can be cultured without collapse for a longer time period of up to 216 hr. With the extended gastruloid culture, the cell viability in gastruloids was studied using flow cytometry to ensure that the viability of cells in the gastruloid were not compromised when the gastruloid became bulkier with the extended culture. The Flk-1/GFP expression in the gastruloid over time, from 72 to 216 hr, was also studied using flow cytometry and fluorescence microscopy.

Apart from the gastruloid disaggregation, which had already been solved by using the ultra-low attachment coated U-bottom 96-well plate, heterogeneity of the stemness in the starting ES cell population is another issue which may undermine the consistency of results. 2iLIF pretreatment can reprogram the ES cells from naïve back to a ground state, and was applied from 24 to 72hr to confirm the optimal length of 2iLIF pretreatment in order to raise the highest haematopoietic potential in gastruloids. Chapter Three demonstrated that Shh could give rise to more $CD41^+$ cells in gastruloids, therefore the 24-hour pulse of Shh was applied in either 120 hr, 144 hr or 168 hr to optimise the time point of addition of Shh into gastruloid culture.

Gastruloids were immuno-fluorescence stained with CD45, c-Kit and CD31 antibodies and examined under confocal microscopy to identify any possible formation of haematopoietic structures. Animal engraftment has been widely applied in haematopoietic studies as a functional assay to confirm the reconstitution capacity of the hematopoietic stem cells. To examine the *in vivo* reconstitution capacity of the $CD45^+$ gastruloid cells, unsorted and $CD45^+$ sorted gastruloid cells were injected into irradiated mice. Flow cytometry was performed on week 9 and week 16 bone marrow and spleen cells from the culled mice to investigate any short-term and long-term engraftment.

4.2 Extending haemogenic gastruloid protocol to the 216 hr

4.2.1 Extending the gastruloid protocol to 216 hr with a new plate

Although culturing gastruloids treated with VEGF and FGF_2 resulted in haematopoietic development in gastruloids at the 168 hr, some gastruloids had the sign of disaggregation. ES cells migrated from the gastruloid and differentiated into fibroblast-like cells at the bottom of the wells since 120 hr in all culture conditions. When the culture reached 144 hr, some gastruloids lost shape and eventually collapsed to the bottom (Figure 4.2.1). The gastruloids become heavier as they grow, which may facilitate the cells to disassociate from the gastruloid and attach to the surface of the well in the plate. The cells attachment triggers the gastruloid to disintegrate and finally collapse in on the well, and most (>80%) of the gastruloids collapsed after 168hr (n=5). The collapse of the gastruloid is opportunistic and undermine inconsistency to the results, while also limiting the gastruloid protocol only up to 168 hr.

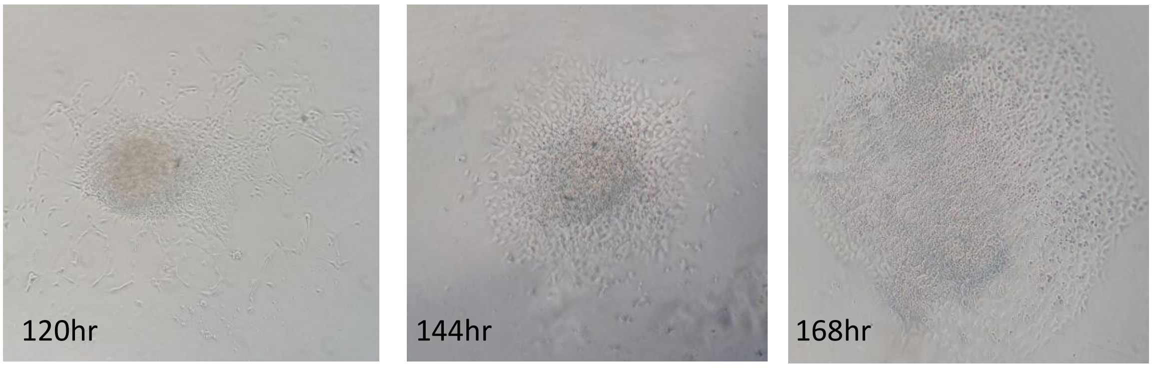

Figure 4.2.1. Images of the disaggregation of gastruloids at 120, 144 and 168hr.

Representative image of ES cells migrate and differentiate into fibroblast-like cells at the bottom of the wells of Greiner CELLSTAR 96-well plates (650185, Greiner) since 120 hr (left). Images of Disaggregation of the gastruloid at 144 hr (middle) and 168hr (right). (Magnification: 20x)

Some gastruloid protocols suggests placing the gastruloid plate on a shaker in the incubator from 120hr to enable the gastruloids to grow and prevent it from collapsing (Beccari *et al.*, 2018). Another possible solution could be using cell culture plates to prevent cell attachment where standard hydrophobic surfaces of the well are insufficient to prevent collapse. The Greiner CELLSTAR 96-well plates (650185, Greiner) are plates with standard hydrophobic surfaces, while Corning Costar ultra-low attachment 96-well plates (174927, Costar) or CELLSTAR® Cell-repellent PS cell culture plates (650970, Greiner) have cell repellent coating on the surface of the wells.

The Costar ultra-low attachment 96-well plates (174927, Costar) were tested against Greiner CELLSTAR 96-well plates (650185, Greiner) to identify whether the cell-repellent plate can prevent gastruloid collapse when extending the protocol. The surface of the wells of the ultra-low attachment plate was treated with a hydrophilic, neutrally charged coating. This coating is designed to inhibit the immobilisation of the cells and arrest the cells into the suspended state for organoid formation. Using the Costar ultra-low attachment plate resulted in a great improvement in preventing the occurrence of disaggregation (Figure 4.2.2 A and B).

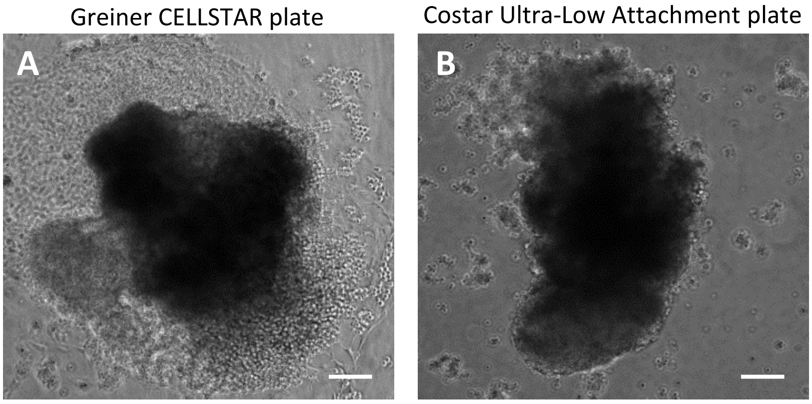

Figure 4.2.2. Images of 216hr gastruloids using ultra-low attachment plates.

Representative image of gastruloids cultured with (A) Greiner CELLSTAR 96-well plates or (B) Costar Ultra-low attachment plate. (Magnification: 20x) (scale bar: 100um) (n=3).

Greiner CELLSTAR® Cell-repellent PS cell culture plates (650970, Greiner) were also tested with Corning Costar ultra-low attachment 96-well plates (174927, Costar) to ensure a plate from a different brand would not affect the growth of the gastruloids cultured. Both plates prevented the occurrence of disaggregation, and gastruloids cultured using these plates had no significant difference in terms of shape and size (Figure 4.2.3 A and B).

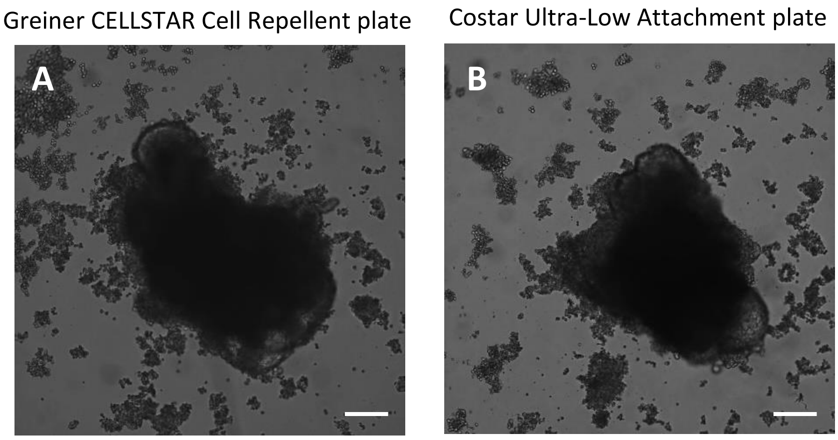

Figure 4.2.3. Images of 216hr gastruloids cultured with different brand low attachment plates.

Representative images of gastruloids cultured with (A) Greiner CELLSTAR cell repellent plates or (B) Costar Ultra-low attachment plate (Magnification: 20x) (scale bar: 100um) (n=3).

4.2.2 Viability and Flk-1/GFP expression of gastruloid cells in the extended culture

Although the gastruloid culture can be extended to 216 hr with Greiner CELLSTAR® Cell-repellent PS cell culture plates (650970, Greiner) or Corning Costar ultra-low attachment 96-well plates (174927, Costar), the viability of gastruloids grown with this extended culture may reduce. The gastruloid is a cluster of cells and as it becomes larger and more intricate, the diffusion of gases, nutrients, and signalling molecules to cells in the gastruloid may be compromised, leading to cell death. The reduced diffusion efficiency is a significant and common limitation in tissue engineering, particularly for avascular tissues culture (Rademakers *et al.*, 2019). Compromised diffusion of gases and nutrients reduces the viability of the gastruloid but also causes the gastruloid to fail to maintain an optimal microenvironment, which hampers the haematopoietic differentiation potential of the gastruloid.

Hoechst 58 (33258) was used as a viability dye to qualitatively study the change in viability of gastruloid cells with the extended protocol. Hoechst 58 is a bisbenzimide DNA intercalator that emits blue fluorescence when bound to double-stranded DNA. Hoechst 58 cannot penetrate the intact cell membrane of living cells, thus the cells will be Hoechst 58 negative or very dim in fluorescence. When the cells become necrotic, they will begin losing maintenance of the membrane, meaning Hoechst 58 will be able to penetrate the damaged cell membrane and stain the DNA resulting in bright fluorescence. Apart from using flow cytometry to understand more about the viability of the cells, the GFP/Flk-1 fluorescence can also be studied to understand if haematopoietic differentiation is compromised in the extended protocol.

Gastruloids were cultured for 216 hours and were collected every 24 hours from 120 hr. Gastruloid cells were stained with Hoechst 58 and analysed using flow cytometry. The viability only dropped from 77% (120 hr) to 64% (216 hr), suggesting the gastruloids were healthy in the extended culture protocol and that their viability was not greatly compromised (Figure 4.2.4).

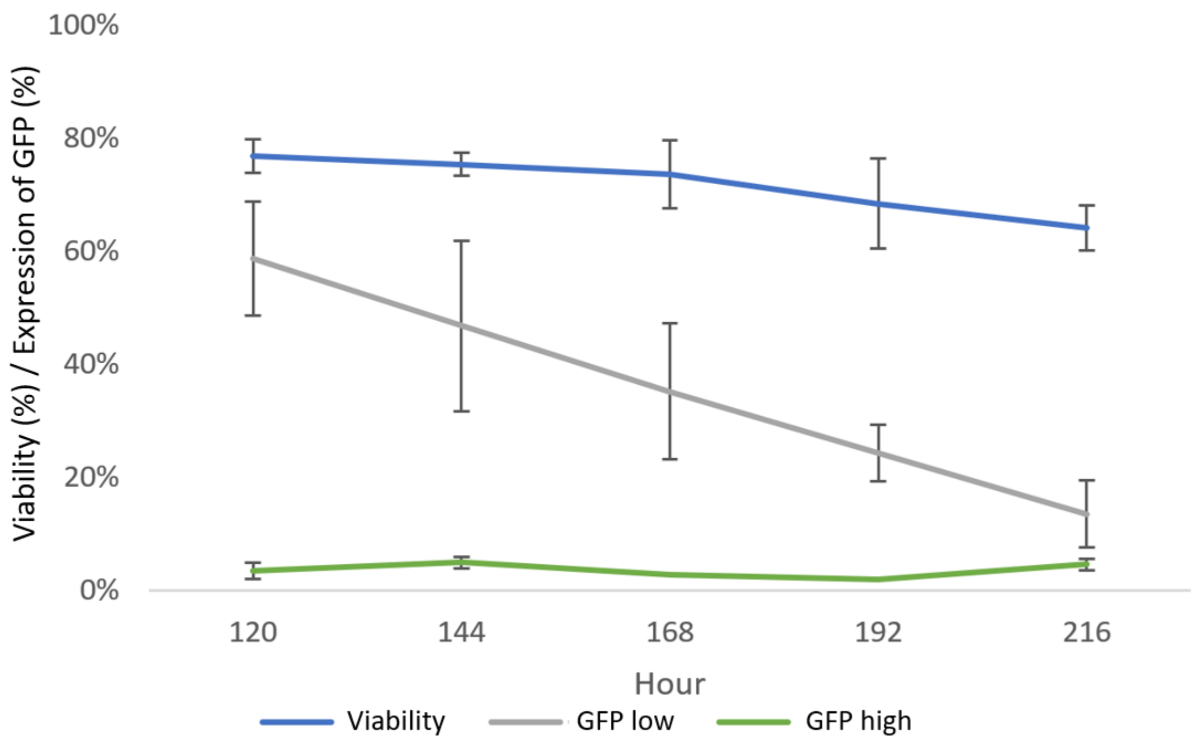

Figure 4.2.4. Line graph showing the viability, expressions of GFP_{Low} and GFP_{High} of gastruloids from 120 to 216 hr

The viability (blue) of gastruloids was measured using Hoechst 58 with flow cytometry. The expressions of GFP_{Low} (grey) and GFP_{High} (light green) of gastruloids from the 120 to 216 hr were estimated using flow cytometry (n=3).

Regarding GFP/Flk-1 fluorescence, the GFP_{low} peaked (59%) at 120 hr and continuously decreased, reaching 14% at 216 hr (Figure 4.2.4). As prescribed previously, Flk-1 is critical to the initiation of haematopoiesis as it is involved in the movement of cells from the posterior primitive streak to the yolk sac and, possibly, to the intraembryonic sites of definitive haematopoiesis. Consequently, Flk-1 is expected to be highly expressed in the haemogenic endothelium at the early stage, and downregulation should begin with the onset of haematopoiesis when the haematopoietic progenitors are maturing (Shalaby *et al.*, 1997). The confirmed expression of GFP_{Low}, suggests that the gastruloid has formed GFP_{Low} expressing haemogenic endothelium, and that these cells have undergone subsequent haematopoiesis resulting in a decrease in GFP_{Low} signals at the late stage. In addition to the GFP_{Low} population, GFP_{High} cells were also present in the gastruloid, but its expression was consistently only around 3-5% throughout 120 to 216 hr (Figure 4.2.4). Flk-1 is the marker of haematopoietic and endothelial progenitors and is also related to other progenitors such as vascular or cardiac progenitors. Since these GFP_{High} cells are maintained throughout the culture, they may belong to other non-haematopoietic progenitors.

4.2.3 Fluorescence microscopic images and video of gastruloid throughout 72 to 216 hr

Fluorescence images demonstrate that gastruloids have a polarised pattern of Flk-1 at 96 hr, and that the gastruloids become internally structured from 144 hr. Since flow cytometry analysis displayed that Flk-1 expression changed during the culture in the extended protocol, indicating that structures in the gastruloid may further alter with the progress of haematopoietic differentiation. Gastruloids were cultured for 216 hours, and images of the gastruloids were taken using fluorescence microscopy from 72 to 216 hr.

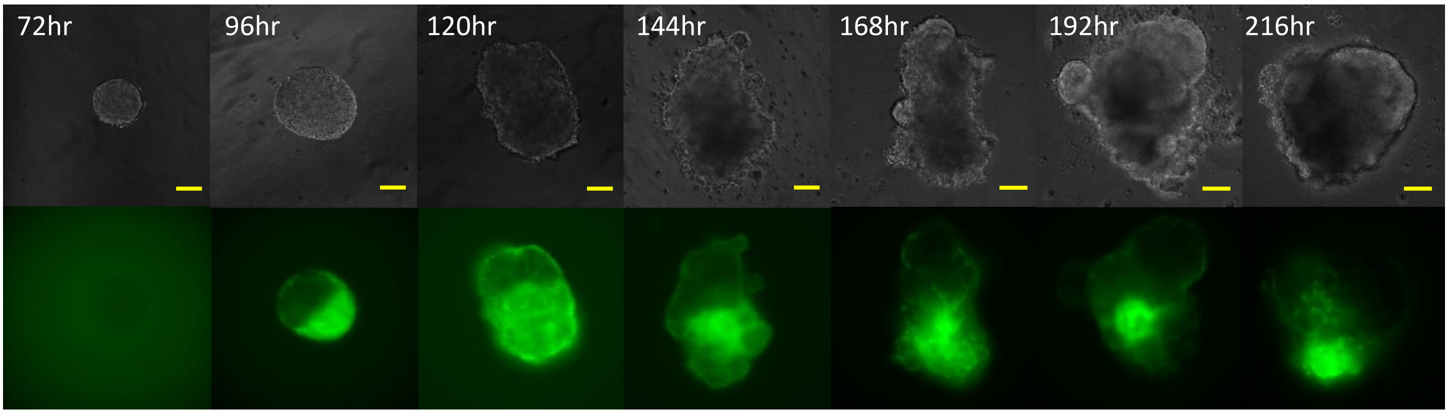

Figure 4.2.5. Fluorescence images of gastruloids over time from 72 to 216 hr.

Bright-field (top panels) and GFP fluorescence (bottom panels) microscopy images of a representative gastruloid from 72 to 216 hr. Culture condition: A+C pulse between 48 and 72 hr followed by VEGF + FGF_2 between 72 and 216 hr (magnification: 20x) (scale bar: 100um).

Gastruloids at 72 hr showed a spheroid shape (~200 um) but had no expression or very subtle expression of GFP/Flk-1. After a further 24 hours, the gastruloid doubled in size (~300 um) and displayed polarised GFP fluorescence, indicating the initiation of mesodermal differentiation (Figure 4.2.5). The gastruloid grew to ~400 um and elongated into the ovoid shape in 120 hr. Additionally, the GFP fluorescence was even more upregulated and exhibited granular patterns. At 144 hr, the gastruloid expanded further, and some parts budded out. The GFP fluorescence was also reorganised and centralised, outlining lumen-like structures.

At 168 hr, several budding structures differentiated to contain a sac-like, shiny structure. The bright GFP signals were maintained, and the lumen structures further formed smaller compartments. At 196 hr, the gastruloid began growing laterally and GFP fluorescence centralised at the core of the gastruloid (Figure 4.2.5). Finally, at 216 hr, the bright GFP signals focused at one end of the gastruloid, and most of the dim GFP signals diminished.

The fluorescence images reflect the flow cytometry results, that the dim GFP peak at 120 hr, and throughout the culture, the signal decreases with the progress of differentiation which forms structures in the gastruloid. The fluorescence images also revealed that bright GFP structures are maintained, which is also consistent with the flow cytometry results.

Apart from the growth of the gastruloid and the development of the internal structures, it has also been found that some gastruloids have signs of cardiac differentiation, indicated by a twitching part reassembling heart beating. Gastruloids with this twitching part were first seen at 168 hr, but the twitching is very subtle and rare (average 2.94% of gastruloids, SD=3.94%) (Figure 4.2.6 A). While at 192 hr, more gastruloids (average 12.50%, SD=8.77%) developed a cardiac-like contractile focus, and the beating was stronger and more regular (Figure 4.2.6 B). Further gastruloids displayed heart-like beating at 216 hr (average 17.50%, SD=11.10%) and are more rhythmic than at 192 hr. Some gastruloids had multiple beating foci, which contacted and relaxed rhythmically in turn, indicated by the yellow and red lines (Figure 4.2.6 C).

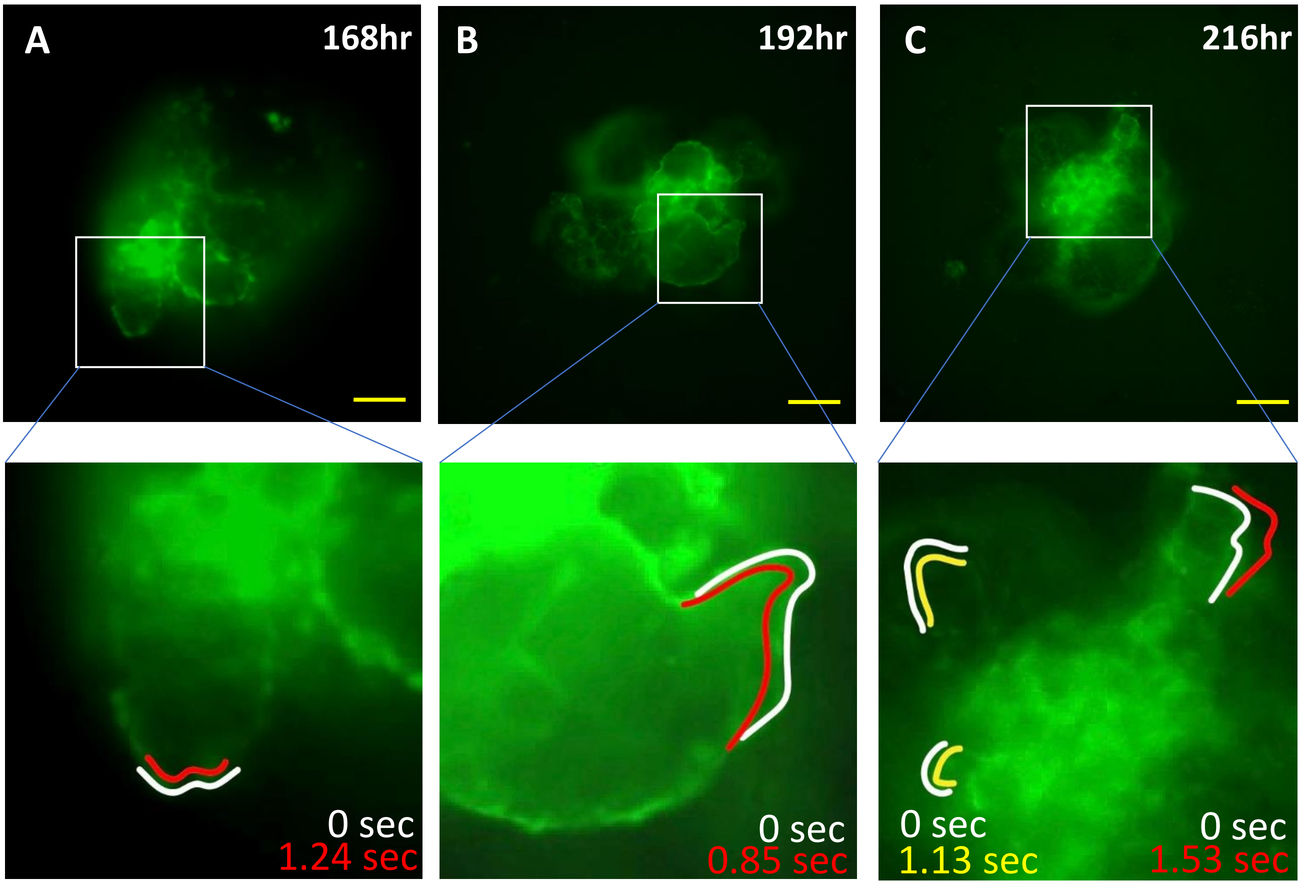

Figure 4.2.6. Screenshots from fluorescence videos showing the beating of gastruloids across time

Representative images from GFP fluorescence video showing the cardiac beating part of a gastruloid at the 168 hr, 192 hr and 216 hr. Culture condition: A+C pulse between 48 and 72 hr followed by VEGF + FGF_2 between 72 to 216 hr (magnification: 20x) (scale bar: 100um).

Most contractile foci were only present at lumen-like compartments and/or sac-like structures. The differentiation of the twitching and beating part of the gastruloid was not GFP fluorescence dependence, since the beating structure can be either GFP^-, GFP_{dim} or GFP_{bright}. The differentiation of cardiac-like twitching and beating foci in the gastruloid indicated that the gastruloid at 168 hr reach the day E8- E9, as this is the typical start time of the onset of the heart beating in mouse embryos (Chen *et al.*, 2010). Aside from indicating the corresponding embryonic stage of the gastruloids, the presence of a cardiac-like beating suggests the derivation and differentiation of the lateral plate mesoderm, which produces cardiac, endothelial, and haematopoietic cell progenitors. Altogether, these data showed that extending the culture to 192hr help develop gastruloid to the time equivalent to the embryonic day with the onset of haematopoiesis.

4.3 Optimising the cytokine schedule in the extended protocol

4.3.1 24-hour 2iLIF pretreatment promotes the Flk-1/GFP and CD45 expression of gastruloid cells

The issue of gastruloid disaggregation can be improved by using the cell repellent surface plate to extend the protocol. However, the ES cells of the gastruloid differentiate into fibroblast-like cells suggesting that the cells may have a different state of pluripotency after culturing in S+L medium for several passages. Such ES cells may have partially committed to differentiation, become heterogeneous and consequently, do not uniformly contribute to maintaining the aggregation of the gastruloid, leading to the inability to maintain a gastruloid culture. 2iLIF can be applied to restrict ES cells to a naive state of pluripotency to ensure the starting population for gastruloid aggregation is more homogeneous and undifferentiated (Ying *et al.*, 2008).

2iLIF is a serum-free medium based on N2B27 medium with two inhibitors (2i), CHIR99201 (Chi) and PD03, alongside leukaemia inhibitory factor (LIF). Chi is a GSK3 inhibitor that leads to the stabilisation and nuclear translocation of β-catenin, which subsequently abrogates the repression of the pluripotency network and maintains self-renewal (Ye *et al.*, 2012). However, Chi is insufficient, and the effect of PD03 is additionally required to maintain the self-renewal of ES cells (Miyanari & Torres-Padilla, 2012). PD03 is a MEK inhibitor and promotes the expression of Nanog, which enhances the self-renewal-promoting effect (Ye *et al.*, 2013). LIF belongs to the class of IL-6, and it activates STAT3 to inhibit ES cell differentiation and promotes self-renewal (Tosolini & Jouneau, 2016). 2iLIF pretreatment can help to generate a homogeneous population by reprogramming ES cells from primed to naïve state of inner cell mass-like ground pluripotency before beginning the differentiation culture. A homogeneous cell population could reduce disaggregation and promote haematopoietic differentiation by having more gastruloids with higher pluripotency in the extended gastruloid culture.

In order to understand whether applying 2iLIF pretreatment can help promote the haematopoietic differentiation, ES cells were either pretreated with 24-hour, 48-hour or 72-hours of 2iLIF and compared to a control group with no 2iLIF pretreatment (Figure 4.3.1). Microscopic images were taken to identify if the ES cells' morphology was altered in response to 2iLIF pretreatment. At 192 hr, gastruloid cells were taken for flow cytometry to assess the expression of haematopoietic markers such as GFP/Flk-1 and CD45.

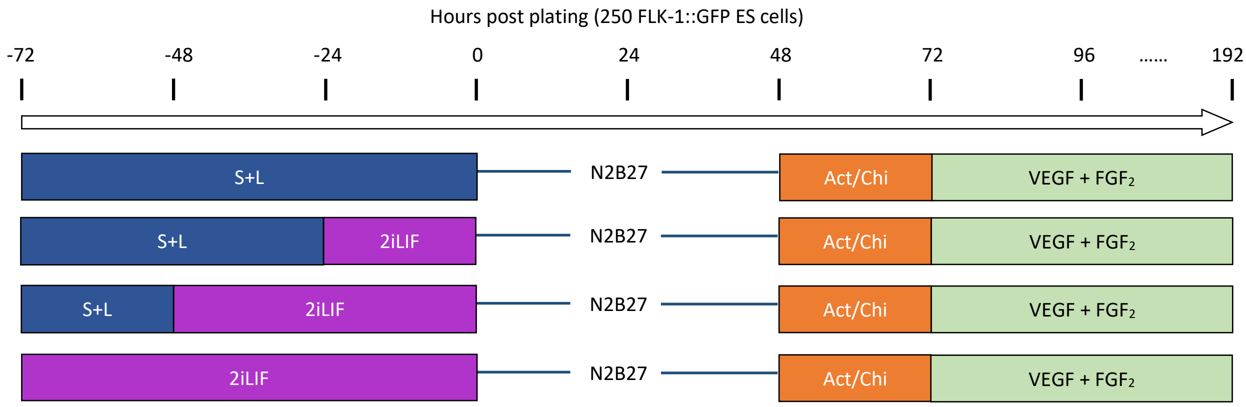

Figure 4.3.1. The culture scheme of gastruloids used to investigate understand if the pre-treatment promotes haematopoietic differentiation at 192hr.

Morphological characterisation of ES cells during culture is essential in stem cell research to indicate differentiation status. The ES cells cultured for three days with S+L had an abundance of spontaneously differentiating cells in the cultures, which were fully attached and in flat and spreading morphology (Figure 4.3.2 A). While after 24-hour with 2iLIF, ES cells appeared to be more homogeneously organised into ball-shaped colonies (Figure 4.3.2 B). This morphology became dominant after 48-hour with 2iLIF. Pretreating ES cells with 2iLIF for 72 hours resulted in well-demarcated, ball-shaped, refractile colonies (Figure 4.3.2 C and D).

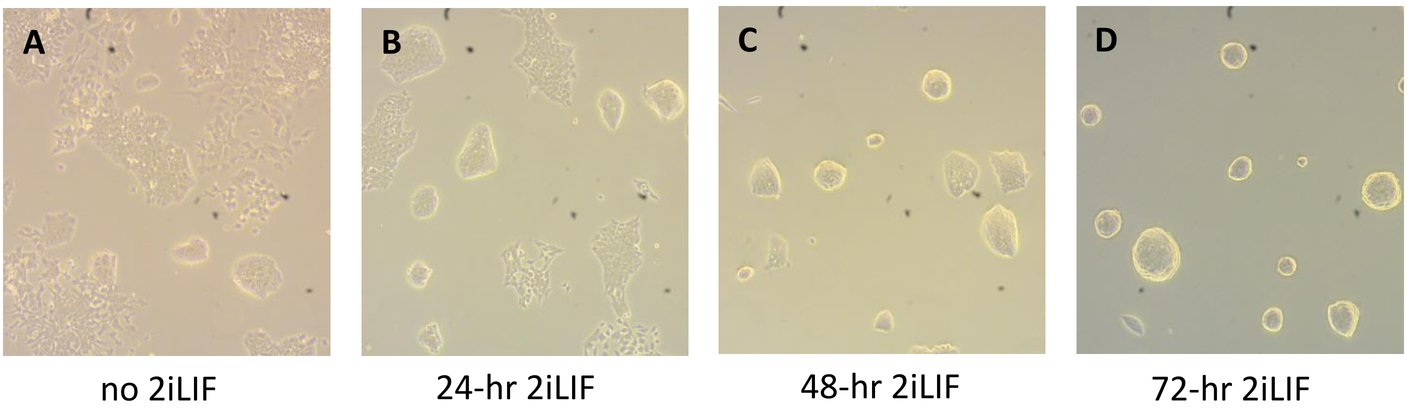

Figure 4.3.2 Microscopic images of mouse ES cells with 2iLIF pretreatment for different time

Representative microscopic images of mouse ES cells pretreated with A) no 2iLIF, B) 24-hour 2iLIF, C) 48-hour 2iLIF and D) 72-hour 2iLIF (magnification: 10x).

Although the morphologies of ES cells demonstrated that 2iLIF would affect the differentiation status of ES cells, these ES cells need to be investigated in gastruloid differentiation to understand the extent to which 2iLIF pretreatment affects the haematopoietic potential of gastruloids. The expression of Flk-1/GFP and CD45 in gastruloids was analysed with flow cytometry to discover whether 2iLIF alters the haematopoietic potential of gastruloids. At 144 hr, the gastruloid formed with 24-hour-pretreated gastruloid cells exhibited improved Flk-1/GFP expression (~90%) compared to the control (~67%) (Figure 4.3.3 A and B; Figure 4.3.4). This result shows that 2iLIF primes the ES cells to be more committed to mesodermal differentiation by slightly improving the homogeneity of ES cells. While pretreating the ES cells with an additional 24 or 48 hours did not improve the Flk-1/GFP expression, pretreating ES cells for more than 24 hours may drive the ES cells back towards their ground state, which would impede the differentiation of gastruloid cells (Figure 4.3.3 C and D).

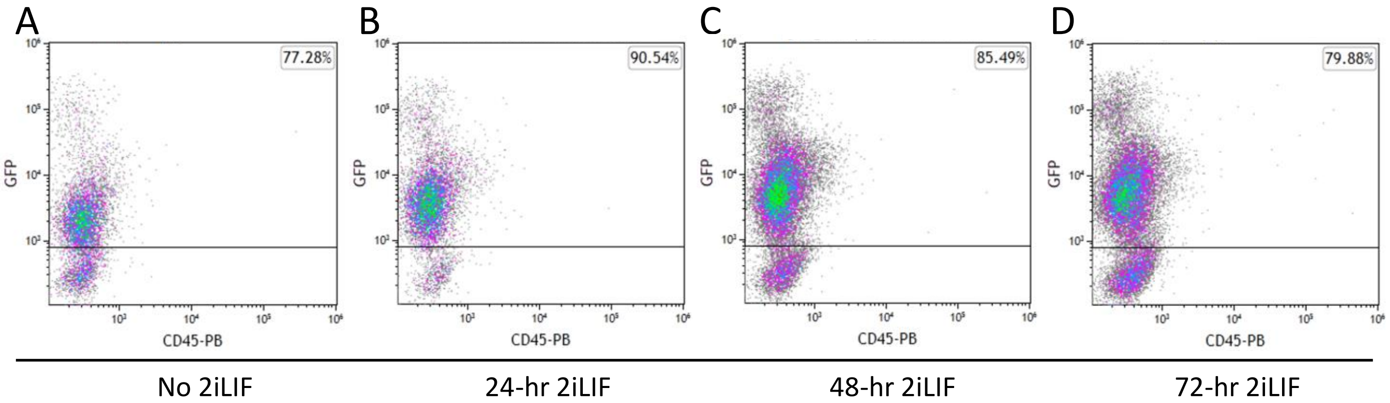

Figure 4.3.3 Flow cytometry result of 144 hr gastruloids with 2iLIF pretreatment for different time

Representative flow cytometry dot plots of the 144 hr CD45-PB antibody-stained gastruloid cells showing the relative fluorescence intensity of the cells expressing GFP fluorescence with no pretreatment (A), 2iLIF pretreatment for 24 hr (B), 48 hr (C) and 72 hr(D), n=2.

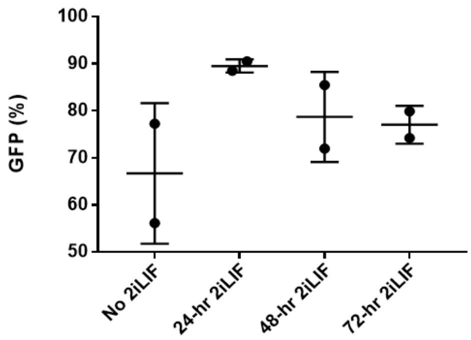

Figure 4.3.4 Summarised flow cytometry result of the 144 hr gastruloids with 2iLIF pretreatment

Data are from the flow cytometry result of the 144 hr gastruloid showing the relative fluorescence intensity of the cells expressing GFP fluorescence with no pretreatment, 2iLIF pretreatment for 24 hr, 48 hr and 72 hr (n=2, mean±SD, student's t-test p=0.1645 at 24-hr 2iLIF).

There is a significant difference in Flk-1/GFP and CD45 expression in gastruloids in the control group compared with the 2iLIF pretreated group at 192 hr (Figure 4.3.5). However, only the gastruloid formed from 24-hour-pretreated ES cells showed significantly higher CD45 expression, suggesting that 24-hour 2iLIF pretreatment can promote the formation of hematopoietic progenitors in gastruloids (Figure 4.3.6 A and B). However, over-extended exposure to 2iLIF compromised the assistance of 2iLIF in hematopoietic activities as cells were driven too close their ground state (Figure 4.3.6 A and B).

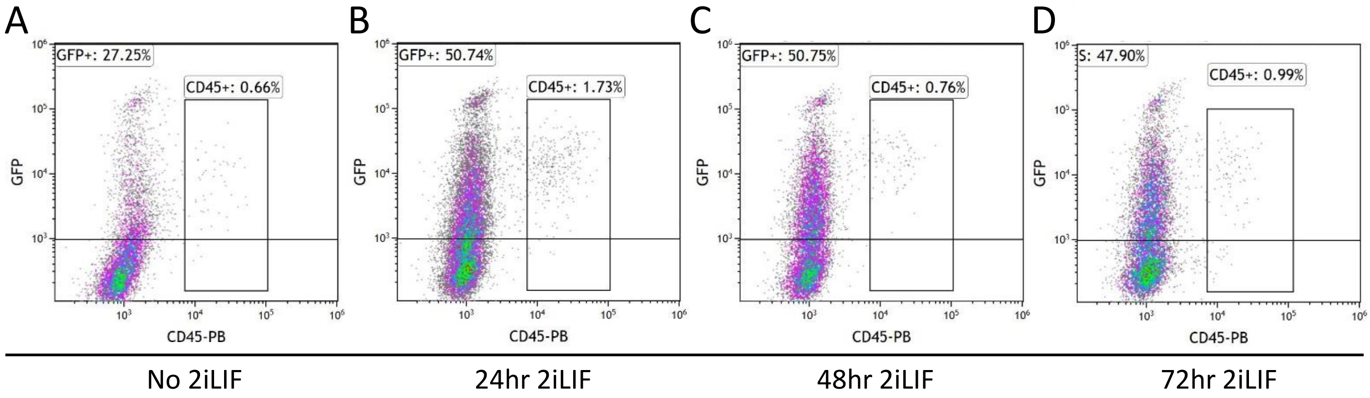

Figure 4.3.5 Flow cytometry results of 192 hr gastruloids with 2iLIF pretreatment for different time

Representative flow cytometry dot plots of CD45-PB antibody-stained 192 hr gastruloid cells showing the relative fluorescence intensity of the cells expressing GFP fluorescence and CD45 with no pretreatment (A), 2iLIF pretreatment for 24 hr (B), 48 hr (C) and 72 hr(D) (n=2).

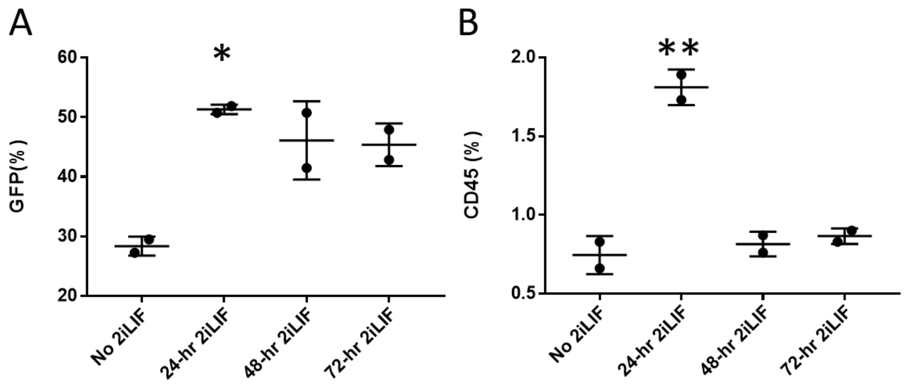

Figure 4.3.6 Summarised flow cytometry result of the 192 hr gastruloids with 2iLIF pretreatment

*Data are from the flow cytometry result of the 192 hr gastruloid showing the relative fluorescence intensity of the cells expressing (A) GFP fluorescence and (B) CD45 with no pretreatment, 2iLIF pretreatment for 24 hr, 48 hr and 72 hr (n=2, mean±SD, paired t-test p=0.0030 *at 24-hr 2iLIF and p=0.0118 **at 24-hr 2iLIF).*

4.3.2 More VeCAD$^+$ and CD45$^+$ cells in gastruloid at 192 hr can be stimulated by Shh between 144 and 168 hr

The previous study demonstrated that adding Shh promotes the Flk-1^{High}CD41^{Low} and Flk-1^{Low}CD41^{High} population in gastruloids at 144 hr (Figure 3.4.12). Such populations may contain definitive haematopoietic precursors, and they may further transform into CD45$^+$ cells when the gastruloid culture is extended. Although it is shown that adding Shh can promote haematopoietic differentiation, previous experiments have only tested between 120 and 144 hr, and it is worth discovering the optimal time to add Shh to the gastruloid culture. Gastruloids were cultured with Shh added at either 120 hr, 144 hr or 168 hr. All gastruloids were subsequently harvested for flow cytometry analysis for hematopoietic markers CD41, CD45, c-Kit, GFP/Flk-1 and VeCAD (Figure 4.3.7).

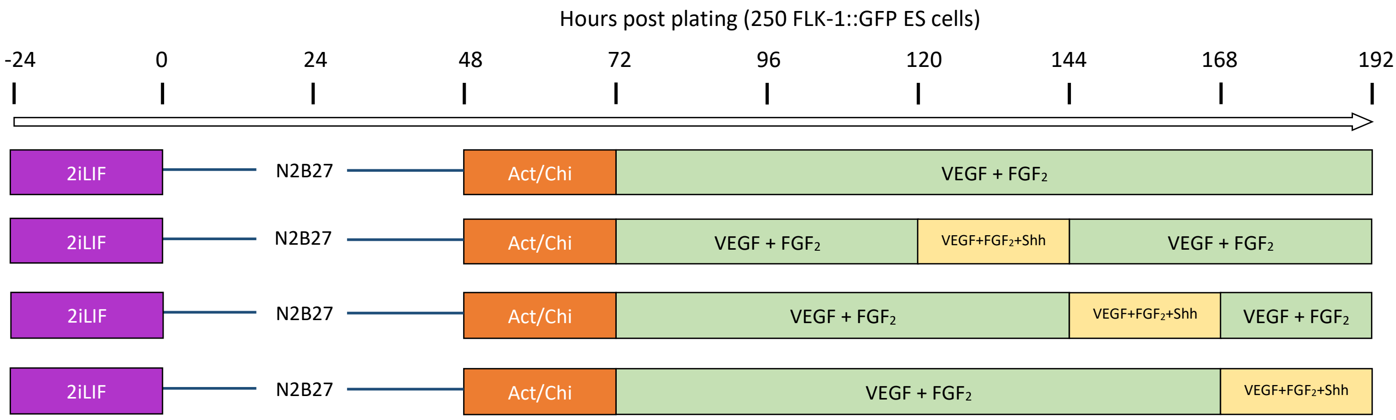

Figure 4.3.7. The culture scheme of gastruloids used to investigate if Shh can promote the formation of CD45 and CD41 expressing cells at 192hr

The flow cytometry results revealed that GFP^{Low} and GFP^{High} expression patterns were still observed in the gastruloids at 192 hr, but adding Shh at any time point (120 hr, 144 hr or 168 hr) increased the GFP^{High} subpopulation but not both GFP^{Low} (Figure 4.3.9 B and C). A small population of CD45$^+$ cells appeared in all gastruloids at 192 hr in all conditions but had no significant difference across experimental groups (Figure 4.3.8; Figure 4.3.7A). This suggests that the expression of CD45 in gastruloid cells at 192 hr may not be related to Shh (Figure 4.3.8; Figure 4.3.9). Flk-1$^+$ vascular endothelium gives rise to express endothelial cell marker CD31 and vascular endothelial cadherin (VeCAD). Mouse embryo-derived VeCAD$^+$ endothelial cells can differentiate into myeloid and lymphoid cells *in vitro* and even generate HSCs to colonise the hematopoietic sites of the embryo *in vivo* (Nishikawa *et al*., 1998;

Zovein *et al*., 2008). Some VeCAD$^+$ endothelium cells will commit to haematopoiesis and differentiate to CD45$^+$ cells, indicative of type 2 pre-HSCs.

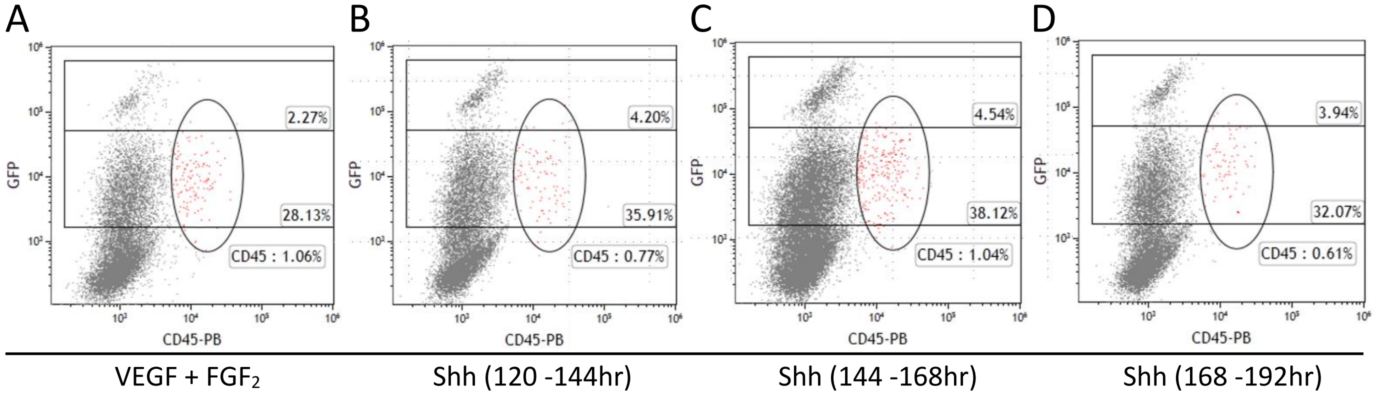

Figure 4.3.8. Flow cytometry results of 192 hr gastruloids cultured with Shh at different time

Representative flow cytometry dot plots At 192 hr showing GFP^{Low} and GFP^{High} populations in CD45-PB antibody-stained gastruloids cultured (A) with VEGF+FGF$_2$ and (B) with Shh added between 120 and 144 hr, (C) 144 and 168 hr and (D) 168 and 192 hr. CD45 expressing cells are coloured in red (n=3).

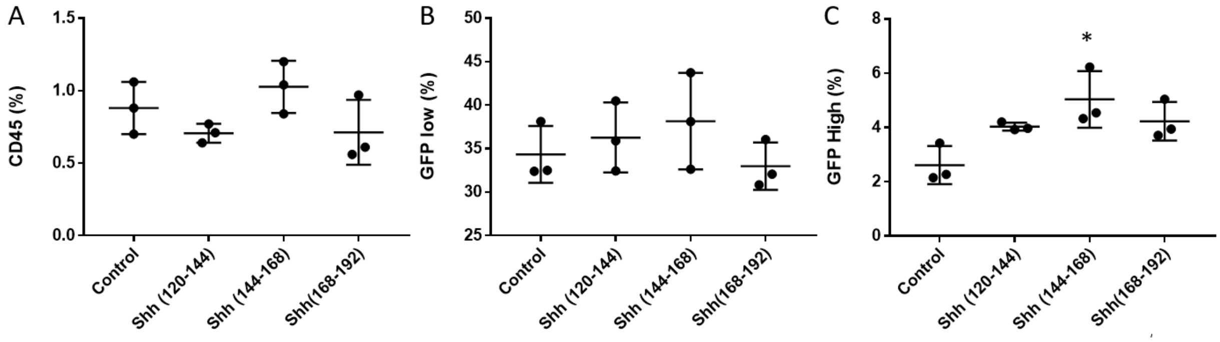

Figure 4.3.9. Summarised flow cytometry result of the 192 hr gastruloids with Shh at different time

*Data are from the flow cytometry result of the 192 hr gastruloid on (A) CD45, (B) GFP^{Low} and (C) GFP^{High} populations. Gastruloids cultured with VEGF+FGF$_2$ (control) and Shh added between 120 and 144 hr, 144 and 168 hr and 168 and 192 hr (n=3, mean$\pm$SD, student's t-test p=0.0065 *at Shh(144-168) on GFP^{High}).*

Although all culture conditions had CD45 expression, only gastruloids treated with Shh between 144 and 168 hr displayed significant expression of VeCAD$^+$ cells (Figure 4.3.10 C; Figure 4.3.11 A and B). In addition, a portion of VeCAD$^+$ cells were also CD45$^+$ which may be related to type 2 pre-HSCs (Figure 4.3.11 B). The CD45$^+$ VeCAD$^+$ population has been confirmed in the AGM region, and it is believed that this population is equivalent to type 2 pre-HSCs, which can develop into long-term repopulating definitive HSCs (Rybtsov *et al*., 2011). The emergence of CD45$^+$ VeCAD$^+$ cells suggests that the gastruloid protocol can generate a type 2 pre-HSCs-like population under the tight temporal control of Shh activity.

To further characterise the cells expressing CD45 and VeCAD, 1) $CD45^{+}VeCAD^{-}$ (blue), 2) $CD45^{+}VeCAD^{+}$ (red) and 3) $CD45^{-}VeCAD^{+}$ (green) cells were annotated and gated to study their expression of CD41 and c-kit. Results showed that most $CD45^{+}$ cells (red and blue) are either $CD41^{low}$ or $CD41^{-}$ populations (Figure 4.3.12). Definitive haematopoiesis is a stepwise process that happens through sequential upregulation of CD41 and CD45, followed by the emergence of long-term definitive HSCs. The occurrence of $CD41^{low/-}CD45^{+}$ cells indicates that the transformation of $CD41^{low}CD45^{-}$ type 1 pre-HSCs to $CD41^{low}CD45^{+}$ type 2-HSCs may take place in the gastruloid (Rybtsov *et al*., 2011). After being transformed into $CD45^{+}$ $VeCAD^{+}$ cells, these type 2 pre-HSCs may expand to form a $CD45^{+}$ $VeCAD^{-}$ population by downregulating the expression of VeCAD (Barcia Durán *et al*., 2018).

It has also been found that adding Shh between 144 and 168 hr may maintain the $CD45^{-}$ $VeCAD^{+}$ population, and that this population is divided into two populations, $CD41^{-}$ and $CD41^{+}$ (Figure 4.3.10 C and 4.3.12). The $CD45^{-}$ $VeCAD^{+}$ $CD41^{-}$ cells suggest putative endothelial cells and the $CD45^{-}$ $VeCAD^{+}$ $CD41^{+}$ population indicate the pro-HSCs. The presence of these two populations at 192 hr proves that the gastruloid partly maintain a sustainable haematopoietic hierarchy from endothelial cells, pro-HSCs and type 2 pre-HSCs. However, only two of four repeats displayed the $CD45^{-}$ $VeCAD^{+}$ $CD41^{+}$ population in the gastruloids at 192hr, which means this population was not always maintained in the gastruloid and cell heterogeneity may still exist in the gastruloids at 192 hr.

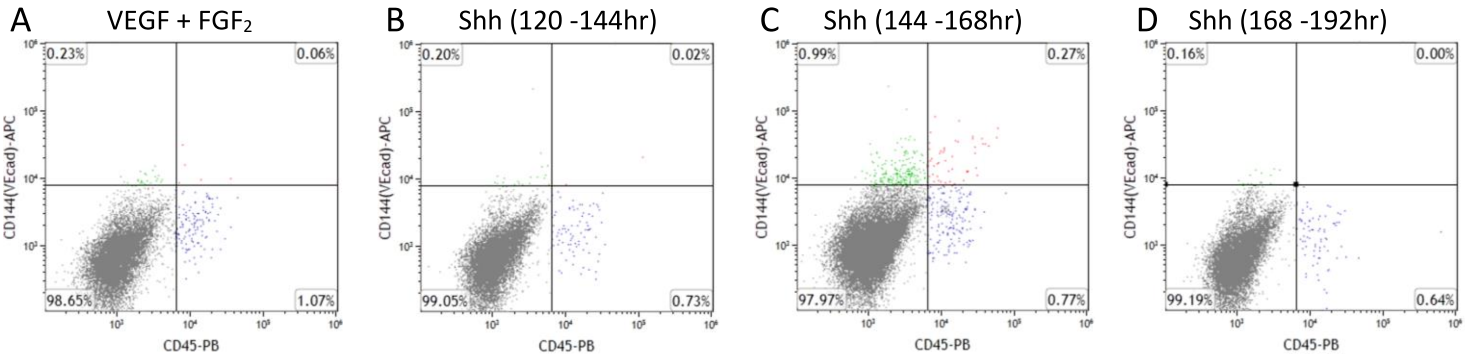

***Figure 4.3.10**. Flow cytometry results of 192 hr gastruloids cultured with Shh at different time (CD45 vs VeCAD)*

Representative flow cytometry dot plots of the 192 hr gastruloids culturedwith VEGF+FGF$_2$ (A) and with Shh added between 120 and 144 hr (B), 144 and 168 hr (C), and 168 and 192 hr (D). $CD45^{+}VeCAD^{-}$ cells are shown in blue, $CD45^{+}VeCAD^{+}$ cells are shown in red and $CD45^{-}VeCAD^{+}$ cells are shown in green. Gastruloids were stained with CD45-PB and VeCAD-APC antibodies (n=2).

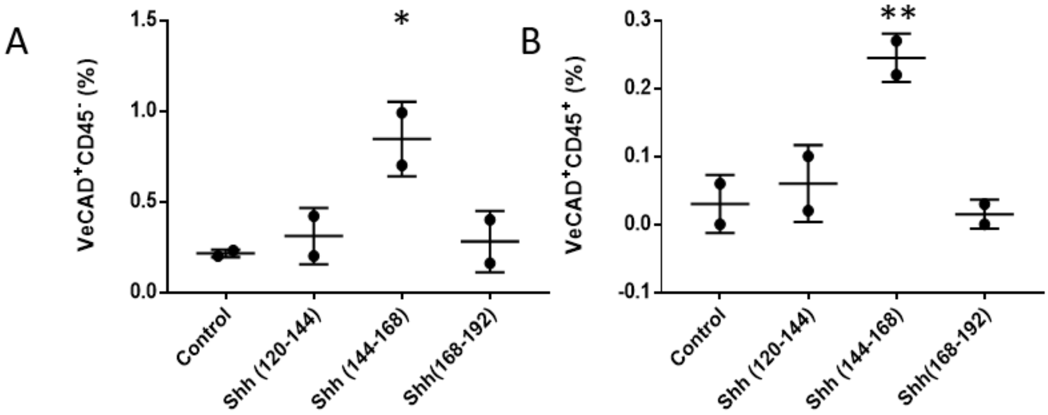

Figure 4.3.11. Summarised flow cytometry result of CD45$^+$VeCAD$^-$ and CD45$^+$VeCAD$^+$ populations in 192 hr gastruloids cultured with Shh at different time

*Data are from the flow cytometry result of the 192 hr gastruloid on (A) CD45$^+$VeCAD$^-$ and (B) CD45$^+$VeCAD$^+$ populations. Gastruloids cultured with VEGF+FGF$_2$ and with Shh added between 120 and 144 hr, 144 and 168 hr and 168 and 192 hr (n=2, mean$\pm$SD, paired t-test p=0.0496 *at Shh (144-168) on CD45$^+$VeCAD$^-$ and p=0.0148 **at Shh (144-168) on CD45$^+$VeCAD$^+$).*

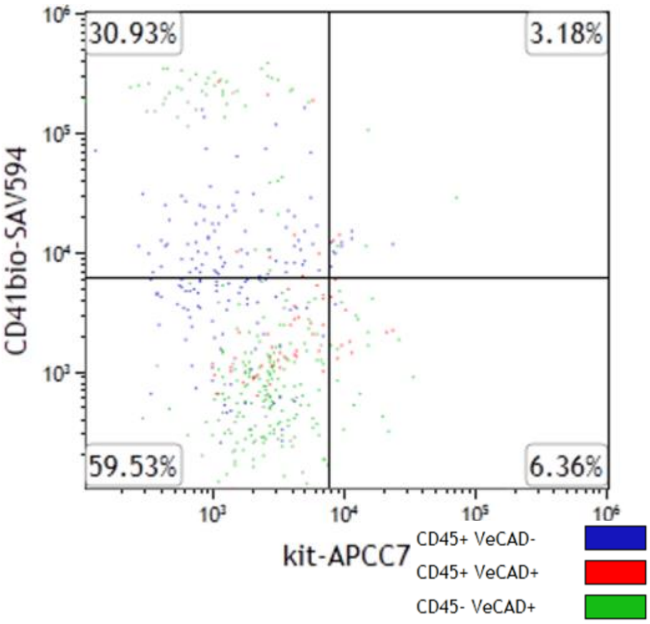

Figure 4.3.12. Flow cytometry result of 192 hr gastruloids cultured with Shh between 144 and 168 hr from Figure 4.3.8 C (cKIT vs CD41)

Representative flow cytometry dot plot of the 192 hr gastruloid cells with Shh added between 144 and 168 hr from Figure 4.3.8 C. 1) CD45$^+$VeCAD$^-$, 2) CD45$^+$VeCAD$^+$, and 3) CD45-VeCAD$^+$ cells were annotated and gated to study their expression of CD41 and c-Kit. CD45$^+$VeCAD$^-$ cells are shown in blue, CD45$^+$VeCAD$^+$ cells are shown in red and CD45$^-$VeCAD$^+$ cells are shown in green. Gastruloid ells were stained with CD45-PB, cKIT-APC/Cy7, CD41-Biotin, Streptavidin Alexa-fluor 594 and VeCAD-APC antibodies (n=4).

4.4 Putative haematopoietic cluster in gastruloid at 192 hr

During haematopoiesis, haematopoietic cells bud out from the endothelium of the dorsal aorta to form a cluster in the AGM. The haemogenic endothelium is believed to transform into pro-HSCs, type 1 pre-HSCs and subsequently into $CD45^+$ type 2 pre-HSCs in the haematopoietic cluster (Hirschi, 2012). The emergence of $CD45^+$ cells in the gastruloid at 192 hr proves that the gastruloid cultures protocol can generate cells with the property of type 2 pre-HSCs, but also indicates that a component similar to the intra-aortic cluster may form in gastruloids as if an AGM. The luminal structure and complex compartments observed in the gastruloid at 144 hr coincides with the emergence of putative $CD41_{Low}$ pro-HSCs at 144 hr, which suggests that a haemogenic cluster may form in the gastruloid (Figure 3.4.12; Figure 4.2.6).

Fluorescence microscopy can inspect the fluorescent component of the gastruloid. However, restricted by the depth of field of the microscope and the enlarging gastruloid, it is challenging to capture the details of the structures formed during the culture. Alternatively, confocal imaging has a controllable depth of field suitable for thick samples, which can be applied to image the spatial arrangement developed in the gastruloid. Gastruloids cultured with VEGF and FGF_2 were collected at 192 hr and stained with c-Kit, CD31 and CD45.2 antibodies.

The confocal image displayed a cluster formed of a lumen which contained c-Kit$^+$ and $CD45^+$ c-Kit$^+$ cells (Figure 4.3.9). The structure reassembled the intra-aortic cluster shown in other publications (Figure 4.3.10) (Medvinsky *et al*., 2011). During cluster formation, active invagination of the endothelial layer of the ventral floor is expected to occur for the formation of pre-HSCs in the AGM. However, no indentation of the lumen was observed in the cluster formed in the gastruloid (Figure 4.3.9). Although the CD31 staining is almost non-specific, it is presented in the figures to show the contrast in the absence of the DAPI staining.

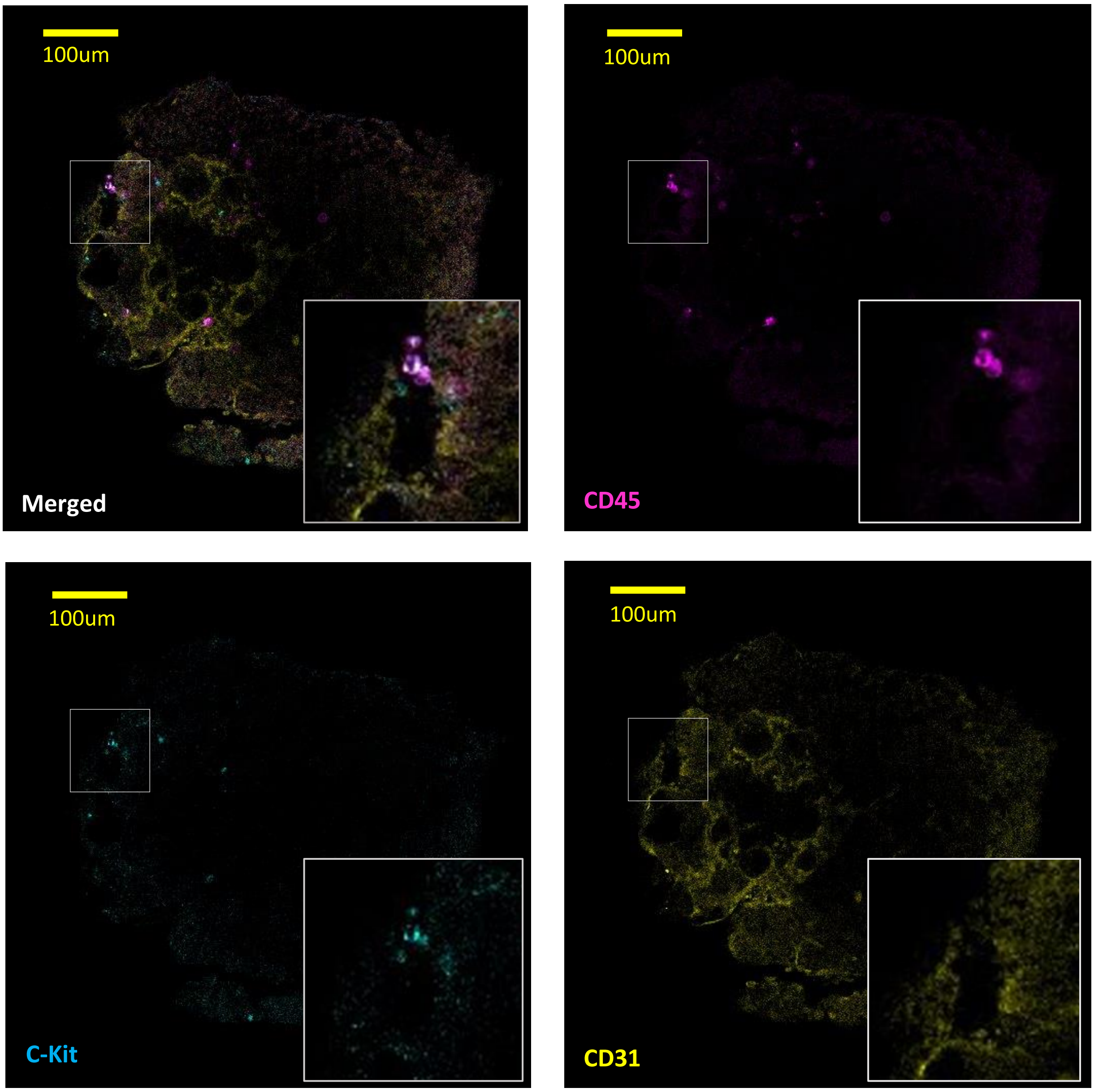

Figure 4.4.1. Confocal images showing the localisation of the putative intra-aortic cluster in the gastruloid at 192 hr.

The whole-mount immunostained gastruloid showing CD45 (magenta), c-Kit (cyan), CD31 (yellow), and merged expression. (Magnification: 20x) (scale bar: 100um). The putative intra-aortic cluster is magnified in the inserts and marked with an asterisk. Gastruloid was first stained with mouse anti-mouse CD45.2-PE, goat anti-mouse cKit-biotin and rat anti-mouse CD31 antibodies and then with anti-goat Alexa-Fluor 568 and anti-rat Alexa-Fluor 488.

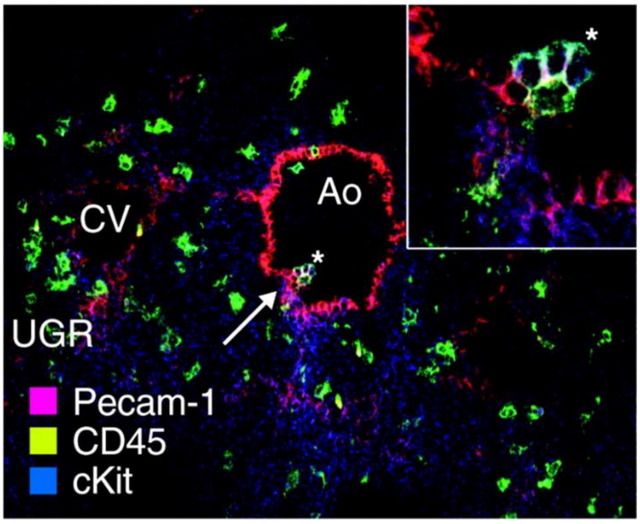

Figure 4.4.2. Image of the mouse's transverse section of the E11.5 AGM region

The image shows the Ao and an intra-aortic cluster that is triple-positive for Pecam-1 (CD31), CD45 and c-Kit (magnified in the insert). Arrow notes the indentation and the asterisk indicates the intra-aortic cluster. Ao, aorta, CV, caudal vein and UGR, urogenital ridges (Medvinsky et al., 2011).

4.5 The 192 hr gastruloid cells show possible week-9 bone marrow engraftment in irradiated mice

After confirming the presence of $CD45^+$ cells and the haematopoietic cluster in gastruloids, it is important to study whether the $CD45^+$ cells formed in the gastruloid can reconstitute haematopoiesis *in vivo* using a transplantation model, in other words, if haemogenic gastruloids generate haematopoietic stem cells. The presence of haematopoietic stem cells needs to be demonstrated experimentally through reconstitution of the hematopoietic system in an irradiated adult recipient. This functional assay is widely applied in haematopoietic studies to verify the presence and identity of haematopoietic stem cells and to check the differentiation capacity of early hematopoietic progenitors.

Before injecting the gastruloid cells into the mouse, the CD45 isotype of the Flk-1::GFP ES cells was confirmed by assessing the presence of CD45.1 or CD45.2. Flk-1::GFP ES cells were plated to culture gastruloids, and at 192 hr, gastruloids were disassociated and stained with CD45.1 PerCP and CD45.2-APC antibodies for flow cytometry. The results suggested that most Flk-1::GFP ES cells were $CD45.2^+$ as this population is quite clear (Figure 4.5.1). Since the allelic variant of the gastruloid is CD45.2, CD45.1 C57BL/6 (B6) mice strains were used for the transplantation experiments.

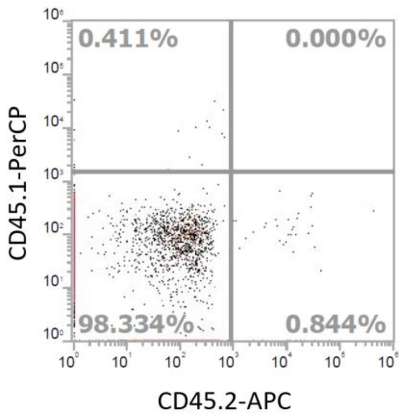

Figure 4.5.1 Flow cytometry result for checking the allelic variant of Flk-1::GFP ES cells

Representative flow cytometry dot plot showing the allelic variant of Flk-1::GFP ES cells was studied using CD45.1-PerCP and CD45.2-APC antibodies to test the disassociated gastruloid cells (n=3).

Irradiation preferentially kills rapidly dividing cells, including bone marrow and other hematopoietic progenitors, but the mice can be rescued by transplantation of a bone marrow allograft. C57BL/6 (B6) is congenic strain and the mice were irradiated and immunosuppressed, allowing engraftment of the gastruloids onto the mice alongside the companion bone marrow cells.

Gastruloids were treated with or without Shh at 144 hr to investigate whether the reconstitution capability of gastruloids was dependent on the Shh. Eight plates of gastruloids were cultured, and Shh was added to four plates. All gastruloids were harvested and dissociated at 192 hr and one plate worth of disassociated gastruloids from each condition were injected into mice (GT7-GT10). Three plates worth of dissociated gastruloids from each condition were sorted with CD45-PE using flow cytometry and were subsequently taken for mouse injection (GT11-GT13) (Table. 4.5.1). The control mouse (GT 14) was not injected with any gastruloid cells.

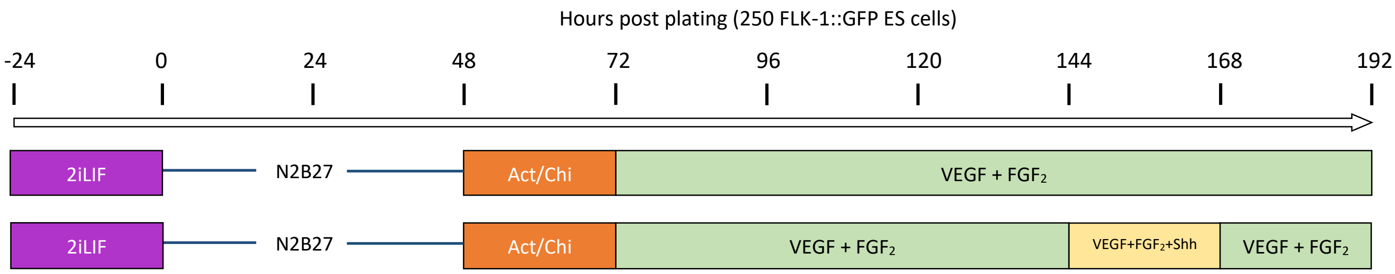

Figure 4.5.2. The culture scheme of gastruloids used to investigate if the gastruloids are Shh dependent on their engraftment in the in vivo model

Mouse	Condition	Cell types	Cells Injected (10^3)	Week 9 Engraftment	Week 16 Engraftment
GT7	No Shh	Bulk Gastruloid cells	600	✓	
GT8	No Shh	Bulk Gastruloid cells	600	Deceased	
GT9	Shh	Bulk Gastruloid cells	590	✓	
GT10	Shh	Bulk Gastruloid cells	590		✓
GT11	Shh	Sorted $CD45^+$ cells	1.64	✓	
GT12	Shh	Sorted $CD45^+$ cells	1.70		✓
GT13	No Shh	Sorted $CD45^+$ cells	1.70		✓
GT14	Control	Control	0	✓	

Table 4.5.1. Table showing the experimental details of the mouse engraftment study into irradiated C57BL/6 (B6) mice

Although mouse GT8 died due to sickness, mice GT7, GT9, GT11 and GT14 were culled on week 9. The bone marrow and spleen were disassociated, and the cells were stained with CD45.1 and CD45.2 antibodies to identify whether gastruloid cells possess short-term engraftment in the animal model. The flow cytometry results exhibited a clear CD45.2 population in the bone marrow from mice injected with gastruloids, independently of Shh treatment (Figure 4.5.3 A, B and C). The CD45.2 populations in the bone marrow from mouse GT7 (without Shh) and GT 9 (Shh) were not significant different, suggesting that Shh may not further enhance the short-term reconstitution capability in the bone marrow (Figure 4.5.3 A and B).

It was also found that the viability of sorted CD45$^+$ cells was not compromised in the sorting procedure, which is why they can also have short-term reconstitution in the mouse bone marrow (Figure 4.5.3 C). However, it seems injecting sorted CD45$^+$ gastruloid cells or bulk gastruloid cells into the mouse bone marrow did not result in a significant difference in the engraftment. This means that the reconstitution capability of CD45$^+$ gastruloid cells was not affected, even when injected into the mouse together with a non-haematopoietic gastruloid, which formed the majority of the injected cells (Figure 4.5.3 B and C).

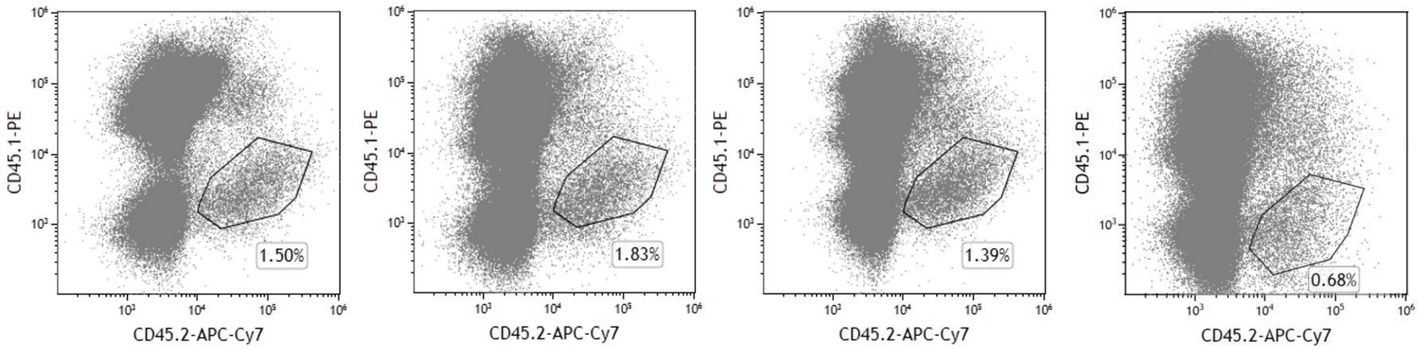

A GT 7 B GT 9 C GT 11 D GT 14

Figure 4.5.3. Flow cytometry results of bone marrow samples for checking short-term engraftment

Mice GT7, GT9, GT11 and GT14 were culled on week 9 and bone marrow cells were stained with CD45.1 PE and CD45.2 APC/Cy7 antibodies for flow cytometry analysis (n=1).

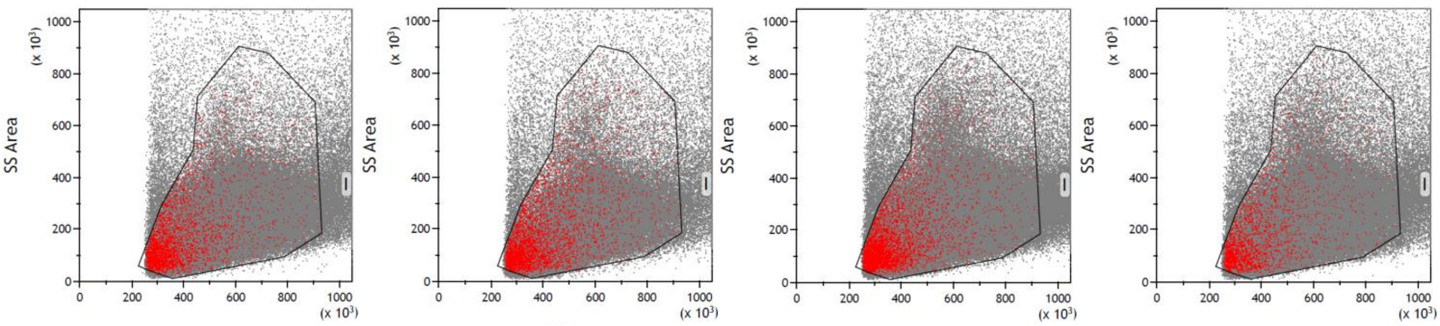

A GT 7 B GT 9 C GT 11 D GT 14

Figure 4.5.4. Results of back gating the CD45.2$^+$cells into the total collected mouse samples

Results of flow cytometry analysis on backgating the bone marrow cells of mice GT7, GT9, GT11 and GT14 from figure 4.5.3. The cells laballed in red are the CD45.2$^+$ cells in figure 4.5.3 and they are backgated to the total collected mouse samples.

Although there was some background CD45.2$^+$ signalling in the control mouse GT14, the percentage was considerably lower than that observed in animals injected with gastruloid cells(Figure 4.5.3 D). All four samples were backgated to the total collected mouse samples, and most of the bone marrow cells in Figure 4.5.3 are at the bottom left corner in Figure 4.5.4, suggesting many of them are cell debris. The spleen was also collected and analysed with flow cytometry. However, no short-term reconstitution by gastruloid cells was observed in any mice, GT7, GT9, nor GT11 (Figure 4.5.5). Mice GT10, GT12 and GT13 were culled at week 16 to investigate the long-term engraftment of gastruloid cells. No sign of reconstitution was detected in the bone marrow or spleen harvested from all mice (Figure 4.5.6; Figure 4.5.7). These results indicate that gastruloid cells cultured by the current protocol could only display short-term engraftment in an *in vivo* model, suggesting that the $CD45^+$ haematopoietic progenitors from gastruloids failed to maintain long-term stemness *in vivo*.

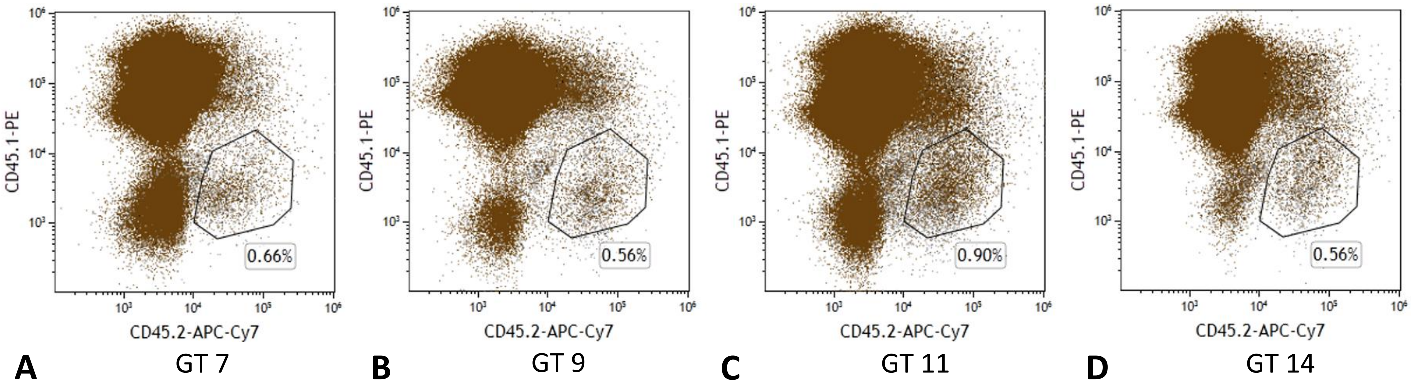

Figure 4.5.5. Flow cytometry results of spleen samples for checking short-term engraftment

Mice GT7, GT9, GT11 and GT14 were culled on week 9 and spleen cells were stained with CD45.1 PE and CD45.2 APC/Cy7 antibodies for flow cytometry analysis (n=1).

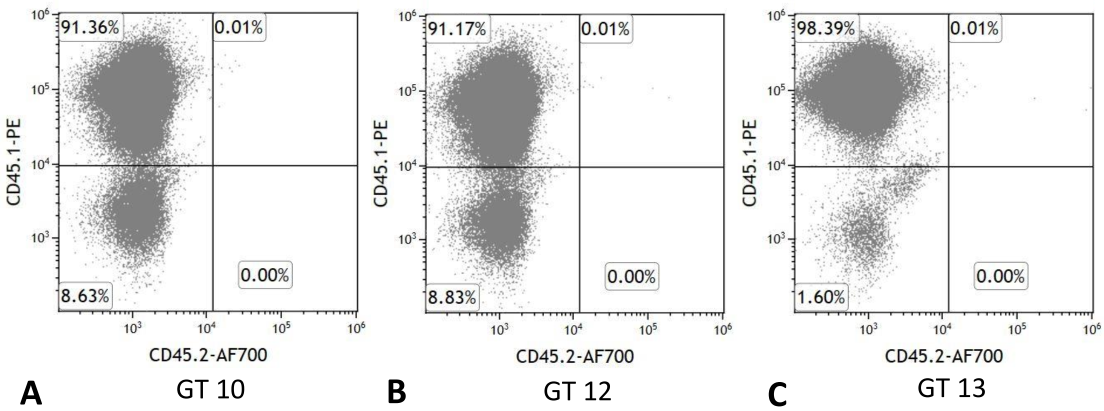

Figure 4.5.6. Flow cytometry results of bone marrow samples for checking long-term engraftment

Mice GT10, GT12, and GT13 were culled on week 16 and bone marrow cells were stained with CD45.1 PE and CD45.2 APC/Cy7 antibodies for flow cytometry analysis (n=1).

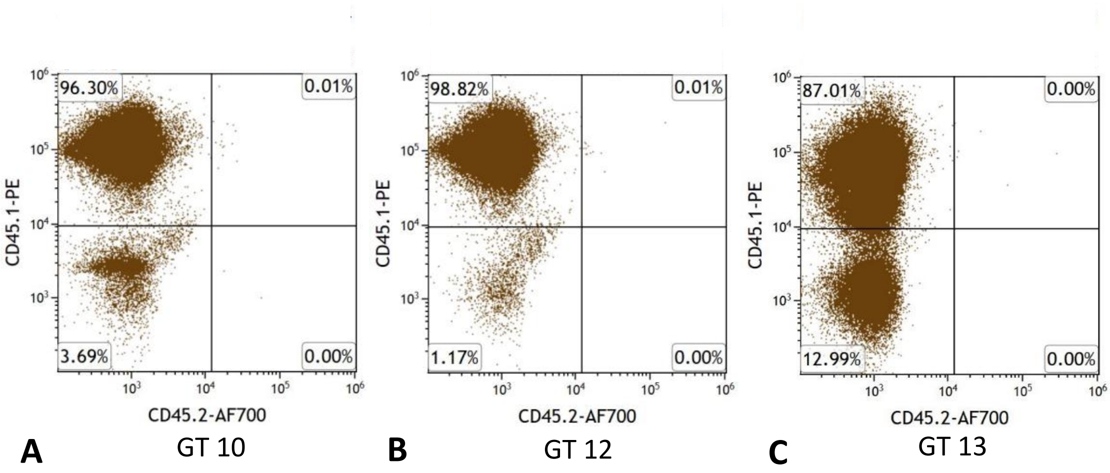

Figure 4.5.7. Flow cytometry results of spleen samples for checking long-term engraftment

Mice GT10, GT12, and GT13 were culled on week 16 and spleen cells were stained with CD45.1 PE and CD45.2 APC/Cy7 antibodies for flow cytometry analysis (n=1).

4.6 Conclusion

One of the highlights of this chapter is the extension of the haemogenic gastruloid protocol up to 216 hr by simply switching to using ultra-low attachment coated U-bottom 96-well plates for gastruloid culture. Other research groups have attempted to extend the protocol by using a shaker to avoid the gastruloid attaching to the bottom of the well but shaking irritates the gastruloids too much, and they only succeeded in extending the protocol to 168 hr (Beccari *et al*., 2018; Rossi *et al*., 2021a). The success of extending the culture to 216 hr without using the shaker has streamlined and simplified the culture protocol allowing other researchers to adopt this protocol.

Another important finding in this chapter is the emergence of $CD45^+$ cells in the gastruloids at 192 hr. The presence of $CD45^+$ cells is a strong indication of gastruloids recapitulating definitive haematopoiesis and forming the type 2 pre-HSCs (Batsivari *et al*., 2017). Together with the visualisation of the haematopoietic clusters in the gastruloid expressing CD45, c-Kit and CD31which reassembled the image of a transverse section of the E11.5 AGM region in mice, these strong proofs indicated and validated the occurrence of haematopoiesis in the gastruloid (Medvinsky *et al.*, 2011; Wang *et al*., 2016)..

Even though $CD45^+$ cells are generated in gastruloid in 192 hr, there are only elusive results from the short-term bone marrow engraftment while other engraftments have failed, undermining this claim weak and undetermined. Since the C57BL/6 (B6) mice were irritated, gastruloid cells were injected with the companion bone marrow cells, which may compete with gastruloid cells for survival, resulting in failure in engraftment. Another possible reason for the failure of engraftment is that the haematopoietic niches in gastruloid may lack homing signalling, such as CXCR4; thus, they cannot home to bone marrow after being injected into the mice. However, mouse engraftment study is still a common assay to test the *in vivo* reconstitution capacity; thus, the engraftment experiment shall be carried out again. Increasing the gastruloid culture time, injecting more gastruloid cells or using other mice without the end of irradiation to validate the haematopoietic potential of gastruloids (Waskow et al., 2002; Yang et al., 2005).

Although the gastruloid culture protocol can be extended to 216 hr, this chapter has focused on the gastruloid at 192 hr because this is the first observation of $CD45^+$ cells. The 216 hr gastruloids also deserve a more detailed characterisation, as they are expected to promote haematopoietic linage commitment and a more developed AGM-like haematopoietic cluster.

In addition, the cytokine schedule of the gastruloid between 168 to 216 hr is yet to be optimised, and shall be the focus of the next chapter.

Chapter	Main Findings
4.2.1	Gastruloid culture can be extended to 216hr using low adherence plate.
4.2.2	Gastruloid is viable throughout 216hr of culture.
4.2.3	Gastruloid shows lumen-like structure throughout 216hr of culture and starts cardiac-like beating since 168hr
4.3.1	Pre-treating mES cells with 2iLIF for 24hr promotes the gastruloids potential in forming CD45+ cells at 192hr
4.3.2	The 24-hr pulse of Shh at 144hr stimulate more VeCAD+ and CD45+ cells in gastruloid at 192hr
4.4	Gastruloid shows putative CD31+, cKIT+ and CD45+ clusters at 192hr
4.5	Cells from 192 hr gastruloid may have short engraftment potential in the irradiated C57BL/6 (B6) mice model.

Table 4.6.1. Summary of the main findings in chapter 4.

Chapter 5: Further optimisation and functional characterisation of haematopoietic production from gastruloid

5.1 Introduction

Since chapter four finalised that the Shh pulse should be added between 144 and 168 hr, this chapter focuses on optimising the cytokine schedule during the last 48 hours and understanding more about the CD45$^+$ cells formed at 192 and 216 hr. Although chapter four demonstrated that adding SCF and Noggin did not enhance the haematopoietic activity in gastruloids at earlier stages, they were added individually or in combination at the beginning of the final 48 hours to investigate whether more CD45 cells were produced. Also, since FGF_2 may restrict the specification of HSCs by countering the BMP activity, FGF_2 was removed in the last 48 hours. The proportion of CD45$^+$ cells in the gastruloids was subsequently measured to probe the FGF_2 effects on the formation of CD45$^+$ type 2 pre-HSCs (Pouget *et al*., 2014). Finally, a panel of TPO, SCF, and Flt-3l was added in the last 24 or 48 hours to observe whether these cytokines could further promote CD45$^+$ cell output in gastruloids.

Gastruloids were individually disassociated to check the percentage of CD45$^+$ cells across gastruloids and determine the gastruloid-to-gastruloid variation in the percentage of CD45$^+$ cells at 192 and 216 hr. Additionally, CD45$^+$ cells at 216 hr were further characterised for the expression of additional candidate stem cell markers Sca-1, EPCR (CD201), and AA4.1 (CD93) within the CD45$^+$ gastruloid population. These surface proteins (Sca-1, EPCR and AA4.1) are either markers of lymphohaematopoietic progenitors, markers to purify pre-HSCs, or have a vital role in HSCs self-renewal. Fluorescence microscopy images of gastruloids at 216 hr were also taken to closely observe haematopoietic cluster development.

Functional assays have been performed to investigate whether CD45$^+$ cells from gastruloids can demonstrate haematopoietic activity. Since CD45$^+$ cells have demonstrated lymphoid potential in the previous CFC assay, CD45$^+$ cells were co-cultured with OP9 and OP9-DL1 to discover if they could differentiate into myeloid-lymphoid lineage-committed progenitors. Whole gastruloids were seeded onto a chick embryo chorioallantoic membrane (CAM), and confocal images were taken to assess gastruloid engraftment of the CAM and the putative survival or expansion of CD45$^+$ cells. Lastly, once the haemogenic gastruloid culture protocol was optimised and finalised, gastruloid cells were injected into non-irradiated mice to further confirm the reconstitution capability of HSCs progenitor cells generated from the gastruloid, with the help of Dr Natacha Bohin and Mr Andrea Tavosanis (Professor Kamil Kranc's Lab, Barts Cancer Centre). Non-irradiated c-Kit mutant NSG mice were particularly selected as unlikely irradiated mice, since their naïve haematopoietic niche is preserved, and we can understand whether lymphoidhaematopoetic cells from the gastruloid can engraft to bone marrow and spleen with such a niche.

5.2 Optimisation of the cytokine schedule between 168 and 216 hr

5.2.1 Addition of SCF and Noggin between 168 and 216 hr not affecting the formation of CD45$^+$ cells at 216 hr

From the previous chapter, the formation of heart-like structures in gastruloids at 168 hr, and the enhanced emergence of candidate CD45$^+$ type 2 pre-HSCs with a 24-hour pulse of Shh at 144 hr, suggests that the 168 hr gastruloids can be regarded as around E10. At this stage, in addition to the Shh signalling in the ventral region of the aorta, SCF and BMP inhibitory signals at the dorsal region are also integral parts of the system for developing HSCs (Souilhol *et al*., 2016). BMP signalling is stage-specific and only active in haematopoietic clusters when pre-HSCs switch from type 1 to type 2, which suggests that Noggin, a BMP inhibitor, can also be applied to gastruloids at 168 hr (Wilkinson *et al*., 2009). Apart from Noggin, SCF is also a crucial haematopoietic factor that has various roles, from the formation of haemogenic endothelium to the emergence of type 2 pre-HSCs (Rybtsov *et al*., 2014).

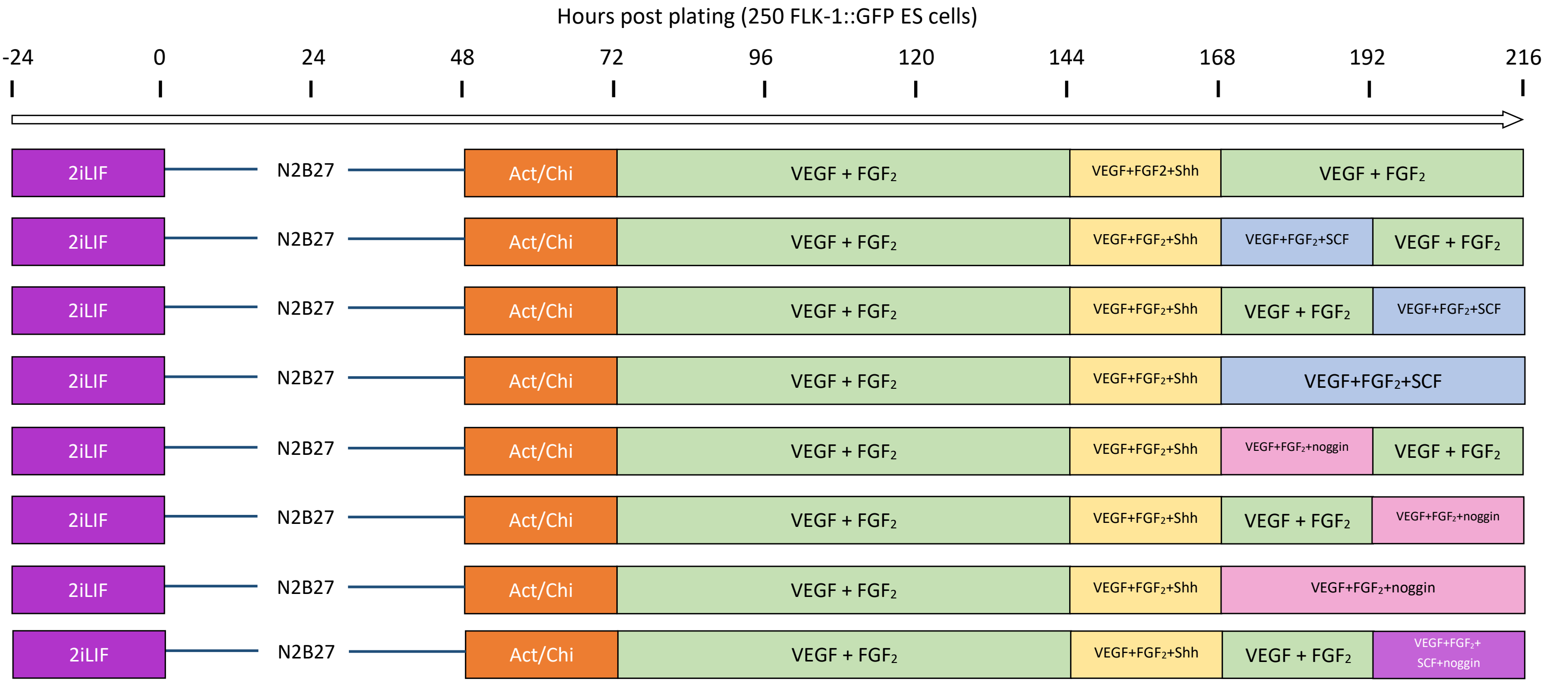

Figure 5.2.1. The culture scheme of gastruloids used to investigate if adding SCF and/or Noggin in the last 24 or 48 hours of culture can generate more CD45$^+$ cells.

To study if SCF could be applied alongside Noggin to create the haematopoietic microenvironment in gastruloids and to optimise the time point of addition, gastruloids were cultured and SCF and Noggin were added individually at either 168 or 192 hr for 24 or 48 hours (Figure 5.2.1). SCF and Noggin were also added together at 192 hr for 24 hours as a trial to observe whether there is any synergy. Gastruloid cells were collected at 216 hr, dissociated, and analysed with flow cytometry for CD45 and GFP expression. Results displayed that neither SCF or Noggin could enhance the GFP expression of gastruloids at 192 hr as there was no significant difference between any of the conditions (Figure 5.2.2 A). Neither SCF nor Noggin could enhance the differentiation of CD45 (Figure 5.2.2 B).

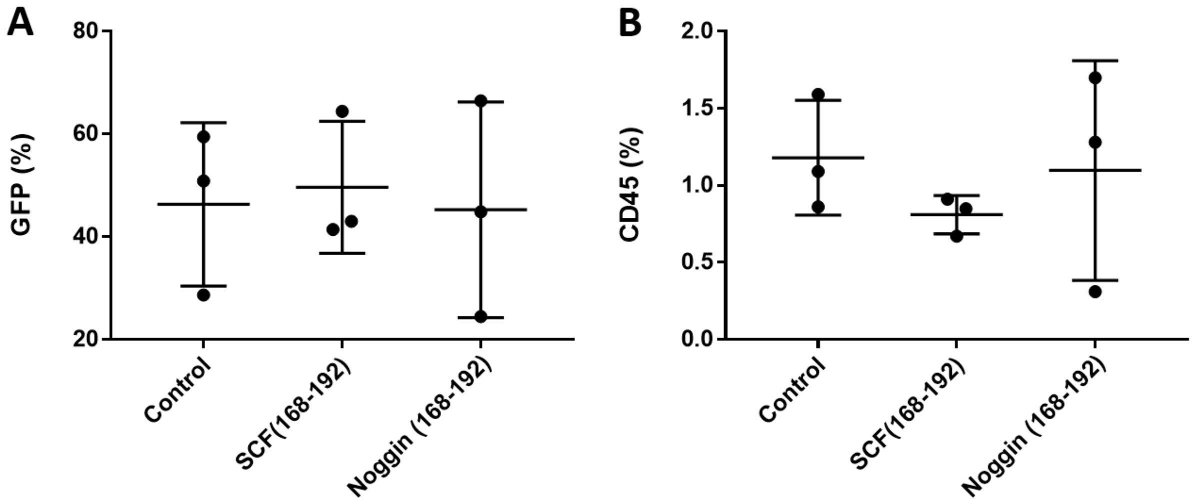

Figure 5.2.2. Summarised flow cytometry result of 192 hr gastruloids cultured with Shh or SCF

Summarised flow cytometry result of the CD45-APC stained 192 hr gastruloid with either SCF or Noggin added at the last 24 hours on (A) GFP expression and (B) CD45 expression (n=4).

Gastruloid cells were also harvested at 216 hr for flow analysis. As with the results at 192 hr, adding SCF and/or Noggin for either 24 or 48 hours, did not change the GFP expression level of gastruloids, suggesting these cytokines do not facilitate or mediate the differentiation of Flk-1 expressing early-stage haemogenic cells (Figure 5.2.3 A). Regarding the differentiation of $CD45^+$ cells in these conditions, the gastruloids treated with SCF or Noggin for either 24 or 48 hours did not display a significant difference in $CD45^+$ cell expression than the gastruloids in the control group (Figure 5.2.3 B).

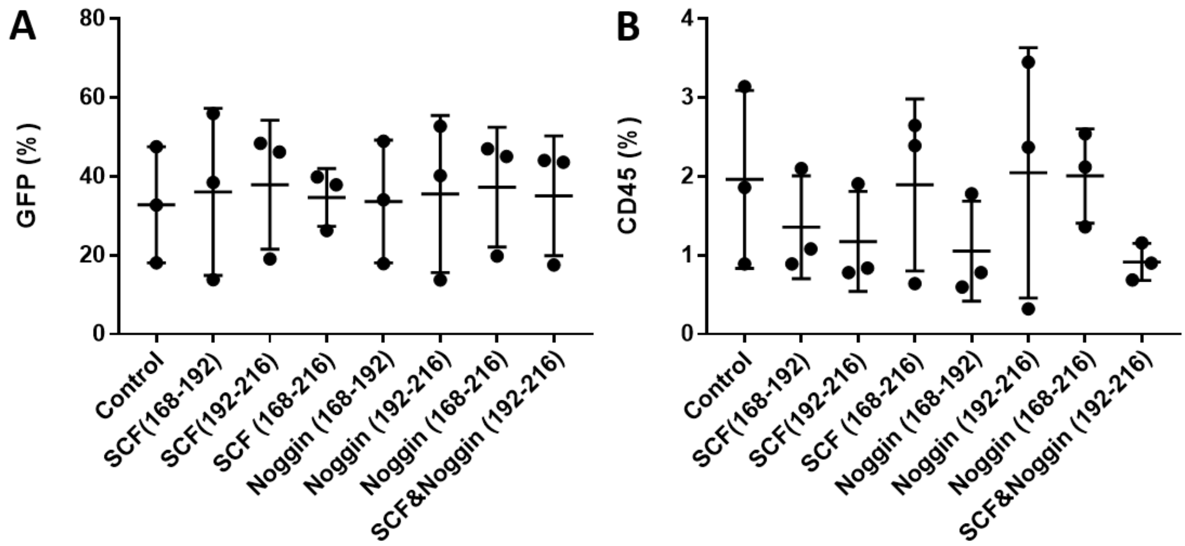

Figure 5.2.3. Summarised flow cytometry result of 216 hr gastruloids cultured with Shh or SCF

Summasired flow cytometry result of the CD45-APC-stained 216 hr gastruloid with either SCF or Noggin at the last 24 or 48 hours on (A) GFP expression and (B) CD45 expression (n=4).

5.2.2 Removal of FGF_2 between 168 and 216 hr not hampering the formation of $CD45^+$ cells at 216 hr

Although adding Noggin did not promote haematopoietic differentiation in the gastruloids during the last 48 hours of culture, it is still worth optimising the addition of BMP-related cytokines as this is a critical haematopoietic signalling pathway. The importance of BMP signalling is well characterised, and FGF_2 regulates the emergence and maintenance of HSCs at the dorsal aorta by counteracting BMP activity. FGF_2 is absent in the aortic region which expresses BMP4, and conversely, BMP4 is absent in the aortic region if FGF_2 is overactivated (Pouget *et al*., 2014). Since the gastruloid is proposed to start forming $CD45^+$ type 2 pre-HSCs from 168 hr, the haematopoietic stem cell specification may be restricted if FGF_2 is added to the culture (Lee *et al*., 2014).

Gastruloids were cultured with or without FGF_2 from 168 hr. Then gastruloids were collected at 216 hr, disassociated, and analysed with flow cytometry for their GFP and CD45 expression (Figure 5.2.4). Results demonstrated that removing FGF_2 from the culture at 168 hr did not change GFP expression, resulted in only an insignificant, subtle increase in the proportion of $CD45^+$ cells (Figure 5.2.5). Although the increase of $CD45^+$ cells caused by FGF_2 removal was insignificant, since FGF_2 may inhibit further haematopoiesis in gastruloids, it is worth removing the FGF_2 from the protocol after 168 hr.

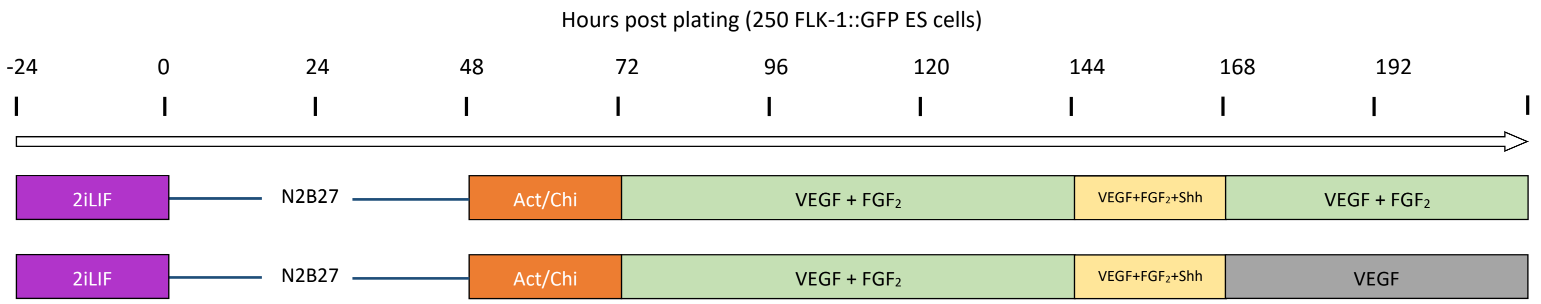

Figure 5.2.4. The culture scheme of 216hr gastruloids used to investigate if removing FGF_2 from gastruloids at 168 hr affects the CD45 differentiation.

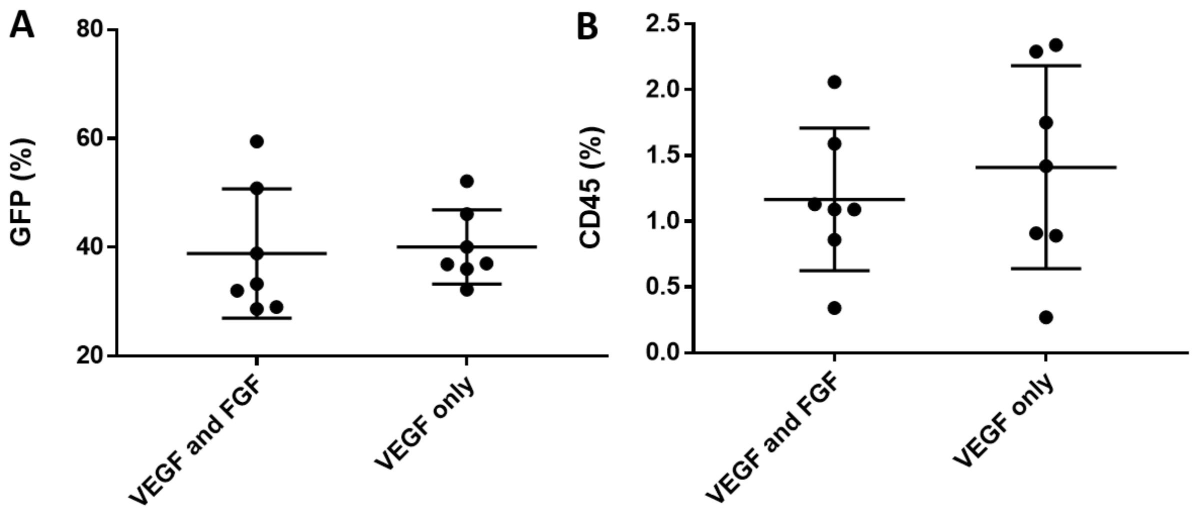

Figure 5.2.5. Summarised flow cytometry result of 216 hr gastruloids cultured without FGF_2 at the last 48 hr

Summarised flow cytometry result of the CD45-APC-stained 216 hr gastruloid with or without FGF_2 in the last 48 hours on (A) GFP expression and (B) CD45 expression (n=7, mean$\pm$SD, student's t-test p=0.5064 at VEGF only).

5.2.3 Adding SCF, TPO and Flt-3l in combination between 168 and 216 hr promoting the formation of CD45$^+$ cells at 216 hr

In addition to removing the FGF_2 from the culture to prevent restriction of haematopoietic stem cell specification, other cytokines including TPO and Flt-3l, may also be considered including, to promote maturation of the CD45$^+$ pre-HSCs at the last 48 hours.

The TPO signalling pathway is vital when the haemogenic endothelial cells transit to HSCs via *Runx1* activation from E10 to E10.5 in the AGM region (Fleury *et al*., 2010). TPO can also stimulate the endothelial cells from the AGM to form haematopoietic cells, suggesting TPO is critical to the formation and maintenance of haematopoietic cell clusters in the AGM (Harada *et al*., 2017). Flt-3l is a haematopoietic growth factor that promotes the proliferation of hematopoietic progenitor cells of both lymphoid and myeloid origin in the foetal liver (Dong *et al*., 2002). A high level of Flt-3l was also found in CD45$^+$ and Ter119$^+$ hematopoietic cells (Yumine *et al*., 2017).

Maintenance and regulation of the embryonic haematopoietic niche includes a panel of cytokines. At E12.5, the gene encoding of three cytokines, SCF, Flt-3l and TPO, was remarkably upregulated in the foetal liver (Yumine *et al*., 2017). Moreover, SCF, Flt3-l and IL3 can successfully maintain the E11.5 *ex vivo* haematopoietic capability of the dissociated and reaggregated AGM region from HSCs (Taoudi *et al*., 2008). Although previously it was found that adding SCF alone or with Noggin could not promote the formation of haematopoietic CD45$^+$ cells in the gastruloid at 216 hr, adding SCF in combination with Flt3-l and TPO has been shown to be critical in the support of haematopoietic differentiation, therefore it would be worth studying them in the gastruloid culture.

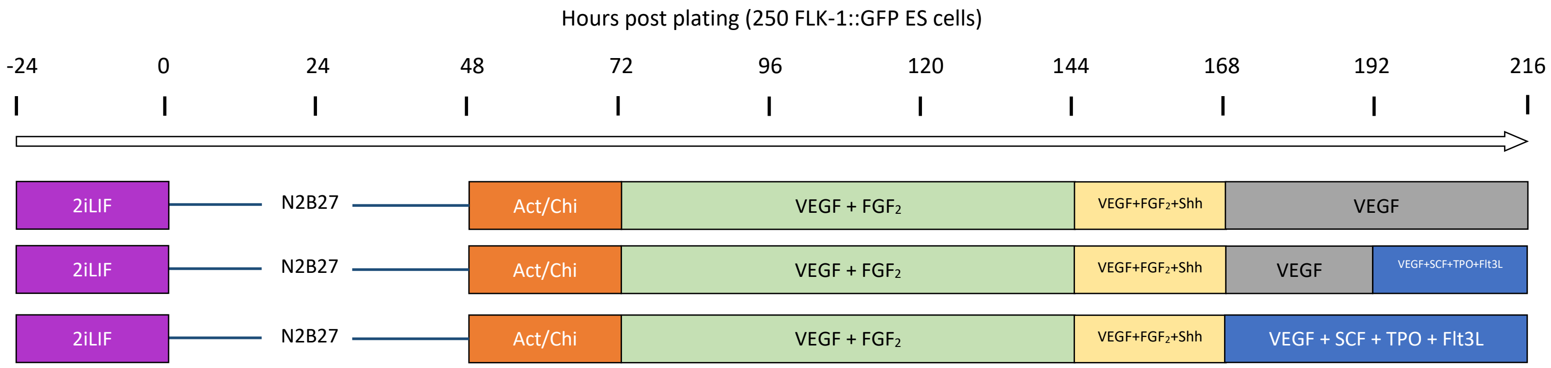

Figure 5.2.6. The culture scheme of gastruloids used to investigate if adding SCF, TPO and Flt-3l to the gastruloids at last 24 or 48 hr affects the CD45 differentiation at 192 hr and 216 hr.

Gastruloids were cultured with or without 3Cy (SCF, TPO and Flt-3l) for the last 24 or 48 hours (Figure 5.2.6). Gastruloids were subsequently collected at 192 and 216 hr for flow cytometry analysis of CD45 expression. Adding these three cytokines did not significantly promote the GFP or CD45 expression in the gastruloid at 192hr (Figure 5.2.7 A and B).

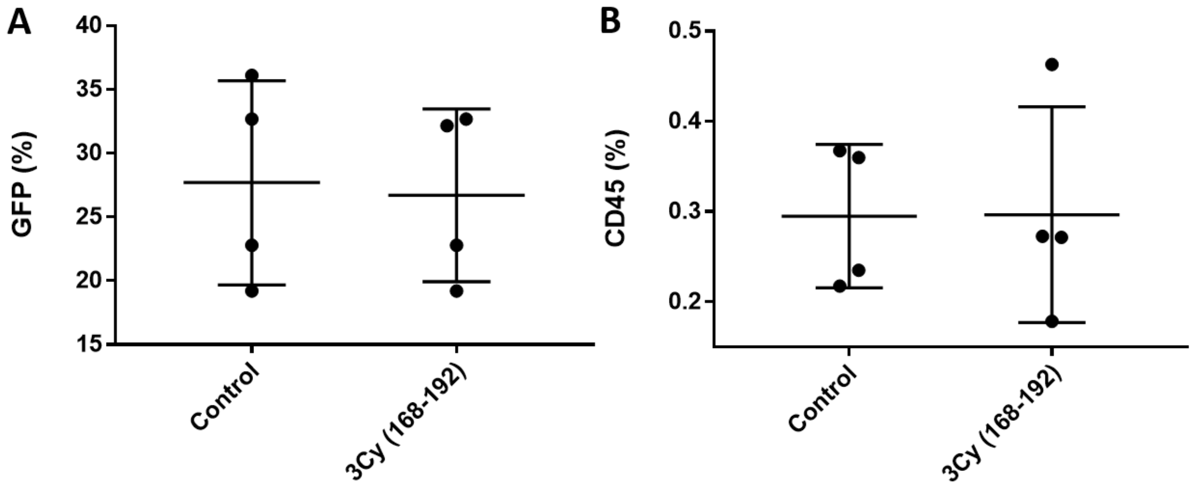

Figure 5.2.7. Summarised flow cytometry result of 192 hr gastruloids cultured with 3Cy (SCF, TPO and Flt-3l) at the last 24 hr

Summarised flow cytometry result of the CD45-APC stained 192 hr gastruloid with 3Cy (SCF, TPO and Flt-3l) added at the last 24 hours on (A) GFP expression and (B) CD45 expression (n=4).

At 216 hr, the results indicated that adding these three cytokines at 168 or 192 hr did not change the proportion of GFP^+ cells (Figure 5.2.8 A). Culturing the gastruloids with these three cytokines from 192 hr showed a minimal increase in the production of $CD45^+$ cells, but such an increase is not significant (Figure 5.2.8 B). The gastruloid treated with three cytokines for 48 hours had a significant boost in the formation of $CD45^+$ cells at 216 hr compared with the control. It has been suggested that stimulating the gastruloids by three cytokines between 192 and 216 hr is essential, but pretreating the gastruloids between 168 and 192 hr can prime the haematopoietic $CD45^-$ cells and promote their transition into $CD45^+$ cells.

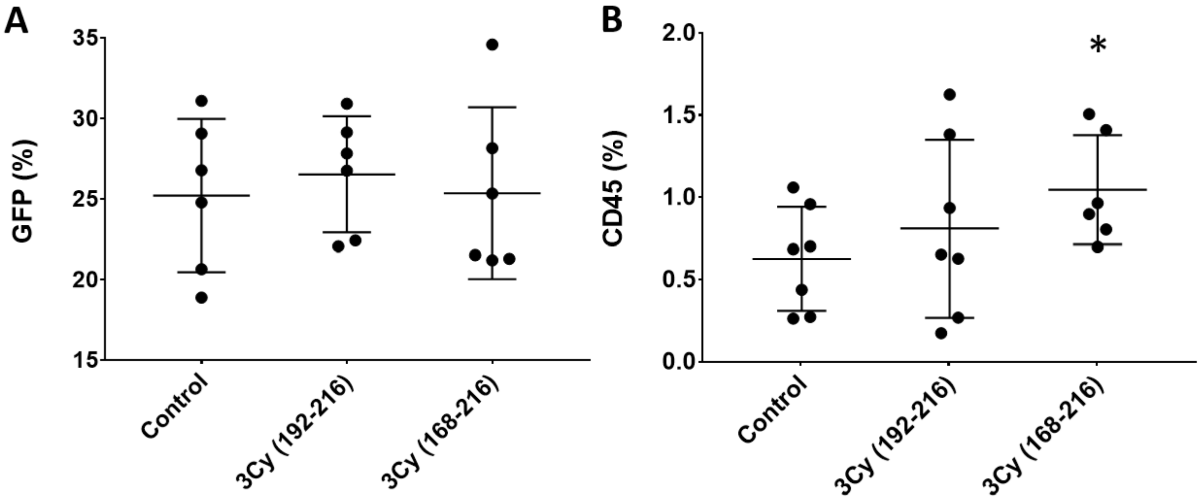

Figure 5.2.8. Summarised flow cytometry result of 216 hr gastruloids cultured with 3Cy (SCF, TPO and Flt-3l) at the last 24 or 48 hr

*Summarised flow cytometry result of the CD45-APC-stained 216 hr gastruloid with 3Cy (SCF, TPO and Flt-3l) added at the last 24 or 48 hours on (A) GFP expression and (B) CD45 expression (n=7, mean± SD, student's t-test p=0.0393 * at 3Cy(168-216).*

5.3 Characterising haematopoietic gastruloid cells formed at 216 hr

5.3.1 $CD45^+$ cells in individual gastruloids at 192 and 216 hr

The expression of CD45 is an important criterion to test the emergence of definitive haematopoietic stem or progenitor cells (HSPCs) from the *in vitro* culture, as CD45 is expressed in most of the haematopoietic cells, except for some mature cell types. For the embryonic haematopoietic study, especially for those focussing on AGM development, $CD45^+$ is a critical marker as it may indicate the emergence of type 2 pre-HSC, which is why it has often been used when optimising the haemogenic gastruloid protocol. $CD45^+$ cells were first observed in the gastruloid at 192 hr, and its expression was maintained at 216 hr. However, the portion of $CD45^+$ cells at 216 hr is not always higher than the portion at 192 hr, suggesting there are gastruloid-to-gastruloid variations, posing the question of which time point is more appropriate for other assays.

Flow cytometry has been carried out frequently to study the expression of CD45 in gastruloids for protocol optimisation, but most of the time, all gastruloids are pooled together for disassociation and antibody staining. Although this practice is quick and standard, the information regarding gastruloid-to-gastruloid variation is lost. In order to assess the variation in the capability to form CD45 in individual gastruloids at 192 and 216 hr, gastruloids were collected at these two-time points, dissociated, and stained with CD45-APC antibodies for flow cytometry.

The result revealed that the 192 hr gastruloids were very heterogeneous and that they either had high or low CD45 expression, while 216 hr had a relatively consistent CD45 expression pattern across gastruloids (Figure 5.3.1). Although in this testing, on average, gastruloids at 192 hr has more $CD45^+$ cells than at 216 hr, the gastruloid-to-gastruloid heterogeneity may be the reason for inconsistent results at 192 hr. However, the range of CD45 expression of gastruloids at 192 hr is greater than that of 216 hr, suggesting that a portion of gastruloids may reach the peak of their haematopoietic potential at 192 hr, begin to lose their CD45 expression and differentiate into other haematopoietic linage cells when they reach 216 hr.

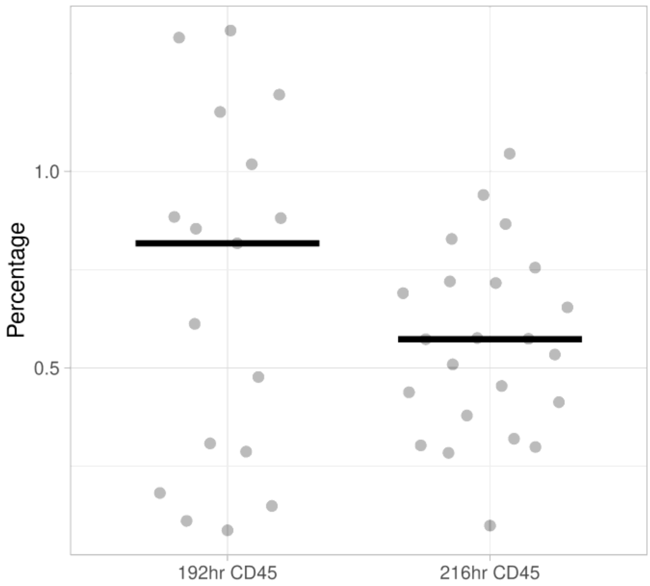

Figure 5.3.1. Summarised flow cytometry result of individual gastruloids at 192 and 216hr (CD45)

Gastruloids were collected and stained indiviaully with CD45-APC antibody on 96 well plate. Summarised flow cytometry result of the CD45 expression of individual gastruloids at 192 hr (n=18) and 216 hr (n=24).

5.3.2 Gastruloid cells at 216 hr expressing Sca-1 and EPCR but not AA4.1

The previous section suggested that gastruloids at 216 hr are relatively more homogeneous than at 192 hr, in terms of the CD45 expression. However, the gastruloid cells under haematopoiesis are supposed to commit to different lineages and consequently, may express different HSC markers, such as Sca-1, EPCR (CD201) and AA4.1 (CD93). By studying the expression of these markers, we can better evaluate the differentiation status of the gastruloids.

Stem cell antigen-1 (Sca-1) plays an important role in haematopoietic stem cell self-renewal and the development of committed progenitors as *Sca-1* knockout results in transplantation defeats in mice (Ito *et al*., 2003). High levels of Sca-1 expression is also a marker of quiescent haematopoietic progenitors (Morcos *et al*., 2017). AA4.1, an early B cell marker, can also mark the lymphohaematopoietic progenitors, distinguishing lymphoid-myeloid progenitors from myeloid-restricted progenitors within the CD45^{+} cell population (Yamane, 2020). AA4.1^{+} Sca-1^{+} Tie-2^{+} lineage foetal liver cells can also provide long-term multilineage reconstitution after transplantation into irradiated mice, establishing AA4.1 as a marker of foetal liver HSCs (Hsu *et al*., 2000). Endothelial protein C receptor (EPCR) is a marker to purify pre-HSCs from the mouse AGM region at the single-cell level at E11 (Zhou *et al*., 2016). EPCR has also been used with SLAM phenotype markers to identify mouse HSCs as half of E-SLAM (EPCR-SLAM) cells in the mouse bone marrow and foetal liver had long-term multilineage repopulating ability when transplanted into mice (Wilson *et al*., 2015).

Since these three HSC markers can capture functional repopulating HSCs, they were selected to dissect the CD45^{+} compartment in the 216 hr gastruloids and search for phenotypic evidence of the presence of HSCs (Figure 5.3.2). For flow cytometry analysis, dissociated gastruloid cells were stained with c-Kit, CD45, Sca-1, EPCR and AA4.1 antibodies. Results from the flow cytometry indicated the specification of Sca-1^{+} CD45^{+} and EPCR^{+} CD45^{+} cells in the 216 hr gastruloid, while AA4.1^{+} CD45^{+} cells were absent (Figure 5.3.3 A). The expression pattern of Sca-1^{+} CD45^{+} cells was considerably more defined than EPCR^{+} CD45^{+} cells, and they may reassemble the progenitors of the phenotype (Lin^{-} CD45^{+} EPCR^{+} Sca-1^{+}) of cells that are found in the AGM region at E10.5 following co-culture (Figure 5.3.5) (Tang *et al*., 2021). In the CD45^{-} compartment, only Sca-l and EPCR markers were expressed in the gastruloid, indicating that there may be some committed progenitors formed, but not early B cell progenitors in the gastruloid (Figure 5.3.3 B; Figure 5.3.5).

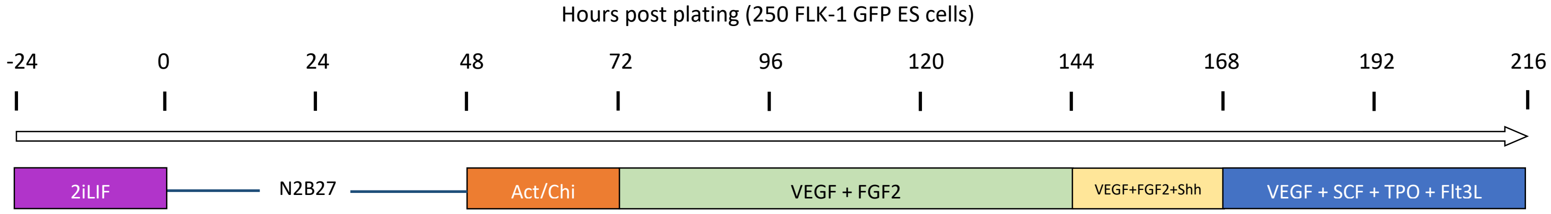

Figure 5.3.2. The culture scheme of used to investigate if 216hr gastruloids express Sca-1, EPCR or AA4.1.

The Sca-1$^+$ and EPCR$^+$ cells were gated to check c-Kit expression. Sca-1$^+$ cells had around ~80% c-Kit$^+$ expression, while EPCR$^+$ cells had around 60% expression regardless of CD45 expression (Figure 5.3.4 A and B). The c-Kit$^+$ CD45$^+$ cells from the mouse AGM are regarded as HSPCs with a long-term repopulating population and enriched LT-HSCs genes. The recapitulation of c-Kit$^+$ CD45$^+$ cells with Sca-1 and EPCR further validates the formation of long-term repopulating HSC progenitors in the AGM (Figure 5.3.4 A) (Pereira *et al.*, 2013).

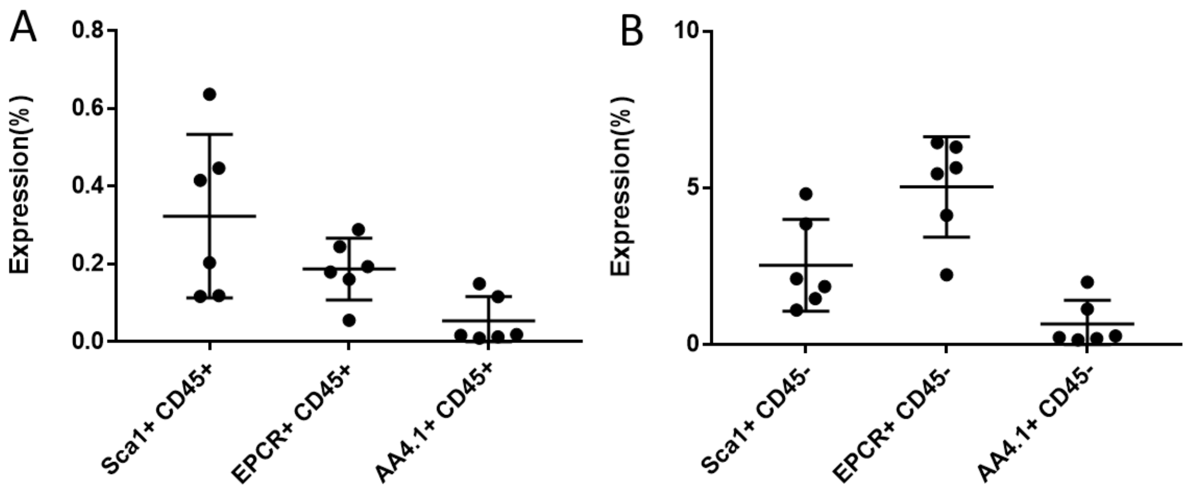

Figure 5.3.3. Summarised flow cytometry result of 216 hr gastruloids on the expression of Sca1, EPCR and AA4.1 with CD45

Summarised cytometry result of the 216 hr gastruloid with on the expression of Sca1, EPCR and AA4.1 which (A) are positive with CD45 and (B) are CD45 negative (n=6).Gastruloids were stained with CD45-APC, Sca1-PE/Cy7, EPCR-PE and AA4.1-PerCP/Cy5.5.

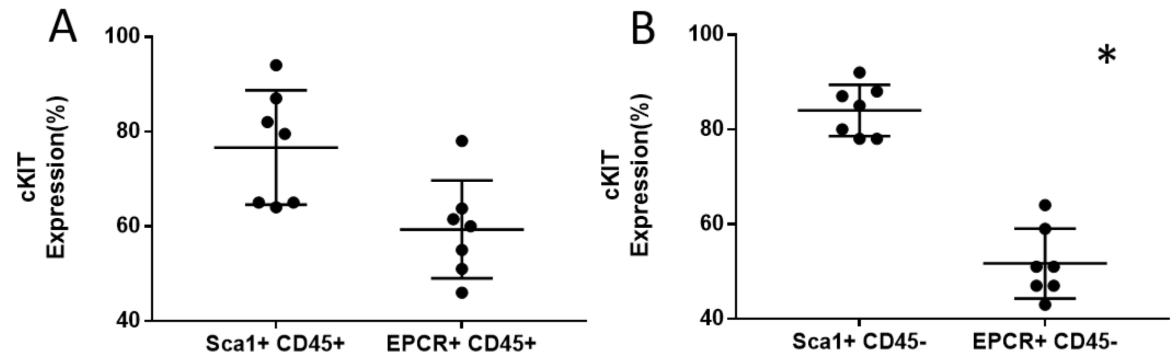

Figure 5.3.4. Summarised flow cytometry result of 216 hr gastruloids on the expression of Sca1 and EPCR with cKIT

*(A) Sca-1$^+$ CD45$^+$ and EPCR$^+$ CD45$^+$ cells and (B) Sca-1$^+$ CD45$^-$ and EPCR$^+$ CD45$^-$ cells from flow cytometry results in the 216 hr gastruloids from figure 5.3.2 have been gated to check the c-Kit expression (n=6, mean$\pm$SD, student's t-test $p<0.0001$ *at EPCR$^+$CD45$^-$).*

Although Sca-1$^+$ CD45$^-$ cells are less expressed than EPCR$^+$ CD45$^-$ cells regarding their expression percentage, the Sca-1$^+$ CD45$^-$ cell population is well separated from the double-negative population, suggesting this Sca-1$^+$ CD45$^-$ cell population is promising (Figure 5.3.3 B; Figure 5.3.5). Apart from their roles in haematopoiesis, Sca-1$^+$ cells are also regarded as a crucial cardiac marker and a vital source for cardiomyocyte renewal. Sca-1 expression is primarily observed in mesoderm-derived cells and represents a subset of vascular endothelial cells in the postnatal heart (Zhang *et al*., 2018). Gastruloids have demonstrated the potential to form cardiac-like heart beating components since 168 hr, which even show rhythmic beating at 216 hr. The Sca-1$^+$ population observed in the flow cytometry result may prove the formation of vascular endothelial cells in the heart beating component formed in gastruloids (Figure 5.3.3; Figure 4.2.7)

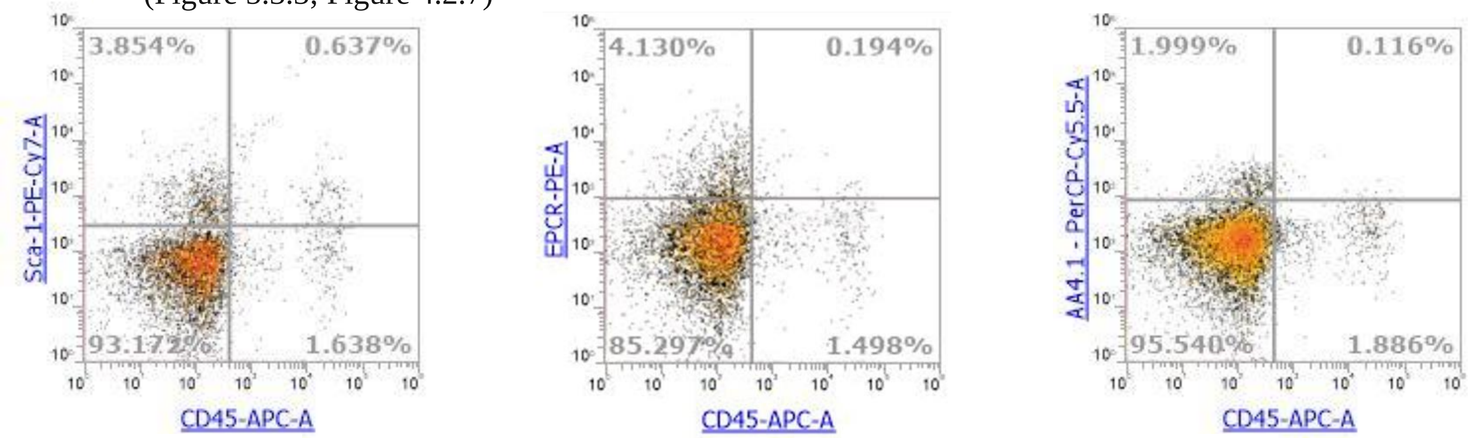

Figure 5.3.5. Flow cytometry results of 216 hr gastruloids on the expression of Sca1, EPCR and AA4.1 with CD45

Representative flow cytometry dot plots of the expression of Sca1, EPCR and AA4.1 with CD45 in the gastruloids at 216 hr (n=6). Gastruloids were stained with CD45-APC, Sca1-PE/Cy7, EPCR-PE and AA4.1-PerCP/Cy5.5.

Since the formation of Sca-1^{+} c-Kit^{+} CD45^{-} cells in the 216 hr gastruloid were shown in figure 4.3.3B, the Sca-1^{+} c-Kit^{+} cells have been particularly studied, and this population can be observed in the flow cytometry dot plot (Figure 5.3.6 A and B).

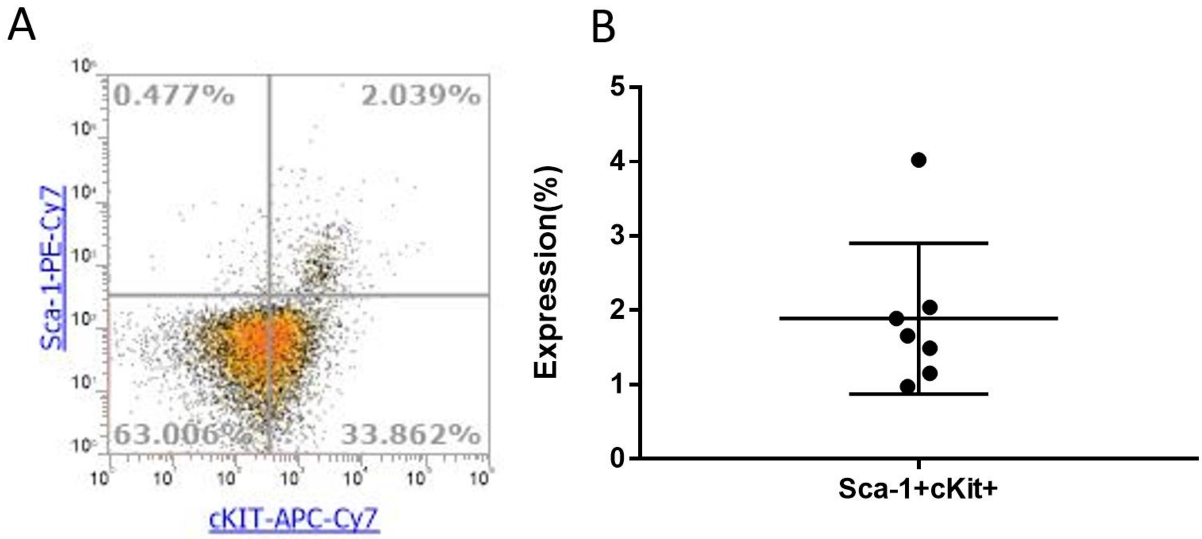

Figure 5.3.6.Flow cytometry result of the experssion of Sca1^{+} c-Kit^{+} cells in 216hr gastruloid

(A) Representative flow cytometry dot plot on the experssion of Sca1^{+} c-Kit^{+} cells in 216hr gastruloid stained ith cKit-APC/Cy7 and Sca-1-PE/Cy7 antibodies. (B) Summarised flow cytometry results of expression of Sca1^{+} c-Kit^{+} cells in the gastruloids at 216 hr (n=7).

5.3.3 Haematopoietic cluster in the 216 hr gastruloid

In chapter 4.4, the 192 hr gastruloid was studied under confocal microscopy, and putative haematopoietic clusters were observed in the gastruloid. These clusters resemble the morphology of the intra-aortic cluster, suggesting that an AGM-like structure may have formed in the gastruloid under the microenvironment established with the haematopoietic cytokines. Although a confocal image was applied to study the haematopoietic cluster in the 192 hr gastruloid, higher magnification such as 20x aided the visualisation of the cluster's details (Figure 4.4.1). In addition, the haemogenic protocol was extended to 216 hr with an extra cytokine panel of SCF, TPO and Flt-3l, and it would be worth revisiting confocal imaging in a higher magnification to study whether the gastruloid is able to form a more clearly defined structure and if such a structure contains more $CD45^+$ or c-Kit^+ cells.

The 216 hr gastruloids were fixed and stained with DAPI, CD45 and c-Kit antibodies, and confocal imaging was performed in 20x magnification. The confocal image clearly showed that the clusters could also form in the 216 hr gastruloid (Figure 5.3.7). With Flk-1 outlining the cluster, c-Kit^+ cells clearly highlighted the lumen inside of the cluster, and some of these c-Kit^+ cells co-expressed the CD45 signals, indicating the formation of phenotypic pre-HSCs in this AGM-like cluster.

This confocal imaging has microscopically validated the results from flow cytometry on the formation of $CD45^+$ c-Kit^+ pre-HSCs in the gastruloid (Figure 5.3.8). Other functional assays such as OP9 co-culture or engraftment study are worth carrying out to further characterise further the haematopoietic potency of the progenitors formed in gastruloids.

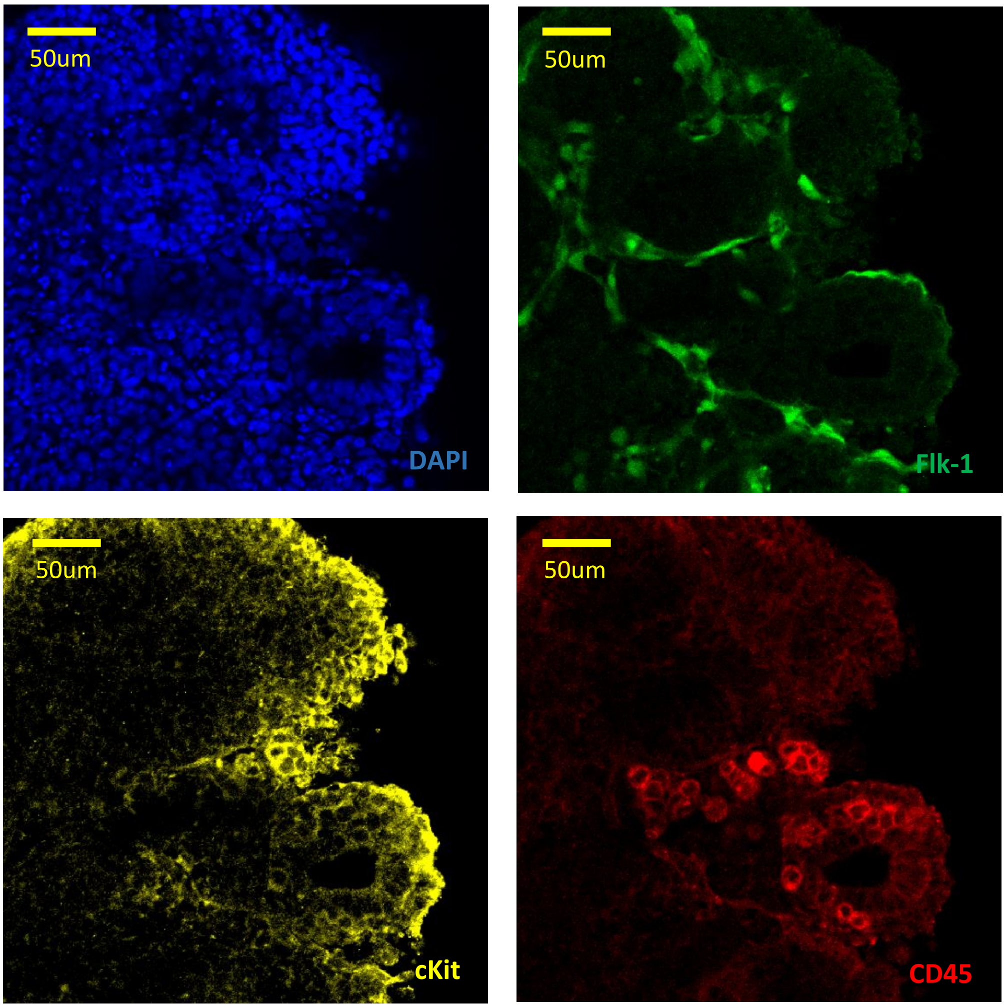

Figure 5.3.7. Localisation of the AGM-like cluster in the 216 hr gastruloid.

Confocal images of a whole-mount immunostained gastruloid showing DAPI (blue) GFP (green) c-Kit (yellow) and CD45 (red) expression. (Magnification: 20x) (scale bar: 50um). Gastruloid was first stained with goat anti-mouse cKit-biotin and rat anti-mouse CD45-biotin antibodies and then with anti-goat Alexa-Fluor 633 and anti-rat Alexa-Fluor 568.

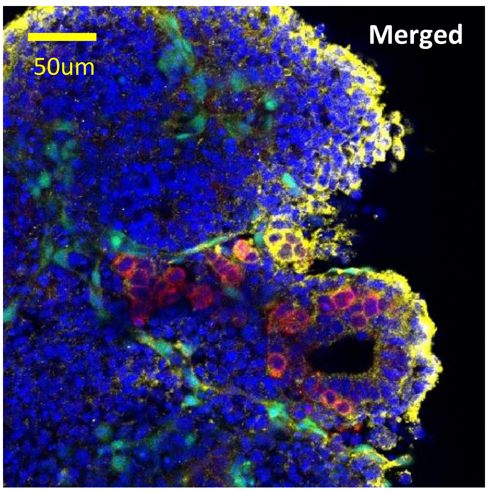

Figure 5.3.8 Merged confocal images of immunostained gastruloid from Figure 5.3.7

Merged confocal images of a whole-mount immunostained gastruloid showing DAPI (blue) GFP (green) c-Kit (yellow) and CD45 (red) expression. (Magnification: 20x) (scale bar: 50um).

5.4 Functional assays to characterising the haematopoietic potentials of CD45$^+$ cells from gastruloid at 192 and 216 hr

5.4.1 Gastruloid at 216 hr occasionally showed lymphohaematopoietic potential and CD45$^+$ cells enrichment in the OP9 co-culturing system

OP9 is a stromal cell line developed from mouse bone marrow, which can support haematopoietic development. With such haemopoietic supportive capacity, OP9 cells are often used as feeder cells in co-culture to support the haematopoietic development of other cells such as ES cells, foetal liver cells, and bone marrow cells, establishing haematopoietic niches. Following co-culturing with OP9 cells, cultured cells display signs of lymphohaematopoietic differentiation generating B cell lineages. OP9 cells have also been further modified into OP9-DL1 cells, which expresses Notch ligand Delta-like 1 (DL1) to support the differentiation of T cell lineages (de Pooter & Zúñiga-Pflücker, 2007).

Gastruloids are shown to be possibly able to generate cells with an identity similar to haematopoietic progenitors, such as CD41$^+$ cells and CD45$^+$ cells. Further functional assays can help to further validate whether definite haematopoiesis is occurring in gastruloids and producing haematopoietic progenitors. Based on the published protocol, gastruloid cells were co-cultured with OP9 and OP9-DL1 stromal cells to examine the lymphoid potential, which is an important benchmark to confirm the emergence of definitive haematopoietic progenitors (Holmes & Zúñiga-Pflücker, 2009).

The 216 hr gastruloids were collected, dissociated, and seeded on the plate pre-seeded with OP9 or OP9-DL1 according to protocol 4 in the published protocol (Holmes & Zúñiga-Pflücker, 2009). This protocol was adapted to study whether the haematopoietic progenitors from gastruloids can demonstrate lymphohaematopoietic differentiation as comparable to bone marrow. The cells were re-seeded without trypsin every three to four days. After the fifth day, one-tenth of the sample cells from the OP9 co-culture were harvested and stained with CD45 and CD19 antibodies. Ter119 and CD11b and antibodies were also occasionally added to determine the presence or absence of myeloid (CD11b), and erythroid (Ter119) markers. CD4 and CD8 antibodies were added to stain the sample cells from the OP9-DL1 co-culture. As a positive control, bone marrow was cultured on OP9 or OP9-DL1 cells.

Culturing gastruloid and bone marrow cells with OP9 cells only worked occasionally. Half of the passage (two out of four passages) found that OP9 cells could enrich $CD45^+$ cells from the gastruloid at day 8, but they decreased shortly after (Table 5.4.1 A). On average, 50% of bone marrow was maintained in OP9 cells at day 8, but this portion decreased with time (Table 5.4.1 A). Although no clear $CD45^+$ $CD19^+$ population was observed, promoted CD19 expression on day 12 and day 16 appeared in one of the passages of bone marrow and gastruloid cells (Table 5.4.1 B). CD11b and Ter119 were tested on another two passages, only one of which presented a $CD11b^+$ $Ter119^-$ gastruloid cell population on days 5, 8 and 12, suggesting possible myeloid differentiation (Figure 5.4.1).

A

	Bone marrow cells			Gastruloid cells		
CD45(%)	Day 8	Day 12	Day 16	Day 8	Day 12	Day 16
R1	98.93	99.02	21.28	70.77	89.00	2.49
R2	34.02	0.72	11.22	63.26	4.92	5.08
R3	39.03	8.91	3.23	4.37	7.29	1.71

B

	Bone marrow cells			Gastruloid cells		
CD19(%)	Day 8	Day 12	Day 16	Day 8	Day 12	Day 16
R1	0.98	37.60	37.5	1.20	50.00	39.76
R2	4.29	5.88	1.46	6.67	0.00	0.62
R3	5.16	0.63	0.80	1.14	16.39	0.99

Table 5.4.1. Summarised flow cytometry result of OP9 cell co-culture with the 216 hr gastruloid cells and bone marrow cells

The 216hr gastruloid cells and bone marrow cells were seeded on the OP9 cells. On days 8, 12 and 16, the expression of (A) CD45 (n=3) and (B) CD19 (n=3) on gastruloid cells and bone marrow cells were studied using flow cytometry with CD45-APC and CD19-PE/Cy7.

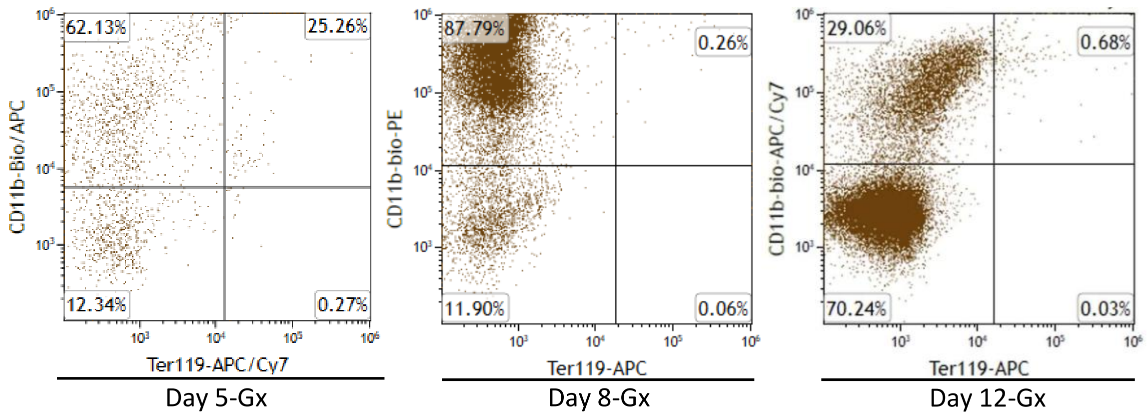

Figure 5.4.1. Flow cytometry results of OP9 cell co-culture of the 216 hr gastruloid cells on days 5, 8 and 12 (Ter119 vs CD11b)

Representative flow cytometry dot plots on OP9 cell co-culture of the 216 hr gastruloid cells on days 5, 8 and 12 for the expression of CD11band Ter119 cells (n=2). Gastruloid were stained with Ter119-APC, CD11b-Bio and Strepavidin-PE. Gx = gastruloid cells.

There was no detection of $CD4^+$ or $CD8^+$ cells in gastruloid-initiated co-cultures at any time point throughout the 16-day OP9-DL1 co-culture (n=3) (Figure 5.4.2). However, the bone marrow also failed to provide clear $CD4^+$ or $CD8^+$ cell populations, which suggests these cultures were not successful. OP9-DL1 cells used in this assay may have been exhausted thus failed to stimulate any haematopoietic differentiation. It remains inconclusive as to whether gastruloid cells have the T-cell lineages differentiation capability.

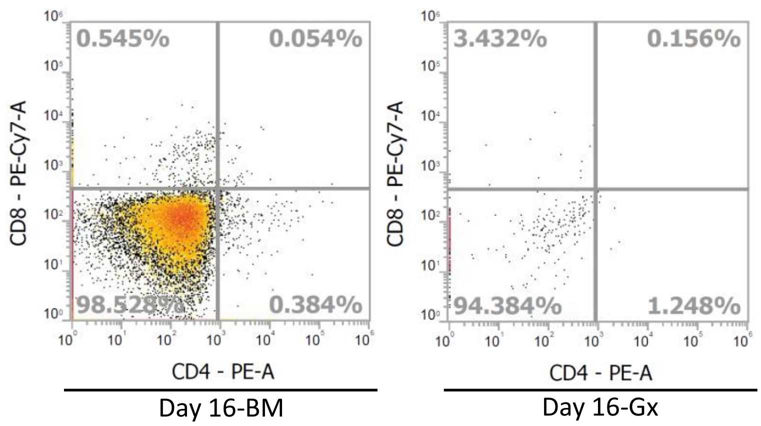

Figure 5.4.2. Flow cytometry results of OP9-DL1 cell co-culture of the 216 hr gastruloid cells on days 16 (CD4 vs CD8)

Representative flow cytometry dot plots on OP9-DL1 cell co-culture of the 216 hr gastruloid cells on day 16 for the expression of CD4 and CD8 (n=3). Gastruloids were stained with CD4-PE and CD8-PE/Cy7. Gx = gastruloid cells.

The discrepant results suggest that OP9 cells used in this assay might have been exhausted and not in a suitable state to stimulate haematopoietic differentiation, or perhaps more practice is required to perform no-trypsin passages to disaggregate cells by pipetting. However, the lymphohaematopoietic potential of the gastruloid cells and the enrichment of $CD45^+$ cells is occasionally visible in some passages. More repeats of this assay with new vials of OP9 and OP9-DL1 cells would further validate the lymphohaematopoietic potential of the haemogenic gastruloids.

5.4.2 Whole gastruloids showing engraftment to and $CD45^+$ cells survival at chick chorioallantoic membrane

The chick embryo chorioallantoic membrane (CAM) assay is a naturally immune-incompetent and reproducible model that has been widely applied in angiogenesis, tumour engraftment, toxicology, and xenograft studies (Ribatti, 2016). CAM is a membrane formed by fusing the mesodermal layer of the chorion with the outer mesodermal layer of the allantois E4 and E5 of embryonic development. The CAM then become a highly vascularised, non-innervated extra-embryonic membrane that can support the weight of the engraftment from E8 to E10 (Ribatti, 2016).

The CAM assay has also been applied in mouse stem cell xenograft studies. It has been discovered that chick embryos can form teratomas by microinjecting mouse ES cells (Haraguchi *et al*., 2015). Mouse ES cells were efficiently incorporated into the body and extra-embryonic tissues of chick embryos, where they formed small clusters. Mouse embryoid bodies were transplanted into the CAM and the implanted graft differentiated into a cluster of compacted epithelial-like cells and fibroblast-like cells. The CAM demonstrated an angiogenic response caused by grafting (Gajović & Gruss, 1998). These studies hint at the possibility of transplanting the whole mouse gastruloid into CAM to test its engraftment capability. Aside from the advantage of the CAM assay being a relatively simple, quick, and low-cost *in vivo* model, the CAM assay allows whole gastruloid engraftment, while mouse transplantation requires the gastruloid to be disassociated into a single-cell suspension for the injection.

The CAM assay has been applied to test if the gastruloid is capable of engrafting and surviving *in vivo*. This assay can provide valuable preliminary results before repeating the mouse transplantation, on whether the gastruloid (especially CD45 cells) can engraft *in vivo*, which is a pivotal criterion to demonstrate that the gastruloid cells can perform similarly as HSC progenitors. Following collection of the gastruloid at 216 hr, gastruloids were stained with Vybrant DiO-dye (Thermo Fisher) and transplanted into the windowed day-7 egg and cultured for another 7 days for the CAM assay (Figure 5.4.3; Figure 5.4.4 A and B). Live imaging was taken on day 14 of the CAM culture alongside further immunofluorescence staining with the CD45.2 PE antibody (Figure 5.4.4 C).

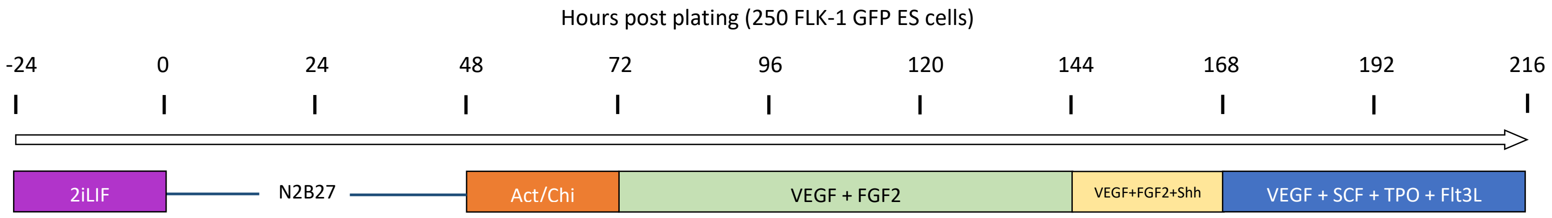

Figure 5.4.3. The culture scheme of gastruloids used to investigate if they can engraft in CAM assay.

In total, 18 eggs were cultured for the CAM assay, but only 8 of them survived the day following transplantation as eggs were eliminated due to contamination, eggshell cracks, or death. After 7-day CAM culture, four eggs had observable gastruloid engraftments on CAM. Perhaps if gastruloids failed to stick and remain on the CAM directly underneath the window at the beginning of the assay, since CAM is wobbly and the chick embryo is in motion, gastruloids may have been pushed to the side or even to the bottom of the egg, preventing the gastruloids from being accessible. Two eggs had gastruloids engrafted next to blood vessels, of which fluorescent images were taken (Figure 5.4.5). In total, five gastruloids were engrafted on CAM in these four eggs with only two of the gastruloids engrafted next to blood vessels. However, whether the gastruloid engraftment initiated the CAM to give an angiogenic response or these simply occurred by coincidence is inconclusive.

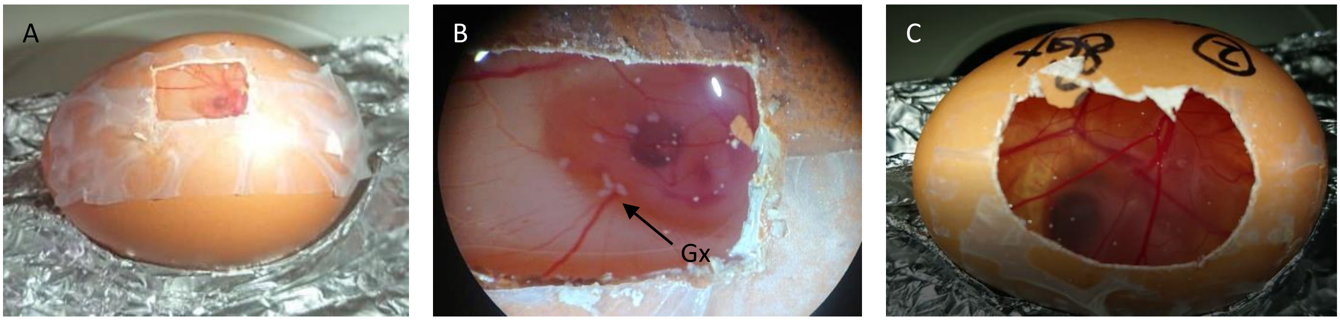

Figure 5.4.4. Images of the egg transplantation of gastruloid on day 0 and 7

(A) Windowed egg at day 0 for the CAM assay. (B) Gastruloid transplantation on the CAM at day 0 (magnification: 2x), Gx =gastruloid. (C) Gastruloid-transplanted egg to be harvested at day 7 for the CAM assay.

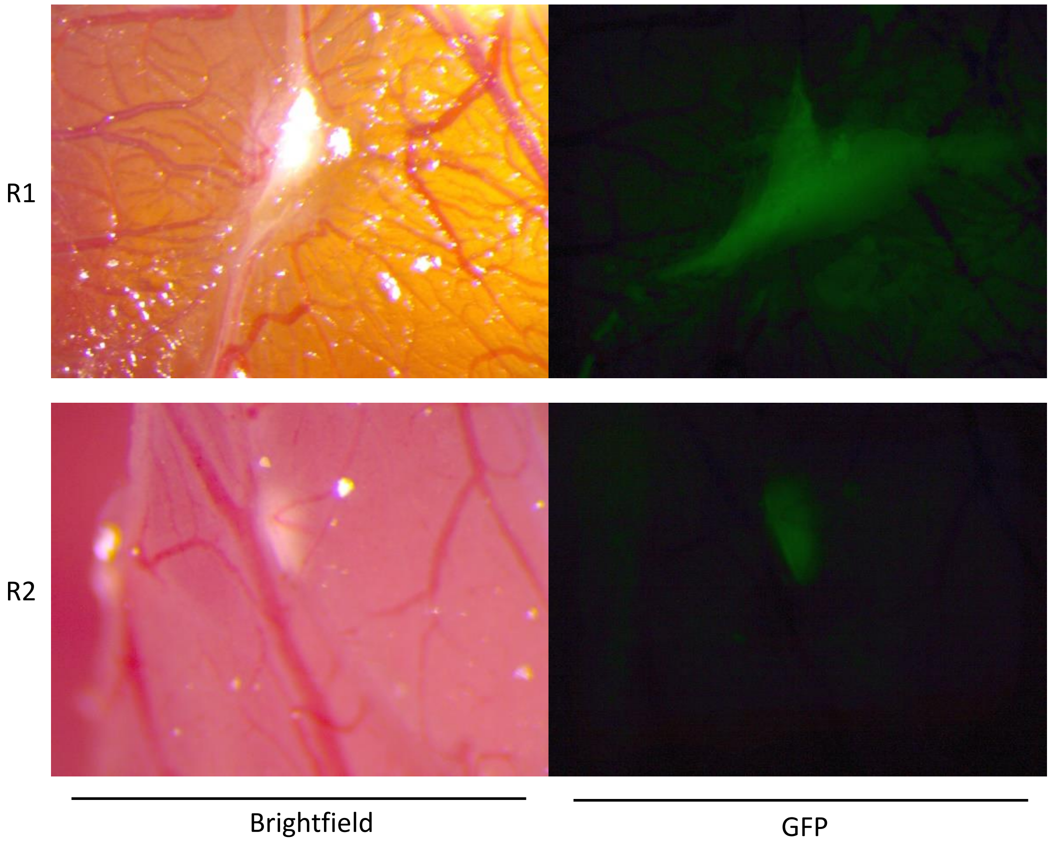

Figure 5.4.5. Fluorescence microscopic images of the gastruloid-initiated clusters on CAM in the egg after a 7-day culture

Gastruloids are stained with Vybrant DiO dye whichshows fluorescence under the GFP/488 channel of fluorescent microscopy (magnification:5x) (n=2).

The CAMs around the engrafted gastruloids were collected and stained with a CD45.2 PE antibody to visualise whether the gastruloid could maintain or expand the CD45^{+} population. Confocal imaging confirmed that the gastruloids engrafted near blood vessels. One CAM sample showed that the gastruloid collapsed and engrafted around the area close to the blood vessels (Figure 5.4.6). However, no CD45^{+} cells were found in these gastruloid micro-clusters on the CAM. The engrafted gastruloid formed an intact cluster for another CAM sample and a significant CD45^{+} cell population was maintained in the gastruloid cluster (Figure 5.4.7). This discovery is significant and positive as it proves that gastruloids can not only engraft on the CAM, but also that CD45^{+} cells from the gastruloid can survive and expand on the CAM if the gastruloid forms an intact cluster to provide a haematopoietic supportive niche.

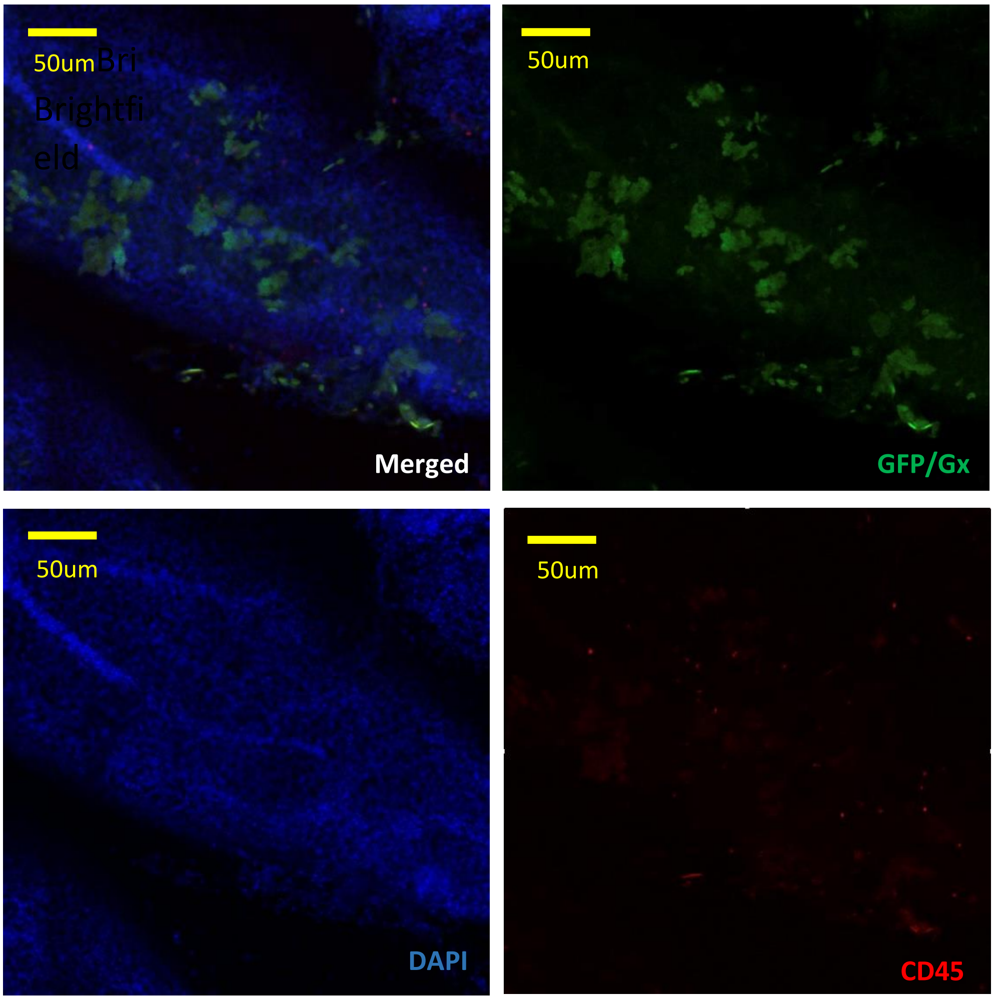

Figure 5.4.6. First confocal image of the gastruloid-initiated clusters on CAM in the egg after a 7-day culture

Gastruloid was stained with Vybrant DiO dye, DAPI and CD45-biotin antibodies and then with anti-rat Alexa-Fluor 568 (magnification: 20x).

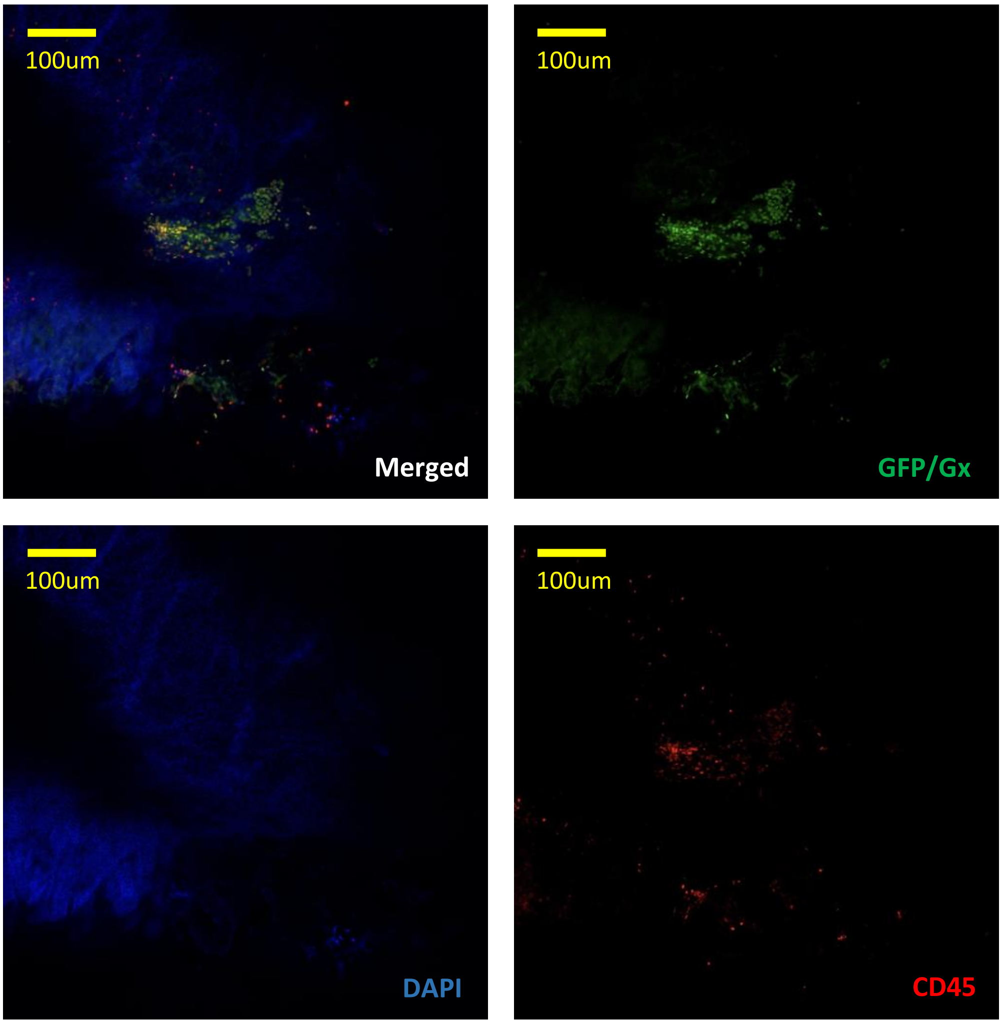

Figure 5.4.7. Second confocal image of the gastruloid-initiated clusters on CAM in the egg after a 7-day culture

Gastruloid was stained with Vybrant DiO dye, DAPI and CD45-biotin antibodies and then with anti-rat Alexa-Fluor 568(magnification: 10x).

5.4.3 No engraftment of the 192 hr gastruloid cells at non-irradiated c-Kit mutant mice

The previous bone transplantation assay (chapter 4.5) showed that gastruloid cells can have short-term bone marrow reconstitution as the CD45.2 cells from the injected gastruloid cells were maintained at the bone marrow of the irradiated mice. Although gastruloid cells cultured with the previous addition scheme only had slight short-term bone marrow reconstitution, it is worth conducting a mouse study on gastruloid cells cultured with the optimised protocol. From chapter 5.2, the addition scheme was optimised by removing the FGF_2 from 168 hr and adding SCF, TPO and Flt-3l. It is expected that gastruloids cultured with this updated protocol may have a better reconstitution capability than that represented in chapter 4.5.

In the previous mouse transplantation, lethally irradiated C57BL/6 (B6) mice were used as the host, while non-irradiated c-Kit mutant mice were used in the current animal transplantation study. C-Kit mutant mice have a hypomorphic mutation on the *c-kit* gene and have haematopoietic defects, which results in their bone marrow showing a decline in pro-B and pro-T cells followed by the loss of common lymphoid progenitors (Waskow *et al*., 2002). The c-Kit mutant mice were not irradiated to preserve their naïve haematopoietic niche for the engraftment of gastruloid lymphoidhaematopoetic cells. Additionally, no companion bone marrow cells were needed when using c-Kit mutant mice, to avoid the competition between the supporting bone marrow cells and gastruloid cells. These considerations made c-Kit mutant mice an ideal candidate to validate whether gastruloid cells could reconstitute into the bone marrow as if lymphoidhaematopoetic progenitors.

The 192 hr gastruloids were collected for the current mouse transplantation assay because gastruloids at 192 hr on average have more CD45 cells than those at 216hr and the CD45 cells at the 192hr may likely be less lineage committed. Gastruloids were disassociated to form a single-cell suspension and cells were injected into 15 c-Kit mutant mice without irradiation, with the assistance of Dr Natacha Bohin (Professor Kamil Kranc's Lab, Barts Cancer Centre) (Table 5.4.2). Each mouse received living gastruloid cells equivalent to 22.5 gastruloids, which contained around 413 $CD45^+$ cells. Four other non-irradiated c-Kit mutant mice were selected as the controls and received 10,000 $CD45.1^+$ $CD45.2^+$ bone marrow mononuclear cells each.

Five experimental and two control group mice were culled to discover whether spleen colony-forming cell (CFU-S) was presented on day 12. The CFU-S assay is a classic assessment for mouse transplantation experiments as CFU-S has been considered the most primitive HSPC capable of colony formation in the irradiated spleen since day 8. However, no colonies were visible on the spleen of either the experimental or control mice and it is presumed that an acute response to irradiation is required for colony formation at day 12 (Figure 5.4.8). Although bone marrow and spleen samples were collected and stained with CD45.1, CD45.2, B220 and CD11b antibodies, no clear sign of CD45.2 engraftment was found in any experimental samples (Figure 5.4.9 A). The control group presumably should contain CD45.1^{+} CD45.2^{+} bone marrow cells, but neither population has appeared in flow cytometry results (Figure 5.4.9 B). Although the CD45.2-PerCP antibody could have lost its specificity to CD45.2 cells, which may cause a silent CD45.2 signal, no colonies were observed on any spleens, validating the absence of the CD45.2 engraftment in the experimental mice (Figure 5.4.8; Figure 5.4.10 A and B).

Mouse	Condition	Day 12 CFU-S	Week 4 Bleeding	Week 7 Engraftment	Week 8 Bleeding	Week 10 Engraftment
48A	Experimental	✓				
48B	Experimental	✓				
48P	Experimental	✓				
48Q	Experimental	✓				
48R	Experimental	✓				
49A	Control	✓				
50D	Control	✓				
49C	Experimental		✓	✓		
49E	Experimental		✓	✓		
49F	Experimental		✓	✓		
49G	Experimental		✓	✓		
49B	Control		✓	✓		
48C	Experimental		✓		✓	✓
48D	Experimental		✓		✓	✓
48M	Experimental		✓		✓	✓
48N	Experimental		✓		✓	✓
48O	Experimental		✓		✓	✓
48L	Experimental		✓		✓	✓
50C	Control		✓		✓	✓

Table 5.4.2. Table showing the experimental details of the mouse engraftment study into non-irradiated cKit mutant mice

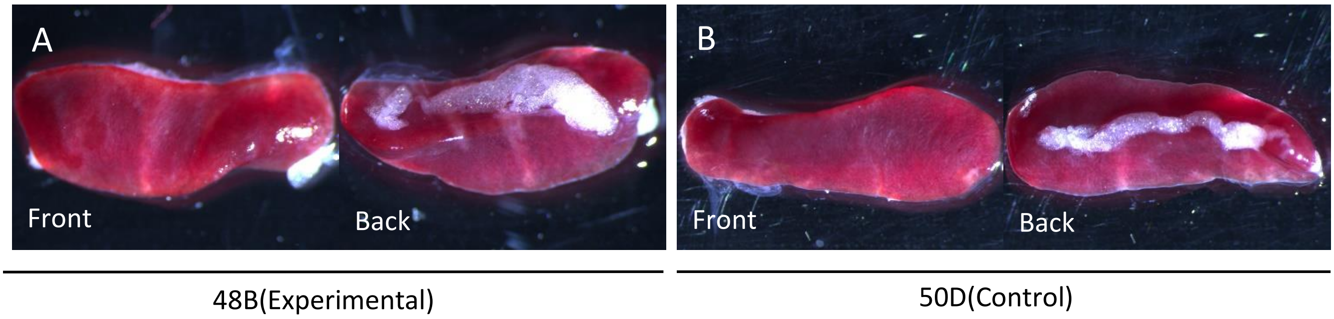

Figure 5.4.8. Images of the spleens collected on day 12.

Representative front and back images of spleen harvested from (A) experimental group (n=5) and (B) control group (n=2).

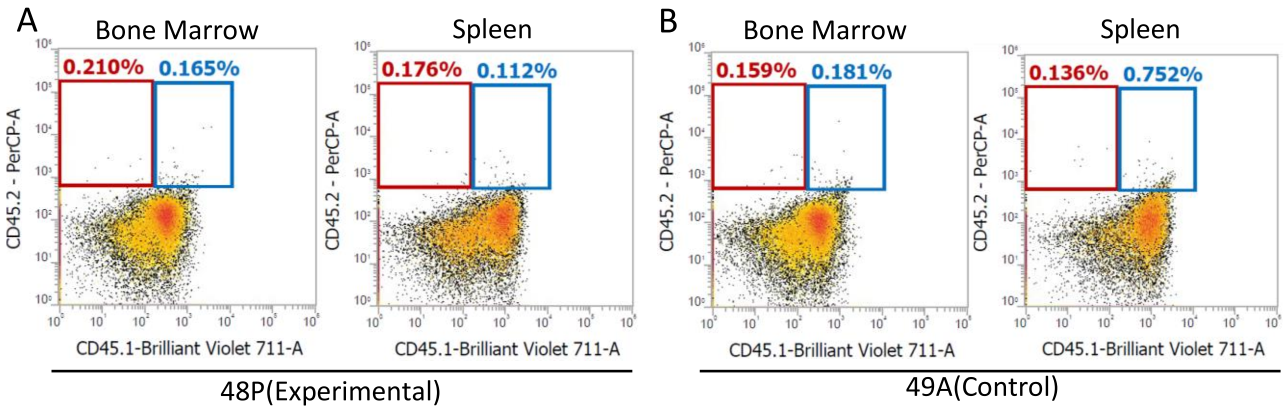

Figure 5.4.9. Flow cytometry result of bone marrow and spleen samples on day 12 for CFU-S assay

Representative flow cytometry results of (A) experimental group (n=5) and (B) control group (n=2) for the expression of CD45.1 and CD45.2 in the bone marrow and spleen on day 12 for the CFU-S assay. Bone marrow and spleen were stained with CD45.1-BV711 nad CD45.2-PerCP antibodies.

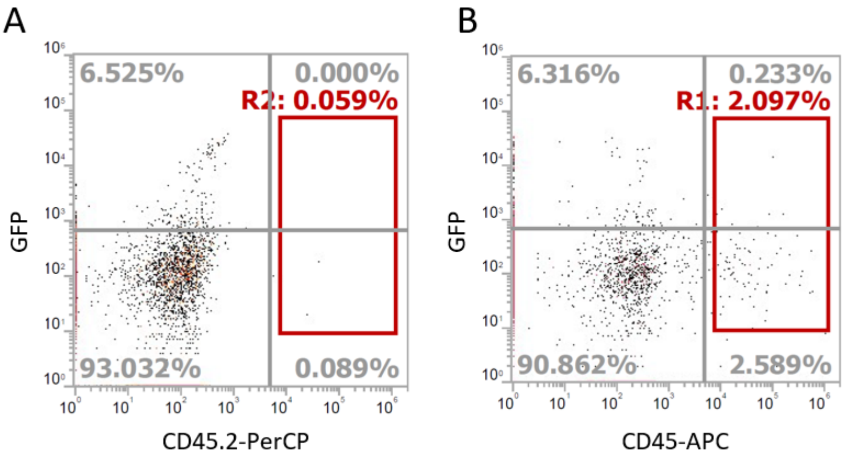

Figure 5.4.10. Flow cytometry results for validation of CD45.2-PerCP antibody

The 216hr gastruloid cells were individually stained with (A) CD45.2 PerCP antibody or (B) CD45-APC antibody for validating the binding of CD45.2 PerCP antibody using flow cytometry (n=2).

On week 4, under the supervision of Dr Natacha Bohin, bleeding was performed on all mice, which included ten experimental and two control mice. There were no significant $CD45.2^+$ cells from the gastruloids which presented in the peripheral blood of the mice, except 49F and 48D which had a very subtle group (Figure 5.4.11). Out of the two control mice, only the mouse 49B had a sign of engraftment, with a significant group of $CD45.1^+$ $CD45.2^+$ cells in its peripheral blood detected by flow cytometry.

On week 7, 5 experimental mice and a control mouse were culled to analyse the bone marrow and spleen. In the spleen of the control mouse 48B, a very promising $CD45.1^+$ $CD45.2^+$ population suggested the success of the bone marrow mononuclear cells in engrafting to the host's spleen (Figure 5.4.12). In the bone marrow of control mouse 48B, there was a much smaller, but still clear $CD45.1^+$ $CD45.2^+$ population (Figure 5.4.12). The $CD45.1^+$ $CD45.2^+$ population in bone marrrow and spleen of control mouse 48B was further gated and $B220^-$ $CD11b^+$ cells were observed, indicating the formation of myeloid linage progenitors. However, no engraftment was observed in the experimental group, either in the bone marrow or spleen, even for the mouse 49F, which appeared to have subtle engraftment in the peripheral blood at week 4 (Figure 5.4.11; Figure 5.4.13).

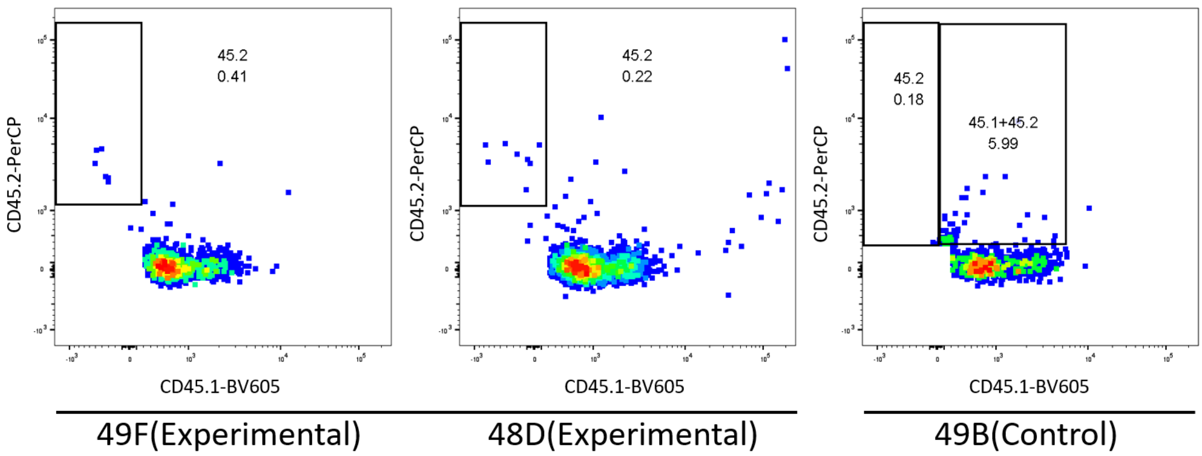

Figure 5.4.11. Flow cytometry result of peripheral blood cell samples on week 4 bleeding assay

Representative flow cytometry dot plots on the experimental mice (n=5) and control mouse (n=2) for the expression of CD45.1 and CD45.2 cells in peripheral blood on week 4. The peripheral blood samples were stained with CD45.1-BV605 and CD45.2-PerCP antibodies.

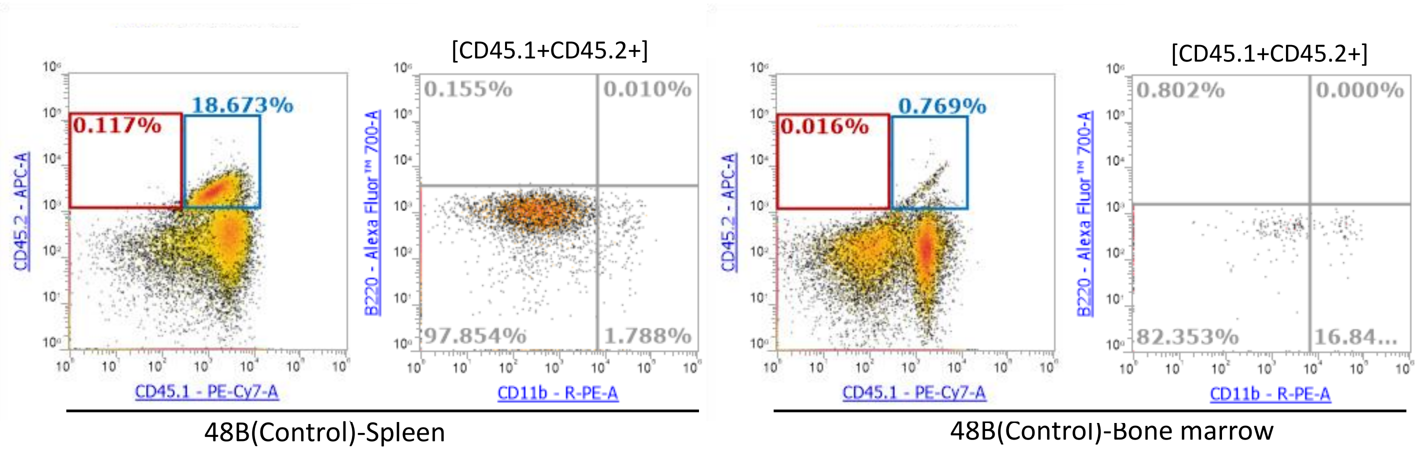

Figure 5.4.12. Flow cytometry result of bone marrow and spleen samples of control mouse 48B on week 7 short-term engraftment assay

Flow cytometry dot plots on the expression of CD45.1 and CD45.2, and the CD45.1$^+$ CD45.2$^+$ gated expression of B220 and CD11b in the spleen and bone marrow of the control mouse 48B on week 7. Bone marrow and spleen cells were stained with CD45.1-PE/Cy7, CD45.2-APC, CD11b-PE and B220-AF700 antibodies.

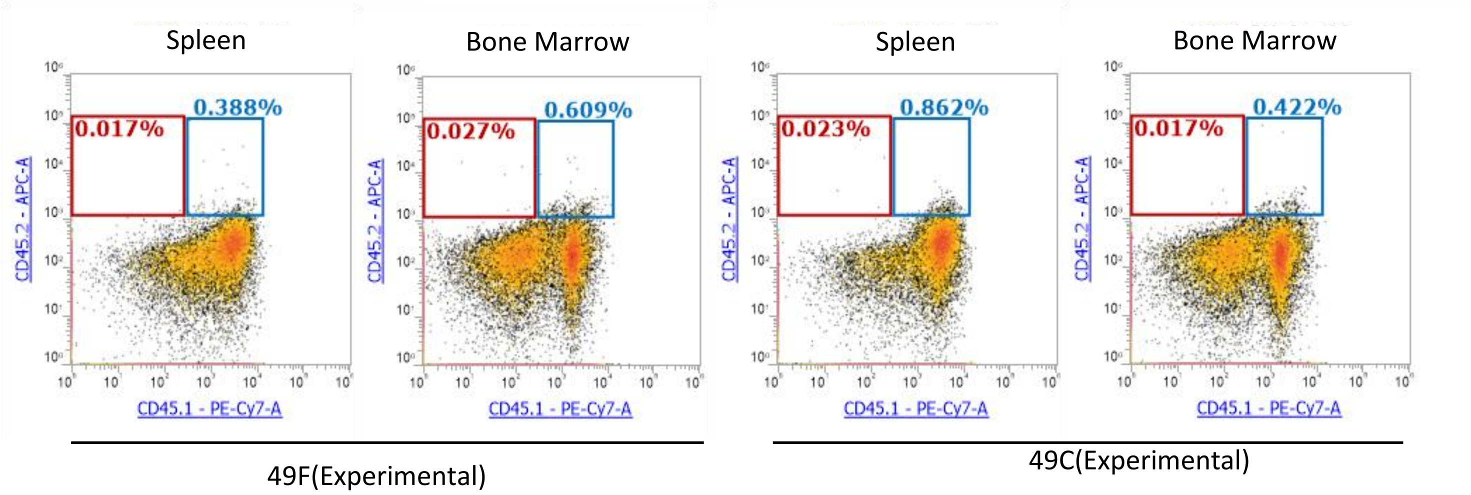

Figure 5.4.13. Flow cytometry result of bone marrow and spleen samples of 49C and 49F on week 7 short-term engraftment assay

Flow cytometry dot plots on the expression of CD45.1 and CD45.2 in the spleen and bone marrow of experimental mice 49C and 49F on week 7. Bone marrow and spleen cells were stained with CD45.1-PE/Cy7 and CD45.2-APC antibodies.

On week 8, bleeding was done on the remaining mice, including six experimental mice and a control mouse, with the assistance of Mr Andrea Tavosanis (Professor Kamil Kranc's Lab, Barts Cancer Centre). No experimental mice had CD45.2$^+$ cells, except for a very minor group in mice 48D and 48N (Figure 5.4.14). No experimental mice had promising results, suggesting that gastruloid cells could not engraft in the peripheral blood of the mice in either week 4 or week 8. Instead, an evident population of CD45.1$^+$ CD45.2$^+$ cells was present in the peripheral blood of control mouse 50C.

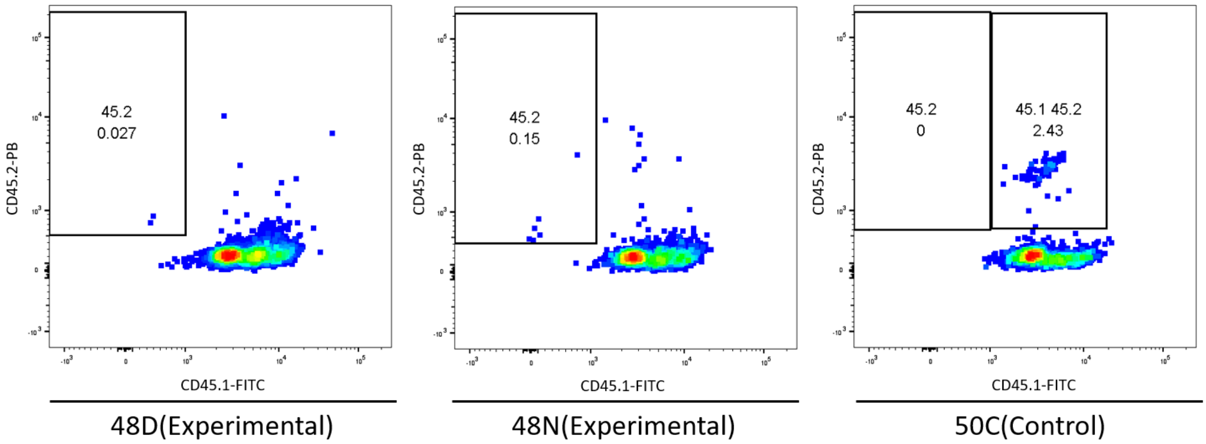

Figure 5.4.14. Flow cytometry result of peripheral blood cell samples on week 8 bleeding assay

Representative dot plot from flow cytometry on the experimental mice (n=4) and control mouse (n=1) for the expression of CD45.1 and CD45.2 cells in peripheral blood on week 8. The peripheral blood samples were stained with CD45.1-BV605 and CD45.2-PerCP antibodies.

On week 10, all remaining mice were culled, including six experimental mice and a control mouse. The control mouse (50C) had an obvious CD45.1^{+}CD45.2^{+} population in the bone marrow and spleen, but this population had declined in comparison to another control mouse (48B), which was culled on week 7 (Figure 5.4.12; Figure 5.4.15). The B220^{-} CD11b^{+} cells were maintained in the CD45.1^{+} CD45.2^{+} population from the spleen of control mouse 50C, and its percentage had almost doubled, suggesting that the myeloid potential of the control mouse had increased (Figure 5.4.12; Figure 5.4.15). None of the experimental mice had CD45.2^{+} cells in their bone marrow or spleen, with the exception of a very minor group in the spleen of mice 48M and 48N (Figure 5.4.16). However, the CD45.1^{+} CD45.2^{+} population was also present in the spleen of mice 48M and 48N, hinting that the CD45.2^{+} cells may simply be background staining. It is undetermined whether there is any long-term engraftment in the spleen of mice.

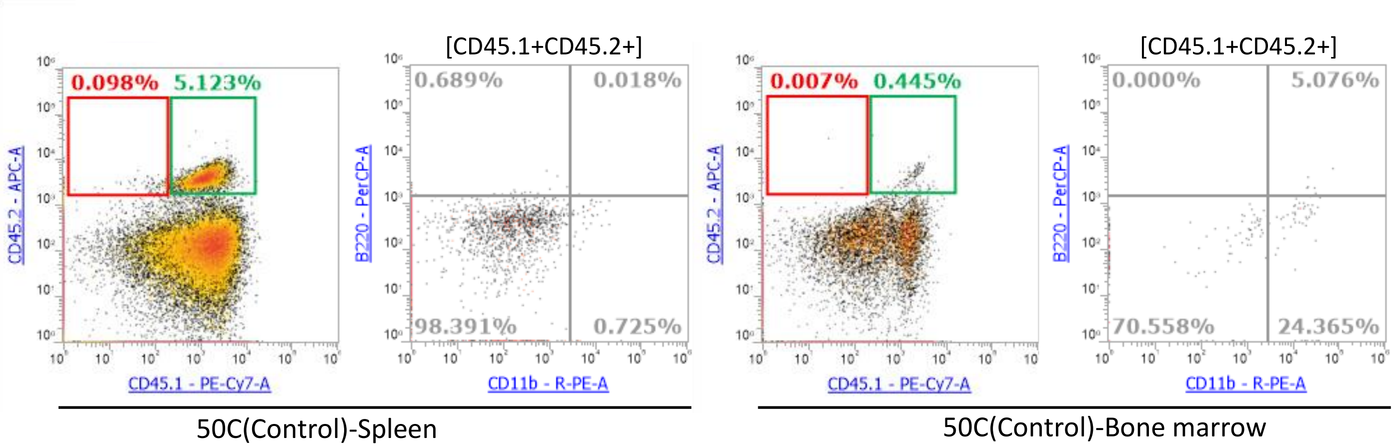

Figure 5.4.15. Flow cytometry result of bone marrow and spleen samples of control mouse 50C on week 10 long-term engraftment assay

Flow cytometry dot plots on the expression of CD45.1 and CD45.2, and the CD45.1⁺ CD45.2⁺ gated expression of B220 and CD11b in the spleen and bone marrow of the control mouse 50C on week 10. Bone marrow and spleen cells were stained with CD45.1-PE/Cy7, CD45.2-APC, CD11b-PE and B220-AF700 antibodies.

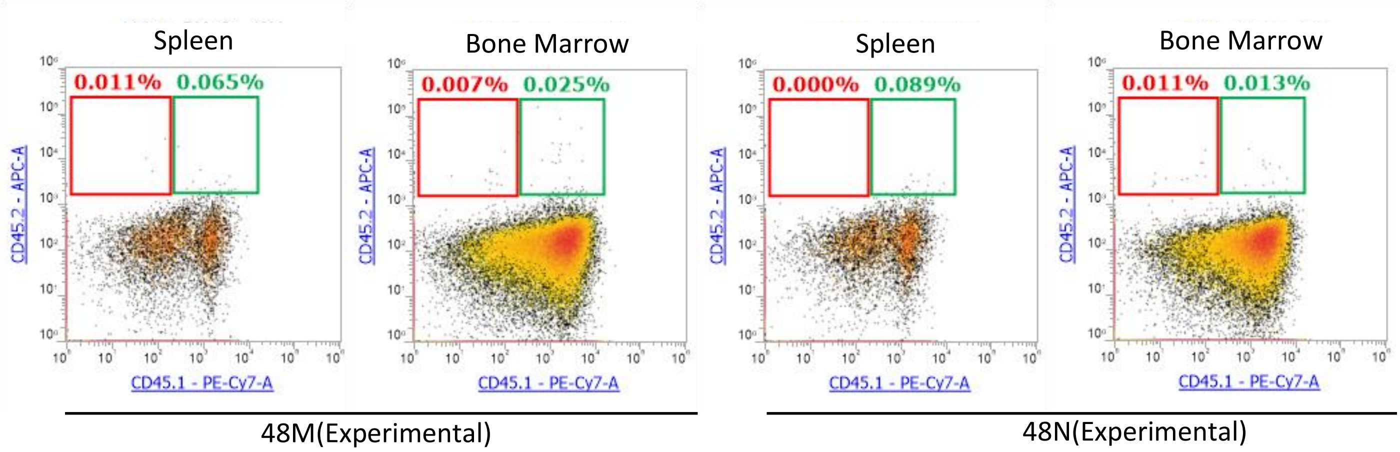

Figure 5.4.16. Flow cytometry result of bone marrow and spleen samples of 48M and 48N on week 10 long-term engraftment assay

Flow cytometry dot plots on the expression of CD45.1 and CD45.2 in the spleen and bone marrow of experimental mice 48M and 48N on week 10. Bone marrow and spleen cells were stained with CD45.1-PE/Cy7 and CD45.2-APC antibodies.

5.5 Conclusion

The cytokine schedule in the last 48 hours of this haemogenic gastruloid protocol has been optimised in this chapter. Although adding SCF and noggin could not promote haematopoietic potential in 144^{th} gastruloid chapter 3, their roles in early haematopoiesis are important thus they have been tested again in the last 48 hrs of the culture. However, they did not promote gastruloids to differentiate more $CD45^+$ cells no matter being added individually or together to the gastruloid. Instead, adding SCF together with TPO and Flt-3l to the gastruloid from 168 hr, can increase the haematopoietic potential and form more $CD45^+$ cells in the gastruloid at 216 hr suggesting a fine control of the haematopoietic niches is needed to stimulate the haematopoiesis in gastruloid

After optimising the cytokine schedule, further works focused on characterising the $CD45^+$ cells. The 192 hr and 216 hr gastruloids were individually disassociated to assess the $CD45^+$ cells in each gastruloid, which demonstrated that the $CD45^+$ cells produced in gastruloids at 192 hr are more diverse, while the 216 hr gastruloids output slightly fewer but more homogeneous $CD45^+$ cells. This result is helpful in determining which time point is the best for the second mouse engraftment study. The number of injected cells is one of the key success factors in mouse engraftment experiments. Although gastruloids produce $CD45^+$ cells with higher homogeneity at 216hr, occasionally the 192 hr gastruloids give more CD45 cells thus 192hr gastruloid will be applied in the second mouse engraftment experiments.

The CAM assay has been applied as a preliminary test before the second mouse engraftment, to confirm if gastruloid (especially CD45 cells) can survive and expand *in vivo*. Although The CAM assay indicated that gastruloids can expand on the vascular endothelium of the egg, and flow cytometry showed promising results of CD45 cells in gastruloid, the injected gastruloid cells still failed to show any signs of engraftment in the second mouse study. No conclusion can be drawn from the animal study on non-irritated c-Kit mutant mice, as it is believed that acute response to irradiation is required for gastruloid cells to form colonies and engraft in the mice. If engraftment study can be repeated, the irradiated C57BL/6 (B6) mice should be considered the optimised gastruloid protocol shall be used to culture gastruloid cells.

Even though the result from the second mouse engraftment study is inconclusive, the haematopoietic cluster in 216 hr gastruloid under confocal imaging and results from OP9 co-culture is fascinating as it evidences the lymphohaematopoietic potential and myeloid potential in the gastruloid. (de Pooter & Zúñiga-Pflücker, 2007).

The haemogenic gastruloid protocol has been finalised in this chapter, and several phenotypical and functional assays were performed to characterise the gastruloid at 216 hr and the $CD45^{+}$ cells. Altogether, these results have indicated that haemogenic gastruloids can not only form haematopoietic clusters similar to the mouse AGM, but also that $CD45^{+}$ cells demonstrate great lymphoid and myeloid potential. Although the animal study could not prove the engraftment capability of the gastruloid cells and OP9 culture was not stable enough to provide statistically robust results, the findings from this chapter are still significant and positive. Since the gastruloid protocol has been finalised, a holistic overview, such as studying the gastruloid over time, would help to estimate if this haemogenic gastruloid protocol can recapitulate the mouse AGM region and model definitive haematopoiesis.

Chapter	Main Findings
5.2.1	Culturing gastruloid with SCF or noggin at the last 48 hr could not promote the formation of CD45+ cells at 216hr.
5.2.2	FGF2 at the last 48 hr could not promote the formation of CD45+ cells at 216hr.
5.2.3	Adding SCF, TPO and Flt-3l together at the last 48 hr could not promote the formation of CD45+ cells at 216hr.
5.3.1	At 192hr, there are gastruloid-to-gastruloid variations in the expression of CD45, but it is more consistent at 216hr.
5.3.2	Gastruloid expresses haematopoietic markers, EPCR and Sca-1, at 216 hr
5.3.3	Gastruloid shows more defined cKIT+ and CD45+ haematopoietic clusters at 216 hr
5.4.1	The CD45 cells from gastruloid can be enriched and lymphohematopoietic marker, CD19, is occasionally expressed in OP9 co-culturing
5.4.2	Whole gastruloid can xeno-engraft and CD45+ cells can survive at chick chorioallantoic membrane.
5.4.3	Cells from 192 hr gastruloid cannot engraft at non-irradiated c-Kit mutant mice

Table 5.5.1. Summary of the main findings in chapter 5.

Chapter 6: Characterisation of haemogenic gastruloids across time from 120 to 216 hr

6.1 Introduction

In the previous chapter, experiments were focused on characterising the development of haematopoietic progenitors in the gastruloid over time.. In chapter 3, the CFC assay was carried out on the gastruloid cells collected at the 144 hr to investigate which cytokines could support more cells with haematopoietic colony-forming capability. The CFC assay was repeated on gastruloids collected from 120 to 216 hr to understand how the haematopoietic colony formation changed with time.

The haematopoetic markers including c-Kit, CD41, CD43 and CD45, were also holistically reviewed to study their expression across time from 96 to 216 hr. The Flk-1::GFP cell line was intensively used to form gastruloids throughout this doctoral project, but this finalised haemogenic gastruloid protocol has not been applied to other cell lines. Therefore, the protocol was applied to E14 cell lines and its derivative Tbra::GFP and on the KH2-based derivative, Sox-17::GFP cell line. The expression of several haematopoietic markers in the gastruloid generated with these cell lines were compared with the gastruloid made with Flk-1::GFP to confirm the transferability and reproducibility of this protocol to other cell lines.

The final experiment of this doctoral project was to use Smart-Seq2, a single cell mRNA sequencing protocol, to study the gene expression patterns of gastruloid cells down to a single cells level across time, from 120 to 216 hr. Additionally, the sequencing data can help to determine whether gastruloids and the AGM have similar haematopoietic signatures at the equivalent comparable time points.

6.2 Time course assessment of haematopoietic gastruloid

6.2.1 CFC assay on gastruloid cells from 120 to 216 hr

HSPCs are capable of differentiating into a full lineage of blood cells. It is helpful to examine the differentiation profile of gastruloid cells to determine whether haematopoiesis has taken place in the gastruloid culture and if the progenitors formed in the gastruloid can differentiate into other, more committed haematopoietic progenitors. The CFC assay is an *in vitro* assay to study the capability of hematopoietic progenitors to differentiate and has previously been used to optimise the cytokine cocktail.

The CFC assay was carried out to examine the change in haematopoietic potential of the progenitors from the gastruloid across time. Five gastruloids were cultured, collected and dissociated every 24 hours from 120 to 216 hr. The gastruloid cells were subsequently seeded in a methylcellulose medium for seven days. Colonies formed in the methylcellulose medium were counted after 7 days of culture, and representative images were taken under the microscope.

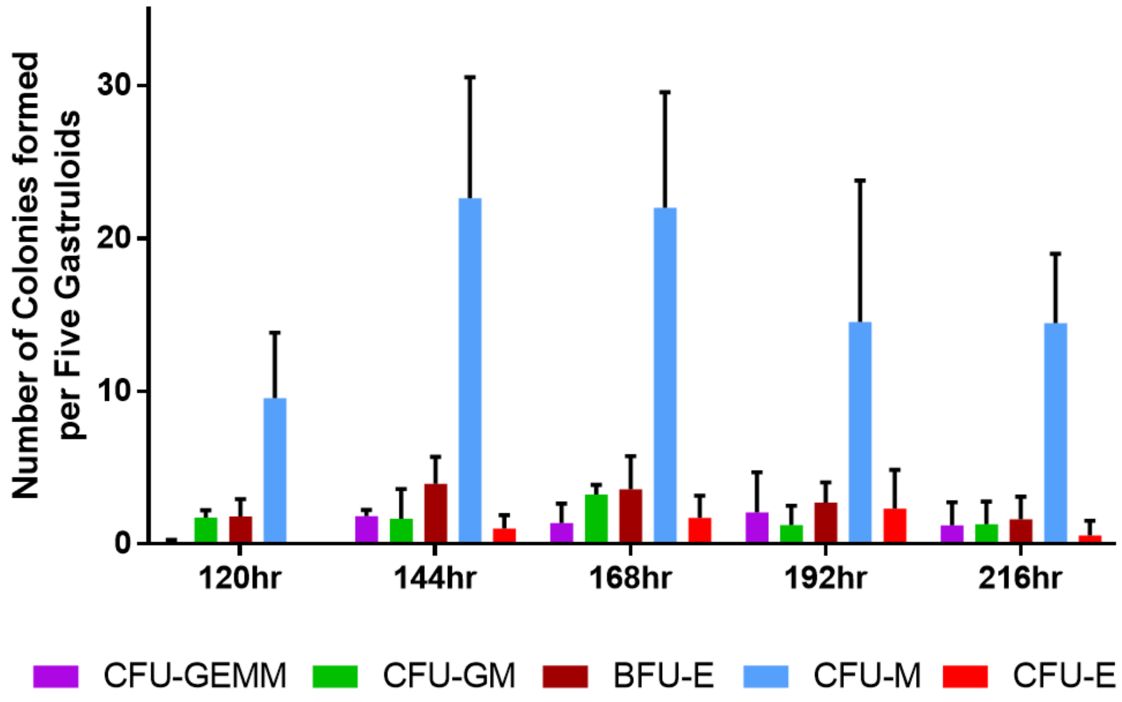

Figure 6.2.1. Summarised CFC assay result of colonies formed by gastruloid across time from 120hr to 216hr

The total number of colonies formed by gastruloids collected from 120 to 216 hr. (n=3, mean±SD). Five gastruloids were collected and plated for the CFC assay at each time point.

Gastruloids at 120 hr formed some CFU-GM and BFU-E colonies and an abundance of CFU-M colonies (Figure 6.2.1). Having both myeloid linage progenitors (CFU-GM and CFU-M) and erythroid lineage progenitors (BFU-E) formed at 120 hr proves gastruloids at this time point are capable of being committed to more than one linage. Gastruloids at 144 hr displayed more CFU-M colonies, and CFU-GEMM and CFU-E colonies began forming in the methylcellulose (Figure 6.2.1; Figure 6.2.2 A, B and C). The CFU-GEMM colony suggests that gastruloids at 144 hr can differentiate into multipotential progenitors. BFU-E is the precursor of CFU-E, and the formation of BFU-E proved that more committed progenitors are formed at this time point. CFU-E is considered to be the earliest erythroid precursor cell that eventually differentiates into erythrocytes.

The number of CFU-M and BFU-E colonies formed at 168 hr did not have significant change compared with 144 hr except the CFU-E, though slightly more CFU-GM and CFU-E colonies formed (Figure 6.2.1; Figure 6.2.2 D). Although CD45$^+$ cells first appeared in the gastruloid since 192 hr , 144hr and 168hr have the most colony-forming potentials among all time points.

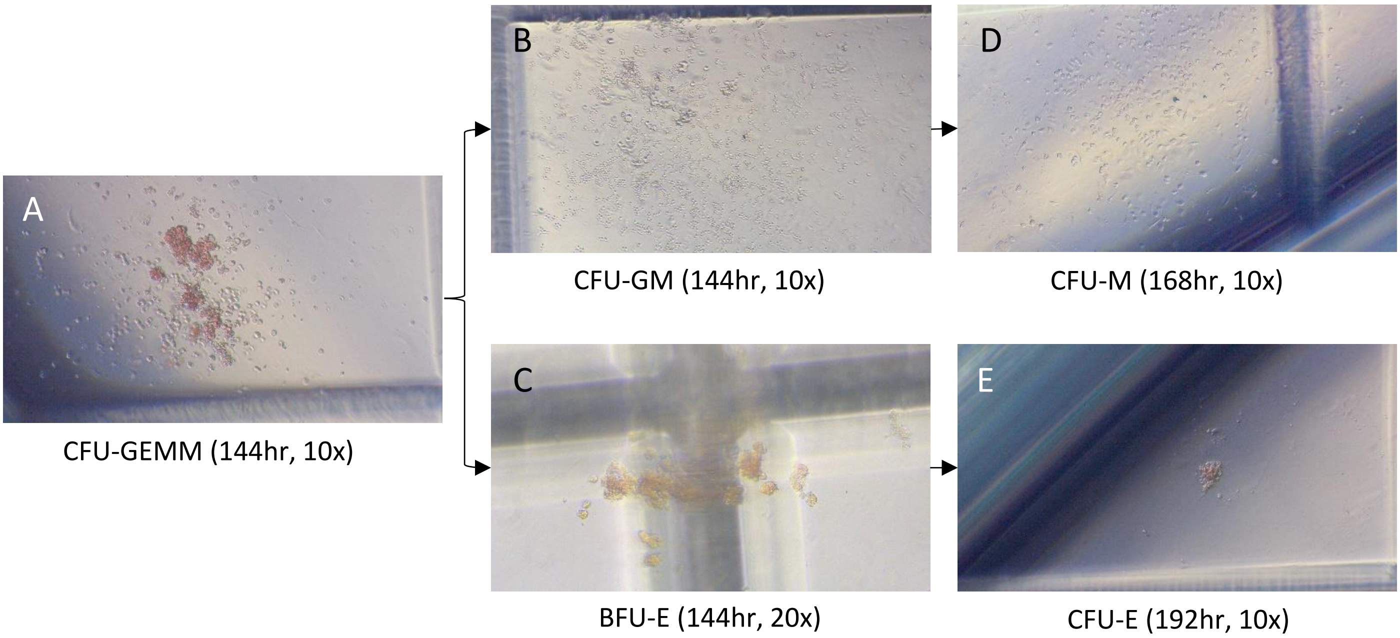

Figure 6.2.2. Representative images of colonies formed by gastruloid cells harvested during 120 to 216 hr.

(A) CFU-GEMM formed at 144 hr (magnification: 10x), (B) CFU-GM formed at 144 hr (magnification: 10x), (C) BFU-E formed at 144 hr (magnification: 20x), (D) CFU-M formed at 168 hr (magnification: 10x) and (E) CFU-E formed at 192 hr (magnification: 10x).

6.2.2 Characterisation of the haematopoietic markers in gastruloid cells across time from 96 to 216 hr

In chapter 3, flow cytometry analysis was carried out to optimise the cytokine addition scheme across 96 to 144 hr. By considering the expression of haematogenic cell surface markers (Flk-1, CD41, CD45, c-Kit and VeCAD) alongside the CFC assay, it was concluded that adding VEGF and FGF_2 to the gastruloid between 96 to 144 hr promoted haematopoiesis. After extending the haemogenic gastruloid protocol and further optimising it by including Shh, SCF, TPO and Flt-3l, it was expected that the updated protocol would be able to promote the establishment of the haematopoietic microenvironment. An overview of the progenitors formed throughout the protocol would reveal how closely the *in vitro* haemogenic gastruloid can resemble the haematopoietic activities in the AGM *in vivo*.

Gastruloids were cultured and collected every 24 hours from 96 to 216 hr. Dissociated gastruloid cells were stained with Sca-1, c-Kit, CD41, CD43 and CD45 antibodies to identify how the profile of haematopoietic progenitors changes across time. The analysis focused on the time-course expression of GFP^{low} cells, GFP^{high} cells, total c-Kit^+ cells, $CD41^+$ cells, $CD43^+$ cells, $CD45^+$ cells and Sca-1^+ cells from 96 to 216 hr. In addition, the expression profile of the subpopulations c-Kit^+ Sca-1^+ cells, $CD41^+$ c-Kit^+ cells, and $CD41^+CD43^+$ cells have been particularly studied to observe whether any haemopoietic progenitors emerge in the gastruloids.

Chapters 3.4 and 4.3 presented two GFP subpopulations, GFP^{low} and GFP^{high} in the gastruloid (Figure 6.2.3 A and B). The emergence of Flk-1/GFP^{low} began at 96 hr and reached the peak at 144 hr (Figure 6.2.3 B). After 144 hr, the Flk-1/GFP^{low} population steadily declined throughout the culture. GFP^{high} cells presented in the gastruloid 24 hours later than GFP^{low} cells, but its portion remained stable (2 to 4%) throughout the culture (Figure 6.2.3 A). Since both $CD41^+$ cells and $CD45^+$ cells belong to the GFP^{low} or GFP^- populations, although Flk-1^+ cells are regarded as mesodermal-lineage cells, only the GFP^{low} population is likely to contain precursors of haematopoietic stem cells, which have a long-term reconstitution capacity in mice (Haruta & Tokodoro, 2001).

Similar to the GFP^{low} population, the expression of c-Kit^+ cells increased with time and reached its peak at 144 hr (Figure 6.2.3 C). After which, the proportion of c-Kit^+ cells declined steadily with time and reached its lowest at 216 hr. c-Kit is a marker for progenitors and endothelial/haemogenic endothelial cells. Therefore, it can be regarded that the gastruloid cells increase their differentiation potential when the mesodermal linage is committed and reaches its peak when some of these mesodermal cells differentiate into CD41^{+} cells at 144 hr. After 144 hr, the gastruloid cells becomes more committed to various lineages causing the overall stemness decrease shown by the decline in c-Kit expression at the later time point of the culture.

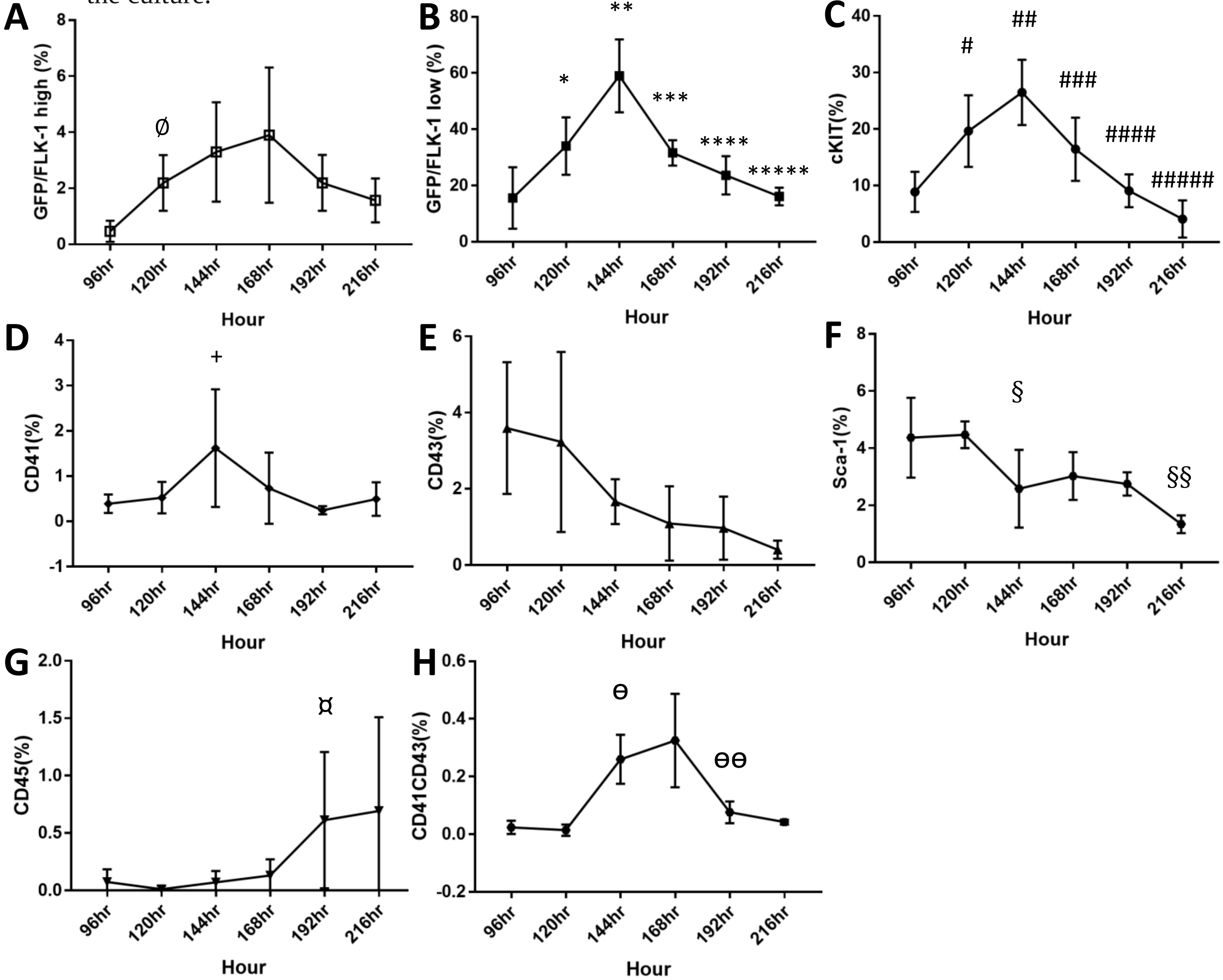

Figure 6.2.3. Overview the expression of haematopoietic markers in gastruloid from 96 to 216 hr

*Flow analysis on the expression of (A) GFP^{high} (n=6, , mean$\pm$SD, student's t-test p=0.0067 Ø at 120 hr), (B) GFP^{low}(n=7 to 13, mean$\pm$SD, student's t-test p=0.0051 * at 120 hr, p<0.0001 ** at 144 hr, p<0.0001 *** at 168 hr, p=0.0096 **** at 192 hr, p=0.0189 at 216hr), (C) c-kit^{+}(n=8 to 12, mean$\pm$SD, student's t-test p=0.0096 # at 144 hr, p=0.0096 ## at 144 hr, p=0.0001 ### at 168 hr, p=0.0046 #### at 192 hr, p=0.0013 ##### at 216 hr), (D) CD41^{+}(n=9 to 14, mean$\pm$SD, student's t-test p=0.0404 + at 144 hr), (E) CD43^{+}(n=6 to 9), (F) Sca-1^{+}(n=5 to 6, mean$\pm$SD, student's t-test p=0.0343 § at 144 hr, test p=0.0003 §§ at 216 hr), (G) CD45^{+}(n=9 to 15, mean$\pm$SD, student's t-test p=0.0091 ¤ at 192 hr) and (H) CD41^{+} CD43^{+} cells (n=5, mean$\pm$SD, student's t-test p<0.0001 ɵ at 144 hr, p=0.0118 ɵɵ at 192 hr) in the gastruloid over time from the 96 to 216 hr. All t-tests were conducted by comparing with the previous time point.*

CD41 is regarded as a critical marker for the transition of hemogenic endothelial cells to a hematopoietic cell fate, and a previous study demonstrated that $CD41^+$ cells began to present in the gastruloid at 144 hr (Figure 3.4.12) (Swiers *et al*., 2013). This time-course analysis generated similar results, that the expression of $CD41^+$ cells reached the peak at 144 hr (Figure 6.2.3 D). The expression of $CD41^+$ cells at 144 hr was highly variable, suggesting that not all gastruloids generate $CD41^+$ cells which implies the heterogeneity of gastruloid cells to form pro-HSCs. Apart from at 144 hr, $CD41^+$ cells were also observed at 168 hr, indicating that the wave of $CD41^+$ progenitor cells/pro-HSCs is likely not a single transient event, but a repeated, continuous process that may happen across 144 to 168 hr and even later (Figure 6.2.3 D).

CD43 is the marker which defines type 1 pre-HSCs in definitive haematopoiesis and a marker of multipotent haematopoietic progenitors in yolk sac haematopoiesis (Inlay *et al*., 2014). CD43 expression is not only related to definite haematopoietic stem cells as a marker of type 1 pre-HSCs ($CD41^+$ $CD43^+$), but is also considered to be related to yolk sac haematopoiesis, in which the $CD43^+$ c-Kit^{high} $Sca1^+$ $CD11A^-$ cells emerging at the E9.5 yolk sac can form erythromyeloid and lymphoid cells (Inlay *et al*., 2014). In the gastruloids, $CD43^+$ cells had the highest expression at 96 hr, which declined during 120 to 144 hr and faded out gradually until the end of the cultures (Figure 6.2.3 E). Since the $CD41^+$ cells were only present in the gastruloids at 144 hr, the $CD43^+$ cells at 96 and 120 hr were probably related to yolk sac haematopoiesis. In addition, $CD41^+$ $CD43^+$ cells were only observed during 144 and 168 hr, suggesting that the $CD41^+$ cells (pro-HSCs) formed in 144 hr have transitioned into $CD41^+CD43^+$ cells (type 1 pre-HSCs) at 168 hr (Figure 6.2.3 H).

Sca-1^+ cells rose since 96 hr, and its expression dropped along with the $CD43^+$ cells at 144 hr (Figure 6.2.3 F). The proportion of Sca-1^+ gastruloid cells remained stable during 144 and 192 hr, but further decreased when it reached 216 hr. Since CD43 has high expression at 96 and 144 hr, the $CD43^+$ cells were further gated to check their expression of Sca-1 and c-Kit. This result indicates that a majority of the $CD43^+$ cells in these 48 hours were $CD43^+$ c-Kit^+ $Sca1^+$ cells, suggesting they may be related to yolk sac haematopoietic progenitors (Inlay *et al*., 2014) (Figure 6.2.4 A). In addition, this also explains the result from the CFC assay. The formation of erythroid (BFU-E), myeloid (GFU-M), and other multipotential progenitor colonies at 120 hr likely originated from the $CD43^+$ c-Kit^+ $Sca1^+$ yolk sac haematopoietic progenitors (Figure 6.2.1). Lastly, since the c-Kit^+ Sca-1^+ population was significant at 192 and 216 hr, they were gated to check their CD43 expression. The result demonstrated that

90% of this c-Kit$^+$ Sca-1$^+$ population do not express CD43, suggesting these populations at 192 and 216 hr are not related to yolk sac haematopoietic progenitors. Alternatively, they mark the endothelial cells with the possibility of becoming haemogenic progenitors, such as LSK cells if they pick up other haematopoietic markers in the future (Figure 6.2.4 B).

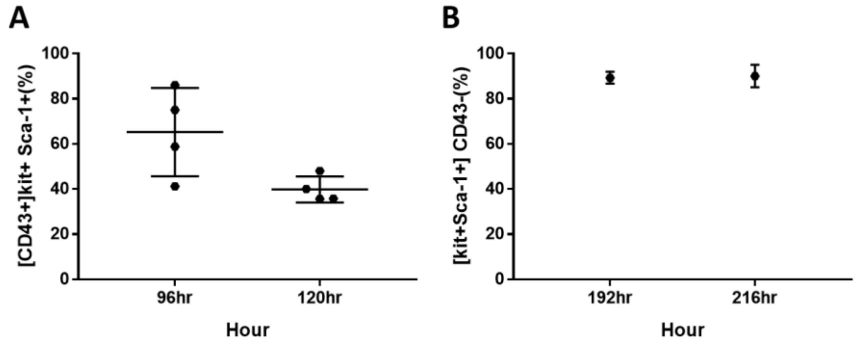

Figure 6.2.4. Comparison of the CD43 expression of cKit$^+$ Sca-1$^+$cells emerged at the early and late culture of haematopoietic gastruloid

Summarised flow analysis result on the (A) CD43$^+$ gated expression of cKit$^+$ Sca-1$^+$ cells in the gastruloid at 96 and 120 hr, and the (B) cKit$^+$ Sca-1$^+$ gated expression of CD43$^-$ cells in the gastruloid at 192 and 216 hr (n=4 or 5).

CD45 is a critical marker for definitive haematopoiesis, which characterises the formation of type 2 pre-HSCs. The time-course experiments showed that gastruloid cells gave rise to CD45$^+$ cells from 192 hr and were maintained at 216 hr, which is consistent with the results from previous chapters (Figure 6.2.3 G). However, the percentage of CD45$^+$ cells at 192 and 216 hr had no significant difference. When summarising the results regarding CD45$^+$ cells at 192 and 216 hr, the peak of CD45 expression could be reached at either of these two time points, suggesting that batch-to-batch and gastruloid-to-gastruloid variation still exists (Figure 5.3.1; Figure 6.2.3 G).

In summary, the time course results from flow cytometry suggest that haematopoietic events, similar to definitive haematopoiesis in the AGM region, occurred in gastruloids cultured with this haemogenic gastruloid protocol (Figure 6.2.5). At 96 hr, mesodermal endothelial cells first formed in the gastruloid, which is implied by the Flk-1/GFP merging at 96 hr (Figure 6.2.6 A). In the following 24-hour, ETH probably happened, meaning that endothelial cells transited to haematopoietic progenitor cells by forming the haemogenic endothelium, shown by the c-Kit$^+$ Flk-1$^+$ cells at 120 hr (Figure 6.2.6 B). At 144 hr, CD41$^+$ cells were generated, and such CD41$^+$ Flk-1$^+$ cells can be regarded as closely related to pro-HSCs, which are formed in the mouse AGM region at E9 (Figure 6.2.6 C). Pro-HSCs are believed to differentiate into type 1 pre-HSCs, which co-express CD41 and CD43 and such CD41$^+$ CD43$^+$ cells were observed in the gastruloid at 144 and 168 hr (Figure 6.2.6 D). Type 2 pre-HSCs, characterised with CD45, formed at 192 and 216 hr indicating that definitive haematopoiesis occurred during 192 and 216 hr by type 1 pre-HSCs (CD41$^+$ CD43$^+$) transforming into type 2 pre-HSCs (CD45$^+$) (Figure 6.2.6 E and F).

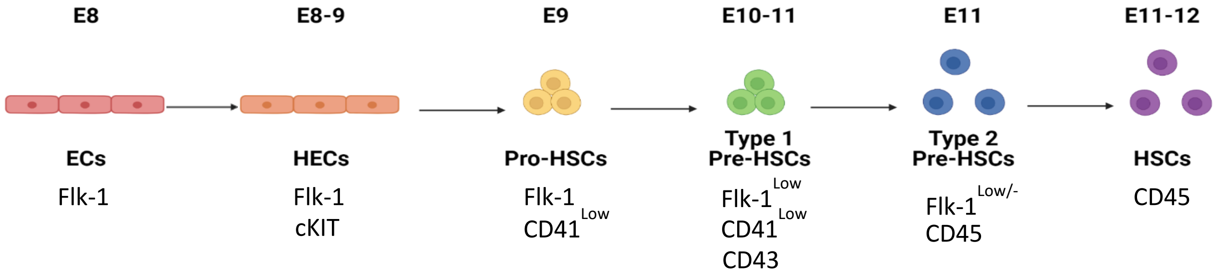

Figure 6.2.5. Stepwise specification of early embryonic haematopoietic progenitor cells at the intra-aorta cluster in the AGM.

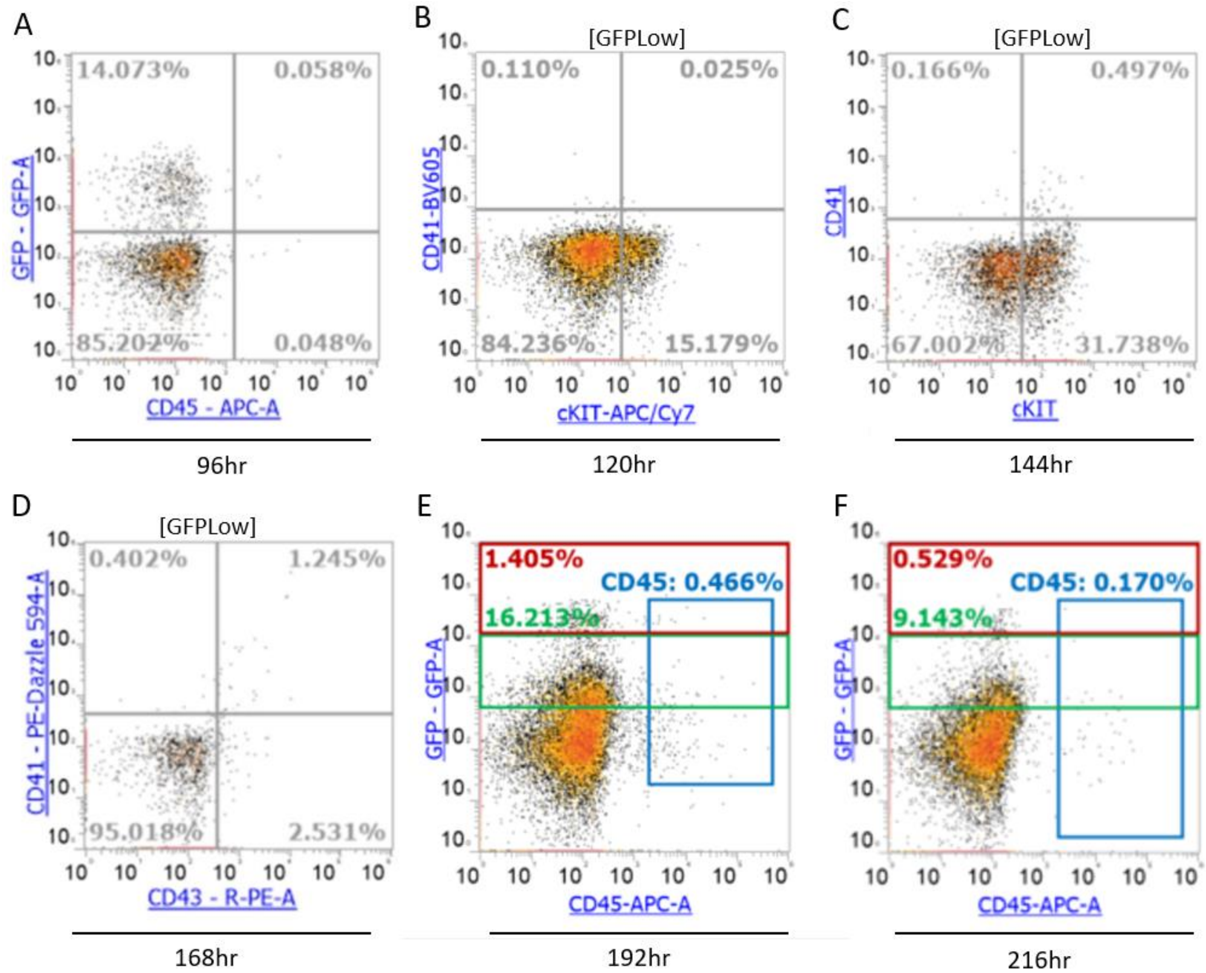

Figure 6.2.6. Representative results of flow analysis illustrating stepwise specification of early embryonic haematopoietic progenitor cells in gastruloid across time

Representative images of flow analysis on the (A) expression of GFP$^+$ cells at 96 hr, (B) GFP^{Low} gated c-Kit$^+$ cells at 120 hr, (C) GFP^{Low} gated CD41$^+$ c-Kit$^+$ cells at 144 hr, (D) GFP^{Low} gated CD41$^+$ CD43$^+$ cells at 168 hr, (E) CD45$^+$ cells at 192 hr and (F) CD45$^+$ cells at 216 hr.

6.2.3 Adaptation of gastruloid protocol into other embryonic stem cells line across time: E14

In this study, the Flk-1::GFP cell line was intensively used as it expresses GFP fluorescence when *Flk-1* transcriptional activities are upregulated. The initiation of Flk-1 expression is an essential marker of mesodermal differentiation, followed by the haematopoietic transition. The Flk-1::GFP ES cell line is generated by inserting the eGFP reporter into the initiation codon of the *Flk-1* locus of the mouse ES cell line E14TG2a. This E14 cell line is the most used, well-characterised, and widespread ES cell line and is often used in stem cell studies. In order to understand if this haemogenic gastruloid protocol, developed mainly on the Flk-1::GFP ES cell line, is applicable to another cell line, the E14 cell line was used to make gastruloids. A time-course study on the expression of CD41, c-Kit and CD45 in the E14 cell line-made gastruloids and Flk-1::GFP cell-generated gastruloids was studied from 120 to 216 hr.

Flow cytometry demonstrated that the E14 cell line-made gastruloids were slightly less committed to forming haematopoietic stem cell progenitors than the Flk-1::GFP cell line-made gastruloids. The E14 cell line could only generate a smaller portion of CD41^{+} cells than the Flk-1::GFP cell line throughout the culture (Figure .6.2.7 A; Figure 6.2.8). The E14 cell line-generated gastruloids also showed marginally, but not statistically significant, less CD45^{+} cells (p=0.0941) (Figure 6.2.7 C; Figure 6.2.9). However, the peak of CD41^{+} cells at 144 hr and that of CD45^{+} cells at 192 hr was still observed, indicating that the wave of pro-HSCs and type 2 pre-HSCs presented in the E14 cell line-made gastruloids (Figure 6.2.7). The E14 cell line-made gastruloids demonstrated similar endothelial signatures as the Flk-1::GFP cell line-made gastruloids, which showed similar expression of c-Kit^{+} cells throughout the culture, except for 144 hr (Figure 6.2.7 B). Altogether these results show that the Flk-1::GFP cells were likely more committed to the mesodermal/endothelial linage, resulting in more pro-HSCs and type 2 pre-HSCs than E14 cells.

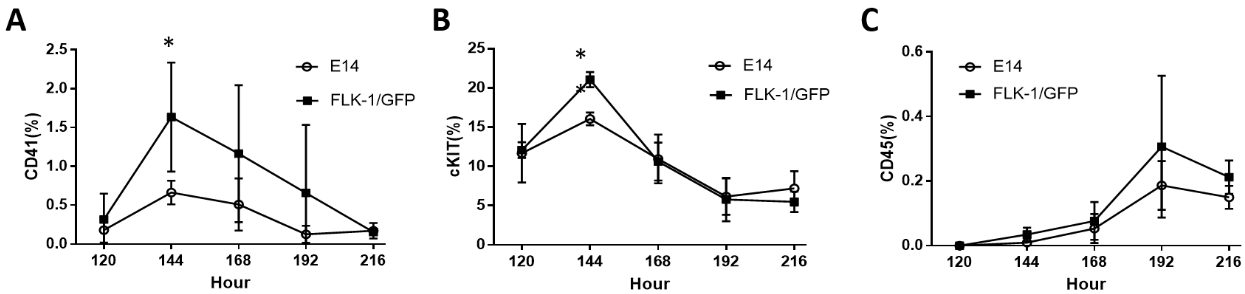

Figure 6.2.7. Summarised flow cytometry results on the expression of CD41, cKit and CD45 in E14 and FLK-1::GFP made gastruloid across time

*Flow analysis on the expression of (A) CD41$^+$, (B) c-Kit$^+$ and (C) CD45$^+$ cells in the E14 cell line-made gastruloids and Flk-1::GFP cell line-made gastruloids over time from 120 to 216 hr (n=5, mean±SD, student's t test p=0.0485 * at CD41 at 144 hr, p=0.0024 ** at c-Kit at 144 hr). All t-tests were conducted by comparing with Flk-1::GFP cell line-made gastruloids in the same time point.*

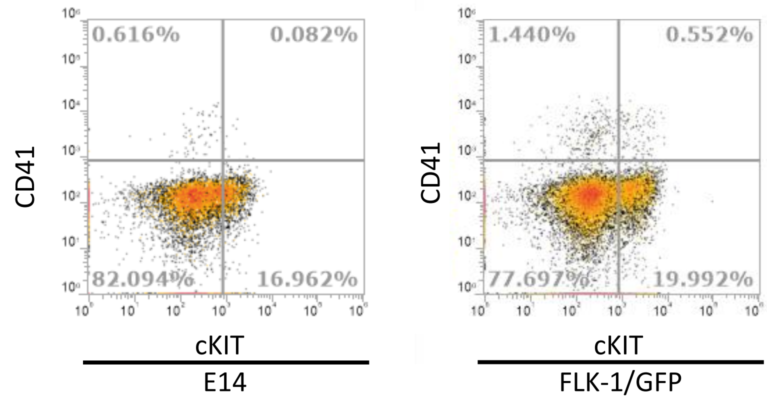

Figure 6.2.8. Flow cytometry dot plots of expression of CD41 and cKit in E14 and FLK-1::GFP made gastruloid at 144hr

Representative images of flow cytometry on the expression of CD41 and c-Kit in the E14 cell line-made gastruloids and Flk-1::GFP cell line-made gastruloids at 144 hr. Both gastruloid cells were stained with CD41-PE Dazzle 594 and cKIT-APC/Cy7.

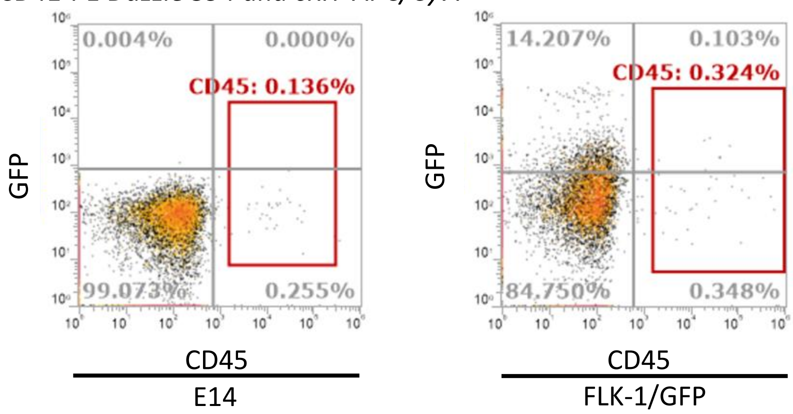

Figure 6.2.9. Flow cytometry dot plots of expression of CD45 in E14 and FLK-1::GFP made gastruloid at 216hr

Representative images of flow cytometry on the expression of CD45 in the E14 cell line-made gastruloids and Flk-1::GFP cell line-made gastruloids at 216 hr. Both gastruloid cells were stained with CD45-APC.

The 216 hr E14 cell line-made gastruloids were taken for confocal imaging to study if there was any emergence of CD45^{+} c-Kit^{+} pre-HSCs and the formation of AGM-like clusters comparable to those formed in Flk-1::GFP gastruloids. Although E14 had not been inserted with any eGFP sequence, the confocal image demonstrated that there were CD45 and c-Kit signals in the E14 gastruloid (Figure 6.2.10; Figure 6.2.11). The c-Kit^{+} cells had outlined a lumen structure and some c-Kit^{+} cells co-expressed a CD45 signal, reassembling the result from the confocal imaging of 216 hr Flk-1::GFP cell line-made gastruloids (Figure 5.3.7).

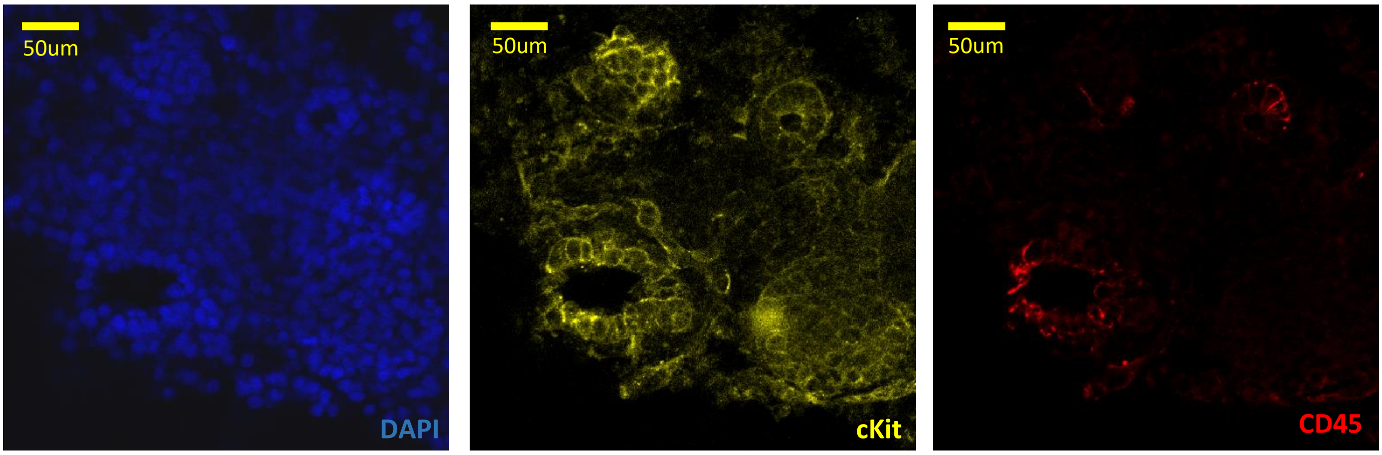

Figure 6.2.10. Localisation of the AGM-like cluster in 216 hr E14 cell line-made gastruloids.

Confocal images of a whole-mount immunostained gastruloid showing DAPI (blue),c-Kit (yellow) and CD45 (red) expression. (Magnification: 20x) (scale bar: 50um). Gastruloid was first stained with goat anti-mouse cKit-biotin and rat anti-mouse CD45-biotin antibodies and then with anti-goat Alexa-Fluor 633 and anti-rat Alexa-Fluor 568.

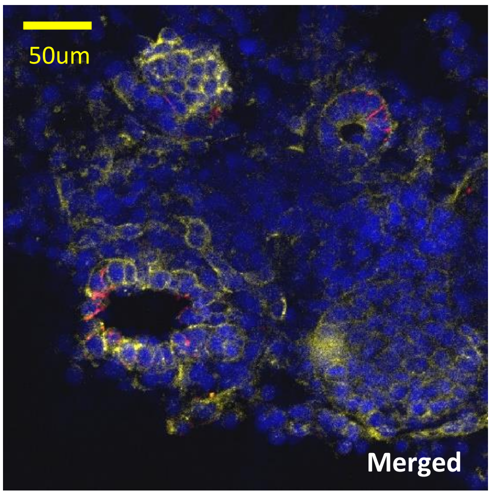

Figure 6.2.11 Merged confocal images of immunostained gastruloid from Figure 6.2.10

Merged confocal images of a whole-mount immunostained gastruloid showing DAPI (blue) GFP (green) c-Kit (yellow) and CD45 (red) expression. (Magnification: 20x) (scale bar: 50um).

6.2.4 Adaptation of gastruloid protocol into other embryonic stem cells line across time: Tbra::GFP and Sox17::GFP

Two other cell lines, Tbra::GFP and Sox17::GFP, were used in other gastruloid studies, thus it would be worth studying the expression of these two genes in the haemogenic gastruloid (Van den Brink *et al*. ,2014; Turner *et al*., 2017). Brachyury (Tbra) plays a vital role in establishing the anterior-posterior axis in the embryo and defining the mesoderm during gastrulation (Marcellini *et al*., 2003). Tbra is essential in establishing the embryonic mesodermal progenitor niche and consequently is regarded as an early mesodermal marker (Martin & Kimelman, 2010). Sox17 is an endodermal marker necessary for the morphogenesis of the gut endoderm and the assembly of the basement membrane which separates the endoderm and mesoderm in the gut (Viotti *et al*., 2014). Sox 17 can also facilitate the *in vitro* differentiation of primitive and definitive endoderm from mouse embryonic stem cells (Qu *et al*., 2008).

As a well characterised and common cell line and being developed into the Flk-1::GFP cell line, the mouse E14 cell line has also been developed to be the TBra::GFP ES cell line, which expresses GFP fluorescence when the *Tbra* gene is initiated. Sox-17::GFP is a cell line developed from the mouse KH2 ES cell line, which expresses GFP fluorescence when the *Sox17* gene is initiated. The expression of Tbra and Sox17 in the ordinary gastruloid protocol were studied. Under conditions that promote the formation of the embryonic mesoderm in embryos, gastruloids exhibited polarised expression of Sox17 and Tbra, and the Tbra expression declined and was restricted to the tip of the gastruloid (van den Brink *et al*., 2014). Since Sox-17::GFP is a cell line derived from KH2 ES cell line, trying the haemogenic gastruloid protocol on Sox-17::GFP cell line can show that this protocol is not only limited to the E14-based cell line.

Tbra::GFP, Sox17::GFP, and Flk-1::GFP cell lines were used to generate gastruloids, and time-course studies on the expression of GFP in these three cell line-made gastruloids were performed from 72 to 216 hr. At 216 hr, gastruloids were collected to study the expression of GFP and CD45. At 72 hr, the Sox17::GFP and TBra::GFP cell line-made gastruloids displayed similar expression of GFP (Figure 6.2.12 A). However, Sox-17/GFP expression (green) was stably maintained in the gastruloids throughout the culture, while Tbra/GFP expression (blue) reached the peak at 96 hr and rapidly diminished within the following 48 hours, when Flk-1/GFP expression (red) peaked at 144 hr (Figure 6.2.12 A). These results demonstrate that gastruloids cultured with the haemogenic gastruloid protocol express Tbra and Sox-17 as the ordinary gastruloid protocol (van den Brink *et al*., 2014).

The timing of the decline of Tbra$^+$ cells also fit well with the formation of Flk-1$^+$ cells, suggesting the differentiation of Tbra$^+$ mesodermal precursors into Flk-1$^+$ common mesodermal progenitors (Figure 6.2.12 A). Sox-17 contributes to the maintenance of haematopoietic cell clusters in the midgestation AGM region, and the SoxF protein is pivotal in controlling the fate decision of HSCs between differentiation and self-renewal during foetal haematopoiesis (Nobuhisa *et al*., 2014). The stable expression of Sox-17 in gastruloids may reassemble the formation of SoxF proteins in the intra-aortic clusters, further indicating the haematopoietic potential of the gastruloid. Finally, the CD45 expression in gastruloids generated with these cell lines did not significantly differ, indicating that gastruloids made with Tbra::GFP and Sox-17::GFP cell lines showed comparable haematopoietic potential as Flk-1::GFP-made gastruloids (Figure 6.2.12 B; Figure 6.2.13). In addition, gastruloids made with the KH2 cell line derivative (Sox-17::GFP) were capable of generating CD45$^+$ cells indicating that this haemogenic gastruloid protocol is not only applicable to the E14 cell line and its derivatives (Tbra::GFP and Flk-1::GFP), but is also transferable to use on other ES cell lines.

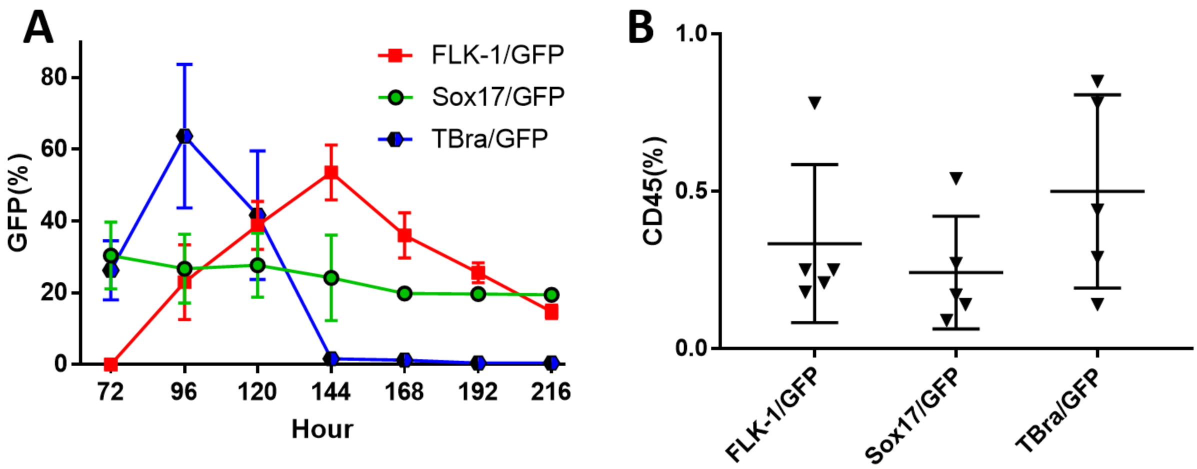

Figure 6.2.12. Summarised flow cytometry results on the expression of GFP across time and CD45 at 216hr in Sox-17::GFP, TBra::GFP and FLK-1::GFP made gastruloid

(A) Flow analysis on the expression of GFP in the Flk-1::GFP (red), Sox-17::GFP (green) and TBra::GFP (blue) cell line-made gastruloids over time from 72 to 216 hr (n=2). (B) Summarised result of flow cytometry on the expression of CD45 in the Flk-1::GFP, Sox-17::GFP and TBra::GFP cell line-made gastruloids at 216 hr after staining with CD45-APC antibody (n=5, mean±SD, student's t test, p=0.5235 at Sox17/GFP and p=0.3771 at Tbra/GFP).

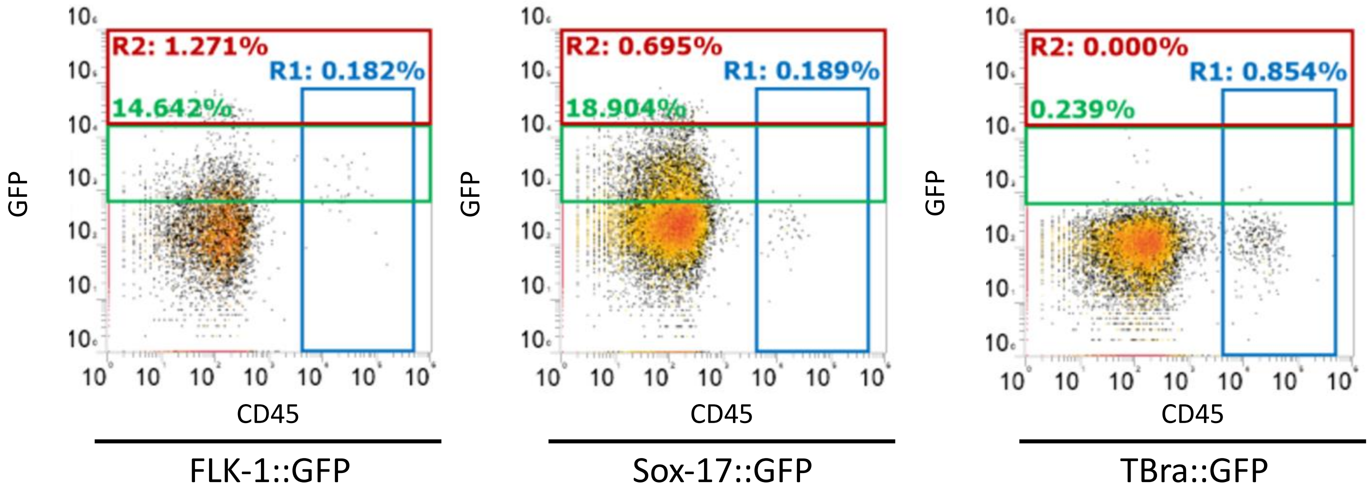

Figure 6.2.13. Flow cytometry results on expression of CD45 in Sox-17::GFP, TBra::GFP and FLK-1::GFP made gastruloid at 216hr

Representative flow cytometry dot plots on the expression of GFP and CD45 in the Flk-1::GFP, Sox-17::GFP and TBra::GFP cell line-made gastruloids at 216 hr (n=5). All gastruloids were stained with CD45-APC antibodies

6.3 Single-cell SMART sequencing

6.3.1 Quality control and construction of a single-cell clustering atlas

Throughout the project on developing the haemogenic gastruloid culture protocol, the gastruloids have been assessed and well characterised with a range of phenotypical analyses and functional assays. These analyses confirmed that the progenitors developed from gastruloids have myeloid- and lymphoid-haematopoietic potential and that the haemogenic gastruloid could recapitulate definitive haematopoiesis from haemogenic endothelial cells to type 2 pre-HSCs, and AGM-like haematopoietic clusters. However, except for the preliminary qPCR analysis on the 120 hr gastruloid, no molecular assays have been applied later than that. Thus, transcriptional changes taking place in the gastruloid after 120 hr remain unknown.

From the qPCR analysis, the gastruloid exhibited upregulated expression of haematopoietic and endothelial markers, which supports the potential of developing the gastruloid for haematopoietic research. Nevertheless, even if additional qPCR analyses were applied to analyse the gastruloids cultured at a later time point, qPCR can only provide limited information of the transcriptional activities, not an overview, which is needed to define the haematopoietic programmes developing in the gastruloids and to compare them with the mouse AGM region.

In order to provide a holistic overview of the gene profile of the gastruloid, gene sequencing analysis was conducted to profile the whole gastruloid cells and sorted gastruloid cells across time (Table 6.2.1). Data were processed and analysed by Dr Gabriel Torregrosa Cortés from Universitat Pompeu Fabra.

Plate	Time	Haematopoetic markers
P1	120hr	Whole Gx populations
P2	144hr	Whole Gx populations
P3	144hr	$CD41^+$ cells
P4	144hr	$Ckit^+$ $Sca\text{-}1^+$ cells
P5	168hr	Whole Gx populations
P6	192hr	Whole Gx populations
P7	192hr	$CD45^+$ cells
P8	192hr	$Ckit^+$ $Sca\text{-}1^+$ cells
P9	216hr	$CD45^+$ cells

Table 6.3.1 Details of the plates sent out fo single-cell SMART sequencing analysis

List of plates of gastruloid cells sent to Centro Nacional de Análisis Genómico for single-cell SMART sequencing analysis. Gx = gastruloid cells.

All samples were first checked with quality control, and they passed the test with low rates of doublets (plot with UMI counts) and <0.1% reads mapping to mitochondrial DNA (Figure 6.3.1). On average, the gene counts of the whole gastruloid had around 3000 to 4000 genes per gastruloid cell, and the 120 hr gastruloid cell displayed nearly double the gene counts (6000 to 8000 cells), and the bimodal distribution can be seen on the plot with UMI counts (Figure 6.3.2; Figure 6.3.1 D). Since the 120 hr is a critical time point for EHT and the emergence of the haemogenic endothelium, it is a stage of lineage diversification involving the priming of many differentiation programmes, resulting in the boost in gene count.

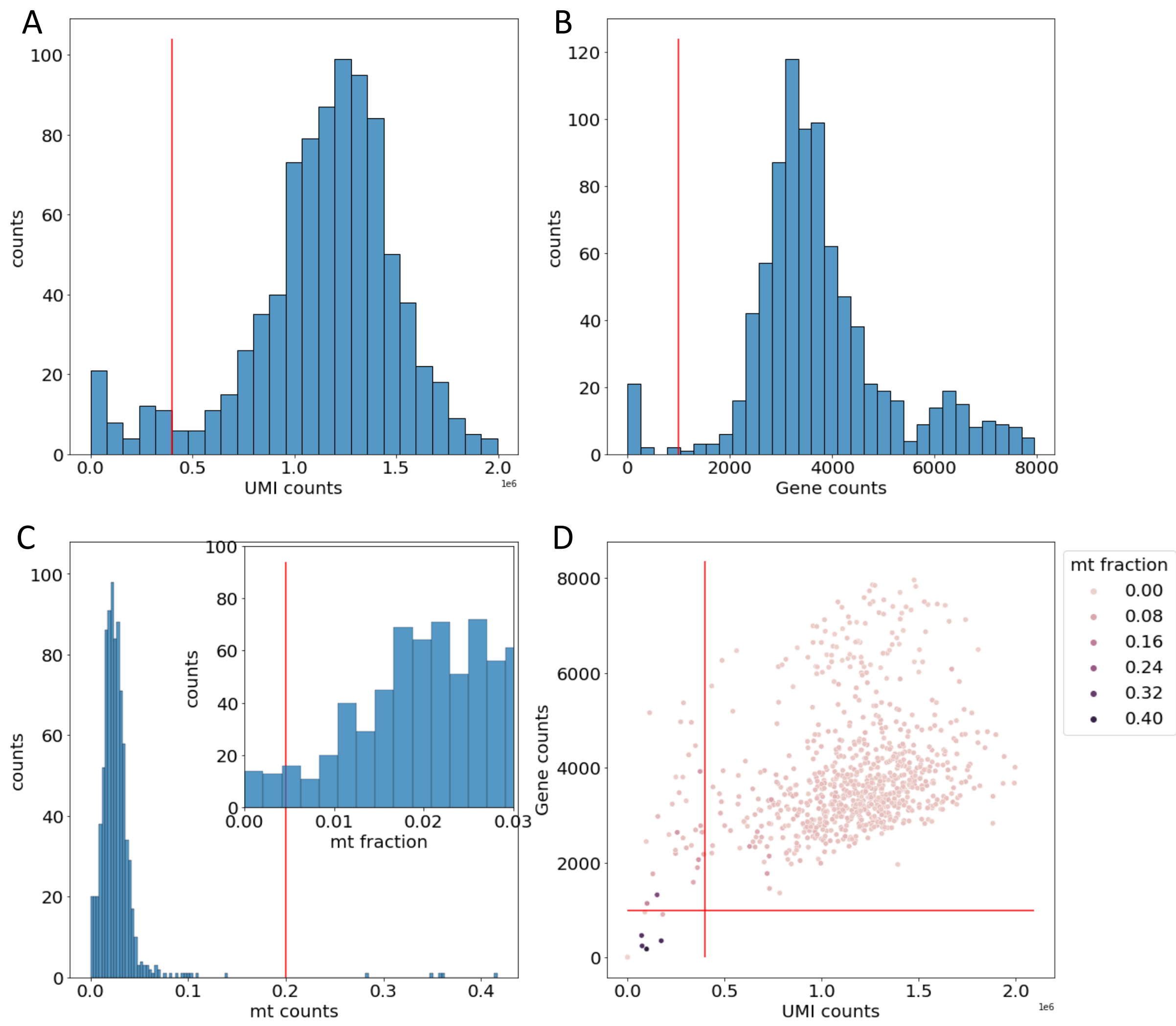

Figure 6.3.1. Plots of quality control metrics with gastruloid samples.

(A) Histogram of the number of unique molecular identifiers (UMIs) detected per cell. (B) Histogram of the number of genes detected per cell. (C) Histograms of mitochondrial (MT) count per cell. The smaller histogram is zoomed-in on MT ratio below 0.03. (D) Number of genes versus the number of UMI coloured by the MT ratio.

After quality control of the gastruloid samples, the gene counts of all cells were normalised to the mean number of gene counts and scaled to log1p to only represent changes in gene expression. The Seurat algorithm with default properties was applied to select the highly variable genes (Satija *et al*., 2015). The elbow method selected the first 10 principal components (PCs) in both the whole and sorted gastruloid subsets as they explain the significantly higher degrees of variance in the data.

The selected data were considered for clustering and differential gene expression analysis. The data from whole gastruloid cells were studied together over time, and the sorted gastruloid cells of c-Kit, CD41 and CD45 at the various time points were considered specifically. These data were projected in 2D, and the UMAP plots of the two data sets were shown with highlighted clusters (Figure 6.3.2 to 6.3.5).

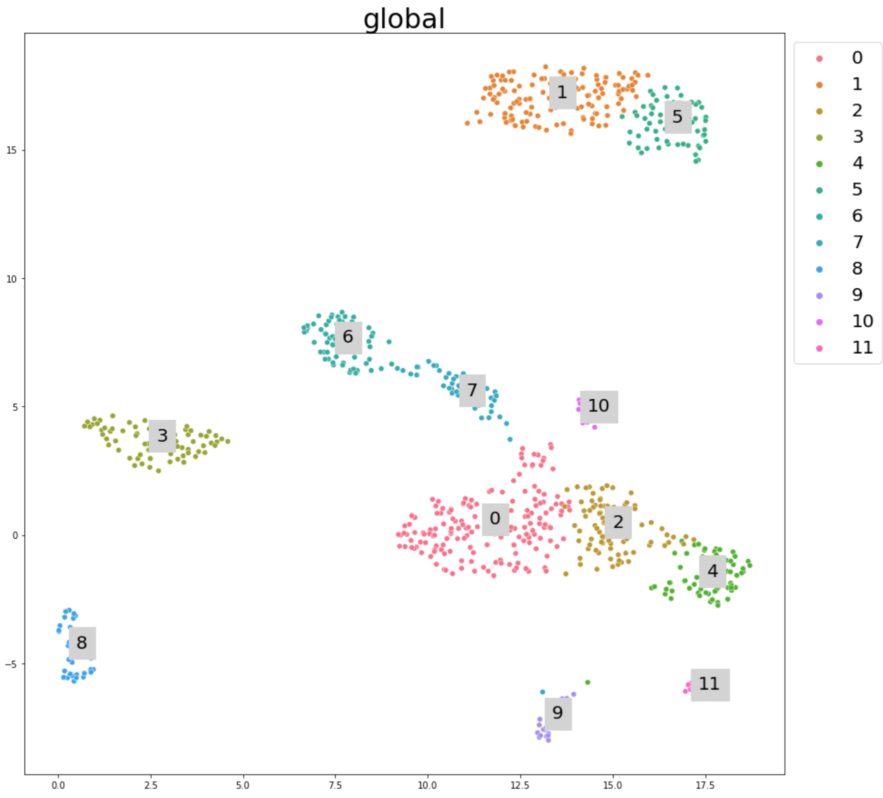

Figure 6.3.2. UMAP plot of the clustering in the whole gastruloid cells data

UMAP plot of the clustering was performed with the Leiden algorithm with a resolution of 0.5 on whole gastruloid cells data.

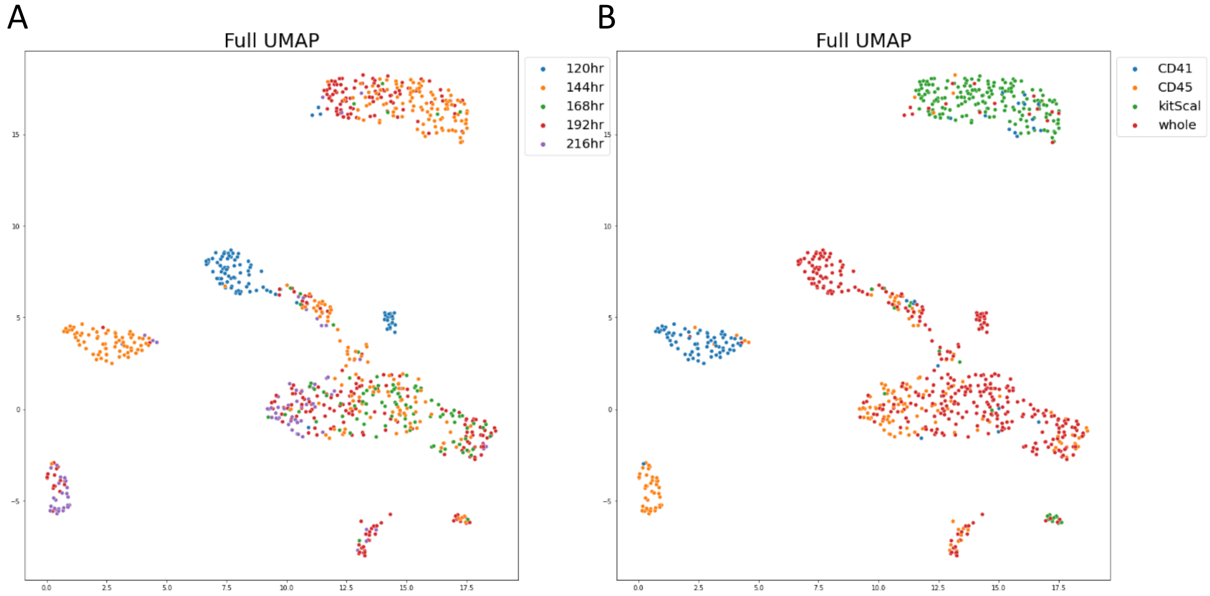

Figure 6.3.3. UMAP plot of the clustering in the whole gastruloid cells data by time and by subpopulations

(A) UMAP plot of the clustering on whole gastruloid cells with data coloured by the time. (B) UMAP plot of the clustering on whole gastruloid cells with data coloured by the subpopulations.

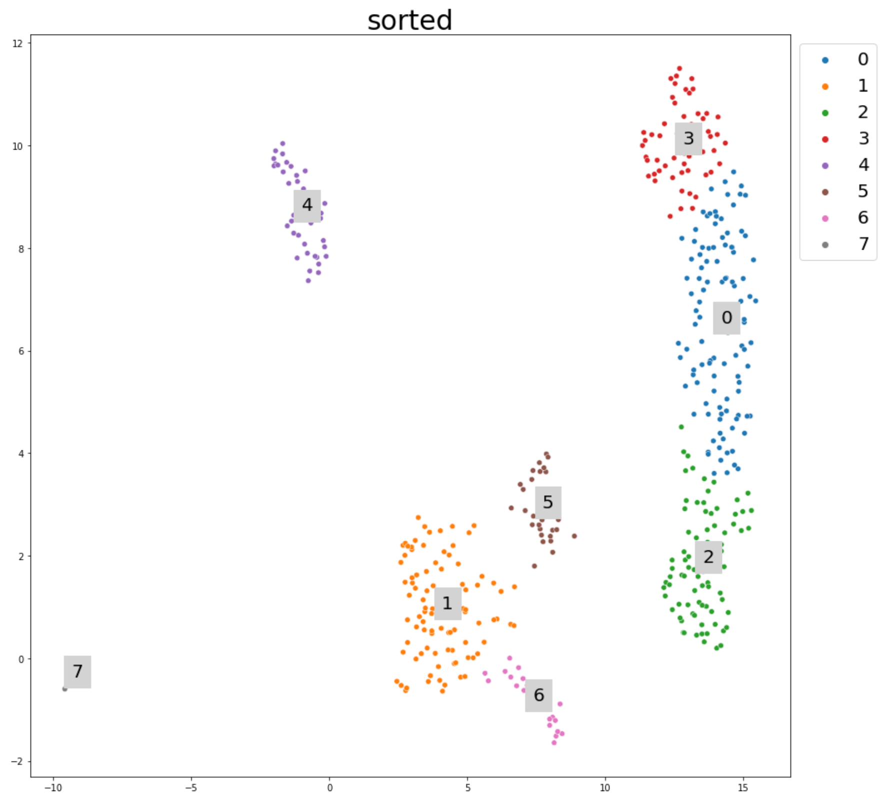

Figure 6.3.4. UMAP plot of the clustering in the sorted gastruloid subpopulation cells data

UMAP plot of the clustering was performed with the Leiden algorithm with a resolution of 0.5 on sorted gastruloid subpopulation cells data.

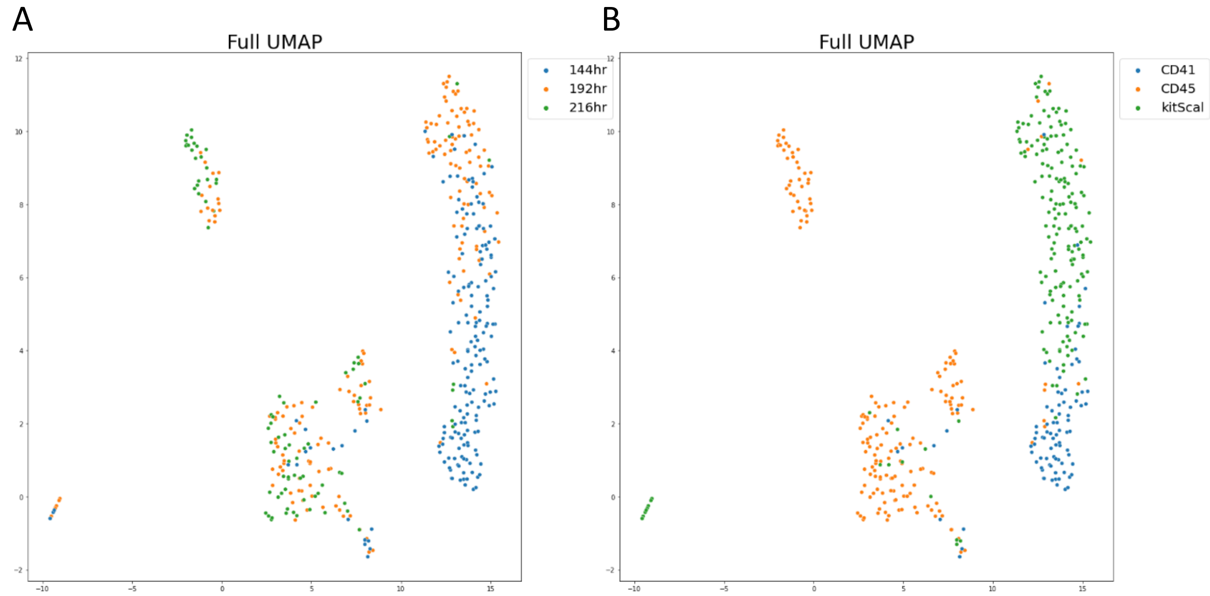

Figure 6.3.5. UMAP plot of the clustering in the sorted gastruloid subpopulation cells databy time and by subpopulations

(A) UMAP plot of the clustering on sorted gastruloid subpopulation cells data, coloured by the time with sorted population available. (B) UMAP plot of the clustering on sorted gastruloid subpopulation cells data, coloured by the subpopulations.

6.3.2 Characterisation of the whole gastruloid cells and sorted gastruloid subpopulation cells by projection to mouse embryo single-cell RNA sequencing data

For the clusters of the sorted gastruloid subpopulation cells, the c-Kit$^+$ clusters are clusters 0, 3 and 7, the CD41$^+$ cell cluster is cluster 2, and the CD45$^+$ clusters are 1, 4 and 5. The cluster-specific gene expressions were calculated as significantly overexpressed genes in that cluster compared with other genes. These clusters had distinctive haematopoetic signatures, c-kit$^+$ clusters expressed an endothelial signature, CD41$^+$ cluster expressed an erythroid programe, and CD45$^+$ clusters have some (less clear-cut) myeloid-lymphoid affiliation (Appendix 1).

After studying the haematopoietic signatures of the clusters, these data were further studied to understand whether gastruloids had potential HSC signatures. The data from whole gastruloid cells and the sorted gastruloid subpopulation cells was compared with the unpublished single-cell RNA sequencing data on mouse embryos from Anna Bigas' group (IMIM, Barcelona). The mouse embryo aorta samples are collected from Gfi1 reporter mice using the same collection strategy shown in a publication (Fadullah, *et al*., 2022). They analysed different subpopulations from the AGM at E10.5 and E11 and discovered that the engraftable HSC could be found in embryo cluster 2 based on functional analysis (Figure 6.3.6 A). However, information about other clusters is not yet available as further data analyses are currently still being conducted by Anna Bigas' group.

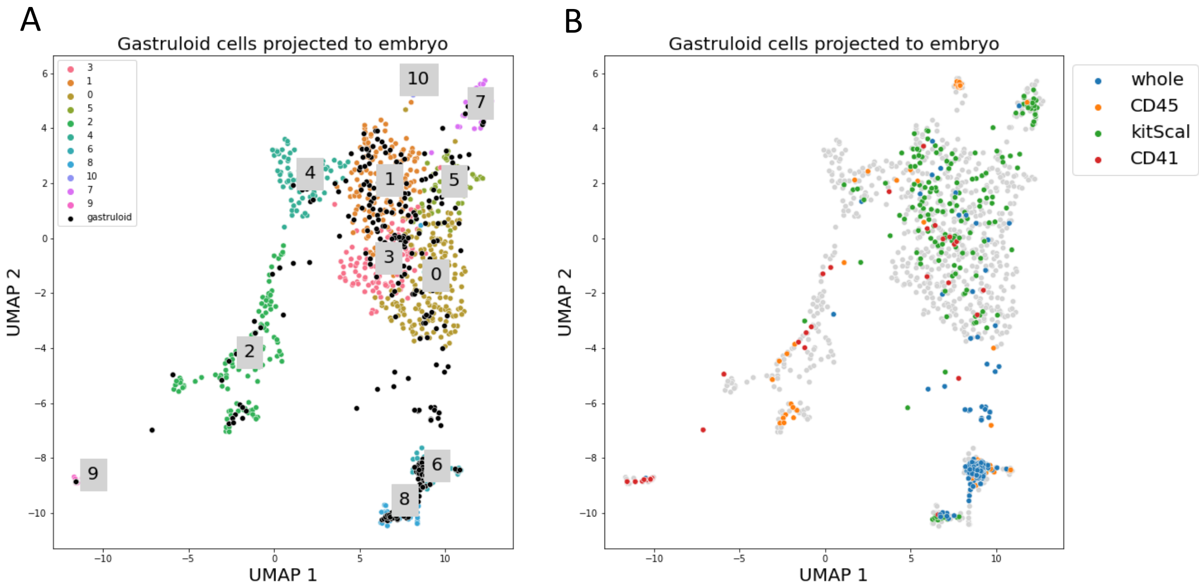

Figure 6.3.6. UMAP plot of the clustering on mouse embryo and with projection of gastruloid data

(A) UMAP plot of the clustering on mouse embryo (Thambyrajah, Lacaud and Bigas, unpublished) (B) UMAP plot of the clustering on mouse embryo with data projection of the whole gastruloid and sorted gastruloid subpopulation cells (CD45$^+$, CD41$^+$ and c-Kit$^+$ Sca-1$^+$).

The clustering data of the subpopulation of gastruloids was projected to that of mouse embryos to study the similarity of gene expression programmes in gastruloids and E10.5 and E11 mouse embryos. Additionally, comparing the clusters between embryos, whole gastruloids, and sorted gastruloid subpopulations, indicated that the closest resemblance is between cluster 8 of the whole gastruloid and the HSC cluster 2 in the embryo. Cluster 8 of the whole gastruloid primarily consists of CD45$^+$ cells, suggesting that the CD45$^+$ cells from gastruloid may show HSC signatures comparable to the AGM from mouse embryos (Figure 6.3.3 B).

The UMAPs have been projected using a KNN regressor with 15 neighbours and the proportion and the distance of cells from the gastruloid clusters can be mapped to the clusters in the embryo using the KNN graph. Clusters 2 and 10 from the embryo had the highest proportion and shortest distance to cluster 8 from the whole gastruloid cells (Figure 6.3.7). KNN method always looks for the closest neighbours independently on how far these cells are from the target cell. Since these two datasets are from different cell types, KNN will still find matches between cell types that are not corresponding to each other just because they are the closest that they found. The cluster 6 from the embryo is not a mixed cluster but it looks transcriptomically more similar to the cells from the gastruloid that are not specifically blood lineages. Thus most part of the whole gastruloid cells map to this region (Figure 6.3.6 B) and selected cells expressing other markers map to other embryo clusters other than this one.

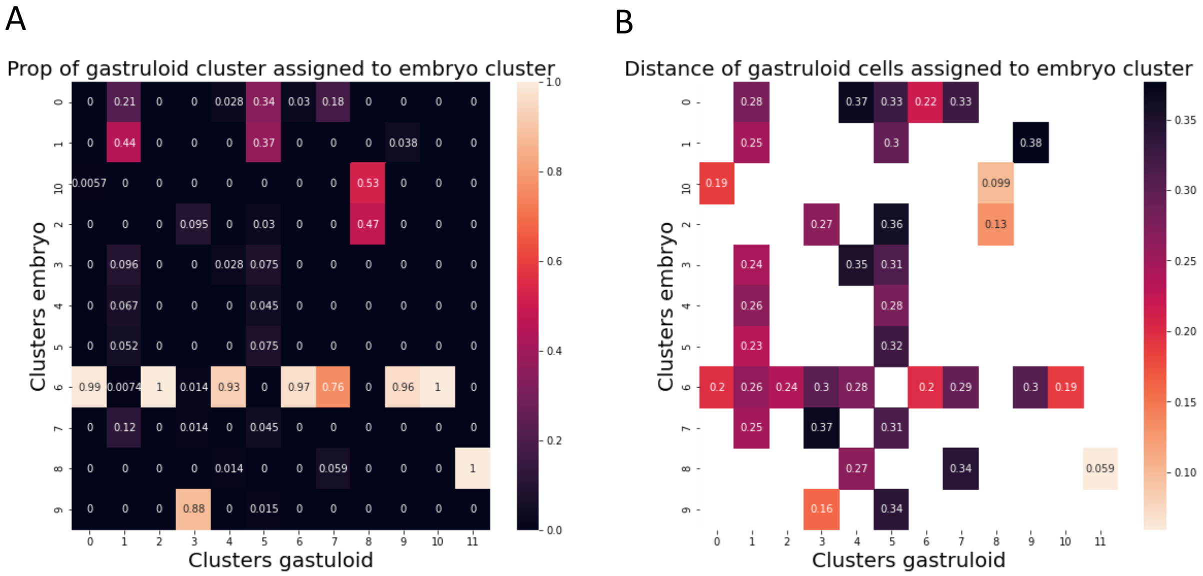

Figure 6.3.7. The proportion and distance matric from whole gastruloid to mouse embryo clusters

(A) The proportion matric shows the proportion of whole gastruloid clusters assigned to the embryo clusters. (B) The distance matric shows the pairwise distances between the whole gastruloid clusters and the embryo clusters.

The differential expression of genes from whole gastruloid clusters are aligned with those of embryo clusters, and the heat map suggests that clusters 2 and 10 from the embryo are highly correlated to cluster 8 of the whole gastruloid (Figure 6.3.8). The top fifty HSC marker genes were selected from the mouse embryo data, and the percentage of whole gastruloid cells expressing these genes in each cluster was accessed. This demonstrated that cluster 8 of the whole gastruloid had the highest percentage of cells expressing HSC marker genes (Figure 6.3.9).

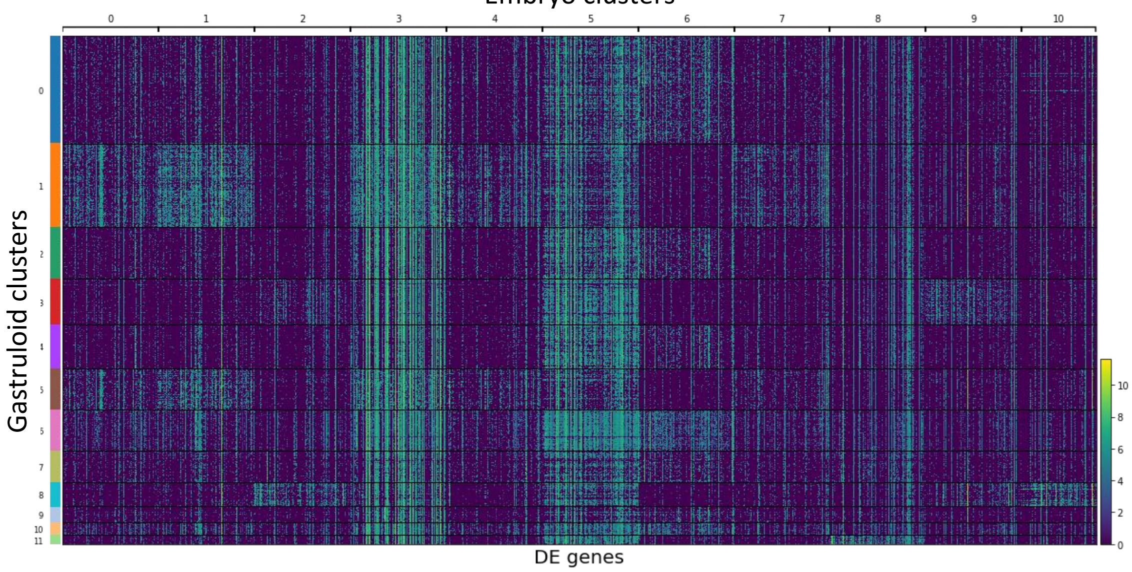

Figure 6.3.8. The heat map from differential expression analysis from whole gastruloid to mouse embryo clusters

This heat map differentially expressed genes from the clusters of the whole gastruloid were compared with those from embryo clusters.

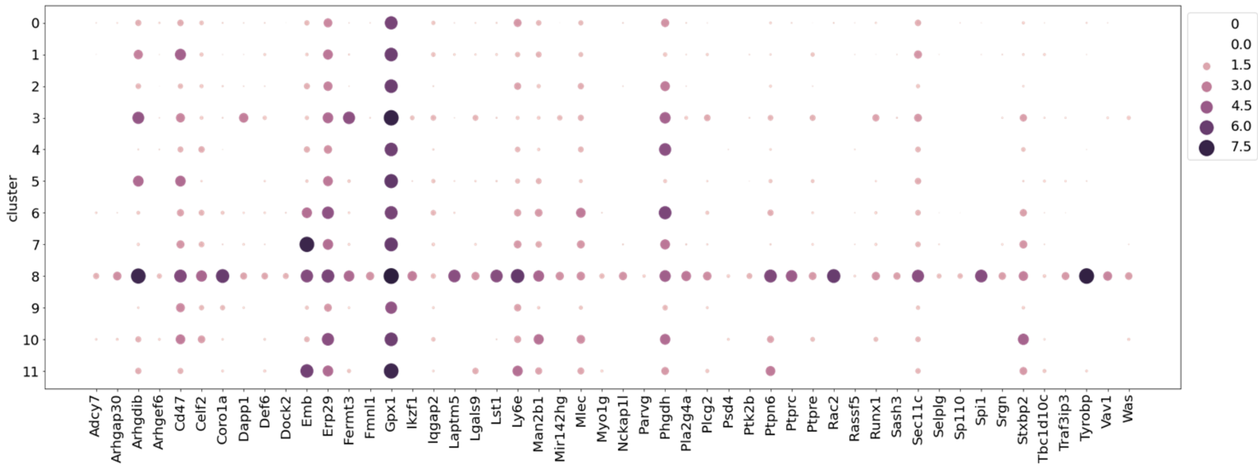

Figure 6.3.9. The split dot plots of the percentage of whole gastruloid cells expressing the HSC marker genes in each cluster.

The size of the dot corresponds to the percentage of cells expressing these genes.

A similar approach was applied to compare the clusters between the embryo and sorted gastruloid subpopulation, which indicated that the closest resemblance was between cluster 4 of the sorted gastruloid subpopulation and the HSC cluster 2 in the embryo. Similar to cluster 8 of the whole gastruloid, cluster 4 of the sorted gastruloid subpopulations not only had the highest proportion and shortest distance to clusters 2 and 10 in the embryo, but also was highly correlated to clusters 2 and 10 in the embryo, based on differential expression analysis (Figure 6.3.10; Figure 6.3.11). The cells from cluster 4 of the sorted gastruloid subpopulations also had the highest percentage of cells expressing HSC marker genes (Figure 6.3.12).

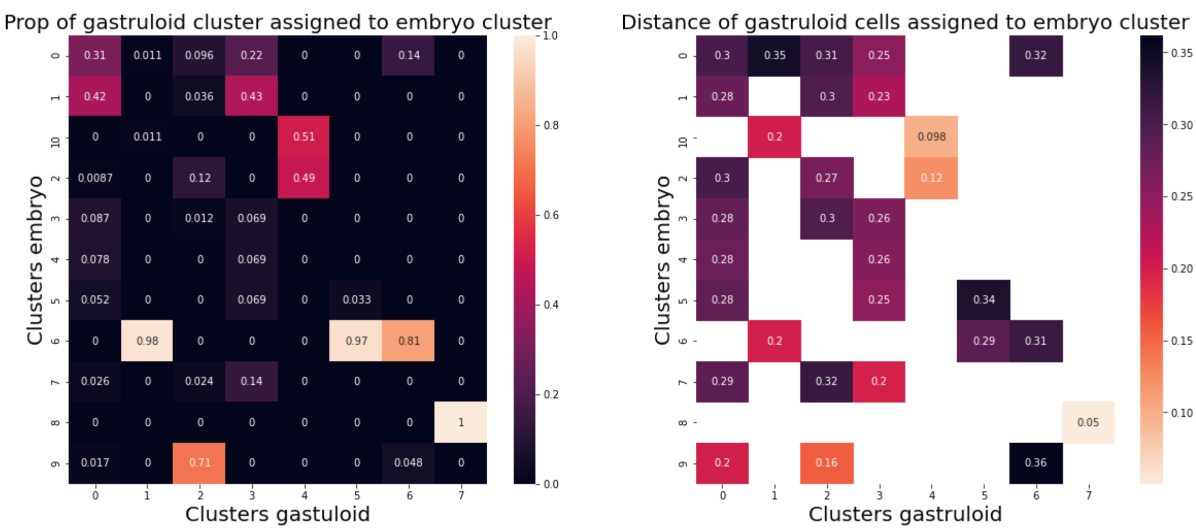

Figure 6.3.10. The proportion and distance matric from sorted gastruloid to mouse embryo clusters

(A) The proportion matric shows the proportion of sorted gastruloid clusters assigned to the embryo clusters. (B) The distance matric shows the pairwise distances between the sorted gastruloid clusters and the embryo clusters.

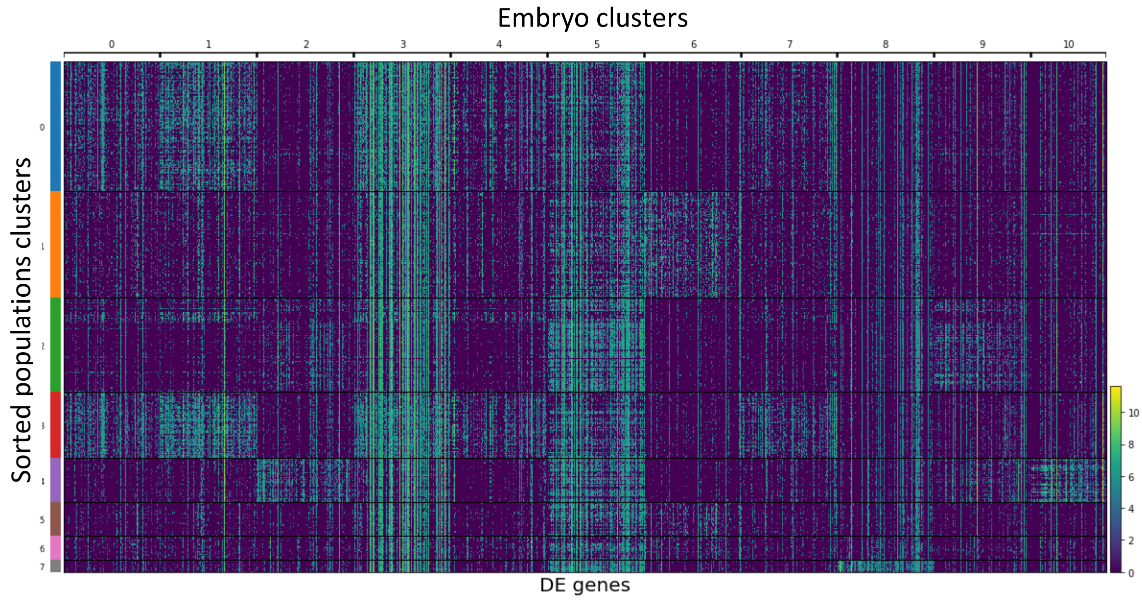

Figure 6.3.11. The heat map from differential expression analysis from sorted gastruloid to mouse embryo clusters

This heat map differentially expressed genes from the clusters of sorted gastruloid subpopulations, was compared with that from embryo clusters.

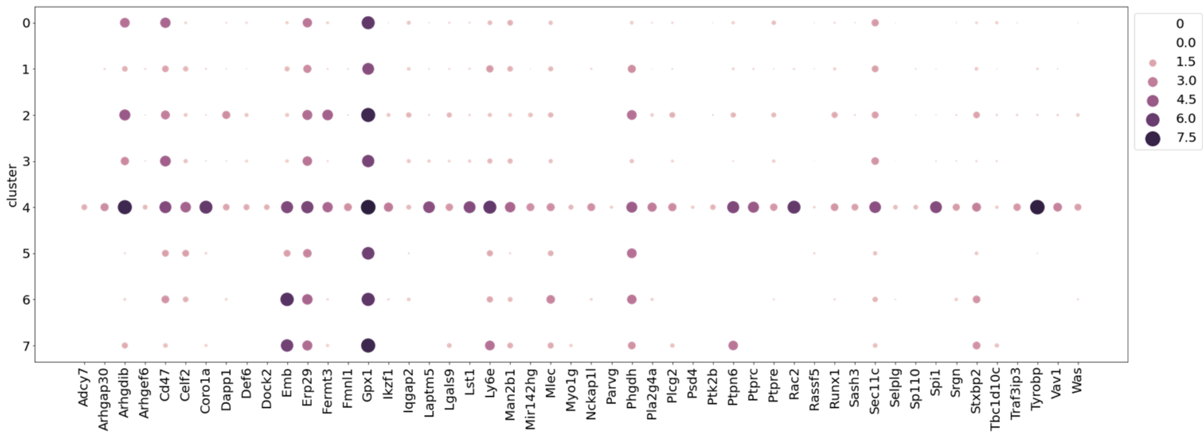

Figure 6.3.12. The split dot plots of the percentage of sorted gastruloid population cells expressing the HSC marker genes in each cluster.

The size of the dot corresponds to the percentage of cells expressing these genes.

With the help of single-cell SMART sequencing, the haematopoietic profile of the gastruloid across time was studied. The results proved that the gastruloid captures the successive generation of CD41$^+$ erythroid progenitors at 144hr, CD45$^+$ myeloid-lymphoid progenitors at 192 and 216 hr, and CD45$^+$ HSC-like cells predominantly from 216 hr. Although previous animal studies did not prove the engraftment capability of gastruloids, the results of this single-cell transcriptional analysis indicate that the further extension of the haemogenic gastruloid protocol may produce HSC-like cells with a high capability to demonstrate robust engraftment *in vivo*.

6.4 Conclusion

In the previous chapter, the gastruloid protocol was extended and optimised, and the progenitor cells formed in the gastruloid were characterised using various assays at selected time points. However, a systemic and holistic overview of gastruloids over time is absent, but is essential for understanding the development of gastruloids and the differentiation activities taking place inside them. Therefore, this chapter aimed to characterise the change of gastruloids across time through phenotypical studies, functional assay and molecular analysis.

. The CFC assay was applied to examine the change of colony-forming ability and haematopoietic potential of gastruloid cells over time. The number of colonies formed and multilineage potentials of gastruloid increase over time and peak when itreaches 168 hr. One of the possible explanations is that the CD45$^+$ type 2 pre-HSCs in the gastruloid at 192 hr and 216 hr switch to myeloid lineage or enter quiescence after plating on CFC assay.

An overview of the changes of haematopoietic markers in gastruloids over time was conducted using flow cytometry. This time-course analysis evidenced that the AGM-like definitive haematopoiesis can be recapitulated in gastruloid in a stepwise manner, from Flk-1$^+$ c-Kit$^+$ haemogenic endothelium, CD41$^+$ pro-HSCs, CD41$^+$ CD43$^+$ type 1 pre-HSCs to CD45$^+$ type 2 pre-HSCs (Goldie *et al*., 2008; Nadin *et al*., 2003; Batsivari *et al*., 2017). This finalised haemogenic gastruloid protocol was also applied to other cell lines to study the transferability and reproducibility of this protocol. Since other mouse embryonic stem cells, such as E14 cells, are more commonly used, it is important to confirm that AGM-like definitive haematopoiesis can also be recapitulated in gastruloid made with other cell lines using this protocol. The gastruloids made with either E14, Tbra::GFP or Sox-17::GFP cells can displayed similar CD41, c-Kit and CD45 expression as Flk-1::GFP-made gastruloids over time. Altogether, these results suggest this protocol can be applied to other mouse ES cell lines, which makes this protocol more accessible and applicable for future haematopoiesis research.

In order to validate whether the haematopoietic activities happening in the gastruloid can transcriptionally recapitulate those in the mouse AGM, single-cell mRNA sequencing Smart-Seq2 was conducted to study the gene expression patterns of gastruloid cells down to the single cells level from 120 to 216 hr. Compared with the unpublished mouse embryo data, it is proved that gastruloids capture a successive generation of CD41$^+$ erythroid progenitors at

144 hr, $CD45^+$ myeloid-lymphoid progenitors at 192 and 216 hr, and $CD45^+$ HSC-like cells predominantly from 216 hr.

Chapter	Main Findings
6.2.1	Gastruloid shows increasing colony formation potentials across time from 120hr to 216hr
6.2.2	The expression of haematopoietic markers in gastruloid changes across time from 96 hr to 216 hr. The expression of 1) Flk-1+ raises from 96hr and drops from 192hr, 2) cKIT+ raises from 96hr and drops from 168hr, 3) CD41+ reaches the peak at 144hr and then diminishes after, 4) CD41+CD43+ only presents at 144 hr and 168 hr, and 5) CD45+ emerges in at 192hr and 216 hr.
6.2.3	This gastruloid culture can be applied to E14 mES cell line. The E14 cell-made gastruloid has haematopoietic marker expression and cluster formation similar to Flk-1::GFP cell-made gastruloid across time.
6.2.4	This gastruloid culture can be applied to the Sox-17::GFP (KH2 mES cell line derivative). The Sox-17::GFP cell-made gastruloid has haematopoietic marker expression similar to Flk-1::GFP cell-made gastruloid across time.
6.3.1	Sorted gastruloid cells of c-Kit, CD41 and CD45 were collected for gene sequencing and passed the quality test.
6.3.2	From the result of single-cell SMART sequencing showed that gastruloid captures the successive generation of, 1) CD41+ erythroid progenitors at 144hr 2) CD45+ myeloid-lymphoid progenitors at 192 and 216 hr, and 3) CD45+ HSC-like cells predominantly from 216 hr.

Table 6.4.1. Summary of the main findings in chapter 6.

Chapter 7: Discussion

7.1 Insights and summaries from the project

7.1.1 Haematopoietic gastruloid protocol as a tool to study mouse definitive haematopoiesis

Currently, mouse early-stage haematopoiesis can only be partly demonstrated using pluripotent stem cells *in vitro* in the incubator, since LT-HSCs have not yet been generated without genetic reprogramming. This lack of a definitive haematopoietic model *in vitro* may be one of the reasons why the microenvironment niche of definitive haematopoiesis is yet to be clearly defined. This thesis has adapted the ordinary gastruloid protocol (Baillie-Johnson *et al*., 2015) into a novel haemogenic gastruloid protocol, which has the potential to be developed as a tool to study definitive haematopoiesis.

The gastruloids cultured from this haemogenic gastruloid protocol can recapitulate the stepwise differentiation of key progenitors in the AGM region. This ranges from the formation of endothelial cells and their transition to haemogenic endothelial cells, the formation of pro-HSCs and the transient appearance of type 1 pre-HSCs to the final formation of type 2 pre-HSCs. Additionally, the progression of such haematopoietic activities occurs at a similar tempo to definitive haematopoiesis in the AGM region in mice. This suggests that haemogenic gastruloids are likely able to mimic definitive haematopoiesis in the gastruloid under strict control of the external signals from cytokines.

Apart from generating haematopoietic cells with definitive surface marker phenotypes, the progenitors generated from the gastruloids included different bipotent and multipotent colony-forming cells at different times, suggesting there is more than one wave of haematopoiesis happening. Results from single-cell SMART sequencing concur with the CFC results by implying there may be more than one wave of haematopoiesis (yolk sac and definite haematopoiesis) taking place in the gastruloid. In addition, confocal imaging displayed the formation of an AGM-like haematopoietic cluster populated with $CD45^+$ cells, which is likely to be where $CD45^+$ type 2 pre-HSCs are generated. The results from the animal studies only demonstrated the gastruloid cells have a short-term engraftment capability, as opposed to long-term engraftment. However, being able to multi-waves of haematopoiesis in addition to the establishment of haematopoietic clusters proved the potential of developing this protocol as a haematopoietic model for research, especially for those investigating the AGM and definitive haematopoiesis.

The endothelial-to-hematopoietic transition (EHT) is the indispensable progress in definitive haematopoiesis in which endothelial cells acquire haematopoietic specification and transit into lineage-committed haemogenic endothelial cells. Haemogenic endothelial cells are a significant source of pro-HSCs and the subsequent definitive haematopoietic progenitors. *Flk-1* genes are required to establish both the endothelium and the haemogenic endothelium. Consequently, *Flk-1*$^{-/-}$ cells cannot develop into endothelial cells or definitive haematopoietic cells and are unable to form blood clusters (Shalaby *et al*., 1997). The gastruloids cultured with the haemogenic gastruloid protocol also recapitulated this phenomenon. Gastruloids not expressing Flk-1 at 96 or 120 hr did not express CD41 (pro-HSCs) at 144 hr, and subsequently there was no emergence of CD45^{+} cells (type 2 pre-HSCs) at 192 or 216 hr in flow cytometry analysis.

Aside from Flk-1, CD41 is another haemopoietic cell marker that characterises the onset of definitive haematopoiesis in mice. By switching the promotor of *ITGA2B*, the gene encoding CD41, the histone modification required for the expression of surface receptors in HSCs can be restructured, affecting megakaryocyte differentiation and definitive haematopoiesis (Dumon *et al*., 2012). In the haemogenic gastruloid protocol, if the gastruloids did not express any CD41 between 120 and 168 hr, no CD45^{+} cells (type 2 pre-HSCs) were generated. Haemogenic gastruloids have some characteristics similar those of the mouse AGM region, particularly regarding the importance of Flk-1 and CD41 in definitive haematopoiesis. This reveals that haemopoietic gastruloids have likely recapitulated the microenvironment of the mouse AGM region and mimic their differentiation profile of haemopoietic progenitors.

Rossi and her colleagues used the cardiogenic gastruloid protocol to culture gastruloids for embryonic blood development in a bioarxiv preprint (Rossi *et al.*, 2021a; Rossi *et al.*, 2021b). However, the absence of Activin/Nodal signalling resulted in neglectable Flk-1 expression (~4%) in their gastruloid, even at 144hr which peaked at ~60% in my haemogenic gastruloid (Rossi *et al.*, 2021b). Even without promising Flk-1 expression, which is essential for the development of the haemogenic endothelium, they claimed the emergence of CD45 and CD41 took place as early as 96 hr, which is equivalent to E8 or E9 (Motoike *et al*., 2003; Rossi *et al.*, 2021b). The recapitulation of stepwise haematopoiesis and the AGM cluster is absent in their preprint, suggesting the haemogenic gastruloid protocol developed by this project has the potential to be developed into a better model of embryonic haematopoiesis.

Finally, as a 3D culture protocol that can likely recapitulate different waves of haematopoiesis, particularly the AGM-like definitive haematopoiesis, this haemogenic gastruloid protocol has great potential to be further developed as a method to maintain HSCs and its progenitors *in vitro*. This protocol has excellent flexibility in engineering and in the control of synthetic niches, allowing it to be a model for research on the HSC niche, which attempts to understand the intrinsic and extrinsic HSC regulators with spatial and temporal variations. Mouse ES cells are easy to genetically engineer, so haemogenic gastruloids can be a robust platform to combine cellular, molecular and gene manipulation techniques such as transgenics, Cre-*LoxP* programming, siRNA, and microRNA for haematopoietic research (Li *et al.*, 2020)

7.1.2 Limitation and future works

Although haemogenic gastruloids have significant potential compared to current culture assays to recapitulate definitive haematopoiesis in the AGM region, limitations still arise due to the limited time of this project, though the research can be continued in future work, while other limitations are due to the nature of 3D organoid cultures *in vitro*.

The development of this haemogenic gastruloid protocol, primarily focused on optimising the cytokine addition scheme temporally in order to attempt to mimic the haematopoietic niches of the AGM region. Most of the work analysed if adding certain cytokines could raise the haematopoietic potential, as well as at which time point and for how long the cytokines are present to give the most promotion of the haematopoietic potential, measured by the formation of $CD41^+$ and/or $CD45^+$ cells. However, the concentration of the cytokines added to the gastruloid was not the focus of this study, and the concentration of the cytokines used in this protocol are based on other established studies and protocols used to study mouse haematopoiesis. Also, with the limited knowledge on the niche of definitive haematopoiesis, it is currently unknown whether the cytokine addition scheme proposed in this protocol can mimic the genuine mouse AGM haematopoietic niches. Additional effort can be spent fine-tuning the concentrations of cytokines to be added to the gastruloid cultures for optimising their promotion of the haematopoietic potential. Furthermore, a fixed concentration of some cytokines, such as VEGF and FGF (5 ng/mL), were applied throughout the cultures, but this will not be the case in the AGM region as the concentration of such transcription factors is expected to be dynamic across different waves of haematopoiesis. In the future, when the haematopoietic niches are better defined, a dynamic range of concentrations of such cytokines can be tested on haemogenic gastruloids to improve the protocol in establishing a microenvironment closer to the genuine haematopoietic niches in the AGM region.

2iLIF is a medium based on N2B27 medium supplemented with Chiron, PD03, and LIF, which can bring the ES cells to a naive state of pluripotency. 2iLIF was utilised to pretreat the mouse ES cells, which ensured that the starting ES cell population for gastruloids were on the same ground. This pretreatment can tackle the batch-to-batch heterogeneity of ES cells and displayed elevated haematopoietic potential of the gastruloid with one day of 2iLIF pretreatment. However, research groups that adapted 2iLIF pretreatments for their gastruloid stated concerns that the 2iLIF medium may have delayed the differentiation of the gastruloid. One of the groups put Chiron and PD03 in the maintenance culture of ES cells, and the gastruloid generated with these ES cells presented at least a 24-hour delay of the gastrulation and differentiation. The Pina group from Brunel University London also observed that practically no heart-beating cluster was formed in the haemogenic gastruloid following the introduction of 2iLIF pretreatment to the protocol. 2iLIF pretreatment remains a mandated step of the current haemogenic gastruloid protocol. Since cardiogenesis and haematopoiesis share many gene regulatory networks, the observation from the Pina group indicates that haematopoiesis in the haemogenic gastruloid may also be compromised. Reviewing the necessity of using the 2iLIF pretreatment in haemogenic gastruloids should be the next step of this project. This could be accomplished by using flow cytometry to compare the formation of haematopoietic progenitors and single-cell RNA sequencing to observe the change in gene expression patterns because of 2iLIF.

Cell sorting is common in haematopoietic studies, which selects the target cell population out of a pool of antibody-stained cells according to the designed gating strategies. However, almost all of the functional assays applied in this project have been carried out without cell sorting, and analyses were based on the whole population of gastruloid cells. A trial was carried out which sorted out $CD45^+$ cells and seeded them on methylcellulose for a CFC assay. However, no cells could survive after sorting, which suggests that the cell sorting environment is probably too harsh for gastruloid cells, leading them to die after sorting. Haematopoietic cells are a minor population and haematopoietic progenitors, such as $CD41^+$ cells and $CD45^+$ cells, are very rare in the gastruloid. The disadvantage of analysing the whole population of gastruloid cells is that it is impossible to perform functional characterisation of the targeted haematopoietic progenitors as they are masked by non-haematopoietic cells, meaning the results of CFC assays are not representative or specific enough. For future work, if the gastruloid cells can be enriched with a stroma co-culture before sorting, or the sorting facility is able to sort haematopoietic progenitors without being compromised, haematopoietic progenitors such as Flk-1^+, $CD41^+$ and $CD45^+$ cells could be seeded on methylcellulose over time to understand their haematopoietic colony-forming capability individually.

Apart from applying sorted haematopoietic progenitors to the CFC assay, another study requiring more extensive testing and optimisation is the animal transplantation study. The animal study tests the reconstitution capability of the proposed haematopoietic progenitors produced in the gastruloid and cells able to engraft in the mouse would be regarded as HSCs. However, the result of the animal studies (chapter 4.5 and 5.4.3) did not provide a strong indication that haematopoietic progenitors produced in the gastruloid are able to engraft *in vivo*. Results from the first animal study (chapter 4.5) revealed that the 192 hr gastruloids had weak short-term bone marrow engraftment and these gastruloids probably only treated with VEGF, FGF and Shh. Therefore, it is expected that the 192 hr gastruloids generated from the optimised protocol may show more evidence to prove their short-term engraftment in the bone marrow and spleen *in vivo*, and even long-term engraftment. However, the second animal study did not provide sufficient evidence to prove its engraftment (chapter 5.4.3). The non-irritated c-Kit mutant mice were used to test the reconstitution capability of gastruloid cells in a naïve haematopoietic niche and avoid the competition between the supporting bone marrow cells and gastruloid cells; however, it appears as though an acute response to irradiation is required for the colon forming and engraftment. A repeat of the animal study with the 192 hr gastruloids is encouraged, but with a similar setting to the first animal study (chapter 4.5), which used irradiated C57BL/6 (B6) mice.

Confocal microscopy is an accessible method to inspect the internal structures formed in the gastruloids as it can image the spatial arrangement of this structure with its controllable depth of field. It was applied to visualise the formation of haematopoietic clusters in the 192 and 216 hr gastruloids and confirmed that these clusters have CD45 and c-Kit expression, and its morphology is similar to the aorta in the AGM region. However, no other hematopoietic markers have been studied, and their spatial information in the gastruloid remain unknown. For future work, hematopoietic markers such as Sca-1, CD41, CD43 and EPCR can also be studied by confocal microscopy to inspect their spatial and temporal arrangement over time, which will be very useful to validate the stepwise haematopoietic differentiation revealed by flow cytometry. The haemogenic gastruloid protocol can also be applied to cell lines with haematopoietic markers, such as the Sca-1::GFP cell line, for directly tracking the emergence of haematopoietic progenitors in the gastruloid with confocal imaging. In addition, since the cardiac progenitors and heart beating components were reported in the haemogenic gastruloids, it is worth further verifying their identities with cardiac morphogenesis markers such as Tbx1, Tbx5, Ecad and cTnT (Rossi *et al.*, 2021a).

Both confocal and fluorescence microscopy are helpful tools to study the cell identity by inspecting the proteins on the surface of the cell membrane with the help of fluorescence labelling. However, these microscopy tools cannot visualise the structure inside of the gastruloids if the proteins have not yet been produced, whilst only the expression of certain genes is upregulated. On such occasions, *in situ* hybridisation can be applied to identify the localisation of specific gene expression using a labelled RNA probe. The RNA probe is designed to hybridise specific RNA transcripts and displays a blue colour (NBT diformazan) under brightfield microscopy or shows fluorescence in RNA-fluorescence *in situ* hybridisation (FISH) under confocal microscopy. It would be worth conducting this assay in the future as it would provide valuable spatial and temporal information regarding haematopoietic gene expression *in situ*.

The above has focused on the limitations of the current haemogenic gastruloid culture protocol and how it can be improved in the immediate future. However, some limitations arise from the 3D nature of organoid culture in recapitulating definitive haematopoiesis in the AGM region, and they are not easy to solve. Firstly, gastruloids have difficulty completely replicating the *in vivo* environment of the living body as the gastruloid is floating in the medium, in which the biochemical and mechanical signalling to indicate the direction is absent to the gastruloid. The lack of directional cues is likely one reasons why the formation of the haematopoietic cluster and heart beating component is inconsistent regarding the location in the gastruloid, even single beating foci are commonly observed, suggesting a level of self-organisation. Secondly, the development of HSCs after the formation of the haematopoietic cluster may be restricted, and the lack of vasculature in gastruloids may lead to a haematopoietic niche different from that *in vivo*. Other embryonic cell types such as stroma cells may be missing in the gastruloids; thus, their contribution to the microenvironment will be lacking in the gastruloid.

7.2 Future applications

7.2.1 Reducing and replacing the use of *in vivo* animals in research

The mouse model is an essential tool for understanding the differentiation and engraftment capacity of haematopoietic progenitors. Hematopoietic cells are only regarded as HSCs if they demonstrate reconstitution to the hematopoietic system of the irradiated adult recipient, and this functional assay has been widely applied in haematopoietic studies. Combined with genetic manipulation techniques, the mouse model has also been used as a full gene knockout model, gene deletion or overexpression model for studying the cellular and molecular genetic processes underlying haematopoiesis.

Although the animal model has a crucial role in bioscience research, society has expressed significant concerns regarding animal use for economic, regulatory, and ethical reasons in recent years. Animal models for research are strictly regulated by law in the UK, and studies must abide by the principles of the 3Rs (replacement, reduction, and refinement) when designing and performing the experiments (MacArthur, 2018). At the same time, animal testing regulations also restrict the extent of experimentation available to research groups conducting haematopoietic studies. As such, the haemogenic gastruloid can be developed as a robust and reproducible *in vitro* haematopoietic model to replace animal studies.

Currently, the *in vitro* culture of the AGM region to produce definitive haematopoietic progenitors remains elusive, consequently mouse models are the primary assay used to study the haematopoietic niches and differentiation in the AGM. The results of this project show that the haemogenic gastruloid protocol can recapitulate the formation of definitive haematopoietic progenitors and the structure in the AGM region. This highlights the promising potential of this protocol to generate an AGM model *in vitro*, reducing the use of animal study. Besides, the available animal models are primarily adult mice, meaning their haematopoietic niches are adult and not embryonic. Although the AGM can be accessed from the mouse embryo model for haematopoetic studies, the amount of material is limiting, and the progress is mainly destructive.

Animal experiments can be expensive and time-consuming, and researchers face difficulty upscaling the study to include a more significant number of replicas. For example, the transplantation experiment conducted in this project took more than 12 weeks, making it challenging to repeat the experiment. Additionally, animals demand extra care in the facility, and many precautional works have to be prepared in advance to ensure the study is conducted without animal cruelty, as required by the animal protection act. In comparison, the procedure and materials required for gastruloid cultures are considerably less than that for animal work. It takes roughly two weeks to culture a haemogenic gastruloid with the features of the AGM region, and the multiple-well culture plate can produce close to a hundred gastruloids at once. It is economical and easy to maintain the haemogenic gastruloid culture and it will be worth developing this protocol as a validation tool for animal models used in haematopoietic studies.

7.2.2 Adapting mouse haemogenic gastruloid protocol to human ES cells

This haemogenic gastruloid culture protocol is able to generate definitive haematopoietic progenitors, but this protocol only applies to mouse ES cells and not to human cells. Adapting the haemogenic gastruloid culture protocol to culture human ES cells would unleash great potential for both research and clinical settings. Other research groups have developed gastruloid protocols using human ES cells to generate gastruloids. Human gastruloids demonstrated features similar to the mouse gastruloid including the formation of three germ layers, axis elongation, and the polarised expression of the mesodermal marker, *BRA* (Moris *et al*., 2020). However, unlike mouse gastruloids, the expression of *BRA* was detected as early as 24 hr in human gastruloids, which is 48 hours earlier than in the mouse gastruloids which demand the Chi pulse between 48 to 72 hr (Van den Brink *et al*., 2014; Moris *et al*., 2020). This variation suggests that the formation of the mesodermal layer in mice and humans have fundamental differences, and the protocol will need significant adaptation for culture of human haemogenic gastruloids.

The AGM region began to form in the mouse embryo at E9, while the counterpart only started to form in the human embryo at 27 dpf (Ivanovs *et al*., 2017). This significant discrepancy in the date of the formation of the AGM region in human and mouse embryos implies that the human gastruloid protocol must be extended accordingly until it is late enough for the generation of the AGM region and definitive haematopoietic progenitors in human gastruloids. Human early haematopoiesis in embryos has not been well characterised due to ethical and technical challenges. However, it is known that the $CD34^{+}$/$CD45^{+}$ cells seeding the human foetal liver in prodefinitive haematopoiesis are equivalent to the yolk sac-derived EMPs and lymphoid progenitors in mice (Ivanovs *et al*., 2017). For definitive haematopoiesis, proHSCs and preHSCs have not yet been defined in humans, but it is known that the human AGM region can generate HSC progenitors with local forming capability without long-term engraftment, prior to the emergence of *bona fide* HSCs (Sinka *et al*., 2012). Although there is a significant difference in human and mouse early haematopoiesis in the embryo, the experience, results, and the cytokine scheme developed from the mouse haemogenic gastruloid protocol can be used as a reference for the development of the human haemogenic gastruloid protocol in the future (Lim *et al*., 2013; Parekh & Crooks, 2013; Choi *et al*., 2019).

Experiments on human embryonic studies are tightly regulated, and the 14-day statutory rule restricts maintaining human embryos *in vitro* for more than 14 days after fertilisation. The 14-day rule was determined as the primitive streak is formed in the human embryo on the 15th day, which is why the experiment must be terminated to prevent the embryo from suffering. Although it is morally important to keep the embryo from suffering as a result of biological experiments, such early termination also challenges the study of haematopoiesis in human embryos since the AGM is only initiated from the 27th day. While there is a discussion on extending the 14-day rule to 28 days, it will take time for academia to reach a consensus on this argument (Cavaliere, 2017). The development of a human haemogenic gastruloid protocol will be groundbreaking as it will provide a great alternative to study human early embryonic haematopoiesis *in vitro*.

To overcome the research limitations introduced by the 14-day rule, researchers developed a mouse model to study *in vivo* haematopoiesis, which did help to develop a more complete understanding of human haematopoiesis. The humanised mouse is a model that uses immunodeficient mouse strains that allows human xenografts and human HSCs show improved engraftment efficiency in newborn or adult NSG (Macchiarini *et al*., 2005). However, one of the main concerns with using the mouse model is the cross-species difference between the mouse hematopoietic microenvironment and the human HSCs and progenitors. Developing a novel human haemogenic gastruloid may provide an established human hematopoietic niche similar to the human body. It would provide human cell-cell interaction, growth factors, and chemokines to promote the appropriate expansion and trafficking of human ES and hematopoietic cells.

7.2.3 Haemogenic gastruloid in drug discovery and development

In drug discovery, preclinical testing is a necessary process that links the discovery of a drug in the laboratory to the human clinical trials for drug development. Preclinical studies include drug formulation, active pharmaceutical ingredient (API) preparation, absorption, distribution, metabolism, excretion (ADME) and efficacy testing, and safety studies. The results of preclinical studies are mandatory to almost all drug regulatory bodies including the FDA, MHRA and EMA, as preclinical studies verify that the drug is effective and is safe to be administrated to patients in the subsequent clinical trials. However, preclinical studies have the lowest success rate (~32%) compared with clinical trials (~50% to 88%), and cost 7 million USD and take 47 months per drug on average in preclinical trials (Takebe *et al.*, 2018; Prasad & Mailankody, 2017). Any assay which could help evaluate drug candidates and terminate early could help to save time and resources so they could be reinvested into other drug discovery projects.

Haemogenic gastruloids could be an excellent tool for preclinical studies, especially in toxicology and safety testing. Many preclinical studies are conducted on animal models, which is expensive and time-consuming, which restricts the size of the studies. Rare adverse side effects are sometimes not reported until the therapeutics are launched, such as myocarditis and pericarditis in the administration of Covid-19 vaccines (Diaz *et al.*, 2021). Gastruloid culture is ideal for high-throughput screening for safety tests because it is comparatively inexpensive, quick, and easy to maintain. Haemogenic gastruloids have haematopoietic and cardiac features which can be utilised before the animal model to investigate whether new drug candidates initiate any possible adverse effects in the haematopoietic and cardiac system. In the future, if haemogenic gastruloids can be further developed to model diseases, it could even be used in drug efficacy testing to assess if the drug candidate can cure or relieve the condition and whether this drug has sufficient efficacy to be worth testing on the animal model in preclinical studies.

Pregnant and lactating women are generally excluded from clinical trials, research, and new treatments due to concerns that the novel drug candidates may harm the development of the foetus and increase the risk of complications for the women. Only around 2% of clinical trials are specifically for pregnant women (Steinberg *et al.*, 2021). However, such exclusion has been regarded as unethical, since it leaves pregnant women unprotected from any new medical treatments. Mantziou and her colleagues recently used mouse and human gastruloids to examine the effects of certain teratogenic substances on gastruloid development (Mantziou *et al*., 2021). If the haemogenic gastruloid protocol could be adapted for human ES cells, which also models early haematopoiesis and cardiogenesis, this would also be a great platform to study whether drug candidates affect early haematopoiesis and cardiogenesis of the foetus. Such a testing platform would provide preliminary teratogenic safety data of the drug candidates and assist the clinical trials officer to make the decision of accepting pregnant women in the clinical trial with no teratogenic risks to the embryo.

Another possible application of the haemogenic gastruloid is using it in combination with organ-on-a-chip (OoC) technology to develop a next-generation drug screening platform. OoC is a technology using a chip fabricated with microchannels in which an organoid is seeded and interconnected with the fluid flow on the chip. Haematogenic gastruloids can be integrated with other embryonic organoids, such as kidney, intestinal, and liver organoids, on the same chip (Editorials, 2021). This OoC would be able to provide a more physiologically relevant system to replicate *in vivo* responses to drug candidates. An embryonic OoC has great potential to replace animal testing in preclinical trials and even potentially redefine the assessments of preclinical trials.

7.2.4 Use case of haemogenic gastruloid: Infant leukaemia disease model

The haemogenic gastruloid culture protocol may be an ideal tool to understand the haematopoietic niches and gene regulatory signalling involved in definitive haematopoiesis, but could also find powerful applications in multiple areas of research in leukaemic haematopoiesis. Leukaemic stem cells (LSCs) are the leukaemic population that are substantially more resistant to chemotherapy and are believed to have a role in maintaining leukaemia. LSCs benefit from the HSCs haematopoietic niches from the vascular endothelium, which supports the survival, proliferation, and homing of LSCs (Ninomiya *et al*., 2007). Although leukaemia is the most common type in child cancer, infant leukaemia for children under the age of a year is a rare malignancy which displays a poor response to chemotherapy. Leukaemia has lack of new treatments and the absence of a research model to understand the underlying disease processes (Brown *et al*., 2019).

Currently, an effective *in vitro* model to study the infant leukaemic haematopoietic microenvironment remains elusive, and the rarity of the conditions poses challenges in obtaining *ex vivo* embryonic tissue to study the foetal origins of infant leukaemia. Critically, haemogenic gastruloids represent a powerful research platform for insights into the mechanistic events in leukaemia, particularly in infant leukaemia, which has a poor prognosis. Haemogenic gastruloids could be the first *in vitro* culture system with the potential to recapitulate the formation of the haemogenic endothelium and the emergence of HSC progenitors within a synchronously specified microenvironment, with spatial and temporal control under leukaemic conditions.

By matching the sequential acquisition of specific combinations of mutations with haematopoietic development, it is possible to dissect the mechanisms of *in utero* leukaemogenesis. The haemogenic gastruloid protocols could be applied to the modelling of leukaemic events, in particular, those more commonly found *in utero* (e.g. MLL/KMT2A, t(7;12), t(1;22) or inv(16) fusion protein), with temporal precision through the use of inducible systems (Meyer *et al*., 2018; Quessada *et al*., 2021). Leukaemic modelling can be achieved through the ectopic delivery of leukaemic fusion genes in retroviral vectors, or by genetic engineering using CRISPR/Cas9 technology. This would allow the detailed study of the timing and specific interactions between primary and distinct additional mutation events, not only because they contribute to leukaemia formation, but also to understand their role in the modification of normal haematopoiesis (Ran *et al*., 2013). If leukaemogenesis could be modelled in the haemogenic gastruloid, which recapitulates leukaemia development by introducing specific mutation events acquired *in utero*, these leukaemic gastruloids could be further engineered as a drug screening tool for personalised medicine. Assuming that different leukaemic mutation patterns underlie distinct responses to chemotherapy and leukaemic gastruloids respond to drug treatment similarly to *in vivo* models, it would be possible to engineer different common mutation events in infant leukaemia using the CRISPR-Cas9 system in the leukaemic gastruloids. Such a personalised leukaemic gastruloid protocol could be applied in high-throughput screening for identifying new drug candidates to improve the chemotherapy response in infant leukaemic patients.

Reference

Acloque, H., Adams, M.S., Fishwick, K., Bronner-Fraser, M., Nieto, M.A. 2009. “Epithelial-mesenchymal transitions: the importance of changing cell state in development and disease.” *Journal of Clinical Investigation* 119 (6): 1438-49.

Alberts, B., Johnson, A., Lewis, J., Raff, M., Roberts, K. & Walters, P. 2002. *Molecular Biology of the Cell (Fourth ed.).* New York and London: Garland Science.

Alemany, A., Florescu, M., Baron, C.S., Peterson-Maduro, J. & van Oudenaarden, A. 2018. “Whole-organism clone tracing using single-cell sequencing.” *Nature.* 556 (7699): 108-112.

Alvarez-Silva, M., Belo-Diabangouaya, P., Salaün, J. & Dieterlen-Lièvre, F. 2003. “Mouse placenta is a major hematopoietic organ.” *Development.* 130 (22): 5437-5444.

Amadei, G., Lau, K.Y.C., De Jonghe, J., Gantner, C.W., Sozen, B., Chan, C., Zhu, M., Kyprianou, C., Hollfelder, F. & Zernicka-Goetz, M. 2021. “Inducible Stem-Cell-Derived Embryos Capture Mouse Morphogenetic Events In Vitro.” *Developmental Cell* 56 (3): 366-382.

Anand, R.K. & Rahn, K.L. 2020. “Interfacing electronic and genetic circuits.” *Nature Chemistry* 12 (1): 14-16.

Audzevich, T., Bashford-Rogers, R., Mabbott, N.A., Frampton, D., Freeman, T.C., Potocnik, A., Kellam, P. & Gilroy, D.W. 2017. “Pre/pro-B cells generate macrophage populations during homeostasis and inflammation. .” *Proceedings of the National Academy of Sciences of the United States of America* 114 (20): E3954-E3963.

Baillie-Johnson, P., van den Brink, S. C., Balayo, T., Turner, D. A., & Martinez Arias, A. (2015). Generation of Aggregates of Mouse Embryonic Stem Cells that Show Symmetry Breaking, Polarization and Emergent Collective Behaviour In Vitro. Journal of visu. 2015. “Generation of Aggregates of Mouse Embryonic Stem Cells that Show Symmetry Breaking, Polarization and Emergent Collective Behaviour In Vitro. .” *Journal of visualized experiments : JoVE* 105: 53252.

Baillie-Johnson, P., van den Brink, S.C., Balayo, T., Turner, D.A. & Martinez Arias, A. 2015. “Generation of Aggregates of Mouse Embryonic Stem Cells that Show Symmetry Breaking, Polarization and Emergent Collective Behaviour In Vitro.” *Journal of Visualized Experiments* (105): 53252.

Barcellos-Hoff, M.H., Aggeler, J., Ram, T.G. & Bissell, M.J. 1989. “Functional differentiation and alveolar morphogenesis of primary mammary cultures on reconstituted basement membrane. .” *Development.* 105 (2): 223-35.

Barcia Durán, J.G., Lis, R., Lu, T.M., Rafii, S. 2018. “In vitro conversion of adult murine endothelial cells to hematopoietic stem cells.” *Nature Protocol* 13 (12): 2758-2780.

Barker, N., Huch, M., Kujala, P., van de Wetering, M., Snippert, H.J., van Es, J.H., Sato, T., Stange, D.E., Begthel, H., van den Born, M., Danenberg, E., van den Brink, S., Korving, J., Abo, A., Peters, P.J., Wright, N., Poulsom, R. & Clevers, H. 2010. “Lgr5(+ve) stem cells drive self-renewal in the stomach and build long-lived gastric units in vitro.” *Cell Stem Cell* 6 (1): 25-36.

Batsivari, A., Rybtsov, S., Souilhol, C., Binagui-Casas, A., Hills, D., Zhao, S., Travers, P. & Medvinsky, A. 2017. “Understanding Hematopoietic Stem Cell Development through Functional Correlation of Their Proliferative Status with the Intra-aortic Cluster Architecture. .” *Stem cell reports* 6 (1549-62): 8.

Beccari, L., Moris, N., Girgin, M., Turner, D.A., Baillie-Johnson, P., Cossy, A.C., Lutolf, M.P., Duboule, D. & Arias, A.M. 2018. “Multi-axial self-organization properties of mouse embryonic stem cells into gastruloids.” *Nature* 562 (7726): 272-276.

Belloc, F., Dumain, P., Boisseau, M.R., Jalloustre, C., Reiffers, J., Bernard, P. & Lacombe, F. 1994. “A flow cytometric method using Hoechst 33342 and propidium iodide for simultaneous cell cycle analysis and apoptosis determination in unfixed cells.” *Cytometry.* 17 (1): 59-65.

Böiers, C., Carrelha, J., Lutteropp, M., Luc, S., Green, J.C., Azzoni, E., Woll, P.S., Mead, A.J., Hultquist, A., Swiers, G., Perdiguero, E.G., Macaulay, I.C., Melchiori, L., Luis, T.C., Kharazi, S., Bouriez-Jones, T., Pontén, A., & Jacobsen, S.E. 2013. “Lymphomyeloid contribution of an immune-restricted progenitor emerging prior to definitive hematopoietic stem cells.” *Cell Stem Cell.* 13 (5): 535-48.

Boj, S.F., Hwang, C.I., Baker, L.A., Chio, I.I., Engle, D.D., Corbo, V., Jager, M., Ponz-Sarvise, M., Tiriac, H., Spector, M.S., Gracanin, A.,Offerhaus, G.J., Vries, R.G., Clevers, H. & Tuveson, D.A. 2015. “Organoid models of human and mouse ductal pancreatic cancer.” *Cells* 160 (1-2): 324-38.

Bonilla, F.A. & Oettgen, H.C. 2010. “Adaptive immunity.” *The Journal of Allergy and Clinical Immunology* 125 (2): S33-40.

Boyer, S.W., Schroeder, A.V., Smith-Berdan, S. & Forsberg, E.C. 2011. “All hematopoietic cells develop from hematopoietic stem cells through Flk2/Flt3-positive progenitor cells.” *Cell Stem Cell.* 9 (1): 64-73.

Brown, P., Pieters, R. & Biondi, A. 2019. “How I treat infant leukemia. .” *Blood* 133 (3): 205-214.

Buenrostro, J.D., Corces, M.R., Lareau, C.A., Wu, B., Schep, A.N., Aryee, M.J., Majeti, R., Chang, H.Y. & Greenleaf, W.J. 2018. “Integrated Single-Cell Analysis Maps the Continuous Regulatory Landscape of Human Hematopoietic Differentiation.” *Cell* 173 (6): 1535-1548.

Burkert, U., von Ruden, T. & Wagner, E.F. 1991. “Early fetal hematopoietic development from in vitro differentiated embryonic stem cells.” *The New biologist.* 3 (7): 698-708.

Canu, G., Athanasiadis, E., Grandy, R.A., Garcia-Bernardo, J., Strzelecka, P.M., Vallier, L., Ortmann, D. & Cvejic, A. 2020. “Analysis of endothelial-to-haematopoietic transition at the single cell level identifies cell cycle regulation as a driver of differentiation.” *Genome Biology* 21: 157.

Cao, J. & Zhao, T. 2016. “Single-cell sequencing delivers hematopoietic stem cell specification.” *Science Bulletin* 61 (18): 1419-21.

Cavaliere, G. 2017. “A 14-day limit for bioethics: the debate over human embryo research.” *BMC Medical Ethics* 18 (1): 38.

Cerdan, C., McIntyre, B. A., Mechael, R., Levadoux-Martin, M., Yang, J., Lee, J. B., & Bhatia, M. 2012. “Activin A Promotes Hematopoietic Fated Mesoderm Development Through

Upregulation of Brachyury in Human Embryonic Stem Cells." *Stem cells and development* 21 (15): 2866-2877.

Chapple, R.H., Tseng, Y.J., Hu, T., Kitano, A., Takeichi, M., Hoegenauer, K.A. & Nakada, D. 2018. "Lineage tracing of murine adult hematopoietic stem cells reveals active contribution to steady-state hematopoiesis." *Blood Advances* 2 (11): 1220-1228.

Chen, F., De Diego, C., Chang, M. G., McHarg, J.L., John, S., Klitzner, T.S. and Weiss, J.N. 2010. "Atrioventricular Conduction and Arrhythmiasat the Initiation of Beating in EmbryonicMouse Hearts." *Developmental Dynamics* 239 (7): 1941-9.

Chen, K.G., Mallon, B.S., Johnson, K.R., Hamilton, R.S., McKay, R.D. & Robey, P.G. 2014. "Developmental insights from early mammalian embryos and core signaling pathways that influence human pluripotent cell growth and differentiation." *Stem cell research.* 12 (3): 610-21.

Choi, J., Baldwin, T.M., Wong, M., Bolden, J.E., Fairfax, K.A., Lucas, E.C., Cole, R., Biben, C., Morgan, C., Ramsay, K.A., Ng, A.P., Kauppi, M., Corcoran, L.M., Shi, W., Wilson, N., Wilson, M.J., Alexander, W.S., Hilton, D.J. & de Graaf ,C.A. 2019. "Haemopedia RNA-seq: a database of gene expression during haematopoiesis in mice and humans." *Nucleic Acids Research* 47 (D1): D780-D785.

Congrains, A., Bianco, J., Rosa, R.G., Mancuso, R.I. & Saad, S.T.O. 2021. "3D Scaffolds to Model the Hematopoietic Stem Cell Niche: Applications and Perspectives." *Materials (Basel)* 14 (3): 569.

Coşkun, S., Chao, H., Vasavada, H., Heydari, K., Gonzales, N., Zhou, X., de Crombrugghe, B. & Hirschi, K.K. 2014. "Development of the fetal bone marrow niche and regulation of HSC quiescence and homing ability by emerging osteolineage cells. ." *Cell Reports* 9 (2): 581-90.

Costa, G., Kouskoff, V. & Lacaud, G. 2012. "Origin of blood cells and HSC production in the embryo." *Trends in immunology.* 33 (5): 215-23.

de Bruijn, M.F., Speck, N.A., Peeters, M.C. & Dzierzak, E. 2000. "Definitive hematopoietic stem cells first develop within the major arterial regions of the mouse embryo." *The EMBO Journal* 19 (11): 2465-74.

de Pooter, R. & Zúñiga-Pflücker, J.C. 2007. "T-cell potential and development in vitro: the OP9-DL1 approach." *Current Opinion in Immunology* 19 (2): 163-8.

Diaz, G.A., Parsons, G.T., Gering, S.K., Meier, A.R., Hutchinson, I.V. & Robicsek, A. 2021. "Myocarditis and Pericarditis After Vaccination for COVID-19." *The Journal of the American Medical Association* 326 (12): 1210-1212.

Ding, L., Saunders, T.L., Enikolopov, G. & Morrison, S.J. 2012. "Endothelial and perivascular cells maintain haematopoietic stem cells." *Nature* 481 (7382): 457-62.

Dong, J., McPherson, C.M. & Stambrook, P.J. 2002. " Flt-3 ligand: a potent dendritic cell stimulator and novel antitumor agent." *Cancer Biology & Therapy* 5: 486-9.

Dontu, G., Abdallah, W.M., Foley, J.M., Jackson, K.W., Clarke, M.F., Kawamura, M.J. & Wicha, M.S. 2003. “In vitro propagation and transcriptional profiling of human mammary stem/progenitor cells.” *Genes & Development* 17 (10): 1253-70.

Dumon, S., Walton, D.S., Volpe, G., Wilson, N., Dassé, E., Del Pozzo, W., Landry, J.R., Turner, B., O'Neill, L.P., Göttgens, B. & Frampton, J. 2012. “Itga2b regulation at the onset of definitive hematopoiesis and commitment to differentiation.” *PLoS One.* 7 (8): e43300.

Durand, C., Robin, C., Bollerot, K., Baron, M.H., Ottersbach, K. & Dzierzak, E. 2007. “Embryonic stromal clones reveal developmental regulators of definitive hematopoietic stem cells.” *Proceedings of the National Academy of Sciences of the United States of America* 104 (52): 20838-43.

Dykstra, B., Kent, D., Bowie, M., McCaffrey, L., Hamilton, M., Lyons, K., Lee, S.J., Brinkman, R. & Eaves, C. 2007. “Long-term propagation of distinct hematopoietic differentiation programs in vivo.” *Cell Stem Cell.* 2 (218-29): 1.

Eaves, C.J. 2015. “Hematopoietic stem cells: concepts, definitions, and the new reality. .” *Blood. 2015 Apr 23;2605-13* 125 (17): 2605-13.

Echelard, Y., Epstein, D.J., St-Jacques, B., Shen, L., Mohler, J., McMahon, J.A. & McMahon, A.P. 1993. “Sonic hedgehog, a member of a family of putative signaling molecules, is implicated in the regulation of CNS polarity.” *Cell* 75 (3): 1417-30.

Editorials. 2021. “The promise of organoids and embryoids.” *Nature Materials* 20 (2): 121.

Ema, M., Takahashi, S. & Rossant, J. 2006. “Deletion of the selection cassette, but not cis-acting elements, in targeted Flk1-lacZ allele reveals Flk1 expression in multipotent mesodermal progenitors.” *Blood.* 107 (1): 111-7.

Era, T., Izumi, N., Hayashi, M., Tada, S., Nishikawa, S. & Nishikawa, S. 2008. “Multiple mesoderm subsets give rise to endothelial cells, whereas hematopoietic cells are differentiated only from a restricted subset in embryonic stem cell differentiation culture.” *Stem Cells.* 26 (2): 401-11.

Fadlullah, M.Z.H., Neo, W.H., Lie-A-Ling, M., Thambyrajah, R., Patel, R., Mevel, R., Aksoy, I., Do Khoa, N., Savatier, P., Fontenille, L., Baker, S.M., Rattray, M., Kouskoff, V., Lacaud, G. 2022. “Murine AGM single-cell profiling identifies a continuum of hemogenic endothelium differentiation marked by ACE.” *Blood* 139 (3): 343-356.

Faltusová, K., Chen, C. L., Heizer, T., Báječný, M., Szikszai, K., Páral, P., Savvulidi, F., Renešová, N., & Nečas, E. 2020. “Altered Erythro-Myeloid Progenitor Cells Are Highly Expanded in Intensively Regenerating Hematopoiesis. .” *Frontiers in cell and developmental biology* 8 (98).

Ferkowicz M. J., Yoder M. C. 2005. “Blood island formation: longstanding observations and modern interpretations.” *Experimental Hematology* 33: 1041-1047.

Ferkowicz, M.J. & Yoder, M.C. 2005. “Blood island formation: longstanding observations and modern interpretations.” *Experimental Hematology* 33 (9): 1041-7.

Flamme, I., Breier, G. & Risau, W. 1995. “Vascular endothelial growth factor (VEGF) and VEGF receptor 2 (flk-1) are expressed during vasculogenesis and vascular differentiation in the quail embryo.” *Developmental Biology* 169 (2): 699-712.

Fleury, M., Petit-Cocault, L., Clay, D. & Souyri, M. 2010. “Mpl receptor defect leads to earlier appearance of hematopoietic cells/hematopoietic stem cells in the Aorta-Gonad-Mesonephros region, with increased apoptosis.” *International Journal of Developmental* 54 (6-7): 1067-1074.

Frame, J.M., Fegan, K.H., Conway, S.J., McGrath, K.E. & Palis, J. 2016. “Definitive Hematopoiesis in the Yolk Sac Emerges from Wnt-Responsive Hemogenic Endothelium Independently of Circulation and Arterial Identity.” *Stem cells* 2 (431-44): 34.

Gajović, S. & Gruss, P. 1998. “Differentiation of the mouse embryoid bodies grafted on the chorioallantoic membrane of the chick embryo.” *The International Journal of Developmental Biology* 42 (2): 225-8.

Gekas, C., Dieterlen-Lievre, F., Orkin, S.H. & Mikkola, H.K. 2005. “The placenta is a niche for hematopoietic stem cells. .” *Developmental cell* 8 (3): 365-75.

Gekas, C., Dieterlen-Lièvre, F., Orkin, S.H. & Mikkola, H.K. 2005. “The placenta is a niche for hematopoietic stem cells.” *Developmental Cell.* 8 (3): 265-275.

Gekas, C., Rhodes, K.E., Van Handel, B., Chhabra, A., Ueno, M. & Mikkola, H.K. 2010. “Hematopoietic stem cell development in the placenta. .” *The International Journal of Developmental Biology* 54 (6-7): 1089-1098.

Gerber, H. P., Malik, A. K., Solar, G. P., Sherman, D., Liang, X. H., Meng, G., Hong, K., Marsters, J. C., & Ferrara, N. 2002. “VEGF regulates haematopoietic stem cell survival by an internal autocrine loop mechanism.” *Nature* 417 (6892): 954-8.

Ginhoux, F & Guilliams, M. 2016. “Tissue-resident macrophage ontogeny and homeostasis.” *Immunity* 44 (3): 439-449.

Ginhoux, F., Lim, S., Hoeffel, G., Low, D. & Huber, T. 2013. “Origin and differentiation of microglia.” *Frontiers in Cellular Neuroscience* (45): 7.

Girgin, M.U., Broguiere, N., Mattolini, L. & Lutolf, M.P. 2021. “Gastruloids generated without exogenous Wnt activation develop anterior neural tissues. .” *Stem Cell Reports.* 16 (5): 1143-1155.

Goldie, L.C,, Lucitti, J.L., Dickinson, M.E., Hirschi, K.K. 2008. “Cell signaling directing the formation and function of hemogenic endothelium during murine embryogenesis.” *Blood* 112 (8): 3194-204.

Gomez Perdiguero, E., Klapproth, K., Schulz, C., Busch, K., Azzoni, E., Crozet, L., Garner, H., Trouillet, C., de Bruijn, M.F., Geissmann, F. & Rodewald, H.R. 2015. “Tissue-resident macrophages originate from yolk-sac-derived erythro-myeloid progenitors.” *Nature* 7540 (547-51): 518.

Guye, P., Ebrahimkhani, M.R., Kipniss, N., Velazquez, J.J., Schoenfeld, E., Kiani, S., Griffith, L.G. & Weiss, R. 2016. “Genetically engineering self-organization of human pluripotent stem cells into a liver bud-like tissue using Gata6.” *Nature Communications* 7: 10243.

Hadland, B. & Yoshimoto, M. 2018. “Many layers of embryonic hematopoiesis: new insights into B-cell ontogeny and the origin of hematopoietic stem cells.” *Experimental Hematology* 60: 1-9.

Harada, K., Nobuhisa, I., Anani, M., Saito, K., & Taga, T. 2017. “Thrombopoietin contributes to the formation and the maintenance of hematopoietic progenitor-containing cell clusters in the aorta-gonad-mesonephros region. .” *Cytokine* (95): 35-42.

Haraguchi, S., Matsubara, Y. & Hosoe, M. 2015. “Chick embryos can form teratomas from microinjected mouse embryonic stem cells.” *Development, Growth & Differentiation* 58: 194-204.

Harrison, R.G. 1906. “Observations on the living developing nerve fiber.” *Experimental Biology and Medicine* 4: 140-143.

Haruta, H., Nagata, Y. & Todokoro, K. 2001. “Role of Flk-1 in mouse hematopoietic stem cells.” *FEBS Letters* 507 (1): 45-8.

He, Q. & Liu, F. 2016. “Unexpected role of inflammatory signaling in hematopoietic stem cell development: its role beyond inflammation.” *Current Opinion in Hematology* 23 (1): 18-22.

Healy, C.P. & Deans, T.L. 2019. “Genetic circuits to engineer tissues with alternative functions.” *Journal of Biological Engineering* 13: 39.

Hirai, H., Samokhvalov, I.M., Fujimoto, T., Nishikawa, S., Imanishi, J. & Nishikawa, S. 2005. “Involvement of Runx1 in the down-regulation of fetal liver kinase-1 expression during transition of endothelial cells to hematopoietic cells.” *Blood* 106 (6): 1948-55.

Hirschi, K.K. 2012. “Hemogenic endothelium during development and beyond.” *Blood* 119 (21): 4823-4827.

Hoeffel, G. & Ginhoux, F. 2018. “Fetal monocytes and the origins of tissue-resident macrophages.” *Cellular Immunology* 330: 5-15.

Hoeffel, G. & Ginhoux, F. 2015. “Ontogeny of Tissue-Resident Macrophages.” *Frontiers in Immunology* 6: 486.

Holmes, R. & Zúñiga-Pflücker, J.C. 2009. “The OP9-DL1 system: generation of T-lymphocytes from embryonic or hematopoietic stem cells in vitro.” *Cold Spring Harbour Protocol* 2.

Hsu, H.C., Ema, H., Osawa, M., Nakamura, Y., Suda, T. & Nakauchi, H. 2000. “Hematopoietic stem cells express Tie-2 receptor in the murine fetal liver.” *Blood.* 96: 3757-3762.

Huber, T.L., Kouskoff, V., Fehling, H.J., Palis, J. & Keller, G. 2004. “Haemangioblast commitment is initiated in the primitive streak of the mouse embryo. .” *Nature.* 432 (7017): 625-30.

Huch, M., Dorrell, C., Boj, S.F., van Es, J.H., Li, V.S., van de Wetering, M., Sato, T., Hamer, K., Sasaki, N., Finegold, M.J., Haft, A., Vries, R.G., Grompe, M. & Clevers, H. 2013. “In vitro expansion of single Lgr5+ liver stem cells induced by Wnt-driven regeneration. ." *Nature.* 494 (7436): 247-50.

Inlay, M.A., Serwold, T., Mosley, A., Fathman, J.W., Dimov, I.K., Seita, J. & Weissman, I.L. 2014. "Identification of multipotent progenitors that emerge prior to hematopoietic stem cells in embryonic development." *Stem Cell Reports* 2 (4): 457-72.

Ito, C.Y., Li, C.Y., Bernstein, A., Dick, J.E. & Stanford, W.L. 2003. "Hematopoietic stem cell and progenitor defects in Sca-1/Ly-6A–null mice." *Blood* 101 (2): 517-23.

Ivanovs, A., Rybtsov, S., Anderson, R.A., Turner, M.L. & Medvinsky, A. 2014. "Identification of the niche and phenotype of the first human hematopoietic stem cells." *Stem cell reports.* 2 (4): 449-56.

Ivanovs, A., Rybtsov, S., Ng, E.S., Stanley, E.G., Elefanty, A.G. & Medvinsky, A. 2017. "Human haematopoietic stem cell development: from the embryo to the dish." *Development.* 144 (13): 2323-37.

Jakobsson, L., Franco, C.A., Bentley, K., Collins, R.T., Ponsioen, B., Aspalter, I.M., Rosewell, I., Busse, M., Thurston, G., Medvinsky, A., Schulte-Merker, S. & Gerhardt, H. 2010. "Endothelial cells dynamically compete for the tip cell position during angiogenic sprouting." *Nature Cell Biology* 12 (10): 943-53.

Kang, H., Mesquitta, W.T., Jung, H.S., Moskvin, O.V., Thomson, J.A. & Slukvin, II. 2018. "GATA2 Is Dispensable for Specification of Hemogenic Endothelium but Promotes Endothelial-to-Hematopoietic Transition. ." *Stem Cell Reports.* 11 (1): 197-211.

Kattman, S.J., Huber, T.L. & Keller, G.M. 2006. "Multipotent flk-1+ cardiovascular progenitor cells give rise to the cardiomyocyte, endothelial, and vascular smooth muscle lineages." *Developmental Cell* 11 (5): 723-32.

Kauts, M.L., Vink, C.S., Dzierzak, E. 2016. "Hematopoietic (stem) cell development - how divergent are the roads taken?" *FEBS letters.* 590 (22): 3975-86.

Kawamoto, H. & Katsura, Y. 2009. "A new paradigm for hematopoietic cell lineages: revision of the classical concept of the myeloid-lymphoid dichotomy. ." *Trends immunology* 30 (5): 193-200.

Kim, S.J., Jung, J.W., Ha, H.Y., Koo, S.K., Kim, E.G. & Kim, J.H. 2017. "Generation of hematopoietic stem cells from human embryonic stem cells using a defined, stepwise, serum-free, and serum replacement-free monolayer culture method." *Blood research.* 52 (1): 37-43.

Kobayashi, M., Shelley, W.C., Seo, W., Vemula, S., Lin, Y., Liu, Y., Kapur, R., Taniuchi, I. & Yoshimoto, M. 2014. "Functional B-1 progenitor cells are present in the hematopoietic stem cell-deficient embryo and depend on Cbfβ for their development. ." *Proceedings of the National Academy of Sciences of the United States of America* 111 (33): 12151-6.

Kondo, M., Wagers, A.J., Manz, M.G., Prohaska, S.S., Scherer, D.C., Beilhack, G.F., Shizuru, J.A. & Weissman, I.L. 2003. "Biology of hematopoietic stem cells and progenitors: implications for clinical application." *Annual Review of Immunology* 21: 759-806.

Kumaravelu, P., Hook, L., Morrison, A.M., Ure, J., Zhao, S., Zuyev, S., Ansell, J. & Medvinsky, A. 2002. "Quantitative developmental anatomy of definitive haematopoietic stem cells/long-term repopulating units (HSC/RUs): role of the aorta-gonad-mesonephros (AGM) region and the yolk sac in colonisation of the mouse embryonic liver." *Development.* 129 (21): 4891-9.

Lacaud, G., Carlsson, L. & Keller, G. 1998. "Identification of a fetal hematopoietic precursor with B cell, T cell, and macrophage potential." *Immunity* 9 (6): 827-38.

Lancaster, M.A., Renner, M., Martin, C.A., Wenzel, D., Bicknell, L.S., Hurles, M.E., Homfray, T., Penninger, J.M., Jackson, A.P. & Knoblich, J.A. 2013. "Cerebral organoids model human brain development and microcephaly. ." *Nature.* 501 (7467): 373-9.

Lancrin, C., Sroczynska, P., Stephenson, C., Allen, T., Kouskoff, V. & Lacaud, G. 2009. "The haemangioblast generates haematopoietic cells through a haemogenic endothelium stage." *Nature* 457 (7231): 892-895.

Laurenti, E. & Göttgens, B. 2018. "From haematopoietic stem cells to complex differentiation landscapes." *Nature* 553 (7689): 418-426.

Lawson, N.D., Vogel, A.M. and Weinstein, B.M. 2002. "Sonic hedgehog and vascular endothelial growth factor act upstream of the Notch pathway during arterial endothelial differentiation. ." *Developmental cell.* 3 (1): 127-36.

Lee, Y., Manegold, J.E., Kim, A.D., Pouget, C., Stachura, D.L., Clements, W.K., and Traver, D. 2014. "FGF signalling specifies haematopoietic stem cells through its regulation of somitic Notch signalling." *Nature communications.* 5 (5583).

Leung, A., Ciau-Uitz, A., Pinheiro, P., Monteiro, R., Zuo, J., Vyas, P., Patient, R. & Porcher, C. 2013. "Uncoupling VEGFA functions in arteriogenesis and hematopoietic stem cell specification." *Developmental cell* 24 (2): 144-58.

Li, H., Yang, Y., Hong, W., Huang, M., Wu, M. & Zhao, X. 2020. "Applications of genome editing technology in the targeted therapy of human diseases: mechanisms, advances and prospects." *Signal transduction and targeted therapy* 5 (1): 1.

Lim, W.F., Inoue-Yokoo, T., Tan, K.S., Lai, M.I. & Sugiyama, D. 2013. "Hematopoietic cell differentiation from embryonic and induced pluripotent stem cells." *Stem Cell Research & Therapy* 4 (3): 71.

Lis, R., Karrasch, C.C., Poulos, M.G., Kunar, B., Redmond, D., Duran, J.G.B., Badwe, C.R., Schachterle, W., Ginsberg, M., Xiang, J., Tabrizi, A.R., Shido, K., Rosenwaks, Z., Elemento, O., Speck, N.A., Butler, J.M., Scandura, J.M. & Rafii, S. 2017. "Conversion of adult endothelium to immunocompetent haematopoietic stem cells." *Nature.* 545 (7655): 439-445.

Lu, C.C., Brennan, J., Robertson, E.J. 2001. "From fertilization to gastrulation: axis formation in the mouse embryo. ." *Current Opinion in Genetics and Development* 11 (4): 384-92.

MacArthur, C. J. 2018. "The 3Rs in research: a contemporary approach to replacement, reduction and refinement." *British Journal of Nutrition* 120 (s1): S1-S7.

Macchiarini, F., Manz, M.G., Palucka, A.K. & Shultz, L.D. 2005. "Humanized mice: are we there yet? ." *Journal of Experimental Medicine* 202 (10): 1307-11.

Mahony, C.B. & Bertrand, J.Y. 2019. “How HSCs Colonize and Expand in the Fetal Niche of the Vertebrate Embryo: An Evolutionary Perspective.” 7: 1-11.

Mantziou, V., Baillie-Benson, P., Jaklin, M., Kustermann, S., Arias, A.M. & Moris, N. 2021. “In vitro teratogenicity testing using a 3D, embryo-like gastruloid system.” *Reproductive Toxicology* 105: 72-90.

Marcellini, S., Technau, U., Smith, J.C. & Lemaire, P. 2003. “Evolution of Brachyury proteins: identification of a novel regulatory domain conserved within Bilateria.” *Developmental Biology* 260 (2): 352-61.

Marcelo, K.L., Goldie, L.C. & Hirschi, K,K. 2103. “Regulation of endothelial cell differentiation and specification.” *Circulation Research* 112 (9): 1272-87.

Marikawa, Y., Tamashiro, D.A., Fujita, T.C. & Alarcón, VB. 2009. “Aggregated P19 mouse embryonal carcinoma cells as a simple in vitro model to study the molecular regulations of mesoderm formation and axial elongation morphogenesis.” *Genesis* 47 (2): 93-106.

Marshall, C.J., Sinclair, J.C., Thrasher, A.J. & Kinnon, C. 2007. “Bone morphogenetic protein 4 modulates c-Kit expression and differentiation potential in murine embryonic aorta-gonad-mesonephros haematopoiesis in vitro.” *British journal of haematology.* 139 (2): 321-30.

Martin, B.L. & Kimelman, D. 2010. “Brachyury establishes the embryonic mesodermal progenitor niche. .” *Genes & Development* 24 (24): 2778-83.

Matano, M., Date, S., Shimokawa, M., Takano, A., Fujii, M., Ohta, Y., Watanabe, T., Kanai, T. & Sato, T. 2015. “Modeling colorectal cancer using CRISPR-Cas9-mediated engineering of human intestinal organoids. .” *Nature Medicine* 21 (3): 256-62.

Matsumoto, K., Isagawa, T., Nishimura, T., Ogaeri, T., Eto, K., Miyazaki, S., Miyazaki, J., Aburatani, H., Nakauchi, H. & Ema, H. 2009. “Stepwise development of hematopoietic stem cells from embryonic stem cells.” *PLoS One.* 3 (e4820): 4.

Maximow, A. 1909. “ntersuchengenuber blut und bindgewebe: 1. Die fruhesten entwicklungs-stadian der Blut- und Bindgewebszellen beim saugetierembryo, bis sum anfang der blutbildung in der leber.” *Arch. Mikr. Anat. Entwicklungsgesch* 4: 159-166.

McGrath, K.E., Frame, J.M., Fegan, K.H., Bowen, J.R., Conway, S.J., Catherman, S.C., Kingsley, P.D., Koniski, A.D. & Palis, J. 2015. “Distinct Sources of Hematopoietic Progenitors Emerge before HSCs and Provide Functional Blood Cells in the Mammalian Embryo.” *Cell Reports* 11 (12): 1892-904.

Medvinsky, A., Rybtsov, S. & Taoudi, S. 2011. “Embryonic origin of the adult hematopoietic system: advances and questions.” *Development* 138 (6): 1017–1031.

Medvinsky, A., Rybtsov, S. and Taoudi, S. 2011. “Embryonic origin of the adult hematopoietic system: advances and questions. .” *Development.* 138 (6): 1017-31.

Meyer, C., Burmeister, T., Gröger, D., Tsaur, G., Fechina, L., Renneville, A., Sutton, R., Venn, N.C., Emerenciano, M., Pombo-de-Oliveira, M.S., Barbieri, Blunck, C., Suarez, L., Cavé, H. & Marschalek, R. 2018. “The MLL recombinome of acute leukemias in 2017.” *Leukemia.* 32 (2): 273-284.

Mikkola, H.K., Orkin, S.H. 2006. “The journey of developing hematopoietic stem cells. .” *Development.* 133 (19): 3733-44.

Minegishi, N., Suzuki, N., Yokomizo, T., Pan, X., Fujimoto, T., Takahashi, S., Hara, T., Miyajima, A., Nishikawa, S. & Yamamoto, M. 2003. “xpression and domain-specific function of GATA-2 during differentiation of the hematopoietic precursor cells in midgestation mouse embryos.” *Blood* 102 (3): 896-905.

Miyanari, Y. & Torres-Padilla, M.E. 2012. “Control of ground-state pluripotency by allelic regulation of Nanog. .” *Nature.* 483 (7390): 470-3.

Morcos, M.N.F., Schoedel, K.B., Hoppe, A., Behrendt, R., Basak, O., Clevers, H.C., Roers, A. & Gerbaulet, A. 2017. “SCA-1 Expression Level Identifies Quiescent Hematopoietic Stem and Progenitor Cells.” *Stem Cell Reports* 8 (6): 1472-1478.

Moris, N., Anlas, K., van den Brink, S.C., Alemany, A., Schröder, J., Ghimire, S., Balayo, T., van Oudenaarden, A. & Martinez Arias, A. 2020. “An in vitro model of early anteroposterior organization during human development.” *Nature* 582 (7812): 410-415.

Morita, Y., Ema, H. & Nakauchi, H. 2010. “Heterogeneity and hierarchy within the most primitive hematopoietic stem cell compartment.” *Journal of Experimental Medicine* 207 (6): 1173-82.

Motoike, T., Markham, D. W., Rossant, J., and Sato, T. N. 2003. “. Evidence for novel fate of Flk1+ progenitor: contribution to muscle lineage. Genesis. 2003;35(3):153-9.” *Genesis* 35 (3): 153-159.

Na Nakorn, T., Traver, D., Weissman, I.L. & Akashi, K. 2002. “Myeloerythroid-restricted progenitors are sufficient to confer radioprotection and provide the majority of day 8 CFU-S.” *Journal of Clinical Investigation* 109 (12): 1579-85.

Nadin, B.M., Goodell, M.A. & Hirschi, K.K. 2003. “Phenotype and hematopoietic potential of side population cells throughout embryonic development.” *Blood* 102 (7): 2436-43.

Nature Methods. 2018. “Method of the Year 2017: Organoids.” *Nature Methods* 15 (1).

Ng, A.P. & Alexander, W.S. 2017. “Haematopoietic stem cells: past, present and future. .” *Cell Death Discovery* 3 (17002).

Nikolic, T., Dingjan, G.M., Leenen, P.J. & Hendriks, R.W. 2002. “A subfraction of B220(+) cells in murine bone marrow and spleen does not belong to the B cell lineage but has dendritic cell characteristics.” *European Journal of Immunology* 32 (3): 686-92.

Ninomiya, M., Abe, A., Katsumi, A., Xu, J., Ito, M., Arai, F., Suda, T., Ito, M., Kiyoi, H., Kinoshita, T. & Naoe, T. 2007. “Homing, proliferation and survival sites of human leukemia cells in vivo in immunodeficient mice.” *Leukemia.* 21 (1): 136-42.

Nishikawa, S.I., Nishikawa, S., Kawamoto, H., Yoshida, H., Kizumoto, M., Kataoka, H. & Katsura, Y. 1998. “In vitro generation of lymphohematopoietic cells from endothelial cells purified from murine embryos. .” *Immunity* 8 (6): 761-9.

Nobuhisa, I., Osawa, M., Uemura, M., Kishikawa, Y., Anani, M., Harada, K., Takagi, H., Saito, K., Kanai-Azuma, M., Kanai, Y., Iwama, A. & Taga, T. 2014. “Sox17-mediated maintenance of fetal intra-aortic hematopoietic cell clusters." *Molecular and Cellular Biology* 34 (11): 1976-90.

Noetzli, L.J., French, S.L., Machlus, K.R. 2019. "New Insights Into the Differentiation of Megakaryocytes From Hematopoietic Progenitors." *Arteriosclerosis, Thrombosis, and Vascular Biology* 39 (7): 1288-1300.

North, T., Gu, T.L,. Stacy, T., Wang, Q., Howard, L., Binder, M., Marín-Padilla, M. & Speck, N.A. 1999. "Cbfa2 is required for the formation of intra-aortic hematopoietic clusters." *Development.* 126 (11): 2563-75.

Notta, F., Zandi, S., Takayama, N., Dobson, S., Gan, O.I., Wilson, G., Kaufmann, K.B., McLeod, J., Laurenti, E., Dunant, C.F., McPherson, J.D., Stein, L.D., Dror, Y. & Dick, J.E. 2016. "Distinct routes of lineage development reshape the human blood hierarchy across ontogeny." *Science* 351 (6269).

Nowotschin, S., & Hadjantonakis, A. 2011. "Cellular dynamics in the early mouse embryo: from axis formation to gastrulation." *Current Opinion in Genetics and Development* 20 (4): 420-427.

Oguro, H., Ding, L. & Morrison, S.J. 2013. "SLAM family markers resolve functionally distinct subpopulations of hematopoietic stem cells and multipotent progenitors." *Cell Stem Cell.* 13 (1): 102-16.

Osawa, M., Hanada, K., Hamada, H. & Nakauchi, H. 1996. "Long-term lymphohematopoietic reconstitution by a single CD34-low/negative hematopoietic stem cell." *Science* 273 (5272): 242-5.

Ottersbach, K. & Dzierzak, E. 2005. "The murine placenta contains hematopoietic stem cells within the vascular labyrinth region." *Developmental Cell* 8 (3): 377-387.

Palis, J., Robertson, S., Kennedy, M., Wall, C. & Keller, G. 1999. "Development of erythroid and myeloid progenitors in the yolk sac and embryo proper of the mouse." *Development* 126 (22): 5073-84.

Parekh, C. & Crooks, G.M. 2013. "Critical differences in hematopoiesis and lymphoid development between humans and mice." *Journal of Clinical Immunology* 33 (4): 711-5.

Pauklin, S., & Vallier, L. 2015. "Activin/Nodal signalling in stem cells. Development." *Development* 142 (4): 607-619.

Pereira, C.F., Chang, B., Qiu, J., Niu, X., Papatsenko, D., Hendry, C.E., Clark, N.R., Nomura-Kitabayashi, A., Kovacic, J.C., Ma'ayan, A., Schaniel, C., Lemischka, I.R. & Moore, K. 2013. "Induction of a hemogenic program in mouse fibroblasts." *Cell Stem Cell.* 13 (2): 205-18.

Petit-Cocault, L., Volle-Challier, C., Fleury, M., Péault, B. & Souyri, M. 2007. "Dual role of Mpl receptor during the establishment of definitive hematopoiesis." *Development.* 134 (16): 3031-40.

Picelli, S., Björklund, Å.K., Faridani, O.R., Sagasser, S., Winberg, G. & Sandberg, R. 2013. "Smart-seq2 for sensitive full-length transcriptome profiling in single cells. ." *Nature Methods* 10 (11): 1096-8.

Pietras, E.M., Reynaud, D., Kang, Y.A., Carlin, D., Calero-Nieto, F.J., Leavitt, A.D., Stuart, J.M., Göttgens, B. & Passegué, E. 2015. “Functionally Distinct Subsets of Lineage-Biased Multipotent Progenitors Control Blood Production in Normal and Regenerative Conditions.” *Cell Stem Cell.* 17 (1): 35-46.

Pimanda, J.E., Donaldson, I.J., de Bruijn, M.F., Kinston, S., Knezevic, K., Huckle, L., Piltz, S., Landry, J.R., Green, A.R., Tannahill, D. & Göttgens, B. 2007. “The SCL transcriptional network and BMP signaling pathway interact to regulate RUNX1 activity.” *Proceedings of the National Academy of Sciences of the United States of America.* 3 (840-5): 104.

Potts, K.S., Sargeant, T.J., Markham, J.F., Shi, W., Biben, C., Josefsson, E.C., Whitehead, L.W., Rogers, K.L., Liakhovitskaia, A., Smyth, G.K., Kile, B.T., Medvinsky, A., Alexander, W.S., Hilton, D.J. & Taoudi, S. 2014. “A lineage of diploid platelet-forming cells precedes polyploid megakaryocyte formation in the mouse embryo.” *Blood* 17 (2725-9): 124.

Pouget, C., Peterkin, T., Simões, F., Lee, Y., Traver, D. & Patient, R. 2014. “FGF signalling restricts haematopoietic stem cell specification via modulation of the BMP pathway.” *Nature Communications* 5 (5588).

Prasad, V. & Mailankody, S. 2017. “Research and Development Spending to Bring a Single Cancer Drug to Market and Revenues After Approval. .” *JAMA Internal Medicine* 177 (11): 1569-1575.

Qu, X.B., Pan, J., Zhang, C. & Huang, S.Y. 2008. “Sox17 facilitates the differentiation of mouse embryonic stem cells into primitive and definitive endoderm in vitro. .” *Development, Growth & Differentiation* 50 (7): 585-93.

Quessada, J., Cuccuini, W., Saultier, P., Loosveld, M., Harrison, C.J. & Lafage-Pochitaloff, M. 2021. “Cytogenetics of Pediatric Acute Myeloid Leukemia: A Review of the Current Knowledge.” *Genes (Basel).* 12 (6): 924.

Rademakers, T., Horvath, J. M., van Blitterswijk, C. A., & LaPointe, V. 2019. “Oxygen and nutrient delivery in tissue engineering: Approaches to graft vascularization.” *Journal of tissue engineering and regenerative medicine* 13 (10): 1815-1829.

Ran, F.A., Hsu, P.D., Wright, J., Agarwala, V., Scott, D.A. & Zhang, F. 2013. “Genome engineering using the CRISPR-Cas9 system.” *Nature Protocols* 8 (11): 2281-2308.

Ribatti, D. 2016. “The chick embryo chorioallantoic membrane (CAM). A multifaceted experimental model.” *Mechanisms of Development* 141: 70-77.

Riddell, J., Gazit, R., Garrison, B.S., Guo, G., Saadatpour, A., Mandal, P.K., Ebina, W., Volchkov, P., Yuan, G.C., Orkin, S.H. & Rossi, D.J. 2014. “Reprogramming committed murine blood cells to induced hematopoietic stem cells with defined factors.” *Cells* 158 (1): 549-64.

Rivron, N.C., Frias-Aldeguer, J., Vrij, E.J., Boisset, J.C., Korving, J., Vivié, J., Truckenmüller, R.K., van Oudenaarden, A., van Blitterswijk, C.A. & Geijsen, N. 2018. “Blastocyst-like structures generated solely from stem cells.” *Nature.* 557 (7703): 106-111.

Robin, C., Bollerot, K., Mendes, S., Haak, E., Crisan, M., Cerisoli, F., Lauw, I., Imanirad, P., Verstegen, M., Cupedo, T. & Dzierzak, E. 2009. “Human placenta is a potent hematopoietic niche containing hematopoietic stem and progenitor cells throughout development." *Cell Stem Cell.* 5 (4): 385-395.

Robinson, S.N., Seina, S.M., Gohr, J.C., Kuszynski, C.A. & Sharp, J.G. 2005. "Evidence for a qualitative hierarchy within the Hoechst-33342 'side population' (SP) of murine bone marrow cells." *Bone Marrow Transplant.* 35 (8): 807-18.

Rossi, G., Broguiere, N., Miyamoto, M., Boni, A., Guiet, R., Girgin, M., Kelly, R.G., Kwon, C. & Lutolf, M.P. 2021a. "Capturing Cardiogenesis in Gastruloids." *Cell Stem Cell* 28 (2): 230-240.

Rossi, G., Giger, S., Hübscher, T. & Lutolf, M.P. 2021b. "Gastruloids as in vitro models of embryonic blood development with spatial and temporal resolution." *biorxiv.*

Rozario, T. & DeSimone, D.W. 2010. "The extracellular matrix in development and morphogenesis: a dynamic view." *Developmental Biology* 341 (1): 126-40.

Rue, P. & Martinez Arias, A. 2015. "Cell dynamics and gene expression control in tissue homeostasis and development." *Molecular systems biology.* 11 (1): 792.

Rybtsov, S., Batsivari, A., Bilotkach, K., Paruzina, D., Senserrich, J., Nerushev, O. & Medvinsky, A. 2014. "Tracing the origin of the HSC hierarchy reveals an SCF-dependent, IL-3-independent CD43(-) embryonic precursor." *Stem cell reports* 3 (3): 489-501.

Rybtsov, S., Ivanovs, A., Zhao, S. & Medvinsky, A. 2016. "Concealed expansion of immature precursors underpins acute burst of adult HSC activity in foetal liver." *Development.* 143 (8): 1284-9.

Rybtsov, S., Sobiesiak, M., Taoudi, S., Souilhol, C., Senserrich, J., Liakhovitskaia, A., Ivanovs, A., Frampton, J., Zhao, S. & Medvinsky, A. 2011. "Hierarchical organization and early hematopoietic specification of the developing HSC lineage in the AGM region." *The Journal of experimental medicine.* 208 (6): 1305-15.

Sabin, F. R. 1920. "Studies on the origin of blood vessels and of red blood corpuscules as seen in the living blastoderm of chicks during the second day of incubation." *Contrib. Embryol.* 9: 213-262.

Sankaran VG, Xu J, & Orkin SH. 2010. "Advances in the understanding of haemoglobin switching." *British journal of haematology.* 181-94: 149(2):.

Satija, R., Farrell, J.A., Gennert, D., Schier, A.F. & Regev, A. 2015. "Spatial reconstruction of single-cell gene expression data." *Nature Biotechnology* 33 (5): 495-502.

Sato, T., Vries, R.G., Snippert, H.J., van de Wetering, M., Barker, N., Stange, D.E., van Es, J.H., Abo, A., Kujala, P., Peters, P.J. & Clevers, H. 2009. "Single Lgr5 stem cells build crypt-villus structures in vitro without a mesenchymal niche." *Nature* 459 (7244): 262-5.

Schwank, G., Koo, B.K., Sasselli, V., Dekkers, J.F., Heo, I., Demircan, T., Sasaki, N., Boymans, S., Cuppen, E., van der Ent, C.K., Nieuwenhuis, E.E., Beekman, J.M. & Clevers, H. 2013. "Functional repair of CFTR by CRISPR/Cas9 in intestinal stem cell organoids of cystic fibrosis patients.Cell Stem Cell." *Cell Stem Cell.* 13 (6): 653-8.

Seco, P., Martins, G.G., Jacinto, A. & Tavares, A.T. 2020. “A Bird's Eye View on the Origin of Aortic Hemogenic Endothelial Cells.” *Frontiers in - Cell and Developmental Biology* 8: 605274.

Shalaby, F., Ho, J., Stanford, W.L., Fischer, K.D., Schuh. A.C., Schwartz, L., Bernstein, A. & Rossant, J. 1997. “A requirement for Flk1 in primitive and definitive hematopoiesis and vasculogenesis.” *Cells* 89 (6): 981-90.

Shav-Tal, Y. & Zipori, D. 2002. “The role of activin a in regulation of hemopoiesis.” *Stem cells.* 20 (6): 493-500.

Shiratori, H. & Hamada, H. 2006. “The left-right axis in the mouse: from origin to morphology.” *Development* 133 (11): 2095-104.

Simian, M., Hirai, Y., Navre, M., Werb, Z., Lochter, A. & Bissell, M.J. 2001. “The interplay of matrix metalloproteinases, morphogens and growth factors is necessary for branching of mammary epithelial cells. .” *Development.* 128 (16): 3117-31.

Simunovic, M., Metzger, J.J., Etoc, F., Yoney, A., Ruzo, A., Martyn, I., Croft, G., You, D.S., Brivanlou, A.H. & Siggia, E.D. 2019. “A 3D model of a human epiblast reveals BMP4-driven symmetry breaking.” *Nature Cell Biology* 21 (7): 900-910.

Sinka, L., Biasch, K., Khazaal, I., Péault, B. & Tavian, M. 2012. “Angiotensin-converting enzyme (CD143) specifies emerging lympho-hematopoietic progenitors in the human embryo.” *Blood* 119 (16): 3712-23.

Skardal, A., Murphy, S.V., Devarasetty, M., Mead, I., Kang, H.W., Seol, Y.J., Aleman, J,, Hall, A.R., Shupe, T.D., Kleensang, A., Dokmeci, M.R., Jackson, J.D., Yoo, J.J., Hartung, T., Khademhosseini, A., Soker, S., Bishop, C.E. & Atala, A. 2017. “Multi-tissue interactions in an integrated three-tissue organ-on-a-chip platform.” *Scientific Reports* 7 (1): 8837.

Souilhol, C., Gonneau, C., Lendinez, J.G., Batsivari, A., Rybtsov, S., Wilson, H., Morgado-Palacin, L., Hills, D., Taoudi, S., Antonchuk, J., Zhao, S. & Medvinsky, A. 2016. “Inductive interactions mediated by interplay of asymmetric signalling underlie development of adult haematopoietic stem cells.” *Nature communications.* 7: 10784.

Steinberg, J.R., Weeks, B.T., Reyes, G.A., Conway Fitzgerald, A., Zhang, W.Y., Lindsay, S.E., Anderson, J.N., Chan, K., Richardson, M.T., Magnani, C.J., Igbinosa, I., Girsen, A., El-Sayed, Y.Y., Turner, B.E. & Lyell, D.J. 2021. “The obstetrical research landscape: a cross-sectional analysis of clinical trials from 2007-2020.” *American Journal of Obstetrics & Gynecology MFM* 3 (1).

STEMCELL Technologies Inc. 2018. *MethoCult™ GF M3434.* https://www.stemcell.com/methocult-gf-m3534.html.

Suchting, S., Freitas, C., le Noble, F., Benedito, R., Bréant, C., Duarte, A. & Eichmann, A. 2007. “The Notch ligand Delta-like 4 negatively regulates endothelial tip cell formation and vessel branching.” *Proceedings of the National Academy of Sciences of the United States of America.* 104 (9): 3225-30.

Sugimura, R., Jha, D.K., Han, A., Soria-Valles, C., da Rocha, E.L., Lu, Y.F., Goettel, J.A., Serrao, E., Rowe, R.G., Malleshaiah, M., Wong, I., Sousa, P., Zhu, T.N., Ditadi, A., Keller, G., Engelman, A.N., Snapper, S.B., Doulatov, S. & Daley, G.Q. 2017. "Haematopoietic stem and progenitor cells from human pluripotent stem cells." *Natures* 545 (7655): 432-438.

Sugimura, R., Jha, D.K., Han, A., Soria-Valles, C., da Rocha, E.L., Lu, Y.F., Goettel, J.A., Serrao, E., Rowe, R.G., Malleshaiah, M., Wong, I., Sousa, P., Zhu, T.N., Ditadi, A., Keller, G., Engelman, A.N., Snapper, S.B., Doulatov, S. & Daley, G.Q. 2017. "Haematopoietic stem and progenitor cells from human pluripotent stem cells." *Nature* (Nature) 545 (7655): 432-438.

Sun, J., Ramos, A., Chapman, B., Johnnidis, J.B., Le, L., Ho, Y.J., Klein, A., Hofmann, O. & Camargo, F.D. 2014. "Clonal dynamics of native haematopoiesis." *Nature* 514 (7522): 322-7.

Swiers, G., Rode, C., Azzoni, E. & de Bruijn, M.F. 2013. "A short history of hemogenic endothelium." *Blood Cells, Molecules and Diseases* 51 (4): 206-12.

Tabor, J.J., Salis, H.M., Simpson, Z.B., Chevalier, A.A., Levskaya, A., Marcotte, E.M., Voigt, C.A. & Ellington, A.D. 2009. "A synthetic genetic edge detection program." *Cells* 137 (7): 1272-81.

Takebe, T., Imai, R. & Ono, S. 2018. "The Current Status of Drug Discovery and Development as Originated in United States Academia: The Influence of Industrial and Academic Collaboration on Drug Discovery and Development." *Clinical and Translational Science* 11 (6): 597-606.

Tam, P.P. & Loebel, D.A. 2007. "Gene function in mouse embryogenesis: get set for gastrulation." *Nature Reviews Genetics* 8 (5): 368-381.

Tang, W., He, J., Huang, T., Bai, Z., Wang, C., Wang, H., Yang, R., Ni, Y., Hou, J., Wang, J., Zhou, J., Yao, Y., Gong, Y., Hou, S., Liu, B, & Lan. Y. 2021. "Hlf Expression Marks Early Emergence of Hematopoietic Stem Cell Precursors With Adult Repopulating Potential and Fate." *Frontiers in Cell and Developmental Biology* 9 (728057).

Taoudi, S., Gonneau, C., Moore, K., Sheridan, J.M., Blackburn, C.C., Taylor, E. & Medvinsky, A. 2008. "Extensive hematopoietic stem cell generation in the AGM region via maturation of VE-cadherin+CD45+ pre-definitive HSCs." *Cell Stem Cell.* 3 (3): 99-108.

Tober, J., Koniski, A., McGrath, K.E., Vemishetti, R., Emerson, R., de Mesy-Bentley, K.K., Waugh, R. & Palis, J. 2007. "The megakaryocyte lineage originates from hemangioblast precursors and is an integral component both of primitive and of definitive hematopoiesis. ." *Blood* 109 (4): 1433-41.

Tosolini M, Jouneau A. 2016. "Acquiring Ground State Pluripotency: Switching Mouse Embryonic Stem Cells from Serum/LIF Medium to 2i/LIF Medium. ." *Methods in molecular biology.* 1341: 41-8.

Trowbridge, J.J., Scott, M.P. & Bhatia, M. 2006. "Hedgehog modulates cell cycle regulators in stem cells to control hematopoietic regeneration." *Proceedings of the National Academy of Sciences of the United States of America.* 103 (38): 14134-9.

Turner, D. A., Baillie-Johnson, P., & Martinez Arias, A. 2016. “Organoids and the genetically encoded self-assembly of embryonic stem cells.” *BioEssays : news and reviews in molecular, cellular and developmental biology* 38 (2): 181-191.

Turner, D. A., Girgin, M., Alonso-Crisostomo, L., Trivedi, V., Baillie-Johnson, P., Glodowski, C. R., Hayward, P. C., Collignon, J., Gustavsen, C., Serup, P., Steventon, B., P Lutolf, M., & Arias, A. M. 2017. “Anteroposterior polarity and elongation in the absence of extra-embryonic tissues and of spatially localised signalling in gastruloids: mammalian embryonic organoids.” *Development* 144 (21): 28943906.

van den Brink, S.C. & van Oudenaarden, A. 2021. “D gastruloids: a novel frontier in stem cell-based in vitro modeling of mammalian gastrulation.” *Trends in Cell Biology* 31 (9): 747-759.

van den Brink, S.C., Alemany, A., van Batenburg, V., Moris, N., Blotenburg, M., Vivié, J., Baillie-Johnson, P., Nichols, J., Sonnen, K.F., Martinez Arias, A. & van Oudenaarden, A. 2020. “Single-cell and spatial transcriptomics reveal somitogenesis in gastruloids.” *Nature* 582 (7812): 405-409.

van den Brink, S.C., Baillie-Johnson, P., Balayo, T., Hadjantonakis, A.K., Nowotschin, S., Turner, D.A. & Martinez Arias, A. 2014. “Symmetry breaking, germ layer specification and axial organisation in aggregates of mouse embryonic stem cells.” *Development.* 141 (22): 4231-42.

Veenvliet, J.V., Bolondi, A., Kretzmer, H., Haut, L., Scholze-Wittler, M., Schifferl, D., Koch, F., Guignard, L., Kumar, A.S., Pustet, M., Heimann, S., Buschow, R., Wittler, L., Timmermann, B., Meissner, A. & Herrmann, B.G. 2020. “Mouse embryonic stem cells self-organize into trunk-like structures with neural tube and somites.” *Science* 370 (6522).

Viotti, M., Nowotschin, S. & Hadjantonakis, A.K. 2014. “SOX17 links gut endoderm morphogenesis and germ layer segregation. .” *Nature Cell Biology* 16 (12): 1146-56.

Vogeli, K. M., Jin, S. W., Martin, G. R. & Stainier, D. Y. 2006. “A common progenitor for hematopoietic and endothelial lineages in the zebrafish gastrula.” *Nature* 443: 337-339.

Wang, P.W., Khan, S., Nguyen, T., Kingshott, P. & Wong, R.C.B. 2018. “Topographical Modulation of Pluripotency and Differentiation of Human Embryonic Stem Cells.” *IEEE Transactions on Nanotechnology.* 17 (3).

Wang, X. & Rivière, I. 2017. “Genetic Engineering and Manufacturing of Hematopoietic Stem Cells.” *Molecular Therapy – Methods & Clinical Development* 5: 96-105.

Wang, X., Gong, Y. & Ema, H. 2016. “Chasing the precursor of functional hematopoietic stem cells at the single cell levels in mouse embryos.” *Journal of hematology & oncology* 9 (1): 58.

Wang, Y., Yates, F., Naveiras, O., Ernst, P. & Daley, G.Q. 2005. “Embryonic stem cell-derived hematopoietic stem cells. .” *Proceedings of the National Academy of Sciences of the United States of America.* 102 (52): 19081-6.

Warmflash, A., Sorre, B., Etoc, F., Siggia, E.D. & Brivanlou, A.H. 2014. “A method to recapitulate early embryonic spatial patterning in human embryonic stem cells.” *Nature Methods* 11 (8): 847-54.

Waskow, C., Paul, S., Haller, C., Gassmann, M. & Rodewald H.R. 2002. “Viable c-Kit(W/W) mutants reveal pivotal role for c-kit in the maintenance of lymphopoiesis. .” *Immunity* 17 (3): 277-88.

Wiles, M.V. & Keller, G. 1991. “Multiple hematopoietic lineages develop from embryonic stem (ES) cells in culture.” *Development* 111 (2): 259-67.

Wilkinson, R.N., Pouget, C., Gering, M., Russell, A.J., Davies, S.G., Kimelman, D. & Patient, R. 2009. “Hedgehog and Bmp polarize hematopoietic stem cell emergence in the zebrafish dorsal aorta.” *Developmental Cell* 16 (6): 909-16.

Wilson, A. and Trumpp, A. 2006. “Bone-marrow haematopoietic-stem-cell niches.” *Nature Reviews Immunology* 6 (2): 93-106.

Wilson, N.K., Kent, D.G., Buettner, F., Shehata, M., Macaulay, I.C., Calero-Nieto, F.J., Sánchez Castillo, M., Oedekoven, C.A., Diamanti, E., Schulte, R., Ponting, C.P., Voet, T., Caldas, C., Stingl, J., Green, A.R., Theis, F.J. & Göttgens, B. 2015. “Combined Single-Cell Functional and Gene Expression Analysis Resolves Heterogeneity within Stem Cell Populations.” *Cell Stem Cell* 16 (6): 712-24.

Xue, L., Cai, J.Y., Ma, J., Huang, Z., Guo, M.X., Fu, L.Z., Shi, Y.B. & Li, W.X. 2013. “Global expression profiling reveals genetic programs underlying the developmental divergence between mouse and human embryogenesis.” *BMC Genomics* 14: 568.

Yamaguchi, T.P., Dumont, D.J., Conlon, R.A., Breitman, M.L. & Rossant, J. 1993. “flk-1, an flt-related receptor tyrosine kinase is an early marker for endothelial cell precursors.” *Development.* 118 (2): 489-98.

Yamamoto, R., Morita, Y., Ooehara, J., Hamanaka, S., Onodera, M., Rudolph, K.L,, Ema, H. & Nakauchi, H. 2013. “Clonal analysis unveils self-renewing lineage-restricted progenitors generated directly from hematopoietic stem cells.” *Cell.* 154 (5): 1112-1126.

Yamane, T. 2020. “Cellular Basis of Embryonic Hematopoiesis and Its Implications in Prenatal Erythropoiesis.” *International Journal of Molecular Sciences* 21 (24): 9346.

Yang, L., Bryder, D., Adolfsson, J., Nygren, J., Månsson, R., Sigvardsson, M. & Jacobsen, S,E. 2005. “Identification of Lin(-)Sca1(+)kit(+)CD34(+)Flt3- short-term hematopoietic stem cells capable of rapidly reconstituting and rescuing myeloablated transplant recipients. .” *Blood.* 105 (7): 2717-23.

Ye, H., Wang, X., Li, Z., Zhou, F., Li, X., Ni, Y., Zhang, W., Tang, F., Liu, B. & Lan, Y. 2017. “Clonal analysis reveals remarkable functional heterogeneity during hematopoietic stem cell emergence.” *Cell Research - Nature* 27 (8): 1065-1068.

Ye, S., Li, P., Tong, C. & Ying, Q,L. 2013. “Embryonic stem cell self-renewal pathways converge on the transcription factor Tfcp2l1. .” *The EMBO journal.* 32 (19): 2548-60.

Ye, S., Tan, L., Yang, R., Fang, B., Qu, S., Schulze, E.N., Song, H., Ying, Q. & Li, P. 2012. “Pleiotropy of glycogen synthase kinase-3 inhibition by CHIR99021 promotes self-renewal of embryonic stem cells from refractory mouse strains. .” *PLoS One.* 7 (4): e35892.

Ying, Q.L., Wray, J., Nichols, J., Batlle-Morera, L., Doble, B., Woodgett, J., Cohen, P. and Smith, A. 2008. "The ground state of embryonic stem cell self-renewal." *Nature* 453 (7194): 519-23.

Yokota, T. 2019. ""Hierarchy" and "Holacracy"; A Paradigm of the Hematopoietic System." *Cells* 8 (10): 1138.

Yoshida, H., Takakura, N., Hirashima, M., Kataoka, H., Tsuchida, K., Nishikawa, S. & Nishikawa, S. 1998. "Hematopoietic tissues, as a playground of receptor tyrosine kinases of the PDGF-receptor family. ." *Developmental and comparative immunology.* 22 (3): 321-32.

Yoshimoto, M., Montecino-Rodriguez, E., Ferkowicz, M.J., Porayette, P., Shelley, W.C., Conway, S.J., Dorshkind, K. & Yoder, M.C. 2011. "Embryonic day 9 yolk sac and intra-embryonic hemogenic endothelium independently generate a B-1 and marginal zone progenitor lacking B-2 potential." *Proceedings of the National Academy of Sciences of the United States of America* 108 (4): 1468-73.

Yumine, A., Fraser, S.T. & Sugiyama, D. 2017. "Regulation of the embryonic erythropoietic niche: a future perspective." *Blood Research* 52 (1): 10-17.

Yzaguirre, A.D., Howell, E.D., Li, Y., Liu, Z. & Speck, N.A. 2018. "Runx1 is sufficient for blood cell formation from non-hemogenic endothelial cells in vivo only during early embryogenesis. ." *Development.* 145 (2).

Zeigler, B.M., Sugiyama, D., Chen, M., Guo, Y., Downs, K.M. & Speck, N.A. 2006. "The allantois and chorion, when isolated before circulation or chorio-allantoic fusion, have hematopoietic potential." *Development.* 133 (21): 4183-4192.

Zhang, L., Sultana, N., Yan, J., Yang, F., Chen, F., Chepurko, E., Yang, F.C., Du, Q., Zangi, L., Xu, M., Bu, L. & Cai, C.L. 2018. "Cardiac Sca-1+ Cells Are Not Intrinsic Stem Cells for Myocardial Development, Renewal, and Repair. ." *Circulation.* 138 (25): 2919-2930.

Zhang, Y., Gao, S., Xia, J. & Liu, F. 2018. "Hematopoietic Hierarchy - An Updated Roadmap." *Trends in Cell Biology* 28 (12): 976-986.

Zhou, F., Li, X., Wang, W., Zhu, P., Zhou, J., He, W., Ding, M., Xiong, F., Zheng, X., Li, Z., Ni, Y., Mu, X., Wen, L., Cheng, T., Lan, Y., Yuan, W., Tang, F. & Liu, B. 2016. "Tracing haematopoietic stem cell formation at single-cell resolution." *Nature* 533 (7604): 487-92.

Zovein, A.C., Hofmann, J.J., Lynch, M., French, W.J., Turlo, K.A., Yang, Y., Becker, M.S., Zanetta, L., Dejana, E., Gasson, J.C., Tallquist, M.D. & Iruela-Arispe, M.L. 2008. "Fate tracing reveals the endothelial origin of hematopoietic stem cells." *Cell Stem Cell* 3 (6): 625-36.

Zriwil, A., Böiers, C., Kristiansen, T.A., Wittmann, L., Yuan, J., Nerlov, C., Sitnicka, E. & Jacobsen, S.E.W. 2018. "Direct role of FLT3 in regulation of early lymphoid progenitors." *British Journal of Haematology* 183 (4): 588-600.

Appendix 1: Differential gene expression profile of clusters in whole gastruloid cells

Cluster 0

	names	logfoldchanges	pvals	pvals_adj	scores
0	Mfap2	5.765777111	2.18329E-52	6.44638E-48	15.23155689
1	Col3a1	7.835797787	2.59605E-45	3.83254E-41	14.12682056
2	Ptn	5.77524519	4.08929E-40	4.02468E-36	13.25738144
3	Mdk	2.637127876	1.09202E-37	8.06078E-34	12.83151817
4	Dlk1	4.397938728	3.11979E-35	1.8423E-31	12.38579464
5	Ldhb	4.153129101	1.92414E-32	9.46869E-29	11.85937119
6	Selenow	0.903362751	2.2973E-32	9.69E-29	11.84451962
7	Gpc3	4.780353069	9.40698E-30	3.47188E-26	11.32919121
8	Nr2f2	3.345435143	2.17343E-28	7.1303E-25	11.05076981
9	Tceal9	1.21217525	1.81136E-25	5.34823E-22	10.42986965
10	Peg3	4.670468807	1.55907E-23	4.18483E-20	9.99774456
11	Nrep	2.742598295	8.81222E-23	2.16825E-19	9.824715614
12	Serf1	1.727099061	1.21251E-22	2.75388E-19	9.792508125
13	Cd63	1.713794827	1.97047E-22	4.15573E-19	9.743301392
14	Ubb	0.533239841	1.09618E-21	2.15773E-18	9.567409515
15	Cald1	3.084106684	1.69697E-20	2.7836E-17	9.279862404
16	Vcan	3.697408676	8.15299E-20	1.14631E-16	9.111127853
17	H3f3a	0.491853297	1.26709E-19	1.70055E-16	9.063173294
18	Lgals1	3.251943111	1.41193E-19	1.81255E-16	9.051363945
19	Ubb-ps	0.521561205	1.2779E-18	1.50925E-15	8.807656288
20	Cnpy2	1.187075734	1.89047E-18	2.14685E-15	8.763638496
21	Elob	0.547889292	2.55482E-18	2.79384E-15	8.729640961
22	Crabp1	3.978772163	4.88183E-18	5.14789E-15	8.656099319
23	Cdkn1c	2.992989063	7.32165E-18	7.45445E-15	8.609755516
24	H2az2	1.043007851	1.7056E-16	1.52605E-13	8.24115181
25	S100a11	2.224305391	1.90507E-16	1.65438E-13	8.227910995
26	Igf2r	2.089465141	2.13703E-16	1.80279E-13	8.214133263
27	Mir100hg	3.725611925	6.08384E-16	4.85491E-13	8.087626457
28	Ssbp2	2.474800825	1.00789E-15	7.83128E-13	8.025895119
29	H3f3b	0.429152608	1.81947E-15	1.37748E-12	7.953068733
30	Nfia	2.609124899	3.32885E-15	2.39726E-12	7.877916336
31	Cdh11	3.531437159	5.14392E-15	3.61618E-12	7.823341846
32	Sox11	2.708812952	8.08364E-15	5.55064E-12	7.766262054
33	Ndufa2	0.529096305	3.6266E-14	2.27828E-11	7.573729038
34	Id2	3.234766483	5.11321E-14	3.12357E-11	7.528995514
35	Ndufa7	0.518001437	5.18374E-14	3.12357E-11	7.527206421
36	Bex3	0.671791136	9.10293E-14	5.27006E-11	7.453306675
37	Ndufa11	0.608435154	1.10935E-13	6.29899E-11	7.427182198
38	Atpif1	0.470828146	1.7655E-13	9.65336E-11	7.365450382
39	Sem1	0.430667967	2.50294E-13	1.34367E-10	7.318748474
40	Pbx1	2.492703915	3.18861E-13	1.59571E-10	7.286182404

41	Atp5k	0.574067116	6.43233E-13	3.16535E-10	7.190989971
42	Ifitm2	0.923475862	6.80507E-13	3.29388E-10	7.183295727
43	Ddr2	5.016016483	1.20078E-12	5.53974E-10	7.105280399
44	Sumo2	0.460650057	1.27119E-12	5.77433E-10	7.097407341
45	Cdc26	0.937741041	1.85727E-12	7.83396E-10	7.044800758
46	Ldhb-ps	1.860113621	2.03714E-12	8.47163E-10	7.031917572
47	Dynlt1f	0.661754131	2.85872E-12	1.17231E-09	6.984500408
48	Slc25a4	0.580094516	3.53518E-12	1.39173E-09	6.954618454
49	Nfib	3.057936192	5.8734E-12	2.28182E-09	6.882687092
50	Tceal8	0.703961551	7.69919E-12	2.95229E-09	6.844037056
51	Grb10	2.104910374	7.91375E-12	2.99566E-09	6.840100765
52	Prrx1	3.592445374	1.20193E-11	4.43604E-09	6.779978752
53	Fstl1	2.416189671	1.26764E-11	4.62079E-09	6.772284985
54	Ndufc1	0.554803967	3.57434E-11	1.23611E-08	6.620728016
55	Rcn3	2.53062892	4.63917E-11	1.57444E-08	6.582078457
56	Epha7	2.848917007	5.87015E-11	1.91837E-08	6.547007084
57	Atp5o	0.440324545	5.91248E-11	1.91837E-08	6.545933723
58	Gm8524	1.233863473	1.10258E-10	3.39113E-08	6.452172279
59	H3f3c	0.9387725	1.22031E-10	3.71453E-08	6.436784267
60	Sdhb	0.439727157	1.37594E-10	4.14551E-08	6.418532848
61	Serpinf1	2.90552187	1.46602E-10	4.37229E-08	6.40887022
62	Ppib	0.519019306	1.56185E-10	4.57438E-08	6.399208069
63	AA465934	0.782134771	1.58026E-10	4.57438E-08	6.397418499
64	Gabarap	0.593080699	1.69721E-10	4.86524E-08	6.386503696
65	Cxcl12	3.426754951	1.72927E-10	4.90945E-08	6.383640766
66	Cdk4	0.637463093	2.19102E-10	6.04599E-08	6.347317219
67	Runx1t1	2.553274393	2.28463E-10	6.24593E-08	6.340875626
68	Morf4l1	0.320247203	2.7725E-10	7.44188E-08	6.310993671
69	Psme2	0.524793863	3.3849E-10	9.00384E-08	6.28003788
70	Pdcd5	0.518820643	5.75448E-10	1.4522E-07	6.197012901
71	Prdx2	0.578963101	6.00828E-10	1.5034E-07	6.190213203
72	Pdcd5-ps	0.674346626	6.1882E-10	1.5354E-07	6.18556118
73	Cstb	0.868446767	1.10407E-09	2.6503E-07	6.093589306
74	Gm1673	1.414129972	1.1494E-09	2.73687E-07	6.087147236
75	Ube2b	0.852597177	1.42515E-09	3.3396E-07	6.052613258
76	Atp5md	0.400977015	1.44588E-09	3.3615E-07	6.050287247
77	Tshz2	2.176579714	1.73789E-09	3.94308E-07	6.020584106
78	Gm48564	0.625104249	1.74945E-09	3.94308E-07	6.019510746
79	Gm10257	0.983030319	2.33972E-09	5.0796E-07	5.972271919
80	Ndufa13	0.408075243	2.59638E-09	5.51515E-07	5.955273151
81	Rcn2	1.538591027	3.75557E-09	7.70047E-07	5.894614697
82	Cd63-ps	1.370856285	5.00462E-09	1.0121E-06	5.847018242
83	Mrpl27	0.637200058	5.55994E-09	1.10176E-06	5.829483032
84	Fbn2	2.258244276	6.40351E-09	1.26047E-06	5.80586338
85	Ift43	1.581894755	8.64347E-09	1.62552E-06	5.755404472
86	Cox6c	0.35112223	9.16157E-09	1.69065E-06	5.74556303
87	Rab34	2.236210585	9.41688E-09	1.72697E-06	5.74091053
88	Ndufb11	0.438793093	1.21883E-08	2.16789E-06	5.697072029

89	Tmem167	0.508457661	1.48995E-08	2.59319E-06	5.662716389
90	Cd302	2.747842312	1.49306E-08	2.59319E-06	5.662358761
91	Flywch2	2.742832661	1.72371E-08	2.95896E-06	5.637665749
92	Sec61b	0.342725486	2.05146E-08	3.44155E-06	5.60760498
93	Hsd17b10	0.429923534	2.21889E-08	3.70141E-06	5.594006062
94	Lsm7	0.512138665	2.23727E-08	3.70944E-06	5.592574596
95	Sec61g	0.382838011	2.24883E-08	3.70944E-06	5.59168005
96	Sumo1	0.329417408	2.7904E-08	4.47768E-06	5.554103851
97	Gm48553	0.566881776	2.8423E-08	4.53632E-06	5.550882816
98	Psme2b	0.688486397	2.9762E-08	4.72448E-06	5.542830944
99	Hsbp1	0.393163502	3.14818E-08	4.97076E-06	5.532989502
100	Selenom	1.632234573	3.41913E-08	5.31333E-06	5.518496037
101	Gsta4	1.723656178	3.61954E-08	5.59532E-06	5.50847578
102	Tmsb10	0.765278399	4.09637E-08	6.17089E-06	5.486645699
103	Gm13835	0.414547414	5.24475E-08	7.7043E-06	5.442807198
104	Sec11a	0.587906361	5.33509E-08	7.7982E-06	5.439764977
105	Son	0.398689359	5.87424E-08	8.5021E-06	5.422587395
106	Ndufa3	0.451021284	6.16326E-08	8.8769E-06	5.413998604
107	Mir99ahg	2.177998066	7.18658E-08	1.02015E-05	5.386442661
108	Atp5j	0.325748324	7.37485E-08	1.04187E-05	5.381790638
109	Id3	1.957551956	7.80448E-08	1.09211E-05	5.371591568
110	Tbca	0.404655337	1.11665E-07	1.54067E-05	5.306638241
111	Gm48513	0.71945411	1.29074E-07	1.74701E-05	5.280156136
112	Marcks	1.370960355	1.29579E-07	1.74701E-05	5.279440403
113	Maged2	1.658889294	1.49385E-07	1.97791E-05	5.253316402
114	Ppdpf	0.539349198	1.62705E-07	2.14465E-05	5.237569809
115	Col11a1	2.644356012	1.70447E-07	2.22682E-05	5.228981018
116	Dnmt3a	1.493674517	1.93246E-07	2.45939E-05	5.205719948
117	Prdx2-ps1	0.765054762	2.01029E-07	2.54746E-05	5.198383331
118	Gm9844	0.84551549	2.17723E-07	2.74722E-05	5.183532238
119	Ccnd2	1.831178427	2.25806E-07	2.79495E-05	5.17673254
120	Nme4	1.291540504	2.58161E-07	3.16284E-05	5.1516819
121	Npc2	0.881944656	2.61383E-07	3.18909E-05	5.149355888
122	Atraid	0.830575526	3.49805E-07	4.14793E-05	5.094422817
123	Nedd8	0.365179151	4.16363E-07	4.87839E-05	5.061320305
124	Lhfpl2	2.670580149	4.49629E-07	5.22668E-05	5.046647549
125	Malat1	0.630489469	4.69838E-07	5.41891E-05	5.038237572
126	Col1a1	4.910087585	5.10054E-07	5.85987E-05	5.022491455
127	Tmem258	0.353377491	5.56675E-07	6.29747E-05	5.005671978
128	Gm43584	0.720086038	5.70279E-07	6.37805E-05	5.001019478
129	Tmem45a	4.801992893	5.92934E-07	6.55692E-05	4.993504524
130	Polr2i	0.780315399	6.04585E-07	6.66081E-05	4.989746571
131	Ssbp1	0.558056116	6.39692E-07	6.99539E-05	4.978831768
132	Ndufa5	0.368986845	7.57898E-07	8.12277E-05	4.94590807
133	Fkbp7	1.845104098	7.59291E-07	8.12277E-05	4.945549965
134	Zfp637	1.581789494	7.71947E-07	8.19874E-05	4.942329407
135	Gm8034	0.828495622	8.269E-07	8.75091E-05	4.928909302
136	Cetn3	0.212873727	8.49142E-07	8.92234E-05	4.92372036

137	Tspan3	1.091364264	8.8804E-07	9.2085E-05	4.914952278
138	Atp5j2	0.310187161	8.88852E-07	9.2085E-05	4.914773464
139	Sfrp1	2.715226889	9.56131E-07	9.73473E-05	4.900458813
140	Btf3l4	0.548585534	9.92486E-07	0.000100701	4.893122673
141	Gm12350	0.784413278	1.00155E-06	0.000100928	4.891333103
142	Snai2	2.668122768	1.01715E-06	0.000102151	4.888291359
143	Chd3	2.303780794	1.03768E-06	0.000103509	4.884354591
144	Gtf2h5	0.307059586	1.13923E-06	0.000112123	4.865924358
145	Rbms3	2.89618969	1.16739E-06	0.000114513	4.861093521
146	Notch2	1.504871607	1.20816E-06	0.00011773	4.854293823
147	Dynlt1c	0.410476595	1.35827E-06	0.000131489	4.831032276
148	Timm8b	0.482252359	1.36561E-06	0.000131768	4.829958916
149	Rps26	0.25014627	1.44377E-06	0.000138405	4.818864822
150	Dynlt1b	0.321228802	1.53856E-06	0.000147015	4.806160927
151	Pdlim7	1.159523726	2.12824E-06	0.000199839	4.740849972
152	Grcc10	0.582122505	2.15471E-06	0.000201049	4.738344669
153	Tmem256	0.413947999	2.15852E-06	0.000201049	4.737987041
154	Tecr	0.272918522	2.69601E-06	0.000245901	4.692716599
155	Gpx8	1.805543661	2.69837E-06	0.000245901	4.692537785
156	Prdx4	0.500409961	3.00687E-06	0.000269851	4.670350075
157	Ncam1	1.977977872	3.24604E-06	0.000288683	4.654603958
158	C1d	0.347497612	3.33167E-06	0.000294524	4.649235725
159	Ss18l2	0.827405632	3.47621E-06	0.000305472	4.640468121
160	Snrnp27	0.332988054	3.56148E-06	0.000311922	4.635457993
161	Skp1	0.360181212	3.57074E-06	0.000311922	4.634921074
162	Ostc	0.148463681	3.58311E-06	0.00031208	4.634205341
163	Airn	2.222911835	3.61111E-06	0.000313593	4.632595062
164	Fxyd1	3.782881021	3.72841E-06	0.000320948	4.625974178
165	Psmb6	0.301089913	3.80317E-06	0.000326328	4.621859074
166	Tpm1	1.003771544	3.94679E-06	0.000334865	4.614164829
167	Pfdn5	0.310957909	3.98779E-06	0.000337374	4.612017632
168	Rpl22l1	0.385078818	4.00155E-06	0.000337571	4.611301899
169	Fundc2	0.635160387	4.01535E-06	0.00033777	4.610586166
170	Mrpl14	0.375000477	4.19899E-06	0.000350225	4.601281643
171	Foxp2	2.738044262	4.79946E-06	0.000394732	4.573368073
172	Cox7c	0.242189527	4.81589E-06	0.000394983	4.57265234
173	Mrpl21	0.544032037	5.00021E-06	0.000405594	4.564779282
174	Ndufs3	0.319942832	5.38015E-06	0.000432845	4.549390793
175	D8Ertd738e	0.176464945	5.77783E-06	0.000460218	4.534360409
176	Atp6v1g1	0.341582894	5.87161E-06	0.000462699	4.53096056
177	Fbln1	1.813119769	6.39507E-06	0.000490386	4.512888432
178	Romo1	0.274419367	6.52587E-06	0.000496605	4.508594036
179	Pafah1b3	0.885916352	6.58112E-06	0.000499522	4.506804466
180	Hmga2	1.384887815	6.74957E-06	0.000509688	4.50143671
181	Gstp1	0.843772829	7.15881E-06	0.000534663	4.488911152
182	Arl3	1.453784823	8.11713E-06	0.000594706	4.462070942
183	Erh	0.24999103	8.42074E-06	0.000610886	4.454197884
184	H3f3a-ps2	0.541863501	8.81553E-06	0.000637959	4.444356441

185	Spcs1	0.257063061	9.21265E-06	0.000658626	4.434873104
186	Eny2	0.35142839	1.00838E-05	0.000714579	4.415369511
187	Lpar1	2.193490267	1.00921E-05	0.000714579	4.41519022
188	Psma3	0.277642012	1.0397E-05	0.000730906	4.408748627
189	Oaz1	0.335968792	1.10696E-05	0.000767235	4.395149708
190	Igf2	0.829127312	1.19396E-05	0.000816038	4.378687859
191	Septin7	0.441097617	1.19985E-05	0.000818173	4.377614498
192	Cst3	0.389516979	1.22171E-05	0.000827342	4.373677731
193	Alx1	3.169857979	1.28115E-05	0.00086112	4.363299847
194	Sfr1	0.325306743	1.28325E-05	0.00086112	4.362941742
195	Dynll1	0.23815468	1.31943E-05	0.0008794	4.356858253
196	Gli3	1.837790132	1.4269E-05	0.000940417	4.339680195
197	Vps72	0.719394088	1.43856E-05	0.00094389	4.337891102
198	Meis1	1.780497074	1.48372E-05	0.000967071	4.331091404
199	Parm1	2.389503241	1.53271E-05	0.00099243	4.323934078

Cluster 1

	names	**logfoldchange**	**pvals**	**pvals_adj**	**scores**
0	Ecscr	10.13255	7.39E-64	2.18E-59	16.87071
1	Gimap6	9.228951	4.15E-62	6.13E-58	16.63107
2	Cldn5	9.756306	8.92E-62	8.78E-58	16.5852
3	Gng11	7.747735	3.96E-57	2.93E-53	15.92935
4	Elk3	7.158746	1.16E-56	6.87E-53	15.86193
5	Emcn	9.306989	2.06E-56	1.01E-52	15.82595
6	Kdr	7.367974	5.35E-56	2.25E-52	15.76584
7	Egfl7	6.799891	6.93E-56	2.56E-52	15.74943
8	Ramp2	7.9305	1.07E-55	3.52E-52	15.72175
9	F11r	7.372057	2.71E-54	7.99E-51	15.51592
10	Icam2	9.089886	4.51E-54	1.21E-50	15.48309
11	Vim	4.646353	1.52E-53	3.74E-50	15.4048
12	S1pr1	7.162066	2.98E-53	6.76E-50	15.3613
13	Plxnd1	6.99908	2.05E-51	4.32E-48	15.08448
14	Ctla2a	7.855728	1.25E-50	2.46E-47	14.96466
15	BC028528	6.208576	3.44E-50	6.36E-47	14.89704
16	Tspan18	6.801633	5.53E-50	9.6E-47	14.86541
17	Sparc	6.428199	6.92E-50	1.13E-46	14.85038
18	Col4a1	6.736255	1.2E-48	1.87E-45	14.6578
19	Myct1	7.439823	5.28E-48	7.79E-45	14.55696
20	Fkbp1a	2.221012	1.96E-47	2.76E-44	14.4668
21	Vamp5	6.97346	3.55E-47	4.76E-44	14.42607
22	Cdh5	7.053743	1.02E-46	1.32E-43	14.35271
23	Gmfg	6.967991	4.05E-46	4.99E-43	14.25701
24	Gngt2	6.835515	6.9E-46	8.15E-43	14.21984
25	Pcdh17	5.732253	9.88E-46	1.12E-42	14.19473
26	Plk2	6.754151	3.5E-45	3.83E-42	14.10576
27	Crip2	6.883645	1.02E-44	1.07E-41	14.03042
28	Stab1	7.258633	2.57E-43	2.62E-40	13.79928

29	Tmsb4x	3.153737	1.3E-42	1.28E-39	13.68223
30	Tmsb10	1.65593	4.69E-42	4.46E-39	13.58851
31	Anxa5	4.86014	6.36E-42	5.86E-39	13.56617
32	Tpm4	3.27705	7.02E-42	6.28E-39	13.55885
33	Arhgap18	6.975946	9.47E-41	8.22E-38	13.36667
34	Sox18	7.567988	2.05E-40	1.73E-37	13.30913
35	Cd93	7.726384	2.15E-40	1.77E-37	13.30537
36	Efna1	7.101407	4.35E-40	3.47E-37	13.25278
37	Flt4	6.544598	1.29E-39	1E-36	13.17092
38	Igfbp4	5.032798	1.49E-39	1.13E-36	13.16005
39	Cd34	7.24974	2.56E-39	1.89E-36	13.11912
40	Col18a1	5.606128	1.07E-38	7.73E-36	13.00997
41	Rhoc	4.69724	1.76E-38	1.24E-35	12.97201
42	S100a13	5.138379	2.17E-38	1.49E-35	12.95619
43	Ets2	5.174747	2.29E-38	1.54E-35	12.95184
44	Col4a2	5.843853	2.35E-38	1.54E-35	12.94987
45	Klhl4	7.392093	3.34E-38	2.14E-35	12.92298
46	Lxn	4.778404	1.18E-37	7.32E-35	12.8257
47	Gm8034	1.964532	1.19E-37	7.32E-35	12.82491
48	Calm1	1.410034	3.05E-37	1.84E-34	12.75175
49	Sat1	5.722626	4.29E-37	2.53E-34	12.72506
50	Thsd1	6.638296	4.8E-37	2.78E-34	12.71636
51	Crem	5.732615	1.07E-36	6.09E-34	12.65328
52	Gm16104	5.028234	1.27E-36	7.06E-34	12.64023
53	Madcam1	8.033079	3.03E-36	1.66E-33	12.57143
54	Msn	5.093144	1.36E-35	7.29E-33	12.4524
55	Anxa2	5.904167	3.04E-35	1.6E-32	12.38794
56	Rasgrp3	6.309357	4.13E-35	2.14E-32	12.36322
57	Clec1b	6.9491	5.12E-35	2.61E-32	12.34602
58	Ostf1	5.258152	6.24E-35	3.12E-32	12.33001
59	Ppic	3.666491	6.45E-35	3.17E-32	12.32743
60	Gm3788	2.01579	8.36E-35	4.05E-32	12.30648
61	Igfbp3	6.620741	1.27E-34	5.94E-32	12.27286
62	Tax1bp3	3.765452	1.56E-34	7.21E-32	12.25586
63	B2m	3.13278	2.34E-34	1.06E-31	12.22304
64	Anxa6	5.73005	2.36E-34	1.06E-31	12.22225
65	Upp1	6.453378	2.96E-34	1.3E-31	12.20406
66	Igf1	5.983839	3.09E-34	1.34E-31	12.2005
67	Esam	7.394323	1.09E-33	4.58E-31	12.09768
68	Gnai2	3.821138	2.09E-33	8.71E-31	12.0437
69	Mef2c	4.970781	3.29E-33	1.35E-30	12.00633
70	Ssu72	2.16184	8.41E-33	3.31E-30	11.92843
71	Mmrn2	6.58931	1.11E-32	4.29E-30	11.90569
72	Cd38	6.415323	1.99E-32	7.64E-30	11.85646
73	Ipo11	4.780359	6.7E-32	2.54E-29	11.75443
74	Rab11a	2.777457	9.92E-32	3.71E-29	11.72122
75	Sh3bgrl3	1.833782	1.13E-31	4.12E-29	11.71014
76	Fli1	4.312791	1.36E-31	4.9E-29	11.69452

77	Rasip1	5.4911	2.27E-31	8.08E-29	11.65083
78	Myl6	1.111045	4.47E-31	1.57E-28	11.59309
79	Sox7	6.820633	7.32E-31	2.54E-28	11.55078
80	Gm9844	1.740221	8.75E-31	3E-28	11.53536
81	Cyb5a	2.286221	3.02E-30	1.01E-27	11.42819
82	Ets1	5.209648	3.14E-30	1.04E-27	11.42503
83	Sptbn1	4.049684	3.75E-30	1.23E-27	11.40941
84	Myo1b	4.574349	3.63E-29	1.18E-26	11.2103
85	Prcp	5.169239	4.09E-29	1.31E-26	11.19962
86	Tek	6.926417	4.94E-29	1.55E-26	11.18301
87	Ralb	4.026374	5.89E-29	1.83E-26	11.16739
88	Myzap	5.881882	9.66E-29	2.97E-26	11.1233
89	Pfn1	0.88621	1.25E-28	3.8E-26	11.10037
90	Tagln2	4.905603	1.47E-28	4.42E-26	11.08593
91	Gng2	3.907295	1.82E-28	5.42E-26	11.06675
92	Mpzl1	4.482674	2.54E-28	7.51E-26	11.0367
93	Gm7809	2.127632	7.62E-28	2.2E-25	10.93764
94	Arap3	5.645366	1.87E-27	5.35E-25	10.85598
95	Cd59a	4.395111	2.52E-27	7.15E-25	10.82869
96	Lama4	6.45706	2.59E-27	7.3E-25	10.82593
97	Actr2	1.552538	5.36E-27	1.49E-24	10.75929
98	Tnfaip8l1	5.765085	7.74E-27	2.14E-24	10.72529
99	Apold1	5.983686	8.6E-27	2.35E-24	10.7156
100	Anxa3	5.622103	1.35E-26	3.65E-24	10.67388
101	2810025M15Ri	3.236642	1.8E-26	4.83E-24	10.64699
102	Ptprm	5.874312	9.72E-26	2.56E-23	10.48881
103	Cd81	2.415479	9.99E-26	2.61E-23	10.48624
104	Hspg2	4.471336	1.03E-25	2.67E-23	10.48347
105	Actb	0.756468	2.31E-25	5.93E-23	10.40675
106	Tspan13	4.108732	2.77E-25	7.06E-23	10.38935
107	Flt1	5.223666	3.66E-25	9.12E-23	10.36286
108	Gng5	0.804465	5.01E-25	1.23E-22	10.33281
109	Lpar6	3.944043	6.54E-25	1.6E-22	10.3071
110	Arhgap29	4.743003	7.78E-25	1.88E-22	10.29049
111	Tpm3	2.083204	1.34E-24	3.22E-22	10.2379
112	Pde4b	6.129373	1.52E-24	3.58E-22	10.22604
113	Tmem88	5.370419	1.56E-24	3.66E-22	10.22327
114	Myl12a	1.206321	1.59E-24	3.69E-22	10.22169
115	Dram2	3.962819	2.64E-24	6.08E-22	10.17225
116	Itga6	4.833939	2.8E-24	6.42E-22	10.16632
117	Cd9	4.524724	3.13E-24	7.1E-22	10.15565
118	Slc39a1	2.590738	3.94E-24	8.88E-22	10.13311
119	Bmp2k	3.622265	4.38E-24	9.81E-22	10.12263
120	Pon2	4.763168	5.09E-24	1.13E-21	10.10799
121	Arhgap31	5.198553	6.47E-24	1.43E-21	10.08447
122	Prex2	4.893996	1.14E-23	2.47E-21	10.0289
123	Rhoj	5.538572	1.2E-23	2.58E-21	10.02396
124	Cdc42ep1	4.48086	1.56E-23	3.34E-21	9.997665

125	Adam10	3.441006	2.97E-23	6.24E-21	9.933801
126	Itm2b	2.339893	2.98E-23	6.24E-21	9.933405
127	Ppp1r16b	5.93398	3.22E-23	6.69E-21	9.925694
128	Gpihbp1	6.587339	5.05E-23	1.04E-20	9.880613
129	Cavin1	5.838245	7.22E-23	1.48E-20	9.844825
130	Prkar1a	2.154485	8.04E-23	1.64E-20	9.83395
131	Sema6d	4.99857	1.19E-22	2.41E-20	9.794209
132	Fxyd5	5.37884	1.2E-22	2.42E-20	9.79322
133	mt-Co1	0.731054	1.45E-22	2.89E-20	9.774436
134	Dusp6	4.082879	2.14E-22	4.18E-20	9.735089
135	Pea15a	4.123814	2.94E-22	5.72E-20	9.702465
136	Calcrl	4.085967	5.3E-22	1.02E-19	9.642357
137	Vamp8	3.021415	5.44E-22	1.04E-19	9.639588
138	Arpc5	2.805289	6.26E-22	1.19E-19	9.625154
139	Nid1	4.822831	6.96E-22	1.32E-19	9.61428
140	Tcf4	3.229485	1.07E-21	2E-19	9.570386
141	Ccdc85b	3.873783	1.28E-21	2.35E-19	9.551602
142	Gm5526	1.50237	1.28E-21	2.35E-19	9.551207
143	Rcsd1	5.246755	1.33E-21	2.42E-19	9.54745
144	Tnfaip1	3.98518	1.34E-21	2.43E-19	9.546461
145	Nfkbia	3.973304	2.58E-21	4.64E-19	9.478642
146	Sri	2.058103	2.66E-21	4.76E-19	9.475281
147	Clic1	2.06911	3.37E-21	5.99E-19	9.450565
148	Gm17018	2.894474	8.31E-21	1.44E-18	9.355659
149	Ica1	4.521407	8.79E-21	1.52E-18	9.349727
150	Tmem255a	6.104815	8.92E-21	1.53E-18	9.348145
151	Eng	4.632308	1.45E-20	2.47E-18	9.296342
152	Itm2a	4.254959	1.56E-20	2.63E-18	9.288828
153	Timp3	4.863348	1.82E-20	3.06E-18	9.27222
154	Sh3bp5	4.737452	2.08E-20	3.47E-18	9.258181
155	Selenop	4.285906	3.6E-20	5.98E-18	9.19926
156	Lamb1	4.205217	3.85E-20	6.35E-18	9.192142
157	Pomp	0.94352	5.41E-20	8.87E-18	9.155562
158	Arpc2	1.68656	5.71E-20	9.32E-18	9.149632
159	Exoc3l4	4.589641	6.04E-20	9.79E-18	9.1437
160	Gm26862	3.610636	7.95E-20	1.28E-17	9.113843
161	Serf2	0.624206	9.49E-20	1.51E-17	9.094665
162	Litaf	3.697378	1.38E-19	2.17E-17	9.053933
163	N4bp3	5.76443	1.99E-19	3.1E-17	9.013993
164	Cavin3	5.32631	2.77E-19	4.3E-17	8.977612
165	Plvap	4.878501	3.19E-19	4.93E-17	8.961992
166	Grap	5.618803	3.33E-19	5.12E-17	8.957247
167	Trp53i11	4.368176	5.09E-19	7.78E-17	8.910386
168	Dock6	4.414527	9.11E-19	1.39E-16	8.845533
169	Aplp2	3.700111	9.44E-19	1.43E-16	8.841578
170	Creg1	3.483154	9.5E-19	1.43E-16	8.840788
171	Arhgef15	5.108475	9.57E-19	1.43E-16	8.839997
172	Kank3	4.63396	1.02E-18	1.52E-16	8.833076

173	Maged2	3.408616	1.13E-18	1.68E-16	8.821015
174	Cfl1	0.569978	1.69E-18	2.48E-16	8.77633
175	Dad1	0.99582	3.25E-18	4.7E-16	8.702382
176	Cd59b	2.505214	3.31E-18	4.76E-16	8.700404
177	Igf2	1.872859	3.4E-18	4.87E-16	8.697241
178	Ptpn18	3.134391	3.7E-18	5.27E-16	8.68775
179	Akap12	3.810518	3.74E-18	5.3E-16	8.686563
180	Bcl6b	5.940448	4.32E-18	6.11E-16	8.669955
181	Lrrc70	4.889184	4.6E-18	6.47E-16	8.662837
182	AC149090.1	2.880519	5.62E-18	7.86E-16	8.640099
183	Cmtm3	3.357815	6.28E-18	8.75E-16	8.627247
184	Lcp1	4.410617	6.39E-18	8.86E-16	8.62527
185	Tacc1	2.971044	8E-18	1.1E-15	8.599566
186	Snx3	1.573326	1.19E-17	1.63E-15	8.553694
187	Sdcbp	2.276987	1.21E-17	1.65E-15	8.551519
188	Ctsb	2.988908	1.36E-17	1.85E-15	8.538074
189	F2r	3.425481	1.57E-17	2.12E-15	8.521663
190	Malat1	1.108655	1.62E-17	2.18E-15	8.518104
191	Ctsl	2.307704	1.71E-17	2.29E-15	8.511777
192	Gnpda2	3.571329	2.31E-17	3.07E-15	8.476977
193	Ppp1r11	1.662303	3.05E-17	4.02E-15	8.444551
194	Gmfg-ps	3.015754	3.75E-17	4.92E-15	8.420429
195	Map4k4	3.159405	4.77E-17	6.23E-15	8.392352
196	Sipa1	4.146157	4.9E-17	6.37E-15	8.389189
197	Dysf	6.226363	5.25E-17	6.8E-15	8.380884
198	Klhl6	4.425582	5.27E-17	6.8E-15	8.380488
199	Hmcn1	3.165554	5.51E-17	7.07E-15	8.375348

Cluster 2

	names	**logfoldchanges**	**pvals**	**pvals_adj**	**scores**
0	H2az2	1.567811	2.19E-23	4.29E-19	9.963988
1	Mdk	2.64093	2.9E-23	4.29E-19	9.935931
2	Ranbp1	1.238363	1.52E-19	1.5E-15	9.042955
3	Hmgb1	0.799167	3.01E-19	2.22E-15	8.96846
4	H2az1	1.299954	4.14E-19	2.45E-15	8.933147
5	Psmb6	0.778946	5.32E-18	2.62E-14	8.646292
6	Ran	1.115508	2.14E-17	9.05E-14	8.485692
7	Cdk4	1.029176	3.06E-17	1.13E-13	8.444091
8	Apex1	1.636404	1.27E-15	4.18E-12	7.997118
9	Naca	0.555755	1.72E-15	5.08E-12	7.959871
10	Fkbp3	0.962356	4.31E-15	1.16E-11	7.845709
11	Sumo2	0.540831	4.98E-15	1.23E-11	7.827327
12	Pclaf	3.514961	6.18E-15	1.33E-11	7.800238
13	Snrpb	1.133441	6.32E-15	1.33E-11	7.797336
14	Ptn	4.429893	2.04E-14	4.01E-11	7.648345
15	Gm6563	1.198999	3.12E-14	5.76E-11	7.593199
16	Stmn1	0.970699	4.46E-14	7.75E-11	7.546761

17	Sdhb	1.044307	7.43E-14	1.22E-10	7.480005
18	Nme1	1.114907	9.79E-14	1.52E-10	7.443725
19	Oaz1	0.692158	1.03E-13	1.53E-10	7.436469
20	Ppia	0.460742	1.17E-13	1.64E-10	7.420506
21	Sumo1	0.691353	2.06E-13	2.77E-10	7.344801
22	Gm15387	1.024072	3.59E-13	4.61E-10	7.270064
23	Skp1	0.778289	3.82E-13	4.7E-10	7.26184
24	Sarnp	1.17888	6.44E-13	7.61E-10	7.190731
25	Gm10282	0.852473	7.61E-13	8.64E-10	7.167996
26	Mrpl42	1.315554	8.34E-13	9.12E-10	7.155418
27	H3f3a	0.551285	9.4E-13	9.92E-10	7.138971
28	Cks1b	1.566283	1.07E-12	1.09E-09	7.121557
29	Gm10123	0.470134	1.19E-12	1.17E-09	7.107045
30	Erh	0.609872	2.2E-12	2.03E-09	7.02094
31	Ldhb	3.632052	2.53E-12	2.26E-09	7.001832
32	Snrpa1	1.46767	7.58E-12	6.58E-09	6.846312
33	Crabp2	4.275135	1.23E-11	1.04E-08	6.77617
34	Hmgn2	0.785079	1.28E-11	1.05E-08	6.770365
35	Id2	4.043922	1.42E-11	1.13E-08	6.756337
36	Selenoh	1.304481	1.49E-11	1.15E-08	6.749322
37	Hspe1	0.921127	1.96E-11	1.41E-08	6.70893
38	Chchd2	0.510191	2.51E-11	1.73E-08	6.67265
39	Gm1673	2.301661	2.61E-11	1.75E-08	6.667329
40	Ndufa12	0.773475	2.67E-11	1.75E-08	6.663459
41	Dctpp1	1.675945	3.22E-11	2.01E-08	6.63637
42	Hint1	0.78768	3.27E-11	2.01E-08	6.633952
43	Gm8186	0.604596	6.69E-11	4.03E-08	6.52753
44	Srsf7	0.692544	1.31E-10	7.71E-08	6.426429
45	Snrpd2	0.681554	2.46E-10	1.37E-07	6.329198
46	Snrpg	0.546178	4.32E-10	2.32E-07	6.242126
47	Cct5	0.859882	5.01E-10	2.64E-07	6.218906
48	Psma7	0.556056	7.64E-10	3.96E-07	6.152151
49	Gm11223	0.827804	8.32E-10	4.24E-07	6.138606
50	Gm26585	0.829591	9.15E-10	4.58E-07	6.12361
51	Snrpe	0.604825	9.63E-10	4.74E-07	6.115387
52	Hmgb1-ps8	0.825495	9.9E-10	4.79E-07	6.111033
53	Nmral1	2.830117	1.1E-09	5.24E-07	6.094102
54	Bex3	0.926094	1.32E-09	6.2E-07	6.064595
55	Atp5o	0.534841	1.36E-09	6.29E-07	6.059757
56	Nutf2	0.854451	1.88E-09	8.56E-07	6.007514
57	Psma3	0.561079	2.07E-09	9.13E-07	5.992034
58	Dynlt1f	0.979497	2.47E-09	1.07E-06	5.963252
59	Hsp90aa1	0.648748	2.56E-09	1.08E-06	5.957689
60	D8Ertd738e	0.776351	3.39E-09	1.39E-06	5.911734
61	Ndufa12-ps	0.734393	3.46E-09	1.4E-06	5.908348
62	Elob	0.515052	4.13E-09	1.65E-06	5.87884
63	Ube2i	0.592	4.34E-09	1.68E-06	5.870858
64	Rps9	0.349694	5.05E-09	1.91E-06	5.845462

65	Hmgb1-ps2	1.114823	6.77E-09	2.53E-06	5.796605
66	Nedd8	0.59131	7.66E-09	2.79E-06	5.775805
67	Psma1	0.899749	7.84E-09	2.82E-06	5.771935
68	Cdc26	1.146101	9.74E-09	3.42E-06	5.73517
69	Ubb	0.467047	1.03E-08	3.55E-06	5.725979
70	Prdx2	0.670347	1.05E-08	3.55E-06	5.723077
71	Rpl18	0.42936	1.22E-08	4.09E-06	5.696955
72	Rps3a2	0.409479	1.25E-08	4.1E-06	5.693086
73	Psma2	0.496256	1.25E-08	4.1E-06	5.692602
74	Rpl21	0.413176	1.27E-08	4.11E-06	5.690667
75	Ywhae	0.545413	1.52E-08	4.87E-06	5.659708
76	Park7	0.628175	1.66E-08	5.28E-06	5.643744
77	Nasp	2.229621	2.09E-08	6.56E-06	5.604562
78	Gm21596	0.694939	3.66E-08	1.11E-05	5.506606
79	Mdh1	0.978765	3.66E-08	1.11E-05	5.506606
80	Tipin	1.950162	3.98E-08	1.19E-05	5.49161
81	Dcakd	1.666847	4.17E-08	1.23E-05	5.483628
82	Hnrnpc	0.806616	4.79E-08	1.4E-05	5.458958
83	Btf3	0.513831	5.13E-08	1.47E-05	5.446864
84	Gm15428	1.680062	6.23E-08	1.72E-05	5.412035
85	Gm6394	0.398165	6.35E-08	1.74E-05	5.408649
86	Lsm7	0.630379	6.77E-08	1.84E-05	5.397039
87	AA465934	1.079916	7.6E-08	2.02E-05	5.376481
88	Ndufab1	0.619755	7.7E-08	2.03E-05	5.374062
89	Rps3a1	0.376579	7.83E-08	2.05E-05	5.370917
90	H3f3b	0.485227	8.9E-08	2.28E-05	5.34794
91	Ndufa7	0.552871	9.2E-08	2.34E-05	5.341893
92	Gm13577	0.993815	9.94E-08	2.49E-05	5.327865
93	Psmc1	0.912467	1.01E-07	2.51E-05	5.324963
94	Psmb2	0.572792	1.16E-07	2.8E-05	5.300292
95	Gpc3	3.300072	1.25E-07	3E-05	5.286264
96	Gm13835	0.525133	1.46E-07	3.46E-05	5.256998
97	Ube2n	0.690221	1.65E-07	3.87E-05	5.234988
98	Rpl27	0.396428	1.73E-07	3.99E-05	5.226281
99	Lsm3	1.054702	2.02E-07	4.63E-05	5.197257
100	Rps14	0.311584	2.29E-07	5.12E-05	5.174037
101	Rps3a3	0.348492	2.33E-07	5.14E-05	5.170651
102	Gm6724	0.773662	2.36E-07	5.16E-05	5.168716
103	Eloc	0.806488	2.44E-07	5.27E-05	5.162427
104	Mif	0.492797	2.51E-07	5.38E-05	5.156622
105	Hsd17b10	0.779051	2.73E-07	5.79E-05	5.141385
106	Crabp1	3.125324	3.01E-07	6.31E-05	5.122761
107	Rps11	0.375561	3.25E-07	6.76E-05	5.108249
108	Hmgn1	0.664032	3.4E-07	7.03E-05	5.099542
109	Sem1	0.451802	3.68E-07	7.43E-05	5.08503
110	Rpl23a	0.425791	4.34E-07	8.59E-05	5.053587
111	Psmc4	0.585447	4.4E-07	8.65E-05	5.050926
112	Tecr	0.744344	5.25E-07	9.99E-05	5.017065

113	Atp5pb	0.642101	5.34E-07	0.0001	5.013679
114	Atpif1	0.472326	5.47E-07	0.000102	5.009083
115	Cops4	0.917194	5.81E-07	0.000107	4.997474
116	Acat2	1.765788	5.93E-07	0.000109	4.993362
117	Dlk1	2.081675	6.76E-07	0.000123	4.968207
118	Snu13	0.976313	7.09E-07	0.000128	4.958775
119	Snrpert	0.557049	7.33E-07	0.000132	4.952486
120	Elof1	1.371397	7.47E-07	0.000134	4.948617
121	Ssb	0.691766	7.87E-07	0.000138	4.938458
122	Sap18	0.537589	8.29E-07	0.000145	4.928299
123	Uchl3	1.378352	8.63E-07	0.000149	4.920559
124	Peg3	3.232491	8.7E-07	0.000149	4.918867
125	Rpl7	0.386073	8.87E-07	0.000151	4.915238
126	Gsta4	2.102345	8.88E-07	0.000151	4.914997
127	Ndufa2	0.514365	9.25E-07	0.000156	4.907015
128	Psma5	0.751144	9.91E-07	0.000161	4.89347
129	Srsf3	0.592424	1.03E-06	0.000165	4.886698
130	Lsm8	0.857828	1.08E-06	0.000174	4.875572
131	Rpl5	0.359705	1.16E-06	0.000185	4.862511
132	Ptges3	0.726689	1.22E-06	0.000194	4.852353
133	Cct8	0.690121	1.29E-06	0.000201	4.841711
134	Lsm4	0.896508	1.29E-06	0.000201	4.841469
135	Vdac3	0.842505	1.36E-06	0.00021	4.831069
136	Rps15	0.367972	1.37E-06	0.00021	4.829618
137	Nsmce2	1.133309	1.42E-06	0.000217	4.822845
138	Rps6	0.344802	1.49E-06	0.000227	4.812203
139	Anapc13	0.79211	1.5E-06	0.000227	4.811719
140	Brix1	0.864985	1.57E-06	0.000236	4.802528
141	Atp5c1	0.554346	1.65E-06	0.000245	4.79237
142	Psmc2	0.758383	1.71E-06	0.000252	4.78463
143	Rps4x	0.403271	1.79E-06	0.000262	4.775439
144	Gm10095	0.409204	1.89E-06	0.000275	4.764797
145	Rps25	0.314428	1.93E-06	0.000279	4.760927
146	Mfap2	2.699361	2.08E-06	0.000297	4.745689
147	Phb	0.94542	2.16E-06	0.000306	4.738191
148	Eif3m	0.622692	2.27E-06	0.00032	4.728033
149	Cacybp	1.190323	2.34E-06	0.000328	4.721986
150	Emg1	1.417134	2.45E-06	0.000343	4.71207
151	Serf1	1.087349	2.58E-06	0.000359	4.701911
152	Tcp1	0.919428	2.7E-06	0.000372	4.69272
153	Cd24a	2.641933	2.7E-06	0.000372	4.69272
154	Polr2j	0.592735	2.89E-06	0.000396	4.678692
155	Rpl6	0.304295	3.14E-06	0.000427	4.661761
156	Tmem167	0.997574	3.38E-06	0.000453	4.646523
157	Psmb7	0.703743	3.43E-06	0.000458	4.643137
158	Pafah1b3	1.395236	3.49E-06	0.000464	4.639751
159	Hmgb1-ps4	1.206266	3.61E-06	0.000478	4.632737
160	Dbi	0.724462	3.72E-06	0.000488	4.626448

161	Rps5	0.371278	4.18E-06	0.000538	4.602262
162	Clns1a	0.960597	4.19E-06	0.000538	4.601778
163	Rpl13	0.285786	4.41E-06	0.000561	4.591136
164	Prdx1	0.478913	4.46E-06	0.000563	4.588717
165	Cetn3	0.782411	4.74E-06	0.000591	4.57614
166	Thyn1	1.104614	4.88E-06	0.000605	4.570093
167	Mrps18c	0.729335	5.08E-06	0.000624	4.561628
168	Cox5a	0.638701	5.29E-06	0.000648	4.55292
169	Tceal8	1.157489	6.76E-06	0.00081	4.501161
170	Psmc6	0.920209	6.77E-06	0.00081	4.500677
171	Eif2s1	1.092386	7.06E-06	0.000833	4.49197
172	Eef1d	0.841328	7.14E-06	0.00084	4.489551
173	Gm15459	0.454126	7.38E-06	0.000862	4.482295
174	Wdr61	1.160473	7.71E-06	0.000893	4.473104
175	Cct7	0.984	8.18E-06	0.00094	4.460527
176	Dut	1.788944	8.19E-06	0.00094	4.460285
177	Ift46	1.93916	8.77E-06	0.001003	4.445531
178	Bccip	1.095539	8.87E-06	0.001011	4.443112
179	Prps1	2.215073	9.03E-06	0.001021	4.439242
180	Fcf1	0.810831	9.46E-06	0.001066	4.429084
181	Ywhaq	0.60418	9.96E-06	0.00111	4.417958
182	Rps16	0.334058	1.07E-05	0.001179	4.402479
183	Psmc5	0.85931	1.1E-05	0.001205	4.39619
184	Cox7a2	0.500871	1.11E-05	0.001214	4.393772
185	Cox7c	0.402527	1.16E-05	0.001261	4.384581
186	Txnl4a	1.029377	1.21E-05	0.001314	4.374906
187	Rsl24d1	1.188865	1.32E-05	0.001417	4.356524
188	Ndufa4	0.529626	1.36E-05	0.001446	4.350719
189	Hspa8	0.413678	1.41E-05	0.001499	4.342012
190	Ubb-ps	0.368846	1.44E-05	0.001524	4.337174
191	Oaz1-ps	0.717695	1.68E-05	0.001743	4.303313
192	Eif2b2	1.666861	1.75E-05	0.001798	4.294122
193	Fkbp4	1.341908	1.8E-05	0.001839	4.288317
194	Eif4a3	0.854622	1.84E-05	0.001865	4.282996
195	Set	0.817235	1.93E-05	0.001947	4.272595
196	Cnpy2	0.536997	1.94E-05	0.001947	4.27187
197	Bcas2	0.954496	1.95E-05	0.001953	4.270419
198	Psmb3	0.189846	2.03E-05	0.002021	4.261228
199	Banf1	0.429728	2.35E-05	0.002312	4.228817

Cluster 3

	names	logfoldchanges	pvals	pvals_adj	scores
0	Car2	8.635583	5.77E-40	1.7E-35	13.23154
1	Smim1	8.845968	3.42E-38	5.06E-34	12.92105
2	Nfe2	10.59639	4.37E-37	2.58E-33	12.7237
3	Tspan32	10.91873	6.34E-35	2.68E-31	12.32874
4	Hbb-bh1	16.45304	1.58E-33	5.81E-30	12.06714

5	Fth1	1.788708	4.16E-33	1.23E-29	11.98702
6	Gfi1b	10.4964	1.25E-32	3.35E-29	11.89564
7	Rgs10	8.196259	4.76E-32	1.08E-28	11.78327
8	Rps2	1.081434	1.69E-31	3.55E-28	11.67628
9	Fermt3	8.470946	1.84E-31	3.63E-28	11.6686
10	Prkar2b	7.071903	2.24E-31	4.13E-28	11.65222
11	Prdx3	4.397731	7.85E-31	1.36E-27	11.54471
12	Rpl14	0.914139	1.77E-30	2.61E-27	11.47457
13	Rap1b	5.555245	9.92E-30	1.33E-26	11.32458
14	Urod	4.979169	4.58E-28	5.88E-25	10.98362
15	Gpx1	2.30235	1.78E-27	2.19E-24	10.86025
16	Bola3	2.790505	1.2E-25	1.37E-22	10.46862
17	Rplp0	0.727966	1.27E-25	1.39E-22	10.4635
18	Tmem14c	3.421284	1.46E-25	1.54E-22	10.45019
19	H2az1	1.576423	2.1E-25	2.14E-22	10.41589
20	Rbm38	4.764688	2.32E-25	2.28E-22	10.40641
21	Snrnp25	3.825399	1.05E-24	1E-21	10.26128
22	Srm	4.132054	1.84E-24	1.65E-21	10.20702
23	Sptb	7.373595	1.09E-23	9.21E-21	10.03296
24	Lyl1	5.972642	1.38E-23	1.1E-20	10.00966
25	Hmbs	4.394652	2.29E-23	1.78E-20	9.959749
26	Rplp1	0.771379	3.98E-23	3.01E-20	9.90446
27	Rpl6	0.621555	4.3E-23	3.17E-20	9.896781
28	Blvrb	5.269103	6.47E-23	4.66E-20	9.855825
29	Rpl19	0.690758	8.01E-23	5.63E-20	9.834324
30	Asns	5.000963	1.2E-22	8.21E-20	9.793881
31	Hbb-bs	36.51742	1.23E-22	8.27E-20	9.79081
32	Gclm	5.99859	1.5E-22	9.85E-20	9.770844
33	Fech	5.780544	1.95E-22	1.25E-19	9.744224
34	Rpl4	0.684834	2.19E-22	1.38E-19	9.732449
35	Glrx5	4.534212	1.38E-21	8.15E-19	9.543544
36	Gm10076	0.622729	4.44E-21	2.57E-18	9.421702
37	Gypa	35.91552	5.11E-21	2.85E-18	9.406857
38	Hbb-bt	33.87194	5.11E-21	2.85E-18	9.406857
39	Hbb-y	12.24995	6.16E-21	3.32E-18	9.387147
40	Nt5c3	4.902548	6.18E-21	3.32E-18	9.38689
41	Hba-a2	12.66993	7.41E-21	3.91E-18	9.367693
42	Rpl23a	0.83005	1.31E-20	6.66E-18	9.30754
43	Rpl18	0.693196	1.7E-20	8.49E-18	9.279896
44	Gm8730	0.643823	2.11E-20	1.04E-17	9.256859
45	Eif5a	0.958166	2.29E-20	1.11E-17	9.247643
46	Snca	8.787775	3.02E-20	1.44E-17	9.218207
47	Gata1	11.50918	3.86E-20	1.81E-17	9.191842
48	Gm29718	2.805613	4.23E-20	1.95E-17	9.182116
49	Hba-a1	14.0669	4.72E-20	2.14E-17	9.170341
50	Rps11	0.701244	6.6E-20	2.95E-17	9.133993
51	Creg1	4.606606	7.79E-20	3.38E-17	9.116076
52	Atp5g1	1.018587	9.84E-20	4.21E-17	9.090734

53	Tnfaip8	5.299805	1.44E-19	6.09E-17	9.049011
54	Cox8a	0.89259	1.89E-19	7.76E-17	9.01932
55	Rplp2	0.791804	3.87E-19	1.57E-16	8.940481
56	C1qbp	1.958825	1.27E-18	4.93E-16	8.808401
57	Eif4ebp1	2.687138	1.39E-18	5.26E-16	8.798162
58	Rps18	0.626927	1.44E-18	5.39E-16	8.794066
59	Gypc	6.313212	2.45E-18	8.84E-16	8.73417
60	Rpl14-ps1	0.90194	3.55E-18	1.23E-15	8.692447
61	Emp3	4.998025	3.91E-18	1.34E-15	8.68144
62	Dhrs11	5.68095	4.95E-18	1.64E-15	8.654564
63	Rpl12	1.169203	5.96E-18	1.93E-15	8.633318
64	Cnbp	0.692343	9.4E-18	3.02E-15	8.5811
65	Syngr1	5.647251	1.14E-17	3.63E-15	8.558576
66	Rasgrp2	5.545842	1.56E-17	4.89E-15	8.522739
67	Gm7536	0.89909	1.58E-17	4.91E-15	8.521204
68	Hbb-bh0	34.37945	2.99E-17	9.1E-15	8.446973
69	Hsp90aa1	0.679204	3.02E-17	9.11E-15	8.445693
70	Supt4a	1.52415	3.52E-17	1.05E-14	8.428031
71	Dut	2.689906	4.34E-17	1.27E-14	8.403459
72	Pa2g4	2.049014	7.3E-17	2.11E-14	8.342026
73	Rpl13	0.514083	8.95E-17	2.57E-14	8.317965
74	Rpl17	0.793436	9.38E-17	2.66E-14	8.312333
75	Klf1	13.07752	1.62E-16	4.52E-14	8.247061
76	Tlcd1	5.279214	1.82E-16	5.02E-14	8.233495
77	Rps11-ps1	1.122735	2.51E-16	6.78E-14	8.194843
78	Gm9625	0.573186	2.58E-16	6.86E-14	8.191516
79	Inka1	4.344687	3.1E-16	8.16E-14	8.169502
80	Nop10	1.171321	3.46E-16	9.03E-14	8.156192
81	Psmb10	4.180947	3.57E-16	9.16E-14	8.152352
82	Alad	3.960818	5.12E-16	1.29E-13	8.108582
83	Cenpw	2.792401	5.18E-16	1.3E-13	8.107303
84	Crlf3	4.594499	5.75E-16	1.43E-13	8.094503
85	Gm14165	0.641844	1.33E-15	3.16E-13	7.99186
86	Rps13-ps1	0.66369	1.53E-15	3.62E-13	7.974454
87	Atp5b	0.649188	1.71E-15	4E-13	7.960888
88	Rpl27	0.556079	1.72E-15	4E-13	7.96012
89	Timm8a1	2.724022	2.44E-15	5.49E-13	7.916862
90	Ran	0.846938	3E-15	6.72E-13	7.890752
91	Gpx4	0.982886	3.83E-15	8.51E-13	7.860292
92	Hba-x	14.16088	4.06E-15	8.88E-13	7.853125
93	Rpl15-ps6	0.538263	4.06E-15	8.88E-13	7.853125
94	Cacybp	1.746218	1.13E-14	2.41E-12	7.723349
95	F10	8.227283	1.17E-14	2.48E-12	7.718741
96	Syngr2	4.439024	1.21E-14	2.53E-12	7.715414
97	Rack1	0.778345	1.23E-14	2.56E-12	7.712854
98	Adgrg1	6.021271	1.41E-14	2.91E-12	7.695704
99	Dapp1	6.839829	1.43E-14	2.93E-12	7.693913
100	Ubash3b	4.474391	1.67E-14	3.4E-12	7.673947

101	Chchd10	3.671857	1.73E-14	3.5E-12	7.66934
102	Sod2	2.929115	1.86E-14	3.75E-12	7.659613
103	Abcg2	4.142716	1.88E-14	3.75E-12	7.658589
104	Phlda1	2.654779	1.9E-14	3.77E-12	7.657053
105	Ftl2-ps	0.676387	2.38E-14	4.62E-12	7.628385
106	Banf1	0.773928	2.63E-14	5.08E-12	7.61533
107	Hdgf	3.377824	2.84E-14	5.45E-12	7.605347
108	Mpl	8.889615	2.99E-14	5.68E-12	7.598692
109	Rpl21	0.585043	3E-14	5.68E-12	7.59818
110	Rps8	0.614599	4.32E-14	8.02E-12	7.551082
111	Bcas2	1.671559	4.7E-14	8.67E-12	7.540075
112	Prkca	4.951284	4.91E-14	9.01E-12	7.534188
113	Tnni1	5.985558	6.56E-14	1.19E-11	7.496305
114	Galk1	2.779412	6.96E-14	1.25E-11	7.488626
115	Arhgdib	4.535917	7.7E-14	1.38E-11	7.475315
116	Cbfa2t3	4.709668	8.39E-14	1.49E-11	7.464052
117	Rps16	0.547287	8.66E-14	1.53E-11	7.459957
118	Smim3	5.201	8.82E-14	1.55E-11	7.457397
119	Npm1	0.46286	9.63E-14	1.67E-11	7.445879
120	Gpx4-ps2	1.022684	1.06E-13	1.82E-11	7.433336
121	Rps3a2	0.507655	1.1E-13	1.87E-11	7.428729
122	Alas2	7.491059	1.18E-13	2E-11	7.419002
123	Slc25a5	1.391953	1.43E-13	2.39E-11	7.393917
124	Prdx2	0.984765	1.8E-13	2.98E-11	7.363201
125	Rpl17-ps5	1.580072	1.83E-13	3.02E-11	7.360385
126	Hspe1	0.918594	1.87E-13	3.07E-11	7.357569
127	Rab5if	2.744026	1.91E-13	3.12E-11	7.354753
128	Tomm20	0.989964	2.57E-13	4.13E-11	7.315079
129	Rnaseh2a	3.227996	2.61E-13	4.17E-11	7.313031
130	Lmo2	4.56215	3.06E-13	4.86E-11	7.291529
131	Rpl41	0.43951	3.37E-13	5.32E-11	7.278731
132	Esd	1.448678	3.79E-13	5.92E-11	7.262861
133	Rpl31	0.56506	3.82E-13	5.93E-11	7.261837
134	Gm10180	0.934351	3.83E-13	5.93E-11	7.261325
135	Prkab1	4.026531	3.95E-13	6.08E-11	7.25723
136	Uqcr11	0.623487	4.48E-13	6.82E-11	7.24008
137	Polr2e	1.356236	5.21E-13	7.85E-11	7.219602
138	Pnpo	4.429209	5.58E-13	8.36E-11	7.210387
139	Gm12918	0.751363	5.61E-13	8.37E-11	7.20962
140	Tubb4b	3.418442	5.77E-13	8.56E-11	7.20578
141	Rpl39	0.673492	5.87E-13	8.67E-11	7.203476
142	Naa10	2.45029	6.05E-13	8.89E-11	7.19938
143	Rida	3.133531	6.64E-13	9.62E-11	7.186582
144	Mrpl12	2.044658	7.16E-13	1.03E-10	7.176343
145	Rab27b	7.013857	7.2E-13	1.03E-10	7.175576
146	Cenpp	3.835104	7.23E-13	1.03E-10	7.175064
147	Adk	3.730431	9.21E-13	1.29E-10	7.141788
148	Ddx39a	2.44606	1.19E-12	1.66E-10	7.106208

149	Rps7	0.432262	1.69E-12	2.33E-10	7.057574
150	Rps27l	0.697245	1.82E-12	2.46E-10	7.047847
151	Hscb	3.407769	1.94E-12	2.61E-10	7.038376
152	Ndufa6	1.034939	2.12E-12	2.83E-10	7.026346
153	Rpl7a	0.631033	2.77E-12	3.63E-10	6.988974
154	Rpl15	0.431278	2.91E-12	3.81E-10	6.981807
155	Rpl28	0.622827	3.29E-12	4.27E-10	6.964913
156	Polr2l	0.913528	3.38E-12	4.38E-10	6.960818
157	Mrpl38	3.190891	3.42E-12	4.41E-10	6.959282
158	Gmnn	3.353625	3.56E-12	4.57E-10	6.95365
159	Mrto4	2.570126	4.85E-12	6.17E-10	6.90988
160	Cited4	10.7623	5.26E-12	6.67E-10	6.898361
161	Idi1	3.287218	5.35E-12	6.75E-10	6.896058
162	Gm13841	0.926584	5.63E-12	7.08E-10	6.888634
163	Rpsa	0.680279	7.14E-12	8.89E-10	6.854846
164	Mllt3	4.117335	7.44E-12	9.23E-10	6.848959
165	Rps7-ps3	0.466795	8.45E-12	1.03E-09	6.830785
166	Tk1	3.740421	8.45E-12	1.03E-09	6.830785
167	Rps23	0.436763	8.75E-12	1.06E-09	6.825666
168	Psat1	3.860573	8.88E-12	1.07E-09	6.823618
169	Rpl8	0.636736	9.64E-12	1.15E-09	6.811844
170	Nhp2	1.241418	9.74E-12	1.15E-09	6.810308
171	Mfsd2b	7.698064	1.11E-11	1.3E-09	6.791878
172	Anp32b	2.289677	1.29E-11	1.5E-09	6.769865
173	Rpl30	0.633525	1.31E-11	1.51E-09	6.767817
174	Aldh9a1	3.896382	1.35E-11	1.56E-09	6.762698
175	Rpl27a	0.584427	1.55E-11	1.78E-09	6.743244
176	Rps13	0.508909	1.8E-11	2.05E-09	6.721743
177	Acadm	3.827672	1.87E-11	2.13E-09	6.715856
178	Dtymk	1.307742	1.89E-11	2.14E-09	6.714576
179	Nars	2.270959	2.02E-11	2.28E-09	6.704849
180	Ccnb2	4.250588	2.58E-11	2.88E-09	6.669013
181	Lyar	2.751183	2.71E-11	3.02E-09	6.66159
182	Ssx2ip	4.416946	2.8E-11	3.11E-09	6.656726
183	Mrpl57	2.195415	3.1E-11	3.43E-09	6.641624
184	Wdr12	3.434066	3.48E-11	3.83E-09	6.624731
185	Cmc2	2.993935	3.51E-11	3.85E-09	6.623451
186	Psma5	0.741841	3.53E-11	3.86E-09	6.622427
187	Birc5	4.123659	3.76E-11	4.08E-09	6.613212
188	Rps27a	0.454332	3.76E-11	4.08E-09	6.613212
189	Grap2	7.511945	4.26E-11	4.61E-09	6.594782
190	Rpl36	0.514879	4.59E-11	4.95E-09	6.583519
191	mmu-mir-	0.886721	4.72E-11	5.07E-09	6.579424
192	Hbq1b	32.89119	6.7E-11	7.09E-09	6.527206
193	Mnd1	3.642286	7.17E-11	7.51E-09	6.516968
194	Syce2	2.878147	7.71E-11	8.04E-09	6.506217
195	Mcrip2	4.094943	8.65E-11	8.99E-09	6.488811
196	Rps21	0.647084	8.68E-11	8.99E-09	6.488299

197	Mrps24	2.025206	1E-10	1.03E-08	6.466798
198	Cycs	0.821541	1.09E-10	1.11E-08	6.453487
199	Nol7	2.350447	1.14E-10	1.15E-08	6.4476

Cluster 4

	names	**logfoldchange**	**pvals**	**pvals_adj**	**scores**
0	Fabp7	10.90343	1.49E-36	4.39E-32	12.62766
1	Pantr1	9.317763	1.79E-33	2.65E-29	12.05651
2	Crabp2	6.763683	7.77E-26	7.65E-22	10.50996
3	Gm10282	1.329047	8.63E-25	6.37E-21	10.28046
4	Hmgn2	1.219074	8.25E-23	4.87E-19	9.831364
5	H2az2	1.564673	2.47E-21	1.22E-17	9.482936
6	Hoxb5os	5.473426	5.4E-21	2.28E-17	9.401045
7	Msi1	3.628365	1.41E-20	5.19E-17	9.299854
8	Fkbp3	1.038153	5.04E-20	1.65E-16	9.163196
9	Phyhipl	7.75562	1.15E-19	3.4E-16	9.073481
10	Pclaf	4.353074	3.46E-19	9.29E-16	8.952991
11	Hoxc9	5.737115	5.81E-19	1.43E-15	8.895615
12	Fez1	7.245499	1.58E-18	3.58E-15	8.783993
13	Ckb	5.533312	1.33E-17	2.81E-14	8.540928
14	Rfc4	3.349877	5.62E-17	1.11E-13	8.372972
15	Dek	2.972485	7.65E-17	1.41E-13	8.33646
16	Ranbp1	1.225281	1.59E-16	2.75E-13	8.249875
17	H2az1	1.279947	4.12E-16	6.75E-13	8.135123
18	Gm6724	1.354813	6.94E-16	1.08E-12	8.071488
19	Id2	4.77001	1.37E-15	2.02E-12	7.988554
20	Tuba1a	1.686199	1.64E-15	2.25E-12	7.966125
21	Set	1.282867	1.68E-15	2.25E-12	7.963256
22	Gm10182	1.398855	1.75E-14	2.15E-11	7.66777
23	Dbi	1.179067	1.94E-14	2.29E-11	7.65473
24	Erh	0.676451	2.35E-14	2.67E-11	7.629694
25	Gm10357	1.341306	3.58E-14	3.77E-11	7.575447
26	Nutf2	1.062352	5.28E-14	4.96E-11	7.524852
27	Ccnd2	3.150557	5.3E-14	4.96E-11	7.524331
28	Pdpn	4.962125	5.37E-14	4.96E-11	7.522505
29	Gm3226	1.255029	6.76E-14	5.7E-11	7.492513
30	Rrm2	4.286268	7.42E-14	6.08E-11	7.480255
31	Id3	3.155979	8.31E-14	6.63E-11	7.46539
32	Selenoh	1.236223	1.19E-13	9.23E-11	7.418185
33	Bex1	3.146286	1.34E-13	9.92E-11	7.401755
34	Dnajc9	3.230208	1.72E-13	1.21E-10	7.368894
35	Snrpe	0.720618	2.66E-13	1.83E-10	7.310475
36	Lgr4	3.726773	4E-13	2.68E-10	7.255707
37	Bex2	3.211454	6.9E-13	4.43E-10	7.181379
38	Nmral1	3.463235	8.53E-13	5.36E-10	7.15243
39	Bex4	3.365764	1.02E-12	6.3E-10	7.127132
40	Kif21a	4.919539	1.32E-12	7.94E-10	7.092446

41	Ppa1	2.964403	1.38E-12	8E-10	7.086448
42	Gm7931	1.500719	1.38E-12	8E-10	7.085926
43	Ssb	0.926987	2.32E-12	1.29E-09	7.013685
44	Gm12892	2.87404	2.43E-12	1.33E-09	7.007426
45	Ywhae	0.625703	4.09E-12	2.2E-09	6.93388
46	Snrnp40	2.367065	4.38E-12	2.31E-09	6.924491
47	Dctpp1	1.786986	4.73E-12	2.45E-09	6.913538
48	Pax6	5.638889	4.81E-12	2.45E-09	6.91093
49	Ran	0.904629	6.65E-12	3.22E-09	6.865029
50	Phgdh	3.725828	8.36E-12	3.98E-09	6.832168
51	Hmgb3	2.092553	9.45E-12	4.43E-09	6.814694
52	Ddx39a	2.674942	9.96E-12	4.59E-09	6.807131
53	C130071C03Ri	6.530902	1.05E-11	4.78E-09	6.799307
54	Slc25a5	1.510888	2.38E-11	1.06E-08	6.680644
55	Ptges3	1.186793	2.43E-11	1.07E-08	6.677253
56	Psat1	3.674057	2.58E-11	1.12E-08	6.668647
57	Srsf3	1.075358	3.13E-11	1.3E-08	6.64022
58	Srsf7	0.962926	3.75E-11	1.54E-08	6.613618
59	Vta1	2.273549	4.44E-11	1.77E-08	6.588582
60	Mrpl28	1.882703	4.45E-11	1.77E-08	6.588321
61	Jpt1	1.509255	4.5E-11	1.77E-08	6.586495
62	Ndufa12	0.845639	5E-11	1.9E-08	6.570847
63	Pdzph1	8.319316	5.01E-11	1.9E-08	6.570586
64	Hes5	7.015276	6.8E-11	2.51E-08	6.524946
65	Gm9761	1.227683	1.07E-10	3.84E-08	6.457399
66	Sox9	3.194508	1.09E-10	3.88E-08	6.454009
67	Hmgn2-ps1	1.402331	1.87E-10	6.42E-08	6.371596
68	Ppp1r1a	4.561817	2.75E-10	9.34E-08	6.312134
69	Lsm3	1.474591	4.13E-10	1.37E-07	6.24902
70	Snrpert	0.714636	4.28E-10	1.41E-07	6.243283
71	Ccnd1	3.721339	6.28E-10	1.99E-07	6.183299
72	Pbk	3.752992	6.63E-10	2.08E-07	6.174692
73	Asf1b	3.620376	7.45E-10	2.32E-07	6.156176
74	Pcna-ps2	1.944932	7.61E-10	2.34E-07	6.152785
75	Ddx39b	1.776095	8.13E-10	2.45E-07	6.142353
76	Banf1	0.848233	8.5E-10	2.51E-07	6.135312
77	Ptn	4.288039	9.29E-10	2.69E-07	6.121228
78	Hnrnpc	0.60889	9.44E-10	2.71E-07	6.11862
79	Cdca8	3.412848	9.93E-10	2.82E-07	6.110536
80	Sumo2	0.611937	1.15E-09	3.23E-07	6.087325
81	Snrpd1	1.210302	1.25E-09	3.45E-07	6.074285
82	Cenpm	3.048215	1.32E-09	3.62E-07	6.064374
83	Pou3f2	6.426069	1.39E-09	3.77E-07	6.056289
84	Sfrp2	4.306846	1.46E-09	3.91E-07	6.049248
85	Gm1673	2.151376	1.68E-09	4.46E-07	6.026297
86	Psmc4	1.137957	1.85E-09	4.89E-07	6.010128
87	Spc24	2.992829	3.75E-09	9.46E-07	5.894854
88	Hmgn1	0.771867	5.09E-09	1.26E-06	5.844259

89	Ndufa12-ps	0.789899	6.12E-09	1.48E-06	5.813485
90	Ift27	2.623118	6.61E-09	1.59E-06	5.800445
91	Gm14150	1.090949	6.95E-09	1.66E-06	5.792099
92	Pcna	2.284526	9.44E-09	2.18E-06	5.740461
93	Dcakd	2.177249	1.01E-08	2.31E-06	5.728986
94	Nme1	0.827829	1.13E-08	2.55E-06	5.710469
95	Mir219a-2	4.60873	1.2E-08	2.68E-06	5.699776
96	Cops4	1.301336	1.32E-08	2.91E-06	5.683607
97	Cdk4	0.809208	1.53E-08	3.29E-06	5.65857
98	Gm15428	1.847175	1.68E-08	3.6E-06	5.641879
99	Tuba1b	1.020262	1.74E-08	3.71E-06	5.63562
100	Bub3	1.54612	2.12E-08	4.38E-06	5.602237
101	Cks1b	1.489154	2.77E-08	5.64E-06	5.555293
102	Sox11	2.955196	2.8E-08	5.67E-06	5.553207
103	Pebp1	0.805354	2.85E-08	5.72E-06	5.550599
104	H2ac24	1.786602	2.96E-08	5.91E-06	5.543557
105	Psmb7	0.808015	3.13E-08	6.2E-06	5.534168
106	Psmb6	0.551775	3.2E-08	6.29E-06	5.530256
107	Spc25	3.244346	3.26E-08	6.38E-06	5.526605
108	Acat2	2.065393	3.76E-08	7.3E-06	5.501829
109	Hmgb2	1.060722	7.19E-08	1.34E-05	5.386295
110	Lsm6	1.143853	7.73E-08	1.43E-05	5.373255
111	Dnajc19	1.113459	8.26E-08	1.52E-05	5.361258
112	Hoxa2	3.605594	8.54E-08	1.56E-05	5.35526
113	Snrpb	0.8096	8.91E-08	1.61E-05	5.347697
114	Map1b	3.066524	9.42E-08	1.7E-05	5.337525
115	Tipin	1.715204	1.03E-07	1.84E-05	5.320834
116	Macroh2a1	1.531444	1.21E-07	2.11E-05	5.292146
117	Nusap1	3.418004	1.31E-07	2.27E-05	5.276759
118	Gm13461	0.952882	1.36E-07	2.34E-05	5.2705
119	Sox2	4.377653	1.49E-07	2.54E-05	5.253809
120	Eif1ax	1.113332	1.52E-07	2.56E-05	5.250157
121	Dtx4	4.507979	1.56E-07	2.62E-05	5.244942
122	Zfp706	0.87828	1.85E-07	3E-05	5.214167
123	Ppih	1.854099	1.9E-07	3.07E-05	5.208691
124	Slc7a11	1.322368	1.92E-07	3.08E-05	5.206865
125	Psmc1	0.612941	1.93E-07	3.08E-05	5.206082
126	Ccnb1	3.456063	1.97E-07	3.13E-05	5.20217
127	Hax1	1.856101	2.08E-07	3.27E-05	5.19226
128	Hint1	0.543408	2.31E-07	3.57E-05	5.172439
129	Itgb3bp	2.381182	2.36E-07	3.6E-05	5.168788
130	Calm3	1.308215	2.51E-07	3.77E-05	5.157313
131	Cct5	0.636893	2.73E-07	4.06E-05	5.140882
132	Gm11585	1.473648	3.03E-07	4.47E-05	5.121844
133	Hnrnpa1	0.69061	3.18E-07	4.67E-05	5.112455
134	Gcat	2.135326	3.6E-07	5.25E-05	5.088984
135	Uchl1	2.75826	3.61E-07	5.25E-05	5.088462
136	Jam2	4.271733	3.64E-07	5.27E-05	5.086897

137	Idh1	2.114126	3.66E-07	5.28E-05	5.085593
138	Ube2n	0.638434	3.85E-07	5.51E-05	5.076465
139	Dpysl2	2.378098	4.29E-07	6.03E-05	5.055601
140	Mad2l1	2.793401	4.29E-07	6.03E-05	5.055601
141	Ccdc85c	1.998164	4.49E-07	6.28E-05	5.046995
142	Msmo1	2.496282	4.85E-07	6.72E-05	5.032129
143	Ptges3-ps	1.696621	4.92E-07	6.78E-05	5.029521
144	Magoh	1.224959	4.98E-07	6.84E-05	5.027174
145	Glo1	0.926097	5.07E-07	6.91E-05	5.023784
146	Hpf1	1.889903	5.08E-07	6.91E-05	5.023262
147	Lsm1	2.135627	5.37E-07	7.22E-05	5.012569
148	Gm7901	2.044373	5.38E-07	7.22E-05	5.012308
149	Taf13	2.407503	6.01E-07	8.03E-05	4.990923
150	Gm7879	1.400563	6.07E-07	8.08E-05	4.988836
151	H2ac11	1.681651	6.31E-07	8.35E-05	4.981534
152	Lsm5	0.882522	7.45E-07	9.53E-05	4.949195
153	Pax3	4.209631	7.97E-07	0.000101	4.936155
154	Tra2b	1.00928	8.1E-07	0.000102	4.933025
155	Gm5560	1.296827	8.27E-07	0.000104	4.928853
156	Nxt1	2.12056	8.29E-07	0.000104	4.928331
157	Mir124-2hg	4.673793	9.12E-07	0.000112	4.909814
158	Inip	2.383967	9.39E-07	0.000115	4.904077
159	Gm3756	1.037133	9.58E-07	0.000116	4.900165
160	Nutf2-ps1	1.111041	9.9E-07	0.000119	4.893644
161	Psmd6	1.287976	1.13E-06	0.000135	4.867826
162	Psip1	2.168785	1.16E-06	0.000138	4.862349
163	Prps1	2.423175	1.18E-06	0.00014	4.858437
164	Tsn	1.032054	1.25E-06	0.000146	4.848004
165	Ldhb	3.102366	1.51E-06	0.000175	4.809928
166	Scoc	1.952434	1.57E-06	0.00018	4.801582
167	Hoxa9	4.501713	1.58E-06	0.00018	4.801322
168	Fam181a	6.788868	1.71E-06	0.000194	4.784891
169	Mir99ahg	2.78174	1.76E-06	0.000198	4.779153
170	Gmnn	2.310211	1.79E-06	0.0002	4.775763
171	Rbp1	2.43163	1.92E-06	0.000213	4.76194
172	Lsm4	1.185522	2.13E-06	0.000235	4.740555
173	Hat1	2.188586	2.15E-06	0.000236	4.73899
174	Tagln3	3.53275	2.18E-06	0.000238	4.736382
175	Tecr	0.784531	2.2E-06	0.000239	4.734035
176	Paics	1.590545	2.2E-06	0.000239	4.733774
177	Glo1-ps	1.019735	2.23E-06	0.000241	4.731688
178	Exosc8	1.369519	2.31E-06	0.000248	4.723864
179	Skp1	0.449181	2.43E-06	0.00026	4.713953
180	Slitrk2	5.024508	2.5E-06	0.000266	4.708216
181	Prim1	2.455222	2.52E-06	0.000267	4.706651
182	Ednrb	3.587053	2.56E-06	0.000271	4.703
183	Gm9531	1.207029	2.62E-06	0.000276	4.698566
184	Aimp2	1.560129	2.68E-06	0.000282	4.693611

185	Siva1	1.395425	2.7E-06	0.000283	4.692046
186	Birc5	2.8065	3.23E-06	0.000334	4.655795
187	Psmb2	0.434203	3.29E-06	0.000339	4.652144
188	Smc2	2.334566	3.45E-06	0.000354	4.641973
189	Park7	0.61434	4.07E-06	0.000412	4.607547
190	Ndufb6	0.5527	4.31E-06	0.000432	4.596072
191	Gm13237	1.060164	4.32E-06	0.000433	4.59529
192	Tmem107	2.095294	4.67E-06	0.000466	4.57912
193	Gm4739	1.071886	4.83E-06	0.00048	4.572079
194	Iftap	2.014341	5.24E-06	0.000518	4.554866
195	Fabp5	1.765709	5.35E-06	0.000526	4.550693
196	Ppdpf	1.204854	5.56E-06	0.000546	4.542347
197	Top2a	2.837294	5.87E-06	0.000567	4.530872
198	Cdca3	2.560781	6.01E-06	0.000576	4.526178
199	Pea15a	2.568769	6.04E-06	0.000577	4.525135

Cluster 5

	names	**logfoldchange**	**pvals**	**pvals_adj**	**scores**
0	Kdr	6.699491	2.36E-28	5.36E-24	11.04329
1	Egfl7	6.30223	4.88E-28	5.36E-24	10.97796
2	Ramp2	7.223934	5.44E-28	5.36E-24	10.96805
3	Gmfg	6.574931	1.56E-26	1.15E-22	10.66039
4	Ecscr	8.231786	1.69E-25	9.97E-22	10.43654
5	Gng11	6.74606	3.48E-24	1.71E-20	10.14522
6	Crip2	6.494689	4.1E-23	1.73E-19	9.901557
7	Vamp5	6.01403	5.03E-22	1.86E-18	9.647718
8	Emcn	7.455289	8.37E-22	2.75E-18	9.595238
9	Ctla2a	6.197967	8.64E-21	2.55E-17	9.351574
10	S1pr1	5.794592	1.2E-20	3.21E-17	9.317033
11	Sh3bgrl3	1.904094	1.44E-20	3.54E-17	9.297486
12	Fkbp1a	1.897612	3.05E-20	6.93E-17	9.217158
13	Myct1	5.963454	1.09E-19	2.3E-16	9.079529
14	Calm1	1.354794	1.51E-19	2.97E-16	9.044184
15	Sparc	5.447987	4.87E-19	8.27E-16	8.915123
16	Gimap6	6.385767	4.97E-19	8.27E-16	8.912981
17	Tspan18	5.325819	5.04E-19	8.27E-16	8.911374
18	2810025M15Ri	3.63396	6.03E-19	8.61E-16	8.89156
19	Pfn1	0.963925	6.23E-19	8.61E-16	8.887811
20	Pcdh17	4.723882	6.54E-19	8.61E-16	8.882456
21	Pomp	1.299847	6.9E-19	8.61E-16	8.876565
22	Gngt2	5.538896	6.93E-19	8.61E-16	8.87603
23	Cfl1	0.767777	7E-19	8.61E-16	8.874959
24	Efna1	6.055964	1.58E-18	1.86E-15	8.783919
25	Lpar6	4.163206	4.94E-18	5.6E-15	8.654859
26	Cyb5a	2.030964	9.79E-18	1.07E-14	8.576405
27	Cdh5	4.587255	1.33E-17	1.41E-14	8.540792
28	Tmsb4x	2.694097	5.43E-17	5.53E-14	8.376922

29	Icam2	6.415874	8.82E-17	8.52E-14	8.319621
30	Clec1b	6.133705	8.94E-17	8.52E-14	8.318014
31	Serf2	0.784379	9.4E-17	8.67E-14	8.312123
32	BC028528	4.633504	1.84E-16	1.64E-13	8.23233
33	Myl6	1.080949	2.03E-16	1.76E-13	8.22055
34	Anxa5	3.930605	3.71E-16	3.13E-13	8.147718
35	Cldn5	6.069607	5.07E-16	4.16E-13	8.109695
36	Vim	3.601532	2.08E-15	1.62E-12	7.936186
37	Cd59a	4.311301	2.28E-15	1.69E-12	7.924941
38	Ifitm3	3.259902	2.29E-15	1.69E-12	7.924405
39	B2m	2.821444	2.38E-15	1.72E-12	7.919585
40	Rpl18a	0.52417	3.54E-15	2.49E-12	7.870317
41	Anxa6	4.878581	4.09E-15	2.81E-12	7.852109
42	Cd38	5.544962	7.58E-15	4.97E-12	7.774458
43	Madcam1	6.36649	8.9E-15	5.71E-12	7.754108
44	Tpm4	2.76349	9.28E-15	5.83E-12	7.748753
45	Igf1	4.999424	1.08E-14	6.61E-12	7.73001
46	Fli1	3.742805	1.82E-14	1.09E-11	7.66307
47	Rab11a	2.323793	1.94E-14	1.15E-11	7.654501
48	Sat1	4.662456	3.11E-14	1.8E-11	7.593451
49	Lxn	3.72728	3.72E-14	2.11E-11	7.570424
50	Upp1	5.237711	4.19E-14	2.34E-11	7.554894
51	Ipo11	4.117624	4.55E-14	2.49E-11	7.544183
52	Elk3	4.403181	7.75E-14	4.16E-11	7.474566
53	Tmsb10	1.290503	1.02E-13	5.38E-11	7.43815
54	Tmem88	5.102287	1.4E-13	7.25E-11	7.396379
55	Rhoc	3.781082	1.5E-13	7.62E-11	7.387007
56	Tax1bp3	3.186612	1.52E-13	7.62E-11	7.385133
57	Plk2	4.970672	1.62E-13	7.98E-11	7.376832
58	Anxa2	4.930645	2.44E-13	1.18E-10	7.321941
59	Anxa3	5.106768	3.57E-13	1.7E-10	7.271067
60	Dad1	0.994515	5.09E-13	2.35E-10	7.222869
61	Igfbp4	3.716338	6.44E-13	2.88E-10	7.190738
62	Cd93	4.903094	8.74E-13	3.85E-10	7.148967
63	Myl12a	1.106766	9.09E-13	3.89E-10	7.143612
64	Ifitm2	1.21607	1.03E-12	4.34E-10	7.126475
65	Rpl10	0.529886	3.77E-12	1.57E-09	6.945468
66	Actr2	1.406072	4.18E-12	1.71E-09	6.931009
67	Gm9844	1.413773	4.95E-12	1.96E-09	6.906911
68	Prdx1	0.854544	4.97E-12	1.96E-09	6.906375
69	Rps19	0.473429	4.98E-12	1.96E-09	6.906107
70	Ralb	3.426432	7.5E-12	2.88E-09	6.847735
71	Ost4	0.842435	8.28E-12	3.14E-09	6.833544
72	Snx3	1.634619	1.01E-11	3.77E-09	6.805161
73	Ndufa8	1.339911	1.12E-11	4.1E-09	6.790702
74	Ssu72	1.524868	1.32E-11	4.75E-09	6.766603
75	Ppic	2.775954	1.64E-11	5.83E-09	6.735008
76	S100a10	3.546268	2.01E-11	7E-09	6.705019

77	Vamp8	2.643414	2.28E-11	7.82E-09	6.687078
78	Clic1	1.888134	2.77E-11	9.39E-09	6.658428
79	Actb	0.635756	3.24E-11	1.07E-08	6.6354
80	Stab1	4.461632	3.45E-11	1.13E-08	6.626029
81	Esam	4.598891	4.71E-11	1.53E-08	6.579974
82	Gm16104	3.475883	5.16E-11	1.66E-08	6.566318
83	Ostf1	3.794145	5.43E-11	1.72E-08	6.558553
84	F11r	4.192273	5.48E-11	1.72E-08	6.557214
85	Arhgap18	4.556589	5.74E-11	1.79E-08	6.550252
86	Msn	3.596561	6.4E-11	1.97E-08	6.534186
87	Med10	1.463681	1.11E-10	3.38E-08	6.45118
88	Klhl4	4.847602	1.12E-10	3.38E-08	6.449574
89	Selenop	3.814207	1.22E-10	3.64E-08	6.436721
90	S100a13	3.450904	1.34E-10	3.95E-08	6.422798
91	Gm6969	1.246925	1.42E-10	4.14E-08	6.414229
92	Cd59b	2.355251	1.91E-10	5.46E-08	6.36871
93	Gm8730	0.484383	1.98E-10	5.62E-08	6.362819
94	Sri	1.651292	2.04E-10	5.73E-08	6.358535
95	Arpc5	2.410164	2.07E-10	5.75E-08	6.356393
96	Plxnd1	3.466819	2.13E-10	5.88E-08	6.351573
97	Myzap	3.768792	2.3E-10	6.23E-08	6.339792
98	Gng12	2.90001	4.96E-10	1.31E-07	6.22037
99	Gm9625	0.478253	8.82E-10	2.29E-07	6.129331
100	Prkar1a	1.499436	9.65E-10	2.47E-07	6.115139
101	Gm8034	1.297529	9.7E-10	2.47E-07	6.114336
102	Flt4	3.842582	1.13E-09	2.85E-07	6.089702
103	Col4a1	3.682598	1.32E-09	3.27E-07	6.065068
104	Sox7	4.629787	1.49E-09	3.68E-07	6.044986
105	Rplp0	0.467991	1.79E-09	4.37E-07	6.0158
106	Cd34	4.289789	1.99E-09	4.81E-07	5.998663
107	Maged2	2.840537	2E-09	4.81E-07	5.997592
108	Cox7a2l	1.211567	2.63E-09	6.26E-07	5.953144
109	Gng5	0.641702	3.55E-09	8.39E-07	5.903876
110	Rpl15-ps6	0.482345	4.44E-09	1.02E-06	5.866925
111	Gm3788	1.391224	4.86E-09	1.1E-06	5.85193
112	Mrpl17	1.373598	5.71E-09	1.29E-06	5.825154
113	Arpc2	1.484863	7.23E-09	1.58E-06	5.785525
114	Rps20	0.524993	7.73E-09	1.68E-06	5.774279
115	Rabac1	2.2818	7.95E-09	1.71E-06	5.769459
116	Ets2	2.792832	8.89E-09	1.89E-06	5.750716
117	Exoc3l4	3.608808	9.11E-09	1.91E-06	5.746432
118	Cdc42	0.979025	9.11E-09	1.91E-06	5.746432
119	Lrrc70	4.282761	9.68E-09	2.01E-06	5.736257
120	Rps19-ps1	0.655134	1.34E-08	2.73E-06	5.681098
121	Rps19-ps2	0.654993	1.34E-08	2.73E-06	5.680562
122	Sox18	4.069135	1.42E-08	2.87E-06	5.671191
123	Rasip1	3.532028	1.5E-08	3.01E-06	5.661551
124	Cd81	1.748555	1.52E-08	3.04E-06	5.659142

125	Gm7809	1.464669	1.62E-08	3.22E-06	5.647896
126	Cd9	3.393897	1.69E-08	3.33E-06	5.640934
127	Nfkbia	3.215608	1.82E-08	3.55E-06	5.628617
128	Cox4i1	0.487702	1.93E-08	3.75E-06	5.617907
129	Tspan13	2.79996	2.52E-08	4.83E-06	5.571851
130	Gm15427	0.532352	3.2E-08	6.1E-06	5.53008
131	Creg1	2.808028	3.44E-08	6.52E-06	5.517228
132	Gmfg-ps	2.169209	3.77E-08	7.1E-06	5.501163
133	Selenok	1.081795	4.07E-08	7.57E-06	5.487774
134	Gnai2	2.332614	5.35E-08	9.69E-06	5.43931
135	Sub1	0.52322	5.55E-08	9.94E-06	5.432615
136	Itm2a	3.182107	7.58E-08	1.34E-05	5.376921
137	Samsn1	3.85781	7.64E-08	1.34E-05	5.375314
138	Gm5526	1.154954	7.82E-08	1.37E-05	5.371298
139	Calm2	0.660611	7.95E-08	1.38E-05	5.368352
140	Rps16	0.441528	8.61E-08	1.47E-05	5.353893
141	Rpl35	0.419822	8.95E-08	1.52E-05	5.346931
142	Rps6	0.388331	1.04E-07	1.75E-05	5.319084
143	Mpzl1	3.041956	1.08E-07	1.8E-05	5.313194
144	Eef1a1	0.348172	1.11E-07	1.83E-05	5.308374
145	Mef2c	2.675583	1.13E-07	1.85E-05	5.304625
146	Atox1	0.858731	1.2E-07	1.96E-05	5.293379
147	Gchfr	3.461347	1.27E-07	2.05E-05	5.28374
148	Apoe	3.242131	1.57E-07	2.52E-05	5.244111
149	Col4a2	3.038051	1.9E-07	3.01E-05	5.208499
150	Pecam1	4.060782	2.46E-07	3.82E-05	5.160837
151	Igfbp3	3.580813	2.56E-07	3.95E-05	5.153608
152	Pon2	3.256155	2.88E-07	4.39E-05	5.130848
153	Col18a1	2.932457	3.89E-07	5.72E-05	5.074082
154	Flt1	3.540919	4.04E-07	5.87E-05	5.067121
155	Chmp2a	1.282475	4.67E-07	6.72E-05	5.039541
156	Gm10123	0.39108	4.92E-07	7.02E-05	5.029366
157	Krtcap2	0.71509	5.84E-07	8.21E-05	4.996432
158	Ppia	0.367938	5.88E-07	8.23E-05	4.995093
159	Utp11	1.521749	6.36E-07	8.86E-05	4.97983
160	Ccdc85b	2.772176	6.41E-07	8.88E-05	4.978492
161	Prcp	3.06406	8.35E-07	0.000114	4.927082
162	Bmp2k	2.466761	8.74E-07	0.000118	4.917977
163	Klhl6	3.669033	1E-06	0.000134	4.891737
164	Rsu1	2.05326	1.34E-06	0.000178	4.833365
165	Tmem50a	1.048184	1.36E-06	0.000178	4.830687
166	Ets1	2.869721	1.47E-06	0.00019	4.815157
167	Uqcrh	0.542111	1.86E-06	0.000233	4.768031
168	Cox6b1	0.415062	2E-06	0.000248	4.753036
169	Gng2	2.165619	2.08E-06	0.000254	4.745539
170	Ctsl	1.98398	2.15E-06	0.00026	4.738577
171	Tm2d3	1.91289	2.16E-06	0.000261	4.737506
172	Sptbn1	2.195015	2.35E-06	0.000281	4.720369

173	Arhgdib	2.961584	2.46E-06	0.000293	4.711266
174	Ptpn18	2.506166	2.73E-06	0.000324	4.689845
175	Gm17018	1.661287	2.8E-06	0.000329	4.685025
176	Crem	2.817792	2.87E-06	0.000334	4.680205
177	Rpl32	0.367322	3.41E-06	0.000394	4.644325
178	Gm6278	0.552257	3.57E-06	0.000408	4.635221
179	Capza2	0.808978	4.21E-06	0.000474	4.600948
180	Tnfaip8l1	3.341588	4.4E-06	0.000495	4.591308
181	Rpl15-ps2	0.443537	4.54E-06	0.000508	4.584882
182	Eng	2.92906	5.09E-06	0.000563	4.561051
183	Map1lc3b	0.884355	5.21E-06	0.000575	4.555964
184	Tie1	3.304748	5.91E-06	0.000641	4.529723
185	Depp1	4.423108	6.44E-06	0.000691	4.511516
186	Rpl18-ps1	0.790515	6.57E-06	0.0007	4.507231
187	Bcap31	0.926275	7.01E-06	0.000737	4.493308
188	Ap2s1	0.689547	7.1E-06	0.000741	4.49063
189	Sdcbp	1.337562	7.39E-06	0.000763	4.482061
190	Mtarc2	2.121225	7.7E-06	0.000793	4.473226
191	Tagln2	2.607643	8.29E-06	0.000845	4.457428
192	Itga6	2.806329	9.78E-06	0.000965	4.422083
193	Gpihbp1	3.493402	1.01E-05	0.000996	4.414586
194	Tmem204	3.92884	1.02E-05	0.001	4.412979
195	Naa38	1.244728	1.13E-05	0.001089	4.391558
196	mt-Co1	0.44874	1.17E-05	0.001123	4.383525
197	Gm6192	0.54246	1.51E-05	0.00141	4.327295
198	Kit	2.780764	1.64E-05	0.001513	4.309088
199	Ppp1r11	1.325118	1.74E-05	0.001578	4.296235

Cluster 6

	names	logfoldchange	pvals	pvals_adj	scores
0	Pkm	2.091221	1.63E-34	1.6E-30	12.25244
1	Hmga1	4.513479	1.99E-34	1.6E-30	12.23627
2	Ptbp1	7.680706	2.71E-34	1.6E-30	12.21119
3	Eef2	3.774256	6.9E-34	2.91E-30	12.1349
4	Hmga1b	4.435226	5.84E-32	1.33E-28	11.76608
5	Hsp90ab1	0.993951	1.76E-31	3.46E-28	11.6728
6	Fscn1	3.915244	4.22E-30	5.75E-27	11.39915
7	Ptma	1.215979	4.42E-30	5.75E-27	11.3951
8	Ddb1	4.807075	6.45E-30	7.28E-27	11.36221
9	Polr2m	5.270305	7.57E-30	7.71E-27	11.34819
10	Rbm14	6.42043	9.51E-30	9.17E-27	11.32824
11	Rn18s	1.038427	9.63E-30	9.17E-27	11.32716
12	Ewsr1	5.062407	1.04E-29	9.62E-27	11.32015
13	Acly	5.852371	1.08E-29	9.68E-27	11.31692
14	Mid1	5.042693	2.33E-29	1.96E-26	11.24952
15	Pfkl	4.858015	3.59E-29	2.79E-26	11.21123
16	Macroh2a2	6.47045	5.86E-29	4.02E-26	11.16783

17	Tkt	6.206285	7.72E-29	5.07E-26	11.14329
18	Eftud2	6.297004	3.07E-28	1.81E-25	11.01981
19	Ilf3	5.303805	3.64E-28	2.07E-25	11.00445
20	Mta2	6.294112	8.31E-28	4.3E-25	10.92976
21	Wdr6	6.829177	8.92E-28	4.46E-25	10.9233
22	Cdca7	5.604793	9.64E-28	4.74E-25	10.91628
23	Igf2bp1	5.188745	1.17E-27	5.67E-25	10.89849
24	Peg3	5.887171	2E-27	9.38E-25	10.84969
25	G3bp1	3.795239	3.29E-27	1.52E-24	10.80413
26	Lin28a	7.142814	4.62E-27	2.07E-24	10.77285
27	Prtg	6.196465	7.65E-27	3.22E-24	10.72648
28	Uhrf1	5.943652	1.16E-26	4.68E-24	10.6882
29	Kmt2d	4.657602	1.4E-26	5.5E-24	10.67068
30	Arhgdia	3.572128	2.2E-26	8.33E-24	10.62835
31	Meox1	8.364664	4.49E-26	1.64E-23	10.56149
32	Caprin1	4.494909	6.34E-26	2.28E-23	10.52913
33	Nedd4	1.861061	7.11E-26	2.5E-23	10.51835
34	Vars	5.862569	7.4E-26	2.57E-23	10.51457
35	Parp1	4.94745	8.81E-26	2.99E-23	10.49813
36	Ppp2r5d	6.069171	8.81E-26	2.99E-23	10.49813
37	Tmem250-ps	5.743812	1.57E-25	5.03E-23	10.44367
38	Mcm7	4.909959	2.3E-25	7.22E-23	10.40727
39	Ado	6.299663	5.79E-25	1.74E-22	10.31884
40	Srsf4	5.441862	5.86E-25	1.75E-22	10.31776
41	Ivns1abp	5.009802	7.93E-25	2.32E-22	10.28865
42	Med25	5.362672	1.16E-24	3.27E-22	10.25171
43	Eef1a1	0.694809	1.25E-24	3.49E-22	10.24443
44	Anp32e	5.059182	1.4E-24	3.86E-22	10.23392
45	Atxn2l	5.183694	1.61E-24	4.36E-22	10.22017
46	Vcp	2.788811	1.74E-24	4.67E-22	10.21262
47	Fbln1	6.297845	2.84E-24	7.48E-22	10.16517
48	Fubp1	3.621347	3.19E-24	8.32E-22	10.15384
49	Msh2	5.900664	4.08E-24	1.04E-21	10.12958
50	Igf2bp2	5.395679	4.78E-24	1.21E-21	10.11421
51	Skp2	6.107861	7.38E-24	1.81E-21	10.07161
52	Usp10	5.288013	7.56E-24	1.84E-21	10.06919
53	Mcm2	5.50312	9.49E-24	2.28E-21	10.04681
54	Actn4	5.482248	1.27E-23	3.02E-21	10.01823
55	Prrc2a	4.867848	1.34E-23	3.17E-21	10.01257
56	Dpp3	5.885443	1.65E-23	3.78E-21	9.992081
57	Jpt2	5.478982	1.68E-23	3.81E-21	9.990463
58	Sall4	6.078403	2.41E-23	5.36E-21	9.954336
59	Ubap2l	3.690068	2.48E-23	5.47E-21	9.95164
60	Hnrnpm	3.746213	2.6E-23	5.7E-21	9.946787
61	Sf1	4.782264	4.34E-23	9.35E-21	9.895832
62	Rcc1	6.41703	4.6E-23	9.85E-21	9.8899
63	Sdc1	6.417004	5.17E-23	1.09E-20	9.878307
64	Hdgfl2	5.514261	5.41E-23	1.13E-20	9.873724

65	Trim71	4.463145	6.03E-23	1.25E-20	9.86294
66	Fus	4.353868	6.48E-23	1.34E-20	9.85566
67	Sinhcaf	4.274806	7.63E-23	1.53E-20	9.839215
68	Eif4b	4.731696	7.69E-23	1.53E-20	9.838407
69	Zfp444	5.285275	7.73E-23	1.53E-20	9.837867
70	Sf3b3	4.778815	1.18E-22	2.24E-20	9.795269
71	Prmt5	5.91886	1.22E-22	2.3E-20	9.791764
72	Pcbp4	5.33224	1.31E-22	2.44E-20	9.785025
73	Hnrnpk	1.071002	1.41E-22	2.61E-20	9.777475
74	Dbn1	5.188077	1.56E-22	2.85E-20	9.767231
75	Hnrnpa1	1.139464	1.84E-22	3.35E-20	9.750515
76	Nono	2.974584	1.95E-22	3.52E-20	9.744584
77	Sf3b2	3.549356	2.39E-22	4.26E-20	9.723555
78	Api5	4.980108	3.08E-22	5.39E-20	9.697673
79	Ppp6r3	5.585454	3.46E-22	6.02E-20	9.68581
80	Gga2	5.752847	3.75E-22	6.47E-20	9.677722
81	Pgam1	1.908964	5.1E-22	8.76E-20	9.646178
82	Flywch1	5.897439	6.36E-22	1.07E-19	9.623531
83	Bap1	6.012265	7.84E-22	1.31E-19	9.601963
84	Glyr1	5.232578	7.91E-22	1.31E-19	9.601154
85	Cdip1	5.574697	9.95E-22	1.61E-19	9.577429
86	Gart	5.533324	1.14E-21	1.84E-19	9.56314
87	Poldip2	5.441425	1.18E-21	1.88E-19	9.559635
88	Igf2bp3	4.913635	1.18E-21	1.88E-19	9.559635
89	Ss18	5.693196	1.21E-21	1.91E-19	9.557478
90	Lmnb1	5.738132	1.44E-21	2.26E-19	9.539145
91	Maged1	3.601831	1.92E-21	2.98E-19	9.509489
92	Cherp	4.968214	2.38E-21	3.64E-19	9.486842
93	Cadm1	5.738364	3.77E-21	5.65E-19	9.438852
94	Chd7	4.833207	5E-21	7.42E-19	9.409196
95	Tubb5	1.388052	5.08E-21	7.5E-19	9.407578
96	Mat2a	4.467215	5.12E-21	7.52E-19	9.40677
97	Fndc3c1	5.606801	1.09E-20	1.59E-18	9.326697
98	Gas1	5.172493	1.11E-20	1.61E-18	9.325079
99	Thop1	5.742736	1.16E-20	1.67E-18	9.320496
100	Ncapd2	5.420811	1.27E-20	1.82E-18	9.31052
101	Tnpo3	5.340878	1.32E-20	1.88E-18	9.306746
102	2410002F23Ri	5.272708	1.43E-20	2.03E-18	9.298119
103	Zfp266	4.944135	1.61E-20	2.26E-18	9.285447
104	Rbm10	5.506952	1.76E-20	2.46E-18	9.276011
105	Ssrp1	4.063566	1.78E-20	2.48E-18	9.274663
106	Washc2	5.505299	2.03E-20	2.82E-18	9.260644
107	Mcm5	5.405131	2.26E-20	3.09E-18	9.24932
108	Tdg-ps2	4.251974	2.36E-20	3.22E-18	9.244468
109	Psmd3	5.206229	2.39E-20	3.24E-18	9.243119
110	Nup62	5.450163	2.43E-20	3.28E-18	9.241502
111	Ccar2	5.60586	3.13E-20	4.21E-18	9.214272
112	Uba1	4.541854	3.22E-20	4.3E-18	9.211307

113	Dgcr2	4.996744	3.3E-20	4.38E-18	9.208879
114	Mau2	5.197659	3.34E-20	4.42E-18	9.207532
115	Rnf187	4.983776	3.39E-20	4.47E-18	9.205914
116	Slc35a4	5.692321	3.42E-20	4.49E-18	9.204836
117	Ubap2	4.326185	3.78E-20	4.94E-18	9.194052
118	Lbr	4.431511	3.94E-20	5.1E-18	9.189738
119	Ptbp2	5.17094	4.84E-20	6.21E-18	9.16763
120	Rrs1	5.190121	5.06E-20	6.46E-18	9.162777
121	Cdh2	4.925791	5.7E-20	7.23E-18	9.149837
122	Cpsf1	5.26235	6.79E-20	8.53E-18	9.130964
123	Akt2	5.486713	7.32E-20	9.15E-18	9.122876
124	Rcbtb1	5.298103	7.84E-20	9.69E-18	9.115327
125	Cnot9	5.027221	9.91E-20	1.21E-17	9.089984
126	Map2k6	5.331026	1.02E-19	1.24E-17	9.087019
127	Cbx2	5.34669	1.03E-19	1.25E-17	9.08567
128	Dlst	5.524407	1.04E-19	1.25E-17	9.085132
129	Pold1	5.932019	1.04E-19	1.25E-17	9.084592
130	Trim59	5.194643	1.09E-19	1.3E-17	9.07947
131	Dhx8	5.101639	1.15E-19	1.37E-17	9.073808
132	Lef1	5.170368	1.16E-19	1.37E-17	9.07246
133	Smarcc1	4.495918	1.17E-19	1.37E-17	9.07219
134	Rnf10	4.224489	1.26E-19	1.47E-17	9.064102
135	Septin9	4.378401	1.29E-19	1.5E-17	9.061406
136	Fkbp4	2.640061	1.3E-19	1.5E-17	9.060328
137	Nasp	3.301641	1.31E-19	1.5E-17	9.059789
138	Clptm1	5.29279	1.31E-19	1.5E-17	9.059789
139	Psmd13	5.305234	1.31E-19	1.5E-17	9.059519
140	Tuba1b	1.511733	1.44E-19	1.64E-17	9.049005
141	Amd1	4.872625	1.6E-19	1.81E-17	9.037681
142	Mbtps1	5.387632	1.64E-19	1.85E-17	9.034716
143	Xrcc1	5.305973	1.72E-19	1.93E-17	9.029862
144	Dele1	4.985093	1.92E-19	2.14E-17	9.01773
145	Qrich1	5.178531	2E-19	2.21E-17	9.013147
146	Aldh2	5.976215	2.18E-19	2.4E-17	9.003711
147	Tcof1	4.427985	2.21E-19	2.43E-17	9.002093
148	Mapk1ip1l	4.175064	2.29E-19	2.5E-17	8.998319
149	Ythdf3	5.274049	2.3E-19	2.5E-17	8.998049
150	Cpsf6	4.344285	2.5E-19	2.72E-17	8.988613
151	Drosha	4.635047	2.58E-19	2.8E-17	8.985108
152	Igdcc3	4.730368	3.13E-19	3.34E-17	8.964079
153	Gm14150	1.594702	3.31E-19	3.5E-17	8.957878
154	Tmem132a	5.815127	3.77E-19	3.96E-17	8.943589
155	Rcl1	5.558025	3.93E-19	4.11E-17	8.939006
156	Aco2	5.136077	3.98E-19	4.15E-17	8.937657
157	Klhl12	5.583378	4E-19	4.16E-17	8.936849
158	Fto	5.278587	4.25E-19	4.38E-17	8.930378
159	Usp29	4.524129	4.45E-19	4.57E-17	8.925256
160	Hsph1	5.362514	4.48E-19	4.58E-17	8.924447

161	Lrrc41	4.88748	4.5E-19	4.58E-17	8.923908
162	Brd3	3.606472	4.84E-19	4.89E-17	8.91582
163	Elp3	5.483804	4.87E-19	4.89E-17	8.91528
164	Cnot3	3.48126	4.88E-19	4.89E-17	8.91501
165	Slc16a3	5.395383	4.89E-19	4.89E-17	8.914742
166	Mybbp1a	4.515697	5.06E-19	5.05E-17	8.910967
167	Ipo9	5.143374	5.35E-19	5.32E-17	8.904766
168	Smpd4	5.150097	5.42E-19	5.37E-17	8.903418
169	Tdg	3.857324	5.7E-19	5.63E-17	8.897757
170	Calu	5.092409	6.03E-19	5.93E-17	8.891555
171	Gcn1	4.653046	6.54E-19	6.42E-17	8.882389
172	Supt16	4.002156	6.59E-19	6.44E-17	8.88158
173	Tgif2	4.645227	7.24E-19	7.04E-17	8.871065
174	Bckdk	5.306599	8.92E-19	8.63E-17	8.847879
175	Ubxn7	5.17522	9.87E-19	9.52E-17	8.836556
176	Gm6560	2.022698	1E-18	9.62E-17	8.834669
177	Eif4g1	4.141088	1.02E-18	9.78E-17	8.832512
178	Eif2s3x	4.221396	1.12E-18	1.07E-16	8.821998
179	Rpa1	5.302275	1.19E-18	1.13E-16	8.815527
180	Elovl6	5.137054	1.27E-18	1.21E-16	8.807978
181	Dnajc10	4.874942	1.31E-18	1.24E-16	8.804743
182	Dcaf8	5.011095	1.31E-18	1.24E-16	8.804473
183	Top3b	5.444086	1.4E-18	1.31E-16	8.797733
184	Fads1	4.826596	1.4E-18	1.31E-16	8.797463
185	Dvl2	4.749563	1.42E-18	1.32E-16	8.796115
186	Cdk16	5.570993	1.45E-18	1.34E-16	8.793689
187	Snd1	4.139148	1.56E-18	1.44E-16	8.785601
188	Champ1	5.413248	1.64E-18	1.5E-16	8.779939
189	9530068E07Ri	5.266033	1.71E-18	1.57E-16	8.774817
190	Mcm3	4.955498	1.91E-18	1.74E-16	8.762685
191	Rrm1	4.835902	1.97E-18	1.79E-16	8.75891
192	Nap1l4	4.047822	2.03E-18	1.84E-16	8.755674
193	Tox4	4.915113	2.58E-18	2.32E-16	8.728714
194	Cand1	5.00858	2.73E-18	2.45E-16	8.722243
195	Akap8	5.1061	2.79E-18	2.49E-16	8.719817
196	Ldlrad3	5.751093	3.13E-18	2.78E-16	8.706607
197	Chtop	4.359191	3.18E-18	2.82E-16	8.704989
198	Col26a1	5.362186	3.65E-18	3.22E-16	8.689082
199	Brd2	4.547816	3.79E-18	3.33E-16	8.685039

Cluster 7

	names	logfoldchange	pvals	pvals_adj	scores
0	Emb	9.162507	7.09E-27	2.09E-22	10.73341
1	Krt18	10.2607	1.1E-23	1.63E-19	10.03184
2	Krt8	9.980689	3.59E-23	3.53E-19	9.91491
3	Spint2	6.674073	3.43E-22	2.53E-18	9.686825
4	Cldn6	11.48319	1.33E-19	7.88E-16	9.057538

5	Bex4	4.833158	3.08E-19	1.52E-15	8.965817
6	Bex1	4.546189	4.93E-19	1.83E-15	8.913883
7	Epcam	9.116387	4.97E-19	1.83E-15	8.912971
8	Slc2a3	6.987286	8.39E-18	2.75E-14	8.594076
9	Mdk	2.575802	6.24E-15	1.84E-11	7.798964
10	Tceal9	1.395864	6.73E-14	1.81E-10	7.493128
11	Gm4322	3.28021	9.57E-14	2.36E-10	7.446661
12	Igfbp2	4.956985	7E-13	1.59E-09	7.179396
13	Cldn7	9.000674	3.38E-12	7.12E-09	6.961029
14	Gm12245	3.480314	5E-12	9.85E-09	6.90545
15	Cd24a	3.984417	7.19E-11	1.33E-07	6.516701
16	Spink1	10.69788	3.07E-10	5.34E-07	6.294993
17	Slc16a1	5.49692	4.07E-10	6.68E-07	6.251259
18	Cystm1	5.522563	4.56E-10	6.7E-07	6.233644
19	Cpm	6.156616	4.72E-10	6.7E-07	6.228177
20	Rbp4	9.645524	5.26E-10	7.06E-07	6.211169
21	Gpc3	4.393733	5.62E-10	7.21E-07	6.200843
22	Fkbp11	3.943494	9.63E-10	1.18E-06	6.115501
23	Tpm1	3.066305	1.69E-09	1.92E-06	6.025299
24	Bsg	1.238066	1.78E-09	1.95E-06	6.016795
25	Bex2	3.009089	2.44E-09	2.58E-06	5.965164
26	Ptprf	3.90021	5.31E-09	4.9E-06	5.836999
27	Apela	6.871733	1.49E-08	1.29E-05	5.663277
28	Grb10	3.003147	2.16E-08	1.82E-05	5.59889
29	Tspan7	3.849892	3.37E-08	2.76E-05	5.521141
30	Chchd10	3.137785	7.36E-08	5.88E-05	5.382041
31	Paip1	2.724828	9.93E-08	7.67E-05	5.327981
32	Fn1	3.445779	1.01E-07	7.67E-05	5.324337
33	Lrpap1	2.804233	1.18E-07	8.51E-05	5.296395
34	9030622O22Ri	10.40524	2.56E-07	0.000172	5.153044
35	Kif21a	3.876872	2.77E-07	0.000182	5.138466
36	Cpn1	9.130176	2.86E-07	0.000183	5.132696
37	Pcbd1	4.328848	5.09E-07	0.000313	5.023057
38	Apoe	3.567567	5.47E-07	0.00033	5.009086
39	Txndc12	2.090861	6.24E-07	0.000369	4.983574
40	Tmem254a	3.217826	7.9E-07	0.000448	4.937714
41	Ifitm1	4.013414	8.37E-07	0.000458	4.926477
42	Enpp1	6.124966	9.19E-07	0.000493	4.908254
43	S100a10	3.080097	9.39E-07	0.000495	4.904002
44	Car14	3.685795	1.12E-06	0.000559	4.869987
45	Cltc	2.357912	1.21E-06	0.000593	4.854801
46	Cdkn1a	3.231663	1.82E-06	0.000851	4.772799
47	Dnase2a	3.894557	1.94E-06	0.000893	4.760044
48	Vamp8	2.04836	2.05E-06	0.000918	4.748199
49	Trh	6.66328	2.74E-06	0.001171	4.689583
50	Anxa4	3.309709	2.79E-06	0.001174	4.685939
51	Stard10	4.995352	2.89E-06	0.001184	4.678649
52	Cmtm8	4.536616	3.06E-06	0.001239	4.666501

53	Prxl2a	4.028406	3.49E-06	0.001392	4.639775
54	Pdcd4	1.724784	3.68E-06	0.001448	4.628841
55	Ndufs6	0.69543	3.86E-06	0.001469	4.618515
56	Krt7	7.595947	3.87E-06	0.001469	4.618211
57	Apoa1	9.311026	3.88E-06	0.001469	4.617604
58	Cd63	1.370079	3.97E-06	0.001485	4.612745
59	Mreg	5.042728	4.03E-06	0.001486	4.610011
60	Ndufa7	0.526326	4.39E-06	0.001602	4.591789
61	Amot	3.590557	4.52E-06	0.001629	4.585714
62	Id1	3.059707	4.85E-06	0.001726	4.571136
63	Otx2	5.307656	4.95E-06	0.00174	4.566885
64	Serf1	1.539546	5.11E-06	0.001775	4.560203
65	Tma7	0.439378	6.47E-06	0.002147	4.510395
66	Rnase4	4.177794	7.16E-06	0.002324	4.488831
67	Gm47283	1.263542	7.57E-06	0.00243	4.476986
68	Igfbp5	3.230622	8.6E-06	0.002731	4.449652
69	Frem2	5.340683	1.14E-05	0.003472	4.388607
70	Rdx	1.767134	1.41E-05	0.004155	4.342747
71	Mapk13	6.408644	1.72E-05	0.004897	4.298405
72	Amer1	2.888767	1.84E-05	0.005166	4.283827
73	Cadm1	2.930537	2.01E-05	0.005599	4.263782
74	Dhx40	3.219988	2.25E-05	0.006207	4.238574
75	Hes1	1.802627	2.58E-05	0.006856	4.2079
76	Ezr	3.449797	3.05E-05	0.007823	4.169936
77	Romo1	0.618064	3.08E-05	0.007849	4.167202
78	Ktn1	1.859283	4.56E-05	0.010937	4.077304
79	Clic6	6.256474	4.68E-05	0.011061	4.070926
80	Malat1	0.889801	4.86E-05	0.011395	4.062119
81	Mettl26	2.466598	5.01E-05	0.011649	4.055133
82	Atp6v1f	0.520416	5.44E-05	0.012558	4.035696
83	Col4a1	2.774086	5.49E-05	0.012574	4.03357
84	Tln2	2.880229	5.71E-05	0.012938	4.024459
85	Tma7-ps	0.469357	5.74E-05	0.012938	4.023244
86	S100a1	3.589607	5.86E-05	0.013107	4.018384
87	Gprc5c	2.332241	6.19E-05	0.013629	4.005629
88	Slc2a1	2.644197	6.48E-05	0.014168	3.994695
89	Ociad2	3.600201	6.54E-05	0.014208	3.992265
90	Gfpt2	3.537929	6.66E-05	0.014324	3.988014
91	Ssbp1	0.822617	6.71E-05	0.014324	3.986191
92	Abhd2	1.554196	6.77E-05	0.014324	3.984369
93	Ndufa13	0.459343	6.79E-05	0.014324	3.983458
94	Krt8-ps	4.232512	7.24E-05	0.014948	3.968272
95	Sms	2.082937	7.43E-05	0.015122	3.962198
96	Ctsz	2.45179	7.63E-05	0.01532	3.95582
97	Gcsh	1.282605	8.86E-05	0.017338	3.919982
98	Anapc13	0.642054	9.24E-05	0.017837	3.909656
99	H2bu2	2.831978	9.62E-05	0.018448	3.899938
100	Afdn	2.164631	9.82E-05	0.0187	3.895078

101	Soat1	2.360124	9.99E-05	0.018909	3.890826
102	Dzip3	2.249596	0.000108	0.020297	3.871996
103	Atp7b	3.992928	0.000114	0.020989	3.859241
104	mt-Nd2	0.898013	0.000128	0.02312	3.829477
105	Tmc4	3.821296	0.00013	0.023322	3.825832
106	Ctsl	1.782404	0.000148	0.02607	3.794247
107	Fam162a	1.200225	0.000155	0.026688	3.783617
108	Mea1	0.750442	0.000171	0.029113	3.759016
109	Tnks2	2.21287	0.000171	0.029113	3.759016
110	Lama5	4.293011	0.000178	0.030064	3.748083
111	Tmprss2	10.35769	0.00018	0.030087	3.745046
112	Cdh1	7.644528	0.000198	0.032543	3.721053
113	Mrpl15	1.222037	0.000203	0.033111	3.715282
114	Atox1	0.396319	0.000209	0.033973	3.707386
115	Epb41l3	2.914014	0.00022	0.035444	3.695237
116	Sall4	2.584095	0.000239	0.037705	3.673978
117	Rtn4	2.418882	0.000243	0.037887	3.670029
118	Gm10736	0.336488	0.000263	0.040169	3.649681
119	Crb3	6.477871	0.00027	0.040691	3.642695
120	Gm14443	2.358287	0.000284	0.042324	3.629636
121	Fkbp4	1.480798	0.000287	0.042609	3.626599
122	Acsl3	2.373864	0.000292	0.04315	3.622043
123	Bex3	0.582998	0.000317	0.046265	3.601391
124	Adi1	2.233937	0.000327	0.047511	3.593191
125	Pafah1b3	1.261069	0.000333	0.048224	3.588028
126	Akr1c13	3.174997	0.000335	0.048269	3.586509
127	Ubl5	0.548875	0.000346	0.049319	3.578309
128	Snhg20	1.77996	0.000404	0.055449	3.537612
129	Tnks	2.363003	0.000409	0.055893	3.534271
130	Col2a1	2.92796	0.000411	0.055893	3.533056
131	Ifi30	3.098968	0.000424	0.057191	3.524552
132	Ttr	32.49994	0.000429	0.057462	3.521515
133	Rnf128	4.973	0.000446	0.059066	3.511189
134	Rbm47	3.985939	0.000463	0.060926	3.50147
135	Tpd52	2.40904	0.000523	0.067438	3.46867
136	Hk2	1.633318	0.00062	0.077957	3.422506
137	Luzp1	1.616872	0.000645	0.080129	3.411876
138	Cited1	4.190455	0.000674	0.082892	3.400031
139	Rab11fip4	4.485671	0.000706	0.084602	3.387275
140	Pfdn1	0.102029	0.000711	0.084602	3.385453
141	Gpx3	2.357234	0.000748	0.087253	3.371483
142	Epb41l5	2.295077	0.000748	0.087253	3.371483
143	Espn	4.127735	0.000764	0.088846	3.365408
144	Eola1	2.114381	0.000788	0.090908	3.356905
145	Prtg	2.12513	0.000795	0.091353	3.354475
146	Vmp1	1.718075	0.00082	0.093837	3.345971
147	Rabgap1l	3.243957	0.000849	0.096537	3.336252
148	Rimklb	2.295755	0.00085	0.096537	3.335948

149	Chmp2b	2.115076	0.000855	0.096694	3.33443
150	Mgst1	2.212507	0.000879	0.099096	3.326534
151	Sorl1	3.791641	0.000885	0.099367	3.324711
152	Zfp329	2.083311	0.000922	0.101628	3.31317
153	Cxadr	2.656174	0.000959	0.104504	3.302237
154	Tmsb15b1	1.362231	0.000963	0.104571	3.301022
155	Foxa2	30.86683	0.001014	0.109216	3.286747
156	Peg3	2.887093	0.001095	0.115851	3.26488
157	Tjp2	2.538985	0.001099	0.115851	3.263969
158	Cst3	0.906297	0.00113	0.118697	3.256073
159	Gsta4	1.824095	0.001144	0.119215	3.252428
160	Ap1m2	7.194605	0.001229	0.127277	3.23208
161	Rbpms	1.978484	0.001251	0.128733	3.226917
162	Gm10076	0.250549	0.0013	0.132814	3.215983
163	App	2.119498	0.001349	0.136872	3.205353
164	Tcf7l2	1.603266	0.001409	0.142424	3.192901
165	Nav2	3.6032	0.001446	0.145715	3.185308
166	Krt19	6.381273	0.00147	0.147677	3.180449
167	Podxl	3.310487	0.001548	0.153874	3.165567
168	Cyp26a1	3.687703	0.001561	0.154643	3.163138
169	Kdm5b	1.6907	0.001582	0.155709	3.159189
170	Prss12	5.745147	0.001672	0.162367	3.143093
171	Pla2g12a	2.470531	0.00171	0.164489	3.136411
172	Pgrmc1	1.085167	0.001846	0.173949	3.113937
173	Col4a2	2.191201	0.00185	0.173949	3.113329
174	Pdgfa	3.916225	0.001869	0.17519	3.110292
175	Ddt	1.289184	0.00189	0.176064	3.106951
176	Smim14	1.336017	0.00192	0.177659	3.102396
177	Patj	3.176487	0.001931	0.177659	3.100574
178	Akr1c12	3.463457	0.001945	0.178382	3.098448
179	Acot13	1.204072	0.001996	0.180762	3.090855
180	Nenf	1.601414	0.002004	0.180948	3.08964
181	Cspp1	1.718089	0.002052	0.184123	3.082654
182	Grb7	5.065187	0.002068	0.18451	3.080225
183	Lpgat1	2.449465	0.002096	0.186408	3.076277
184	Hcfc1r1	1.225262	0.002199	0.194944	3.062002
185	Tmed10	1.016708	0.00232	0.202647	3.045906
186	Pigf	1.948261	0.002372	0.206393	3.039224
187	AC160336.1	0.972919	0.002447	0.211884	3.029809
188	Dnmt3b	2.293763	0.002494	0.214085	3.024039
189	Cstb	0.61514	0.00253	0.215236	3.019787
190	Atpif1	0.191619	0.002542	0.215293	3.018268
191	Rps28	0.314958	0.002545	0.215293	3.017964
192	Gm3511	0.519442	0.002555	0.215541	3.01675
193	Notch2	1.569358	0.002729	0.22763	2.996705
194	Ftl1	0.220222	0.002773	0.230633	2.991845
195	Pwwp3b	2.494063	0.00284	0.235536	2.984556
196	Bpnt2	1.841793	0.002851	0.235811	2.983341

197	Spint1	6.367459	0.002903	0.239387	2.977875
198	Strbp	1.618574	0.002929	0.240858	2.975141
199	Gyg	2.14761	0.00299	0.242775	2.968763

Cluster 8

	names	logfoldchanges	pvals	pvals_adj	scores
0	Fcer1g	14.89111	1.41E-26	2.12E-22	10.66993
1	Tyrobp	15.43467	1.44E-26	2.12E-22	10.66788
2	Lsp1	12.8769	2.67E-25	2.08E-21	10.39308
3	Arhgdib	8.217549	2.81E-25	2.08E-21	10.38797
4	Spi1	14.0107	3.77E-24	2.13E-20	10.13735
5	Evi2a	13.3216	4.34E-24	2.13E-20	10.12373
6	Laptm5	11.04171	6.9E-24	2.55E-20	10.0781
7	B2m	4.601311	2.66E-23	8.73E-20	9.944614
8	Cd52	14.3868	5.75E-23	1.54E-19	9.867657
9	Coro1a	11.44126	8.93E-23	2.2E-19	9.823389
10	Cd53	12.59442	9.98E-23	2.27E-19	9.812152
11	Tmsb4x	3.841702	1.01E-21	2.14E-18	9.575489
12	Lst1	10.70796	1.37E-21	2.6E-18	9.544161
13	Gpx1	2.705132	1.41E-21	2.6E-18	9.541436
14	Tnni2	11.13759	1.57E-21	2.74E-18	9.529859
15	Alox5ap	8.607179	5.43E-21	8.91E-18	9.40046
16	Plek	9.813076	8.37E-21	1.3E-17	9.35483
17	Rac2	14.20454	1.02E-20	1.5E-17	9.334399
18	Arpc2	2.757329	1.3E-20	1.78E-17	9.307838
19	Ly6e	7.23063	1.33E-20	1.78E-17	9.305795
20	Cyba	5.87812	2.49E-20	2.95E-17	9.238712
21	Ighm	15.72897	1.16E-19	1.27E-16	9.072878
22	Bcl2a1d	14.37576	1.16E-19	1.27E-16	9.072878
23	Bcl2a1a	11.32266	1.39E-19	1.47E-16	9.053127
24	Ptpn18	5.636287	3.02E-19	3.07E-16	8.967997
25	Ptpn6	8.395747	7.48E-19	7.36E-16	8.867542
26	Cst3	2.393426	8.32E-19	7.93E-16	8.855624
27	Arpc5	3.78856	1.29E-18	1.19E-15	8.806249
28	Mir142hg	6.54074	1.88E-18	1.68E-15	8.764364
29	Prdx5	3.890584	4.6E-18	3.99E-15	8.662889
30	Fth1	2.061659	9.45E-18	7.97E-15	8.580482
31	Actr2	2.055981	1.38E-17	1.13E-14	8.536896
32	Ccl6	12.93886	1.53E-17	1.22E-14	8.524636
33	Bcl2a1b	11.05297	1.66E-17	1.29E-14	8.515102
34	Ptprc	12.04049	1.77E-17	1.34E-14	8.508291
35	Rgs2	7.236438	1.89E-17	1.4E-14	8.500119
36	Lcp1	7.562403	2.58E-17	1.84E-14	8.464364
37	Fyb	8.885916	3.9E-17	2.61E-14	8.41601
38	Mef2c	6.035414	5.34E-17	3.51E-14	8.378893
39	Ucp2	6.212273	8.5E-17	5.46E-14	8.324069
40	Sh3bgrl3	2.0814	2.22E-16	1.38E-13	8.209312

41	Capg	8.533355	2.25E-16	1.38E-13	8.207951
42	Hpgds	10.18303	3.91E-16	2.36E-13	8.141209
43	Sec11c	5.712256	1.26E-15	7.27E-13	7.99887
44	Cap1	3.872108	1.31E-15	7.41E-13	7.994103
45	Stap1	11.88075	1.39E-15	7.77E-13	7.98593
46	Ctsc	8.313072	3.04E-15	1.63E-12	7.889222
47	Serp1	4.568999	7.52E-15	3.89E-12	7.775487
48	Acsl5	6.688488	8.15E-15	4.13E-12	7.765272
49	Pfn1	1.069754	1.23E-14	6E-12	7.712831
50	Ccl9	12.2475	1.24E-14	6E-12	7.71181
51	Emp3	5.819128	2.27E-14	1.06E-11	7.634511
52	Lilr4b	9.124662	3.01E-14	1.39E-11	7.597735
53	Lpl	9.043269	3.51E-14	1.59E-11	7.577984
54	Mbnl1	5.309615	3.82E-14	1.71E-11	7.567088
55	Gsn	7.519361	3.9E-14	1.72E-11	7.564363
56	Dok2	8.75062	4.36E-14	1.89E-11	7.549721
57	Sat1	5.582178	6.95E-14	2.97E-11	7.488768
58	Clec12a	12.39075	8.64E-14	3.61E-11	7.460164
59	Ccl3	13.04641	8.69E-14	3.61E-11	7.459483
60	Actb	1.029191	9.24E-14	3.79E-11	7.45131
61	Psme2	2.070302	1.58E-13	6.31E-11	7.380141
62	Bin2	9.133897	2.21E-13	8.69E-11	7.335533
63	H2aj	2.023386	2.66E-13	1.04E-10	7.310334
64	Fam111a	5.429118	2.94E-13	1.13E-10	7.297053
65	Capza2	2.247466	3.33E-13	1.26E-10	7.280368
66	Celf2	5.703544	7.42E-13	2.77E-10	7.171401
67	Sirpa	6.715609	7.5E-13	2.77E-10	7.170039
68	Atp6v0b	3.191671	1.29E-12	4.6E-10	7.095124
69	Ikzf1	8.073382	1.77E-12	6.13E-10	7.051877
70	Erp29	3.459505	2.69E-12	9.13E-10	6.992967
71	Dhrs3	6.059551	2.87E-12	9.62E-10	6.984114
72	Ncf4	7.917556	3.36E-12	1.11E-09	6.961979
73	Psme2b	1.850248	3.93E-12	1.29E-09	6.939505
74	Ciao2a	2.212754	4.02E-12	1.3E-09	6.93644
75	Fxyd5	5.861995	4.08E-12	1.31E-09	6.934397
76	Vamp8	3.325215	4.33E-12	1.38E-09	6.925884
77	Apbb1ip	9.485664	5.19E-12	1.63E-09	6.900345
78	Emb	5.686172	5.42E-12	1.68E-09	6.894216
79	Tpd52	5.356892	5.99E-12	1.84E-09	6.879914
80	Csf1r	9.361346	6.43E-12	1.94E-09	6.869698
81	Lyn	5.51965	1.44E-11	4.09E-09	6.753921
82	Ptgs1	8.101775	1.65E-11	4.64E-09	6.73417
83	Tln1	3.593334	1.83E-11	5.09E-09	6.719187
84	Psmb8	34.2721	2.49E-11	6.79E-09	6.674238
85	Cd47	4.553866	2.57E-11	6.95E-09	6.669471
86	Ctss	10.99995	3.1E-11	8.31E-09	6.641889
87	Ostf1	4.963435	3.94E-11	1.05E-08	6.606474
88	Gmfg	5.587478	5.4E-11	1.41E-08	6.559482

89	Llph	2.342757	5.74E-11	1.49E-08	6.550288
90	Fermt3	5.805609	6.23E-11	1.6E-08	6.538029
91	Tagln2	5.063447	8.51E-11	2.11E-08	6.491378
92	Rnf141	4.802979	8.6E-11	2.12E-08	6.489675
93	Cyrib	4.972408	8.74E-11	2.13E-08	6.487291
94	Rnase4	6.462112	9.7E-11	2.35E-08	6.471627
95	Inpp5d	5.534241	1.02E-10	2.44E-08	6.464477
96	Rhog	4.550004	1.12E-10	2.67E-08	6.449493
97	Ctsz	4.348932	1.18E-10	2.8E-08	6.441321
98	Cox6a1	0.799902	1.29E-10	3E-08	6.428381
99	Cenpx	1.948174	1.39E-10	3.19E-08	6.416803
100	Gpr183	5.979378	1.44E-10	3.28E-08	6.411355
101	Ncf1	12.88117	1.54E-10	3.45E-08	6.401139
102	Asb2	10.8522	1.68E-10	3.73E-08	6.388199
103	Nrros	6.402763	1.7E-10	3.75E-08	6.386156
104	Fcgr2b	10.13376	1.79E-10	3.92E-08	6.377984
105	Cx3cr1	10.70406	1.83E-10	3.98E-08	6.374578
106	Atp6v0e	2.121302	1.96E-10	4.18E-08	6.364363
107	Nop10	1.111998	1.96E-10	4.18E-08	6.364363
108	Cd9	4.79368	2.07E-10	4.36E-08	6.35619
109	Irf8	8.991838	2.1E-10	4.39E-08	6.354147
110	Ssr4	2.809431	2.23E-10	4.6E-08	6.344613
111	Ndufv3	1.186017	2.32E-10	4.76E-08	6.338483
112	Il2rg	5.836224	2.46E-10	5E-08	6.329629
113	Irf5	7.915766	3.68E-10	7.34E-08	6.266973
114	Ncf2	7.647069	5.91E-10	1.17E-07	6.192739
115	Man2b1	4.928539	5.94E-10	1.17E-07	6.192059
116	Psme1	2.453579	6.73E-10	1.32E-07	6.172308
117	H2-D1	5.512917	7.99E-10	1.55E-07	6.145066
118	P2ry12	10.79797	9.43E-10	1.81E-07	6.118846
119	Gm14414	1.055803	9.9E-10	1.89E-07	6.111014
120	C1qb	11.41315	1.01E-09	1.91E-07	6.107949
121	Rps8-ps5	1.053604	1.2E-09	2.26E-07	6.080367
122	Gusb	4.764458	1.24E-09	2.32E-07	6.074919
123	Rgs18	9.34026	1.25E-09	2.33E-07	6.073216
124	C3ar1	9.225263	1.52E-09	2.8E-07	6.042229
125	mt-Atp6	1.468759	1.61E-09	2.95E-07	6.032694
126	Gpsm3	5.32481	1.62E-09	2.95E-07	6.032013
127	Atp5g1	0.835868	1.8E-09	3.27E-07	6.014647
128	Cox8a	0.800495	1.91E-09	3.44E-07	6.005452
129	Tubb2a	4.907592	2.11E-09	3.78E-07	5.989107
130	Ckb	4.89228	2.2E-09	3.91E-07	5.982296
131	Slc25a5	1.494123	3.22E-09	5.59E-07	5.919981
132	Tomm5	1.873714	3.62E-09	6.25E-07	5.900571
133	Gm13493	0.938497	4.31E-09	7.27E-07	5.871967
134	Samhd1	5.017545	5.12E-09	8.53E-07	5.843364
135	Stxbp2	3.890211	5.29E-09	8.77E-07	5.837915
136	Ccl4	10.11913	5.67E-09	9.35E-07	5.826337

137	Fcgr3	9.504742	5.76E-09	9.45E-07	5.823613
138	Fmnl1	8.647916	5.9E-09	9.57E-07	5.819527
139	Clta	1.563618	6.07E-09	9.74E-07	5.81476
140	Vav1	8.944102	6.07E-09	9.74E-07	5.81476
141	Cyth4	8.74909	6.17E-09	9.85E-07	5.812036
142	Hacd2	3.56555	6.4E-09	1.01E-06	5.805906
143	Apobec1	8.614032	6.43E-09	1.01E-06	5.805225
144	Arhgap30	8.333953	6.51E-09	1.02E-06	5.803182
145	Lamp1	3.545217	6.87E-09	1.07E-06	5.793988
146	Zc3hav1	4.473379	6.9E-09	1.07E-06	5.793307
147	Rgs19	4.113978	7.81E-09	1.2E-06	5.772535
148	Stk17b	5.359155	8E-09	1.22E-06	5.768449
149	Tmem176b	4.300371	8.02E-09	1.22E-06	5.768108
150	AI413582	4.18725	9.05E-09	1.36E-06	5.747677
151	Tspo	4.636514	1.06E-08	1.57E-06	5.721457
152	Pla2g4a	8.002504	1.11E-08	1.64E-06	5.712603
153	Ndufb1	1.004867	1.24E-08	1.82E-06	5.693534
154	Arrb2	3.704433	1.24E-08	1.82E-06	5.693534
155	Tmem176a	4.479406	1.25E-08	1.82E-06	5.692852
156	Lcp2	6.218205	1.29E-08	1.85E-06	5.687745
157	Tubb6	4.052484	1.32E-08	1.9E-06	5.682978
158	Efhd2	5.77341	1.43E-08	2.02E-06	5.669697
159	Rps25	0.598232	1.44E-08	2.02E-06	5.669016
160	Gm12892	2.925794	1.54E-08	2.15E-06	5.657438
161	Bcap29	4.257458	1.55E-08	2.16E-06	5.656076
162	Ntpcr	4.286482	1.55E-08	2.16E-06	5.655395
163	Aup1	3.402777	1.59E-08	2.2E-06	5.651309
164	S100a11	3.003717	1.62E-08	2.23E-06	5.647904
165	Llph-ps2	1.885046	1.78E-08	2.43E-06	5.63224
166	Arpc1b	4.109355	1.79E-08	2.44E-06	5.630877
167	Rogdi	4.023961	2.25E-08	3.05E-06	5.591377
168	Uqcr10	0.67341	2.37E-08	3.2E-06	5.582523
169	Pnp	3.060984	2.58E-08	3.47E-06	5.567541
170	Rap1b	3.815514	2.69E-08	3.6E-06	5.56039
171	Pnp2	2.385346	2.88E-08	3.83E-06	5.548471
172	Ftl1-ps2	1.112658	3.08E-08	4.07E-06	5.536893
173	Ncoa3	3.542079	3.08E-08	4.07E-06	5.536553
174	Blvra	4.140058	3.13E-08	4.1E-06	5.534169
175	Ctsb	3.314658	3.18E-08	4.15E-06	5.531445
176	Lyz2	8.808681	3.28E-08	4.26E-06	5.525997
177	Cd68	6.694997	3.33E-08	4.31E-06	5.523273
178	Tacc1	3.214368	3.46E-08	4.44E-06	5.516462
179	Gm15590	1.592848	3.51E-08	4.49E-06	5.513738
180	Maf	4.546831	3.78E-08	4.81E-06	5.500798
181	Sting1	6.293325	4.5E-08	5.67E-06	5.470151
182	Unc93b1	7.244037	4.7E-08	5.9E-06	5.462319
183	Tspan4	4.488451	4.74E-08	5.91E-06	5.460617
184	Rgs10	5.062329	5.1E-08	6.28E-06	5.447677

185	Tsc22d4	3.318076	5.5E-08	6.71E-06	5.434396
186	Snx5	2.904134	6.01E-08	7.28E-06	5.418392
187	Aim2	5.317474	6.66E-08	8.03E-06	5.400003
188	Skap2	3.84456	6.69E-08	8.03E-06	5.399323
189	Snx2	2.175998	7.68E-08	9.14E-06	5.374465
190	Lamtor1	2.84731	8.08E-08	9.58E-06	5.36527
191	Bid	4.801245	8.95E-08	1.05E-05	5.346882
192	Ccr2	9.910639	1.14E-07	1.32E-05	5.302614
193	Samsn1	4.492594	1.22E-07	1.41E-05	5.290355
194	Rps29	0.528906	1.28E-07	1.47E-05	5.281502
195	Gm10925	1.333727	1.29E-07	1.47E-05	5.280821
196	Uchl5	2.675387	1.3E-07	1.47E-05	5.279118
197	Lmo2	4.228471	1.32E-07	1.49E-05	5.276053
198	Gm14303	0.892546	1.38E-07	1.56E-05	5.267881
199	Hexb	4.200613	1.39E-07	1.56E-05	5.266178

Cluster 9

	names	**logfoldchange**	**pvals**	**pvals_adj**	**scores**
0	Tubb3	11.64696	1.44E-16	4.26E-12	8.261115
1	Tagln3	9.475524	7.97E-16	1.18E-11	8.054723
2	Tuba1a	3.088256	2.21E-15	2.17E-11	7.92913
3	Elavl4	10.66286	3.42E-15	2.52E-11	7.874706
4	Sox11	5.883125	1.11E-14	6.57E-11	7.725668
5	Map2	9.576751	5.46E-14	2.36E-10	7.520532
6	Mllt11	7.24116	5.6E-14	2.36E-10	7.517183
7	Gm11223	1.909958	4.63E-13	1.71E-09	7.235854
8	Stmn1	1.910703	5.74E-13	1.88E-09	7.206549
9	Slc7a11	3.191718	1.47E-12	4.33E-09	7.077606
10	Hoxb5os	6.628241	2.05E-12	5.52E-09	7.030718
11	Dpysl3	7.655765	4.76E-12	1.17E-08	6.91266
12	Stmn3	9.481903	6.2E-12	1.41E-08	6.874982
13	Dynlt1b	1.545562	1.57E-11	3.32E-08	6.741016
14	Dcx	10.14891	4.13E-11	7.61E-08	6.599514
15	Crmp1	7.86601	4.84E-11	8.41E-08	6.575651
16	Crabp2	6.901302	6.58E-11	1.08E-07	6.530019
17	H2bu2	6.260839	1.15E-10	1.7E-07	6.445453
18	Idh1	3.946639	7.26E-10	8.04E-07	6.160356
19	Tppp3	6.898785	7.35E-10	8.04E-07	6.158263
20	H3f3b	0.967986	8.35E-10	8.8E-07	6.138168
21	Gsk3b	2.884843	1.16E-09	1.18E-06	6.085837
22	Hoxc9	5.654434	1.56E-09	1.44E-06	6.038112
23	Nhlh2	12.09603	1.94E-09	1.69E-06	6.002527
24	Bex2	3.484719	5.81E-09	4.52E-06	5.822091
25	Dynlt1c	1.386188	6.28E-09	4.53E-06	5.809113
26	Syt11	6.63266	6.7E-09	4.53E-06	5.798228
27	Ckb	6.139281	6.74E-09	4.53E-06	5.797391
28	Crabp1	6.570335	7.4E-09	4.86E-06	5.781482

29	Dynlt1-ps1	1.857769	8.18E-09	5.14E-06	5.764737
30	Calm2	1.236356	1.07E-08	6.31E-06	5.719523
31	Clasp2	4.105808	1.29E-08	7.35E-06	5.686869
32	Vbp1	2.299663	1.35E-08	7.5E-06	5.680171
33	Msi1	3.211843	1.84E-08	9.69E-06	5.626584
34	Fabp5	2.555749	1.9E-08	9.85E-06	5.620723
35	Dcc	9.318904	2.02E-08	1.03E-05	5.610257
36	Gm3226	1.5538	3.71E-08	1.74E-05	5.50434
37	Jpt1	1.411938	3.91E-08	1.81E-05	5.494711
38	Rtn1	8.207048	5E-08	2.23E-05	5.451172
39	Dpysl2	3.457711	5.67E-08	2.41E-05	5.428984
40	Kif5c	6.296965	5.72E-08	2.41E-05	5.427309
41	Mir124-2hg	7.5646	6.48E-08	2.66E-05	5.405121
42	Gm12892	3.535706	7.26E-08	2.94E-05	5.384607
43	Phyhipl	6.905872	7.75E-08	3.05E-05	5.372885
44	Orc4	3.440933	9.93E-08	3.71E-05	5.32809
45	Dynlrb1	1.255599	1.05E-07	3.86E-05	5.318461
46	Cd24a	4.241416	1.2E-07	4.32E-05	5.293343
47	Cdkn1c	4.243355	1.47E-07	5.12E-05	5.255665
48	Gm6166	2.105061	1.54E-07	5.3E-05	5.247292
49	Malat1	1.521058	1.62E-07	5.48E-05	5.238919
50	Gdi1	3.885928	1.82E-07	6.03E-05	5.217149
51	Selenok	1.210701	2.97E-07	9.63E-05	5.125466
52	Ldhb	3.901373	3.23E-07	0.000103	5.109558
53	Dctn3	1.951278	3.29E-07	0.000103	5.10579
54	Stmn2	8.057827	3.46E-07	0.000107	5.09658
55	Olfm2	7.0301	4.31E-07	0.00013	5.054715
56	Srgap3	6.821203	4.35E-07	0.00013	5.053041
57	mt-Atp6	1.571334	4.52E-07	0.000132	5.045505
58	Sox4	3.666016	4.99E-07	0.000143	5.026666
59	Cirbp	3.276955	5.11E-07	0.000144	5.022061
60	Atp6v1g1	0.847497	5.26E-07	0.000145	5.016619
61	Ube2n	1.069383	6.19E-07	0.000168	4.98522
62	Cox5a	1.272564	6.27E-07	0.000168	4.982708
63	Sst	10.51478	6.91E-07	0.000181	4.96387
64	Ptprs	3.119848	7.39E-07	0.000188	4.950891
65	Dpysl4	6.47801	7.55E-07	0.00019	4.946705
66	Klc1	5.16725	7.68E-07	0.000191	4.943356
67	Ina	8.499858	8.08E-07	0.000197	4.933309
68	Ank2	5.430244	8.79E-07	0.000213	4.916981
69	Gm1673	2.690179	9.76E-07	0.000232	4.896468
70	Scg5	8.039833	1.03E-06	0.000242	4.885164
71	Mien1	2.320257	1.17E-06	0.000272	4.860464
72	Ube2b	1.777196	1.27E-06	0.00029	4.844975
73	1500004A13Ri	5.964126	1.49E-06	0.000336	4.812739
74	Fam110a	5.731923	1.66E-06	0.000368	4.790969
75	Pantr1	5.542741	1.78E-06	0.000387	4.776735
76	Paip2	1.042883	1.88E-06	0.000404	4.766269

77	Uchl1	4.277286	2.1E-06	0.000443	4.743662
78	Gng3	7.074158	2.12E-06	0.000443	4.741988
79	Cfl2	2.842466	2.32E-06	0.000478	4.723149
80	Gm10925	1.467511	2.95E-06	0.000581	4.674167
81	Carhsp1	3.229189	3.01E-06	0.000588	4.6704
82	Cadm1	4.548067	3.13E-06	0.000608	4.662027
83	Ubb-ps	0.649421	3.85E-06	0.000715	4.619325
84	mt-Co1	0.668269	4.21E-06	0.000776	4.600904
85	Nrep	2.558518	4.56E-06	0.000826	4.584159
86	Nefl	6.44206	5.01E-06	0.000882	4.564483
87	Serf1	1.69756	5.18E-06	0.000905	4.557365
88	Map1b	3.703279	5.82E-06	0.000994	4.532666
89	Map1lc3b	1.43804	5.86E-06	0.000994	4.53141
90	Sema4b	3.930913	5.99E-06	0.00101	4.526804
91	H3f3a	0.569149	6.6E-06	0.001092	4.506291
92	Tsg101	1.571216	6.62E-06	0.001092	4.505454
93	Atat1	3.770633	6.98E-06	0.001146	4.49415
94	Ftl1	0.621208	7.11E-06	0.00116	4.490382
95	Dynlt1a	1.939142	1.1E-05	0.001709	4.396606
96	Gabarapl2	1.379833	1.21E-05	0.001848	4.376092
97	Iqsec1	3.448852	1.24E-05	0.001893	4.369813
98	Atp6v0c	1.218271	1.49E-05	0.002204	4.330879
99	Lhx1os	6.123482	1.6E-05	0.002349	4.314552
100	Rgmb	5.128072	1.68E-05	0.00246	4.303248
101	Srrm4	7.380738	2E-05	0.002897	4.264733
102	Hoxd3os1	4.275418	2.43E-05	0.003456	4.220775
103	Snap25	7.382293	2.77E-05	0.003817	4.191889
104	Ftl2-ps	0.563902	2.94E-05	0.004	4.178073
105	Kif21a	4.223324	3.13E-05	0.004212	4.163839
106	Macroh2a1	1.822071	3.14E-05	0.004212	4.163002
107	Ubb	0.589182	3.15E-05	0.004212	4.162165
108	Fez1	5.229174	3.51E-05	0.0046	4.137884
109	Atp5l	0.819312	3.51E-05	0.0046	4.137884
110	Calm1	1.065466	3.94E-05	0.005055	4.11109
111	Atp6v0c-ps2	1.190769	4.01E-05	0.005125	4.106904
112	Nkain4	6.608373	4.09E-05	0.005184	4.102299
113	Celf4	6.18786	4.3E-05	0.005361	4.090577
114	Pafah1b3	1.950576	5.1E-05	0.006151	4.050806
115	Ywhae	0.460261	5.1E-05	0.006151	4.050806
116	Ncam1	3.579345	5.46E-05	0.006556	4.034897
117	Acot7	4.291027	6.08E-05	0.007236	4.009778
118	Nova1	5.198222	6.4E-05	0.007493	3.997638
119	Ctnna2	5.532549	6.48E-05	0.0075	3.994707
120	Cartpt	11.70799	6.57E-05	0.007548	3.991358
121	Ndufa1	0.708653	6.96E-05	0.007907	3.977543
122	Ccdc85c	2.482447	7.09E-05	0.007986	3.973356
123	Sf3b6	0.925068	7.15E-05	0.008026	3.971263
124	Vta1	1.933966	7.23E-05	0.008081	3.968751

125	Basp1	2.946798	7.68E-05	0.008401	3.954099
126	Ftl1-ps2	0.779433	7.83E-05	0.008533	3.949493
127	Chrna4	7.852851	8.14E-05	0.00877	3.940283
128	Myl12b	2.220583	8.2E-05	0.008799	3.938609
129	Mir219a-2	4.009035	8.93E-05	0.009479	3.918095
130	Cnn3	1.701482	0.000106	0.010915	3.877068
131	Psmc5	1.224206	0.000107	0.011027	3.873719
132	Hsbp1	0.592299	0.000115	0.01149	3.856973
133	Prr13	2.737623	0.000117	0.01161	3.852787
134	Mrpl34	1.018178	0.000127	0.012372	3.83311
135	Ywhaq	0.773969	0.00013	0.012566	3.826831
136	Vps28	1.458021	0.000137	0.013159	3.813853
137	Napa	1.59499	0.000143	0.01362	3.802131
138	Ldhb-ps	1.948965	0.000151	0.014145	3.789571
139	Micu3	3.288532	0.000151	0.014148	3.788734
140	Tmsb4x	2.048828	0.00018	0.016222	3.746032
141	Ift43	2.598565	0.000193	0.017243	3.727612
142	Rab3a	4.825655	0.000195	0.017363	3.7251
143	Pid1	6.017548	0.000199	0.017606	3.720076
144	Ip6k2	2.562211	0.0002	0.017618	3.718402
145	Gm7172	2.413176	0.000228	0.019803	3.685747
146	Gm14328	1.519304	0.000237	0.020241	3.6757
147	Prdx2	0.771653	0.000248	0.02113	3.663978
148	Sh3rf1	3.602396	0.000279	0.02317	3.633836
149	mt-Cytb	0.841151	0.000285	0.023483	3.628812
150	Prdx2-ps1	1.218574	0.00029	0.023839	3.624207
151	Ttc3	1.709368	0.000295	0.0242	3.619601
152	Btf3l4	0.750778	0.000297	0.024289	3.617927
153	Gm13453	1.107321	0.000302	0.024466	3.61374
154	Scg3	7.893869	0.00031	0.024782	3.607042
155	Dner	7.267956	0.00033	0.026146	3.590715
156	Robo3	7.0371	0.000344	0.026927	3.57983
157	Psmc1	1.188733	0.000349	0.027146	3.575644
158	Rcn2	2.068368	0.000356	0.027411	3.571039
159	Gm2423	1.046186	0.000356	0.027411	3.571039
160	Gdf11	3.843598	0.000375	0.028703	3.556805
161	Mgst3	2.674178	0.000377	0.028703	3.555968
162	Miat	6.266991	0.000403	0.030036	3.537966
163	Tmem181b-ps	2.149942	0.000408	0.030171	3.535035
164	Lhx1	4.757032	0.000434	0.031822	3.51829
165	Ebf1	3.433727	0.000438	0.031995	3.516196
166	Gm28661	1.257792	0.000474	0.03394	3.495264
167	Rbfox2	3.112734	0.000474	0.03394	3.495264
168	Psmb1	0.594352	0.00051	0.035665	3.475588
169	Vps72	1.270777	0.00052	0.036223	3.470145
170	Gm12346	0.979828	0.000553	0.037952	3.453818
171	Gap43	3.998296	0.000567	0.038636	3.44712
172	Tubb2b	2.578293	0.000574	0.038938	3.443771

173	Hoxb7	4.478681	0.000577	0.03909	3.442096
174	1500011B03Ri	1.752054	0.000584	0.039306	3.439166
175	Gm2830	1.993542	0.000586	0.039338	3.43791
176	Pou2f2	5.252562	0.00059	0.039403	3.436235
177	Sbk1	4.138393	0.00059	0.039403	3.436235
178	Soga3	5.604654	0.000604	0.040145	3.429955
179	mt-Co2	1.17743	0.000608	0.040365	3.427862
180	Skp1	0.669997	0.000622	0.040969	3.422001
181	Trappc4	0.759866	0.000664	0.043093	3.404
182	Eif1ad	1.804547	0.000689	0.04451	3.393952
183	Lamtor5	1.465699	0.000696	0.044735	3.391021
184	Cdk2ap1	2.585168	0.000698	0.044735	3.390184
185	Tsg101-ps	1.63159	0.000698	0.044735	3.390184
186	Tspan3	1.804647	0.000702	0.044814	3.388928
187	Ank3	3.497264	0.000718	0.045487	3.382649
188	Ndufb9	0.237572	0.000751	0.047006	3.370089
189	Taf13	2.496758	0.000763	0.047524	3.365903
190	Mapk6	2.64915	0.000776	0.048222	3.361298
191	H2aw	2.397044	0.000794	0.048918	3.355018
192	Eif5	0.580198	0.000898	0.054219	3.320689
193	Ccl27a	2.959459	0.000975	0.057687	3.297664
194	Rnd3	3.100568	0.000988	0.058232	3.293896
195	Ywhaq-ps3	1.258546	0.001003	0.058871	3.28971
196	Nxph4	7.122077	0.001024	0.059752	3.283849
197	Atp6v1e1	1.858225	0.00103	0.059872	3.282174
198	Ndufb8	0.56677	0.001033	0.059932	3.281337
199	Kdm6b	1.548129	0.001042	0.060349	3.278825

Cluster 10

	names	**logfoldchange**	**pvals**	**pvals_adj**	**scores**
0	Kifc2	8.675134	3.4E-14	5.09E-10	7.582072
1	Foxh1	10.27841	3.45E-14	5.09E-10	7.58017
2	Capn6	10.81505	9.69E-14	9.53E-10	7.445116
3	Fscn1	4.364839	1.17E-12	7.24E-09	7.10843
4	Msx1	9.509843	1.52E-12	7.24E-09	7.072765
5	Nrp1	7.327863	1.8E-12	7.24E-09	7.049463
6	Eef1a1	1.015645	1.81E-12	7.24E-09	7.048512
7	Ahnak	8.804278	1.96E-12	7.24E-09	7.037099
8	Has2	7.822373	2.33E-12	7.4E-09	7.013322
9	Wdr6	7.500875	2.51E-12	7.4E-09	7.00286
10	Krt18	9.485285	4.57E-12	1.23E-08	6.918213
11	Hsp90ab1	1.085592	5.13E-12	1.26E-08	6.902044
12	Rps6ka6	8.267362	6.99E-12	1.59E-08	6.857819
13	Mxra8	8.184712	7.52E-12	1.59E-08	6.847357
14	Tbx20	10.20214	8.28E-12	1.63E-08	6.833566
15	Ddb1	5.025863	1.04E-11	1.93E-08	6.800278
16	Krt8	9.741396	1.27E-11	2.2E-08	6.772221

17	Plin3	6.173733	1.95E-11	3.19E-08	6.709925
18	Zc3hav1	6.932303	2.13E-11	3.31E-08	6.696609
19	Nedd4	2.098731	3.42E-11	4.81E-08	6.62718
20	Ctnna1	4.661543	3.63E-11	4.87E-08	6.61862
21	Ugdh	7.292529	4.67E-11	5.64E-08	6.581052
22	Arhgdia	3.753692	4.78E-11	5.64E-08	6.577724
23	Ptbp1	6.864378	5.53E-11	6.28E-08	6.555849
24	Maged1	4.067627	6.32E-11	6.67E-08	6.535876
25	Kalrn	5.966492	1.09E-10	1.03E-07	6.454557
26	Amot	7.280025	1.19E-10	1.1E-07	6.440767
27	Ptpn13	6.78672	1.33E-10	1.16E-07	6.423647
28	Klf6	6.786787	1.46E-10	1.23E-07	6.409381
29	Asb4	7.661754	1.75E-10	1.4E-07	6.381799
30	Msx2	9.407429	1.86E-10	1.44E-07	6.372764
31	Bmp5	8.970885	2E-10	1.51E-07	6.361351
32	Eef2	3.47507	2.31E-10	1.71E-07	6.339
33	Dsp	9.249816	2.94E-10	2.11E-07	6.301908
34	Calcoco1	6.076922	2.99E-10	2.11E-07	6.299055
35	Rbpms2	6.772962	3.59E-10	2.43E-07	6.270998
36	Acly	5.657589	3.87E-10	2.52E-07	6.259109
37	Bmp4	7.696944	3.92E-10	2.52E-07	6.257207
38	Caprin1	4.651098	4.29E-10	2.7E-07	6.24294
39	Peg3	5.89539	4.59E-10	2.82E-07	6.232479
40	Pitx2	6.896807	6.29E-10	3.57E-07	6.183022
41	Rn18s	0.941485	7.53E-10	4.12E-07	6.15449
42	Gm13456	1.189693	8.19E-10	4.32E-07	6.141174
43	Gpc3	5.890942	9.8E-10	4.99E-07	6.112641
44	Hand1	11.58522	1.14E-09	5.63E-07	6.088864
45	Anapc2	5.873424	1.14E-09	5.63E-07	6.087913
46	Dpp3	6.228012	1.18E-09	5.7E-07	6.083158
47	Cdh11	6.678866	1.59E-09	7.13E-07	6.034652
48	Psap	6.196062	1.62E-09	7.15E-07	6.031799
49	Epb41l3	6.816213	1.67E-09	7.15E-07	6.027044
50	Arhgap1	6.144167	1.78E-09	7.49E-07	6.017057
51	Sqstm1	4.829702	1.81E-09	7.54E-07	6.013728
52	Pik3ip1	6.806642	2.21E-09	8.65E-07	5.981867
53	Tkt	5.773845	2.23E-09	8.65E-07	5.98044
54	Mical1	6.866526	2.34E-09	8.66E-07	5.972356
55	Actb	1.033444	2.35E-09	8.66E-07	5.97188
56	Sall4	6.019967	2.5E-09	9.12E-07	5.961419
57	Tiparp	6.298049	2.6E-09	9.38E-07	5.954761
58	Calu	5.510706	2.67E-09	9.48E-07	5.950956
59	Map1b	5.129534	2.74E-09	9.62E-07	5.946677
60	S100a10	5.279528	2.91E-09	9.99E-07	5.93669
61	Igf2bp1	4.940722	3.17E-09	1.06E-06	5.922424
62	Copa	5.674263	3.48E-09	1.15E-06	5.907207
63	Vstm2b	7.21383	3.77E-09	1.22E-06	5.893891
64	Arfgap1	5.819795	3.93E-09	1.25E-06	5.887234

65	Supt5	5.00617	3.98E-09	1.25E-06	5.884856
66	Dok4	6.665965	4.12E-09	1.28E-06	5.879149
67	Epha7	6.418819	4.22E-09	1.3E-06	5.875345
68	Vwa5a	7.440865	4.77E-09	1.4E-06	5.854897
69	Slc6a6	6.350348	5.26E-09	1.52E-06	5.838728
70	Pfkl	4.397896	5.57E-09	1.57E-06	5.829217
71	Serinc3	5.567536	5.76E-09	1.61E-06	5.823511
72	Jup	5.804911	5.91E-09	1.61E-06	5.819231
73	Macroh2a2	5.81392	6.01E-09	1.61E-06	5.816378
74	Soat1	6.00949	6.07E-09	1.61E-06	5.814951
75	Gulp1	5.770767	6.17E-09	1.61E-06	5.812098
76	Bag3	6.447661	6.64E-09	1.69E-06	5.799734
77	Tspan12	6.2792	7.07E-09	1.74E-06	5.789272
78	Cgnl1	5.694084	7.09E-09	1.74E-06	5.788796
79	Ywhaz	1.296843	7.52E-09	1.81E-06	5.77881
80	Dbn1	5.195023	7.72E-09	1.82E-06	5.77453
81	Elovl6	5.665433	8.33E-09	1.92E-06	5.76169
82	6330403K07Ri	6.177174	8.42E-09	1.93E-06	5.759788
83	Herc1	5.488039	8.71E-09	1.98E-06	5.754081
84	Pkm	1.558912	9.91E-09	2.23E-06	5.732206
85	Slc2a1	5.527514	1.2E-08	2.6E-06	5.699869
86	Med25	5.415984	1.21E-08	2.61E-06	5.697967
87	Tmem119	6.332988	1.25E-08	2.67E-06	5.692736
88	Ythdf3	5.678058	1.32E-08	2.81E-06	5.683225
89	Mta2	5.525108	1.44E-08	2.97E-06	5.668483
90	Ppp2r5d	5.582069	1.64E-08	3.27E-06	5.646133
91	Glyr1	5.324415	1.7E-08	3.35E-06	5.639951
92	Psmd2	3.637287	1.74E-08	3.38E-06	5.636147
93	Jun	5.043815	1.8E-08	3.47E-06	5.63044
94	Atxn2l	5.026344	1.82E-08	3.48E-06	5.628538
95	Nono	2.967011	1.89E-08	3.58E-06	5.62188
96	Ppic	3.706167	2.03E-08	3.79E-06	5.609516
97	Pmp22	6.547189	2.05E-08	3.8E-06	5.608089
98	Tbx3	7.978587	2.13E-08	3.92E-06	5.601432
99	Gga2	5.612346	2.23E-08	4.04E-06	5.593348
100	Dpysl2	3.950923	2.23E-08	4.04E-06	5.593348
101	Klhdc8b	6.361504	2.25E-08	4.04E-06	5.591445
102	Arhgef40	5.042484	2.25E-08	4.04E-06	5.591445
103	Gpx3	5.935216	2.36E-08	4.2E-06	5.583361
104	Rbms3	5.504446	2.44E-08	4.3E-06	5.577179
105	Mmp11	5.985828	2.5E-08	4.34E-06	5.573375
106	Arf1	2.427187	2.5E-08	4.34E-06	5.573375
107	Decr2	4.519858	2.76E-08	4.75E-06	5.556255
108	Pcyt1b	6.087221	2.94E-08	4.96E-06	5.544842
109	Pdlim3	8.256145	3.21E-08	5.32E-06	5.529624
110	Rsrp1	3.356256	3.24E-08	5.32E-06	5.527722
111	Igfbp2	5.738441	3.61E-08	5.9E-06	5.508701
112	Slc25a24	5.69863	3.84E-08	6.16E-06	5.498239

113	Zfp512	5.617682	4.11E-08	6.53E-06	5.485875
114	Tmem88	6.028281	4.18E-08	6.6E-06	5.483021
115	Ttll12	5.63076	4.67E-08	7.29E-06	5.463524
116	Dlst	5.602069	4.78E-08	7.43E-06	5.459244
117	Aldh2	5.981245	5.29E-08	8.14E-06	5.441174
118	Add1	4.759153	5.38E-08	8.23E-06	5.43832
119	Bcar3	6.774376	5.47E-08	8.28E-06	5.435467
120	Tuba1a	2.039428	5.47E-08	8.28E-06	5.435467
121	9530068E07Ri	5.568334	5.58E-08	8.41E-06	5.431663
122	Usp22	4.471157	5.76E-08	8.58E-06	5.425956
123	Gata3	6.999135	5.78E-08	8.58E-06	5.42548
124	Rab6a	4.870518	5.83E-08	8.6E-06	5.424054
125	Usp5	5.635971	5.89E-08	8.61E-06	5.422152
126	Zfp281	5.393638	5.89E-08	8.61E-06	5.422152
127	Zfp568	5.291046	5.92E-08	8.61E-06	5.421201
128	Mfap4	5.984408	5.95E-08	8.61E-06	5.420249
129	Epb41l5	5.299188	6.11E-08	8.8E-06	5.415494
130	Kctd10	5.171334	6.21E-08	8.9E-06	5.412641
131	Hnrnpk	1.112143	6.28E-08	8.95E-06	5.410738
132	Rara	4.366373	6.58E-08	9.3E-06	5.402179
133	Vcp	2.612072	6.58E-08	9.3E-06	5.402179
134	Ccdc43	5.469473	6.69E-08	9.4E-06	5.399326
135	Spata13	5.269371	6.91E-08	9.62E-06	5.393619
136	Psen1	5.769789	6.98E-08	9.63E-06	5.391717
137	Sec23a	5.734513	7.02E-08	9.63E-06	5.390766
138	Polg	5.916185	7.48E-08	1.02E-05	5.379353
139	Cyp51	5.543325	7.53E-08	1.03E-05	5.377926
140	Myadm	5.598609	7.63E-08	1.03E-05	5.375548
141	Zfp975	5.657871	7.68E-08	1.03E-05	5.374598
142	Epb41l1	6.872775	7.84E-08	1.05E-05	5.370793
143	Rcn1	5.264824	8.01E-08	1.06E-05	5.366989
144	Stau1	5.297383	8.66E-08	1.15E-05	5.352722
145	Rbms2	4.988176	9.42E-08	1.24E-05	5.337505
146	Oaz2	4.695685	9.62E-08	1.26E-05	5.333701
147	Bcl9	5.020891	9.9E-08	1.29E-05	5.32847
148	Fastk	4.726591	1.01E-07	1.3E-05	5.325616
149	Map3k1	5.380433	1.02E-07	1.31E-05	5.323714
150	Mrtfb	4.863702	1.06E-07	1.35E-05	5.316581
151	Alpl	7.0474	1.08E-07	1.38E-05	5.312301
152	Ube2h	5.146295	1.11E-07	1.41E-05	5.30707
153	Khdrbs1	4.781673	1.15E-07	1.43E-05	5.301839
154	Zfp260	5.771806	1.16E-07	1.43E-05	5.299461
155	Ccdc6	5.350977	1.16E-07	1.43E-05	5.299461
156	Pcmtd2	5.232072	1.17E-07	1.44E-05	5.297559
157	Unc5c	6.744335	1.22E-07	1.49E-05	5.28995
158	Prtg	5.230804	1.24E-07	1.5E-05	5.288048
159	Myh9	3.986733	1.25E-07	1.51E-05	5.286146
160	Mogat2	6.058337	1.28E-07	1.54E-05	5.281391

161	Rcn3	5.159553	1.3E-07	1.54E-05	5.279489
162	Vcan	5.395155	1.3E-07	1.54E-05	5.279489
163	Pltp	6.659964	1.34E-07	1.58E-05	5.273782
164	Slc38a4	5.903561	1.4E-07	1.63E-05	5.265698
165	Fbh1	5.554591	1.41E-07	1.64E-05	5.26332
166	Cfc1	8.813383	1.44E-07	1.66E-05	5.260467
167	Atp1b2	8.701133	1.48E-07	1.71E-05	5.25476
168	Gtf2i	4.500795	1.5E-07	1.72E-05	5.252858
169	Mbtps1	5.411428	1.53E-07	1.75E-05	5.248578
170	P4hb	2.629802	1.57E-07	1.77E-05	5.244298
171	Mapk3	5.102497	1.59E-07	1.79E-05	5.242396
172	Trim71	4.15499	1.66E-07	1.86E-05	5.233836
173	Lamp1	4.379057	1.71E-07	1.91E-05	5.22813
174	Cmtm7	4.971313	1.83E-07	2.02E-05	5.215765
175	Brox	4.995789	1.86E-07	2.05E-05	5.212913
176	Dcaf8	5.029554	1.88E-07	2.07E-05	5.210535
177	Rbpms	4.67049	2.21E-07	2.36E-05	5.181051
178	Fus	4.029266	2.23E-07	2.38E-05	5.178673
179	Itm2c	4.991342	2.26E-07	2.4E-05	5.176771
180	Marchf7	4.936597	2.38E-07	2.51E-05	5.16726
181	Rbm14	5.045571	2.4E-07	2.52E-05	5.165358
182	Zfp317	5.058708	2.46E-07	2.56E-05	5.160603
183	Cacnb3	6.043767	2.5E-07	2.59E-05	5.157749
184	Lrrc8a	4.604636	2.54E-07	2.62E-05	5.154896
185	Ubap2l	3.457551	2.56E-07	2.64E-05	5.152994
186	Txnip	5.214175	2.63E-07	2.7E-05	5.148239
187	Ddost	4.655184	2.67E-07	2.73E-05	5.145385
188	Micu2	5.028473	2.7E-07	2.75E-05	5.143007
189	Prdm6	7.308706	2.79E-07	2.82E-05	5.136826
190	Surf4	4.706206	2.81E-07	2.82E-05	5.135874
191	Igf2r	3.289851	2.85E-07	2.85E-05	5.133021
192	F2r	5.086312	2.94E-07	2.91E-05	5.127315
193	Shc1	5.19882	2.95E-07	2.92E-05	5.126363
194	Uba1	4.405078	3.03E-07	2.95E-05	5.121608
195	Gas6	7.52063	3.03E-07	2.95E-05	5.121608
196	Gnai3	4.971645	3.03E-07	2.95E-05	5.121608
197	Hsd11b2	5.692038	3.11E-07	3.01E-05	5.116853
198	Trp53inp1	5.535141	3.11E-07	3.01E-05	5.116853
199	Apbb1	5.678485	3.15E-07	3.03E-05	5.113999

Cluster 11

	names	**logfoldchange**	**pvals**	**pvals_adj**	**scores**
0	Dppa5a	19.55639	3.08E-11	1.78E-07	6.642836
1	Utf1	16.44828	3.1E-11	1.78E-07	6.641741
2	Hsp90aa1	2.6145	3.1E-11	1.78E-07	6.641741
3	Zfp988	8.525683	3.34E-11	1.78E-07	6.630793
4	Gdf3	12.8089	4.02E-11	1.78E-07	6.603423

5	Zfp989	8.123189	4.46E-11	1.78E-07	6.588095
6	Hat1	5.246332	4.52E-11	1.78E-07	6.585906
7	Hspb1	11.49114	4.83E-11	1.78E-07	6.576052
8	Mt1	8.411995	1.26E-10	3.78E-07	6.431535
9	Dhx16	9.123885	1.28E-10	3.78E-07	6.429346
10	Gm5844	3.345029	1.42E-10	3.8E-07	6.414018
11	Gm12346	3.111342	2.56E-10	6.31E-07	6.323148
12	Zfp978	6.716705	3.1E-10	7.05E-07	6.293588
13	Gstm3	8.092233	3.73E-10	7.86E-07	6.265122
14	Rps4l	4.337697	4.47E-10	8.66E-07	6.236657
15	Ooep	36.5192	5.65E-10	8.66E-07	6.19998
16	Dppa5b	15.66967	5.67E-10	8.66E-07	6.199433
17	Dppa5c	15.57384	5.67E-10	8.66E-07	6.199433
18	Zfp640	13.36697	5.81E-10	8.66E-07	6.195601
19	Hsf2bp	13.47513	6.14E-10	8.66E-07	6.186842
20	Gm10323	12.07339	6.16E-10	8.66E-07	6.186295
21	Zfp987	8.729202	6.76E-10	8.96E-07	6.171515
22	Gm9531	4.063797	6.98E-10	8.96E-07	6.166588
23	Mt2	7.770206	7.37E-10	9.07E-07	6.15783
24	Gm21411	9.118598	7.93E-10	9.36E-07	6.146334
25	Zfp534	8.10736	8.52E-10	9.68E-07	6.134839
26	Zfp980	8.368474	8.98E-10	9.82E-07	6.126627
27	Ifitm1	8.498003	1.01E-09	1.07E-06	6.107468
28	Gsta4	4.568464	1.06E-09	1.08E-06	6.099804
29	Rnf17	9.903798	1.23E-09	1.2E-06	6.076265
30	Rex2	7.175059	1.26E-09	1.2E-06	6.071886
31	Gm13147	7.145277	1.31E-09	1.21E-06	6.065865
32	Ash2l	6.954955	1.6E-09	1.4E-06	6.034115
33	Zfp600	6.952096	1.61E-09	1.4E-06	6.032473
34	Set	2.285067	1.84E-09	1.55E-06	6.011124
35	Rps11	1.070416	2.09E-09	1.72E-06	5.990322
36	Pmm1	7.029451	2.41E-09	1.92E-06	5.96733
37	Trap1a	9.911162	3.54E-09	2.75E-06	5.904378
38	Gstm1	6.614618	4.48E-09	3.39E-06	5.865512
39	Exosc5	4.639562	5.24E-09	3.87E-06	5.839236
40	Crip1	6.66315	6.51E-09	4.69E-06	5.803107
41	Gpx4	2.032769	7.76E-09	5.46E-06	5.773547
42	Zfp42-ps1	34.89792	8.56E-09	5.48E-06	5.757125
43	L1td1	36.36898	8.56E-09	5.48E-06	5.757125
44	Fbxo15	14.99512	8.67E-09	5.48E-06	5.754935
45	Zfp42	15.4722	8.72E-09	5.48E-06	5.75384
46	Tdrd12	12.04144	9.61E-09	5.91E-06	5.737418
47	Gstp2	4.389824	1.09E-08	6.59E-06	5.715521
48	Zfp985	6.548778	1.13E-08	6.65E-06	5.710595
49	Hspbap1	7.421922	1.46E-08	8.34E-06	5.666255
50	Chchd10	6.377284	1.47E-08	8.34E-06	5.66516
51	Sema4b	5.238691	1.62E-08	9E-06	5.648737
52	Avpi1	6.900627	1.78E-08	9.58E-06	5.631768

53	Castor1	9.253726	1.96E-08	1.03E-05	5.615892
54	Gm8935	6.771241	2.02E-08	1.04E-05	5.610418
55	Dppa4	8.276161	2.04E-08	1.04E-05	5.608776
56	Cystm1	7.500287	2.33E-08	1.15E-05	5.585238
57	Mkrn1	6.87779	2.45E-08	1.19E-05	5.576479
58	Zfp990	6.905921	2.53E-08	1.21E-05	5.571005
59	Rpl4	0.845012	3.29E-08	1.54E-05	5.525023
60	Rdm1	6.796847	3.44E-08	1.57E-05	5.517359
61	Platr14	8.686018	3.46E-08	1.57E-05	5.516264
62	Zfp986	5.44296	3.66E-08	1.64E-05	5.50641
63	Zfp981	6.682911	4.63E-08	2.04E-05	5.464807
64	Gpx4-ps2	2.003311	6.3E-08	2.73E-05	5.410066
65	Impa2	6.479185	6.38E-08	2.73E-05	5.407876
66	Zfp982	6.274151	6.66E-08	2.81E-05	5.400213
67	Msh6	6.500622	7.43E-08	3.09E-05	5.380506
68	Ahsa1	3.494861	9.24E-08	3.74E-05	5.341092
69	Triml2	35.8778	1.07E-07	4.23E-05	5.314269
70	Epp13	14.67638	1.08E-07	4.23E-05	5.312627
71	Gjb3	13.49933	1.1E-07	4.23E-05	5.30989
72	Zfp998	13.33344	1.1E-07	4.23E-05	5.308795
73	Dppa2	13.0479	1.13E-07	4.26E-05	5.304963
74	Tdh	12.56946	1.15E-07	4.26E-05	5.301131
75	Snrpn	3.696166	1.15E-07	4.26E-05	5.300584
76	Tdgf1	12.11536	1.17E-07	4.27E-05	5.297847
77	Mylpf	7.530043	1.19E-07	4.28E-05	5.29511
78	Folr1	12.56325	1.2E-07	4.28E-05	5.29292
79	Nanog	11.35934	1.26E-07	4.44E-05	5.284162
80	Rhox5	10.35442	1.52E-07	5.23E-05	5.249674
81	Prorp	7.176745	1.55E-07	5.25E-05	5.246937
82	Zfp936	9.184155	1.56E-07	5.25E-05	5.244748
83	Ifitm3	4.504132	1.58E-07	5.25E-05	5.242558
84	Ncl	1.775862	1.85E-07	5.99E-05	5.214093
85	Prdx1	1.389691	1.93E-07	6.18E-05	5.206429
86	Sgo2a	6.209964	2.02E-07	6.34E-05	5.19767
87	Sod2	3.931917	2.2E-07	6.85E-05	5.181248
88	Aldoa	1.560468	2.41E-07	7.4E-05	5.164825
89	Eif2s2	1.885732	3.02E-07	9.1E-05	5.122128
90	Eed	5.705243	3.07E-07	9.17E-05	5.118843
91	H2-Bl	8.05184	3.52E-07	0.000104	5.093115
92	Cox7a1	5.555618	3.66E-07	0.000107	5.085999
93	Ccdc58	2.787418	3.92E-07	0.000113	5.072861
94	Dpy30	2.050945	3.99E-07	0.000114	5.069576
95	Eno1b	1.343017	4.15E-07	0.000118	5.061913
96	Tipin	3.225538	5.22E-07	0.000147	5.018119
97	Gstm2	6.084443	5.83E-07	0.000162	4.99677
98	Spp1	8.902124	6.2E-07	0.000171	4.984727
99	Fbxo5	6.281551	6.38E-07	0.000175	4.979253
100	Mnd1	5.631255	6.62E-07	0.000179	4.972137

101	Tpd52	5.788288	6.66E-07	0.000179	4.971042
102	Rpl18	0.761527	6.97E-07	0.000185	4.962284
103	Amt	4.232429	7.37E-07	0.000194	4.951335
104	Esco2	5.785213	7.73E-07	0.000202	4.942029
105	Emb	6.274261	8.11E-07	0.000208	4.932723
106	Slc25a39	3.812108	1.03E-06	0.000262	4.885646
107	Mageb16	12.71621	1.12E-06	0.00028	4.869224
108	Sox15	12.69384	1.13E-06	0.00028	4.868129
109	Gm7896	11.26307	1.16E-06	0.000284	4.862655
110	Plac9a	11.71564	1.16E-06	0.000284	4.86156
111	Rbpms2	5.993192	1.2E-06	0.000291	4.854991
112	Syce2	4.255769	1.24E-06	0.000299	4.848422
113	Morc1	10.92047	1.27E-06	0.000303	4.844043
114	Gstp1	3.321166	1.3E-06	0.000307	4.839664
115	Rfc5	5.307767	1.34E-06	0.000315	4.833095
116	Gm32885	10.20479	1.38E-06	0.000321	4.827621
117	Ldhb	4.738996	1.47E-06	0.000339	4.815577
118	Ccne1	5.898022	1.65E-06	0.000378	4.792038
119	EU599041	8.621638	1.66E-06	0.000378	4.790396
120	Oard1	4.070868	1.74E-06	0.000391	4.781638
121	Apoc1	7.601678	1.89E-06	0.000416	4.765215
122	Gm6871	8.596428	1.89E-06	0.000416	4.765215
123	Apoe	5.762068	1.98E-06	0.000433	4.755362
124	Tcea3	8.02399	2.02E-06	0.000439	4.750983
125	Agtrap	5.587259	2.05E-06	0.000441	4.748793
126	Ddx39a	3.549262	2.08E-06	0.000444	4.745509
127	Eif4ebp1	2.8701	2.09E-06	0.000444	4.744414
128	Rrp9	5.250481	2.16E-06	0.000448	4.737845
129	Dkc1	4.921897	2.17E-06	0.000448	4.73675
130	Slc2a3	6.492867	2.17E-06	0.000448	4.73675
131	Gm19705	7.264834	2.17E-06	0.000448	4.73675
132	Bclaf3	6.056878	2.29E-06	0.00047	4.725802
133	Mreg	7.423326	2.47E-06	0.000503	4.710474
134	Cenpm	4.758256	2.61E-06	0.000527	4.699526
135	Sycp3	7.481345	2.64E-06	0.000529	4.697336
136	Got1	5.726187	2.67E-06	0.00053	4.694599
137	Pin1	2.260652	2.68E-06	0.00053	4.694052
138	Mtf2	4.637374	2.69E-06	0.00053	4.692957
139	Rpp25	7.248552	2.8E-06	0.000547	4.685293
140	Rad51	5.908062	3E-06	0.000582	4.671061
141	Eef1e1	3.667468	3.06E-06	0.000591	4.666681
142	Rplp2	0.915694	3.23E-06	0.000619	4.655733
143	Mif4gd	6.012185	3.3E-06	0.000628	4.651354
144	Fkbp3	1.199346	3.35E-06	0.000634	4.648069
145	Rpl21	0.75284	3.4E-06	0.00064	4.644785
146	Uchl3	3.169562	3.59E-06	0.000671	4.633837
147	Hells	4.487775	3.8E-06	0.000701	4.621794
148	Plekhf2	5.23779	3.82E-06	0.000701	4.620699

149	Sall4	5.437467	3.93E-06	0.000706	4.615225
150	1810037I17Ri	2.366686	3.93E-06	0.000706	4.615225
151	Cox6b2	4.35006	3.95E-06	0.000706	4.61413
152	Alpl	7.6741	3.95E-06	0.000706	4.61413
153	Rps5	0.802247	4.45E-06	0.000783	4.588949
154	Rhebl1	6.14777	4.54E-06	0.000793	4.585117
155	Eno1	1.169378	4.84E-06	0.000836	4.571432
156	Cisd1	2.656952	5E-06	0.000858	4.564863
157	Pa2g4	2.585407	5.58E-06	0.000952	4.541872
158	Lactb2	5.288075	5.66E-06	0.000961	4.538587
159	Socs2	5.701669	5.9E-06	0.000996	4.529829
160	Gpx1	1.776373	6.72E-06	0.001127	4.502458
161	Rpl19	0.652663	7.04E-06	0.001174	4.492605
162	Ckb	5.987537	7.44E-06	0.001235	4.480562
163	Vangl1	5.618545	7.72E-06	0.001273	4.472898
164	Rad50	5.189858	7.8E-06	0.001279	4.470708
165	Hspe1	1.369197	8.08E-06	0.001311	4.463044
166	Gm14409	4.906376	8.16E-06	0.001317	4.460855
167	Atad2	4.874942	8.5E-06	0.001365	4.452096
168	Rif1	4.951343	8.99E-06	0.001435	4.440053
169	Cct8	1.405397	9.27E-06	0.001464	4.433484
170	Nudc	2.266816	9.27E-06	0.001464	4.433484
171	Rhox9	35.0439	9.49E-06	0.001482	4.428557
172	Gm48218	31.52622	9.49E-06	0.001482	4.428557
173	Rrp1b	5.240944	9.58E-06	0.001489	4.426368
174	Syngr1	5.362042	9.63E-06	0.001489	4.425273
175	Tdgf1-ps1	10.00698	1.02E-05	0.001566	4.41323
176	Mymx	11.05446	1.02E-05	0.001566	4.412135
177	Rnaseh2b	3.953123	1.03E-05	0.001574	4.409945
178	Gart	4.946982	1.05E-05	0.00159	4.406661
179	Nop58	3.407099	1.07E-05	0.001618	4.401734
180	Zfp268	3.49475	1.09E-05	0.00163	4.39845
181	Alg13	5.097321	1.09E-05	0.00163	4.397902
182	Tfap2c	9.173427	1.1E-05	0.00163	4.39626
183	Asns	5.276968	1.11E-05	0.00163	4.394071
184	Zfp979	5.970556	1.12E-05	0.00163	4.393523
185	Platr22	9.19153	1.14E-05	0.001664	4.388049
186	Cct3	2.304844	1.15E-05	0.001668	4.386407
187	Tcea1	2.832305	1.17E-05	0.001685	4.383122
188	Jade1	6.067031	1.21E-05	0.001737	4.375459
189	Mrpl40	2.889115	1.28E-05	0.001818	4.363416
190	Paics	2.473578	1.32E-05	0.001864	4.356847
191	Park7	1.253043	1.33E-05	0.001865	4.355752
192	Slc50a1	6.30502	1.35E-05	0.001884	4.352467
193	Gm7239	3.933854	1.37E-05	0.001913	4.348088
194	Atp5b	0.904299	1.4E-05	0.001942	4.343709
195	Gm12411	1.957037	1.41E-05	0.001943	4.342614
196	Wfdc2	8.501524	1.43E-05	0.001963	4.339329

197	Rrp15	3.823384	1.44E-05	0.001973	4.33714
198	Etfb	1.706523	1.52E-05	0.002075	4.325097
199	Nanos3	7.688163	1.54E-05	0.00208	4.323454

Appendix 2: Differential gene expression profile of clusters in sorted gastruloid populations

Cluster 0

	names	logfoldchange	pvals	pvals_adj	scores
0	Kdr	6.506680965	2.8E-36	8.26408E-32	12.57775
1	Egfl7	5.455970764	3.99E-33	4.51298E-29	11.99047
2	Ecscr	7.864098549	4.59E-33	4.51298E-29	11.97887
3	Ramp2	6.826596737	1.62E-32	1.19827E-28	11.8736
4	Crip2	6.546727657	1.21E-30	7.12999E-27	11.50764
5	S1pr1	5.663964748	1.46E-29	6.52834E-26	11.29047
6	Emcn	7.503074646	1.55E-29	6.52834E-26	11.28549
7	Pcdh17	4.942258835	6.68E-29	2.46535E-25	11.15618
8	Vamp5	5.619348526	7.71E-28	2.52937E-24	10.93652
9	Cyb5a	2.243031979	1.06E-27	3.1333E-24	10.90751
10	Gng11	6.039817333	2.75E-27	7.39054E-24	10.82048
11	Tpm4	3.642393112	5.77E-27	1.41901E-23	10.75251
12	Myct1	5.661606789	6.96E-27	1.58174E-23	10.7351
13	Gngt2	5.268237114	8.79E-27	1.85432E-23	10.71355
14	Ctla2a	5.872848034	1.46E-26	2.88044E-23	10.6663
15	Icam2	6.605639935	5.76E-26	1.06234E-22	10.53824
16	Cldn5	6.686191082	1.04E-25	1.80175E-22	10.4827
17	Elk3	5.1925807	1.42E-25	2.32191E-22	10.45327
18	Gimap6	6.105171204	1.56E-25	2.42166E-22	10.44416
19	Gmfg	5.111363411	2.3E-25	3.39125E-22	10.40727
20	Tspan18	5.07407093	9.29E-25	1.30574E-21	10.2734
21	2810025M15Ri	3.863187551	1.97E-24	2.64842E-21	10.20046
22	Cfl1	0.74022454	2.09E-24	2.68919E-21	10.19466
23	Fkbp1a	1.989429712	6.87E-24	8.45057E-21	10.07861
24	Tax1bp3	4.044154644	2.32E-23	2.73663E-20	9.958421
25	Sparc	5.003171921	6.19E-23	7.03268E-20	9.860196
26	BC028528	4.671416283	7.04E-23	7.69605E-20	9.847348
27	Vim	4.164870262	1.21E-22	1.27691E-19	9.792641
28	Efna1	5.719002724	1.71E-22	1.73873E-19	9.757827
29	Madcam1	6.612471104	2.49E-22	2.44593E-19	9.719697
30	Anxa6	5.108458996	2.9E-22	2.76261E-19	9.703948
31	Esam	5.828527927	5.82E-22	5.24963E-19	9.632663
32	Igf1	5.114806175	5.87E-22	5.24963E-19	9.631834
33	Rhoc	4.279094696	3.08E-21	2.6784E-18	9.459837
34	Lpar6	4.213635921	3.43E-21	2.89557E-18	9.448647
35	Cd38	5.482663155	5.78E-21	4.74035E-18	9.393939

36	Upp1	5.438038349	6.11E-21	4.87347E-18	9.388137
37	Plk2	5.390010834	8.2E-21	6.37076E-18	9.357053
38	Lxn	3.817265034	1.02E-20	7.72973E-18	9.333843
39	Cdh5	4.438087463	1.15E-20	8.50744E-18	9.320995
40	Clec1b	5.405128479	1.84E-20	1.32476E-17	9.271261
41	Cd93	5.375285625	2.61E-20	1.83346E-17	9.233961
42	Myl6	0.915291905	2.69E-20	1.84713E-17	9.230645
43	Anxa5	3.998630524	3.19E-20	2.13986E-17	9.21241
44	F11r	4.743068695	8.65E-20	5.59752E-17	9.104652
45	Tmsb10	1.503835201	8.72E-20	5.59752E-17	9.103824
46	Ppic	2.782493591	1.53E-19	9.62109E-17	9.042485
47	Ipo11	4.359438896	1.63E-19	1.00098E-16	9.035853
48	Arhgap18	4.995991707	2.44E-19	1.46945E-16	8.991508
49	Col4a1	4.933027744	2.54E-19	1.50104E-16	8.986948
50	Gm7809	2.207137823	2.6E-19	1.50527E-16	8.984462
51	Tmem88	5.263142109	2.77E-19	1.57396E-16	8.977416
52	Calm1	1.201856494	5.51E-19	3.06744E-16	8.901571
53	Gm16104	3.604610205	5.76E-19	3.14859E-16	8.896598
54	Sh3bgrl3	1.403345108	6.16E-19	3.30609E-16	8.889138
55	Serf2	0.602291584	7.87E-19	4.15177E-16	8.861784
56	Sat1	4.452129841	1.13E-18	5.86748E-16	8.821168
57	Sox7	5.323067665	1.63E-18	8.28124E-16	8.780552
58	Pomp	1.002554536	2.14E-18	1.06881E-15	8.749883
59	Ralb	3.603682518	2.67E-18	1.3145E-15	8.724601
60	Maged2	4.117428303	3.31E-18	1.60433E-15	8.700149
61	Fli1	3.499928474	5.09E-18	2.42596E-15	8.651243
62	Pfn1	0.743850172	6.91E-18	3.23728E-15	8.616429
63	Mest	4.298707008	1.6E-17	7.39605E-15	8.519448
64	Gm9844	1.585216999	2.95E-17	1.33946E-14	8.448577
65	Gng5	0.720275521	3.22E-17	1.44149E-14	8.438216
66	Plxnd1	3.869094133	4.62E-17	2.03674E-14	8.395942
67	Igfbp4	3.865940332	5.55E-17	2.4103E-14	8.374391
68	Cd34	4.741774082	2.93E-16	1.25265E-13	8.176283
69	Msn	3.953718185	3.42E-16	1.4411E-13	8.157633
70	Sox18	4.64749527	3.74E-16	1.55326E-13	8.146857
71	Klhl4	4.853282452	1.31E-15	5.36019E-13	7.993925
72	Nfkbia	3.86320734	2.82E-15	1.1408E-12	7.898601
73	Med10	1.968821526	3.43E-15	1.36886E-12	7.874148
74	S100a13	3.304959297	3.64E-15	1.4336E-12	7.866688
75	Actb	0.744532645	3.83E-15	1.48675E-12	7.860472
76	Myl12a	0.915666342	4.64E-15	1.7774E-12	7.836433
77	Tmsb4x	2.428822279	4.82E-15	1.82545E-12	7.83146
78	Eef1a1	0.439662755	6.03E-15	2.25443E-12	7.803277
79	Rab11a	1.930768967	1.27E-14	4.68812E-12	7.708783
80	Rasip1	3.626634121	1.77E-14	6.46339E-12	7.666094
81	Gng2	3.437739849	2.1E-14	7.5747E-12	7.644128
82	Ssu72	1.73728323	2.83E-14	1.00571E-11	7.605999
83	Anxa2	4.286088943	3.87E-14	1.35934E-11	7.565382

84	Ifitm3	2.601436853	4.51E-14	1.547E-11	7.545489
85	Myzap	3.904131651	5.81E-14	1.97121E-11	7.512333
86	Igfbp3	4.405722618	7.34E-14	2.46232E-11	7.481664
87	Cd59a	3.251862764	8.54E-14	2.8321E-11	7.46177
88	Gm3788	1.527945995	8.7E-14	2.854E-11	7.459283
89	Anxa3	4.438415527	9.38E-14	3.0438E-11	7.449337
90	Prkar1a	1.789250016	1.15E-13	3.64026E-11	7.422812
91	Tnfaip8l1	4.290662289	1.29E-13	4.05598E-11	7.407063
92	Gm8034	1.510367155	1.35E-13	4.19263E-11	7.40126
93	Flt4	3.694597244	3.7E-13	1.13761E-10	7.266149
94	Gm6969	1.237524271	4.08E-13	1.24186E-10	7.252887
95	Col4a2	3.620854378	4.47E-13	1.34731E-10	7.240453
96	Cd81	2.176116228	5.94E-13	1.77082E-10	7.20191
97	Prdx1	0.756319761	6.37E-13	1.87273E-10	7.192377
98	Gm17018	2.646014214	6.41E-13	1.87273E-10	7.191548
99	Tpm3	1.55022192	8.31E-13	2.38279E-10	7.155905
100	Rasgrp3	3.78387022	8.72E-13	2.47672E-10	7.149274
101	Clic1	1.636865139	8.86E-13	2.49044E-10	7.147202
102	Ccdc85b	3.312912464	1.31E-12	3.63608E-10	7.093738
103	Pea15a	3.493954659	1.95E-12	5.37365E-10	7.038201
104	Ostf1	3.219917536	6.93E-12	1.89369E-09	6.859159
105	Col18a1	3.353395939	7.51E-12	2.03495E-09	6.847554
106	Stab1	3.719629049	7.64E-12	2.05179E-09	6.845068
107	Map1lc3b	1.191874743	7.96E-12	2.11064E-09	6.839265
108	Cnn3	2.811840773	8.01E-12	2.11064E-09	6.838436
109	Ets1	3.432804585	1.02E-11	2.64234E-09	6.803622
110	Myo1b	3.446021557	1.23E-11	3.1662E-09	6.776268
111	Mmrn2	3.581376314	1.46E-11	3.72699E-09	6.751401
112	Sh3bp5	3.793699265	1.84E-11	4.64153E-09	6.718246
113	Mef2c	3.001022577	2.22E-11	5.566E-09	6.690477
114	Cdc42	0.907656848	2.26E-11	5.59793E-09	6.688405
115	F2r	3.14485383	2.7E-11	6.65187E-09	6.66188
116	Crem	3.214345217	2.83E-11	6.9013E-09	6.655249
117	Cox7a2l	1.185435295	3.06E-11	7.4062E-09	6.643644
118	Pon2	3.326257944	3.32E-11	7.96988E-09	6.631625
119	Ost4	0.610956073	3.98E-11	9.48549E-09	6.604686
120	Cyb5r3	2.7032938	4.92E-11	1.15408E-08	6.573188
121	S100a10	2.644625664	5.72E-11	1.33046E-08	6.550807
122	Tspan13	3.101764202	6.13E-11	1.41484E-08	6.540446
123	Thsd1	3.263783216	7.34E-11	1.68038E-08	6.513507
124	Mpzl1	3.374783039	1.35E-10	3.03311E-08	6.421913
125	Lamtor5	0.968488336	1.45E-10	3.21525E-08	6.410723
126	Ets2	2.640538454	1.47E-10	3.24373E-08	6.408237
127	Exoc3l4	3.32836318	1.5E-10	3.27263E-08	6.40575
128	Ifitm2	0.9661448	1.51E-10	3.28405E-08	6.404092
129	B2m	2.185770512	1.58E-10	3.4048E-08	6.39746
130	Sri	1.426451921	2.32E-10	4.90287E-08	6.338194
131	Tnfaip1	3.307447433	2.4E-10	5.0277E-08	6.333221

132	Rpl18a	0.328091174	2.9E-10	6.03921E-08	6.303795
133	Mrpl17	1.254534721	3.22E-10	6.65567E-08	6.287631
134	Selenok	0.922331989	3.39E-10	6.95303E-08	6.279757
135	Fscn1	2.166368723	3.53E-10	7.18664E-08	6.27354
136	Ppp1r11	1.847926259	3.87E-10	7.83388E-08	6.259034
137	Selenop	3.401938915	5.02E-10	1.00869E-07	6.218418
138	Gng12	2.481963634	6.43E-10	1.28321E-07	6.17946
139	Prex2	3.400365114	7.77E-10	1.5391E-07	6.149619
140	Ctnna1	2.458896875	9.52E-10	1.8735E-07	6.117292
141	Gpihbp1	3.746053457	1.29E-09	2.50974E-07	6.068387
142	Gnai2	2.247630596	1.44E-09	2.77115E-07	6.051394
143	Lrrc70	3.517051697	1.55E-09	2.96625E-07	6.039375
144	Carhsp1	2.337401628	1.56E-09	2.97754E-07	6.037717
145	Ctsl	2.411734581	1.64E-09	3.10627E-07	6.029843
146	Itga6	3.118855953	2.4E-09	4.48585E-07	5.96809
147	Tcf4	2.445042133	2.72E-09	5.04729E-07	5.947782
148	Akap12	2.984956503	2.77E-09	5.11832E-07	5.944466
149	Arhgap31	3.253683567	2.89E-09	5.29654E-07	5.937835
150	Arpc5	2.100915909	3.1E-09	5.64945E-07	5.92623
151	Ap2s1	1.075586438	3.14E-09	5.68605E-07	5.924158
152	Flt1	3.18346262	3.72E-09	6.70591E-07	5.895975
153	Pecam1	3.63617444	4.02E-09	7.18607E-07	5.883542
154	Prcp	2.99450922	4.55E-09	8.09428E-07	5.862819
155	Mob4	1.77391243	5.19E-09	9.18207E-07	5.840853
156	Tagln2	2.726030588	5.44E-09	9.56897E-07	5.832979
157	Pde4b	3.425668716	6.38E-09	1.10178E-06	5.806454
158	Gm7105	0.644061267	1.06E-08	1.78011E-06	5.720663
159	Arhgap29	3.050396204	1.15E-08	1.91826E-06	5.706986
160	Arhgef15	3.509582758	1.19E-08	1.97357E-06	5.701183
161	Tmem255a	3.692226887	1.27E-08	2.09051E-06	5.690408
162	Gm6192	0.627742231	1.29E-08	2.10794E-06	5.687507
163	Igf2	1.446081519	1.53E-08	2.47575E-06	5.657666
164	Cmtm3	2.524704695	1.87E-08	2.98341E-06	5.623681
165	Hspg2	2.534617424	1.96E-08	3.10574E-06	5.615807
166	Cdc42ep1	3.029368877	1.98E-08	3.11721E-06	5.61332
167	Rhoj	3.176445484	2.08E-08	3.24505E-06	5.605445
168	Fermt2	2.696951628	2.12E-08	3.29035E-06	5.60213
169	Sema6d	3.056746721	2.13E-08	3.29387E-06	5.600886
170	Cd40	3.520795107	2.14E-08	3.29387E-06	5.600058
171	Lama4	3.473444939	2.15E-08	3.29387E-06	5.599228
172	Snx3	1.290406108	2.48E-08	3.74256E-06	5.574362
173	Dapk2	3.789911509	2.61E-08	3.91429E-06	5.565658
174	Sdcbp	1.833813548	2.8E-08	4.15119E-06	5.553639
175	Gnpda2	2.63415122	2.98E-08	4.39295E-06	5.542863
176	Ica1	2.862958908	3.35E-08	4.89509E-06	5.522141
177	Dad1	0.753082275	4.18E-08	6.07598E-06	5.483182
178	Cd59b	1.683097959	4.4E-08	6.36454E-06	5.474064
179	Plvap	3.261902809	4.42E-08	6.36454E-06	5.473236

180	Dusp6	2.719984293	5.35E-08	7.6689E-06	5.43925
181	Gm9625	0.375201255	6.12E-08	8.7317E-06	5.415213
182	Cnn2	2.610804796	7.69E-08	1.08165E-05	5.374182
183	Actr2	1.019580364	7.82E-08	1.09399E-05	5.371281
184	Sox17	3.45685792	8.45E-08	1.17723E-05	5.35719
185	Unc5b	2.970165253	9.39E-08	1.29573E-05	5.338125
186	Tie1	2.994224548	9.97E-08	1.36859E-05	5.327349
187	Calm2	0.567817152	1.06E-07	1.43874E-05	5.316573
188	Gtf2e2	1.504506707	1.16E-07	1.55777E-05	5.30041
189	Sptbn1	2.214957476	1.25E-07	1.66739E-05	5.286318
190	Dram2	2.518917084	1.34E-07	1.78044E-05	5.27347
191	Calcrl	2.494779348	1.41E-07	1.8301E-05	5.263524
192	Gm8730	0.346639007	1.41E-07	1.8301E-05	5.263524
193	Laptm4b	2.233781815	1.47E-07	1.88902E-05	5.256892
194	Gm5526	0.816396236	1.71E-07	2.18746E-05	5.227881
195	Vamp8	1.833362579	1.72E-07	2.18746E-05	5.227052
196	Rras	3.116301775	1.73E-07	2.18746E-05	5.226637
197	Rplp0	0.365141302	1.91E-07	2.40877E-05	5.207987
198	Depp1	4.245811939	2.21E-07	2.74882E-05	5.181048
199	Arpc2	1.229080081	2.51E-07	3.10678E-05	5.156595

Cluster 1

	names	**logfoldchange**	**pvals**	**pvals_adj**	**scores**
0	Mfap2	8.078842	5.4E-36	1.03E-31	12.52573
1	Ptn	9.571926	6.95E-36	1.03E-31	12.50572
2	Gpc3	8.047338	1.06E-34	1.05E-30	12.28691
3	Mdk	4.047952	4.05E-34	2.99E-30	12.1784
4	Col3a1	11.50937	1.1E-33	6.5E-30	12.09657
5	Selenow	1.091038	9.78E-27	4.13E-23	10.70369
6	Peg3	6.273399	3.29E-26	1.21E-22	10.59073
7	Ldhb	6.297367	1.29E-25	4.23E-22	10.4622
8	Dlk1	6.442353	5.3E-25	1.56E-21	10.32745
9	Nr2f2	4.692106	1.36E-22	3.35E-19	9.780878
10	Crabp1	6.479832	2.21E-18	3.84E-15	8.745998
11	Cdh11	7.409396	2.57E-18	4.21E-15	8.729099
12	Sox11	4.793374	2.82E-18	4.38E-15	8.718426
13	H2az2	1.537858	5.27E-18	7.79E-15	8.647269
14	Id2	5.862352	6.12E-18	8.6E-15	8.63037
15	Grb10	3.83451	1.15E-17	1.48E-14	8.557879
16	Tceal9	1.477946	5.19E-17	6.13E-14	8.382212
17	Vcan	5.997202	2.42E-16	2.56E-13	8.198985
18	Cd63	2.066626	1.03E-15	1.02E-12	8.022873
19	Nfia	3.41832	1.54E-15	1.38E-12	7.973953
20	Igf2r	2.924111	1.79E-15	1.55E-12	7.955275
21	Cd24a	4.381194	2.59E-15	2.07E-12	7.909023
22	Nrep	3.974251	3.04E-15	2.36E-12	7.889455
23	Rcn3	4.66181	5.22E-15	3.86E-12	7.821412

24	Cdkn1c	4.073452	9.2E-15	6.63E-12	7.749811
25	Mir100hg	5.757419	1.53E-14	1.05E-11	7.68488
26	Cald1	3.797871	1.89E-14	1.27E-11	7.658197
27	H3f3b	0.474531	5.58E-14	3.43E-11	7.517663
28	Fstl1	3.774685	6.43E-14	3.88E-11	7.498984
29	Pbx1	3.843937	7.72E-14	4.56E-11	7.474969
30	Gm48564	1.137482	1.1E-13	6.35E-11	7.428718
31	Ncam1	5.63466	2.23E-13	1.17E-10	7.334435
32	Serf1	2.030739	2.62E-13	1.33E-10	7.312644
33	Notch2	3.507307	3.58E-13	1.79E-10	7.270395
34	Epha7	5.510889	1.63E-12	7.07E-10	7.063152
35	Gm48553	1.086875	2.02E-12	8.41E-10	7.032911
36	H3f3a	0.582272	2.39E-12	9.79E-10	7.009785
37	Gm1673	2.69034	4.6E-12	1.84E-09	6.917282
38	Elob	0.519319	6.14E-12	2.39E-09	6.876367
39	Lgals1	3.599351	7.78E-12	2.94E-09	6.842568
40	Tspan3	2.471145	1.08E-11	4.04E-09	6.795427
41	Rcn2	2.85778	1.85E-11	6.59E-09	6.717155
42	Ssbp2	3.098222	2.08E-11	7.31E-09	6.700255
43	Bex3	0.996683	3.52E-11	1.16E-08	6.622873
44	Ubb	0.459124	9.92E-11	2.99E-08	6.468108
45	Mir99ahg	3.763883	1.03E-10	3.06E-08	6.463216
46	Ldhb-ps	2.703897	1.08E-10	3.2E-08	6.454766
47	Ccnd2	3.102695	2.28E-10	6.28E-08	6.341361
48	Prrx1	7.829174	4.01E-10	1.07E-07	6.253749
49	Cdk4	0.829459	5.57E-10	1.43E-07	6.202161
50	Ddr2	9.465952	7.1E-10	1.81E-07	6.163915
51	Ndufa7	0.63772	7.9E-10	1.99E-07	6.147015
52	Cnpy2	1.289367	8.64E-10	2.14E-07	6.132783
53	Id3	3.21494	1.16E-09	2.85E-07	6.086087
54	Fbn2	3.727582	2.26E-09	5.29E-07	5.978019
55	Fbln1	4.558397	2.51E-09	5.78E-07	5.961119
56	Tuba1a	1.538772	2.84E-09	6.45E-07	5.940661
57	Rab34	3.951605	2.89E-09	6.52E-07	5.937549
58	Gsta4	3.040617	3.68E-09	8.05E-07	5.897968
59	Meis1	3.974829	3.96E-09	8.59E-07	5.88596
60	Sfrp1	5.873985	5.09E-09	1.07E-06	5.844156
61	Arl3	3.176317	5.11E-09	1.07E-06	5.843711
62	Cdc26	1.184026	5.3E-09	1.1E-06	5.837485
63	Nedd4	1.164224	5.8E-09	1.19E-06	5.822364
64	Gm48513	1.114681	8.32E-09	1.66E-06	5.761881
65	Ubb-ps	0.438761	1.03E-08	2E-06	5.725414
66	Ptprs	2.254628	1.08E-08	2.09E-06	5.717409
67	Col1a1	10.54424	1.28E-08	2.42E-06	5.688946
68	Tshz2	3.020052	2.42E-08	4.36E-06	5.578654
69	Marcks	2.237911	2.74E-08	4.77E-06	5.557307
70	Cd63-ps	1.702005	2.75E-08	4.77E-06	5.556862
71	Gm43584	1.107863	3.22E-08	5.53E-06	5.528844

72	Selenom	2.197565	3.64E-08	6.21E-06	5.507498
73	Nfib	3.33767	3.78E-08	6.41E-06	5.500827
74	Rnd3	3.426872	5.23E-08	8.67E-06	5.443457
75	P4hb	1.178381	6.35E-08	1.04E-05	5.408768
76	H3f3c	1.102645	7.44E-08	1.19E-05	5.380306
77	Matr3	1.805991	8.05E-08	1.28E-05	5.366075
78	Ppdpf	0.813738	8.68E-08	1.36E-05	5.352288
79	Sec61g	0.474411	8.79E-08	1.37E-05	5.350064
80	Cxcl12	5.583465	9.28E-08	1.43E-05	5.340281
81	Gpx8	3.077188	1.47E-07	2.2E-05	5.256227
82	Ndufa3	0.501556	1.9E-07	2.67E-05	5.208641
83	Igsf3	2.597898	2E-07	2.79E-05	5.199747
84	Slc7a11	1.335072	2.01E-07	2.79E-05	5.197968
85	Ift43	2.261681	2.08E-07	2.87E-05	5.191741
86	Cox6c	0.410299	2.22E-07	3E-05	5.180179
87	Gm10257	1.170054	2.46E-07	3.31E-05	5.161056
88	Atp5k	0.568234	2.81E-07	3.77E-05	5.135706
89	Fzd2	4.23698	3E-07	4E-05	5.123698
90	Son	0.493629	3.07E-07	4.07E-05	5.118806
91	Meis2	3.111117	3.12E-07	4.11E-05	5.116138
92	S100a11	2.090598	3.35E-07	4.37E-05	5.102796
93	Pcolce	6.80208	3.4E-07	4.43E-05	5.099683
94	Serpinf1	3.654219	3.54E-07	4.59E-05	5.092123
95	Ndufa11	0.466283	4.25E-07	5.38E-05	5.057434
96	Fxyd1	5.873778	5.46E-07	6.69E-05	5.009404
97	Slc25a4	0.453316	5.85E-07	7.11E-05	4.996062
98	Morf4l1	0.371887	6.43E-07	7.72E-05	4.977828
99	Gli3	3.28701	7.16E-07	8.48E-05	4.956926
100	Gm46996	1.040946	7.74E-07	9.03E-05	4.941805
101	Col11a1	4.493642	7.88E-07	9.16E-05	4.938247
102	Tpm1	1.705895	8.14E-07	9.42E-05	4.932021
103	Sec11a	0.916611	8.44E-07	9.73E-05	4.924905
104	Bsg	0.741976	1.04E-06	0.00012	4.883101
105	Pafah1b3	1.719184	1.14E-06	0.00013	4.865312
106	Foxp2	4.558505	1.19E-06	0.000135	4.857307
107	Fam162a	1.000749	1.22E-06	0.000137	4.852859
108	Tmem132c	5.319074	1.51E-06	0.000167	4.810166
109	Pebp1	0.499496	1.88E-06	0.000204	4.766138
110	Runx1t1	3.275226	1.97E-06	0.000212	4.756799
111	Snai2	5.319785	2.06E-06	0.000221	4.747904
112	Ube2b	0.853154	2.22E-06	0.000235	4.731894
113	Tceal8	0.65977	2.22E-06	0.000235	4.731894
114	Ndufa2	0.393945	2.47E-06	0.000259	4.710547
115	Maged1	1.995513	2.5E-06	0.000261	4.707879
116	Flywch2	3.902938	2.67E-06	0.000276	4.694537
117	Rbms3	5.488811	2.88E-06	0.000296	4.678971
118	6330403K07Ri	5.433258	2.97E-06	0.000304	4.672745
119	Cthrc1	5.650695	3.25E-06	0.00033	4.654511

120	Zfp36l1	1.325313	3.35E-06	0.000339	4.64784
121	Gm8524	1.257326	3.38E-06	0.000339	4.646506
122	Tmem45a	6.867054	3.43E-06	0.000343	4.642949
123	Hmgn1	0.596098	3.49E-06	0.000346	4.639391
124	Serpine2	2.883312	3.52E-06	0.000348	4.637612
125	Lgr4	2.685007	3.73E-06	0.000366	4.626049
126	Marcksl1	1.532779	3.78E-06	0.000369	4.623381
127	Cstb	0.813384	3.82E-06	0.000371	4.620712
128	Sem1	0.338948	3.84E-06	0.000372	4.619823
129	Gas1	4.15102	3.91E-06	0.000377	4.616265
130	AA465934	0.771092	3.97E-06	0.000378	4.613152
131	Pja1	2.45948	4.44E-06	0.000418	4.589581
132	Lhfpl2	4.548635	4.51E-06	0.000423	4.586468
133	Macroh2a2	3.363315	5.05E-06	0.000464	4.562898
134	Atp5o	0.363061	5.22E-06	0.000476	4.555782
135	Sox9	3.342577	5.22E-06	0.000476	4.555782
136	Dynlt1f	0.68075	5.54E-06	0.000498	4.54333
137	Atpif1	0.341452	5.68E-06	0.00051	4.537993
138	Nme4	1.831363	5.87E-06	0.000526	4.530878
139	Crabp2	3.482337	5.99E-06	0.000532	4.526875
140	H3f3a-ps2	0.773462	6.2E-06	0.00055	4.519314
141	Gm2710	1.375337	6.36E-06	0.000562	4.513978
142	Ric1	1.865445	6.55E-06	0.000577	4.507751
143	Dnmt3a	1.894682	6.89E-06	0.0006	4.497078
144	Tcf12	2.721484	7.09E-06	0.000616	4.490852
145	Ednra	6.445711	8.16E-06	0.000706	4.461055
146	Pcdh18	6.172351	8.22E-06	0.00071	4.459276
147	Pdlim4	4.367821	8.7E-06	0.000744	4.447269
148	Sfr1	0.577997	8.84E-06	0.000755	4.443711
149	Pdcd5-ps	0.582325	8.9E-06	0.000757	4.442377
150	Tenm3	3.537405	1.06E-05	0.000878	4.405465
151	Atat1	2.754528	1.15E-05	0.000944	4.386786
152	Gm6421	0.974538	1.28E-05	0.001047	4.362771
153	Gm16399	1.134204	1.36E-05	0.001103	4.350763
154	Higd1a	0.670782	1.44E-05	0.001166	4.337421
155	Gm26585	0.742109	1.46E-05	0.001175	4.335197
156	Fkbp3	0.341399	1.47E-05	0.001181	4.333419
157	Mrpl27	0.679241	1.79E-05	0.001404	4.289835
158	Lum	32.63814	1.81E-05	0.00142	4.286722
159	Pdcd5	0.365317	1.83E-05	0.001431	4.284499
160	Tspan7	3.390369	1.85E-05	0.00144	4.28183
161	Postn	6.390187	1.91E-05	0.001479	4.274715
162	Parm1	3.509808	2.09E-05	0.001597	4.254702
163	Hnrnpa1	0.578003	2.18E-05	0.001652	4.245363
164	Lsm7	0.539899	2.46E-05	0.001818	4.218679
165	Hmgb1-ps8	0.721655	2.48E-05	0.001826	4.2169
166	Map1lc3a	2.433875	2.82E-05	0.002045	4.187548
167	Pip4p2	1.955792	2.96E-05	0.002103	4.176875

168	Atraid	1.051172	3.01E-05	0.002135	4.172872
169	Hmgn3	2.63463	3.07E-05	0.002171	4.16798
170	Copz2	2.73546	3.16E-05	0.002215	4.161754
171	Id1	2.869927	3.33E-05	0.002322	4.149302
172	Zfp637	1.97417	3.6E-05	0.00248	4.131513
173	Col1a2	31.67134	3.66E-05	0.002507	4.127955
174	Adgrl2	2.305318	3.7E-05	0.00252	4.125731
175	Cd248	9.535515	4.17E-05	0.0028	4.097713
176	Fn1	2.092853	4.66E-05	0.003101	4.071919
177	Sulf1	4.229969	4.81E-05	0.00319	4.064804
178	Prdx2	0.590977	5.13E-05	0.003373	4.049683
179	Skp1	0.505083	5.19E-05	0.003404	4.047015
180	Pdcd4	1.180948	5.43E-05	0.003546	4.036341
181	Gsk3b	1.405313	5.51E-05	0.00359	4.032784
182	Pnisr	1.637241	5.52E-05	0.00359	4.032339
183	Nenf	1.697983	5.53E-05	0.00359	4.031894
184	Cd302	2.709584	6.62E-05	0.004166	3.989645
185	Ftl1-ps2	0.373015	6.93E-05	0.004329	3.978527
186	Gm12350	0.846713	7.33E-05	0.004511	3.965185
187	Sema5a	5.471694	7.5E-05	0.004604	3.959848
188	Btf3l4	0.685069	7.53E-05	0.004611	3.958959
189	Sumo2	0.184237	7.61E-05	0.004653	3.95629
190	Tgfb2	2.798151	7.84E-05	0.004774	3.949175
191	Chd3	3.045731	8.37E-05	0.005042	3.933609
192	Dhrs4	2.32344	8.76E-05	0.005259	3.922491
193	Col5a1	3.964366	9.06E-05	0.005415	3.914486
194	Mrfap1	0.562259	9.37E-05	0.005552	3.906481
195	Gm10177	0.767762	9.79E-05	0.005791	3.895808
196	Igfbp5	2.569548	9.84E-05	0.005811	3.894473
197	Alx1	6.871073	0.000102	0.006016	3.885579
198	Dnm1	4.954052	0.000112	0.006588	3.862008
199	Bmp4	3.57379	0.000115	0.00672	3.856672

Cluster 2

	names	logfoldchanges	pvals	pvals_adj	scores
0	Rps2	1.126426	9.63E-32	2.84E-27	11.72375
1	Car2	6.269699	1.95E-28	2.88E-24	11.06041
2	Rplp0	0.780225	2.67E-27	2.63E-23	10.82314
3	Nfe2	8.787044	6.26E-26	3.08E-22	10.5304
4	Smim1	7.702193	7.59E-26	3.2E-22	10.51222
5	Tspan32	8.779597	1.04E-25	3.82E-22	10.48285
6	Prdx3	3.862645	2.93E-24	8.64E-21	10.16214
7	Hbb-bh1	12.49063	1.97E-23	4.59E-20	9.974741
8	H2az1	1.68105	2.02E-23	4.59E-20	9.971944
9	Rpl6	0.620078	4.27E-23	8.82E-20	9.89736
10	Gm8730	0.693339	4.52E-23	8.82E-20	9.891766
11	Prkar2b	5.865782	3.14E-22	5.14E-19	9.695982

12	Gfi1b	7.954546	3.8E-22	5.9E-19	9.676403
13	Rpl14	0.745087	3.19E-21	4.48E-18	9.456379
14	Rgs10	6.379258	1.77E-20	2.27E-17	9.275512
15	Rpl4	0.691084	4.33E-20	5.33E-17	9.179484
16	Fermt3	6.325633	4.76E-20	5.6E-17	9.169229
17	Snrnp25	3.783823	5.76E-20	6.3E-17	9.148718
18	Fth1	1.239084	1.04E-19	1.06E-16	9.084389
19	Urod	4.259409	2.79E-19	2.75E-16	8.976707
20	Gm10076	0.604015	6.9E-19	6.37E-16	8.876485
21	Eif5a	1.136764	1.86E-18	1.61E-15	8.76554
22	Gm9625	0.61625	2.07E-18	1.75E-15	8.753421
23	Tmem14c	2.935585	3.62E-18	2.97E-15	8.690023
24	Rap1b	3.950756	4.75E-18	3.69E-15	8.659258
25	Rbm38	4.198781	6.12E-18	4.63E-15	8.630356
26	Srm	3.84296	1.35E-17	9.75E-15	8.53899
27	Gm7536	0.936904	4.09E-17	2.87E-14	8.410332
28	Rpl18	0.659144	4.72E-17	3.17E-14	8.39355
29	Rplp1	0.621863	6.32E-17	4.15E-14	8.359055
30	Rpl23a	0.798984	1.01E-16	6.46E-14	8.304049
31	Rps18	0.547822	1.48E-16	9.08E-14	8.258366
32	Gm14165	0.650567	1.92E-16	1.16E-13	8.226667
33	Dut	3.13582	2.97E-16	1.72E-13	8.174459
34	Rps11	0.594246	4.9E-16	2.73E-13	8.113858
35	Gclm	5.135078	6.46E-16	3.47E-13	8.080296
36	Sptb	5.907373	8.31E-16	4.3E-13	8.049529
37	Lyl1	4.376452	8.34E-16	4.3E-13	8.049064
38	Rpl19	0.55072	8.44E-16	4.3E-13	8.047665
39	Hmbs	3.782857	8.9E-16	4.45E-13	8.041139
40	Nt5c3	4.333445	9.18E-16	4.52E-13	8.03741
41	Blvrb	4.2667	1.18E-15	5.73E-13	8.006177
42	Asns	4.273234	1.21E-15	5.74E-13	8.003846
43	Hbb-bs	10.37971	1.27E-15	5.96E-13	7.99732
44	Rps3a2	0.522985	1.3E-15	6E-13	7.994524
45	Cnbp	0.782121	1.47E-15	6.67E-13	7.979607
46	Ran	0.829518	1.91E-15	8.55E-13	7.946976
47	Hsp90aa1	0.798425	2.95E-15	1.28E-12	7.892902
48	Gpx1	1.781171	3.89E-15	1.66E-12	7.858407
49	Glrx5	3.828538	4.93E-15	2.05E-12	7.828573
50	Hbb-y	8.992119	6.96E-15	2.85E-12	7.785221
51	Hba-a2	9.931821	7.33E-15	2.96E-12	7.778695
52	Hmga1	3.083145	8.15E-15	3.25E-12	7.765176
53	Rpl13	0.474307	1.24E-14	4.81E-12	7.712035
54	Prdx2	1.161646	1.53E-14	5.87E-12	7.684998
55	Supt4a	1.422976	1.67E-14	6.24E-12	7.67381
56	Hbb-bt	8.910347	1.94E-14	7.18E-12	7.654232
57	Npm1	0.54981	2E-14	7.3E-12	7.650503
58	Gypa	9.708699	2.25E-14	8.09E-12	7.635586
59	Phb2	2.337938	2.35E-14	8.35E-12	7.629992

60	Dhrs11	5.003287	2.61E-14	9.16E-12	7.616473
61	Hba-a1	11.0868	3.18E-14	1.1E-11	7.590835
62	Fech	4.951027	3.52E-14	1.21E-11	7.577783
63	Syngr1	4.941998	5.03E-14	1.71E-11	7.531168
64	Rpl14-ps1	0.776177	5.21E-14	1.75E-11	7.526506
65	Bola3	2.027587	6.23E-14	2.07E-11	7.503198
66	Rpsa	0.789076	8.04E-14	2.58E-11	7.469635
67	Hmga1b	3.122141	9.33E-14	2.96E-11	7.450057
68	Atp5b	0.691649	1.43E-13	4.44E-11	7.393652
69	Rplp2	0.605399	1.67E-13	5.09E-11	7.372675
70	Psma5	1.074189	3.62E-13	1.05E-10	7.269189
71	Pa2g4	1.755269	4.18E-13	1.2E-10	7.249611
72	Gata1	7.93885	4.33E-13	1.23E-10	7.244949
73	Gm29718	2.31556	4.55E-13	1.28E-10	7.237957
74	Rpl12	1.17706	5.46E-13	1.51E-10	7.213251
75	Snca	6.685535	7.63E-13	2.09E-10	7.167568
76	Idi1	3.594314	1.01E-12	2.73E-10	7.129344
77	Rack1	0.722506	1.24E-12	3.34E-10	7.100442
78	Inka1	3.707702	1.4E-12	3.73E-10	7.083661
79	Bcas2	1.691169	1.48E-12	3.89E-10	7.076668
80	Alad	3.541004	2.14E-12	5.45E-10	7.024925
81	Cenpw	2.644337	2.27E-12	5.74E-10	7.016534
82	Rpl21	0.575689	2.5E-12	6.24E-10	7.003482
83	Hbb-bh0	10.28397	2.51E-12	6.24E-10	7.00255
84	Tlcd1	5.001825	2.69E-12	6.61E-10	6.993227
85	Gypc	4.876232	2.98E-12	7.27E-10	6.978776
86	Gmnn	3.626406	3.37E-12	8.08E-10	6.961528
87	Rpl15-ps6	0.469726	3.87E-12	9.21E-10	6.94195
88	Rasgrp2	4.122292	4.3E-12	1.02E-09	6.927033
89	Adgrg1	5.396792	5.43E-12	1.26E-09	6.893936
90	C1qbp	1.740397	5.61E-12	1.29E-09	6.889275
91	Tnfaip8	4.320175	6.73E-12	1.52E-09	6.86317
92	Klf1	8.868122	1.06E-11	2.3E-09	6.797442
93	Crlf3	3.882323	1.6E-11	3.42E-09	6.738708
94	Gm10180	0.885436	1.77E-11	3.76E-09	6.723791
95	Rpl17	0.674257	2.24E-11	4.66E-09	6.689295
96	Timm8a1	2.461226	2.61E-11	5.39E-09	6.66692
97	Rps16	0.440853	3.08E-11	6.32E-09	6.64268
98	Rps7	0.397056	3.43E-11	6.98E-09	6.626831
99	Prkab1	3.770135	3.65E-11	7.39E-09	6.617507
100	Rpl7a	0.681531	3.75E-11	7.52E-09	6.613778
101	Rps13-ps1	0.514294	3.87E-11	7.71E-09	6.609117
102	Adk	3.716173	4.2E-11	8.31E-09	6.596997
103	Prkca	4.874525	4.28E-11	8.42E-09	6.5942
104	Hspe1	0.965798	4.41E-11	8.63E-09	6.589539
105	Gpx4	0.896648	4.55E-11	8.84E-09	6.584877
106	Atp5g1	0.47868	5.98E-11	1.14E-08	6.544322
107	Naa10	2.421285	6.05E-11	1.15E-08	6.542457

108	Mllt3	4.583915	6.46E-11	1.21E-08	6.532668
109	Banf1	0.684105	6.81E-11	1.26E-08	6.524743
110	Hdgf	2.959201	6.96E-11	1.28E-08	6.52148
111	Rnaseh2a	3.150112	7.36E-11	1.35E-08	6.513089
112	Gm12918	0.685493	7.78E-11	1.42E-08	6.504699
113	Rps8	0.51052	7.93E-11	1.43E-08	6.501902
114	Hba-x	10.63244	1.07E-10	1.9E-08	6.457151
115	Rps3a1	0.403438	1.13E-10	2.01E-08	6.447828
116	Ccnb2	4.260113	1.47E-10	2.56E-08	6.408671
117	Psmb10	3.528898	1.53E-10	2.63E-08	6.402145
118	Tnni1	5.515869	1.64E-10	2.8E-08	6.391423
119	Siva1	2.384382	1.7E-10	2.89E-08	6.385829
120	Rps2-ps10	1.159827	1.76E-10	2.96E-08	6.380702
121	Rps7-ps3	0.412793	1.91E-10	3.18E-08	6.368582
122	Birc5	4.335502	1.92E-10	3.18E-08	6.36765
123	Aldh9a1	3.882932	2.25E-10	3.71E-08	6.34341
124	Psat1	3.811304	2.37E-10	3.87E-08	6.335019
125	Eif4ebp1	1.852228	2.46E-10	3.99E-08	6.329425
126	Rpl27	0.387689	3.09E-10	4.94E-08	6.293997
127	Mpl	6.671333	3.26E-10	5.17E-08	6.286073
128	Psmg1	2.537361	3.54E-10	5.59E-08	6.27302
129	Spc24	3.6079	3.73E-10	5.85E-08	6.265096
130	Tk1	3.753032	4.1E-10	6.37E-08	6.250179
131	Wdr12	3.543524	4.36E-10	6.68E-08	6.24039
132	Rpl15	0.377394	4.65E-10	7.07E-08	6.2306
133	Idi1-ps1	2.252805	4.9E-10	7.38E-08	6.22221
134	Tubb4b	2.774056	4.99E-10	7.48E-08	6.219413
135	Sod2	2.673355	5.05E-10	7.53E-08	6.217548
136	F10	6.470833	5.08E-10	7.54E-08	6.216616
137	Rpl8	0.636289	5.17E-10	7.63E-08	6.213819
138	Mrpl12	2.095451	5.26E-10	7.73E-08	6.211022
139	Esd	1.391264	5.59E-10	8.12E-08	6.201699
140	Ddx39a	2.221441	5.86E-10	8.44E-08	6.194241
141	Nop10	0.912723	6.21E-10	8.91E-08	6.184917
142	Rps4x	0.430243	6.29E-10	8.97E-08	6.183053
143	Creg1	3.020155	6.53E-10	9.23E-08	6.176993
144	Gpx4-ps2	0.900084	6.91E-10	9.67E-08	6.168136
145	Pnpo	4.242919	7.33E-10	1.02E-07	6.158813
146	Hspd1	2.441746	8.24E-10	1.13E-07	6.140167
147	Eef1d	1.374887	8.27E-10	1.13E-07	6.139701
148	Tmem97	3.349498	8.59E-10	1.17E-07	6.133641
149	Dtymk	1.391826	8.69E-10	1.18E-07	6.131776
150	Rpl41	0.369296	1E-09	1.34E-07	6.109401
151	Rps3a3	0.374962	1.07E-09	1.42E-07	6.099145
152	Alas2	6.62755	1.17E-09	1.56E-07	6.084229
153	Ncl	0.949034	1.23E-09	1.62E-07	6.07677
154	Cacybp	1.541999	1.38E-09	1.8E-07	6.058124
155	Rps15	0.457529	1.76E-09	2.25E-07	6.018967

156	Rida	2.930541	1.79E-09	2.28E-07	6.01617
157	Rpl27a	0.546576	1.89E-09	2.4E-07	6.006847
158	Rpl17-ps5	1.292183	1.9E-09	2.4E-07	6.006381
159	Mcrip2	3.744006	2.09E-09	2.63E-07	5.990532
160	Tomm20	0.836675	2.23E-09	2.78E-07	5.97981
161	Cited4	9.152649	2.33E-09	2.88E-07	5.973284
162	Anp32b	1.980193	2.39E-09	2.96E-07	5.968623
163	Gm6136	0.559637	2.59E-09	3.16E-07	5.95557
164	Cenpp	3.440278	2.95E-09	3.57E-07	5.934127
165	Cmc2	2.912182	3.2E-09	3.85E-07	5.921075
166	Rps9	0.35556	3.31E-09	3.97E-07	5.915481
167	Lyar	2.743583	3.46E-09	4.14E-07	5.908023
168	Dapp1	5.160131	4.24E-09	5.03E-07	5.87446
169	Mrto4	2.223122	4.27E-09	5.04E-07	5.873528
170	Mrpl18	1.545996	4.51E-09	5.31E-07	5.864204
171	Rps6	0.374523	4.67E-09	5.45E-07	5.858611
172	Rpl39	0.586661	5.22E-09	6.07E-07	5.839964
173	Phlda1	2.168778	5.71E-09	6.59E-07	5.825047
174	Cox8a	0.539461	6E-09	6.9E-07	5.816657
175	Rps11-ps1	0.703653	6.1E-09	6.99E-07	5.81386
176	Uqcr11	0.434399	6.24E-09	7.12E-07	5.810131
177	Emp3	3.313099	7.46E-09	8.44E-07	5.780297
178	Mrpl38	2.784315	7.65E-09	8.62E-07	5.776102
179	Cbfa2t3	3.302224	9.2E-09	1.02E-06	5.744869
180	Gm13841	0.815224	9.61E-09	1.06E-06	5.737411
181	Rpl30	0.562293	9.83E-09	1.08E-06	5.733682
182	Polr2l	0.688855	1.16E-08	1.27E-06	5.705246
183	Ccnb1	4.086851	1.19E-08	1.29E-06	5.701517
184	Nop58	2.581418	1.21E-08	1.31E-06	5.698254
185	Psph	3.441099	1.26E-08	1.36E-06	5.691728
186	Cenpm	3.263858	1.36E-08	1.46E-06	5.677743
187	Ssx2ip	3.512206	1.55E-08	1.63E-06	5.655834
188	Hat1	2.617465	1.65E-08	1.72E-06	5.645113
189	Nhp2	1.339865	1.73E-08	1.8E-06	5.636722
190	Nol7	2.232532	1.8E-08	1.85E-06	5.630196
191	Mrps22	3.030515	1.88E-08	1.92E-06	5.622737
192	Pbk	3.752199	1.89E-08	1.92E-06	5.621805
193	Epb41	3.063017	1.95E-08	1.97E-06	5.616211
194	Smim3	4.001722	1.97E-08	1.98E-06	5.614347
195	Ubash3b	3.153639	1.97E-08	1.98E-06	5.614347
196	Nars	2.164851	2.03E-08	2.03E-06	5.609685
197	Abcg2	3.181288	2.12E-08	2.11E-06	5.602226
198	Cdca3	3.306586	2.13E-08	2.11E-06	5.601294
199	Pgp	2.847989	2.19E-08	2.16E-06	5.596632

Cluster 3

	names	logfoldchanges	pvals	pvals_adj	scores

0	Stab1	6.267481	8.51E-21	2.31E-16	9.353085
1	Cldn5	7.043855	1.57E-20	2.31E-16	9.288331
2	Gimap6	6.738095	7.26E-20	7.14E-16	9.12375
3	Gng11	5.833598	2.92E-19	2.16E-15	8.97158
4	Ecscr	7.113791	4.41E-19	2.6E-15	8.926252
5	Cdh5	5.343144	6.4E-18	3.15E-14	8.625149
6	Col18a1	5.05652	1.88E-17	7.93E-14	8.501039
7	Vim	3.878645	4.42E-17	1.46E-13	8.401211
8	Emcn	6.857253	4.44E-17	1.46E-13	8.400671
9	F11r	5.451866	8.35E-17	2.46E-13	8.326204
10	Flt4	5.225201	1.18E-16	3.18E-13	8.284655
11	AC149090.1	4.177705	1.56E-16	3.84E-13	8.251738
12	Adam10	4.101573	2.32E-16	5.27E-13	8.204252
13	Col4a1	5.537569	2.65E-16	5.6E-13	8.188064
14	Icam2	6.125907	5.95E-16	1.17E-12	8.090394
15	Plxnd1	4.833035	1.19E-15	2.19E-12	8.005675
16	Crem	5.077752	1.66E-15	2.88E-12	7.964664
17	Ets2	4.361156	2.15E-15	3.53E-12	7.932288
18	Plk2	5.806499	2.73E-15	4.24E-12	7.902609
19	Dusp6	5.139098	2.94E-15	4.34E-12	7.893436
20	Aplp2	4.782713	3.32E-15	4.67E-12	7.878327
21	Elk3	5.197196	4.08E-15	5.48E-12	7.852426
22	Apold1	5.313384	7.4E-15	9.5E-12	7.77742
23	Col4a2	5.028481	1.06E-14	1.31E-11	7.731553
24	Ptprm	5.570803	1.42E-14	1.66E-11	7.694859
25	Thsd1	5.322308	1.46E-14	1.66E-11	7.691082
26	S1pr1	4.767356	1.72E-14	1.88E-11	7.670037
27	Ramp2	5.588894	2.07E-14	2.18E-11	7.646294
28	Kdr	5.442187	2.16E-14	2.2E-11	7.640898
29	BC028528	4.406247	2.44E-14	2.4E-11	7.625249
30	Myo1b	5.03686	2.99E-14	2.85E-11	7.598808
31	Egfl7	4.428941	4.53E-14	4.18E-11	7.544847
32	Rhoc	4.35197	7.43E-14	6.65E-11	7.480093
33	Ctla2a	4.998816	1.56E-13	1.32E-10	7.381884
34	Tmsb10	1.488274	1.79E-13	1.47E-10	7.363537
35	Fkbp1a	1.818097	1.97E-13	1.57E-10	7.350587
36	N4bp3	4.865861	2.14E-13	1.62E-10	7.339795
37	Gnai2	3.232047	2.14E-13	1.62E-10	7.339795
38	Tspan18	4.60133	2.36E-13	1.74E-10	7.326844
39	Msn	4.237173	2.53E-13	1.82E-10	7.317131
40	Mpzl1	4.845843	2.58E-13	1.82E-10	7.314433
41	Klhl4	5.291047	4.33E-13	2.97E-10	7.244823
42	Cd93	5.210036	5.37E-13	3.6E-10	7.215684
43	Pcdh17	4.156701	5.67E-13	3.72E-10	7.208129
44	Lama4	5.222069	7.66E-13	4.92E-10	7.167119
45	Prcp	4.804883	8.48E-13	5.33E-10	7.153089
46	Ssu72	1.896743	9.18E-13	5.65E-10	7.142297
47	Gm8034	1.722968	1.49E-12	8.98E-10	7.075385

48	Efna1	5.438113	2.1E-12	1.24E-09	7.027899
49	Septin10	3.663727	2.35E-12	1.36E-09	7.011711
50	Arhgap18	4.876781	2.67E-12	1.52E-09	6.993904
51	Myct1	4.809508	2.88E-12	1.6E-09	6.983651
52	Igfbp4	4.191808	2.99E-12	1.63E-09	6.978255
53	Sox18	5.039123	3.52E-12	1.89E-09	6.955052
54	Prex2	4.678831	4.25E-12	2.24E-09	6.928611
55	Sparc	4.255767	5.92E-12	3.01E-09	6.881665
56	Igfbp3	5.118019	6.68E-12	3.34E-09	6.864397
57	Arhgap29	4.277863	7.04E-12	3.46E-09	6.856843
58	Trp53i11	4.589141	7.91E-12	3.8E-09	6.840115
59	Tspan13	4.129591	7.97E-12	3.8E-09	6.839035
60	Anxa5	3.929622	1.33E-11	6.22E-09	6.765648
61	Gm3788	1.651496	1.64E-11	7.57E-09	6.73489
62	Mmrn2	4.55393	2.04E-11	9.27E-09	6.703053
63	Rcsd1	4.581777	2.68E-11	1.2E-08	6.663122
64	Vamp5	4.387187	3.24E-11	1.43E-08	6.635062
65	Piezo2	5.298486	4.41E-11	1.91E-08	6.589735
66	Nid1	4.420197	4.54E-11	1.91E-08	6.585418
67	Gngt2	4.161729	4.54E-11	1.91E-08	6.585418
68	Itga6	4.242196	4.98E-11	2.07E-08	6.571388
69	Pisd-ps1	3.371125	5.56E-11	2.28E-08	6.5552
70	Arap3	4.111127	5.8E-11	2.35E-08	6.548724
71	Hmcn1	3.494577	6.17E-11	2.46E-08	6.539551
72	Pde4b	4.991525	6.42E-11	2.53E-08	6.533615
73	Tpm4	2.986181	7.85E-11	3.05E-08	6.503397
74	Tcf4	3.485335	1.02E-10	3.91E-08	6.464005
75	Cd34	4.696427	1.11E-10	4.22E-08	6.450515
76	Slc39a1	2.323677	1.23E-10	4.59E-08	6.435406
77	Cavin1	4.494801	1.24E-10	4.59E-08	6.433787
78	Myzap	4.149162	1.36E-10	4.96E-08	6.420297
79	Ppfibp1	4.217731	1.4E-10	5.06E-08	6.41544
80	Sptbn1	3.23664	1.58E-10	5.61E-08	6.397633
81	Actr2	1.243104	1.66E-10	5.83E-08	6.390079
82	Dock6	4.318654	1.75E-10	6.09E-08	6.381445
83	Pald1	4.80147	1.83E-10	6.28E-08	6.374969
84	Tmsb4x	2.306951	2.14E-10	7.25E-08	6.351226
85	Ptk2	4.15125	2.36E-10	7.91E-08	6.336117
86	Timp3	4.494486	2.39E-10	7.93E-08	6.333959
87	Lamb1	4.319705	2.56E-10	8.37E-08	6.323167
88	Cav1	5.966188	2.58E-10	8.37E-08	6.322087
89	Lxn	3.553857	2.9E-10	9.22E-08	6.30428
90	Gap43	4.773582	2.91E-10	9.22E-08	6.303741
91	Gm16104	3.101245	3.25E-10	1.02E-07	6.286473
92	Tek	4.589684	4.65E-10	1.45E-07	6.230353
93	Map4k4	3.555311	5.41E-10	1.65E-07	6.206611
94	Crip2	4.566567	5.92E-10	1.78E-07	6.192581
95	Anxa6	4.386734	6.69E-10	1.99E-07	6.173155

96	Smtn	4.196329	6.74E-10	1.99E-07	6.172075
97	Unc5b	4.221274	8.44E-10	2.44E-07	6.136461
98	Calm1	1.027892	9.09E-10	2.61E-07	6.12459
99	Gng2	3.570812	9.79E-10	2.75E-07	6.112718
100	Rasgrp3	4.229566	1.1E-09	3.06E-07	6.094371
101	Klf10	3.75373	1.33E-09	3.65E-07	6.064153
102	Igf2	1.90798	1.34E-09	3.65E-07	6.063074
103	Gm7809	1.854186	1.52E-09	4.11E-07	6.042569
104	S100a13	3.189734	1.58E-09	4.25E-07	6.035554
105	Bcl6b	4.593291	1.69E-09	4.45E-07	6.025301
106	Tnfaip1	4.025288	1.74E-09	4.54E-07	6.020445
107	Malat1	1.308689	1.8E-09	4.67E-07	6.014509
108	Gpihbp1	4.855876	1.95E-09	4.97E-07	6.001558
109	Gm9844	1.354137	2.09E-09	5.27E-07	5.990766
110	Tax1bp3	3.296644	3.02E-09	7.56E-07	5.93033
111	Leprot	3.540551	3.25E-09	8.06E-07	5.918458
112	Stx6	3.61496	3.29E-09	8.1E-07	5.9163
113	Litaf	3.78594	3.97E-09	9.6E-07	5.885542
114	Afdn	3.234202	4.53E-09	1.09E-06	5.863418
115	Ctnna1	3.20406	4.9E-09	1.17E-06	5.850467
116	Ipo11	3.518202	5.44E-09	1.28E-06	5.8332
117	Madcam1	4.985184	5.54E-09	1.29E-06	5.829962
118	Gmfg	3.916923	6.07E-09	1.4E-06	5.814853
119	Ets1	3.697853	6.64E-09	1.52E-06	5.799744
120	Sat1	4.034286	7.53E-09	1.71E-06	5.778699
121	Nisch	2.951228	7.85E-09	1.77E-06	5.771684
122	Esam	4.451885	7.98E-09	1.78E-06	5.768986
123	Pde4d	4.171006	8.37E-09	1.86E-06	5.760891
124	Creb3	3.910841	9.45E-09	2.08E-06	5.740386
125	Frmd4b	3.990766	9.78E-09	2.14E-06	5.734451
126	Garre1	3.198421	1.01E-08	2.19E-06	5.729594
127	Rasip1	3.225524	1.08E-08	2.33E-06	5.717183
128	Ica1	3.84178	1.17E-08	2.5E-06	5.704232
129	Actb	0.705813	1.29E-08	2.74E-06	5.687504
130	Arhgap31	3.373819	1.39E-08	2.92E-06	5.675093
131	Cmtm3	3.588323	1.46E-08	3.02E-06	5.66592
132	Abhd4	3.864932	1.51E-08	3.09E-06	5.660524
133	Ece1	3.834337	1.55E-08	3.15E-06	5.656207
134	Sox7	4.2416	1.59E-08	3.22E-06	5.65135
135	Exoc3l4	3.345753	1.8E-08	3.59E-06	5.630306
136	Fxyd5	3.936335	1.99E-08	3.94E-06	5.613038
137	Ppic	2.467122	2.16E-08	4.24E-06	5.599008
138	Mast4	3.136896	2.69E-08	5.25E-06	5.560696
139	Pam	2.806909	2.75E-08	5.33E-06	5.556919
140	Nfia	2.682853	3.16E-08	6.11E-06	5.532096
141	Nts	5.729747	3.2E-08	6.14E-06	5.529938
142	Gm26862	2.529574	3.69E-08	7.03E-06	5.505116
143	Zfp57	3.7031	4.14E-08	7.79E-06	5.484611

144	Upp1	4.157408	4.49E-08	8.38E-06	5.470581
145	Pea15a	3.630087	4.64E-08	8.59E-06	5.464645
146	Sh2d3c	3.823811	4.65E-08	8.59E-06	5.464105
147	Rbpms	3.265391	4.71E-08	8.64E-06	5.461947
148	Ostf1	3.052866	5.07E-08	9.23E-06	5.448996
149	Cavin3	3.918721	5.5E-08	9.96E-06	5.434427
150	Grap	4.186732	5.58E-08	1E-05	5.431729
151	Hspg2	3.081365	5.75E-08	1.03E-05	5.426332
152	Amotl1	3.464702	6.15E-08	1.09E-05	5.414461
153	Zscan26	2.996847	6.63E-08	1.17E-05	5.400971
154	Arglu1	1.301959	7.21E-08	1.25E-05	5.385862
155	Kank3	3.516739	7.23E-08	1.25E-05	5.385322
156	Cdc42ep1	3.636268	7.23E-08	1.25E-05	5.385322
157	Slc7a7	4.730946	7.63E-08	1.31E-05	5.375609
158	Selenop	3.607648	9.02E-08	1.54E-05	5.345391
159	Anxa2	3.86781	9.24E-08	1.57E-05	5.341074
160	Ctsl	2.32974	9.72E-08	1.63E-05	5.331901
161	Pxdn	3.513141	1.02E-07	1.7E-05	5.323806
162	Cd38	3.91115	1.15E-07	1.91E-05	5.300603
163	Swap70	3.71958	1.17E-07	1.93E-05	5.297905
164	Adipor1	3.221794	1.19E-07	1.94E-05	5.295746
165	Lrrc8d	2.279637	1.22E-07	1.99E-05	5.29089
166	Ppp1r16b	3.835269	1.25E-07	2.02E-05	5.286573
167	Flt1	3.512752	1.26E-07	2.03E-05	5.284955
168	Rhoj	3.722475	1.35E-07	2.17E-05	5.272004
169	Tmem88	3.804763	1.39E-07	2.22E-05	5.266608
170	Lrrc58	2.800148	1.47E-07	2.34E-05	5.255816
171	Mbnl2	3.060274	1.57E-07	2.47E-05	5.243944
172	Gng5	0.587561	1.63E-07	2.53E-05	5.237469
173	Ctnnb1	2.468498	1.64E-07	2.53E-05	5.236389
174	Ednrb	4.106769	1.87E-07	2.84E-05	5.212107
175	Stt3b	3.322567	1.92E-07	2.9E-05	5.20725
176	Map1b	3.651391	2.05E-07	3.09E-05	5.194839
177	Plekhg1	3.921551	2.2E-07	3.29E-05	5.181889
178	Irf2	3.328245	2.31E-07	3.44E-05	5.172715
179	Fli1	2.700447	2.35E-07	3.48E-05	5.169477
180	Myh9	2.271167	2.42E-07	3.55E-05	5.164082
181	Tnfaip8l1	3.834673	2.42E-07	3.55E-05	5.164082
182	Myh10	3.263031	2.49E-07	3.64E-05	5.158685
183	Plvap	3.48537	2.54E-07	3.7E-05	5.154368
184	Knop1	1.971349	2.6E-07	3.77E-05	5.150052
185	Nrp1	3.51999	2.89E-07	4.12E-05	5.130625
186	Ktn1	2.332281	2.9E-07	4.12E-05	5.129546
187	Dad1	0.78797	3.2E-07	4.52E-05	5.111199
188	Tfpi	3.436445	3.48E-07	4.87E-05	5.095551
189	Rab11a	1.725913	4.14E-07	5.73E-05	5.062634
190	Ralb	2.704907	4.28E-07	5.87E-05	5.056159
191	Myo10	2.935202	4.53E-07	6.16E-05	5.045367

192	Itgb1	2.68347	4.57E-07	6.18E-05	5.043748
193	B2m	2.138925	4.71E-07	6.34E-05	5.037812
194	Tacc1	2.359687	4.72E-07	6.34E-05	5.037272
195	Eng	3.131171	5.09E-07	6.75E-05	5.022703
196	Tagln2	3.030211	5.09E-07	6.75E-05	5.022703
197	Snrk	3.40088	5.15E-07	6.79E-05	5.020545
198	Sema6d	3.683301	5.18E-07	6.8E-05	5.019465
199	Ppp1r2-ps1	1.863037	5.24E-07	6.85E-05	5.017307

Cluster 4

	names	logfoldchange	pvals	pvals_adj	scores
0	Lsp1	13.80933	5.62E-25	6.32E-21	10.32181
1	Fcer1g	14.08376	6.08E-25	6.32E-21	10.3141
2	Tyrobp	14.49745	6.42E-25	6.32E-21	10.30896
3	Evi2a	13.55934	8.95E-24	6.61E-20	10.05252
4	Arhgdib	6.918084	7.59E-23	4.48E-19	9.839787
5	Cd52	13.8936	1.31E-22	5.23E-19	9.784514
6	Spi1	12.55221	1.4E-22	5.23E-19	9.778088
7	Coro1a	12.42553	1.42E-22	5.23E-19	9.776802
8	Cd53	11.97133	3.56E-22	1.08E-18	9.682967
9	Laptm5	10.24008	3.94E-22	1.08E-18	9.672684
10	B2m	3.873299	4.11E-21	1.01E-17	9.429742
11	Tnni2	10.97398	4.97E-21	1.13E-17	9.409819
12	Rac2	13.48525	2.2E-20	4.32E-17	9.252356
13	Lst1	9.81341	5.32E-20	9.83E-17	9.157236
14	Ly6e	7.739422	6.92E-20	1.2E-16	9.128957
15	Ighm	15.0052	2.33E-19	3.64E-16	8.99656
16	Bcl2a1d	13.61992	2.34E-19	3.64E-16	8.995917
17	Bcl2a1a	10.51829	3.23E-19	4.77E-16	8.960568
18	Plek	8.792763	1.32E-18	1.86E-15	8.803749
19	Tmsb4x	3.185782	3.33E-18	4.47E-15	8.699632
20	Gpx1	2.519093	5.41E-18	6.95E-15	8.644359
21	Alox5ap	7.466636	6.51E-18	8.01E-15	8.62315
22	Ptpn6	8.429561	1.94E-17	2.21E-14	8.49718
23	Ccl6	12.55978	2.94E-17	3.21E-14	8.448977
24	Ptpn18	4.736277	3.21E-17	3.38E-14	8.438694
25	Mir142hg	5.647246	3.37E-17	3.43E-14	8.432909
26	Bcl2a1b	10.24218	3.68E-17	3.62E-14	8.422626
27	Ptprc	11.26477	4.11E-17	3.91E-14	8.409772
28	Fyb	8.804829	6.12E-17	5.65E-14	8.362855
29	Cst3	2.289222	8.86E-17	7.93E-14	8.319151
30	Cyba	4.970956	1.13E-16	9.82E-14	8.290229
31	Arpc2	2.247546	2.57E-16	2.17E-13	8.191895
32	Rgs2	7.072653	5.53E-16	4.53E-13	8.099346
33	Hpgds	10.38306	7.19E-16	5.59E-13	8.067211
34	Ucp2	6.023404	7.66E-16	5.71E-13	8.059499
35	Serp1	4.924018	7.74E-16	5.71E-13	8.058213

36	Capg	7.936195	1.54E-15	1.11E-12	7.974019
37	Arpc5	3.005522	2.12E-15	1.49E-12	7.934172
38	Stap1	11.64463	2.51E-15	1.73E-12	7.912962
39	Lcp1	6.546503	3.46E-15	2.32E-12	7.873115
40	Ctsc	8.412772	5.43E-15	3.56E-12	7.816557
41	Ccl9	11.58628	2.32E-14	1.46E-11	7.631458
42	Prdx5	3.179298	2.46E-14	1.52E-11	7.623746
43	Fth1	1.782019	3.35E-14	2.02E-11	7.583899
44	Lpl	9.822574	4.01E-14	2.37E-11	7.560761
45	Emb	6.702011	5.33E-14	3.09E-11	7.523484
46	Psme2	2.218659	6.33E-14	3.6E-11	7.500989
47	Acsl5	6.503191	7.19E-14	4.01E-11	7.484279
48	Gsn	7.53992	8.54E-14	4.67E-11	7.461785
49	Clec12a	11.61346	1.5E-13	7.8E-11	7.387231
50	Ccl3	12.29175	1.51E-13	7.8E-11	7.386589
51	Actr2	1.60267	2.12E-13	1.08E-10	7.340957
52	Sec11c	4.992465	3.26E-13	1.63E-10	7.283113
53	Psme2b	2.005597	4.46E-13	2.2E-10	7.240695
54	Cap1	3.615906	5.76E-13	2.79E-10	7.205989
55	Dok2	8.214165	8.67E-13	4.13E-10	7.150074
56	Lilr4b	8.182674	8.92E-13	4.18E-10	7.146217
57	Mef2c	4.895789	1.1E-12	5.08E-10	7.117296
58	Celf2	5.915879	1.82E-12	8.04E-10	7.047241
59	Sirpa	7.061237	3.96E-12	1.69E-09	6.938624
60	Bin2	8.230127	5.15E-12	2.17E-09	6.901348
61	Ikzf1	7.215935	6.75E-12	2.77E-09	6.862785
62	Apbb1ip	8.783782	9.12E-12	3.69E-09	6.819724
63	Actb	1.030773	9.33E-12	3.72E-09	6.816511
64	Capza2	2.269841	9.58E-12	3.77E-09	6.812654
65	Csf1r	8.882781	1.25E-11	4.78E-09	6.774735
66	Mbnl1	4.694059	1.51E-11	5.64E-09	6.747099
67	Ncf4	7.064679	1.72E-11	6.36E-09	6.727818
68	Tpd52	5.402418	1.83E-11	6.68E-09	6.71882
69	Ciao2a	2.36814	2.51E-11	9.05E-09	6.672545
70	Cyrib	5.488307	2.65E-11	9.43E-09	6.664833
71	Psmb8	34.39128	3.6E-11	1.26E-08	6.619843
72	Dhrs3	5.941807	3.85E-11	1.34E-08	6.60956
73	Ctss	10.19721	5.36E-11	1.84E-08	6.560715
74	Erp29	3.446363	6.15E-11	2.09E-08	6.540148
75	Fam111a	4.896384	6.61E-11	2.22E-08	6.529222
76	Emp3	4.849949	7.75E-11	2.54E-08	6.505442
77	Rnase4	6.739183	1.02E-10	3.27E-08	6.464309
78	Ckb	5.68573	1.16E-10	3.69E-08	6.444386
79	Ctsz	4.552032	2E-10	6.21E-08	6.361477
80	Ncf1	34.08974	2.08E-10	6.41E-08	6.35505
81	Llph	2.490125	2.12E-10	6.45E-08	6.352479
82	Asb2	10.3256	2.43E-10	7.33E-08	6.33127
83	Fcgr2b	9.303332	2.93E-10	8.66E-08	6.302348

84	Ptgs1	7.363107	2.93E-10	8.66E-08	6.302348
85	Cx3cr1	9.896749	3.07E-10	8.97E-08	6.295279
86	Irf8	8.630388	3.29E-10	9.53E-08	6.284352
87	Atp6v0b	2.864743	3.4E-10	9.75E-08	6.279211
88	Irf5	8.587453	4.01E-10	1.13E-07	6.253503
89	Sh3bgrl3	1.398205	5.71E-10	1.58E-07	6.19823
90	Rhog	4.560328	7.65E-10	2.07E-07	6.151956
91	Man2b1	5.115319	1.1E-09	2.95E-07	6.094112
92	P2ry12	11.20249	1.23E-09	3.28E-07	6.076117
93	C1qb	10.62799	1.63E-09	4.29E-07	6.031127
94	H2aj	1.585889	2.38E-09	6.22E-07	5.969428
95	Samhd1	5.425933	2.54E-09	6.57E-07	5.959145
96	H2-D1	5.339693	2.81E-09	7.09E-07	5.942434
97	C3ar1	8.433228	3.18E-09	7.96E-07	5.921868
98	Rogdi	4.532241	3.93E-09	9.74E-07	5.887162
99	Gusb	4.926589	3.96E-09	9.74E-07	5.885876
100	Stk17b	5.867164	4.18E-09	1.02E-06	5.876879
101	Pfn1	0.728474	4.59E-09	1.11E-06	5.861454
102	Il2rg	4.972836	5.63E-09	1.35E-06	5.82739
103	Lamp1	3.754613	5.67E-09	1.35E-06	5.826105
104	Gpsm3	4.801373	6.01E-09	1.42E-06	5.816464
105	Tln1	3.092217	6.85E-09	1.59E-06	5.794612
106	Nrros	5.549898	7.56E-09	1.72E-06	5.777902
107	Gm12892	3.12021	7.74E-09	1.74E-06	5.774046
108	Ncf2	6.829441	8.42E-09	1.87E-06	5.759907
109	Apobec1	8.503153	8.91E-09	1.96E-06	5.750266
110	Arhgap30	8.18575	9.19E-09	2.01E-06	5.745124
111	Ccl4	9.304512	9.54E-09	2.07E-06	5.738698
112	Fcgr3	8.677873	9.76E-09	2.1E-06	5.734841
113	Cyth4	8.256073	9.87E-09	2.11E-06	5.732913
114	Fmnl1	7.798286	1.03E-08	2.18E-06	5.726486
115	Gpr183	4.954983	1.06E-08	2.23E-06	5.721344
116	Vav1	8.104755	1.08E-08	2.24E-06	5.718131
117	Efhd2	6.237694	1.09E-08	2.25E-06	5.716203
118	Stxbp2	3.957082	1.17E-08	2.41E-06	5.703349
119	Rgs18	7.977381	1.42E-08	2.85E-06	5.671214
120	Fermt3	4.848005	1.55E-08	3.09E-06	5.655788
121	Hacd2	3.570426	2.32E-08	4.5E-06	5.586377
122	Cenpx	1.686198	2.41E-08	4.61E-06	5.57995
123	Arrb2	3.657901	2.42E-08	4.62E-06	5.578664
124	Maf	4.727334	2.48E-08	4.66E-06	5.574808
125	Nop10	0.956026	2.48E-08	4.66E-06	5.574808
126	Lyn	4.355632	2.59E-08	4.84E-06	5.567096
127	Inpp5d	4.593271	3.55E-08	6.47E-06	5.511823
128	Cd68	6.747009	4.02E-08	7.24E-06	5.489971
129	Psme1	2.334383	4.26E-08	7.62E-06	5.479688
130	Ndufv3	1.024517	4.78E-08	8.46E-06	5.459121
131	Tspo	4.665426	5.03E-08	8.85E-06	5.450124

132	Ccnd2	3.953094	5.31E-08	9.28E-06	5.440483
133	Unc93b1	7.429646	5.65E-08	9.81E-06	5.429557
134	Rnf141	4.094489	5.69E-08	9.83E-06	5.428272
135	Ntpcr	4.222203	5.73E-08	9.84E-06	5.426986
136	Gm15590	1.54354	6.96E-08	1.17E-05	5.39228
137	Fxyd5	4.372732	7.42E-08	1.24E-05	5.380712
138	Limd2	3.18923	7.53E-08	1.26E-05	5.378141
139	Zc3hav1	4.052634	9.52E-08	1.57E-05	5.335722
140	Atp6v0e	1.696939	1.05E-07	1.72E-05	5.317727
141	Gm13237	1.682025	1.07E-07	1.75E-05	5.31387
142	Arpc1b	3.967141	1.11E-07	1.8E-05	5.307444
143	Pla2g4a	7.070737	1.16E-07	1.86E-05	5.299731
144	Sting1	5.872526	1.24E-07	1.96E-05	5.288162
145	Lamtor1	3.138932	1.24E-07	1.96E-05	5.288162
146	Cd47	3.449714	1.28E-07	2.02E-05	5.281735
147	Cox6a1	0.588654	1.33E-07	2.07E-05	5.275308
148	Snx2	2.480245	1.39E-07	2.15E-05	5.266311
149	Tubb2a	4.446862	1.44E-07	2.21E-05	5.260526
150	Tomm5	1.821605	1.46E-07	2.24E-05	5.257313
151	Bid	4.766768	1.63E-07	2.46E-05	5.236746
152	Ccr2	9.083226	1.7E-07	2.55E-05	5.229033
153	Snx5	3.196796	1.72E-07	2.56E-05	5.227106
154	Aim2	4.904615	1.99E-07	2.93E-05	5.200112
155	Ftl1-ps2	1.02286	2.01E-07	2.94E-05	5.198184
156	Dgkd	3.616871	2.04E-07	2.97E-05	5.195613
157	Clta	1.373987	2.29E-07	3.31E-05	5.174404
158	Tmem176a	4.186665	2.56E-07	3.67E-05	5.153195
159	Llph-ps2	1.755279	2.74E-07	3.91E-05	5.140341
160	Vamp8	2.212757	2.85E-07	4.04E-05	5.133271
161	Sat1	4.31267	2.88E-07	4.04E-05	5.131343
162	Lyz2	7.636794	2.96E-07	4.12E-05	5.126201
163	AI413582	3.734244	3.04E-07	4.21E-05	5.121059
164	Mtdh	3.018123	3.58E-07	4.91E-05	5.09021
165	Gm14414	0.87599	3.63E-07	4.93E-05	5.087639
166	Rps25	0.495633	3.73E-07	5.05E-05	5.082497
167	Rps8-ps5	0.872672	4.41E-07	5.92E-05	5.050362
168	Hexb	4.151143	4.59E-07	6.13E-05	5.04265
169	Ly86	33.93171	4.88E-07	6.46E-05	5.031081
170	Ncoa3	3.416151	4.94E-07	6.52E-05	5.02851
171	Aup1	3.278739	5.11E-07	6.71E-05	5.022083
172	Slc25a5	1.388657	5.23E-07	6.81E-05	5.017584
173	Tmem176b	3.928689	5.92E-07	7.53E-05	4.993804
174	Tubb6	3.90028	5.96E-07	7.54E-05	4.992519
175	Dock8	5.315291	5.98E-07	7.54E-05	4.991876
176	Cd200r1	6.38553	6.45E-07	8.08E-05	4.977094
177	Ssr4	2.262955	6.63E-07	8.26E-05	4.971952
178	Rgs19	3.890948	6.9E-07	8.56E-05	4.96424
179	C1qc	8.623336	6.99E-07	8.6E-05	4.961669

180	Lcp2	4.977981	7.39E-07	9.02E-05	4.950743
181	Ctsb	2.955204	7.64E-07	9.28E-05	4.944316
182	Plcg2	4.554075	8.35E-07	0.000101	4.926963
183	Ccdc107	3.417867	8.63E-07	0.000104	4.920536
184	Pnp2	2.120869	9.19E-07	0.00011	4.908325
185	Fam174a	4.246845	9.28E-07	0.000111	4.906397
186	Psmg4	2.242455	9.78E-07	0.000116	4.896113
187	Skap2	3.645547	1.04E-06	0.000122	4.883259
188	Uchl5	2.555083	1.08E-06	0.000126	4.87619
189	Bcap29	3.710515	1.21E-06	0.00014	4.853695
190	Pnp	2.712692	1.26E-06	0.000145	4.846625
191	Fam107b	3.768439	1.28E-06	0.000147	4.843412
192	Rbfa	3.530923	1.32E-06	0.00015	4.836985
193	Atp5g1	0.671416	1.43E-06	0.000161	4.820917
194	Abhd12	4.426269	1.57E-06	0.000176	4.801636
195	Cox8a	0.578066	1.85E-06	0.000205	4.768858
196	Aif1	33.32258	1.88E-06	0.000207	4.766287
197	Pclaf	3.768788	2.04E-06	0.000224	4.748934
198	Sdf2l1	3.778544	2.13E-06	0.000232	4.740579
199	BC035044	9.545719	2.16E-06	0.000234	4.738008

Cluster 5

	names	**logfoldchange**	**pvals**	**pvals_adj**	**scores**
0	Tuba1a	3.112799	3.83E-16	1.13E-11	8.143744
1	Pantr1	10.13978	5.03E-15	6.45E-11	7.82623
2	Hoxb5os	8.886349	6.55E-15	6.45E-11	7.792884
3	Msi1	4.891134	2.57E-13	1.82E-09	7.315162
4	Crabp2	8.661035	6.56E-13	3.23E-09	7.188301
5	H2az2	1.933524	2.48E-12	1.05E-08	7.004171
6	Phyhipl	11.07128	2.55E-11	9.4E-08	6.670709
7	Gm3226	1.768046	3.89E-11	1.27E-07	6.608366
8	Slc7a11	2.81474	6.39E-11	1.89E-07	6.534424
9	Id2	6.803831	1.63E-10	4.36E-07	6.393064
10	Bex2	4.683426	2.35E-10	5.78E-07	6.336521
11	Fzd3	6.09263	7.67E-10	1.57E-06	6.151666
12	Ckb	6.238082	9.46E-10	1.75E-06	6.11832
13	Sox11	5.484923	1.05E-09	1.82E-06	6.102372
14	Gm1673	3.698407	1.67E-09	2.74E-06	6.02698
15	Ldhb	5.788892	2.84E-09	4.08E-06	5.940715
16	Hoxc9	7.445294	4.2E-09	5.16E-06	5.876197
17	Cdk4	1.241812	1.12E-08	1.11E-05	5.710915
18	Fez1	9.189658	1.16E-08	1.11E-05	5.705116
19	Hmgn1	1.369059	1.21E-08	1.12E-05	5.697866
20	Cd24a	5.091159	2.08E-08	1.76E-05	5.605077
21	Sumo2	0.811765	3.29E-08	2.62E-05	5.525336
22	Fabp7	8.463347	4.82E-08	3.51E-05	5.457918
23	Map1b	4.719631	4.88E-08	3.51E-05	5.455744

24	Fkbp3	1.116893	6.17E-08	4.14E-05	5.413698
25	C130071C03Ri	8.204184	6.38E-08	4.18E-05	5.407899
26	Ywhae	0.805137	8.32E-08	5.34E-05	5.360054
27	Tspan3	3.002568	1.23E-07	7.66E-05	5.289012
28	Pdpn	5.950022	1.24E-07	7.66E-05	5.286837
29	Vta1	2.762578	1.7E-07	9.84E-05	5.229568
30	Ptges3	1.332013	2.2E-07	0.000121	5.181724
31	Gm10282	1.124007	2.49E-07	0.000124	5.158526
32	Hmgn2	1.049162	3.26E-07	0.000155	5.107782
33	Set	1.533406	3.71E-07	0.000169	5.083135
34	Lgr4	4.406689	4.26E-07	0.00019	5.057038
35	Hoxb7	6.765952	5.87E-07	0.000255	4.99542
36	Dpysl2	3.05415	7.03E-07	0.000301	4.960624
37	Ranbp1	1.093404	8.06E-07	0.000335	4.933802
38	Jpt1	1.583887	8.88E-07	0.000359	4.914954
39	Ccdc85c	3.050987	1.18E-06	0.000455	4.859135
40	Gm10241	1.668656	1.18E-06	0.000455	4.859135
41	Tagln3	6.85298	1.19E-06	0.000455	4.85696
42	Pafah1b3	2.499304	1.21E-06	0.000455	4.854061
43	Gm14150	1.42858	1.26E-06	0.000455	4.845361
44	Ppp1r1a	6.153374	1.27E-06	0.000455	4.844636
45	Uchl1	4.527705	1.43E-06	0.000491	4.820714
46	Nutf2	1.133701	1.52E-06	0.000509	4.809115
47	Gm20075	2.612427	1.79E-06	0.000587	4.775769
48	Hmgb3	2.633063	1.88E-06	0.000611	4.76562
49	Gm6724	1.321851	1.91E-06	0.000611	4.762721
50	Kif21a	5.641863	2.21E-06	0.00069	4.732999
51	Gm12892	3.132959	2.22E-06	0.00069	4.732274
52	Cnn3	2.605013	2.58E-06	0.000774	4.701828
53	Skp1	0.785171	2.67E-06	0.000789	4.694578
54	Btf3l4	1.467165	3.47E-06	0.000964	4.640934
55	Tsen34	3.367158	4.31E-06	0.001146	4.595989
56	Fkbp4	2.818443	4.65E-06	0.001202	4.580041
57	Rcn2	3.355799	4.75E-06	0.001208	4.575691
58	Gm10182	1.349289	5.17E-06	0.001295	4.557569
59	Mir219a-2	6.931077	6.34E-06	0.001519	4.514798
60	Cops4	1.676813	6.6E-06	0.00156	4.506099
61	Tecr	1.197432	6.93E-06	0.00161	4.49595
62	Dctpp1	1.978812	7.21E-06	0.001651	4.487251
63	Slitrk2	7.477974	7.34E-06	0.001667	4.483627
64	Ube2n	0.648928	7.46E-06	0.001682	4.480002
65	Erh	0.547138	7.83E-06	0.001751	4.469853
66	Ccnd1	4.030972	9.33E-06	0.002025	4.432158
67	Ldhb-ps	2.450915	1.05E-05	0.00222	4.40606
68	Oaz1	0.738931	1.07E-05	0.002234	4.403161
69	Marcksl1	2.109691	1.08E-05	0.002248	4.400261
70	Nutf2-ps1	1.538426	1.1E-05	0.002262	4.397361
71	Ptn	4.951902	1.37E-05	0.002703	4.348067

72	Ywhaq	0.602704	1.43E-05	0.002794	4.339368
73	Selenoh	1.314815	1.62E-05	0.003156	4.311096
74	Idh1	3.03348	1.65E-05	0.003166	4.307471
75	Scoc	2.7946	1.74E-05	0.003315	4.295873
76	Hmgn2-ps1	1.454566	2.62E-05	0.004798	4.204533
77	Tppp3	5.819443	2.63E-05	0.004799	4.203083
78	Pebp1	1.121829	2.67E-05	0.004802	4.200183
79	Gm7931	1.494589	2.67E-05	0.004802	4.200183
80	Nabp2	2.615809	2.71E-05	0.00482	4.196558
81	Rfc4	2.864002	3.01E-05	0.005199	4.172636
82	Vps72	2.249205	3.09E-05	0.005302	4.166837
83	Ank2	5.323596	3.66E-05	0.006044	4.127691
84	Stmn1	1.152107	3.71E-05	0.006087	4.124792
85	H2bu2	4.621233	3.78E-05	0.006135	4.120442
86	H2az1	1.078267	3.78E-05	0.006135	4.120442
87	Srsf3	1.195112	3.81E-05	0.00614	4.118992
88	Hnrnpa1	0.861346	3.9E-05	0.006161	4.113193
89	Ube2i	0.759415	4.21E-05	0.006573	4.095795
90	Hoxa7	6.206512	4.34E-05	0.00671	4.088545
91	Ilf2	2.164034	4.74E-05	0.007209	4.068248
92	Scd2	2.489131	4.98E-05	0.007461	4.056649
93	Gmps	2.47006	5.18E-05	0.007729	4.047225
94	Atxn7l3b	2.454643	5.25E-05	0.007742	4.044325
95	Taf13	2.943539	5.3E-05	0.007742	4.04215
96	Mettl9	3.171354	5.3E-05	0.007742	4.04215
97	Id3	3.040217	5.38E-05	0.007809	4.038526
98	Epha3	6.006306	5.4E-05	0.007809	4.037801
99	Rnd3	3.888723	5.53E-05	0.007951	4.032002
100	Bex1	2.620454	5.55E-05	0.007951	4.031277
101	Ift43	3.157686	5.63E-05	0.008036	4.027652
102	Sf3b4	1.82462	5.67E-05	0.008047	4.026203
103	Sumo1	0.687299	5.74E-05	0.008069	4.023303
104	Sdhb	0.968591	6.18E-05	0.008563	4.005905
105	Zfp422	3.327343	6.39E-05	0.008694	3.997931
106	Mllt11	3.785148	6.57E-05	0.008896	3.991406
107	Map2	5.636636	6.77E-05	0.009089	3.984157
108	Nudt21	2.283218	6.9E-05	0.009215	3.979808
109	1500011B03Rik	2.426278	7.51E-05	0.009785	3.95951
110	Dpysl3	4.570975	8.17E-05	0.010359	3.939212
111	Tmem126a	2.211728	8.32E-05	0.010459	3.934863
112	Calm3	1.495602	8.32E-05	0.010459	3.934863
113	Gm12669	1.101153	8.53E-05	0.010624	3.929063
114	Id1	3.933952	9.19E-05	0.011358	3.91094
115	Nudt2	2.61042	9.67E-05	0.011853	3.898617
116	Snrnp40	2.246668	9.73E-05	0.011874	3.897167
117	Acat2	2.085474	9.79E-05	0.011897	3.895717
118	Ptges3-ps	2.13676	9.85E-05	0.011919	3.894267
119	Elob	0.455172	0.000101	0.01223	3.887018

120	Dek	2.24342	0.000105	0.012472	3.878319
121	Hnrnpk	0.699594	0.000105	0.012472	3.878319
122	Gm11223	1.047617	0.000126	0.014751	3.833374
123	Sf3b6	1.584017	0.000136	0.015555	3.814526
124	Ift27	2.788405	0.000143	0.016239	3.802927
125	Psip1	2.869688	0.000152	0.017085	3.788429
126	1110004F10Rik	1.184555	0.000156	0.017406	3.781905
127	Itpa-ps1	1.68916	0.000161	0.017874	3.773206
128	Ak6	2.1894	0.000161	0.017874	3.773206
129	Gm12346	1.120776	0.000179	0.01949	3.747108
130	Nme1	0.738486	0.000183	0.01964	3.741309
131	Cadm1	3.778311	0.000185	0.01974	3.73841
132	Crabp1	4.391505	0.000187	0.019897	3.73551
133	Pax6	5.755103	0.000188	0.01994	3.73406
134	Bex3	0.991627	0.000191	0.020157	3.730435
135	Srgap3	5.826255	0.000201	0.021076	3.717387
136	Gcat	2.786188	0.000202	0.021122	3.715937
137	Elavl4	6.16518	0.000208	0.02157	3.709413
138	Macroh2a1	1.715354	0.000227	0.023174	3.68694
139	Dcakd	1.990415	0.000228	0.023174	3.686215
140	Ppa1	2.435441	0.00024	0.02421	3.672442
141	Cox14	1.612533	0.000256	0.025678	3.656494
142	Snrpb	0.735868	0.000261	0.026014	3.651419
143	Tubb5	0.935295	0.000271	0.026805	3.641995
144	Gm6104	1.880049	0.00028	0.027632	3.633296
145	Mcm7	2.75866	0.000297	0.029018	3.618073
146	Psmc4	1.187384	0.000298	0.02907	3.616623
147	Tfam	2.994359	0.000299	0.02907	3.615898
148	Oaz1-ps	0.989103	0.000301	0.029138	3.614448
149	Fabp5	2.322074	0.000307	0.02952	3.609374
150	Igfbp2	3.540987	0.000307	0.02952	3.609374
151	Hoxc8	7.158695	0.000317	0.030243	3.6014
152	Csrnp3	5.076364	0.000341	0.032262	3.581827
153	Pcbp4	3.214658	0.000342	0.032262	3.581102
154	1500004A13Rik	5.42136	0.000343	0.032262	3.580377
155	Gm3375	1.0207	0.000366	0.033611	3.563704
156	Mir124-2hg	6.862181	0.000382	0.034719	3.552105
157	Dtx4	3.97198	0.000406	0.036636	3.536157
158	Zcrb1	1.738237	0.000421	0.037406	3.526733
159	Zfp24	3.249394	0.000422	0.037406	3.526008
160	Ndufa12	0.547881	0.000434	0.038214	3.518759
161	Psmb6	0.43707	0.000436	0.038309	3.517309
162	Gm7964	0.87799	0.000489	0.042566	3.486862
163	Slc25a5	1.144203	0.000526	0.045522	3.46729
164	Gsk3b	1.352764	0.000553	0.047493	3.453516
165	Selenof	1.224124	0.000581	0.049555	3.440468
166	Cct7	1.287962	0.000589	0.049925	3.436843
167	Tceal8	1.179106	0.000633	0.053208	3.41727

168	1110051M20Ri	3.367679	0.000641	0.053767	3.413646
169	Oard1	2.171944	0.00066	0.05505	3.405671
170	Psmb7	0.906746	0.000678	0.05637	3.398422
171	Rbmx2	2.563536	0.000705	0.058324	3.387548
172	Psmb5	0.957034	0.000726	0.059875	3.379574
173	Snrpd1	0.957582	0.000753	0.060933	3.369426
174	Tmem128	2.21946	0.000759	0.061248	3.367251
175	Cox7a2	0.468113	0.000773	0.062045	3.362176
176	Psma2	0.584899	0.000781	0.06253	3.359277
177	Lsm1	2.185152	0.00079	0.06268	3.356377
178	Nmral1	2.959794	0.000819	0.064672	3.346228
179	Mdh1	0.853569	0.00083	0.065171	3.342603
180	Gm6166	1.56356	0.000836	0.065336	3.340429
181	Mcrip1	1.680632	0.000886	0.06829	3.324481
182	Mrpl28	1.300804	0.000904	0.069362	3.318681
183	Atxn10	1.473084	0.000912	0.069723	3.316506
184	Park7	1.040769	0.000933	0.070818	3.309982
185	Tra2b	1.143027	0.000967	0.072682	3.299833
186	Gm3756	1.207509	0.000993	0.074205	3.292584
187	H3f3a	0.427654	0.001034	0.076742	3.280985
188	Cuedc2	1.932782	0.001037	0.076746	3.28026
189	Ttc3	1.901844	0.001045	0.077147	3.278086
190	Taldo1	1.802166	0.001061	0.077954	3.273736
191	Morf4l1	0.699144	0.0011	0.080218	3.263587
192	Pfn2	3.662939	0.001117	0.080843	3.259238
193	Tsn	1.073667	0.001149	0.08274	3.251264
194	Gm2423	0.938987	0.001158	0.08297	3.249089
195	Gins4	2.092812	0.001173	0.083628	3.245464
196	Hnrnph3	2.599179	0.001182	0.083864	3.243289
197	Bud31	1.070665	0.001197	0.084531	3.239665
198	Tubb3	6.54004	0.001218	0.085434	3.234591
199	Snrpe	0.392105	0.001243	0.086569	3.228791

Cluster 6

	names	logfoldchange	pvals	pvals_adj	scores
0	Krt18	13.62258	1.2E-14	3.55E-10	7.715961
1	Bex1	6.425617	4.08E-13	6.02E-09	7.253004
2	Bex4	6.780579	7.01E-13	6.9E-09	7.179274
3	Spint2	7.143277	2.98E-12	2.09E-08	6.978658
4	Krt8	12.61284	3.53E-12	2.09E-08	6.954653
5	Gm4322	4.785615	3.19E-11	1.57E-07	6.637442
6	Cldn6	12.3842	4.68E-11	1.74E-07	6.580858
7	Epcam	11.12765	4.7E-11	1.74E-07	6.58
8	Tceal9	2.110339	2.26E-10	6.98E-07	6.34252
9	Mdk	4.010919	2.36E-10	6.98E-07	6.335661
10	Gpc3	7.614751	4.06E-10	1.09E-06	6.251643
11	Emb	8.197596	8.07E-10	1.98E-06	6.14362

12	Cd24a	6.064405	4.56E-09	1.04E-05	5.862416
13	Cldn7	8.937833	7.43E-09	1.57E-05	5.78097
14	Slc2a3	7.456512	8.87E-09	1.75E-05	5.750963
15	Bex2	4.681201	1.87E-08	3.44E-05	5.624078
16	Gm12245	4.663246	3.04E-08	4.98E-05	5.539203
17	Bsg	1.792501	1.65E-07	0.000257	5.234851
18	Slc16a1	7.415864	2.39E-07	0.000336	5.166265
19	Fn1	5.058377	3.44E-07	0.000461	5.097679
20	Igfbp2	5.402403	1.27E-06	0.001504	4.843909
21	Tpm1	3.315536	1.83E-06	0.001924	4.771894
22	Cpm	7.515709	4.36E-06	0.00415	4.593569
23	Ptprf	5.184138	4.81E-06	0.004436	4.572993
24	Bex3	1.309531	5.22E-06	0.004531	4.555847
25	Ifitm1	6.03811	5.8E-06	0.004757	4.533556
26	Peg3	4.802827	7.51E-06	0.005836	4.478687
27	Stard10	6.190578	7.88E-06	0.005966	4.468399
28	Spink1	12.4489	1.04E-05	0.0075	4.408386
29	Pcbd1	5.103175	1.11E-05	0.007632	4.394669
30	Abhd2	2.473706	1.14E-05	0.007632	4.389524
31	Rbp4	12.02915	1.16E-05	0.007632	4.385238
32	Krt7	8.887983	1.31E-05	0.008433	4.357803
33	Ndufs6	1.198032	3.46E-05	0.018916	4.140899
34	Rdx	2.665482	3.56E-05	0.019135	4.134041
35	Cystm1	6.139397	4.74E-05	0.024584	4.068026
36	Gprc5c	3.425399	4.76E-05	0.024584	4.067169
37	Prtg	5.040532	4.83E-05	0.024584	4.06374
38	9030622O22Ri	33.29642	5.01E-05	0.025071	4.055166
39	Apoa1	11.93852	5.59E-05	0.027512	4.029447
40	Gm3511	1.070658	6.24E-05	0.029222	4.003726
41	Cadm1	4.982379	6.8E-05	0.030626	3.983151
42	Apela	7.887582	6.95E-05	0.030626	3.978007
43	Mapk13	7.756365	7.69E-05	0.033371	3.954001
44	Grb10	3.42835	8.83E-05	0.036738	3.920566
45	Ndufa7	0.578877	9.38E-05	0.037709	3.905991
46	Arxes2	3.728087	0.000125	0.048013	3.83569
47	Gpx3	4.369236	0.000156	0.05543	3.780821
48	Mreg	5.403128	0.000157	0.05543	3.779106
49	Sinhcaf	3.269458	0.000179	0.06085	3.746528
50	Cdkn1a	3.888386	0.000182	0.060986	3.743098
51	Fgfr2	6.0034	0.0002	0.064167	3.719093
52	Kif21a	4.658435	0.000203	0.064563	3.714807
53	Fat1	4.831544	0.000244	0.074511	3.668511
54	Cdh1	9.899414	0.000245	0.074511	3.667654
55	Cpn1	8.232468	0.000269	0.079106	3.643648
56	Tspan7	4.259104	0.000271	0.079106	3.641934
57	Gm47283	1.582605	0.000309	0.086889	3.607641
58	Lsr	7.16386	0.000309	0.086889	3.607641
59	Gja1	3.488226	0.000328	0.090478	3.592209

60	Gm4204	1.338384	0.000362	0.098004	3.566489
61	Cd320	3.577122	0.000377	0.101068	3.555344
62	Lrpap1	2.907894	0.00038	0.101068	3.553629
63	Enpp1	6.614944	0.000412	0.107685	3.532196
64	Prxl2a	5.03277	0.000437	0.111191	3.516764
65	Txndc12	2.636366	0.000483	0.119686	3.490186
66	Id2	4.64345	0.000487	0.119686	3.487615
67	Usp34	3.434334	0.00049	0.119686	3.4859
68	Arxes1	2.656027	0.00055	0.132079	3.455036
69	Ifi30	4.688863	0.000579	0.13784	3.441319
70	Fkbp4	1.93326	0.000628	0.147267	3.419028
71	Notch2	2.885748	0.000653	0.150545	3.40874
72	Emid1	5.639513	0.000724	0.164364	3.380448
73	Eola1	3.313193	0.000744	0.167518	3.372732
74	Slc25a17	2.994769	0.000749	0.167518	3.371018
75	Fzr1	4.032135	0.000761	0.168864	3.366731
76	Cd63	1.721018	0.000785	0.17289	3.358158
77	Paip1	2.882768	0.000853	0.182745	3.33501
78	Id1	4.053518	0.000869	0.182745	3.329866
79	Fkbp11	3.29558	0.000913	0.186027	3.316149
80	Tmc4	4.515265	0.000927	0.186027	3.311862
81	Apoe	3.445594	0.000953	0.18878	3.304146
82	Spint1	8.332045	0.001025	0.200427	3.28357
83	Clic6	8.270582	0.001057	0.201278	3.274997
84	Lama5	8.077248	0.001057	0.201278	3.274997
85	Cmtm8	4.958876	0.001136	0.210997	3.254421
86	Acsl4	2.838701	0.001178	0.214717	3.244133
87	Fermt1	6.901757	0.001178	0.214717	3.244133
88	AC168314.1	3.038761	0.001214	0.217891	3.23556
89	Pdcd4	2.098536	0.001232	0.217891	3.231273
90	Tmem254a	3.336244	0.001244	0.218552	3.228701
91	Prdx4	1.270949	0.001281	0.222545	3.220128
92	Ginm1	2.87046	0.001289	0.222571	3.218413
93	Afdn	2.751726	0.00141	0.240564	3.192693
94	Cep164	2.773758	0.001474	0.248625	3.179833
95	Vkorc1	1.754516	0.001474	0.248625	3.179833
96	Micos13	0.649325	0.0015	0.250955	3.17469
97	Dzip3	2.957646	0.001531	0.254004	3.168688
98	Acsl3	3.539355	0.001638	0.265811	3.14897
99	Mgst1	3.4388	0.001672	0.269159	3.142968
100	Igfbp5	3.674217	0.001677	0.269159	3.142111
101	Anapc13	0.89655	0.001874	0.294292	3.109532
102	Dbi	0.361272	0.001935	0.302218	3.100102
103	Pfdn1	0.542414	0.002026	0.311571	3.086385
104	Hmga2	2.783693	0.002061	0.313228	3.081241
105	S100a1	4.313678	0.002073	0.313228	3.079526
106	Fnbp1l	2.586606	0.002079	0.313228	3.078669
107	Ptrh2	2.331836	0.002109	0.314555	3.074382

108	Hes1	2.033994	0.002171	0.320478	3.065809
109	Gsta4	2.774821	0.002247	0.326779	3.055521
110	Ndufa13	0.318911	0.002325	0.333243	3.045233
111	Dnase2a	4.099137	0.002426	0.346095	3.032373
112	Ddt	2.106027	0.002532	0.359396	3.019513
113	Gm10076	0.385397	0.00259	0.365859	3.012654
114	Tmed10	1.626941	0.00285	0.395021	2.983505
115	Chchd10	2.467245	0.003081	0.417344	2.9595
116	H2bu2	3.520848	0.003116	0.420086	2.95607
117	Nedd4	1.299322	0.003151	0.421819	2.952641
118	Ttr	33.83985	0.003186	0.421819	2.949212
119	Mllt10	2.667991	0.003186	0.421819	2.949212
120	Tmprss2	33.09555	0.003186	0.421819	2.949212
121	Cks1b	1.550332	0.003423	0.445277	2.926921
122	Atpif1	0.460646	0.003423	0.445277	2.926921
123	Airn	3.652656	0.0035	0.45122	2.920063
124	Hsf2	1.907254	0.003627	0.462122	2.908917
125	Sall4	3.619781	0.003647	0.462122	2.907203
126	Prss12	7.763638	0.003647	0.462122	2.907203
127	Romo1	0.617769	0.004012	0.497756	2.877196
128	C230062I16Rik	0.718654	0.004089	0.503078	2.871195
129	Kmt2a	3.266673	0.004282	0.509871	2.85662
130	Car14	4.284277	0.004282	0.509871	2.85662
131	Cst3	1.290065	0.004305	0.509871	2.854906
132	Amer1	3.298965	0.004387	0.511979	2.848904
133	mt-Nd2	0.993609	0.004495	0.518386	2.841188
134	Hint2	1.718736	0.004495	0.518386	2.841188
135	Strbp	2.909234	0.004543	0.521949	2.837759
136	Frem2	6.090268	0.004568	0.522293	2.836045
137	Gcsh	1.702479	0.004592	0.522293	2.83433
138	Cited1	6.425243	0.004617	0.522293	2.832615
139	Kcnq1ot1	2.695573	0.004679	0.527318	2.828329
140	Hacd2	2.494715	0.004755	0.531795	2.823184
141	Tspan12	3.485066	0.004923	0.542991	2.812039
142	Aff4	3.181144	0.004962	0.542991	2.809467
143	Cdh6	5.778325	0.004989	0.542991	2.807753
144	Pabpc4	2.387775	0.005002	0.542991	2.806895
145	Sipa1l1	3.59275	0.005056	0.546789	2.803466
146	Ubn2	2.8448	0.005192	0.555398	2.794893
147	Rbm47	3.789236	0.005331	0.56113	2.786319
148	Hnrnpa1	0.707192	0.005331	0.56113	2.786319
149	Nap1l1	0.971608	0.005359	0.56113	2.784605
150	Ldhb	3.53642	0.005561	0.571147	2.772602
151	Col2a1	4.243024	0.005739	0.578359	2.762314
152	Tjp2	3.35369	0.005785	0.57898	2.759742
153	Greb1l	3.891699	0.00583	0.581582	2.75717
154	Cspp1	2.541731	0.006176	0.604513	2.738309
155	Rab15	5.010239	0.006224	0.604513	2.735737

156	Yeats2	3.064716	0.006306	0.610426	2.73145
157	Nav2	4.741385	0.006372	0.614793	2.728021
158	Vamp8	1.844157	0.006421	0.616117	2.725449
159	H2az2	0.987854	0.006505	0.616117	2.721162
160	1810058I24Rik	0.371436	0.006539	0.616117	2.719448
161	Serf1	1.507762	0.006539	0.616117	2.719448
162	Tln2	3.333372	0.006573	0.616117	2.717733
163	Ctnnal1	3.726063	0.006573	0.616117	2.717733
164	Spin2c	4.312592	0.006711	0.616608	2.710874
165	Zfp553	3.744532	0.006711	0.616608	2.710874
166	Spry2	2.221474	0.006745	0.616608	2.70916
167	Pgrmc1	1.932115	0.006745	0.616608	2.70916
168	Tma7-ps	0.382251	0.00725	0.646684	2.685154
169	Ubfd1	2.445455	0.007287	0.647764	2.68344
170	Wac	2.900269	0.007362	0.650808	2.680011
171	Rps28	0.421066	0.0074	0.652197	2.678296
172	Fhl1	3.134858	0.007438	0.653593	2.676581
173	Gm10163	1.16006	0.007827	0.673777	2.659435
174	Tmed10-ps	1.319018	0.007988	0.681659	2.652576
175	Ctsl	2.420092	0.008131	0.685944	2.646575
176	Scpep1	2.964057	0.008319	0.699533	2.638859
177	Actn1	2.521354	0.00834	0.699533	2.638001
178	Dlg3	4.428174	0.008618	0.720817	2.626856
179	Asah1	2.304886	0.008705	0.724012	2.623427
180	Mta3	2.838481	0.008793	0.727236	2.619998
181	Hk2	2.058267	0.009268	0.76016	2.601994
182	Hnrnpl	1.743148	0.009646	0.778144	2.588276
183	Nepn	33.17271	0.009864	0.789105	2.58056
184	Bpnt2	2.502848	0.010062	0.791928	2.573702
185	Polg	3.523127	0.010112	0.791928	2.571987
186	Tma7	0.280523	0.010162	0.793754	2.570272
187	Fbxl5	2.829422	0.010365	0.79904	2.563414
188	Prss8	8.429451	0.010365	0.79904	2.563414
189	Mif	0.52147	0.010888	0.826438	2.546267
190	Snhg18	3.218986	0.010888	0.826438	2.546267
191	Hs2st1	3.372186	0.011324	0.855093	2.53255
192	Tpd52	2.591922	0.011547	0.865246	2.525691
193	Lamp1	2.065115	0.011547	0.865246	2.525691
194	Soat1	2.497262	0.011575	0.865246	2.524834
195	Cxadr	4.043965	0.011632	0.867076	2.523119
196	Krt19	7.144201	0.011717	0.867076	2.520547
197	Dpp4	7.4169	0.011717	0.867076	2.520547
198	Lrrc42	2.97291	0.012241	0.894634	2.505116
199	Mlec	3.054119	0.01239	0.896657	2.500829

Cluster 7

	names	logfoldchange	pvals	pvals_adj	scores

0	Zfp640	14.93927	1.45E-08	3.74E-05	5.667794
1	Utf1	39.04129	1.45E-08	3.74E-05	5.667794
2	Gm10323	34.74613	1.45E-08	3.74E-05	5.667794
3	Hsp90aa1	2.976665	1.45E-08	3.74E-05	5.667794
4	Dppa5a	22.29659	1.45E-08	3.74E-05	5.667794
5	Dppa5c	36.38777	1.45E-08	3.74E-05	5.667794
6	Dppa5b	36.51495	1.45E-08	3.74E-05	5.667794
7	Zfp988	8.67569	1.49E-08	3.74E-05	5.66311
8	Zfp987	9.968847	1.53E-08	3.74E-05	5.658426
9	Mt2	8.378753	1.57E-08	3.74E-05	5.653742
10	Zfp534	9.061399	1.64E-08	3.74E-05	5.646716
11	Zfp989	8.478951	1.68E-08	3.74E-05	5.642032
12	Hat1	5.480129	1.75E-08	3.74E-05	5.635005
13	Gdf3	12.21379	1.98E-08	3.74E-05	5.613927
14	Hspb1	11.59082	2E-08	3.74E-05	5.611585
15	Zfp980	8.668576	2.26E-08	3.74E-05	5.590507
16	Rnf17	10.36617	2.33E-08	3.74E-05	5.585822
17	Dhx16	9.751678	2.42E-08	3.74E-05	5.578796
18	Gm12346	3.206242	2.49E-08	3.74E-05	5.574112
19	Zfp600	7.220263	2.56E-08	3.74E-05	5.569428
20	Rex2	7.105829	2.66E-08	3.74E-05	5.562402
21	Mt1	8.594644	3.87E-08	5.19E-05	5.496824
22	Gm5844	3.52556	4.84E-08	6.12E-05	5.457009
23	Gm9531	4.139726	4.97E-08	6.12E-05	5.452324
24	Rps4l	4.519779	8.17E-08	9.52E-05	5.363326
25	Sall4	8.029579	8.38E-08	9.52E-05	5.358642
26	Set	2.813726	9.67E-08	9.76E-05	5.33288
27	Gpx4	2.033101	9.79E-08	9.76E-05	5.330537
28	Gm7239	4.876083	9.79E-08	9.76E-05	5.330537
29	Zfp978	6.565437	9.92E-08	9.76E-05	5.328195
30	Gsta4	5.721265	1.38E-07	0.000132	5.267302
31	Ifitm1	9.094862	1.55E-07	0.000143	5.246223
32	Gstm3	7.280513	2.24E-07	0.000192	5.178303
33	L1td1	36.61232	2.57E-07	0.000192	5.15254
34	Zfp42-ps1	35.29716	2.57E-07	0.000192	5.15254
35	Gjb3	36.96218	2.57E-07	0.000192	5.15254
36	Ooep	36.159	2.57E-07	0.000192	5.15254
37	Fbxo15	15.95356	2.59E-07	0.000192	5.15137
38	Zfp42	15.84551	2.6E-07	0.000192	5.150198
39	Hsf2bp	13.84336	2.75E-07	0.000198	5.139659
40	Gm21411	9.560641	3.14E-07	0.000215	5.115067
41	Ash2l	7.305645	3.14E-07	0.000215	5.115067
42	Rhox5	10.98466	3.36E-07	0.000225	5.102186
43	Rps11	1.000249	3.59E-07	0.000236	5.089304
44	Gm13147	7.241745	4.3E-07	0.000276	5.055345
45	Rdm1	7.733162	5.39E-07	0.000338	5.012017
46	Sema4b	5.598844	6.95E-07	0.000427	4.962833
47	Platr14	9.130917	8.17E-07	0.000492	4.931215

48	Zfp982	7.011193	8.47E-07	0.0005	4.924189
49	Pmm1	6.91297	8.73E-07	0.000505	4.918334
50	Gpx4-ps2	1.882322	9.05E-07	0.000514	4.911308
51	Plekhf2	6.466645	9.83E-07	0.000548	4.894913
52	Ncl	2.02478	1.25E-06	0.000682	4.848072
53	Sgo2a	6.922009	1.34E-06	0.000718	4.83402
54	Crip1	6.117563	1.39E-06	0.000722	4.826993
55	Zfp981	6.567304	1.39E-06	0.000722	4.825822
56	Trap1a	9.472869	1.48E-06	0.000753	4.814112
57	Gstm1	6.591983	1.6E-06	0.000781	4.798889
58	Hspbap1	7.921915	1.81E-06	0.00086	4.773126
59	Eno1b	1.575909	1.84E-06	0.00086	4.770784
60	Mylpf	8.106943	1.92E-06	0.000873	4.761416
61	Exosc5	4.570781	1.92E-06	0.000873	4.761416
62	Prorp	7.745321	2.06E-06	0.000922	4.747364
63	Msh6	6.963081	2.21E-06	0.000973	4.733311
64	Cystm1	7.774092	2.3E-06	0.000999	4.725114
65	Ahsa1	3.971832	2.34E-06	0.001001	4.721601
66	Zfp985	6.820132	2.41E-06	0.001016	4.715745
67	Mkrn1	7.006548	2.59E-06	0.001079	4.700522
68	Avpi1	6.965318	2.72E-06	0.001114	4.691154
69	Chchd10	5.657485	3.22E-06	0.001254	4.656023
70	Zfp990	6.722894	3.35E-06	0.001254	4.647826
71	Got1	7.039282	3.37E-06	0.001254	4.646655
72	Prdx1	1.428162	3.41E-06	0.001254	4.644312
73	Ldhb	6.764972	3.41E-06	0.001254	4.644312
74	Mageb16	34.57302	3.53E-06	0.001254	4.637286
75	Gm48218	32.1502	3.53E-06	0.001254	4.637286
76	Rhebl1	7.539674	3.53E-06	0.001254	4.637286
77	Tdgf1	36.52496	3.53E-06	0.001254	4.637286
78	Tdrd12	14.11284	3.57E-06	0.001254	4.634944
79	Epp13	13.77035	3.57E-06	0.001254	4.634944
80	Zfp998	13.63848	3.61E-06	0.001254	4.632602
81	Hsp90ab1	0.914676	3.65E-06	0.001254	4.63026
82	Folr1	13.49632	3.65E-06	0.001254	4.63026
83	Dppa2	12.69923	3.74E-06	0.001268	4.625576
84	Tdh	12.62452	3.78E-06	0.001268	4.623234
85	Dkc1	5.746046	3.91E-06	0.001297	4.616208
86	Morc1	10.89381	4.23E-06	0.001387	4.599813
87	Zfp936	9.922492	4.28E-06	0.001388	4.597471
88	Castor1	10.2161	4.32E-06	0.001388	4.595129
89	Rbpms2	7.153695	4.4E-06	0.001396	4.591616
90	Gm19705	8.854065	4.68E-06	0.001454	4.578735
91	Cct8	1.7519	4.84E-06	0.001488	4.571709
92	Pkm	1.422024	4.95E-06	0.001506	4.567024
93	Tcea3	8.904812	5.29E-06	0.001594	4.552972
94	Gm8935	7.338925	5.41E-06	0.001613	4.548288
95	Bclaf3	7.13883	5.5E-06	0.001624	4.544775

96	Eed	6.162572	5.72E-06	0.001671	4.536578
97	Cox7a1	5.548902	6.08E-06	0.001757	4.523696
98	Rpp25	8.152907	6.18E-06	0.001757	4.520183
99	Fkbp3	1.356212	6.25E-06	0.001757	4.517841
100	Nup62cl	9.842926	6.25E-06	0.001757	4.517841
101	Zfp268	4.139915	6.86E-06	0.001911	4.497933
102	Sycp3	7.991748	7.45E-06	0.002037	4.480368
103	Gstp2	3.939583	7.45E-06	0.002037	4.480368
104	Snrpn	3.852643	7.87E-06	0.002113	4.468658
105	Rpl4	0.818196	8.22E-06	0.002187	4.45929
106	Rpa1	6.487917	8.4E-06	0.002216	4.454606
107	Eno1	1.381361	8.88E-06	0.002319	4.442895
108	Emb	6.707668	9.07E-06	0.002349	4.438211
109	Tipin	3.630633	9.47E-06	0.002432	4.428843
110	Ccne1	6.624501	9.89E-06	0.002518	4.419475
111	Fbxo5	6.672192	1.01E-05	0.002538	4.415961
112	Zfp986	5.10436	1.19E-05	0.002974	4.379659
113	Sod2	3.920103	1.21E-05	0.002988	4.374975
114	Eif2s2	1.955592	1.21E-05	0.002988	4.374975
115	Dppa4	7.314372	1.3E-05	0.003142	4.359752
116	Amt	4.542546	1.31E-05	0.003142	4.358581
117	Apobec3	7.559472	1.34E-05	0.003184	4.353897
118	Mtf2	5.233094	1.37E-05	0.003211	4.349213
119	Slc2a3	6.932227	1.37E-05	0.003211	4.348042
120	Nup88	5.006198	1.47E-05	0.003369	4.332818
121	Gart	6.040684	1.53E-05	0.003444	4.324621
122	Pfas	4.517802	1.67E-05	0.003712	4.304713
123	Slc25a39	4.060798	1.84E-05	0.004051	4.283635
124	Esco2	6.03191	1.89E-05	0.004129	4.27778
125	Ckb	6.886084	1.99E-05	0.004319	4.266069
126	Atad2	5.757061	2.06E-05	0.004398	4.257872
127	Rrp9	5.67086	2.09E-05	0.004398	4.25553
128	Cct3	2.910199	2.09E-05	0.004398	4.25553
129	Paics	2.965019	2.11E-05	0.004413	4.253188
130	Trp53	2.854244	2.15E-05	0.004475	4.248504
131	Etv5	6.786392	2.2E-05	0.004537	4.24382
132	Impa2	5.72171	2.24E-05	0.004601	4.239136
133	Hells	4.94186	2.46E-05	0.005018	4.218057
134	Pin1	2.343956	2.7E-05	0.00547	4.196979
135	Trim71	4.591649	2.75E-05	0.005509	4.193465
136	Oip5	5.750011	3.12E-05	0.00615	4.164189
137	Rpl18	0.758425	3.29E-05	0.006389	4.152479
138	Gm6366	3.717577	3.64E-05	0.00668	4.129058
139	Oard1	4.496214	3.68E-05	0.00668	4.126717
140	Triml2	35.46326	3.76E-05	0.00668	4.122032
141	Sox15	35.2574	3.76E-05	0.00668	4.122032
142	Gm7896	32.63314	3.76E-05	0.00668	4.122032
143	Rhox6	35.43544	3.76E-05	0.00668	4.122032

144	Rfc5	5.529108	3.76E-05	0.00668	4.122032
145	Rpl39l	35.34986	3.76E-05	0.00668	4.122032
146	Plac9a	33.8698	3.76E-05	0.00668	4.122032
147	Mcm7	5.193804	3.76E-05	0.00668	4.122032
148	Dpy30	2.078153	3.76E-05	0.00668	4.122032
149	Zscan10	34.28442	3.76E-05	0.00668	4.122032
150	Fam169a	5.978704	3.79E-05	0.006708	4.11969
151	Platr3	11.07642	3.85E-05	0.006724	4.116177
152	Tex19.1	11.92341	3.85E-05	0.006724	4.116177
153	Mphosph6	3.997612	3.87E-05	0.006724	4.115006
154	Rad51	6.214905	4.11E-05	0.007044	4.100954
155	Rif1	5.606269	4.16E-05	0.007044	4.098612
156	Mymx	10.60479	4.2E-05	0.007044	4.09627
157	EU599041	9.979774	4.2E-05	0.007044	4.09627
158	Selenoh	2.009045	4.2E-05	0.007044	4.09627
159	Nanog	11.7969	4.24E-05	0.007075	4.093927
160	Gm32885	10.03203	4.31E-05	0.007143	4.090415
161	Nanos3	8.60641	4.76E-05	0.007812	4.066994
162	Chek1	5.736137	4.86E-05	0.007922	4.06231
163	Gm6871	10.06079	4.88E-05	0.007922	4.061139
164	Hspe1	1.578698	4.93E-05	0.007959	4.058796
165	Ccdc58	2.690841	5.08E-05	0.008157	4.05177
166	Gm21399	2.390832	5.32E-05	0.008441	4.041231
167	Mif4gd	6.306891	5.4E-05	0.008522	4.037718
168	Rest	5.240617	5.73E-05	0.008951	4.023665
169	Apoc1	7.274944	5.99E-05	0.009312	4.013126
170	Gm14406	7.043807	6.05E-05	0.009355	4.010784
171	Aldoa	1.253855	6.14E-05	0.009442	4.007271
172	Wfdc2	8.688667	6.17E-05	0.009442	4.0061
173	Fkbp4	3.313618	6.27E-05	0.009487	4.002587
174	Rrm2	5.842585	6.39E-05	0.009627	3.997903
175	Galk1	3.493087	6.52E-05	0.009769	3.993219
176	Rpl21	0.78446	6.71E-05	0.010012	3.986193
177	Cenpm	5.238851	6.85E-05	0.010159	3.981508
178	Mreg	7.28736	6.88E-05	0.010159	3.980337
179	Ncoa3	4.638701	6.98E-05	0.010209	3.976824
180	Ptges3	1.797833	7.05E-05	0.010259	3.974482
181	H2-Bl	7.975427	7.23E-05	0.010412	3.968627
182	Alpl	8.341882	7.3E-05	0.010463	3.966285
183	Ung	5.549717	7.41E-05	0.010516	3.962772
184	Nudc	2.539916	7.41E-05	0.010516	3.962772
185	Gm11914	3.785698	7.44E-05	0.010518	3.961601
186	Gm2423	2.095097	7.48E-05	0.010519	3.96043
187	Sox2	6.992083	7.52E-05	0.010521	3.959259
188	Mrpl15	2.795851	7.86E-05	0.010943	3.94872
189	Zfp984	4.60391	7.93E-05	0.010998	3.946378
190	Mettl3	4.812568	8.29E-05	0.011386	3.935838
191	Ccnb2	5.996067	8.41E-05	0.0115	3.932325

192	Tpd52	5.753098	8.5E-05	0.011559	3.929983
193	Pipox	7.53622	8.54E-05	0.011562	3.928812
194	Mgme1	5.912787	8.66E-05	0.011679	3.925299
195	Brca1	5.464264	8.75E-05	0.011686	3.922957
196	Ubxn1	2.201406	8.75E-05	0.011686	3.922957
197	Hmgn5	4.563861	9.05E-05	0.012036	3.91476
198	Ifitm3	3.949825	9.45E-05	0.01246	3.90422
199	Ppat	5.330444	9.54E-05	0.012525	3.901878